Cardiac manifestations of inherited metabolic disease linked to cellular metabolism of vitamin B12 : study in two murine models of invalidation of Mtr and MMACHC genes

Viola Jepchumba Kosgei

Ecole Doctorale BioSE (Biologie-Santé Environnement)

Thèse

Présentée et soutenue publiquement pour l'obtention du titre de

DOCTEUR DE l'UNIVERSITE DE LORRAINE

Mention : « Sciences de la Vie et de la Sante »

Par

Viola Jepchumba KOSGEI

Manifestations cardiaques des maladies héréditaires du métabolisme cellulaire de la vitamine B12 : étude sur deux modéles murins d'invalidation des génes *Mtr* et *MMACHC*

Cardiac manifestations of inherited metabolic disease linked to cellular metabolism of vitamin B12: study in two murine models of invalidation of *Mtr* and *MMACHC* genes

Le 10 Décembre 2019

Membres du jury :

Rapporteurs :	M. Edward Valerian QUADROS :	PU, Département de Médicine et Anatomie/Biologie Cellulaire Brooklyn, NY, USA
	M. Sébastien BLAISE :	MCU, CNRS UMR/URCA 7369, Reims France
Examinateurs :	M. Jean-Louis GUÉANT :	PU-PH, UMR 1256 INSERM, Nancy France
	Mme. Ebba NEXO :	PU-PH, Département de Biochimie Clinique, Aarhus N, Denmark
	M. Yves JUILLIERE :	PU-PH, CHRU Nancy Département de Cardiologie, France
	Mme. Rosa-Maria GUEANT-RODRIGUEZ :	PU-PH, UMR 1256 INSERM, Nancy France, Directeur de thèse
Invité :	M. Ambrose K. KIPROP :	PU, Département de Chimie et Biochimie, Moi University, Kenya

UMR 1256 INSERM, Laboratoire de Nutrition, Génétique et Exposition aux Risques Environnementaux (NGERE), 9 avenue de la Forêt de Haye-Faculté de Médecine 54500 Vandœuvre-Lès-Nancy.

DEDICATION

I dedicate this Ph.D. Thesis to my beloved mother Francisca Kimoi Chepkong'a, my dear husband Jackson Yator and my dear children Alexis Jerotich and Emmanuel Kiptum.

ACKNOWLEDGEMENT

I wish to express my sincere gratitude to Professor Jean-Louis Guéant, the director of the UMR 1256 laboratory for welcoming me to his laboratory, for financial assistance and facilitating my research work during the three years of my Ph.D. studies. His availability, expertise and scientific prowess, valuable advice, enthusiasm for research enabled me to progress and have pleasure in research. Thanks for having confidence in me and building my career as a researcher. Many thanks for your patience during the correction of the article manuscript and this thesis.

I extend my heartfelt gratitude to my Ph.D. supervisor Professor Rosa-Maria Guéant-Rodriguez of University of Lorraine, for given me the opportunity to pursue my Ph.D. studies and accepting to supervise my work. Many thanks for everything Prof, I will never be able to thank you enough. Her scientific guidance and ideas, valuable advice, availability, encouragement and time that she devoted to me during the three years made me to achieve a lot during my studies. Thanks for facilitating my Ph.D. work, her energy and time she devoted in reading and correcting this thesis. Thanks for inviting me to share the precious Christmas holiday with her family and all the precious moments I spent with her outside the lab. Prof, I was lucky to be your student.

I wish to express my appreciation to the members of the Jury for my Ph.D. thesis defense. My sincere gratitude goes to Professor Edward Valerian QUADROS and Dr. Sébastien BLAISE accepting to be the rapporteurs of my thesis and Professor Ebba NEXO and Professor Yves JUILLIERE for accepting to examine my work.

I am deeply indebted to Professor Ambrose Kiprop the Dean of school of physical and biological sciences of Moi University for being my mentor. His advice, encouragement and facilitating my stay here in France is highly appreciated. I don't have enough words to describe my gratitude. His hard work and enthusiasm for research always inspires me, thanks for being my mentor.

I wish to deeply acknowledge the French government through the French Embassy in Kenya for having awarded me the scholarship to pursue my Ph.D. studies. The facilitation of my studies and my stay in France by Campus France is highly acknowledged. Sincere appreciation to Moi University for the facilitation and having given me the study leave. Thanks for making

it possible to realize my dream of obtaining a Ph.D. This will not only be important for my career development, benefit to Moi University but also to contribute to the knowledge in cardiovascular research for betterment of humanity.

I would like to acknowledge our collaborators for their contribution in my Ph.D. work.
Sincere acknowledgement goes to the L'institute Clinique de la Souris (ICS), Strasbourg for generating the transgenic mice. Many thanks go to Prof. L. Monassier.
Sincere acknowledgement goes to the team of Nancyclotep-GIE Ingénieur d'études imagerie préclinique, Vandoeuvre Les Nancy, France, especially to Dr. Fatiha Maskali their help, patience and collaboration in this work.
Sincere appreciation goes to the Inserm U1116 Défaillance cardiovasculaire aiguë et chronique lab, Vandoeuvre Les Nancy led by Professor Patrick Lacolley for his collaboration in this work and Veronique Laplace for her help.

Many thanks go to all the staff of UMR 1256 laboratory for their expertise, discussion and sympathy during my thesis.

I would like to pass my sincere appreciations to Sébastien Hergalent, the bioinformatic engineer in the UMR 1256 laboratory for analysis of proteomic and transcriptomic data. Thanks to his bioinformatic expertise I acquired a wealth of knowledge in omics studies

My gratitude and appreciation go to Dr. J.M Alberto the chief engineer his great participation in my thesis work. His advice, availability, scientific prowess in biochemistry research and his unwavering support enable me to achieve a lot during my study. I would like to also pass my sincere appreciations to Fatiha Elkhafifi former Master II student for her contribution to towards this work. Many thanks to Remy and Veronique for training me and taking care of the mice, Dr. Céline and Dr. Carol for their contribution to this work. I would like to pass my gratitude to Dr. Natasha and Dr. Shu Fung for their availability and advice. I wish to sincerely thank Dr. Brittany Balint, her expertise in immunohistochemistry, academic advice and correction of the article manuscript, her contribution to my thesis is highly appreciated.
For the administrative personnel, Aline, Dominique and Catherine your assistance is highly appreciated. To Aline, thanks to her jovial character and her motherly love I enjoyed sharing the same office with her, she even went out of her way to teach me French.
I would like to pass my sincere appreciation to my friends and colleague Aline, Racha and Ziad whom I shared the same office together. I appreciate the great moments we spent together. I

wish to also pass my gratitude and friendship to my dear colleagues and friends in the lab Amélia, Aurélie, Céline, Attah, Justine, Jeremy, Linda, Rashka, Pauline, Djseia, Tunay, Philip and Thierry. It was a pleasure to work with you.
I would like to sincerely thank the family of Monique for receiving and hosting me in her house when I first arrived in France and many invitations to their family. My appreciation goes to the family of Natalie for the holidays and invitations to your family. Thanks for being my sister here in France.

I would like to pass my sincere appreciation to my friend and colleague Darlene Antoine. I highly appreciated the great moments we spent together in and outside the laboratory. Darlene many thanks for reading my thesis Manuscript.

I would like to appreciate Father Daniel Muhame for his encouragement and Prayers. Thanks for being there for me big brother.

I thank my entire family for the encouragement, support and the confidence they bestowed on me during my studies in France. I am indebted to my Mum for encouraging me to work hard in my studies and for everything. Many thanks to my beloved husband Jackson, and my dear children Alexis and Emmanuel for their love, patience, support, encouragement and their understanding despite my long absence from home. Thanks to my dear sisters Anita, Caro and brother Ambrose for their support, Koech and Memoi thanks so much for your love, understanding and sacrifice to take care of the kids while I was in France.

TABLE OF CONTENTS

DEDICATION 3
ACKNOWLEDGEMENT 4
TABLE OF CONTENTS 7
LIST OF FIGURES 13
LIST OF TABLES 16
ABBREVIATIONS 17
PUBLICATIONS AND ORAL COMMUNICATIONS 21
Publications 21
Poster presentations 21
Oral Presentations 22
ABSTRACT 24
RÉSUMÉ 25
RÉSUMÉ DE THÉSE EN FRANÇAIS 26
INTRODUCTION 42
1 HEART FAILURE 42
1.1 Definition of heart failure 42
1.2 Classification of heart failure 43
1.2.1 Classification of heart failure on the basis of physical activity and severity of symptoms 43
1.2.2 Classification of heart failure based on structural and functional abnormalities 43
1.2.3 Classification of heart failure based on left ventricular ejection fraction 44
1.3 Cardiac physiology and left ventricular adaptation mechanisms 45
1.3.1 Normal cardiac physiology 45
1.3.2 Left ventricular dysfunction 45
1.3.3 Adaptation mechanism to left ventricular dysfunction and heart failure 46
1.4 Biomakers of heart failure 56
1.5 Causes of heart failure 56
1.6 Genetic cardiomyopathies and heart failure. 57
2 Energy metabolism in the heart 60
2.1 Energy metabolism in normal heart 60
2.1.1 Fatty acid oxidation in normal heart 61
2.1.2 Regulation of fatty acid oxidation 63

2.1.3 Glucose metabolism in normal heart 63
2.1.4 Regulation of glucose oxidation 63
2.2 Energy metabolism in heart failure 64
2.2.1 Glycolysis in heart failure 64
2.2.2 Fatty acid oxidation in heart failure 65
2.2.3 Mediators of impaired fatty acid oxidation in the heart failure 66
2.3 Role of Sirt3 in myocardial mitochondrial energy metabolism 67
3 Impaired remethylation of homocysteine as risk factor for cardiovascular diseases and heart failure 70
3.1 Hyperhomocysteinemia 70
3.1.1 Definition of hyperhomocysteinemia 70
3.1.2 Causes of hyperhomocysteinemia 70
3.1.3 Hyperhomocysteinemia and cardiovascular diseases 72
3.1.4 Pathological mechanisms of homocysteine 74
4 THE ROLE OF METHIONINE SYNTHASE IN THE METABOLISM OF MONOCARBONS AND REMETHYLATION OF HOMOCYSTEINE 78
4.1 Nutritional determinants for the remethylation of homocysteine and synthesis of methionine by methionine synthase 78
4.1.1 Vitamin B12 78
4.1.2 Folates (Vitamin B9) 85
5 Metabolism of mono-carbons, methyl donors and remethylation of homocysteine by methionine synthase 92
5.1 The methionine /homocysteine cycle 92
5.1.1 Substrates and metabolites of methionine/homocysteine cycle 92
i) Remethylation of homocysteine 96
ii) Transsulfuration 97
5.1.2 The Folate Cycle 97
5.2 Methionine synthase and MMACHC proteins 100
5.2.1 Methionine synthase 100
5.2.2 MMACHC protein 107
6 GENETIC DEFECTS AND PATHOLOGIES LINKED TO INTRACELLULAR METABOLISM OF VITAMIN B12 AND REMETHYLATION OF HOMOCYSTEINE 112
6.1 Genetic defects linked to intracellular metabolism of vitamin B 12 112
6.1.1 Classification of inborn errors of intracellular metabolism of vitamin B12 112
6.1.2 Genetic defects affecting the remethylation of homocysteine into methionine by methionine synthase 113

6.1.3 Genetic defects linked to deficiency in synthesis of both adenosyl-cobalamin and methyl cobalamin 116

6.2 Cardiovascular diseases and congenital heart defects linked to genetic defects of vitamin B12 metabolism and remethylation of homocysteine 118

7 TRANSGENIC ANIMAL MODELS TO STUDY DEFECTIVE METABOLISM OF FOLATE AND VITAMIN B12 METABOLISM AND REMETHYLATION OF HOMOCYSTEINE 120

7.1 Mice deficient in methionine synthase reductase (*Mtrr* deficient mice) 120

1.1 Mice deficient in methyltetrahydrofolate reductase (*Mthfr* deficient mice) 120

7.2 Mice deficient in Cystathionine beta synthase (*Cbs* deficient mice) 121

7.3 Betaine-homocysteine methyltransferase knock out mice (*Bhmt* deficient mice) 122

STUDY OBJECTIVES AND HYPOTHESES 123

MATERIALS AND METHODS 126

1 Animals 126

1.1 Generation of the transgenic mice models 126

1.1.1 Generation of Cardiac specific *Mtr* constitutive knock out mice by Cre-Lox System 126

1.1.2 Systemic knock out of *MMACHC* gene mouse model 127

1.2 Genotyping 128

1.2.1 DNA extraction 128

1.2.2 Polymerase chain reaction (PCR) 128

1.3 Sacrificing and harvesting of blood and tissue samples 131

2 Evaluation of cardiac function parameters (hemodynamic and left ventricular function analysis) 131

2.1 Measurement of blood pressure using tail cuff plethysmography 131

2.2 Evaluation of left ventricular function by echocardiography 132

2.3 Evaluation of left ventricular function by Mini-PET 133

3 Determination of the concentration of metabolites of one-carbon metabolism in cardiac tissue 136

3.1 Determination of the concentration of adenylated molecules S-adenosyl homocysteine (SAH) and S-adenosyl methionine (SAM) cardiac tissue using chloroacetaldehyde by LC-MS / MS 136

3.2 Determination of the concentration of folates 137

4 Determination of the concentration levels of free carnitine and acylcarnitine 140

5 Evaluation of methionine synthase enzyme activity in heart tissue 141

6 Real time Polymerase chain reaction 142
6.1 Extraction of RNA 142
6.2 Quantification of RNA 143
6.3 Determination of RNA quality and integrity 143
6.4 Real time Polymerase chain reaction (RT-qPCR) 144
7 Western blot analysis 145
7.1 Extraction and preparation of protein for western blot analysis 145
7.2 Determination of protein concentration using Bicinchoninic acid protein assay reagent 146
7.3 Preparation of protein sample for western blot analysis 146
7.4 Preparation of the sodium dodecyl sulfate polyacrylamide gel 146
7.5 Electrophoresis 149
7.6 Transfer of proteins to the membrane 149
7.7 Immunoblotting 150
8 Immunohistology 152
8.1 Treatment of fixed tissues for histological analysis 152
8.2 Cutting of tissues 152
8.3 Deparaffination of tissue and unmasking of antigens 152
8.4 Immunofluorescence 152
8.5 Picrosirius red staining 153
8.6 Masson's Trichrome staining 154
9 Omics studies 155
9.1 Proteomic analysis by LC-MS / MS 155
9.2 RNA Hi Seq sequencing and transcriptome analysis 155
10 Statistical analysis 157
RESULTS 159
MODEL 1 159
1 Validation of the study Model 159
1.1 Confirmation of the effective deletion of Mtr gene in the cardiomyocytes 159
1.1.1 Expression of *Mtr* gene in the heart 159
1.1.2 Expression of MTR /MS and Cre-recombinase proteins in the heart 160

1.1.3 Evaluation of methionine synthase activity in the heart 161

1.2 Consequences of cardiac specific deletion of *Mtr* gene on one- carbon metabolism (metabolic phenotype). 162

1.2.1 Determination of the concentration of S-adenosyl homocysteine (SAH) and S-adenosyl methionine in heart tissue (SAM). 162

1.2.2 Determination of folate concentration in heart 163

2 Consequences of cardiac specific invalidation of *Mtr* gene on cardiac function parameters (Phenotypic study). 164

2.1 Systolic blood pressure 164

2.2 Evaluation of left ventricular function by Echocardiography 164

2.3 Evaluation of left ventricular function using positron emission tomography (Mini-PET) 167

2.4 Survival rate of *Mtr cKO* 169

2.5 Expression levels of biomarkers of heart failure 170

3 Consequences of cardiac specific invalidation of *Mtr* on expression changes in Omics studies 171

3.1 Transcriptomics 171

3.1.1 Transcriptomic expression profile in the heart 171

3.1.2 Gene ontology enrichment and pathway analysis 173

3.1.2.1 Gene ontology enrichment and pathway analysis of the 1889 under-expressed genes 173

3.1.2.2 Gene ontology enrichment and pathway analysis of the 1889 under-expressed genes by Enrichr 174

3.1.2.3 Gene ontology and pathway analysis of the overexpressed genes in sub-clusters 3 and 4 ... 176

3.1.3 Mapping the dysregulated genes in the myocardium *Mtr cKO* using KEGG pathway database 180

3.2 PROTEOMICS 181

3.2.2 Gene ontology enrichment and pathway analysis of the dysregulated proteins in heart tissues. 181

3.2.3 GO enrichment and pathway analysis of the top 94 dysregulated proteins in the myocardium of *Mtr cKO.* 183

4 Consequences of cardiac specific invalidation of *Mtr* on cardiac remodelling 194

4.2 Cardiac specific deletion of *Mtr* gene induces myocardium hypertrophy 194

5 Consequences of cardiac specific invalidation of *Mtr* gene on energy metabolism in the myocardium 202

5.1 Concentration of acylcarnitine in plasma..... 202

5.2 Expression levels of genes, proteins and regulators of energy metabolism in the heart 204

5.2.1 Cardiac specific invalidation of *Mtr* gene induces dysregulated expression of fatty acid beta oxidation genes and proteins. 204

5.3 Cardiac specific invalidation of *Mtr* gene induces dysregulated expression of genes encoding oxidative phosphorylation and glycolysis enzymes. 206

5.4 Expression levels of regulators of energy metabolism in the heart..... 208

MODEL II : Study of cardiovascular consequences of systemic invalidation of *MMACHC* gene in 5 months old mice..... 210

1. Consequences of systemic invalidation of *MMACHC* gene on cardiac function parameters 210

1.1 .Systolic Blood pressure..... 210

1.2 . Expression levels of biomarkers of heart failure 210

2 Consequences of cardiac specific invalidation of *Mtr* gene on one carbon metabolism 211

CONCLUSION AND PERSPECTIVES..... 219

REFERENCES..... 220

Annex 1:.....Hypertrophic cardiomypathy and systolic dysfunction in mice with cardiac selective invalidation of *methionine synthase* (*Mtr*) is related to impaired energy metabolism, cellular stress and fibrosis..... 300

Annex 2: ..... Figures Kosgei J Viola et al 324

Annex 3: ..... Supplementary data for Kosgei J Viola et al 331

LIST OF FIGURES

Figure 1: **Physiology of ANP and BNP adapted from (Volpe, Carnovali, & Mastromarino, 2016)** .52

Figure 2: **Schematic representation of neurohormonal interaction in heart failure. Adapted from (Brahmbhatt & Cowie, 2018)** 55

Figure 3: **Summary of the aetiologies of heart failure adapted from (Ponikowski et al., 2014).** 57

Figure 4: **An overview of fatty acid beta oxidation in the heart adapted from** (Lopaschuk et al., 2010).....62

Figure 5: **Chemical structure of vitamin B 12. Adapted from (David Watkins & Rosenblatt, 2011)** 80

Figure 6: **Absorption, transport, enterohepatic circulation and intracellular metabolism of vitamin B12. Adapted from (Green et al., 2017).**.....84

Figure 7: **Chemical structure of folate and its derivatives adapted from (Bekaert et al., 2008; Guéant et al., 2013)**.....88

Figure 8: **Folate absorption and distribution in peripheral tissues and liver adapted from (Guéant et al., 2013)** 91

Figure 9: **Chemical structure of methionine**.....92

Figure 10: **Chemical structure of S adenosyl methionine** 93

Figure 11: **Chemical structure of S-adenosyl homocysteine** 94

Figure 12: **Inhibition of methylation reactions by SAH** 94

Figure 13: **Summary of the pathway of synthesis of S-adenosyl methionine, S-adenosyl homocysteine and homocysteine.** 95

Figure 14: **Chemical structure of homocysteine**.....96

Figure 15: **The folate and methionine cycles adapted from (Guéant et al., 2013)** 99

Figure 16: **Diagram showing the modular structure of cobalamin-dependent methionine synthase (Rowena G Matthews, 2001)**.....103

Figure 17: **Ribbon drawing of the homocysteine and methyl tetrahydrofolate binding domains of MetH from T. maritima. Adapted from (Evans et al., 2004b)** 104

Figure 18: **Three dimensional structure of methyl cobalamin binding domain of methionine synthase adapted from (Gruber & Kratky, 2006)** 104

Figure 19: **Three-dimensional structure of the activation domain / Adomet binding domain of methionine synthase adapted from (Dixon et al., 1996)**.....105

Figure 20: **Reactions catalyzed by cobalamin dependent Methionine synthase in the conversion of homocysteine to methionine and N5-MeTHF to THF. Scheme Adapted from (R. G. Matthews, 2001)**.....107

Figure 21: **Structure of the apo-MMACHC protein adapted from (Hannibal et al., 2013; Koutmos et al., 2011)**.....110

Figure 22: **Processing of cobalamins by MMACHC adapted from (Koutmos et al., 2011)**.....111

Figure 23: **Genetic defects of metabolism of vitamin B12 adapted from (Coelho et al., 2008)**.....113

Figure 24: **Cardiac specific invalidation of Mtr gene by Cre -loxP system** 127

Figure 25: **Representation of the MiniPET acquisition process adapted from thesis MM. Garcia 2011** 135
Figure 26: **Expression levels of Mtr gene analyzed by RT-qPCR** 159
Figure 27: **Expression levels of MTR and Cre proteins in the hearts of controls and Mtr cKO analyzed by western blotting** 160
Figure 28: **Expression level of MTR protein in the liver analyzed by western blot** 161
Figure 29: **Activity of Methionine synthase enzyme in the myocardium** 161
Figure 30: **Concentration of metabolites of one-carbon metabolism and remethylation of homocysteine in the heart analyzed using LC-MS/MS.** 162
Figure 31: **Concentration levels of folates in the heart tissue of 5 months old Mtr cKO and control mice** 163
Figure 32: **Systolic blood pressure in 5 months old mice measured using tail cuff plethysmography**. 164
Figure 33: **Cardiac left ventricular function of Mtr cKO and control mice evaluated by transthoracic echocardiography.** 166
Figure 34: **Left ventricular parameters of Mtr cKO and controls assessed by Mini-PET** 168
Figure 35: **Comparison of survival rates of Mtr cKO and control mice.** 169
Figure 36: **Expression levels of biomarkers of heart failure in the heart tissues of Mtr cKO and control mice analyzed by RT-qPCR** 170
Figure 37: **Consequence of cardiac specific deletion of Mtr gene in the transcriptome of the heart**. 172
Figure 38: **PANTHER Gene Ontology term enrichment analysis of the 1889 under-expressed genes in the hearts of Mtr cKO.** 174
Figure 39: **Enrichr Gene Ontology term enrichment analysis for the cluster 2 under-expressed genes in the hearts of Mtr cKO**. 175
Figure 40: **Enrichr GO enrichment analysis for the cluster 2 under-expressed genes in hearts Mtr cKO implicated in response to cellular stress.** 176
Figure 41: **Enrichr Gene Ontology term enrichment analysis for the 418 overexpressed genes (Sub-cluster 3) in the hearts of Mtr cKO** 178
Figure 42: **PANTHER Gene Ontology term enrichment and pathway analysis for the overexpressed genes (Sub-cluster 4 and sub-cluster 3) in the hearts of Mtr cKO** 180
Figure 43: **Proteomic analysis of dysregulated proteins in the heart of Mtr cKO.** 182
Figure 44: **Venn diagram representing the overlapping between the commonly dysregulated genes and proteins in the hearts of Mtr cKO mice.** 188
Figure 45: **Enrichr GO biological processes of the 59 positively overexpressed proteins in the hearts of Mtr cKO in comparison to controls.** 189
Figure 46: **Enrichr GO biological processes and molecular functions associated with the 90 positively under-expressed proteins in the hearts of Mtr cKO.** 190
Figure 47: **Enrichr GO cellular components and the KEGG pathways associated with the 90 under-expressed proteins in the heart of Mtr cKO.** 191

Figure 48: **Graphical representation of the positively and negatively correlated genes-proteins in *Mtr cKO* analyzed by Spearman correlation.** 193
Figure 49: **Deletion of *Mtr cKO* in the heart induces cardiac hypertrophy.** 195
Figure 50: **KEGG pathway showing the dysregulated genes in the Mtr cKO associated with the development of hypertrophic cardiomyopathy.** 195
Figure 51: **Cardiac specific deletion of Mtr gene induces interstitial fibrosis in the myocardium evidenced by increased collagen deposition in the myocardium.** 197
Figure 52: **Cardiac specific deletion of Mtr gene induces interstitial fibrosis in the myocardium evidenced by increased expression of MMP2 in the myocardium of Mtr cKO.** 198
Figure 53: **Cardiac specific deletion of Mtr gene induces cellular stress** 200
Figure 54: **Subcellular localization of HNRNPA1, HuR/ ELAV1 and Y14 RNA binding proteins in the left ventricles of Mtr cKO and controls evaluated by immunofluorescence** 201
Figure 55: **Plasma acylcarnitine concentration levels and expression of CD36 in hearts Mtr cKO and control mice.** 203
Figure 56: **KEGG pathway showing dysregulated expression of genes encoding enzymes involved in fatty acid oxidation in the hearts of Mtr cKO.** 204
Figure 57: **Cardiac invalidation of Mtr induces dysregulated expression of oxidative phosphorylation and glycolytic genes and proteins.** 207
Figure 58: **KEGG pathway showing dysregulated genes involved oxidative phosphorylation in the hearts of Mtr cKO. Shown in green are downregulated genes and red are upregulated genes.** 208
Figure 59: **Silencing of MS in the heart impairs energy metabolism by decreasing the expression of Sirt3 protein.** 209
Figure 60: **Systolic blood pressure in the MACHC $^{+/+}$ and MMACHC $^{+/-}$ mice measured using tail cuff plethysmography** 210
Figure 61: **Expression levels of biomarkers of heart failure in the hearts of MMACHC $^{+/-}$ and MMACHC $^{+/+}$ mice.** 211
Figure 62: **Concentration of Vitamin B12 in the hearts of 21 days old MMACHC $^{+/+}$ and MMACHC $^{+/-}$ mice analyzed by LC-MS/MS.** 212

LIST OF TABLES

Table 1: **Recommended vitamin B12 nutritional intake for the French population**.....79

Table 2: **Recommended folate nutritional intake for the French population**.....86

Table 3: **The reaction volumes of KAPA kit reagents used for extraction for genomic DNA for genotyping.**.....128

Table 4: **PCR KAPA kit conditions**.....129

Table 5: **PCR Conditions for genotyping**.....130

Table 6: **Sequences of primers used for genotyping**.....131

Table 7: **Sequences and conditions of primers used for RT-qPCR**.....145

Table 8: **Concentration of polyacrylamide gels for different sizes of proteins**.....147

Table 9: **Conditions for preparation of the stacking and separation gels for PAGE**.....148

Table 10: **List of antibodies used for western blotting analysis**.....151

Table 11: **Left ventricular parameters of Mtr cKO and control mice evaluated by echocardiography.**.....165

Table 12: **Left ventricular parameters of Mtr cKO and control mice assessed by Mini-PET scan.**167

Table 13: **Enrichr Gene ontology term enrichment analysis for the 887 overexpressed genes (Sub-cluster 4) in the hearts of Mtr cKO**.....179

Table 14: **Cardiovascular diseases associated with the 34 differentially expressed proteins in the myocardium of Mtr cKO analysis achieved using Open Targets platform.**.....183

Table 15: **Metabolic diseases associated with the top 94 dysregulated proteins**.....184

Table 16: **Genetic diseases associated with the top 94 dysregulated proteins**.....185

Table 17: **Correlation analysis of the proteome and transcriptome.**.....192

Table 18: **Transcriptomics data showing dysregulated genes involved in fatty acid beta oxidation, oxidative phosphorylation and glycolysis in the myocardium of Mtr cKO.**.....205

ABBREVIATIONS

5-MeTHF: 5-Methyltetrahyrofolate

AA: Amino acid

ABCD4 protein: ATP-binding cassette (ABC) carry D4

ACC: Acetyl CoA carboxylase

ACC/AHA: American College of Cardiology / American Heart Association

AdoCbl: Adenosyl cobalamin

ADP: Adenosine diphosphate

ANP: Atrial natriuretic peptide

AT1: Angiotensin receptor 1

AT2: Angiotensin receptor 2

ATP: Adenosine triphosphate

BHMT: Betaine-homocysteine methyltransferase

BNP: Brain natriuretic peptide

cAMP: Cyclic Adenosine Monophosphate

Cbl: Cobalamin

CblC: Combined methylmalonic aciduria and homocystinuria, CblC type

CblE: homocystinuria-megaloblastic anemia, CblE complementation type / methylcobalamin deficiency CblE type

CblG: Homocystinuria-megaloblastic anemia, CblG complementation type / CblG complementation type methionine synthase deficiency

CBS: Cystathionine β-synthase

CNCbl: Cyanocobalamin

CO: Cardiac output

CPT1: Carnitine palmitoyl transferase 1

CPT2: Carnitine palmitoyl transferase 2

CTH: Cystathionine γ-lyase

CYL: Cystathionine γ-lyase

DCM: Dilated cardiomyopathy

DHF: Dihydrofolate

DHFR: Dihydrofolate reductase

DMB: Dimethylenzimidazole

DNA: Deoxyribonucleic acid

EDV: End diastolic volume

EPI: Epinephrine

ESC: European society of cardiology

ESV: End systolic Volume

ETC: Electron transport chain

FABPpm: Fatty acid binding protein

FACS: Fatty acyl CoA synthetase

FAD: Flavin adenine diglutamate

FADH2: Flavin adenine dinucleotide

FAT/CD36: Fatty acid translocase

FATP: Fatty acid transport protein

FDR: False discovery rate

FGCP: Intestinal folylpolyglutamate carboxypeptidase

FGPS: Folypolyglutamate synthase

FMG: Folate monoglutamates

FMN: Flavin monoglutamate

FPG: Folate polyglutamates

FR: Folate receptor

GCPII: Glutamate carboxypeptidase

GH: γ-glutamyl hydrolase

GSH: Glutathione

HCM: Hypertrophic cardiomyopathy

Hcy: Homocysteine

HF-mEF: Heart failure with medium range ejection fraction

HF-pEF: Heart failure with preserved ejection fraction

HF-rEF: Heart failure with reduced ejection fraction

HF: Heart failure

HHcy: Hyperhomocysteinemia

HR: Heart rate

IF: intrinsic factor

KEGG: Kyoto Encyclopedia of Genes and Genomes

LCAD: Long chain acyl-CoA dehydrogenase

LMBD1: Lysosomal membrane transport 1

LVEF: Left ventricular ejection fraction

LVFS: Left ventricular franctional shortening

MAP: Mean arterial pressure

MAPK: Mitogen activated protein kinase

MAT: Methionine adenosyltransferase

MCAD: Medium chain acyl-CoA dehydrogenase

MCD: Malonyl CoA decarboxylase

MCM: MéthylmalonylCoA mutase

Mecbl: Methyl cobalamin

Met: Methionine

MMA: Methylmalonic acid

MMACHC: methylmalonic aciduria homocystinuria type C

MMADHC: Methylmalonic aciduria and homocystinuria type D

MMP2: Matrix metallopeptidase 2

MS: Methionine synthase

MTHFR: Methylene tetrahydrofolate reductase

MTR: Methionine synthase

MTRR: 5 methyltetrahydrofolate-homocysteine methyltransferase reductase

MUT: Methylmalonic coenzyme A mutase

MYBPC3: Myosin binding protein C

MYH6: alpha myosin heavy chain

MYH7: beta Myosin heavy chain

MYL3: Myosin light chain 3

N5-MeTHF: N5-methyltetrahydrofolate

N5,10-MeTHF: N5,10-methylene tetrahydrofolate

NADH: Nicotinamide adenine dinucleotide

NADPH: Nicotinamide adenine

NE: Norepinephrine

NO: Nitric oxide

NTD: Neural tube defects

NYAH: New York Heart Association

OHCbl: Hydroxy cobalamin

PCFT: Proton-coupled folate transporter

PCr: Phosphocreatine

PCR: Polymerase Chain Reaction

PDH: Pyruvate dehydrogenase

PFK1: Phosphofructokinase 1

PGC1 α: Peroxisome proliferator-activated receptor-γ co-activator-1

RAAS: Renin angiotensin aldosterone system

RCM: Restrictive cardiomyopathy

RFC: Reduced Folate Receptor

RNA: Ribonucleic acid

RT-qPCR: Real time quantitative polymerase chain reaction

S-FBP: Soluble Folate Binding Proteins

SAH: S- adenosyl homocysteine

SAHH: S- adenosyl homocysteine hydrolase

SAM: S-adenosyl methionine

SBP: Systolic blood pressure

SDH: SDH sub-unit of succinate dehydrogenase

SDS-PAGE: Sodium Dodecyl Sulfate Polyacrylamide Gel Electrophoresis

SHMT: Serine hydroxymethyltransferase

SIRT1: NAD- deacetylase sirtuin-1

SIRT3: NAD- deacetylase sirtuin-3

SNS: Sympathetic nervous system

SV: Stroke volume

TAGs: Triglycerides

TCA: Tricarboxylic acid cycle

TCblR: Transcobalamin Receptor

TCII: Transcobalamin

TGFβ: Transforming Growth Factor β

THF: Tetrahydrofolate

VLDL: Very low-density lipoproteins

α MHC: alpha myosin heavy chain

β MHC: Beta myosin heavy chain

μm: Micrometer

μM: Micromolar

PUBLICATIONS AND ORAL COMMUNICATIONS

Publications

Viola J. Kosgei, Carole Arnold, Sébastien Hergalant, Brittany Balint, Jean-Michel Camadro, Fatiha Elkhafifi, Patrick Lacolley, Luc Monnasier, Fatiha Maskali, Jean-Louis Guéant [1*], Rosa-Maria Guéant-Rodriguez* Hypertrophic cardiomypathy and systolic dysfunction in mice with heart selective invalidation of *methionine synthase* (*Mtr*) is related to impaired energy metabolism, cellular stress and fibrosis. (Ready for submission).

Brittany Balint*, **Viola Kosgei Jepchumba**, Jean-Louis Gueant, Rosa-Maria Gueant-Rodriguez. The harmful effects of homocysteine on the arterial wall (Submitted Biochimie Journal).

Poster presentations

Viola .J. Kosgei, C. Arnold, S. Hergalant,B. Balint, F. Elkhafifi, P. Lacolley, L. Monassier, F. Maskali, J.L. Guéant[1], R.M. Guéant-Rodriguez. *Cardiac manifestations of inherited metabolic disease linked to cellular vitamin B12 (cobalamin) uptake: study in murine model of invalidation of Mtr gene in the heart.* Award winning poster presentation in the 12th International conference on One carbon metabolism, B vitamins and Homocysteiene, Montrbrió del Camp, **Catalonia Spain, 2019**.

Kosgei .J. Viola, F.Elkhafifi, P. Lacolley, R. Umoret, J.L Guéant, R.M Guéant-Rodriguez. *Cardiac manifestations of inherited metabolic disease linked to cellular vitamin B12 uptake: Study in murine model of invalidation of Mtr gene in the heart.* 29th European Days of the French Society of Cardiology, **Paris, France, 2019.**

Kosgei .J. Viola, P. Lacolley, P.Y Marie, J.L. Guéant, R.M. Guéant-Rodriguez. *Cardiac manifestations of inherited metabolic disease linked to cellular vitamin B12 uptake study in two murine models of invalidation of Mtr and Mmachc genes.* Journée de rentrée de l'École doctoral Biologie-Santé-Environnement (BioSE), **Nancy, France, 2017**.

Oral Presentations

Kosgei . J. Viola, C. Arnold, S. Hergalant, B. Balint, F. Elkhafifi, P. Lacolley, L. Monassier, M. Fatiha, J.L. Guéant, R.M. Guéant-Rodriguez. *Cardiac manifestations of inherited metabolic disease linked to cellular vitamin B12 (cobalamin) uptake: study in murine model of invalidation of Mtr gene in the heart.* Workshop de présentation de travaux de recherche des FHU(s) Cartage et Arrimage en partenariat avec le projet Lorraine Université d'Excellence (LUE) Impact Geenage, **Nancy, France, 2019.**

Kosgei .J. Viola, C. Arnold, F. Elkhafifi, P. Lacolley, L. Monassier, M. Fatiha, J.L. Guéant, R.M. Guéant-Rodriguez. *Cardiac consequences of constitutive invalidation of Mtr gene (methionine synthase) in mice*. Workshop de présentation de travaux de recherche des FHU(s) Cartage et Arrimage en partenariat avec le projet Lorraine Université d'Excellence (LUE) Impact Geenage, **Nancy, France, 2018.**

Kosgei .J. Viola, C. Arnold, F. Elkhafifi, S. Hergalant, P. Lacolley, L. Monassier, M. Fatiha, J.L. Guéant, R.M. Guéant-Rodriguez. *Cardiac manifestations of inherited metabolic disease linked to cellular vitamin B12 (cobalamin) uptake: study in murine model of invalidation of Mtr gene in the heart.* Journée de la Recherche Master Sciences du Vivant (JRM), **Nancy France 2018**.

Viola .J. Kosgei, C. Arnold, F. Elkhafifi, P. Lacolley, S. Hergalant, L. Monassier, M. Fatiha, J.L. Guéant, R.M. Guéant-Rodriguez. *Cardiac manifestations of inherited metabolic disease linked to cellular vitamin B12 (cobalamin) uptake: study in murine model of invalidation of Mtr gene in the heart*. Journee scientific de école doctoral

one C
B vitamins and Homocysteine
12th International Conference
Montbrió
2019

This is to certify that the Prize for best Student Poster

at the *12th International Conference on One Carbon Metabolism, B Vitamins and Homocysteine,* held by the Unit of Preventive Medicine and Public Health, Universitat Rovira i Virgili, in Montbrió del Camp, Catalonia, Spain from June 9th to June 16th 2019

was awarded to Viola Kosgei, University of Lorraine, for the presentation:

"Cardiac manifestations of inherited metabolic disease linked to cellular vitamin B12 (cobalamin) uptake: study in murine model of invalidation of Mtr gene in the heart".

Michelle Murphy

Chair homocysteine2019

Unit of Preventive Medicine & Public Health,

Faculty of Medicine & Health Sciences

Universitat Rovira i Virgili

UNIVERSITAT ROVIRA i VIRGILI

ABSTRACT

Heart failure (HF) is one of the most common cause of morbidity and mortality in Western countries and its incidence is increasing in developing countries. Inherited genetic defects are one of the major causes of primary cardiomyopathies and heart failure. Deficiency in folates and vitamin B12 (cobalamin) during gestation and lactation cause a fetal programming effect with metabolic cardiomyopathy related to decreased synthesis of methionine and impaired remethylation (RM) of homocysteine. Methionine is the precursor for the S-adenosyl methionine, the universal methyl donor for transmethylation reactions and epigenomic regulatory mechanisms of gene expression. Inborn errors of cobalamin metabolism, including CblG caused by mutations of *MTR* gene, which encodes methionine synthase (that catalyzes vitamin B12 dependent remethylation of homocysteine to methionine), and CblC caused by mutations of *MMACHC* gene cause cardiometabolic decompensation in infants. However, cardiac consequences and mechanisms underlying this process in adults are unknown. The aim of this Ph.D. project was to investigate the cardiac functional, metabolic and molecular consequences of the inhibition of methionine synthesis in a transgenic mouse model of constitutive cardiac specific invalidation of *Mtr* gene and systemic invalidation of *MMACHC* gene. As results, we found that the selective *Mtr* invalidation in the heart produces cardiomyopathy with heart failure, myocardium hypertrophy and systolic dysfunction in young adult mice. At the tissue and molecular levels, the observed cardiomyopathy was related to impaired energy metabolism with disruption of fatty acid oxidation and oxidative phosphorylation, cellular stress and cardiac remodeling with fibrosis. Impaired energy metabolism was linked to decreased expression of Sirt3. The mis-localization and nuclear sequestration of hnRNPA1 could explain part of the expression changes of genes and proteins. These findings suggest a further need to evaluate whether CblG could be a new genetic cause of primary heart failure in adult patients.

Key words: Vitamin B12, methionine synthase, cardiomyopathy, heart failure, cardiac hypertrophy, energy metabolism, *MMACHC, MTR*

RÉSUMÉ

L'insuffisance cardiaque est l'une des causes les plus courantes de morbidité et de mortalité dans les pays occidentaux et son incidence augmente dans les pays en développement. Les anomalies génétiques héréditaires sont l'une des principales causes des cardiomyopathies primitives et de l'insuffisance cardiaque. Une carence en folates et en vitamine B12 (cobalamine) au cours de la gestation et de l'allaitement entraîne un effet de programmation fœtale avec une cardiomyopathie métabolique liée à une diminution de la synthèse de méthionine et à une altération de la réméthylation de l'homocystéine. La méthionine est le précurseur de la S-adénosyl méthionine, le donneur de méthyle universel utilisé pour les réactions de transméthylation et les mécanismes de régulation épigénomique de l'expression génique. Les défauts génétiques du métabolisme de la cobalamine, y compris la CblG causée par des mutations du gène *MTR*, qui code pour la méthionine synthase (qui catalyse la reméthylation de l'homocystéine dépendante de la vitamine B12 en méthionine), et CblC causée par des mutations du gène *MMACHC* provoquent une décompensation cardiométabolique chez les nourrissons. Cependant, les conséquences cardiaques et les mécanismes sous-jacents à ce processus chez l'adulte sont inconnus. Le but de ce projet de doctorat consistait à étudier les conséquences fonctionnelles, métaboliques et moléculaires cardiaques de l'inhibition de la synthèse de la méthionine dans un modèle murin transgénique d'invalidation constitutive du gène *Mtr* par spécificité cardiaque et invalidation systémique du gène *MMACHC*. Nous avons constaté que l'invalidation sélective de *Mtr* dans le cœur produisait une cardiomyopathie avec insuffisance cardiaque, une hypertrophie du myocarde et un dysfonctionnement systolique chez les jeunes souris adultes. Au niveau tissulaire et moléculaire, la cardiomyopathie observée était liée à une altération du métabolisme énergétique avec perturbation de l'oxydation des acides gras et de la phosphorylation oxydative, au stress cellulaire et au remodelage cardiaque avec fibrose. Un métabolisme énergétique altéré, il était lié à une diminution de l'expression de Sirt3. La mauvaise localisation et la séquestration nucléaire de hnRNPA1 pourraient expliquer une partie des modifications de l'expression des gènes et des protéines. Ces résultats suggèrent un mécanisme de cardiomyopathie chez jeunes adultes CblG.

Mots-clés : Vitamine B12, méthionine synthase, cardiomyopathie, insuffisance cardiaque, hypertrophie cardiaque, métabolisme énergétique, *MMACHC, MTR*

RÉSUMÉ DE THÉSE EN FRANÇAIS

1. Introduction

L'insuffisance cardiaque (IC), un large spectre de maladies du myocarde, est l'une des causes les plus courantes de morbidité et de mortalité dans les pays occidentaux et son incidence augmente dans les pays en développement (Bui et al., 2011; Ziaeian & Fonarow, 2016). À l'échelle mondiale, la prévalence de l'IC est estimée à plus de 37,7 millions d'individus (Bui et al., 2011; Ziaeian & Fonarow, 2016). Les personnes âgées de > 65 ans sont les plus touchées par cette maladie (van Riet et al., 2016).

L'IC est défini comme un syndrome clinique complexe provoqué par des anomalies structurelles et fonctionnelles cardiaques qui compromettent la capacité ventriculaire du cœur à remplir ou à éjecter un volume suffisant de sang (Hunt et al., 2009; Yancy Clyde W. et al., 2013). Dans l'IC, le cœur est incapable d'éjecter un débit de sang dans la circulation, et par conséquent, il ne fournit donc pas suffisamment d'oxygène et de nutriments aux tissus périphériques pour répondre aux besoins métaboliques de l'organisme même en présence d'une pression de remplissage normale ou excessive (Dickstein et al., 2008; McMurray et al., 2012).

Selon les directives de *l'American College of Cardiology Foundation/ American Heart Association* (ACCF / AHA) et de l'*European Society of Cardiology* (ESC) en matière de diagnostic et de traitement de l'insuffisance cardiaque, l'IC est défini comme un syndrome clinique dans lequel les patients présentent cardinalement des symptômes comprenant un essoufflement, dyspnée et fatigue, qui peuvent limiter leur capacité à faire une activité physique, et présentent un œdème périphérique et / ou congestion pulmonaire et / ou splanchnique en raison de la rétention d'eau (Yancy Clyde W. et al., 2013).

Les patients insuffisants cardiaques peuvent également présenter des signes comprenant une augmentation de la pression veineuse jugulaire, un déplacement de l'apex et des crépitants pulmonaires (Dickstein et al., 2008; McMurray et al., 2012; Ponikowski et al., 2016; Yancy et al., 2013). Ces symptômes affectent la capacité fonctionnelle et la qualité de vie des patients atteints d'insuffisance cardiaque (Dickstein et al., 2008; McMurray et al., 2012; Ponikowski et al., 2016; Yancy et al., 2013). Avant que ces symptômes ne deviennent évidents, les patients atteints d'IC peuvent présenter des anomalies structurelles et fonctionnelles cardiaques asymptomatiques, notamment une dysfonction diastolique ou systolique du ventricule gauche (Ponikowski et al., 2016).

La fraction d'éjection ventriculaire gauche (FEVG) est la mesure utilisée pour décrire l'insuffisance cardiaque et est définie comme le pourcentage de volume de sang éjecté dans la circulation lorsque les ventricules se contractent pendant la systole par rapport au volume sanguin restant dans la chambre lorsque les ventricules se relâchent pendant la diastole.

La FEVG est mesurée à l'aide de diverses techniques de diagnostic, notamment : l'échocardiographie, la résonance magnétique cardiaque ou Pas des isotopes (Jessup et al., 2016).

Selon l'ESC (Ponikowski et al., 2016). et l'ACCF / AHA (Yancy Clyde W. et al., 2013) sur la base de la FEVG, l'insuffisance cardiaque peut être phénotypiquement classée dans les catégories suivantes:

a. Insuffisance cardiaque avec fraction d'éjection basse (IC/FEb) avec une FE < 40 %

b. Insuffisance cardiaque avec fraction d'éjection moyenne (IC/FEm) avec FE > 40 -49 %

c. Insuffisance cardiaque avec fraction d'éjection préservée (IC/FEp) avec une FE > 50% (Lam & Solomon, 2014; Ponikowski et al., 2016).

IC systolique est un autre terme utilisé pour IC/FEb, des thérapies efficaces ont été identifiées pour le traitement et la gestion de ce type d'IC. IC/FEp est également connu sous le nom l'insuffisance cardiaque diastolique. Il est plus complexe de diagnostiquer les patients avec IC/FEp que ceux avec IC/FEb. Des divers outils de diagnostic sont utilisés pour diagnostiquer la IC. Ils incluent la mesure des peptides natriurétiques; Les peptides natriurétiques auriculaires (ANP) et les peptides natriurétiques ventriculaires (BNP) dans le plasma et l'utilisation d'outils d'imagerie cardiaque tels que l'échocardiographie transthoracique, la tomographie par émission de positrons, la résonance magnétique cardiaque, entre autres (Ponikowski et al., 2016). L' IC/FEp est très prévalent par rapport à l' IC/FEb, des études cliniques ont montré que, chez les personnes âgées de plus de 60 ans, l' IC/FEp est plus fréquent chez les femmes par rapport aux hommes (van Riet et al., 2016).

L'IC est un syndrome multifactoriel et ses principales étiologies comprennent : l'hypertension, la maladie coronarienne, le diabète, la cardiopathie valvulaire, l'hypertension pulmonaire, la cardiopathie congestive, ainsi que d'autres cardiomyopathies moins fréquentes : la cardiopathie congénitale et l'obésité (Blair et al., 2013; Butler et al., 2011; Pazos-López et al., 2011).

L'hypertension et les cardiopathies ischémiques sont les principales étiologies de l'insuffisance cardiaque dans les pays à revenu élevé. En revanche, dans les pays à faible revenu comme ceux d'Afrique et d'Asie, la cardiopathie rhumatismale est un problème de santé majeure, tandis qu'en Amérique du Sud, la maladie de Chagas (une maladie parasitaire tropicale causée par Trypanosoma cruz) reste la principale cause d'IC, (Brahmbhatt & Cowie, 2018; Ziaeian &

Fonarow, 2016). De plus, l'hypertension est la principale cause d'insuffisance cardiaque chez les Africains et les Afro-Américains (Brahmbhatt & Cowie, 2018; Ziaeian & Fonarow, 2016). En outre, l'IC peut résulter de certains troubles métaboliques ou d'anomalies de l'endocarde, du myocarde, des grands vaisseaux du péricarde et des valves cardiaques (Yancy et al., 2013). La majorité des patients IC présentent un dysfonctionnement diastolique et / ou systolique du ventricule gauche (VG) causé par des troubles du myocarde (Ponikowski et al., 2016; Yancy et al., 2013a). Une dégradation du métabolisme énergétique mitochondrial myocardique contribue également à la pathogenèse de l'insuffisance cardiaque (Azevedo et al., 2013; Karwi et al., 2018). Les maladies métaboliques héréditaires constituent également les principales causes de myocardiopathies et d'insuffisance cardiaque. Les myocardiopathies regroupent l'ensemble de maladies cardiaques qui affectent le muscle cardiaque (Seferović et al., 2019) et constituent également l'une des causes les plus courantes d'insuffisance cardiaque d'origine génétique.

Selon le comité de l'*American Heart Association*, les myocardiopathies peuvent être considérées comme primaires ou secondaires. Les myocardiopathies primaires se produisent lorsque les maladies ne concernent que les muscles cardiaques et les maladies secondaires lorsque la cardiomyopathie est associée à des troubles multisystémiques (Maron et al., 2006; McKenna, Maron, & Thiene, 2017). Les cardiomyopathies primaires comprennent : la myocardiopathie dilatée (CMD), la cardiomyopathie arythmogène (CMA), les cardiomyopathies hypertrophiques (CMH) et la myocardiopathie restrictive (CMR) (Elliott et al., 2008; Fu & Eisen, 2018; Seferović et al., 2019). Les causes des myocardiopathies primaires peuvent être génétiques, non génétiques ou acquises.

Dans la CMD, les patients présentent une altération de la fonction systolique ventriculaire gauche et une hypertrophie / dilatation des ventricules gauches ou des deux ventricules (Seferović et al., 2019). À l'échelle mondiale, le CMD est l'une des principales causes d'IC avec une fraction d'éjection basse (Seferović et al., 2019). Cette myocardiopathie est le sous-type le plus courant de maladies myocardiques avec une prévalence de 1 : 2500. Environ 20 à 30 % des cas de CMD familiale ont été rapportés. Leur hérédité est liée au chromosome X, avec une forme de transmission autosomique dominante ou récessive (Pinto et al., 2016). Le DCM est le facteur causal le plus courant de transplantation cardiaque chez les enfants et les adultes souffrant d'insuffisance cardiaque avancée (Maron et al., 2006b; Seferović et al., 2019; Tayal, Prasad, & Cook, 2017). La CMD a été observée à tous les âges confondus et est causée par des facteurs multifactoriels, incluant les facteurs génétiques. En effet, de variantes rares génétiques

dans plus de 50 gènes ont été identifiés et associés à la CMD (Hershberger, Hedges, & Morales, 2013; McNally & Mestroni, 2017; Tayal et al., 2017). Ces gènes codent pour des protéines impliquées dans diverses fonctions structurelles et cellulaires, la majorité étant liée au sarcomère.

Les mutations les plus importantes associées à la CMD qui ont été identifiées dans le sarcomère comprennent: le gène *TTN* codant pour la troponine T2 (qui est le variant le plus prévalent de la CMD), les gènes *MYH7* et *MYH6* codant pour la chaîne lourde de la bêta et alpha de la myosine respectivement, le gène *MYBPC3* codant pour la protéine C de liaison à myosine cardiaque et gène *LMNA* que code pour codant pour la protéine lamina A (Tayal et al., 2017). Autres mutations liées au CMD dans les gènes du cytosquelette (y compris: DMD, DES et VCL, entre autres), celles qui codent pour canaux ioniques (y compris SCN5A codant pour la sous-unité a de la protéine de canal sodique de type 5 et *ABCC9* codant pour la superfamille C de la cassette ATP 9), et enfant de mutations sur de gènes mitochondriaux (TAZ codant Tafazzin) parmi d'autres (Hershberger et al., 2013; McNally & Mestroni, 2017; Tayal et al., 2017).

Dans les études GWAS (Genome Wide Association Study) spécifiques à la CMD, deux variants communs associés à la CMD ont été identifiés (Smith Nicholas L. et al., 2010; Tayal et al., 2017). Un SNP a été identifié dans le gène BAG3 (Villard et al., 2011) et un autre était situé dans un intron du gène *ZBTB17* codant pour un facteur de transcription Zinc finger and BTB domain-containing protein 17. Parmi les autres variantes identifiés dans les études GWAS associés à l'IC et à la CMD avancées, citons le HSPB7 (Cappola Thomas P. et al., 2010). Les causes non génétiques de CMD comprennent les infections virales telles que le VIH et les maladies parasitaires telles que la maladie de Chagas, la toxicité par certains médicaments, notamment les agents chimiothérapeutiques, les maladies immunitaires à médiation systémique (maladies auto-immunes et auto-inflammatoires), les maladies endocriniennes et métaboliques (Diabète de type 2), le péripartum (IC/FEb à la fin de grossesse) et la toxicité liée à l'abus de drogues (alcool, cocaïne, entre autres) (Pinto et al., 2016; Seferović et al., 2019). La CMD est diagnostiquée par échocardiographie transthoracique. Les patients atteints de CMD présentent généralement une FEVG <45%, une diminution de la fraction de raccourcissement du ventricule gauche (FRVG) <25% et un volume du ventricule gauche diastolique (VDVG) > 117 mL (McNally & Mestroni, 2017).

En outre, la cardiomyopathie hypertrophique (CMH) est l'une des cardiomyopathies les plus courantes caractérisée par l'augmentation de la masse ventriculaire gauche (Seferović et al., 2019). L'hypertrophie cardiaque peut se manifester chez les patients atteints de CMH à la naissance, à la puberté, à l'âge adulte ou plus tard dans les 60 ans. Outre l'augmentation de la masse ventriculaire gauche, les patients atteints de CMH peuvent également présenter une fibrose du myocarde, des anomalies des valvules sous-valvulaires et mitrales, un remodelage auriculaire et un dysfonctionnement micro-vasculaire (Olivotto et al., 2009). La prévalence de la CMH est de 1:500, Les patients atteints de CMH ont une fraction d'éjection ventriculaire gauche préservée; ils peuvent également avoir une diminution de la fraction d'éjection ventriculaire gauche aux derniers stades de la maladie (Seferović et al., 2019). Dans la plupart des cas, les HCM résultent de mutations dans des gènes sarcomériques, notamment *MYBPC3* codant pour la protéine C liant la myosine, *MYH7* codant pour la chaîne lourde de la myosine bêta, *MYL3* codant pour la chaîne légère de la myosine, *TNN13* codant pour la troponine I et *TNNT2* codant pour la troponine T (Lopes & Elliott, 2013; J. Yang, Xu, & Hu, 2015). Les mutations dans *MYH7* et *MYBPC3* sont les mutations les plus courantes associées à plus de 60 % des cas familiaux d'apparition de CMH dans l'enfance. Environ 21 enfants sur 33 atteints de CMH familiale présentaient des mutations dans ces gènes. Les mutations dans *MYH7* et *MYBPC3* sont les mutations sarcomériques les plus courantes associées à plus de 60 % des cas familiaux d'apparition de CMH dans l'enfance. (Morita et al., 2008). Le mode de transmission est autosomique dominante. La mutation dans d'autres gènes tels que *TNN* codant pour la titine et *MYH6* codant pour la chaîne légère de la myosine représente la minorité des cas de CM H (Lopes & Elliott, 2013).Les autres causes non génétiques de CMH comprennent les syndromes de malformation cardiaque, les maladies de stockage lysosomal, les troubles neuromusculaires et mitochondriaux (Seferović et al., 2019).

Enfin, la cardiomyopathie restrictive (CMR) est une myocardiopathie phénotypiquement caractérisée par un dysfonctionnement diastolique sévère et une dilatation des oreillettes avec des ventricules de taille normale ou réduite et des anomalies du remplissage de type restrictif (Lopes & Elliott, 2013; Seferović et al., 2019). Des troubles métaboliques, notamment des déficiences en vitamine B12 et folates, ainsi qu'une altération du métabolisme de l'homocystéine due à des anomalies génétiques de la reméthylation conduisent à une hyperhomocystéinémie. L'homocystéine est un aminoacide soufré non essentiel contenant un acide aminé alpha dérivé du métabolisme de la méthionine et non incorporé dans les protéines (Ganguly & Alam, 2015; Joo, Andronikos, & Saffery, 2011).

Durant les deux dernières décennies, plusieurs études ont mis en évidence une relation entre l'hyperhomocystéinémie et les maladies cardiovasculaires.

Chez les individus en bonne santé, la concentration plasmatique normal d'homocystéine à jeun varie de 5 à 15 µMol / L. Une concentration plasmatique en homocystéine supérieure à 15 µmol / L est appelée hyperhomocystéinémie (HHcy).

Selon le niveau de concentration plasmatiques d'homocystéine, L'HHcy peut être classifiée comme suit :

1). HHcy légère avec des concentrations plasmatiques d'homocystéine (16-30 µMol / L)

2). HHcy modérée avec des concentrations d'homocystéine plasmatiques HHcy (30-100 µMol / L)

3). HHcy sévère avec des concentrations d'homocystéine plasmatique (> 100 µmol / L) (Cheng et al., 2000). L'hyperhomocystéinémie est une affection multifactorielle. Cela est dû à des facteurs tels que : 1). Défauts génétiques des gènes codant par des enzymes impliquées dans le métabolisme de l'homocystéine 2) Consommation excessive de méthionine 3). Déficience en cofacteurs du métabolisme de l'homocystéine (carence en folates, vitamine B12 et vitamine B6) 4) Certaines maladies comme l'insuffisance rénale chronique et l'hypothyroïdie et 5) L'utilisation de certains médicaments comme: metrotexate, antipaludiques et metformine (Froese et al., 2016; Iacobazzi et al., 2014; Kim et al., 2018; David Watkins et al., 2002). Le plus fréquente cause d'HHcy est la carence nutritionnelle en folates (vitamine B9), en vitamine B12 et en vitamine B6. Les folates et la vitamine B12 sont des micronutriments essentiels au développement normal, à la survie et à la régulation de divers processus métaboliques du corps. Ces vitamines donnent des groupes méthyle dans les réactions de reméthylation de l'homocystéine et la synthèse de méthionine dans des réactions catalysées par la méthionine synthase. La vitamine B12 est synthétisée de manière intracellulaire par des bactéries anaérobies et aérobies (Battersby, 1994; Martens et al., 2013). Cependant, les voies de biosynthèse de la vitamine B12 sont absentes chez les organismes supérieurs. Les humains dépendent donc des aliments d'origine animale tels que le bœuf, le foie, le poisson, la volaille, les œufs, le lait, les produits laitiers et les suppléments, qui constituent leur seule source de vitamine B12. La carence en vitamine B12 est causée par des facteurs multifactoriels tels que : faible apport alimentaire, malabsorption et altération du traitement et du transport intracellulaire causés par des mutations génétiques ponctuelles et par de variantes génétiques plus fréquentes (L. H. Allen, 2008; Green et al., 2017). Les besoins quotidiens en vitamine B12 varient avec l'âge. En France, un apport quotidien d'environ 2,4 µg est recommandé. La vitamine B12 est métabolisée via une complexe série de réactions catalysées par une enzyme intracellulaire en

adénosylcobalamine (AdoCbl) et méthylcobalamine (MeCbl), les cofacteurs de la méthylmalonine-CoA mutase mitochondriale et de la méthionine synthase cytoplasmique (Green et al., 2017). La méthyl-cobalamine est un dérivé de la vitamine B12 et du MeTHF du cycle du folate utilisée par la MS comme cofacteur et co-substrat dans les réactions de reméthylation de l'homocystéine mentionnées précédemment. Par conséquent, des carences en vitamine B12 et en folates altèrent la voie de la réméthylation et conduisent à une accumulation de l'homocystéine dans les cellules, qui se diffuse ensuite dans le plasma, entraînant une hyperhomocystéinémie. De faibles niveaux de vitamine B12 entraînent une diminution significative de l'activité de la MS (Brunaud et al., 2003). De même, une carence en vitamine B6 provoque une hyperhomocystéinémie en altérant la transsulfuration de l'homocystéine en cystathionine par la cystathionine bêta synthase (CBS). L'ensemble des concentrations plasmatiques totales en vitamine B12, folates et vitamine B6 sont inversement liées à la concentration plasmatique en homocystéine totale (Ganguly & Alam, 2015; Hankey & Eikelboom, 1999). Lors d'essais cliniques randomisés, la supplémentation en acide folique ou l'enrichissement en acide folique (Almassinokiani et al., 2016; Collaboration d'essais cliniques visant à réduire l'homocystéine, 2005; Zeng et al., 2015) ont permis de réduire efficacement les concentrations d'homocystéine plasmatique totale (McKinley et al., 2001). L'hyperhomocytéinémie provoque un stress oxydatif et constitue un facteur de risque de maladies cardiovasculaires, de cancers, de troubles neurologiques, de troubles du développement congénitaux et de troubles gastro-intestinaux (Ganguly & Alam, 2015; Škovierová et al., 2016; Temple et al., 2000). Les anomalies génétiques des voies de reméthylation liées aux mutations des enzymes méthionine synthase (MS / *MTR*) ou la méthionine synthase réductase (MSR / *MTRR*), et d'autres gènes du métabolisme de la cobalamine (vitamine B12, Cbl), notamment les mutations des gènes *CD320, LMBRD1, ABCD4, MMACHC, MMADHC* et *MTRR* (Coelho et al., 2012; Green et al., 2017; David Watkins et al., 2002b). Et enfin, les carences nutritionnelles en vitamine B12 (cobalamine) et en folates entraînent une diminution de la synthèse de méthionine, ce qui conduit à une diminution de la concentration de la S-adénosyl méthionine (SAM) et à une augmentation de l'homocystéine dans les tissulaire et plasmatique.

La méthionine synthase (MS) humaine, EC.2.1.1.13 (MS, 5-méthyltétrahydrofolate : L-homocystéine S-méthyltransférase) est une protéine cytoplasmique méthyl-transférase codée par le gène *MTR* sur le chromosome humain 1p43 (Leclerc et al., 1996). La MS utilise du 5-méthyltétrahydrofolate (5-Me-THF) et de la méthylcobalamine (un dérivé de la vitamine B12) pour catalyser le transfert du groupe méthyle du 5-Me-THF) à l'homocystéine afin de former

de la méthionine et du tétrahydrofolate (Guéant et al., 2013). La méthionine est le précurseur direct de la S-Adénosyl Méthionine (SAM), donneur universel du groupe méthyle pour la méthylation de multiples métabolites, par exemple les histones, de l'ARN et de l'ADN, qui sont essentiels pour les mécanismes de régulation épigénomique de l'expression des gènes (Forges et al., 2007; Guéant et al., 2013).

En plus, la MS est une protéine modulaire avec différents domaines pour la liaison de l'homocystéine, du méthyl tétrahydrofolate, de la cobalamine et du S adénosyl méthionine (Banerjee & Ragsdale, 2003; Evans et al., 2004; Goulding, Postigo, et Matthews, 1997). La réaction de transméthylation catalysée par MS est importante pour le cycle du folate et de la méthionine. Un déficit en vitamine B12 et une activité altérée de la MS entraînent une augmentation de la concentration cellulaire d'homocystéine et provoquent un phénomène de séquestration de Méthyl-THF, connu sur le nom de 'MeTHF trap'. Cette séquestration est due à une altération de la conversion de MeTHF en THF par la MS, ce qui entraîne une accumulation du pool de MeTHF au détriment d'autres folates cellulaires (R. V Banerjee & Matthews, 2016). Des défauts dans la MS sont donc une de causes d'élévation de l'homocystéine totale dans le plasma et une diminution de la concentration de méthionine. Les mutations du gène *MTR* sont associées au défaut CblG, une erreur innée du métabolisme de la cobalamine. Les manifestations cliniques des patients atteints de CblG incluent : hyperhomocystéinémie, hypométhioninémie, anémie mégaloblastique et retard de développement (Froese & Gravel, 2010c; Leclerc et al., 1996a; D Watkins & Rosenblatt, 1989). CblE est un défaut génétique du métabolisme de la cobalamine causé par une mutation du gène *MTRR* qui conduit à une déficience du système de réduction de la MS dont la présentation clinique est similaire à celle de CblG. Récemment, les polymorphismes des gènes *MTHFR* (C677T) et *MTR* (A2756G) ont été associés de manière significative aux maladies cardovasculaires (Raina et al., 2016).

Des mutations du gène *MMACHC* provoquent également une hyperhomocystéinémie et une acidurie méthylmalonique, elles sont liées à une diminution de la disponibilité de MeCbl et d'AdoCbl. Le gène *MMACHC* OMIM 609831 (hyperhomocystinurie de type C combinée à l'acidurie de méthyle malonique) code pour la protéine 'Methylmalonic aciduria and homocystinuria type C protein' (MMACHC). La protéine MMACHC catalyse la décyanation et la désalkylation de la diatomée cyanocobalamine et de l'alkylcobalamine respectivement pour générer les cobalamines biologiquement actif : [méthylcobalamines (MeCbl) et adénosylcobalamine (AdoCbl)] qui sont des coenzymes pour la MS cytoplasmique et le methymalony-CoA mutase (MUT) que est une protéine mitochondriale (Hannibal, DiBello, et

Jacobsen, 2013). Le dysfonctionnement de la protéine MMACHC entraîne une altération du transport intracellulaire et de la biosynthèse de MeCbl et d'AdoCbl. Le déficit en MMACHC altère donc l'activité de la MS et du MUT, ce qui entraîne l'accumulation d'homocystéine et d'acide méthylmalonique dans le sang et l'urine. L'acidurie méthylmalonique peut être fatale car elle provoque une acidose grave. La protéine MMACHC est essentielle à l'embryogenèse pré-implantatoire et au développement des systèmes cardiaques, respiratoires et nerveux dans l'organogenèse (Garcia 2014 et al ., 2014; Pupavac et al., 2011). Une mutation dans le gène *MMACHC* est à l'origine de l'hyperhomocystinurie combinée de type C de l'acide méthylique malonique (OMIM 277400; CblC), qui est le défaut génétique le plus courante du métabolisme intracellulaire de la cobalamine (Lerner-Ellis et al., 2006).

Les patients CblC présentent une hyperhomocytéinurie et une acidurie méthymalonique combinée, une défaillance multi-systémique, des troubles neurologiques et hématologiques incluant une anémie mégaloblastique. La maladie CblC est hétérogène et présente un début précoce ou tardif grave, une survie et une réponse au traitement (Carrillo-Carrasco, Chandler, & Venditti, 2012). L'analyse protéomique des cellules des patients ayant une mutation CblC met en évidence une expression différentielle de protéines associée à des maladies cardiovasculaires, des troubles neurologiques, des troubles musculaires et du squelette (Hannibal et al., 2012). La cardiomyopathie dilatée prénatale peut être une manifestation de troubles CblC (Bie et al., 2009).

2. Objectifs et hypothèse d'étude

Des essais cliniques et des études de population suggèrent une association entre le déficit en donneurs de méthyle (vitamine B12 et folates) et l'insuffisance cardiaque. Des études menés dans notre laboratoire et d'autres dans la littérature ont démontré une association significative entre une hyperhomocystéinémie, la carence en vitamine B12 et une altération de la fonction systolique ventriculaire gauche (Bokhari et al.,2005; Guéant-Rodriguez et al., 2007). Cependant, on ignore si cette association est la cause ou la conséquence de l'IC et si elle résulte d'une diminution de l'activité de MS et de MMACHC. En outre, les patients atteints de CblG, de CblC et d'autres troubles héréditaires du métabolisme de la vitamine B12 qui entraînent une diminution dramatique de la méthionine synthase peuvent présenter une décompensation létale dramatique au cours des deux premières années de la vie, mais on ne sait rien des conséquences cardiaques à l'âge adulte. Chez l'animal, la carence en folates et en vitamine B12 pendant la grossesse et l'allaitement conduit chez le raton à une cardiomyopathie hypertrophique, le

mécanisme impliqué dans ce modèle était lié à une altération de l'activité des enzymes de la chaîne respiratoire et de l'oxydation des acides gras (Garcia et al., 2011). Les modèles nutritionnels ne permettent pas de comprendre les mécanismes spécifiquement liés à l'activité de la méthionine synthase, y compris ceux liés à la diminution de la S-adénosyl méthionine (SAM) dans les cardiomyopathies observées dans les deux défauts génetiques du métabolisme de la cobalamine : CblC et CblG causés par des mutations dans les gènes *MMACHC* et *MTR*, respectivement.

Le travail de thèse présenté dans ce document était conçu pour comprendre les mécanismes conduisant à une cardiomyopathie hypertrophique d'origine héréditaire, pour ce faire, nous avons utilisé deux modèles de souris transgéniques 1) avec invalidation constitutive spécifique du gène *Mtr* dans les cardiomyocytes (*Mtr cKO*) et 2) avec inhibition systémique du gène *MMACHC* (M*MACHC* $^{+/-}$). Ces 2 modèles nous ont permis d'étudier les conséquences fonctionnelles et métaboliques cardiaques de la synthèse altérée à long terme de la méthionine, de la méthylcobalamine (MeCbl) et de l'adénosylcobalamine (AdoCbl) au cours de fenêtres spécifiques du développement embryo-fœtal.

Les objectifs spécifiques de mon travail de thèse étaient :

1. Évaluer l'efficacité de la suppression du gène *Mtr* dans les cardiomyocytes d'animaux *Mtr cKO*
2. Étudier les conséquences métaboliques et fonctionnelles cardiaques de la voie de reméthylation chez des souris transgéniques présentant une inhibition constitutive spécifique du cœur du gène *Mtr*.
3. Étudier les conséquences métaboliques et fonctionnelles cardiaques de la dégradation des cobalamines chez des souris transgéniques avec invalidation systémique du gène *MMACHC*.

Les hypothèses de mon travail de thèse étaient :

1. L'invalidation constitutive spécifique du gène *Mtr* et l'invalidation systémique du gène *MMACHC* entraînent une altération de la reméthylation de l'homocystéine et une diminution de la synthèse de méthionine et de méthylcobalamine dans le myocarde.
2. L'invalidation constitutive du gène *Mtr* à spécificité cardiaque et l'invalidation systémique du gène *MMACHC* entraînent un déficit sévère du métabolisme énergétique du myocarde, une hypertrophie cardiaque et / ou une insuffisance cardiaque.

3. Méthodologie et résultats principaux

Pour atteindre ces objectifs, les paramètres de la fonction cardiaque ventriculaire gauche chez des souris âgées de 5 mois ont été évalués à l'aide d'une échocardiographie transthoracique et de tomographie par émission de positrons adaptée au petit animal (mini-TEP). La pression artérielle systolique chez des souris conscientes a été mesurée à l'aide d'une pléthysmographie du manchon caudal. La fibrose cardiaque a été évaluée en utilisant la coloration au Masson's trichrome et au rouge picrosirius, le immunoblot et la RT-qPCR. L'analyse transcriptomique a été réalisée par séquençage en profondeur d'ARN (RNA sequencing) et étude protéomique par LC-MS / MS. Les annotations fonctionnelles et l'enrichissement par Ontologie des gènes/Gene Ontology (GO) et l'analyse des voies des données omiques ont été réalisés par des outils bioinformatiques ; PANTHER, Enrichr et Open Target Bioinformatics Resources.

L'immunocoloration, l'immunofluorence et le western blotting ont été utilisés pour évaluer l'expression de gènes et de protéines et la fibrose cardiaque. Les métabolites du métabolisme des monocarbons et énergétique dans les tissus plasmatiques et cardiaques ont été analysés par LC-MS / MS.

Nous avons constaté que l'invalidation constitutive du gène *Mtr* dans le cœur produisait une cardiomyocardiopathie hypertrophique avec dysfonction systolique et hypertension systolique, chez de jeunes souris adultes. L'invalidation sélective de *Mtr* (*Mtr cKO)* dans le myocarde a été mis en évidence par une diminution de l'expression protéique et de l'activité enzymatique de la MS et au niveau métabolique par une diminution du rapport SAM : SAH (**Figure 27** Page 160**, Figure 29** page 161 **et Figure 30** page 162, respectivement). Les études d'échocardiographie transthoracique ont révélé une diminution importante de la fraction d'éjection du ventricule gauche et de la fraction de raccourcissement du VG (38,97 ± 2,07 vs 55,38 ± 3,677, P = 0,002 et 18,79 ± 1,14 vs 28,64 ± 2,40, P = 0,002 respectivement; **Figure 33B** page 166), ainsi qu'une augmentation notable des volumes systoliques et diastoliques du VG (57,33 ± 7,28 vs 26,33 ± 4,00 µL, P = 0,0067 et 81,41 ± 2,90 vs 57,03 ± 5,72 µL, P = 0,0015, respectivement **Table 11** page 165) chez les animaux *Mtr cKO* par rapport aux témoins. Des résultats similaires ont été montrés par Mini-PET. Par ailleurs, la RT-qPCR a mis en évidence une augmentation de l'expression des peptides natriurétiques (ANP et BNP) et une diminution du rapport alpha MHC / beta MHC chez les souris *Mtr cKO* témoignant une défaillance cardiaque **(Figure 36A** page 170**).** L'ensemble des résultats confirment la dysfonction systolique du ventricule gauche chez les souris *Mtr cKO*.

En effet, la cardiomyopathie induite par l'inactivation du gène *Mtr* dans le cœur était liée à une altération du métabolisme énergétique avec perturbation de l'oxydation des acides gras et de la phosphorylation oxidative, du stress cellulaire et du remodelage avec fibrose. Des études biochimiques ont révélé une altération de l'oxydation des acides gras dans le myocarde de *Mtr cKO*, mise en évidence par une augmentation significative des acyl carnitines à chaîne courte et moyenne dans le plasma de *Mtr cKO* par rapport aux souris témoins et par une diminution de l'expression de CD36 ($P = 0.001$ and $P = 0.041$, **Figure 55A** et $P = 0.008$, **Figure 55C** respectivement ; page 203). Les études Omics (transcriptome et protéome), et leur confirmation par western blotting et /ou RT-qPCR ont révélé une différence significative d'expression de gènes et / ou de protéines impliquées dans la glycolyse, la phosphorylation oxydative et l'oxydation des acides gras ($P < 0.05$, **Figure 58 page** 208 et **Figure 57** page 207 respectivement). Il convient de noter la diminution de l'expression de Sirt3 dans le myocarde de *Mtr cKO* ($P = 0{,}008$, **Figure 59** page 209). Sirt3 est un régulateur important du métabolisme énergétique mitochondrial.

Les études par immunohistopathologie et par RT-qPCR ont montré une expression accrue du collagène dans le myocarde de *Mtr cKO* indiquant une fibrose cardiaque (**Figure 51A, 51B et 51C** page 197). La fibrose était liée à une augmentation de l'expression du TGFβ1 (transcription growth factor beta 1) et d'AGTR2 (récepteur 2 de l'angiotensine) et de MMP2 (métalloprotéinase matricielle-2) ($P = 0{,}006$, $P = 0{,}023$ et $P = 0{,}005$, **Figure 51D ;** page 197 respectivement).

Des études d'Omics ont révélé que l'invalidation constitutive du gène *Mtr* dans les cardiomyocytes altérait l'expression de gènes et de protéines dans le myocarde. Le transcriptome cardiaque était constitué de 16539 gènes exprimés. Ces gènes ont été regroupés par *K-means* et ensuite, chacun des regroupements résultants a été analysé à nouveau par un regroupement hiérarchique, ce qui a permis de définir trois signatures géniques fortement corrélées, 2 sur-exprimées et 1 sous-exprimée (**Figure 37,** page 173). La signature sous-exprimé consistait en 1889 gènes. Les annotations fonctionnelles par Enrichr ont révélé que les processus biologiques GO (Ontologie des Gènes) de ces gènes étaient principalement liés à une altération du métabolisme énergétique des mitochondries, à la bêta oxydation des acides gras et au remodelage cardiaque (**Figure 38** page 174 et **Figure 39** page 175). Les deux signatures sur-régulées consistaient en 418 et 887 gènes. Les 418 gènes surexprimés (sub-cluster 3) étaient liés aux mécanismes d'adaptative au stress cellulaire et à l'hypertrophie cardiaque, plus particulièrement liés à la réponse au stress oxydatif, l'autophagie, les stimuli du facteur de croissance, la régulation du signal de facteur de croissance endothélial vasculaire et à

l'organisation de la matrice extracellulaire (P <0,05 ; **Figure 41** page 178). En outre, les 887 gènes surexprimés (sub-cluster 4) ont été impliqués dans les voies d'adaptation du remodelage cardiaque et dans l'altération du métabolisme énergétique des mitochondries (*P* <0,05, **Table 13** page 179).

L'ensemble du protéome cardiaque était constitué d'un total de 1998 protéines détectées, dont 34 protéines exprimées de manière statistiquement significative. Parmi elles, 26 étaient sous-exprimées (changement de pli <0,8, P <0,05) et 8 surexprimées (changement de pli <0,8, *P* <0,05). Les processus biologiques GO les plus importants associés à ces protéines étaient liés au métabolisme énergétique (corps, cétoniques, métabolisme du galactose et biogenèse mitochondriale) et au remodelage du myocarde (différenciation des cellules musculaires, signalisation des récepteurs des facteurs de croissance des fibroblastes, assemblage du protéasome, adhésion cellulaire (**Figure 43B** page 182**)** Les maladies cardiovasculaires associées aux 34 protéines dysrégulées analysé par Open Targets Platform comprenaient les cardiomyopathies génétiques liées à la cardiomyopathie dilatée, à la cardiomyopathie hypertrophique, aux troubles mitochondriaux et à l'insuffisance cardiaque (**Figure 43C** page 182 et **Table 14** page 183).

Pour déterminer si l'invalidation du gène *Mtr* a influencé la localisation sous-cellulaire de 3 protéines de liaison à l'ARN (RBP) liées au stress cellulaire, nous avons évalué par détection immunofluorescence ELVAL1 / HuR, Y14 et hnRNPA1. Nous avons constaté que hnRNPA1 était exclusivement localisé dans le noyau des cardiomyocytes de *Mtr cKO*, alors qu'il était localisé dans le cytoplasme et le dans la région périnucléaire dans les cardiomyocytes des témoins (**Figure 54A,** page 201). Aucune différence n'a été observée de localisation cellulaire des RBP ELVAL1 / HuR et Y14 dans les deux groupes (**Figure 54B et 54C** page 201). La pression artérielle systolique et l'expression de biomarqueurs d'IC étaient comparables entre les animaux MMACHC $^{-/+}$ et MMACHC $^{+/+}$ (**Figure 60**, page 210 et **Figure 61**, page 211).

4. Conclusion

En conclusion, nous avons constaté que l'invalidation sélective de *Mtr* dans le cœur produisait une cardiomyopathie avec hypertrophie cardiaque et dysfonctionnement systolique chez les jeunes souris adultes. Au niveau tissulaire et moléculaire, la cardiomyopathie était liée à la perturbation de l'oxydation des acides gras et de la phosphorylation oxydative, au stress cellulaire et au remodelage avec fibrose. La diminution de l'expression de Sirt3 était cohérente avec le métabolisme énergétique altéré et la localisation erronée de hnRNPA1 pourrait expliquer une partie des modifications de l'expression des gènes et des protéines. Ces résultats

suggèrent de faire un dépistage précoce d'une possible cardiomyopathie chez les patients atteints d'une CblG.

INTRODUCTION

INTRODUCTION

1 HEART FAILURE

1.1 Definition of heart failure

Heart failure (HF), a wide spectrum of myocardial diseases, is one of the most common causes of morbidity and mortality in the Western countries and its incidence is increasing in the developing countries (Bui et al., 2011; Ziaeian & Fonarow, 2016). Globally, the prevalence of HF is estimated to be more than 37.7 million individuals (Bui et al., 2011; Ziaeian & Fonarow, 2016). HF prevalence is high in older population aged > 65 years (van Riet et al., 2016).

HF is defined as a complex clinical syndrome caused by cardiac structural and functional abnormalities that compromise the hearts' ventricular ability to fill with or eject blood (Hunt et al., 2009; Yancy Clyde W. et al., 2013). In HF syndrome, the heart fails to pump sufficient blood into circulation, therefore it fails to supply enough oxygen and nutrients to meet body's metabolic needs despite normal or excessive filling pressure (Dickstein et al., 2008; McMurray et al., 2012).

According to American college of cardiology foundation/ American heart association (ACCF/AHA) and European society of cardiology (ESC) guidelines for diagnosis and treatment of heart failure, HF is defined as a clinical syndrome where patients cardinally presents with symptoms that includes breathlessness, dyspnea and fatigue which may limit their capacity to exercise, and peripheral edema and/or pulmonary and/or splanchnic congestion due to water retention (Yancy Clyde W. et al., 2013). Heart failure patients may also presents with signs that include increased jugular venous pressure, displaces apex beat and pulmonary crackles (Dickstein et al., 2008; McMurray et al., 2012; Ponikowski et al., 2016; Yancy et al., 2013). These symptoms affect the functioning capacity and quality of life of HF patients (Dickstein et al., 2008; McMurray,et al., 2012; Ponikowski et al., 2016; Yancy et al., 2013). Before these symptoms become eminent HF patients can present with asymptomatic cardiac structural and functional abnormalities that includes either left ventricular diastolic or systolic dysfunction (Ponikowski et al., 2016). A wide spectrum of left ventricular functional abnormalities are associated with HF, they range from those with normal ventricular sizes with preserved ejection fraction to severe abnormalities that include dilatation of ventricles with reduced ejection fraction (Yancy et al., 2013). Cardiac structural disorders that may cause HF syndrome includes abnormalities of endocardium, myocardium, pericardium, great vessels and heart valves (Yancy Clyde W. et al., 2013).

1.2 Classification of heart failure

The severity of HF can be classified based on three categories; 1). based on the severity of symptom and ability to execute physical activity, 2). based on heart structure and functional abnormalities or 3. based on left ventricular ejection fraction.

1.2.1 Classification of heart failure on the basis of physical activity and severity of symptoms

According to New York Heart Association (NYHA) functional classification, the severity of heart failure is classified into four classes on the basis of symptoms and ability to carry out physical activities (McMurray et al., 2012; Miller-Davis et al., 2006; Yancy Clyde W. et al., 2013). These classes of patients are:

a. Class I HF patients do not have restriction of physical activity. Ordinary physical activity in these patients does not cause undue dyspnea, palpitation, fatigue or anginal pain.
b. Class II HF patients have slightly restricted physical activity. These patients are comfortable at rest, however when carrying out ordinary activities, they show symptoms of heart failure like dyspnea, palpitation, fatigue or anginal pain
c. Class III HF patients have pronounced restriction of physical activity and are only comfortable at rest. Less than ordinary physical activity in this group cause dyspnea, palpitation, fatigue or anginal pain.
d. Class IV HF patients are unable to carry out any physical activity without discomfort, in this group of patients the discomfort increases if any physical activity is undertaken. These patients have symptoms of the anginal syndrome or heart failure even at rest.

1.2.2 Classification of heart failure based on structural and functional abnormalities

American College of Cardiology / American Heart Association (ACC/AHA) classification of heart failure is based heart muscle structural and functional abnormality. With classification heart failure is classified into four stages (A, B, C and D) (Dickstein et al., 2008; Hunt, 2005; Yancy Clyde W. et al., 2013).

a. **Stage A:** The patients in this stage have a higher risk of developing heart failure however they have no sign or symptoms of heart failure. They also have no identified structural and functional abnormalities including abnormalities of endocardium, myocardium, pericardium great vessels and heart valves.

b. **Stage B:** The patients in this stage have structural heart disease associated with the development of heart failure however, they have no signs or symptoms of heart failure.
c. **Stage C:** The patients in this stage have structural heart disease and they present with symptoms and signs of heart failure.
d. **Stage D:** The patients in this stage have advanced heart disease with pronounced heart failure symptoms even at rest despite maximal medical therapy. These patients therefore require specialized interventions.

An overlap between the different classes of the NYHA and ACC/AHA functional classification and progression of heart have been reported. Pre-HF matches with Stage A, NYHA class I to stage B, NYHA class II and III to stage C and NYHA class IV matches with stage D (Kemp & Conte, 2012).

1.2.3 Classification of heart failure based on left ventricular ejection fraction

The measurements of left ventricular (LV) Ejection fraction (EF) is the term used to describe HF. This measurement is used to assess the left ventricular systolic function. Mathematically, EF is defined as the Stroke Volume (SV) divided by End Diastolic Volume (EDV) where SV equals to EDV minus ESV (End Systolic volume) (**Equation 1**) (McMurray et al., 2012).

***E*quation 1** EF = SV/EDV where SV= (EDV-ESV)

Ventricles are the chambers of the heart that pumps blood and the percentage of blood that is pumped out when the ventricles contracts (when the heart beats) is the left ventricular ejection fraction (LVEF). Therefore, LVEF is the percentage of blood that is ejected into circulation following ventricular contraction during systole with reference to the volume that remains in the ventricles during diastole when the ventricles relax. Patients with systolic dysfunction have reduced contraction and emptying of ventricles. The stroke volume in these patients is maintained by the increase in the diastolic volumes. As consequence, the ventricle become dilated and the heart ejects a small fraction of a larger volume of blood. The more systolic function is depressed the more the EF fraction is reduced from normal and the greater the increase in systolic and diastolic volumes (McMurray et al., 2012). The LVEF is measured using either Echocardiography, cardiac magnetic resonance or radionuclide technique (Jessup et al., 2016).

Based on LVEF, HF is phenotypically classified into:

a. Heart failure with reduced ejection fraction (HFrEF) with an EF < 40 %.
b. Heart failure with mid rage ejection fraction (HFmEF) with EF >40 -49 %.
c. Heart failure with preserved ejection fraction (HFpEF) with an EF >50%

Systolic HF is another term used for HFrEF, efficient therapies have been identified for treatment and management. HFpEF is also known as diastolic heart failure, is more complex to diagnose patients with HFpEF than those with HFrEF. Various diagnostic tools are used to diagnose HF, they include measurement natriuretic peptides in plasma and use of cardiac imaging tools like transthoracic echocardiography, positron emission tomography, cardiac magnetic resonance among others (Ponikowski et al., 2016). HFpEF is highly prevalent than HFrEF in a population above 60 years, however, HFpEF was found to be more common in women while HFrEF was common in men (van Riet et al., 2016).

1.3 Cardiac physiology and left ventricular adaptation mechanisms

1.3.1 Normal cardiac physiology

Cardiac output (CO) is the amount of blood pumped by the heart per minute, it is expressed as litres/minute. In general, CO is about 4 to 8 litres per minute. CO is the product of heart rate (HR) which is the number of beats per minute and SV (Kemp & Conte, 2012a; Klabunde, 2011; Levick, 2013; Vincent, 2008). Apart from HR, other factors that affect CO includes: ventricular wall integrity, synergistic ventricular contraction and valvular competence (Kemp & Conte, 2012a; Vincent, 2008).

The three factors that affects the SV (Kemp & Conte, 2012a) include:

a. **Pre-load** which is the distention of myocardium prior to systole, it involves the extend of stretching of the myocardial fibers at the end of systole, the greater the stretch the more the increase in contraction and the greater the cardiac output.
b. **After-load** which is the force that the ventricles have to overcome in order to eject blood.
c. **Contractility** which is the hearts' ionotrophic state independent of cardiac afterload and preload.

1.3.2 Left ventricular dysfunction

There are two categories of left ventricular dysfunction:

1). Left ventricular systolic dysfunction

2). Left ventricular diastolic dysfunction.

Patients with left ventricular systolic dysfunction have decreased LVEF usually less than 40%, they also have impaired LV ventricular contraction and ejection (Kemp & Conte, 2012; Yancy Clyde W. et al., 2013). LV systolic dysfunction is mainly caused by loss of function of the

myocardium (defects of the heart muscle) as a result of myocardial infarction and ischemic disease and excessive pressure overload due to uncontrolled hypertension. In addition cardiotoxic drugs and cardiotoxins may impair valvular competence and contractility leading to volume overload (Kain et al., 2018; Kemp & Conte, 2012; Ziaeian & Fonarow, 2016). On the other hand patients with LV diastolic dysfunction have LVEF >50% and are characterized with modified extracellular matrix, increased collagen deposition, increased LV stiffening and impaired LV relaxation (Kuznetsova et al., 2009).

Impaired left ventricular function causes a decrease in cardiac output leading to global hypoperfusion. Moreover, left ventricular dysfunction causes increase in both end systolic and end diastolic volumes leading to dilatation and stretching of ventricles. The increase in these volumes in turn causes an augmentation of LV end diastolic pressure leading to increase in left atrial pressure. Consequently, the increased in left atrial pressure augments the pressure of the capillaries in the lungs. Pulmonary hypertension then forces fluids out of pulmonary capillaries leading to pulmonary congestion the main clinical symptom of dyspnea (Kemp & Conte, 2012).

1.3.3 Adaptation mechanism to left ventricular dysfunction and heart failure

Heart failure patients have decreased cardiac output and as a consequence this leads to decreased mean arterial pressure (MAP) and tissue hypoperfusion (Kemp & Conte, 2012). To maintain adequate tissue perfusion and to compensate for the hemodynamic disturbances the body undergoes cardiovascular adaptations. These adaptation mechanisms are divided into: Early / acute compensatory mechanism which is beneficial and the late/ chronic compensatory response mechanisms which are mal-adaptative (Gabriel-Costa, 2018).

1.3.3.1 Early/ acute adaptation mechanisms

Early compensatory mechanisms to ventricular dysfunction include: The Frank-Starling mechanism and hyperactivation of neurohormonal responses.

i) Frank-Starling mechanism

Frank-Starling mechanism is an intrinsic mechanism in the heart that plays an important compensatory role in response to decreased cardiac output during the early stages of heart failure (Delicce, Basit, & Makaryus, 2019a; Ertl, Gaudron, Eilles, Schorb, & Kochsiek, 1991; Gabriel-Costa, 2018a). The Frank-Starling mechanism is based on the relationship between the force generated by contraction in relation to the initial length of the Myocardial fibers. Under normal physiological conditions any increase in the stretching of myocardial fibers results in

an increase in tension in the fibers which consequently leads to greater force of contraction in the ventricles.

This mechanism is a link between the preload which is measured as left ventricular end diastolic volume (LVEDV) and cardiac performance which is measured as CO or SV (Delicce, Basit, & Makaryus, 2019b). According to this mechanism the contractility of the heart changes with the levels of tissue stretching and LVEDV (Ertl et al., 1991).

In normal heart, an increase in preload results in an increase in cardiac performance. However, during systolic heart failure or dilated cardiomyopathy, for any preload the SV is decreased. The decrease in SV consequently leads to decrease in left ventricular ejection fraction and incomplete ventricular emptying hence the observed increase in LVEDV (Delicce et al., 2019; Gabriel-Costa, 2018a). According to Frank-Starling mechanism, the increase in LVEDV induces an increase in myocardial fiber stretching and as a consequence the contractile force of the next systole is enhanced and the cardiac output is restored (Delicce et al., 2019; Ertl et al., 1991).

ii) Neurohormonal activation

Activation of sympathetic (adrenergic) nervous system (SNS) and renin angiotensin aldosterone system (RAAS) are the two well-known compensatory homeostatic responses to decreased cardiac output in heart failure (Hartupee & Mann, 2017a). Other mechanisms involve the actions of hormones that include : vasopressin 1, endothelin 1 and natriuretic peptides. These mechanisms re-establishes cardiac output and blood pressure through various mechanisms that include : increasing retention of salt (Na+) and water, peripheral arterial vasoconstriction and increasing cardiac contractility (Hartupee & Mann, 2017). Neurohormonal interaction in heart failure is summarized in **Figure 2**.

a) Sympathetic nervous system

Sympathetic nervous system (SNS) is involved in a number of cardiovascular actions that include: increase in cardiac contraction and heart rate, reduction of venous capacitance and constriction of resistance vessels (Triposkiadis et al., 2009). The decrease in systemic blood pressure and inhibition of baroreceptor complexes observed in heart failure and myocardial infarction activates the SNS. Activation of SNS establishes cardiac output and blood pressure by enhancing cardiac contractility and peripheral resistance (Gabriel-Costa, 2018).

The cardiovascular reflexes regulate sympathetic flow to the heart and peripheral circulation. In the heart, the main reflex response originates from SNS inhibition that include: aortic arch and carotids baroreceptors and cardiopulmonary baroreceptors and from SNS activation that

include cardiovascular low threshold polymodial receptors and peripheral chemoreceptors (Triposkiadis et al., 2009). The four pathways that mediates the effects of activation of the SNS includes:

1) Norepinephrine (NE) releasing neurons, NE effects results in increased heart rate and contractile strength and increase blood.
2) Epinephrine (EPI) released from adrenal cortex into the circulation.
3) Locally released NE and EPI with effects on peripheral vessels.
4) Circulating NE with effects on several regions.

In systolic dysfunction, the decreased pressure in the aortic arch and carotid bodies increases the activation of the SNS and suppresses the activation of the parasympathetic nervous system. In systolic dysfunction and HFrEF, activation of SNS maintains cardiac output and tissue perfusion by increasing heart rate and stroke volume, increasing sodium and water retention and release of renin (Brahmbhatt & Cowie, 2018). Initially, this response is compensatory, however hyperactivation of SNS lead to progression of heart failure due to catecholamine cardiotoxicity and excessive vasoconstriction which increases the afterload leading to increase in work load of the failing heart (Brahmbhatt & Cowie, 2018). Hyperactivation of SNS is characterized by increased plasma NE, central sympathetic outflow, NE plasma spill over from activated sympathetic nerve fibers and reduced uptake of the adrenergic nerve endings (Brahmbhatt & Cowie, 2018; Hartupee & Mann, 2017; Pepper S. Gregory, 1999).

b) Renin aldosterone angiotensin system

Renin aldosterone angiotensin system (RAAS) plays a crucial role in the pathophysiology of heart failure. Renin is an enzyme synthesized in the kidney by specialized granular cells of the juxtaglomerular apparatus (Brahmbhatt & Cowie, 2018; Hartupee & Mann, 2017b). Renin is released into afferent arteriole in response to various stimuli that include: 1). Increased sympathetic activation, 2). Decreased blood pressure sensed by the baroreceptor cells in the arterial walls and 3). Falling intracellular chloride levels within macula densa cells lining the renal tubules at the end of loop of Henle (Pearse & Cowie, 2014). Direct activation of the beta adrenergic receptors by enhanced catecholamines (NE and EPI) traffic in the kidney further stimulates renin release (Weinberger, Aoi, & Henry, 1975).

Renin cleaves angiotensinogen produced in the liver into angiotensin I which is further cleaved by angiotensin converting enzyme into angiotensin II. The release of aldosterone which is a mineralocorticoid released from adrenal cortex is stimulated by angiotensin II. In the distal convoluted tubules of the kidney, aldosterone enhances the reabsorption of sodium and water

and increases the release of potassium into urine (Pearse & Cowie, 2014). Consequently, activation of RAAS maintain the cardiac output and tissue perfusion by increasing blood pressure and retention of water and sodium, however persistent long-term hyperactivation of RAAS leads to deterioration of cardiac function and adverse cardiac remodelling (Brahmbhatt & Cowie, 2018; Gabriel-Costa, 2018; Hartupee & Mann, 2017). Apart from stimulating the reabsorption of sodium via release of aldosterone, angiotensin II stimulates apoptosis, release of vasopressin and NE, vasoconstriction and cardiac contraction (Brahmbhatt & Cowie, 2018; Kemp & Conte, 2012).

c) Mechanism by which SNS and RAAS regulates cardiac contractility

SNS and RAAS modulates cardiac contraction by regulating posttranslational mechanisms that include phosphorylation, dephosphylation and modulating the activities of contractile and Ca^{2+} handling related proteins (Curran, Hinton, Ríos, Bers, & Shannon, 2007; Gabriel-Costa, 2018a). Noradrenaline and angiotensin II regulate cardiac contraction via various mechanisms. Noradrenaline activates the beta 1 adrenergic Gs-coupled receptors which further enhances protein kinase A (PKA) activity (Freedman & Lefkowitz, 2004; Madamanchi, 2007). PKA phosphorylates proteins that reinforce cardiac contractility that includes: L type Ca^{2+} channels, type 2 ryanodine receptor/RYR2 and sarco/ endoplamic reticulum Ca^{2+} -ATPase/SERCA2. The phosphorylated proteins increase intracellular calcium concentration and enhances Ca^{2+} induced and release mechanisms. Ca^{2+} activates the activity of the calcium calmodulin kinase type 2 (CAM kinase II) which further phosphorylates the above-mentioned proteins to enhance cardiac contractility (Maier, Bers, & Brown, 2007; Wehrens, Lehnart, Reiken, & Marks, 2004; Yang et al., 2003). Furthermore, angiotensin II through angiotensin receptor 1 (AT1) receptor increases intracellular calcium concentration by increasing the inositol triphosphate (IP3) levels and enhancing the activity of protein kinase C (PKC) (Grimm & Brown, 2010; Madamanchi, 2007). In addition, SNS and RAAS reinforces cardiac contractility by phosphorylating phosphatases (Jideama, Crawford, Hussain, & Raynor, 2006).

iii) Natriuretic peptides

Both Atrial natriuretic peptide (ANP) and Brain natriuretic peptides (BNP) has cardioprotective effects as circulating hormones as well as local paracrine and autocrine factors. They play crucial role in the regulation of blood pressure and blood volume. ANP and BNP through its antifibrotic and antihypertrophic effects offer cardioprotective benefits (Nishikimi, Maeda, & Matsuoka, 2006). In fetal heart, ANP is secreted in both atria and ventricle, the levels of ANP

in fetal circulation is higher than in adults (Cameron & Ellmers, 2003). The levels of ANP and BNP expressed by fetal ventricles are higher than those expressed by adult ventricles. Therefore increased expression of ANP in adult ventricles has been perceived as the induction of fetal embryonic gene program associated with ventricular hypertrophy (Cameron & Ellmers, 2003). In mid-gestation natriuretic peptide system plays a critical role in cardiac organogenesis and regulation of blood pressure, water and salt homeostasis. Through its role as a vasodilator of the placenta vasculature, natriuretic peptides regulates the supply of blood to the fetus in the placenta (Cameron & Ellmers, 2003).

a) Atrial natriuretic peptide (ANP)

ANP is a circulating peptide hormone of cardiac origin, it is mainly secreted and stored in the atrium as prohormone (ProANP) in the intracellular granules in the atria of adult heart.

Human ProANP is a 126 aa prohormone and a product of cleavage of 151 aa preprohormone (preproANP) in the sarcoplasmic reticulum (**Figure 1**) (Volpe, Carnovali, & Mastromarino, 2016). The release of the inactive proANP from the intracellular granules in the atria is stimulated by increase in atria stretching in response to several stimulus. Some of this stimuli includes, increase in intravascular volume and intra-atrial pressure (Edwards et al.,1988), angiotensin (Soualmia et al., 1997), and endothelin (Stasch et al., 1989). Once it is released, the ProANP undergoes enzymatic cleavage into the inactive 98 aa fragment NT-ANP and the biological active 28 aa ANP in the C terminal (Volpe et al., 2016a). ANP has short plasma half-life of about 2 minutes whereas for NT-ANP plasma half-life varies depending on the fragment that is measured.

ANP have diuretic, natriuretic and vasorelaxing properties, it inhibits vasoconstricting effects of RAAS and maintains sodium homeostasis. ANP plays a crucial role in preserving compensated state of asymptomatic left ventricular dysfunction (Brandt, Wright, Redfield, & Burnett, 1993).

b) Brain natriuretic peptides (BNP)

BNP is a prohormone synthesized in the ventricles in response to cardiomyocyte stretch. Synthesis of biologically active BNP prohormone involves a number of steps. First, the transcription and translation of the PreproBNP a 134 aa precursor peptide by the cardiomyocytes occurs when the cardiomyocyte membranes are exposed to mechanical stretch or volume overload (Maisel, Duran, & Wettersten, 2018; Sudoh et al., 1989). The preproBNP then undergoes two successive enzymatic cleavage. In the first cleavage, 26 aa peptide is removed to form 108 aa proBNP which is subsequently cleaved by prohormone invertase to

form the inactive 76 aa N-terminal NT-proBNP and 32 aa C-terminal active BNP (**Figure 1**) (Kojima et al., 1989; Maisel et al., 2018). Both BNP and NT-proBNP are released in equal concentration into circulation. BNP and NT-proBNP are not stored in the ventricles rather they are rapidly synthesized in a burst following stimulation and released into circulation. NT-proBNP has a plasma half-life of 120 minutes whereas BNP has a plasma half-life of 20 minutes.

Elevated BNP plasma levels is a marker of heart failure and used to follow disease progression (Kemp & Conte, 2012a). Like ANP, this hormone acts directly on the blood vessels where it cause vasodilation, increase release of salt and water and also inhibit the release of renin, aldosterone and vasopressin hormones (Kemp & Conte, 2012).

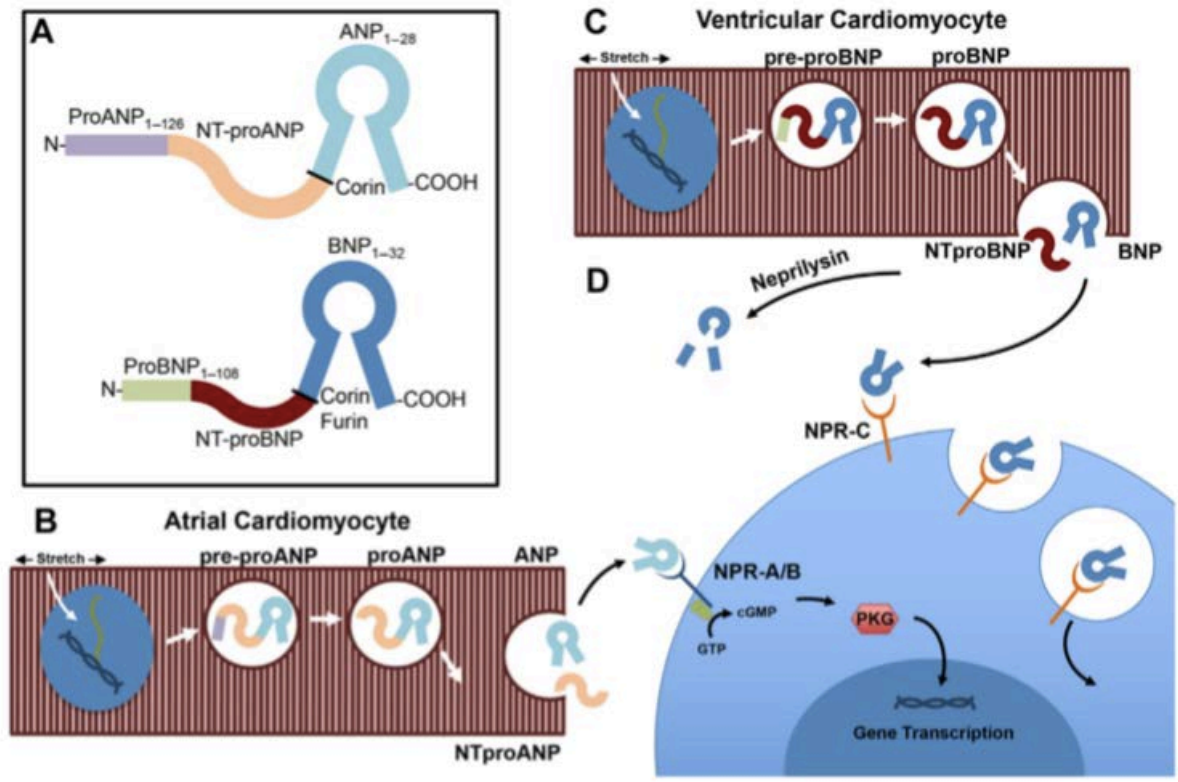

Figure 1: Physiology of ANP and BNP adapted from (Volpe, Carnovali, & Mastromarino, 2016)

A. Molecular structures showing the end-product fragments and enzymatic cleavage sites of ANP and BNP **B).** Schematic illustration of ANP production and processing steps by atrial cardiac myocyte following mechanical stretch stimulation. **C).** Schematic illustration of BNP production and processing steps by atrial cardiac myocyte following mechanical stretch stimulation. **D).** Action of ANP and BNP on target tissues. To carry out its effects both ANP and BNP binds their receptors in the target tissues, NP receptor (NPR)A and NPR-B respectively. Once bound to the receptors, guanosine triphosphate (GTP) is cleaved by cytoplasmic G proteins to form cyclic guanosine monophosphate (cGMP). Intracellular cGMP signaling cascade involving protein kinase G (PKG) is then initiated, consequently resulting in downstream transcription of genes implicated in diuresis, natriuresis and smooth muscle cell relaxation. Finally circulating endogenous peptidases and neprilysin breaks down serum ANP and BNP, additionally these peptides can be breakdown by lysosomes.

iv)Arginine Vasopressin hormone

The arginine vasopressin is an antidiuretic hormone involved in plasma osmoregulation and vasoconstriction. Heart failure patients have increased plasma levels of arginine vasopressin, this increase may contribute to the increase in peripheral vasculature resistance, hyponatremia and edema observed in HF patients (Pearse & Cowie, 2014; Pepper S. Gregory, 1999).

v) Endothelin 1 hormone

Endothelin 1 hormone is an endothelium-derived peptide which is cleaved from a large precursor called big endothelin 1 by endothelin converting enzyme. It has durable arterial and venous vasoconstriction properties (Pepper S. Gregory, 1999). It also stimulates the release of aldosterone as well as promoting retention of water and sodium in the kidney (Pearse & Cowie, 2014). It also enhances the activities of RAAS and arginine vasopressin. Angiotensin II and Epinephrine stimulates the synthesis of endothelin 1.

Increased plasma levels of big endothelin 1 and endothelin 1 has largely been reported in HF patients (Pacher et al., 1993; Rodeheffer et al., 1992; Wei et al., 1994). An increase in plasma endothelin 1 contributes to the maintenance of vascular tone. Interestingly, the increase in plasma big endothelin 1 has been reported to strongly correlate with mortality in HF patients (Perez et al., 2016; Pousset et al., 1997)

1.3.3.2 Late adaptation mechanism

i) Neurohormonal hyperactivation

To maintain tissue perfusion, the neurohormonal adaptive responses are continuously activated, however hyperactivation of the SNS and RAAS are detrimental as they lead to HF progression.

a) Hyperactivation of SNS

Chronic hyperactivation of SNS causes desensitization of the β1 adrenergic receptors and depletion of β1 adrenergic density (M. R. Bristow et al., 1986; Michael R. Bristow et al., 1982; Grimm & Brown, 2010; Lymperopoulos, 2015). Consequently, this results in impaired β1 receptor activation and signalling, decreased cardiac contractility and reduced ionotropic reserve. The decreased β1: β2 resulting from the decreased expression of β1 stimulates intense sympathetic activation which further desensitizes the β1 receptors (Michael R. Bristow et al., 1982; Lucia, Eguchi, & Koch, 2018).

Chronic stimulation of the of the β adrenergic receptors activates signaling pathways involved in the expression of proteins linked to Ca^{2+} handling, excitation-contraction coupling mechanisms and cardiac contraction. Modification in the expression pattern of these proteins

further impairs contractility leading to further decrease in cardiac output (Gabriel-Costa, 2018). Moreover, hyperactivation of SNS induces cardiac remodeling and hypertrophic dilated cardiomyopathy through stimulation of cell growth via Mitogen activated protein Kinase (MAPK) and cell growth signaling pathways (Gabriel-Costa, 2018).

b) Hyperactivation of RAAS

Hyperactivation of RAAS has similar effects as SNS, these effects are mediated by angiotensin II and aldosterone hormones. Autocrine and paracrine effects of angiotensin II on cardiac cells causes alterations in tissue remodeling and cardiac contractility leading to cardiac hypertrophy (Crowley et al., 2006; Kim Shokei et al., 1995; Y.-C. Zhu et al., 2003). In addition, angiotensin II further contributes to the development of cardiac fibrosis, cardiac hypertrophy and remodeling by enhancing the synthesis of inflammatory cytokines, collagen and the production of reactive oxygen species (Sciarretta et al., 2009; Xu et al., 2010).

ii) Cardiac remodelling

Cardiac remodelling involves a group of cellular, molecular and interstitial changes which clinically presents as changes in geometry, size, mass and heart function which occurs in response to cardiac injury or cardiac overload (Cohn, Ferrari, & Sharpe, 2000). Cardiac remodelling is classified into two: 1). Physiological cardiac remodeling which occurs in response to exercise, pregnancy and growth and 2). Pathological cardiac remodeling which occurs in response to excess cardiac overload, biochemical stress, neurohormonal hyperactivation, inflammation, ischemia and ischemic reperfusion (Wu et al., 2017). During cardiac remodelling various changes in heart mass, volume and composition occurs, these changes eventually alters hearts' geometry where the heart becomes more spherical and less elliptical (Cohn et al., 2000).

Initially, these geometric changes are compensatory, they maintain and improve cardiac performance by enhancing stroke volume and cardiac output. In addition, cardiac remodelling enhances cardiac contractility via increase in myocardial wall thickness and ventricular mass. However, cardiac remodelling is progressive in heart failure and at long last, it leads to impaired cardiac ventricular function (Kemp & Conte, 2012). Prolonged remodelling results in myocardial apoptosis and contractile dyssynchrony in the dilated ventricles leading to inefficient pumping of blood. Moreover, continuous enlargement of the heart and myocardium hypertrophy causes fibrosis and increased tension which eventually impairs cardiac contractility (Kemp & Conte, 2012).

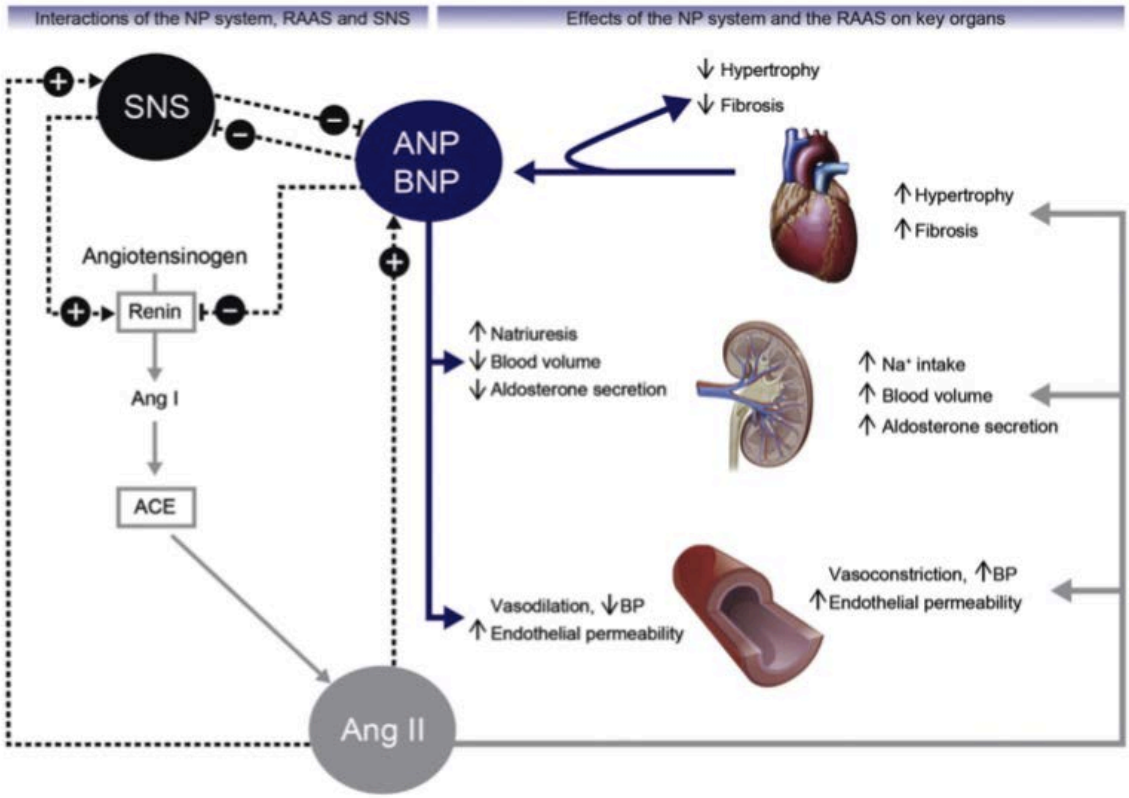

Figure 2: Schematic representation of neurohormonal interaction in heart failure. Adapted from (Brahmbhatt & Cowie, 2018)

1.4 Biomakers of heart failure

Natriuretic peptides (ANP and BNP) are used as clinical biomarkers for diagnosis of acute and chronic HF, ventricular dysfunction, prognosis of HF and most recently in forensic medicine (Baba et al., 2019; Cao et al., 2019; Maisel et al., 2018).

In the year 2016, the ESC guidelines for diagnosis and treatment of acute and chronic heart failure recommends that plasma BNP and NT-proBNP levels should be tested in all patients with suspected HF (Ponikowski et al., 2016). For acute HF the higher values which are considered are: < 100 pg / mL for BNP and < 300 pg / mL for NT-proBNP and < 120 pmol / L for proANP. For normal non acute settings the maximum values are 35 pg / mL for BNP and 125 pg/mL for NT-proBNP (Ponikowski et al., 2016). If the concentration of BNP ranges between 100 and 500 pg / mL clinical judgment should then be used to diagnose HF. On the other hand, if the concentration of BNP is greater than 500 pg / mL, the possibility of cardiac dysfunction or HF is considered and hence HF treatment is rapidly suggested (Cao et al., 2019). Plasma concentration of ANP in healthy subjects is low, it is approximately 20 Pg/ml or 10 fmol/ml of ANP while in HF patients this concentration levels are elevated 10-100 folds (Cody et al., 1986; Lerman et al., 1993). Due to the short half-life of ANP, for diagnosis and prognosis of heart failure the use of BNP and NT-proBNP is preferred. Moreover, due to its short half-life in plasma it is difficult to measure the bioactive form of ANP and therefore its inactive form NT-proANP is measured although the concentrations are higher than active form (Goetze et al., 2015). Heart failure patients have elevated levels of MR-proANP, NT-proANP and BNP, these levels were correlated to the severity of HF and ventricular wall stretch (Januzzi, 2013; Maisel et al., 2002).

1.5 Causes of heart failure

HF is a multifactorial syndrome, its main aetiologies includes: hypertension, coronary heart disease, ischemic cardiomyopathy, diabetes, valvular heart disease, pulmonary hypertension, congestive heart disease, other cardiomyopathies, congenital heart disease and obesity (**Figure 3)**. The aetiologies of heart failure are summarized in Figure 3. Hypertension and ischemic heart disease are the leading aetiologies for HF in high income countries. On the other hand, low-income countries in Africa and Asia, Rheumatic heart disease is a major heart problem, while in South America Chagas diseases (a tropical parasitic disease caused by *Trypanosoma cruz)* remains the main cause of HF (Brahmbhatt & Cowie, 2018; Ziaeian & Fonarow, 2016). In addition, hypertension has been reported to as the main cause of heart failure in Africans and African- Americans (Brahmbhatt & Cowie, 2018; Ziaeian & Fonarow, 2016).

Furthermore, HF may arise from certain metabolic disorders or from abnormalities of endocardium, myocardium, pericardium great vessels and heart valves (Yancy et al., 2013). Majority of HF patients have either Left Ventricular (LV) diastolic and / or systolic dysfunction caused by disorders of the myocardium (Ponikowski et al., 2016; Yancy et al., 2013a). Impaired myocardial mitochondrial energy metabolism also contributes to heart failure (Azevedo et al., 2013; Karwi et al., 2018). Metabolic disorders including deficiencies in vitamin B12 and folate metabolisms as well as impaired metabolism of homocysteine due to genetic defects of remethylation of homocysteine leads to hyperhomocysteinemia. In this study we will focus on hyperhomocysteinemia (the risk factor for cardiovascular diseases) resulting from defects of remethylation of homocysteine and metabolism of vitamin B12.

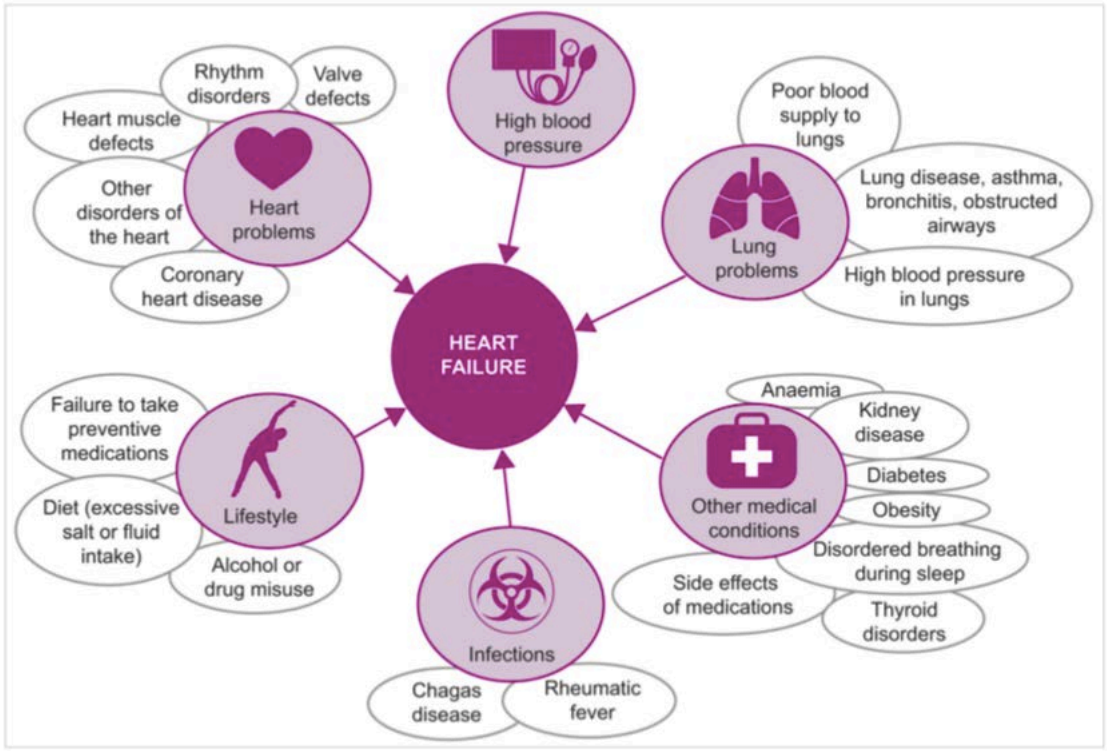

Figure 3: Summary of the aetiologies of heart failure adapted from (Ponikowski et al., 2014).

1.6 Genetic cardiomyopathies and heart failure.

Cardiomyopathies are diverse groups of heart diseases that affect the heart muscle (Seferović et al., 2019). According to committee of American heart association, cardiomyopathies can be considered to be either primary or secondary. Primary cardiomyopathies is when the diseases are only confined to the heart muscles and secondary is when the cardiomyopathy is associated

with multisystemic disorders (Maron et al., 2006; McKenna, Maron, & Thiene, 2017). Primary cardiomyopathies include: dilated cardiomyopathy (DCM), Arrhythmogenic cardiomyopathy (ARVC), hypertrophic cardiomyopathies (HCM) and (RCM) restrictive cardiomyopathy (Elliott et al., 2008; Fu & Eisen, 2018; Seferović et al., 2019). The causes of primary cardiomyopathies can be either genetic, non-genetic or acquired.

In DCM, the patients present with impaired left ventricular systolic function and enlargement / dilatation of the left ventricles or both ventricles (Seferović et al., 2019). Globally, DCM is one of the major causes of HF with reduced ejection fraction (Seferović et al., 2019). It is the most common subtype of myocardial diseases with a prevalence of 1:2500. About 20 to 30 % of familial DCM has been reported, these traits are inherited either through X-linked, autosomal dominance or recessive manner (Pinto et al., 2016). DCM is the most common causal factor for heart transplantation in children and adults with advanced heart failure (Maron et al., 2006b; Seferović et al., 2019; Tayal et al., 2017). DCM has been reported in all ages, it is caused by multifactorial factors including the genetic and non-genetic causes. Rare genetic variants in more than 50 genes have been identified and reported to be associated with DCM (Hershberger et al., 2013; McNally & Mestroni, 2017; Tayal et al., 2017). These genes encode proteins involved in various cellular and structural function with the majority being linked to the sarcomere. The most important mutations associated with DCM that have been identified in the sarcomere include: *TTN* gene encoding troponin T2 (which is the most prevalent variant of DCM), *MYH7* and *MYH6* gene encoding beta and alpha myosin heavy chain respectively and *MYBPC3* encoding cardiac myosin binding protein type C, and in the nuclear envelop is *LMNA* gene encoding nuclear envelop protein (Tayal et al., 2017). Other mutations linked to DCM include the cytoskeleton genes (including: DMD, DES and VCL among others), ion channels (including *SCN5A* encoding sodium channel protein type 5 subunit a and *ABCC9* encoding ATP cassette superfamily C member 9), mitochondrial genes (TAZ encoding Tafazzin) among others (Hershberger et al., 2013; McNally & Mestroni, 2017; Tayal et al., 2017).

In DCM-specific GWA studies, two common variants associated with DCM were identified (Smith Nicholas L. et al., 2010; Tayal et al., 2017) . One SNP was identified in the *BAG3* gene (Villard et al., 2011) and another was located within an intron of *ZBTB17* gene encoding a transcription factor. Other SNP variants identified in GWAS associated with advanced HF and DCM included the *HSPB7* (Cappola Thomas P. et al., 2010). Non genetic causes of DCM include viral infections like HIV and parasitic diseases like Chagas disease, drug toxicity (chemotheraphy), systemic mediated immune diseases (autoimmune and autoinflammatory diseases), endocrine and metabolic diseases (Diabetes mellitus), peripartum (HFrEF at end of

pregnancy) and drug abuse toxicity (alcohol, cocaine among others) (Pinto et al., 2016; Seferović et al., 2019). DCM is diagnosed using transthoracic echocardiography. Patients with DCM usually presents with LVEF < 45%, LVFS < 25 % and EDLV > 117 % (McNally & Mestroni, 2017).

Secondly, HCM is one of the most common cardiomyopathies characterized by the increase in left ventricular mass (Seferović et al., 2019). In patients with HCM, cardiac hypertrophy may present at birth, puberty, adulthood or later in life above the age of 60 years. In addition to the increase in left ventricular mass, patients with HCM may also present with myocardial fibrosis, abnormalities of sub-valvular and mitrial valves, atrial remodeling and microvascular dysfunction (Olivotto et al., 2009). The prevalence of HCM is 1 to 500. These patients have preserved left ventricular ejection fraction, they may also develop reduced LVEF at later stages of the disease (Seferović et al., 2019). In most cases, HCM arise from mutations in sarcomeric genes that includes: *MYBPC3* encoding myosin binding protein C, *MYH7* encoding beta myosin heavy chain, *MYL3* encoding myosin light chain, *TNN13* encoding troponin I and *TNNT2* encoding Troponin T (Lopes & Elliott, 2013; J. Yang et al., 2015). Mutations in *MYH7* and *MYBPC3* are the most common sarcomeric mutations associated with more than 60 % of familial cases of childhood onset of HCM. About 21 out of 33 children with familial HCM were found to have mutations in these sarcomeric genes (Morita et al., 2008).

These traits are inherited in autosomal dominant manner. Mutation in other genes like *TNN* encoding titin and *MYH6* encoding myosin light chain accounts for the minority of cases of HCM (Lopes & Elliott, 2013). Other nongenetic causes of HCM include malformation syndromes, storage disorders, neuromuscular and mitochondrial disorders (Seferović et al., 2019).

Finally, the RCM is a cardiomyopathy that is phenotypically characterized by severe diastolic dysfunction and dilatation of both atria with ventricles with normal or reduced sizes and restrictive feeling abnormalities (Lopes & Elliott, 2013; Seferović et al., 2019). Stiffness of the left ventricles is the hallmark of this cardiomyopathy. Similar genetic mutations observed in the DCM and HCM cause familial RCM (Kaski et al., 2008), other causes include those from systemic disorders (Seferović et al., 2019).

2 Energy metabolism in the heart

2.1 Energy metabolism in normal heart

The heart is one of the body organs with tremendous energy demands. Therefore, the heart continuously produces ATP at high rate in order to meet its energy demands and sustain its contractile function, ionic homeostasis and basal metabolic processes (Seferović et al., 2019). The cardiomyocytes have high metabolic flexibility and they have been described to be omnivorous since they can use different energy substrates like fatty acids, ketones, carbohydrates (glucose and lactate) and amino acids to meet its energy demand (Karwi et al., 2018; Neely & Morgan, 1974). The heart uses fatty acids as its preferred oxidative substrate. The choice of substrate depends on several factors that include energy demand, substrate availability, hormonal status and physiological status (Karwi et al., 2018).

Under normal physiological conditions (normoxia) in the heart, mitochondrial oxidative phosphorylation generates more than 95 % of the ATP used by the heart while glycolysis and to a lesser extent citric acid cycle contributes the remaining 5 % (Doenst, Nguyen, & Abel, 2013). Fatty acid oxidation contributes to about (40-60) % of total energy generated by mitochondrial oxidative phosphorylation while the remaining (20-40) % is from oxidation of the other substrates (glucose, lactate and amino acids) (Karwi et al., 2018).

Adenosyl triphosphate (ATP) and Phosphocreatine (PCr) are the main forms of high energy phosphate metabolites in the heart, their concentrations are (~5µmol/g wet weight) and (~8µmol/g wet weight) respectively (Garcia-Ropero etal., 2019). ATP is the form of energy consumed during cellular reactions, while the PCr is the energy storage compound (Beer et al., 2002). PCr is produced by phosphorylation of creatine from ATP by creatine kinase. Both ATP and PCr are significantly decreased in heart failure (Beer et al., 2002). The rate of consumption of ATP in the heart is 1 mM ATP / second, therefore ATP and PCr should be renewed every 20 seconds (Ventura-Clapier et al., 2011). More than two thirds of ATP produced is used to fuel cardiac contraction and the remaining is used for ion pumps mainly the Ca^{2+} ATPase in the sarcoplasmic reticulum (Garcia-Ropero et al., 2019). ATP hydrolysis rates are high in the heart (~ 0.5 µmol / g wet weight / second) due its continuous contractile function. In addition, high energy ATP pool in the heart is relatively low therefore its depletion occurs within few seconds. Cardiac contractile function therefore depends on continuous ATP production. Thus any alterations in ATP generation impairs cardiac contractile function (Doenst, Nguyen, & Abel, 2013)

2.1.1 Fatty acid oxidation in normal heart

The heart uses fatty acids as the main energy substrate to provide majority of the cofactors required for oxidative phosphorylation where it contribute about (40-60)% of the total energy produced (Doenst et al., 2013b; Fillmore, Mori, & Lopaschuk, 2014; Lopaschuk et al., 2010). Fatty acids for oxidative phosphorylation in the heart originates from hydrolysis of circulating triglycerides (TAGs) covalently bound to either very low density lipoproteins (VLDL) or chylomicrons and from free fatty acid bound to albumin (Augustus et al ., 2003; van der Vusse, van Bilsen, & Glatz, 2000).

Metabolism of fatty acid involves three steps: 1). Uptake across the plasma membrane into the cytosol, 2). Transportation across mitochondrial membrane and 3). Oxidation within mitochondrial matrix (Doenst et al., 2013b). This process is illustrated in **Figure 4**.

i) Uptake of fatty acids into the cardiomyocytes

The uptake of extracellular fatty acids across cardiomyocytes plasma membranes occurs via either passive diffusion or via tissue specific fatty acid transporter proteins that include plasma membrane isoform of fatty acid binding protein (FABPpm), fatty acid translocase (FAT/CD36) and fatty acid transport protein (FATP) (Lopaschuk et al., 2010). The uptake of short chain fatty acid occurs via passive diffusion while the long chain fatty acid is facilitated by the fatty acid transporter proteins. Unlike the FATP and FABPpm, much attention has been put on FAT / CD36 due to the important role it plays in translocation of fatty acids across the sarcolemma of the cardiomyocytes. Moreover, FAT / CD36 also regulates fatty acid uptake as it can translate between the sarcolemma membrane and endosomes (Lopaschuk et al., 2010; Luiken et al., 2004). FAT/CD36 deficiency has been linked to a significant decrease in fatty acid uptake in patients (Nozaki et al., 1999). FAT/CD36 is therefore indispensable for the production of sufficient ATP and also prevention of progression of compensatory cardiac hypertrophy to heart failure (Sung et al., 2017; Umbarawan et al., 2018, p. 36).

ii) Transportation across mitochondrial membrane

Once inside the cytosol, esterification of the fatty acid into long chain fatty acyl CoA is mediated by the ATP dependent fatty acyl CoA synthetase enzyme (Karwi et al., 2018). The long chain acyl CoA are then converted into acyl carnitine by the carnitine palmitoyl transferase 1 (CPT1), this process allows the fatty acid to be shuttled into the mitochondria. Subsequently, the long chain fatty acyl carnitine is transported across inner mitochondrial membrane by the carnitine translocase. The carnitine palmitoyl transferase 2 (CPT2) then converts the long chain fatty acyl carnitine back to fatty acyl CoA (Doenst et al., 2013; Denis McGarry & Brown, 1997; Murthy & Pande, 1984) .

iii) Fatty acid oxidation within mitochondrial matrix

Once inside the mitochondrial matrix, the long chain fatty acyl CoA then enters fatty acid beta oxidation cycle where it generates Acetyl CoA, FADH2 (Flavin adenine dinucleotide) and NADH (nicotinamide adenine dinucleotide) (Fillmore et al., 2014; Lopaschuk et al., 2010). Oxidation of one fatty acid molecule produces 105 ATP molecules, this process consumes 23 molecules of oxygen. Therefore, in comparison to glucose, fatty acids are less efficient energy substrates since it has a Phosphate/Oxygen (P/O) ratio of 2.33 compared to 2.58 in glucose oxidation. Moreover, the esterification of fatty acid into long chain fatty acyl CoA utilizes 2 ATP pi thus further reducing the total energy production from fatty acid beta oxidation (Lopaschuk et al., 2010).

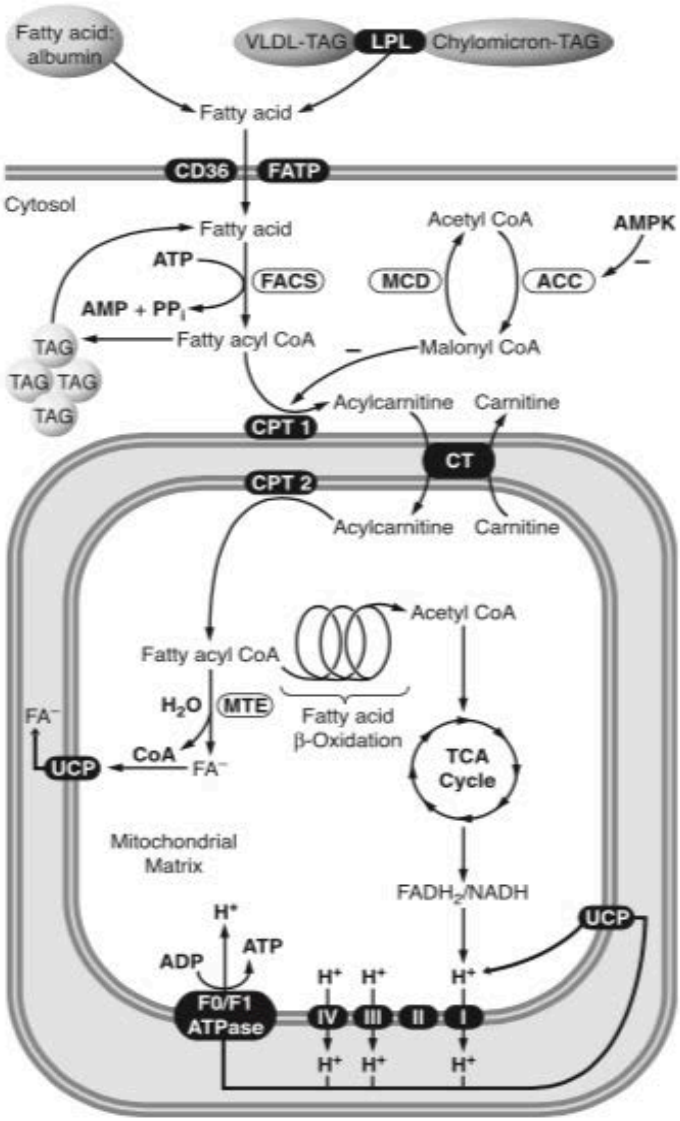

Figure 4: **An overview of fatty acid beta oxidation in the heart adapted from** (Lopaschuk et al., 2010).

2.1.2 Regulation of fatty acid oxidation

Fatty acid oxidation is regulated by a number of factors that include : glucose/ fatty acid cycle and malonyl CoA (Randle et al., 1963). Glucose and fatty oxidation inter-regulate each other via Glucose / fatty acid cycle also known as Randle cycle. Increased glucose oxidation in the heart results in decreased fatty acid oxidation. Fatty acid oxidation is also regulated by Malonyl CoA through inhibition of CPT1 which is the first protein involved in the mitochondrial uptake of long chain fatty acids (McGarry, Leatherman, & Foster, 1978). Cellular levels of malonyl CoA and Acetyl CoA are regulated by malonyl CoA decarboxylase (MCD) and acetyl CoA carboxylase (ACC). MCD catalyzes the decarboxylation of malonyl CoA to acetyl CoA while ACC catalyzes the carboxylation of acetyl CoA to Malonyl CoA. Inhibition of MCD activity results in the accumulation of malonyl CoA which subsequently inhibits the activity of CPT1 resulting in decreased fatty acid oxidation (Dyck et al., 2004; Kolwicz Stephen C. et al., 2012; Stanley et al., 2005).

2.1.3 Glucose metabolism in normal heart

Glycogen stores and exogenous glucose uptake are the main sources of glucose used by the heart. Glycogen pool in the heart is relatively low (about 30 μ Mol / g wet weight). The uptake of glucose into the cardiomyocytes occurs via the insulin-dependent (GLUT4) and insulin independent (GLUT1) transporters (Kraegen et al., 1993). Hexokinase enzyme then phosphorylates the glucose to glucose-6-phosphate (G-6-P) which is metabolized in different pathway. In glycolytic pathway G-6-P is converted to pyruvate, 2 ATP molecules and NADH. The pyruvate can either be transferred to mitochondrial matrix or converted to lactate by lactate dehydrogenase (LDH). G-6-P can also be shuttled to pentose phosphate pathway or used for glycogen synthesis (Karwi et al., 2018). Pyruvate dehydrogenase which is the rate limiting enzyme in glucose oxidation convert pyruvate to acetyl CoA. The latter is used as a substrate for the tricarboxylic acid cycle (Fillmore et al., 2014).

In comparison to fatty acid oxidation, glucose is an efficient substrate for energy production, the phosphate oxygen ratio (P / O) for glucose oxidation is 2.58. To oxidize one molecule of glucose to 31 ATP molecule, only 6 molecules of oxygen are used.

2.1.4 Regulation of glucose oxidation

As mentioned above glucose metabolism is regulated by glucose / fatty acid cycle, increased fatty acid oxidation in the heart inhibit glucose oxidation (Hue & Taegtmeyer, 2009; Randle et al., 1963). Acetyl CoA and NADH produced by fatty acid oxidation inhibit pyruvate dehydrogenase (PDH), the enzyme involved in glucose metabolism. Elevated citrate levels can

inhibit phosphofructokinase 1 (PFK1) a prominent regulatory enzyme in glycolysis. PFK1 catalyzes the conversion of fructose-6- phosphate into fructose 1,6 biphosphate in the third step of glycolysis pathway. Depressed activity of PFK1 subsequently results in increased glucose-6-phosphate which then inhibits hexokinase enzyme that catalyzes the first priming reaction of glycolysis (Fillmore et al., 2014; Parmeggiani & Bowman, 1963). PFK1 activity is also regulated by increase in the levels of fatty acyl CoA (Jenkins et al., 2011).

2.2 Energy metabolism in heart failure

Energy metabolism in heart failure is compromised. It is characterized by impaired mitochondrial function and oxidative capacity which consequently leads to about 40 % reduction in ATP production. A significant decrease in the Pcr and ATP as well as Pcr / ATP ratio was observed in failing human hearts with dilated cardiomyopathy (Beer et al., 2002). Apart from impaired ATP production, mitochondrial TCA cycle activity, metabolic flexibility and oxidative phosphorylation are depressed in heart failure (Akhmedov, Rybin, & Marín-García, 2015; Casademont & Miró, 2002; Karwi et al., 2018a; Neubauer, 2007). The choice of energy substrate during heart failure depends on several factors. Some of these factors include; the model of heart failure and the duration or stage of heart failure (Karwi et al., 2018). In addition, molecular factors including mitochondrial biogenesis, transcriptional control and post transcriptional modification also determine the choice of substrate in HF (Karwi et al., 2018). The alteration of the source of energy substrates and the deficit in energy production are believed to cause depressed cardiac function observed in the failing heart (Fillmore, Mori, & Lopaschuk, 2014).

2.2.1 Glycolysis in heart failure

In heart failure, energy metabolism shifts backward towards fetal energy metabolism which is represented by an increase in glycolysis rates and a decrease in mitochondrial oxidative metabolism (Beer et al., 2002; Fillmore et al., 2014; Lei et al., 2004; Lopaschuk et al., 2010). The glycolysis rates are elevated in order to compensate the decreased mitochondrial oxidative metabolism (Fillmore et al., 2014). Glycolysis generates ATP in absence of oxygen, it is therefore the main source of energy during Ischemia (Jaswal et al., 2011). The decreased oxidation of glucose and increased glycolytic rates in heart failure results in increased uncoupling of glycolysis. Consequently, this leads to increased proton production (Dennis, Gevers, & Opie, 1991; Jaswal et al., 2011). Accumulation of these protons in the cytosol causes intracellular acidosis which lead to reduced cardiac contraction through the inhibition of the slow Ca^{2+} current and desensitization of contractile proteins to Ca^{2+} (Jaswal et al., 2011; Karwi

et al., 2018). The cardiomyocytes try to extrude these protons to the extracellular matrix, however this causes Na+ and Ca^{2+} overload leading to ionic imbalance (Karwi et al., 2018). The altered ionic homeostasis aggravates the limited energy supply in heart failure since the generated ATP is directed towards reestablishment of ionic homeostasis instead of cardiac contractile function hence decreasing cardiac efficiency (Fillmore et al., 2014a). Increase in glucose uptake and glycolysis has been reported in both clinical and experimental heart failure studies (Diakos et al., 2016; Fillmore et al., 2018).

2.2.2 Fatty acid oxidation in heart failure

To date, the changes in fatty acid oxidation in heart failure are not clear. However, in general it is assumed that cardiac fatty acid oxidation is decreased in heart failure (Karwi et al., 2018; Wende et al., 2017).

In experimental studies, a decrease in free fatty acid oxidation was observed in dogs with pacing induced heart failure. However, despite the enhanced glucose oxidation, carbohydrate oxidation was moderately reduced (Lei et al., 2004). Studies in pressure overload (TAC) induced heart failure in mice revealed that fatty acid oxidation was disrupted in hearts of this animals (Byrne et al., 2016; Sung et al., 2015). In agreement with these studies, the work of (Doenst et al., 2010) revealed that impaired fatty acid oxidation preceded congestive heart failure in TAC induced heart failure rats. To the contrary, no change in fatty acid oxidation rates was observed in angiotensin (Mori Jun et al., 2012) and TAC induced (Masoud et al., 2014) heart failure mice.

In the initial stages of HF, fatty acid oxidation in patients with idiopathic dilated cardiomyopathy is decreased. However, the increase in left ventricular dysfunction induce insulin resistance which consequently lead to increase in the uptake and oxidation of fatty acids (Tuunanen et al., 2006). Imbalanced uptake and metabolism of fatty acid could lead to accumulation of lipids and insulin resistance (Zhang et al., 2010).

Increased concentrations of circulating free fatty acids due to increased lipolysis is associated with heart failure. In the failing heart, the increased concentrations of circulating free fatty acids is a key determinant of the rate of fatty acid oxidation in the heart (Karwi et al., 2018). In clinical studies, the elevated levels of free fatty acids in circulation in patients with decompensated heart failure is accompanied with a rise in both myocardial uptake and oxidation of fatty acid (Paolisso et al., 1994; Tuunanen et al., 2006; Tuunanen, Ukkonen, & Knuuti, 2008).

2.2.3 Mediators of impaired fatty acid oxidation in the heart failure

Several mechanisms that mediate the impairment of cardiac fatty acid oxidation in heart failure have been proposed. These mechanisms include; mitochondrial dysfunction, substrate availability, cofactor availability, transcriptional and posttranscriptional modification (PTMs) based mechanisms (Wende et al., 2017).

2.2.3.1 Transcriptional regulation of fatty acid oxidation gene expression

Changes in the transcriptional regulation of fatty acid gene expression levels in heart failure by PPAR isoforms (Madrazo & Kelly, 2008) and PGC1 alpha (Finck & Kelly, 2006; Finck Brian N. & Kelly Daniel P., 2007) which are transcriptional coregulator and coactivators of fatty acid oxidation respectively has been largely studied. PPAR alpha regulates the transcription of a number of genes encoding key fatty acid transporters and fatty acid metabolism enzymes (Barger & Kelly, 2000). In heart failure, PGC1 alpha which plays a crucial role in the mitochondrial biogenesis is downregulated.

A significant decreased expression of the genes encoding the key fatty oxidation enzymes (MCAD and LCAD) and their upstream regulators that include RXR alpha, PPAR alpha, PGC1 alpha have been reported in heart failure (Barger & Kelly, 2000; Osorio Juan Carlos et al., 2002; Razeghi et al., 2001; Sack et al., 1996). An important decrease in the expression of RXR alpha and MCAD proteins and decreased activities of CPT1 and MCAD which are key enzymes in fatty acid oxidation were observed in decompensated pacing induced heart failure in dogs (Osorio et al., 2002).

In the recent past, we showed that methyl donor deficiency impairs fatty acid oxidation in the myocardium of weaning rats through decreased expression of PPAR alpha and ERR alpha and hyperacetylation/hypomethylation of PGC1 alpha (Garcia et al., 2011). The decrease expression of PPAR alpha and ERR alpha induced a significant decreased expression of key proteins involved in fatty acid oxidation that include short chain Acyl CoA dehydrogenase, fatty acid binding protein 3 and trifunctional enzyme subunit alpha complex (Garcia et al., 2011). The expression of PPAR alpha (Karbowska, Kochan, & Smoleński, 2003). PGC1 alpha and ERR (Sihag et al., 2009) were found to be decreased in heart failure patients.

2.2.3.2 Regulation of fatty acid oxidation by posttranslational modifications

Fatty acid oxidation in heart failure may also be altered by PTMs. This modification may include acetylation of lysine in the mitochondria. Acetylation reactions are mediated by either histone or non-histone acetyl transferases which catalyzes acetyl group transfer to lysine

residues of mitochondrial proteins (Xiong & Guan, 2012). GCN5L one of the mitochondrial acetyl transferase that plays a crucial role in the acetylation of mitochondrial proteins. Deacetylation reactions are mediated by the Silent information regulator 2 (Sir) proteins (Sirtuin) (Hirschey et al., 2011; Jing et al., 2013; Schwer & Verdin, 2008). Acetylation of enzymes involved in fatty acid oxidation may directly or indirectly affect the rate of fatty acid oxidation in the heart (Ahn et al., 2008; Chen et al., 2015; Garcia et al., 2011; Hirschey et al., 2011; Jing et al., 2013). The cardiac fatty acid oxidation rates were significantly increased by hyperacetylation of LCAD and Beta-hydroxyacylCoA dehydrogenase enzymes in the mice who were fed with high fat diet (Alrob et al., 2014). Moreover, PTMs of PPAR alpha during heart failure has been reported to impair its activity (Oka Shin-ichi et al., 2015).

2.2.3.3 Substrate and cofactor availability

Utilization of alternative substrates like ketone bodies and glucose during heart failure results in the alteration of fatty acid oxidation via established cofactor and allosteric limitation mechanisms (Wende et al., 2017).

2.3 Role of Sirt3 in myocardial mitochondrial energy metabolism

Sirtuin 3 (Sirt3) is a NAD (+)-dependent deacetylases localized in the mitochondria. It plays a crucial role in the regulation of mitochondrial homeostasis. Sirt3 is the major deacetylase that regulates mitochondrial energy metabolism through reversible deacetylation of key enzymes involved in energy metabolism (Parodi-Rullán, Chapa-Dubocq, & Javadov, 2018; Sun et al., 2018). Fatty acid oxidation, tricarboxylic acid cycle (TCA), oxidative phosphorylation and glucose metabolism are regulated by Sirt3 (Sun et al., 2018). Sirt3 regulates fatty acid oxidation by deacetylating proteins like long chain acyl-CoA dehydrogenase (LCAD) and medium chain acyl-CoA dehydrogenase (MCAD). SIRT3 was shown to activate LCAD *in vitro* and *in vivo*. Sirt3 deficient mice ($Sirt3^{-/-}$) exhibited decreased fatty acid oxidation which was characterized by accumulation of long chain acyl carnitines in liver and plasma and decreased ATP levels during fasting (Hirschey et al., 2010). About 33 % decrease in fatty acid oxidation was observed in Sirt3 deficient mice. In addition, LCAD was found to be hyperacetylated in $Sirt3^{-/-}$ in comparison to wild type mice (Hirschey et al., 2010). Sirt3 plays a crucial role in regulating ATP production by activating the subunits of electron transport chain (ETC). The team of (Ahn et al., 2008) demonstrated that complex 1 activity was inhibited in the mitochondria from liver of $Sirt3^{-/-}$ and mouse embryogenic fibroblasts, it was also found that Nduf9 which is a component of complex 1 was hyperacetylated in $Sirt3^{-/-}$. Furthermore, Sirt3 regulates the

activity of the SDHA subunit of succinate dehydrogenase (SDH) which is a component of complex II of ETC by deacetylation. SDHA was found to be hyperacetylated in Sirt3 KO mice (Finley et al., 2011). Deficiency in Sirt3 was reported to induce a significant reduction in ATP production and impaired oxidative activity in cardiac mitochondria of $Sirt3^{-/-}$ mice (Koentges et al., 2015). Moreover $Sirt3^{-/-}$ mice had severe impaired cardiac contractile function (Koentges et al., 2015). Majority of mitochondrial proteins involved in mitochondrial energy metabolism were more acetylated in hearts of $Sirt3^{-/-}$ in comparison to wild type (Koentges et al., 2015). Of these proteins 50 were linked to ETC subunits including those of complex I, II, III, IV and V, 6 proteins for fatty acid oxidation and transport and 3 proteins for TCA (Koentges et al., 2015). Glycolysis is also indirectly regulated by Sirt3, in absence of Sirt3 cyclophilin D is hyperacetylated. Hexokinase 2 which catalyzes the first step of glycolysis is activated by hyperacetylated cyclophilin D (Wei et al., 2013). The team of also demonstrated the role of Sirt3 in glucose oxidation in skeletal muscle in fed state. Deletion of Sirt3 induced a decreased activity of pyruvate dehydrogenase in skeletal muscle with an increased accumulation of pyruvate (Jing et al., 2013). Pyruvate dehydrogenase plays a crucial role in the glucose oxidation. Sirt3 activates pyruvate dehydrogenase by deacetylating its E1 alpha subunit, this subunit was found to be hyperacetylated in Sirt3 deficient animals (Jing et al., 2013). Sirt3 was also reported to regulate the components of oxidative phosphorylation and TCA cycle (Rardin et al., 2013). Isocitrate dehydrogenase which catalyzes the conversion of citrate to alpha ketoglutarate and generating NADPH in TCA cycle was hyperacetylated in the mitochondria of Sirt3 deficient liver (Rardin et al., 2013).

3 Impaired remethylation of homocysteine as risk factor for cardiovascular diseases and heart failure

3.1 Hyperhomocysteinemia

3.1.1 Definition of hyperhomocysteinemia

Hyperhomocysteinemia is a medical condition distinguished by abnormally elevated plasma total homocysteine levels usually greater than 15 μmol/L. In healthy individuals, normal plasma homocysteine level ranges from (5 -15 μMol/L) when measured in fasted state. Plasma concentration of homocysteine above 15 μMol/L is referred to as hyperhomocysteinemia (HHcy).

Depending on the plasma levels of homocysteine, HHcy can be defined as:

1). Moderate HHcy with (16-30 μMol/L) plasma homocysteine levels

2). Intermediate HHcy (30-100 μMol/L) plasma homocysteine levels

3). Severe HHcy with (> 100 μMol/L) plasma homocysteine level (Cheng et al., 2000).

HHcy induces oxidative stress and is a risk factor for cardiovascular diseases, cancer, neurological disorders, congenital developmental disorders and gastrointestinal disorders (Ganguly & Alam, 2015; Škovierová et al., 2016; Temple et al., 2000). Homocysteine exists in different forms in blood circulation either as disulfides or as mixed sulfides or as free reduced forms or bound to proteins (Iacobazzi et al., 2014). Total plasma homocysteine therefore refers to the total sum of free homocysteine, disulfides or protein bound homocysteine liberated by hydrolysis (Kumar et al., 2017).

3.1.2 Causes of hyperhomocysteinemia

Hyperhomocysteinemia is a multifactorial condition. It is caused by factors that include: 1). Genetic defects and deficiencies in enzymes involved in the metabolism of homocysteine 2). Excess intake of methionine 3). Deficiencies in cofactors of homocysteine metabolism (Deficiency in folates, vitamin B12 and vitamin B6) 4) Certain diseases like chronic renal disease and hypothyroidism and 5) Use of certain drugs like methothrexate and nicotinic acid (Froese et al., 2016; Iacobazzi et al., 2014; Kim et al., 2018; David Watkins et al., 2002).

3.1.2.1 Genetic errors in enzymes involved in cobalamin, folate and homocysteine metabolism

Hyperhomocysteinemia is caused by genetic defects in enzymes involved in cobalamin and folate metabolism and remethylation of homocysteine that include MS (Methionine synthase), MTRR, MMACHC, MMADHC, CD320, (Coelho et al., 2012; Green et al., 2017; David Watkins & Rosenblatt, 2011; David Watkins et al., 2002) cystathionine beta synthase (CBS) and 5- methylene tetrahydrofolate reductase (MTHFR) (Froese et al., 2016; Goyette et al., 1994). Genetic errors of enzymes involved in homocysteine metabolism causes hyperhomocysteienemia by impairing homocysteine remethylation and transsulfuration pathways. Genetic defects of MS, MTRR and MTHFR and MMACHC impairs the remethylation of homocysteine, while those of CBS impairs the homocysteine transsulfuration pathway. MS plays a central role in remethylation of homocysteine to methionine. Genetic defects of MS and MTRR therefore impairs this remethylation pathway leading to accumulation of homocysteine (David Watkins & Rosenblatt, 2011). MTRR also called methionine synthase reductase catalyzes reductive reactivation of MS. Polymorphism of MTRR (A66G) (Gaughan et al., 2001), MTHFR (C677) and MTR (A2756G) (Amouzou et al., 2004; Li et al., 2017) have been shown to be associated with hyperhomocysteinemia.

Remethylation of homocysteine by MS is also hindered by defects of MTHFR which cause decreased availability of MeTHF, the co-substrate for MS reactions. MTHFR enzyme catalyzes the reduction of 5- 10 methylene tetrahydrofolate to 5 methyl tetrahydrofolate the methyl donor in the remethylation of homocysteine by MS. MTHFR deficiency is a common inborn error of folate metabolism characterized by hyperhomocysteinemia, homocystinuria and hypomethioninemia. Single nucleotide polymorphism of MTHFR is the most common genetic defect with high incidence of mild and moderate hyperhomocysteinemia (Ganguly & Alam, 2015). Several mutations have been identified in MTHFR deficient patients (Frosst et al., 1995; Goyette et al, 2018; Yakub et al., 2012). A point mutation involving a substitution of C to T at nucleotide 677 associated with thermo labile MTHFR variant is linked to moderate hyperhomocysteinemia. In order to regulate homocysteine levels, MTHFR patients have a higher folate requirement (Jacques et al., 1996). In the homozygous state, MTHFR c.665C to T was found to be associated with mild hyperhomocysteinemia in plasma (Montjean et al., 2011). The team of Gaughan et al, reported that methionine synthase reductase A66G have significant influence on circulating total homocysteine concentration (Gaughan et al., 2001).

Deficiency in CBS is characterized by impaired conversion of homocysteine to cystathionine therefore leading to accumulation of homocysteine. CBS deficiency (OMIM 236200) is an autosomal recessive disorder caused by mutation in CBS gene EC 4.2.1.22_located in chromosome 21q22. CBS deficient patients if left untreated, their total plasma homocysteine

may increase 10 to 20 fold to as high as 222 μmol/L (Stabler et al., 2013). Recently eight novel mutations in CBS gene were identified in Chinese patients who had between 142-500 mol/L total plasma homocysteine (Li et al., 2018). CBS deficiency is also characterized by increase in methionine levels which subsequently lead to increased SAM levels. Consequently elevated SAM levels allosterically inhibits MTHFR (Froese et al., 2018) via feedback mechanism leading to inhibition of homocysteine remethylation pathway.

3.1.2.2 Nutritional deficiencies linked to hyperhomocysteinemia

Nutritional deficiencies of vitamin B6, folates (vitamin B9) and vitamin B12 (cobalamin) which are cofactors for the enzymes involved metabolism of homocysteine have been linked to etiologies of hyperhomocysteinemia. Mecbl a derivate of vitamin B12 and MeTHF from folate cycle are used by MS as cofactor and co-substrate respectively in the remethylation of homocysteine to methionine. Therefore, deficiencies of vitamin B12 and folate impairs MS homocysteine remethylation pathway leading to accumulation of homocysteine in the cells which further diffuses to plasma leading to hyperhomocysteinemia. Low levels of vitamin B12 cause significant decrease in MS activity (Brunaud et al., 2003). On the other hand, vitamin B6 deficiency cause hyperhomocysteinemia by impairing transsulfuration of homocysteine to cystathionine by CBS. Total plasma levels of vitamin B12, folates and vitamin B6 have been shown to be inversely related to total plasma homocysteine concentration (Ganguly & Alam, 2015; Hankey & Eikelboom, 1999). A close association between vitamin B12 deficiency and hyperhomocysteinemia have been reported (Mahalle et al., 2013; Wang et al., 2019). In clinical randomized trials, folic acid supplementation and folate fortification (Almassinokiani et al., 2016; Homocysteine Lowering Trialists' Collaboration, 2005; Zeng et al., 2015) and low dose vitamin B6 supplementation effectively reduced total plasma homocysteine levels (McKinley et al., 2001).

3.1.3 Hyperhomocysteinemia and cardiovascular diseases

Increased total plasma homocysteine levels is a strong risk factor for the development and progression of cardiovascular diseases (Cybulska & Kłosiewicz-Latoszek, 2015; Ganguly & Alam, 2015; Kim et al., 2018; Peng et al., 2015; Refsum et al., 1998)

Since the discovery of homocysteine in 1937 a lot of experimental and epidemiological studies have been carried out to ascertain the association between elevated plasma homocysteine levels with the development of cardiovascular diseases (Ganguly & Alam, 2015; Kim et al., 2018; Refsum et al., 1998). A positive correction between elevated serum homocysteine levels and atherosclerosis have been reported (Kilmer S. McCully, 2015). In 1969, McCully demonstrated

the association of hyperhomocysteinemia due to impaired cobalamin metabolism to development of the atherosclerosis (McCully, 1969). Homocysteine is one of the factors that play a crucial role in the induction of endothelial dysfunction in atherosclerosis.

Previous work in our laboratory aimed at evaluating the association of plasma homocysteine and left ventricular function in angiographically documented patients revealed a significant association between elevated plasma homocysteine and left ventricular systolic dysfunction (Guéant-Rodriguez et al., 2007). Elevated plasma homocysteine levels is an independent risk factor for development and severity of coronary artery disease in patients scheduled for coronary angiography (Naghshtabrizi, Shakerian, Hajilooi, & Emami, 2012; Shenoy, Mehendale, Prabhu, Shetty, & Rao, 2014). A meta-analysis aimed at investigating the association of serum homocysteine concentration with ischemic heart disease, pulmonary embolism deep vein thrombosis revealed a significant associated of elevated homocysteine with these diseases and that homocysteine was causal (Wald, Law, & Morris, 2002).

In the Framingham heart study, elevated plasma homocysteine was found to independently predict the risk of developing of congestive heart failure in women and men without prior incidence of myocardial infarction (Vasan et al., 2003). The team of (Zhang et al., 2014) found that in the elderly subjects, serum homocysteine is positively associated with central artery stiffness but not with peripheral artery stiffness. In addition, elevated homocysteine was independent predictor of central arterial stiffness (Zhang et al., 2014). Arterial stiffness which is a known strong predictor of future fatal and nonfatal cardiovascular diseases.

In meta-analysis of prospective studies, elevated homocysteine level was reported to be the independent predictor of mortalities from cardiovascular disease and all cause-mortality (Peng et al., 2015; Zhu et al., 2019). In the study by Peng and colleagues, 5μmol/L homocysteine increase caused an increase in the pooled adjusted risk of occurrence of cardiovascular and all cause-deaths (Peng et al., 2015). In chronic heart failure patients, hyperhomocysteinemia was positively associated with decreased survival rate with an increased risk of death at fifth year (Fournier et al., 2015).

Prospective studies in India and Egypt showed that maternal hyperhomocysteinemia is a risk factor for increased incidence of congenital heart defects in the offspring (Malik et al., 2017; Shawky et al., 2018). Additionally, a significant decrease in plasma folate and vitamin B12 was reported in these cases. Elsewhere, elevated amniotic homocysteine levels in 26 patients was reported to be associated with isolated cases of congenital heart defects (Wenstrom et al., 2001). Lowering plasma homocysteine levels by 25 % was found to be effective in reducing cardiovascular risks by 11 to 16 % (Wald et al., 2002).

3.1.4 Pathological mechanisms of homocysteine

Hyperhomocysteinemia contributes to the development and progression of cardiovascular diseases via various mechanisms that include: induction of oxidative stress, endoplasmic reticulum stress, apoptosis and chronic inflammation leading to remodeling of extracellular matrix and endothelial dysfunction.

3.1.4.1 Induction of oxidative stress

Homocysteine induces oxidative stress through a number of mechanisms that include, activation of NADPH oxidases, autooxidation of homocysteine, inhibition of enzymatic activities of antioxidants in the cells and generation of superoxide anion by Nitric oxide synthase (Lehotsky et al., 2015). Below is a detailed description of these mechanisms.

i) Autooxidation of homocysteine

Homocysteine contributes to the development of oxidative stress by generating superoxide radicals. The sulfhydryl (SH) group in homocysteine is highly reactive, it readily self-oxidizes forming disulphide linkage with free thiols producing the superoxide radicals in the process (McDowell & Lang, 2000).

ii) Activation of NADPH oxidases

Homocysteine induces oxidative stress and reduces bioavailability of nitric oxide (NO) in cardiac microvascular endothelial cells by activating the expression of protease activated receptor which induces the upregulated expression of nicotinamide adenine dinucleotide phosphate (NADPH) oxidase and decreasing the expression of thioredoxin (Tyagi et al., 2005). Thioredoxin are antioxidant proteins they catalyze reduction of oxidized proteins through cysteine thiol-disulfide exchange. Homocysteine induces an upregulated expression of NADPH oxidase in microvascular endothelial cells in a dose dependent manner (Tyagi et al., 2005). NADPH oxidase causes oxidative stress by producing superoxide as illustrated in **Equation 1** (Lai & Kan, 2015a).

Equation 1 $NADPH + 2O_2 \longrightarrow NADP^+ + 2O_2^- + H^+$

iii) Accumulation of asymmetric dimethyl arginine

Hyperhomocysteinemia suppresses the expression of dimethyl arginine dimethyl amino hydrolase (DDAH) consequently leading to an increased accumulation of asymmetric dimethyl arginine (ADMA) (Tyagi et al., 2005). DDAH is involved in metabolism and regulation of plasma levels of ADMA (Palm et al., 2007). ADMA is an endogenous inhibitor of nitric oxide synthase (NOS) and a competitive inhibitor of endothelial nitric oxide synthase (eNOS) leading to impaired NO endothelial signaling (Böger et al., 1998). Increased accumulation of ADMA

causes decreased bioavailability of NO (Stühlinger et al., 2001; Tyagi et al., 2005). Clinical studies have demonstrated a strong correlation between ADMA and endothelial dysfunction in patients with hypercholesterolemia.

iv) Generation of superoxide anion by Nitric oxide synthase and reduction of bioavailability of nitric oxide

Elevated homocysteine levels cause uncoupling of eNOS. In this phenomenon the production of NO by eNOS is impaired but its reduction domain remains active and it actively reduces oxygen generating superoxide (Lai & Kan, 2015). The superoxide generated from both uncoupling of eNOS and upregulated expression of NADPH oxidase inactivates the NO produced by the remaining functional eNOS consequently leading to production of peroxynitrite. The peroxynitrite which is a strong oxidizing agent further impairs eNOS function by depleting Tetrahydrobiopterin (BH4) the key cofactor of eNOS oxygenase domain (Lai & Kan, 2015). Elevated plasma homocysteine levels induce oxidative stress by decreasing bioavailability of NO. This soluble gas is produced in vascular cells by three different isoforms of nitric oxide synthase (NOS). Endothelial nitric oxide synthase is the main isoform that produces this gas. NO regulates vascular tone and structure and contractility of cardiomyocytes, other effects of NO in the cardiovascular system include anti-inflammatory effects, prevention of smooth muscle cell proliferation and migration and inhibition of platelet aggregation and adhesion (Desjardins & Balligand, 2006; Tousoulis et al., 2012). Decreased availability of NO cause endothelial dysfunction which is linked to the development of atherosclerosis, hypertension, diabetes and heart failure (Desjardins & Balligand, 2006).

v) Impaired expression of antioxidant enzymes in the cell

Homocysteine induces oxidative stress by impairing the cells' antioxidant capacity by suppressing the expression and activities of antioxidant enzymes like glutathione peroxidase and superoxide dismutase (SOD). In rat vascular smooth muscles cells, high level of homocysteine induced decreased expression and secretion of extracellular SOD mRNA (Nonaka et al.,2001). Several studies have demonstrated the role of homocysteine in suppressing the expression of glutathione peroxidase 1. Homocysteine was found to reduce mRNA expression and activity of the glutathione peroxidase in bovine aortic endothelial cell (Deatrick et al., 2013). Moreover, hyperhomocysteinemia enhanced endothelial dysfunction in glutathione peroxidase deficient mice (Dayal Sanjana et al., 2002).

3.1.4.2 Endoplasmic reticulum stress

Endoplasmic reticulum (ER) is the principle site for correct folding and modification of secretory and transmembrane proteins. Homocysteine induces ER stress by interrupting the formation of disulfide bonds and as a consequence this leads to protein misfolding. Accumulation of misfolded proteins causes ER stress and activates the unfolded protein response (UPR) signaling pathway (Schröder & Kaufman, 2005). UPR induces upregulated expression of ER chaperone proteins and foldase enzyme. High intracellular homocysteine levels have been reported to induce expression of a number of ER stress response genes that include: GRP78, GRP94, HERP, GADD153, GADD45, and ATF-4 (Kokame et al.,2000; Kokame, Kato, & Miyata, 1996; Outinen et al., 1998, 1999). It was recently demonstrated that homocysteine induces endothelial dysfunction via ER stress mediated suppression of intermediate and small calcium potassium channel mechanism (Wang et al., 2015). Chronic ER stress leads to apoptosis. Hyperhomocysteinemia induces ER stress mediated apoptosis in human platelets by enhancing caspase 9 and caspase 3 activities (Zbidi et al., 2010).

3.1.4.3 Protein modification by homocysteinylation

Hyperhomocysteinemia causes posttranslational modification of proteins in a process called homocysteinylation. These types of homocysteinylation are: 1). S-homocysteinylation and 2). N- homocysteinylation. S-homocysteinylation involves the formation of disulfide bond between a free thiol group of homocysteine and another free thiol group from cystine residues of a protein. S-homocysteinylation has a detrimental effect on the thiol dependent redox status of proteins (Škovierová et al., 2016).

N- homocysteinylation is a non-enzyme catalyzed process that involves the formation of amide bond between homocysteine thiolactone and the lysine residues of proteins (Jakubowski, 1999; Jakubowski et al., 2000). Homocysteine thiolactone is a highly reactive cyclic thioester of homocysteine (Jakubowski, 1999, 2008) formed in editing error reaction by methionyl tRNA synthetase (Jakubowski & Goldman, 1993). This reaction prevents translational incorporation of homocysteine to proteins. The proportion of N-homocysteinylation increases with increase in number of lysine residues (Jakubowski, 1999), lysine rich proteins like high density lipoproteins, fibrinogen, low density lipoprotein, albumin, hemoglobin, ferritin antitrypsin, cytochrome c and lysine oxidase are highly susceptible to N-homocysteinylation (Jakubowski, 2008; Sharma, Kumar, & Singh, 2014). The extent of N-homocysteinylation of either acidic or basic protein and the consequence of N- homocysteinylation on the protein structure and functions depends on the proteins' isoelectric point (pI) (Sharma et al., 2014). High intracellular

homocysteine levels are associated with increased formation of homocysteine thiolactone. N-homocysteinylation has detrimental effects on protein function as it causes alteration in proteins structure, damages proteins, impairs proteins folding, increases proteins' susceptibility to oxidative damage and hence results in generation of dysfunctional proteins (Sharma et al., 2014). Introduction of thiol group and inactivation of free amino acid by homocysteinylation affects proteins function by impairing their redox potential leading to oxidative stress (Škovierová et al., 2016). In addition, N- homocysteinylation causes cytotoxicity through various mechanisms that includes: activation of unfolded protein response, inactivation of enzymes, ER stress, enhance protein denaturation and myeloid formation (Sharma et al., 2015). Elevated levels of homocysteine thiolactone and increased protein N-homocysteinylation has been reported in MTHFR and CBS deficient patients with hyperhomocysteinemia (Jakubowski, Boers, & Strauss, 2008). Moreover the team of Jakubowski also demonstrated that nutritional and genetic disorders of folate and homocysteine metabolism causes more than 10 fold increase in N-homocysteinylation of proteins (Jakubowski et al., 2009).

4 THE ROLE OF METHIONINE SYNTHASE IN THE METABOLISM OF MONOCARBONS AND REMETHYLATION OF HOMOCYSTEINE

4.1 Nutritional determinants for the remethylation of homocysteine and synthesis of methionine by methionine synthase

Vitamin B12 (cobalamin) and folates are micronutrients that play crucial role in one-carbon metabolism. They donate methyl groups in the homocysteine remethylation reactions and synthesis of methionine by MS.

4.1.1 Vitamin B12

Vitamin B12 is an essential micronutrient for survival and normal development. Only certain micro-organisms can synthesize vitamin B12. The molecular mechanisms and steps in the vitamin B12 anaerobic and aerobic biosynthetic pathways in bacteria have been identified and fully elucidated (Battersby, 1994; Martens et al., 2013). These biosynthetic pathways are missing in higher organism, therefore humans obtains vitamin B12 mainly from dietary intake of food from animal origin or from vitamin supplements (O'Leary & Samman, 2010). Vitamin B12 is an essential cofactor for enzymatic reactions catalyzed by several classes of enzymes that include: the dehalogenases, adenosylcobalamin-dependent methyltransferases and methyl cobalamin dependent isomerases (Banerjee & Ragsdale, 2003; Gruber, Puffer, & Kräutler, 2011). In humans, vitamin B12 is intracellularly metabolized into two essential coenzymes: methylcobalamin (MeCbl) the cofactor for the reactions catalyzed by cytoplasmic methionine synthase (MS) (Li et al., 1996) and adenosylcobalamin (AdoCbl) the cofactor for the reactions catalyzed by methyl malonyl-CoA mutase (MUT or MCM) (Ledley et al., 1988; Nham, Wilkemeyer, & Ledley, 1990).

4.1.1.1 Vitamin B12 nutritional requirements

As stated above, humans cannot synthesize vitamin B12 therefore dietary intake of vitamin B12 is indispensable. Vitamin B12 is mainly obtained from food products of animal origin like beef, liver, fish, poultry, eggs, milk and milk products. Food from plant origin does not contain vitamin B12. Strict vegetarians may obtain vitamin B12 from vitamin B12 fortified foods that include breakfast cereals, soy-based meat substitutes and rice and soy beverages. Daily vitamin

B12 requirement varies with age, daily intake of about 2.4 µg is the recommended for adults. The recommendations for daily vitamin B12 requirement for the different categories of people in France is summarized in **Table 1**.

Gategory	**2011 (**AFSSA) **(µg/day)**
Adults males	3.4
Adults females	2.4
Old persons > 75 years	3
Pregnant women	2.6

Table 1: **Recommended vitamin B12 nutritional intake for the French population de l'Agence Française de Sécurité Sanitaire des Aliments (AFSSA) (Schlienger, 2011**

4.1.1.2 Structure of vitamin B12

In 1956, the team of Dorothy Hodgkin discovered the three-dimensional structure of vitamin B12 using X-ray Crystallography (1964 Nobel prix in Chemistry) (Hodgkin et al., 1957) . Vitamin B12 is an organometallic voluminous molecule whose structure consists of a central cobalt atom surrounded by a planar corrin ring (**Figure 5)**. The cobalt atom has six ligands. It coordinates with the corrin ring through four planar nitrogen atoms. The two other ligands are the upper beta axial and the lower axial ligands. The lower axial ligand is a 5 ,6 -dimethylbenzimidazole nitrogen (DMB) base which is covalently attached to the corrin ring through the side chain linked to ring D of micro-cycle.

In the upper axial position, the central cobalt atom may coordinate with several different entities (R group), this depends on the modification state of the R group which could be either an hydroxyl group to generate hydroxycobalamin (OHCbl), a methyl group to generate methylcobalamin (MeCbl) cofactor for MS in the remethylation reactions, a cyano group to generate cyanocobalamin (CNCbl) or an adenosyl to generate adenosylcobalamin (AdoCbl) the cofactor for methyl malonyl-CoA mutase (**Figure 5).** Cobalamin cobalt atom may exist in three oxidation states: +1 (Cob(I)alamin) the fully reduced state, +2 (Cob(II)alamin) and +3 (Cob(III)alamin) the fully oxidized state.

Naturally, cobalamins exist in three forms, OHCbl, MeCbl and AdoCbl. CNCbl does not exist naturally as it is a pharmaceutical preparation of vitamin B12.

The reactivity of cobalamin depends on three factors that include:1) the identity of the R group, 2) the coordination of DMB nitrogen in the alpha axial position and 3) the cobalt atom oxidation state. (Froese & Gravel, 2010; Qureshi, Rosenblatt, & Cooperd, 1994; David Watkins & Rosenblatt, 2011).

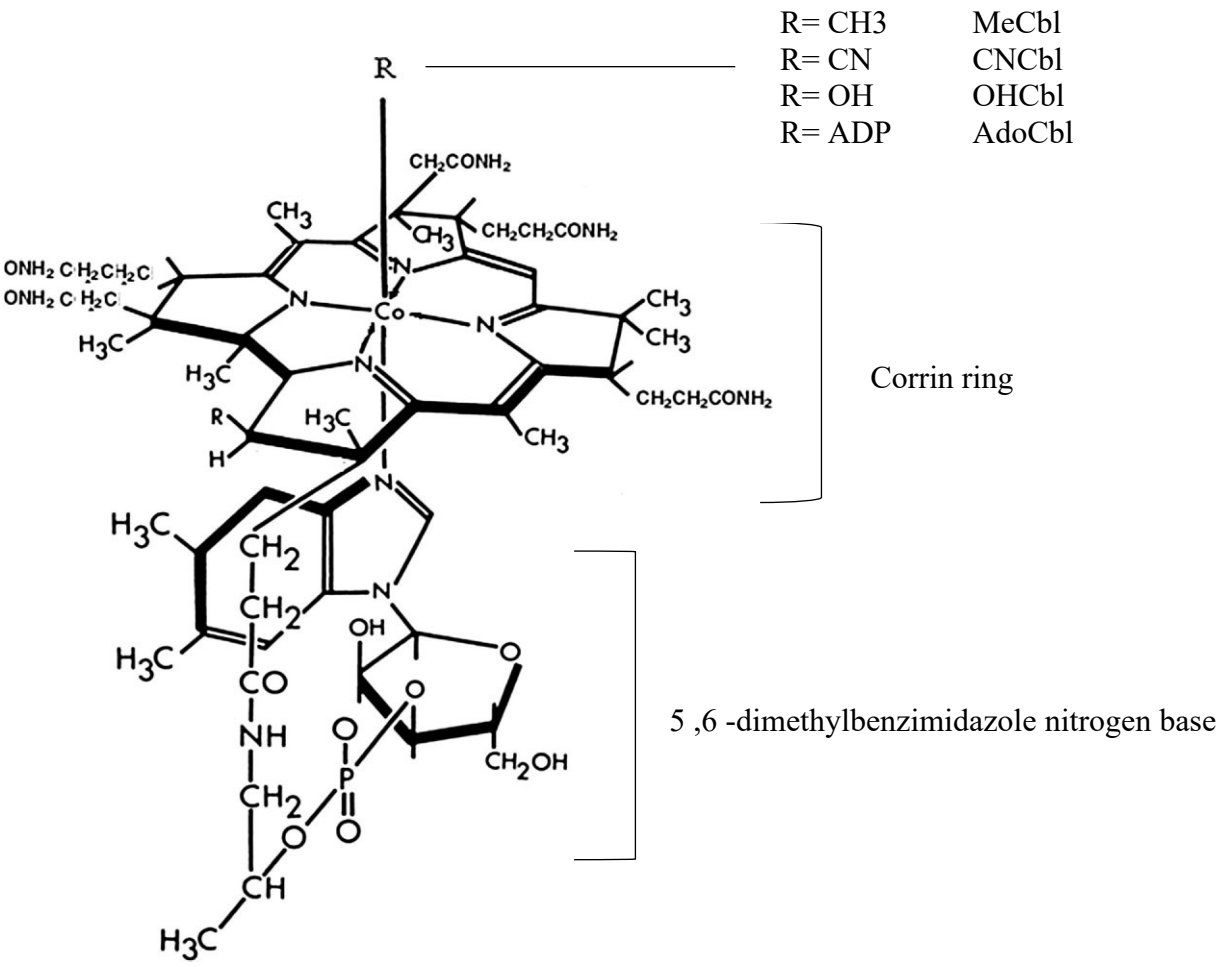

Figure 5: Chemical structure of vitamin B 12. Adapted from (David Watkins & Rosenblatt, 2011)

Vitamin B12 structure consists of a corrin ring with a central cobalt atom which coordinates with a 5,6-dimethylbenzamidazole in the lower axial position and R groups in the upper/ beta position. Designated "R" is the the upper / Beta axial position where a number of different entities including: adenosylcobalamin (AdoCbl), methyl cobalamin (MeCbl), hydroxocobalamin (OHCbl) or Cyanocobalamin (CNCbl) could be bound.

4.1.1.3 Absorption of vitamin B12

In humans, absorption and intracellular metabolism of dietary cobalamins is a delicate and complex multistep process involving a number of cobalamin binding proteins and their

receptors (Green et al., 2017) as shown in **Figure 6**. Following ingestion, cobalamin is liberated from its food carrier proteins in the acidic environment of the stomach by proteolysis mechanism involving pepsin and hydrochloric acid secreted by stomach parietal cells (Nielsen et al., 2012; David Watkins & Rosenblatt, 2011). Subsequently, free cobalamin is exclusively bound by the first cobalamin binding protein called haptocorrin (HC) (also known as transcobalamin I or R binder) in the acidic environment of the stomach to form the Haptocorrin-cobalamin complex (HC-Cbl) (Allen et al ., 1978). HC is a salivary glycoprotein which binds cobalamins with a higher affinity in acidic environment where it protects the bound cobalamin from hydrolytic digestion.

In the alkaline millieu of the duodenum, pancreatic protease digestion releases cobalamin from the HC-Cbl complex after which it associates with intrinsic factor (IF) to form IF-Cbl complex (R. H. Allen et al., 1978). IF is a cobalamin binding protein synthesized and secreted by gastric parietal cells (Hurlimann et al., 1969). IF is highly glycosylated and when bound to cobalamin it is resistant to proteolytic digestion (Hurlimann et al., 1969). IF has high affinity for cobalamins forms with intact lower DMB, it therefore prevents the cellular uptake of degraded cobalamins (Froese & Gravel, 2010).

In distal ileum, IF-Cbl complex internalization occurs via cubam receptor complex mediated endocytosis. Cubam receptor complex has high affinity for IF-Cbl complex. This receptor is expressed on the enterocytes in the ileum and is composed of two proteins :1). A transmembrane protein called amnionless (encoded by *AMN* gene) and 2). A peripheral membrane multiligand binding protein called cubilin (encoded by *CUBN* gene) (Gueant & Chery, 2001; John et al., 2004; Kozyraki & Gofflot, 2007; Nielsen et al., 2012). Mutations in *CUBN* gene localized in chromosome 10 and *AMN* gene localized in chromosome 14 is associated with Imerslund-Gräsbeck disease (Fyfe et al., 2014; John C. Fyfe et al., 2013; Hauck, Tanner, Henker, & Laass, 2008). Inside the cell, lysosomal degradation of IF releases cobalamin into the cytosol. The ATP binding cassete ABC drug transporter also known as multi drug resistant protein 1 (MRP1) then mediates the ATP dependent transport of free cobalamin across the basolateral epithelial membrane of ileum and other cells (Beedholm-Ebsen et al., 2010). Cobalamin is then released into the blood stream for circulation where about 70-80 % of cobalamin is bound to HC and about 20 -30% to transcobalamin (TC) also known as transcobalamin II (TCII). TCII is synthesized in the intestinal villi (Jiang et al., 2013; Quadros & Sequeira, 2013; Quadros et al., 1999) where it facilitates the cellular uptake of cobalamins. Like IF, TCII has high affinity for cobalamins forms with intact lower DMB it therefore prevents cellular uptake of degraded cobalamins.

4.1.1.4 Transport of vitamin B12

In blood, cobalamin is transported bound to two cobalamin specific transporter proteins: haptochorrin (HC) and transcobalamin (TC II) (Burger et al., 1975; Nielsen et al., 2012; Quadros & Sequeira, 2013). Majority of vitamin B12 in blood is bound to HC, this fraction of cobalamin is transported to the liver where it is internalized only in the hepatocyte by asialoglycoprotein receptor mediated endocytosis. Minority of circulating cobalamin (20-30) % is bound to TC; this fraction is available for cellular uptake in the liver and other tissues via TcblR/ CD320 receptor mediated endocytosis (Jiang et al., 2013; Nielsen et al., 2012; Quadros, 2010; Quadros & Sequeira, 2013; Quadros et al., 1999; Green et al., 2017). However in the kidney, the uptake of Cbl-TC complex is facilitated by megalin receptor (Moestrup et al., 1996).

4.1.1.5 Intracellular metabolism of vitamin B12

In mammalian cells, metabolism of cobalamin into the two active coenzymes: AdoCbl and MeCbl is a multistep process involving several proteins as shown in **Figure 6** (Green et al., 2017). Our laboratory recently proposed that intracellular metabolism of cobalamins occurs via multiprotein complex named MS interactome involving MS, MSR, MMACHC and MMDHC. This complex is essential for efficient and safe processing, targeting and trafficking of vitamin B12 from MMACHC to MS for MeCbl synthesis (Bassila et al., 2017).

Endocytosis of cobalamins bound to transcobalamin II (Cbl-TCII) is mediated by transcobalamin receptor (Quadros et al., 2008; Quadros & Sequeira, 2013). Proteolytic degradation of TC in the lysosome frees the cobalamin from the TC-Cbl complex. The free cobalamin is subsequently transported across the lysosomal membrane by two transmembrane proteins LMBD1 and ABCD4 which delivers the free cobalamin to MMACHC protein in the cytoplasm (Deme et al., 2014; Rutsch et al., 2009). The team of Deme has demonstrated that ABD4 and LMBD1 proteins interact with low nanomolar affinity invitro. They also showed that ABD4 and LMBD1 proteins also interact with MMACHC with low nanomolar affinity. This interaction have been proposed to protect the cobalamin from inactivating side reaction and also prevents its dilution in cytoplasmic milieu, therefore facilitating a safe exportation of cobalamin from the lysosome to the cytoplasm (Deme et al., 2014).

In the cytoplasm, MMACHC protein effectuates the decyanation of CNCbl to form cobalamin II; this reaction is important for the conversion of cyanocobalamin into the two active cofactors: MeCbl and AdoCbl (Kim, Gherasim, & Banerjee, 2008). MMACHC is also involved in the processing of alkylcobalamin by dealkylation of a number of substrates that includes the newly internalized natural forms of cobalamins in food; MeCbl or AdoCbl (Kim et al., 2009; Koutmos

et al., 2011; Hannibal et al., 2009). Dietary cobalamins must be processed by the removal of the upper axial ligands before they are delivered to MS and MUT (Hannibal, DiBello, & Jacobsen, 2013). MMACHC binds cobalamins in base off conformations and delivers it to cytoplasmic MMADHC protein. MMACHC has been proposed to interact with MMADHC to form a molecular chaperone for cytoplasmic trafficking of cobalamins (Plesa et al., 2011). To form this molecular chaperone the C terminal domain of MMADHC interacts with MMACHC (Gherasim et al., 2013; Yamada et al., 2015). MMADHC partitions MeCbl into the cytoplasmic MS pathway and AdoCbl into mitochondrial MethylmalonylcoA mutase (MUT) pathway. In the cytoplasmic pathway, MS uses the MeCbl as a cofactor and N5-methyltetrahydrofolate (N5-Me-THF) from folate cycle as cosubstrate to catalyze methyl group transfer from N^5 methyltetrahydrofolate to homocysteine to form methionine and tetrahydrofolate (Banerjee et al., 1990; Rowena G Matthews, 2001). The reactions of MS are detailed in section 5.

In the mitochondria, cobalamin adenosyltransferase (cblB) in collaboration with an unknown cobalamin reductase catalyzes the adenylation of cobalamin II to form adenosylcobalamin (AdoCbl). CblB also transfers the generated AdoCbl MUT (Padovani et al., 2008). MUT uses AdoCbl as cofactor to catalyze the conversion of methylmalonylCoA to succinylCoA (Maiti, Widjaja, & Banerjee, 1999; Takahashi-Iñiguez et al., 2012). SuccinylCoA then enters the Krebs Cycle where it is used as a substrate for gluconeogenesis. It has been proposed that the third mitochondrial protein MMAA (CblA) acts as a gatekeeper ensuring that only Adocbl is bound to MUT. MMAA (CblA) is also crucial in generating mutase bound AdoCbl (Froese & Gravel, 2010).

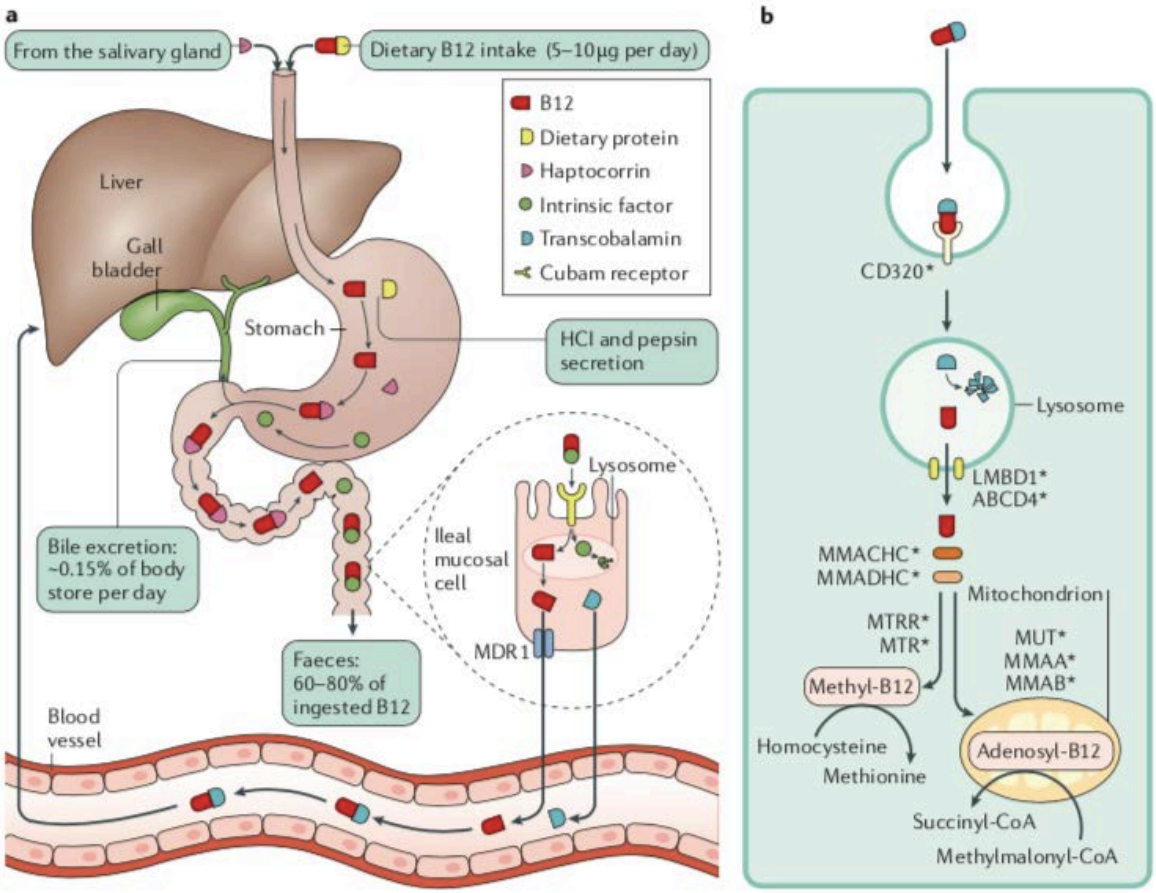

Figure 6: Absorption, transport, enterohepatic circulation and intracellular metabolism of vitamin B12. Adapted from (Green et al., 2017).

a) Vitamin B 12 shown in red is obtained from food of animal origin. After ingestion, vitamin B12 is liberated from its food carrier proteins in the acidic environment of the stomach by proteolysis. The free vitamin B12 then binds to haptocorrin (shown in pink) which protects it from acidic degradation. In the duodenum degradation of haptocorrin releases the vitamin and the change in pH favors the binding of the vitamin to gastric intrinsic factor (IF) (shown in green) to form the vitamin B12 -IF complex. Cubam mediated endocytosis facilitates the uptake of Vitamin B12-IF complex in the enterocytes of the distal ileum. In the enterocytes, lysosomal degradation of B12-IF complex releases the vitamin which then exits the basolateral membrane of the enterocytes in a process mediated by the multidrug resistance protein 1 (MRP1). In blood circulation, majority of vitamin B12 is transported to various tissues bound to transcobalamin (shown in light blue). In the liver, majority of vitamin is stored while some is excreted in the bile and it undergoes enterohepatic circulation.

b) Cellular uptake of vitamin B12 in all tissues is facilitated by the CD320 receptor the uptake of MeCbl and AdoCbl is a complex multistep process involving several proteins encoded by the

genes shown in hysterics (*). Mutations in these genes are associated with inborn errors of cobalamin metabolism.

4.1.2 Folates (Vitamin B9)

Folate is a generic term for water soluble-vitamin B9 also called pteroglyglutamic acid. It is an essential micronutrient that is required for normal cellular function, human health and development. Folates plays a crucial role in metabolism of monocarbons as well as in epigenetic and epigenomic regulatory mechanisms (Guéant et al., 2013; Salbaum & Kappen, 2012). In these mechanisms, folate metabolism is an important determinant for the flux of monocarbon for synthesis of SAM which is the universal methyl donor for transmethylation reactions in the cell (Guéant et al., 2013). Furthermore, folate is the metabolic precursor for THF which is a coenzyme involved in the synthesis of purines and pyrimidines which are the constituents for synthesis deoxyribonucleic acid (DNA) and ribonucleic acid (RNA). In addition, MeTHF another folate derivative is a co-substrate in the remethylation of homocysteine by MS (Banerjee & Matthews, 1990).

4.1.2.1 Nutritional requirements

Folates are not synthesized by humans therefore they must be obtained from dietary intake. Food sources rich in folates includes: green leafy vegetables (spinach , broccoli, kales and sprouts), brewers' yeast, fruits, dried grains (beans and peas) and liver (Salbaum & Kappen, 2012). Limited access to folate rich foods has been reported in a larger percentage of the population in lower socioeconomic groups. Daily folate requirement varies with age, sex and physiological state. To date, no consensus on the recommended dietary allowance (RDA) for folates has been achieved. However, majority of countries the recommended folate RDA is 300 µg/ day for adults and adolescence, (150 – 250) µg/ day for children and for women of childbearing age is 400µg/day. The French population RDA for folates for different ages is summarized in Table 1. The US food and nutrition board recommend an RDA of 400µg/day for folic acid in adults (*Report of the Dietary Guidelines Advisory Committee on the Dietary Guidelines for Americans,* 2010)

Caterogy	RDA 2011 (µg/day)
Adults males	330
Adults females	300
Old persons > 75 years	350
Pregnant women	400

Table 2: **Recommended folate nutritional intake for the French population de l'Agence Française de Sécurité Sanitaire des Aliments (AFSSA) (Schlienger, 2011)**

4.1.2.2 Folate (vitamin B9) deficiency

To date, folate deficiency is one of the most common nutritional deficiencies in the world. Therefore, it is an important public health problem. Folate deficiency can be caused by several factors, the major one being due to low folate dietary intake, other causes include genetic defects of metabolism and intestinal absorption of ingested folates (Fowler, 1998; Lanzkowsky, 1970; Qiu et al., 2006), increased use of folates especially during pregnancy and impaired metabolism due to drug interaction. Pathological liver conditions have also been reported to cause folate deficiency (Scaglione & Panzavolta, 2014).

Folate deficiency during pregnancy causes adverse pregnancy outcomes that includes neural tube defects (NTDs) and congenital heart defects (Botto, Mulinare, & Erickson, 2000; Czeizel et al., 2013; Durand, Prost, & Blache, 1998; Safi, Joyeux, & Chalouhi, 2012). NTDs are defects that affect the central nervous system during human development resulting from failure of closure of the neural tube. NTDs are known to be the most frequent congenital abnormalities which includes Spina bifida (disorders affecting the spinal cord which can either be closed or open), Anencephaly (defects of the brain, little or no brain), Encephalocele (defects of the skull) and Craniorachischisis (caused by total neurulation failure) (Imbard, Benoist, & Blom, 2013).

Adequate intake of folates is crucial factor in preventing development of some NTDs and congenital heart defects. For this reason, systematic folate supplementation in pregnant women has been put in place, a significant protective effects of this supplementation in preventing NTDs and congenital heart defects has been reported (Botto et al., 2000; De-Regil, Peña-Rosas, Fernández-Gaxiola, & Rayco-Solon, 2015; Gomes, Lopes, & Pinto, 2016). The French Agency for food, environmental and occupational health and safety recommend folic acid

supplementation of 440 µg/day for women during periconceptional period (eight weeks before and after conception). Fortification of primary foods with folic acid has significantly decreased the prevalence of NTDs and stroke mortality (Crider, Bailey, & Berry, 2011; De Wals et al., 2007; Hertrampf & Cortes, 2004; Honein, Paulozzi et al., 2001). Folate deficiency has also been linked to other diseases that includes cardiovascular diseases, anaemia, neuropsychiatric disorders and cancer (Blom & Smulders, 2011; Kim, 2004; Lee et al., 2011).

4.1.2.3 Structure of vitamin B9

The chemical structure of folate molecule is composed of a pteridine base conjugated to glutamic acid and P-Aminobenzoic acid as shown in **Figure 7A** (Ducker & Rabinowitz, 2017; Guéant et al., 2013). This basic structure of folates is shared by different folate species. However, they are differentiated by the Pteridine oxidation level, number of glutamate residues and the nature of attached mono-carbon unit (Rébeillé et al., 2006). The Pteridine ring of folates can exist in different oxidation states: either as dihydrofolate (DHF) and tetrahydrofolate (THF) which are the reduced forms of folates or as fully oxidized forms (Bekaert et al., 2008). In folates, one carbon group at different oxidation levels can be carried on the N5 or N10 position. The cellular folate pool consists of different molecules. The biologically active forms of folates occur in reduced forms and they include DHF and THF and the derivatives of THF that includes 5-formylTHF, 10 FormylTHF, 5,10-MethenylTHF, 5,10-MethyleneTHF shown in **Figure 7B** (Bekaert et al., 2008). Oxidized forms of folates like folic acid does not occur naturally, therefore folic acid must be reduced before it enters the folate cycle.

A.

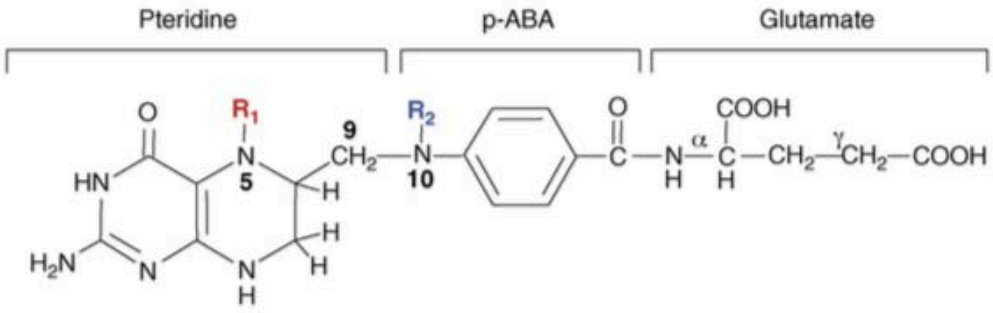

R_1	R_2	Folate species
H	H	THF
CHO	H	5-formyl-THF
H	CHO	10-formyl-THF
CH_3	H	5-methyl-THF
$-CH_2-$		5,10-methylene-THF
=CH–		5,10-methenyl-THF

B.

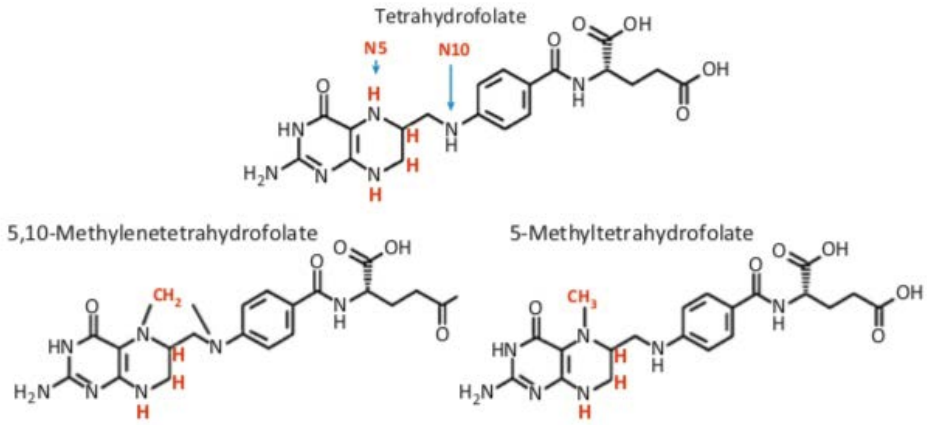

Figure 7: Chemical structure of folate and its derivatives adapted from (Bekaert et al., 2008; Guéant et al., 2013)

A. The basic structure of folate molecule is composed of pteridine ring, P-Aminobenzoic acid (p-ABA) and glutamate. Approximately six residues of gamma linked polyglutamyl tails can be attached to the first glutamate. R1and R2 are the N5 and N10 positions where C1 units at various oxidative levels can be attached. The structural formula of the various naturally occurring C1 units of folates are shown.

B. The chemical structures of naturally occurring folates (tetrahydrofolate, 5,10 Methylene tetrahydrofolate and 5, Methyl tetrahydrofolate) are shown.

4.1.2.4 Absorption and transport of folates

The process of absorption of dietary folates is shown in **Figure 8**. Mechanisms of absorption of folates depends on the pH and substrate specificity. In order to absorb the folates from diet, polyglutamates which are the main forms of dietary folates are first hydrolyzed into monoglutamate in a reaction catalyzed by folylpolyglutamate carboxypeptidase (FGCP) enzyme. FGCP is expressed in the apical brush border of the intestines (Blom & Smulders, 2011; Radziejewska & Chmurzynska, 2019). The FGCP is encoded by the glutamate carboxypeptidase II gene (GCPII) (Chandler et al., 1991). Another enzyme with glutamyl hydrolysis activity is called Gamma -glutamyl hydrolase. This enzyme is expressed in folate storage tissues like kidney and liver, it also plays a crucial role in homeostasis of folates by hydrolyzing intracellular polyglutamates especially in cases of decrease dietary uptake of folates (Schneider & Ryan, 2006). Monoglutamates are the main forms of folates that cross the cell membrane and are also the only forms of folates in blood circulation (Radziejewska & Chmurzynska, 2019).

The absorption of the monoglutamylated folates that includes folic acid, N5-MethylTHF and N5-formylTHF occurs in the duodenum or in the upper part of the jejunum and is mediated by the high affinity proton coupled folate receptor (PCFT1) encoded by SLC46A1 gene (Qiu et al., 2006). PCFT functions optimally in acidic environment, the absorption of folates by PCFT occurs via transmembrane gradient. In man, PCFT is expressed in majority of the body organs like duodenum, jejunum, kidney, placenta, liver, brain, spleen and lungs (Radziejewska & Chmurzynska, 2019; R. Zhao, Matherly, & Goldman, 2009). Reduced folate carrier (RFC) encoded by SLC19A1 gene is another transporter involved in folate absorption, it has high affinity K_t of (2-7 μM) for reduced folates like N5-MethylTHF and N5-formylTHF and low affinity Ki of (100-200 μM) for folic acid and it optimally functions at neutral pH (Radziejewska & Chmurzynska, 2019; Visentin et al., 2014).

Multidrug resistance proteins (MRPs) belonging to the ATP binding cassette transporters (ABC) are also involved in folate absorption. MRPs mediates absorption of folate in a mechanism that is opposite that of PCFT, they are high capacity pumps with low affinity for folates. Absorption of folates by MRPs is facilitated by hydrolysis of ATP (Zhao et al.,2011). MRP2 and MRP3 proteins are expressed on the apical membranes of epithelial cells. The other ABC transporters MRP3 and MPR5 are involved in the exportation of folates outside the cells into the blood stream for its delivery to the liver. MRP3 and MPR5 are expressed on the basomembranes of epithelial cells (Visentin et al., 2014).

Once inside the cells, the monoglutamates undergoes polyglutamylation to enable for its longer retention in the cells. In addition, polyglutamated folates have also been reported to be better substrate for folate dependent enzymes (Cho et al., 2007). In the enterocytes, monoglutamates are first reduced to THF by dihydrofolate reductase after which they are converted to N5-Methyl THF before they are released into portal vein (Smulders & Stehouwer, 2005). N5-methyl THF is the main form of folates in circulation.

The transport of folates and uptake in the peripheral tissues occurs through three systems. These transport systems include: the reduced folate carrier (RFC), high affinity folate receptors and proton coupled folate transporter (PCFT). The RFC is the main folate transporter that delivers the folates to systemic tissues (Visentin et al., 2014). In the high affinity folate receptors, three folate receptors (FRs) expressed on the cell surface includes: FRα (with high affinity for THF and MeTHF, FRß and FRγ, they are anchored to the cell surface by glycosylphosphoinositol dormains (Zhao et al., 2011, Kamen & Smith, 2004). In addition to its role in absorption of folates described above, PCFT is also involved in the transport of folates via electrogenic and proton coupled mechanism at low pH (Qiu et al., 2006)

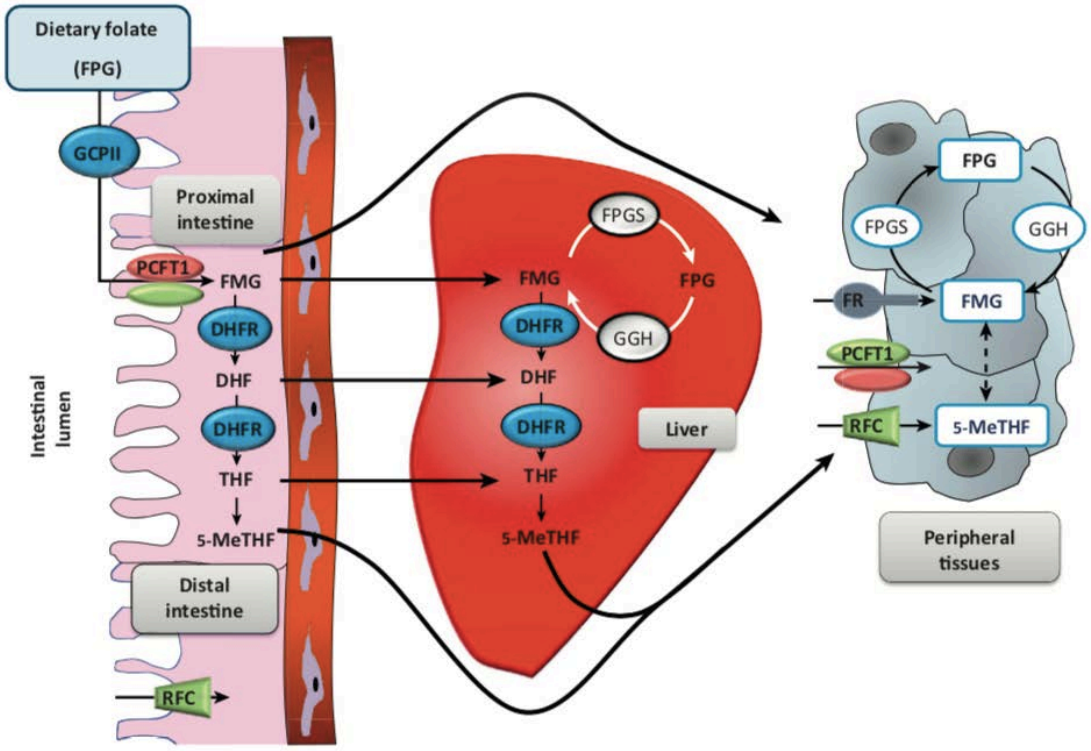

Figure 8*:* **Folate absorption and distribution in peripheral tissues and liver adapted from (Guéant et al., 2013)**

After hydrolysis of dietary folate polyglutamate (FPG) to folate monoglutamate (FMG) by glutamate carboxypeptidase II (GCPII), Proton coupled folate transporter (PCFT1) facilitates the absorption of FMG on the proximal intestine. Subsequently the absorbed FMG are reduced into THF by Dihydrofolate reductase (DHFR) via Dihydrofolate (DHF). Methyl group is then added to the THF to form the N5-MeTHF, the major form of folate in blood circulation. Folate uptake in the peripheral tissues and the liver is facilitated by three systems of folate transport proteins they include: PCFT1, Reduced Folate carrier (RFC) and Folate Receptors (FRs). Once inside the cells, Folylpoly gamma glutamate synthetase (FPGS) catalyzes the polyglutamylation of folate, on the other hand gamma glutamyl hydrolase (GGH) hydrolyses FPG to FMG.

5 Metabolism of mono-carbons, methyl donors and remethylation of homocysteine by methionine synthase

5.1 The methionine /homocysteine cycle

5.1.1 Substrates and metabolites of methionine/homocysteine cycle

5.1.1.1 Methionine

Methionine is an essential sulfur-containing alpha amino acid. It is composed of unbranched hydrophobic side chain and is the only amino acid with thioether (C-S-C) bonding (**Figure 9**). It plays a crucial role in the metabolism and health of all organisms including humans. It is a proteinogenic amino acid involved in the initiation of translation. Apart from its central role as precursor for S-adenosyl homocysteine (SAM), other functions of methionine include: biosynthesis of proteins, biosynthesis of other amino acid like taurine and cysteine and as redox sensor in some proteins , stabilization of protein interaction and structural role (Ferla & Patrick, 2014). Methionine in the cell mainly originates from degradation of endogenous proteins and remethylation pathways by MS and BHMT.

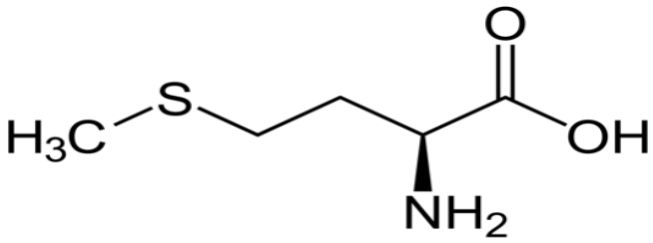

Figure 9: Chemical structure of methionine

5.1.1.2 S- adenosyl methionine and transmethylation reactions

S-adenosyl methionine (SAM) is a metabolite produced throughout the body, however, it is mostly produced and consumed in the liver where about 50 % of the daily methionine uptake is converted into SAM. The chemical structure of SAM is shown in **Figure 10**. S-adenosyl methyl transferases catalyzes the transfer of adenosyl group from Adenosyl triphosphate (ATP) to methionine to form SAM. There are three isoforms of S-adenosyl methyl transferase (MAT) which are: MAT I, MATII and MATIII **Figure 14**. Of these isoforms, MAT I and MAT III are expressed in hepatocytes while MAT II is expressed in extrahepatic tissues (Guéant et al., 2013). SAM is a universal methyl group donor for transmethylation reactions of histones, nucleic acids (DNA and RNA), proteins, phospholipids, glycine and other small molecules. These transmethylation reactions by SAM play an important role in epigenomic and epigenetic

regulatory mechanisms (Guéant, et al., 2013). In these transmethylation reactions, methyl group transfer from SAM is catalyzed by methyltransferases (MT) and each of these reactions produces S-adenosylhomocysteine (SAH), which in turn is an inhibitor of most of these methyltransferases. S-adenosyl homocysteine hydrolase (SAHH) is crucial as it catalyzes the reversible hydrolysis of SAH to homocysteine and adenosine. Increased cellular concentration of SAM regulates the activity of MTHFR. SAM is an allosteric inhibitor of MTHFR, this inhibition is competitively relieved by SAH (Guéant, Namour, et al., 2013). Recently, multisite phosphorylation of N-terminal of MTHFR have been reported to coordinate with SAM binding to regulate the activity of this enzyme (Zheng et al., 2019). The Inhibition of MTHFR causes an important decreased synthesis of MeTHF the cosubstrate in the remethylation reactions catalyzed by MS. As consequence the MTHFR inhibition impairs MS activity.

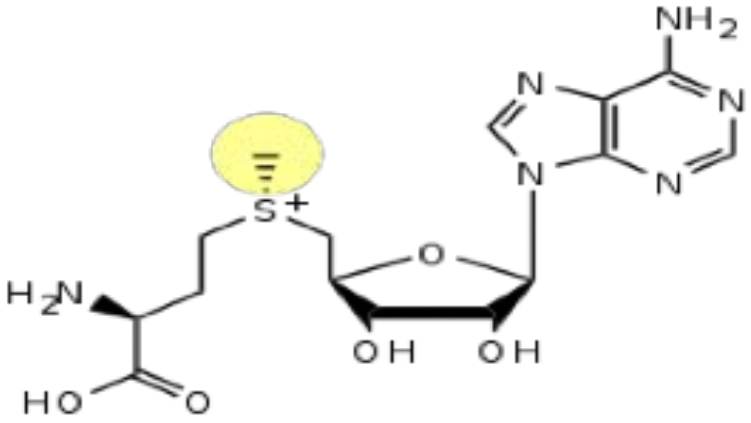

Figure 10: Chemical structure of S adenosyl methionine

5.1.1.3 S-adenosyl homocysteine

S-adenosyl homocysteine (SAH) (**Figure 11**) is a product of SAM-dependent methyl transferase transmethylation reactions. It is hydrolyzed into homocysteine and adenosine in a reversible reaction catalyzed by S-adenosyl homocysteine hydrolase (SAHH) (Turner et al., 2000) (**Figure 13)**. The SAH is a competitive inhibitor of transmethylation reactions through its inhibition of the SAM dependent methyl transferase (Chiang & Cantoni, 1979; Turner et al., 2000) (**Figure 12)**. To avoid cellular accumulation of SAH, rapid hydrolysis of SAH into homocysteine and adenosine is necessary. In the recent past, the team of (Xiao et al., 2015) reported that inefficient removal of homocysteine and adenosine due to genetic and nutritional disturbances causes a reversal of the SAH hydrolase reactions thus leading to accumulation of SAH in the cells. At equilibrium, SAH hydrolase reversible reaction favors the formation of SAH if homocysteine and adenosine are not eliminated.

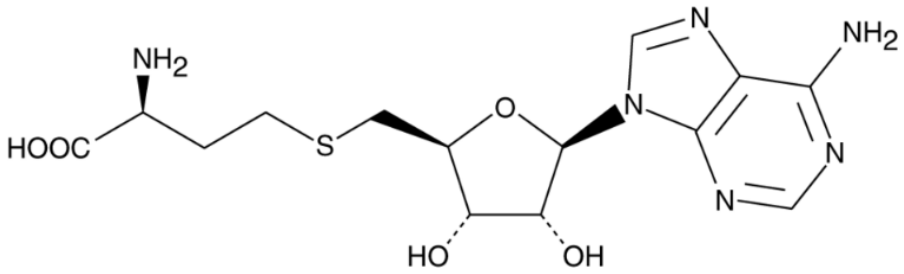

Figure 11: Chemical structure of S-adenosyl homocysteine

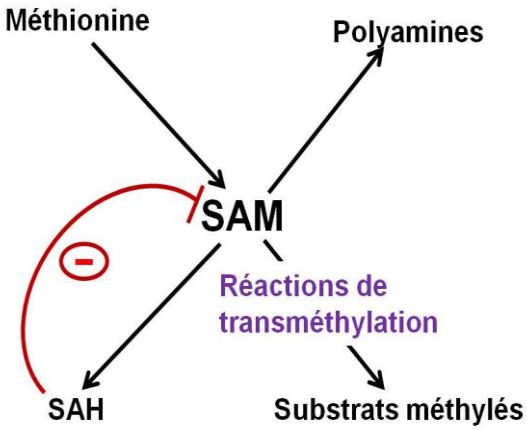

Figure 12: Inhibition of methylation reactions by SAH

5.1.1.4 SAM:SAH ratio

The ratio of SAM:SAH is an indicator of methylation capacity of the cell (Cantoni & Chiang, 1980). Impaired elimination of homocysteine by remethylation results in cellular accumulation of SAH therefore resulting in decreased SAM:SAH ratio. As mentioned earlier, SAH is an allosteric inhibitor of methyltransferases (Turner et al., 2000). Being allosteric inhibitors of MTHFR and methyltransferases, SAM and SAH therefore play a crucial role in regulating folate and methionine metabolism. Folate and vitamin B12 deficiency during gestation and lactation induced an increase in SAH consequently resulting in decreased SAM:SAH ratio in the myocardium of weaning pubs (Garcia et al., 2011).

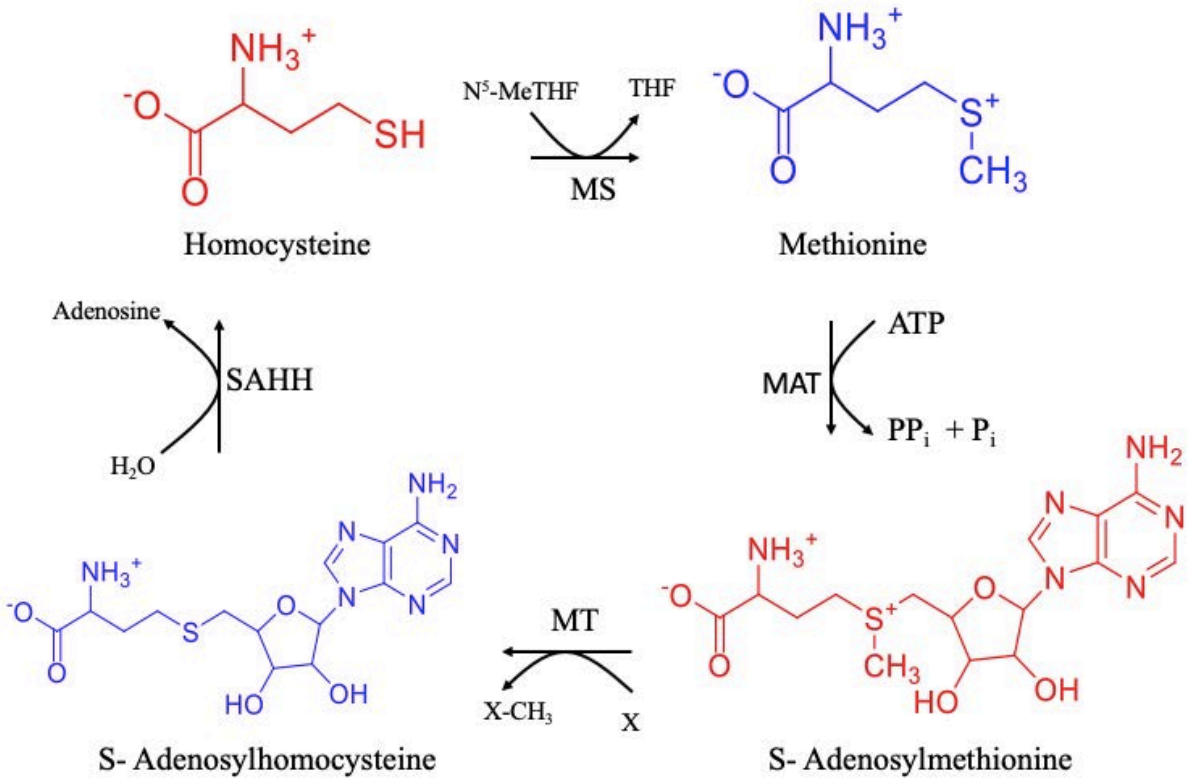

Figure 13: Summary of the pathway of synthesis of S-adenosyl methionine, S-adenosyl homocysteine and homocysteine.

MS = methionine synthase, MAT = Methionine adenosyltransferase, MT = methyltransferase and SAHH = S-Adenosyl homocysteine hydrolase.

5.1.1.5 Homocysteine

Homocysteine is a non-essential non-proteinogenic sulfhydryl containing alpha amino acid derived from metabolism of dietary methionine **Figure 14** (Ganguly & Alam, 2015; Joo et al., 2011). It was first isolated in early 1930s by Byron Riegel and Vincent du Vigneaud. It is an intermediate product in the biosynthesis of methionine and cysteine via remethylation reaction and transsulfuration pathway respectively. Through the biosynthesis of SAM which is the universal methyl donor, homocysteine plays crucial role as a key determinant for methylation cycle (Handy, Castro, & Loscalzo, 2011). Homocysteine can exist in different forms in plasma :1). 1% as free thiols, 2). 70 to 80 % as protein bound homocysteine i.e disulphide bounded to albumin or 3). 20 to 30 % as oxidized homocysteine i.e either as mixed disulphide where homocysteine is bound to cysteine (Homocysteine -Cysteine) or as disulphide where homocysteine is bound to another homocysteine molecules (Homocysteine -Homocysteine) and 4). Bound to other thiols, homocysteine thiolactone (Clarke et al., 1991; Ganguly & Alam,

2015). Elevated cellular homocysteine level is toxic to cells. Cytotoxicity of homocysteine occurs via various mechanisms that includes production of increased levels of ionized calcium, reactive oxygen species and modification of proteins by homocysteinylation (Boldyrev, 2009; Škovierová et al., 2016).

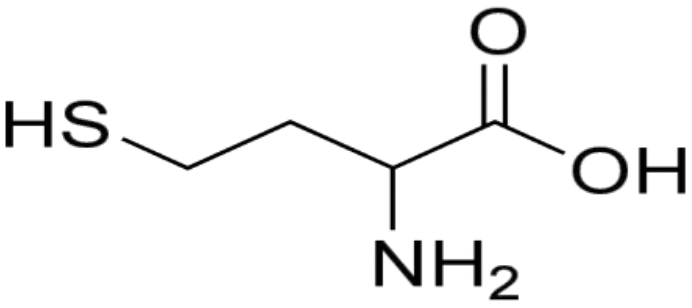

Figure 14: Chemical structure of homocysteine

5.1.1.5.1 Biosynthesis and metabolism of homocysteine

All mammalian cells synthesize homocysteine from dietary methionine and hydrolysis of S-adenosyl Homocysteine (SAH) by S-adenosyl homocysteine hydrolase enzyme (SAHH) **(Figure 13 and 15).** Reversible hydrolysis of SAH to homocysteine is at a branch point between two key metabolic pathways; 1). The remethylation of homocysteine to methionine and 2). The transsufuration of homocysteine to cystathionine (Guéant et al.,2013).

Given that elevated intracellular accumulation of homocysteine is toxic, to prevent this accumulation in the cells, homocysteine is either remethylated into methionine by cobalamin or non-cobalamin dependent pathways or is irreversibly degraded into cystathionine by transsulfuration reactions. Moreover, excess homocysteine can also be exported to the extracellular fluids.

i) Remethylation of homocysteine

Under normal physiological conditions, about half of homocysteine is remethylated to methionine. Two distinct enzymatic reactions for remethylation of homocysteine to methionine have been described. The principal pathway is the folate / vitamin B12 dependent remethylation of homocysteine which is catalyzed by methionine synthase (MS/MTR; EC 2.1.1.13) (Li et al., 1996), the reaction mechanisms of this pathway are described in chapter 5.2.1. In this reactions MS utilizes 5 methyl tetrahydrofolate (5-MeTHF), from folates as a co-substrate and methyl cobalamin (MeCbl; a derivative of vitamin B12) as cofactor to catalyze methyl group transfer from 5-MeTHF to homocysteine generating methionine and tetrahydrofolate (THF) (Banerjee et al., 1990; Rowena G Matthews, 2001). In humans, MS is ubiqutinously expressed in tissues that include kidney, skeletal, muscle heart and liver (Chen et al., 1997). The 5-MeTHF is a

product of metabolism of 5,10 methyleneTHF by folate cycle enzyme methylenetetrahydrofolate reductase (MTHFR; EC 1.5.1.20). The 5-MeTHF is an important folate because it links the folate cycle to homocysteine metabolism. MTHFR deficiency and decreased MeTHF impairs the remethylation of homocysteine. Methyl group transfer reactions catalyzed by cobalamin dependent MS plays three important roles in the cells:

a) Elimination of cellular homocysteine
b) Generation of THF cofactor for DNA synthesis
c) Synthesis of methionine the precursor for SAM, the universal methyl donor for transmethylation reactions.

The second pathway for remethylation of homocysteine to methionine is independent of folates and vitamin B12 and is catalyzed by Betaine homocysteine 5 Methyl transferase (5-BHMT; EC 2.1.15) (Guéant et al., 2013; Škovierová et al., 2016). In this pathway, BHMT uses betaine (a production of choline oxidation) as a methyl donor in the remethylation of homocysteine to form methionine and N,N Dimethylglycine (Bertolo & McBreairty, 2013). Unlike MS dependent remethylation of homocysteine, BHMT pathway is detected only in the liver and kidney (Sunden et al.,1997).

ii) Transsulfuration

Homocysteine transsulfuration pathway involves two vitamin B6 dependent enzymes: Cystathionine ß synthase (CBS; EC 4.2.1.22) and Cystathionine γ lyase (CTH; EC 4.4.1.1.). These enzymes catalyze the irreversible degradation of homocysteine to cysteine using pyridoxial 5 phosphate the active form of vitamin B6 as cofactor. In this pathway, homocysteine and serine are condensed by CBS to cystathionine, subsequently the resulting cystathionine is hydrolyzed into alpha ketoglutarate and cysteine by CTH as shown in **Figure 15** (Blom & Smulders, 2011; Guéant et al., 2013). Cysteine is an amino acid essential for the biosynthesis of proteins, CoenzymeA and Glutathione (GSH) (Stipanuk, Dominy, Lee, & Coloso, 2006). GSH is a strong antioxidant which offers protection against oxidative stress and also against xenobiotics and their metabolites (X. Yu & Long, 2016). In humans, CBS is expressed in the kidney, brain, liver and ovary.

5.1.2 The Folate Cycle

In the folate cycle **(Figure 15),** 5-methyltetrahydrofolate is the methyl donor for the remethylation of homocysteine to methionine. The 5-MeTHF links the folate cycle to methionine/homocysteine cycle. Folates enters the cell mainly as MeTHF thus making B12 dependent MS the rate limiting step for the cellular accumulation of folates (Lucock, 2000).

Flavin adenine dinucleotide (FAD) dependent methylene tetrahydrofolate reductase (MTHFR) catalyzes the conversion of 5,10 methylene tetrahydrofolate to 5-MeTHF. Following methyl group transfer to homocysteine, 5-MeTHF is converted to tetrahydrofolate (THF). The B6 dependent serine hydroxy methyltransferase (SHMT) then directly converts the formed THF into 5,10-methyleneTHF. In this reaction, SHMT uses serine as methyl donor and pyridoxal phosphate as cofactor (Blom & Smulders, 2011). Alternatively, methylenetetrahydrofolate dehydrogenase (MTHFD1) catalyzes the conversion of THF to 5-methylene tetrahydrofolate via 10 formyl tetrahydrofolate and 5,10 methenylTHF. MTHFD1 has various enzymatic activities include formyl tetrahydrofolate synthetase, methylenetetrahydrofolate dehydrogenase and methenyl tetrahydrofolate cyclo-hydrolase activities. The 10-formyl tetrahydrofolate plays a crucial role as methyl donor for purine synthesis. On the other hand, the 5,10 methenyl THF is used by thymidylate synthase (TYMS) as a cofactor in the synthesis of deoxythymidine 5' monophosphate (dTMP) from 5 monophosphate dUMP (Blom & Smulders, 2011). TYMS reactions leads to the formation of 7,8-dihydrofolate (7,8-DHF) which is subsequently reduced back to THF by dihydrofolate reductase (DHFR) (Lucock, 2000). In addition to its role in dTMP synthesis, 5-10 MethyleneTHF can be reduced by B12 dependent methylenetetrahydrofolate reductase (MTHFR) to 5 Methyl THF. The MTHFR competes with TYMS for 5,10 methylene THF therefore MTHFR plays a crucial role in regulating 5 methyl THF available for remethylation of homocysteine.

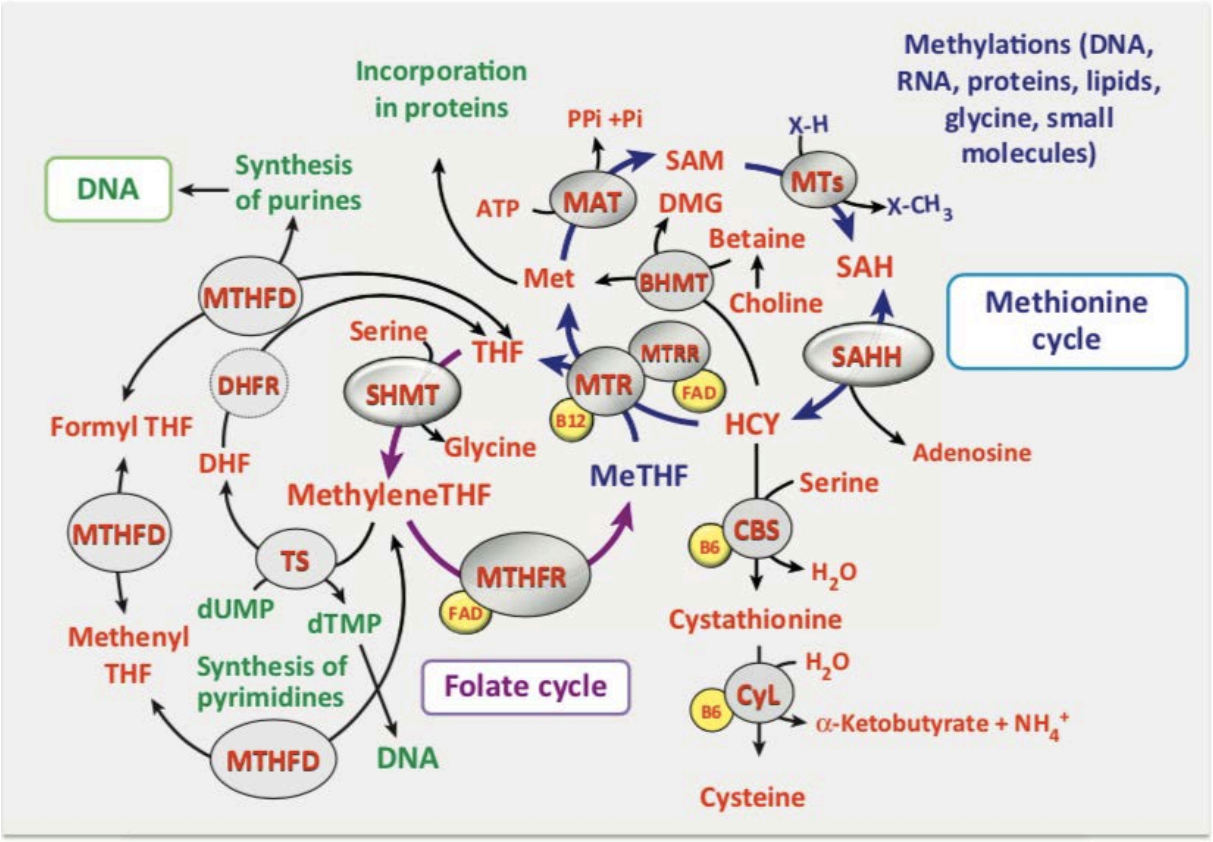

Figure 15: **The folate and methionine cycles adapted from (Guéant et al., 2013)**

In methionine cycle, MS uses MeTHF from folate cycle as methyl donor and methyl cobalamin from vitamin B12 as cofactor to catalyze the remethylation of homocysteine to methionine and THF. Alternatively, homocysteine can remethylated to methionine (met) and N, N Dimethylglycine (DMG) in a reaction catalyzed by betaine homocysteine methyl transferase (BHMT). Once methionine has been formed, methionine adenosyl transferase (MAT) then catalyzes the formation of S-Adenosyl methionine (SAM) from methionine using ATP. SAM is a universal Methyl donor for transmethylation reactions of RNA, DNA, proteins and lipids. The transmethylation reactions are catalyzed by methyltransferases (MTs), in this reactions SAM is converted into SAH. S-adenosyl homocysteine hydrolase (SAHH) then catalyzes the reversible hydrolysis of SAH to homocysteine and adenosine. Finally, the formed homocysteine is either remethylated by MS or BMHT into methionine or is irreversibly metabolized into cysteine by the two vitamin B6 dependent cystathionine beta synthase (CBS) and cystathionine lyase (CYL). For the folate cycle, MTHFR which is vitamin B12 dependent enzyme catalyzes the reduction of 5,10 MethyleneTHF to form 5-MeTHF. The folate cycle via THF plays a crucial role in DNA synthesis. One carbon group from 10-formylTHF are used for purine biosynthesis while the MethyleneTHF is a cofactor for pyrimidine synthesis.

5.2 Methionine synthase and MMACHC proteins

5.2.1 Methionine synthase

Human Methionine synthase EC.2.1.1.13 (MS, 5-methyl- tetrahydrofolate: L-homocysteine S-methyltransferase) is a cytoplasmic protein encoded by *MTR* gene on human chromosome 1p43 (Leclerc et al., 1996). As mentioned earlier MS utilizes (5-MeTHF) as a co-substrate and methyl cobalamin (MeCbl) a derivative of vitamin B12 (cobalamin) as a cofactor to catalyze methyl group transfer from N^5 methyl tetrahydrofolate (N5-MeTHF) to homocysteine to form methionine and THF (Banerjee et al., 1990; Rowena G Matthews, 2001). Methionine is used by methionine adenosyl transferase (MAT) / S-adenosyl methionine synthase (EC. 2.5.1.6) as a precusor for the synthesis of S-Adenosyl methionine (SAM) the universal methyl donor for epigenomic and epigenetic regulatory mechanisms (Guéant et al., 2013).

MS reactions intersect the folate and methionine cycles shown above in **Figure 15**. These reactions are essential for the normal functioning of the two cycles. Decreased MS activity resulting from vitamin B12 deficiency (Brunaud et al., 2003) leads to MeTHF trap, a phenomenon in which deficiency in vitamin B12 impairs the remethylation of homocysteine and blocks the conversion of MeTHF to THF (Guéant et al., 2013). Consequently, this leads to the accumulation of MeTHF pool at the expense of other cellular folates (Banerjee et al., 1990). MeTHF trap disrupts the synthesis of THF, a reduced folate intermediate essential for DNA synthesis. Folate trap due to vitamin B12 deficiency and MS dysfunction therefore impairs the synthesis of DNA by blocking sufficient supply of reduced folates for DNA (Guéant et al., 2013). As mentioned earlier in 5.1.1.5, remethylation of homocysteine into methionine by MS is crucial in preventing cellular accumulation of homocysteine. Defects in MS activity causes elevated plasma total homocysteine and decreased methionine levels.

Mutations in *MTR* is associated with the CblG disease an inborn error of cobalamin metabolism. Clinical manifestations of CblG patients includes:hyperhomocysteinemia, hypomethioninemia, megaloblastic anaemia and developmental delay (Froese & Gravel, 2010; Leclerc et al., 1996; Tuchman et al., 1988). CblE is the second disorder of methionine synthase caused by deficiency in MS reducing system the methionine synthase reductase (MTRR) (Ruiz-Mercado et al., 2016). Clinical presentations of CblE are similar to those of CblG. Recently MTHFR (C677T) and MTR (A2756G) gene polymorphims have been shown to be significantly associated with cardovascular diseases (Raina et al., 2016).

In adult humans, MS is highly expressed in the heart followed by the pancrease and skeletal muscle, it is also expressed in the brain , placenta, lungs, liver, kidney and the pancrease (Chen

et al., 1997). Among other enzymes, MS is highly expressed in embrogenic developmental stage particular in the brain ,liver, lungs wnad kidneys where the expression levels is the highest (Chen et al., 1997).

5.2.1.1 MTR gene

Human methionine synthase is encoded by *MTR* gene which is localized at chromosome 1 in position 1q43 (Leclerc, 1996). The coding region is composed of 33 exons and 32 introns. The 3795 base pairs coding sequence encodes a 1265 amino acids protein in length with a predicted molecular mass of 141000 Da (Leclerc et al., 1996).

In mice, MS gene is localized at chromosome 13. The coding region is composed of 33 exons and 33 introns. The MS coding sequences contains 8294 base pairs encoding a protein of 1253 amino acids with a predicted molecular mass of 139069 Da.

Human MS amino acid sequence is 55 % identical with cobalamin dependent MS (metH) from *E.coli* (Li et al., 1996), 64 % and 92 % identical to MS from *Caenorhabditis elegans* (Li et al., 1996) and rat (Yamada, Tobimatsu, & Toraya, 1998) respectively.

5.2.1.2 Methionine synthase protein structure

MS is a modular protein with four different functional domains arranged in a linear manner. From the extreme N terminal to the extreme C terminal the domains are arranged as follows: the homocysteine and methyl tetrahydrofolate binding and activation domain, the cobalamin prosthetic group binding domain and the AdoMet-binding domains for enzyme reactivation (**Figure 16**) (Dixon et al ., 1996; Goulding et al., 1997; Rowena G Matthews, 2001; Yamada & Koutmos, 2018).

Wild type recombinant vitamin B12 dependent MS (MetH) comprising of 2-1227 residues and truncated MetH were overexpressed, purified and characterized in *Escherichia coli* by Goulding and colleagues. The molecular weight of the MetH is 136 kDa. Limited trypsin proteolysis enabled the study of the different functional regions of MetH. The truncated 70 kDa N-terminal MetH comprising the 2-649 amino acid residues was obtained from heterogeneous expression of truncated MetH gene. Trypsin proteolytic digestion of this N terminal fragment revealed the first two modules of MetH. The first module which is made up of 2-253 amino acid residues is the homocysteine binding and activation domain (**Figure 16** and **Figure 17)**. This domain catalyzes the transfer of a methyl group from the MeCbl to the bound acceptor (homocysteine) to generate cob(I)alamin and methionine (Goulding et al., 1997). The second module which is made up of 354-649 amino acid residues (**Figure 16 and Figure 17**) is the

MeTHF binding and activation domain. It catalyzes methyl group transfer from the bound MeTHF to the exogenous cob(I)alamin to form tetrahydrofolate (Goulding et al., 1997; Matthews, 2001). Crystallographic studies of the homocysteine and MeTHF binding domains of MetH from *Thermotoga maritima* revealed that the two domains are tightly packed $(\beta\alpha)_8$ barrels (Evans et al., 2004b). These domains strongly associate during catalysis. The homocysteine and MeTHF domains' active sites are located close to the C terminal of their respective barrel strands and are separated by a distance of around 50 Å (AngstrÖm) from each other.

The third module is for binding MeCbl, it is located in the 28 kDa fragment (Banerjee et al., 1989; Luschinsky et al., 1992). This module is made up of two structurally different domains: the cap domain and the Rossmann domain (cob domain) shown in (**Figure 18)** (Drennan, Matthews, & Ludwig, 1994). The cap domain is an amino terminal four alpha helix bundle which interacts with the upper/beta face of MeCbl through hydrophobic interaction (Drennan et al., 1994). The cap protects the methyl group of MeCbl from the surrounding milieu. The Rossman domain is composed of 4 to 5 alpha helices surrounding 5 parallel beta sheets hence forming the 5 alpha / beta fold which associates with the lower/alpha surface of cobalamin and the dimethylbenzimidazole nucleotide base (DMB) (Drennan et al., 1994). During catalysis, the cobalamin binding domain shuttles back and forth between the homocysteine and MeTHF active sites to complete a catalytic cycle (Evans et al., 2004b).

The fourth module is the 38 kDa adenosyl methionine (Ado-met) binding domain, this domain is important for reductive reactivation of the inactivated methionine synthase **(Figure 19**). Occasionally after every 100 to 2000 turnovers during catalysis the highly nucleophilic cob(I)alamin is oxidized to Cob(II)alamin (inactive form of the cofactor) which renders the enzyme inactive. This domain is located at the extreme C terminal of the enzyme. This process of reductive reactivation of oxidized MS involves the transfer of methyl group from Ado-met and transfer of electrons from FAD and FMN redox centers of methionine synthase reductase. The reducing equivalent for this reaction are obtained from oxidation of NADPH (Wolthers et al., 2007).

The X-ray structures for the Ado-met binding domain of both human MS (Wolthers et al., 2007) and *E.coli* MetH (Melinda M. Dixon et al., 1996) has been resolved. This domain is a C shaped structure with a mix of alpha and beta regions in its center, dominated by the bent antiparallel beta sheets with a beta meander on the upper region (Melinda M. Dixon et al., 1996; Wolthers

et al., 2007). The center of the inner surface of C is the Ado-met binding site. In order to carry out methyl group transfer from adenosyl methionine to cobalamin(ii), larger areas of both the cobalamin binding domain and the reactivation domain must come in contact (Ludwig & Matthews, 1997). During the activation conformation of MS, the four-helix bundle cap domain is displaced by 26 A and a 63 ° rotation to allow for the interaction between the cobalamin and activation (Ado-met) domain. The human MS activation domain have been shown to associates with the human methionine synthase reductase FMN-binding domain (Wolthers et al., 2007).

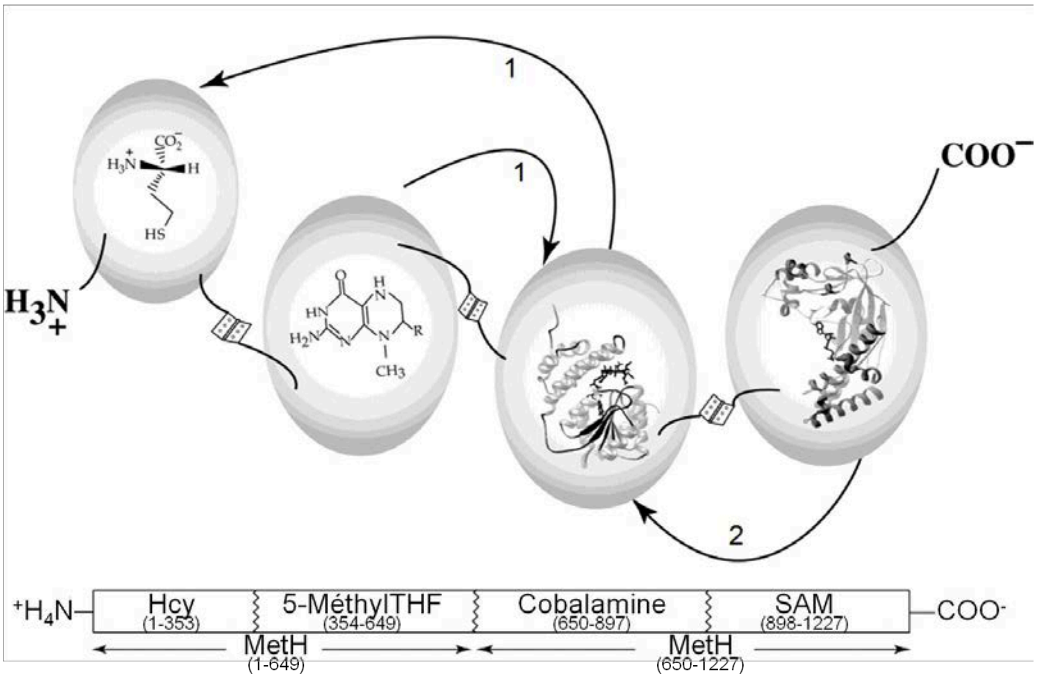

Figure 16: Diagram showing the modular structure of cobalamin-dependent methionine synthase (Rowena G Matthews, 2001)

In the diagram 1) is the Catalytic half reaction and 2) is the reductive methylation. Shown as hinges are the flexible linkers that connect the four modules. The linkers allow the three substrate-binding modules to contact the cobalamin-binding module to transfer methyl groups to and from the cobalamin. The region of the amino acid sequence comprising each module is shown below the diagram is the amino acid sequences of the different modules of MS from *E.coli.* From extreme left the first domain is homocysteine binding and activation, followed by MeTHF binding and activation domain, then the Methyl cobalamin (MeCbl) binding domain and finally S-adenosyl methionine (SAM) binding reactivation domain.

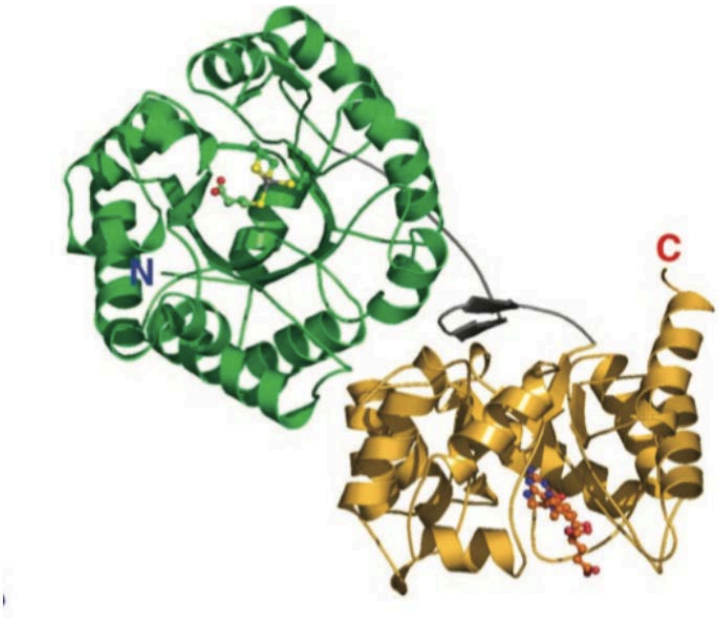

***Figure 17: Ribbon drawing of the homocysteine and methyl tetrahydrofolate binding domains of MetH from* T. maritima. Adapted from (Evans et al., 2004b)**

Shown in green at the N terminal is the homocysteine barrel, in gray is the linker and in gold in the C terminal is the folate barrel. Homocysteine and MeTHF are shown as ball and stick models.

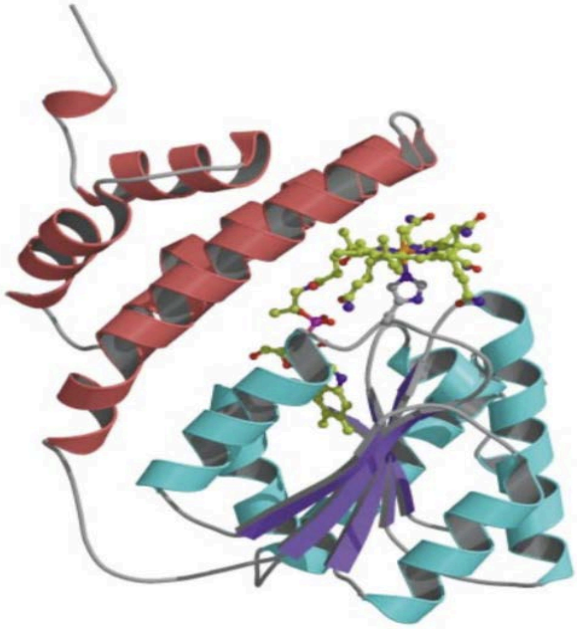

Figure 18: Three dimensional structure of methyl cobalamin binding domain of methionine synthase adapted from (Gruber & Kratky, 2006)

The N-terminal helical domain shown in red is the vitamin B12 binding fragment, methyl cobalamin is shown in ball and sticks.

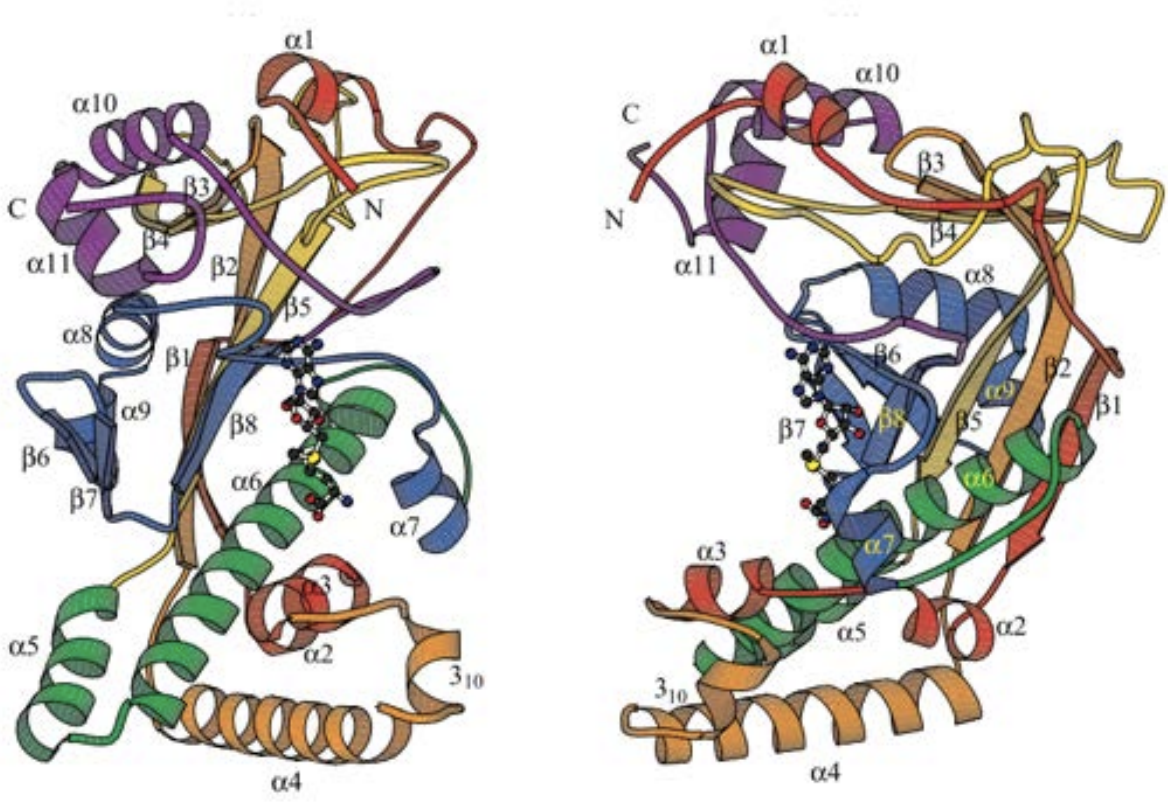

Figure 19: Three-dimensional structure of the activation domain / Adomet binding domain of methionine synthase adapted from (Dixon et al., 1996)

Starting from the N terminus the fold of the backbone has been colored red, orange, yellow, green, blue and finally violet at the C terminus. The substrate adenosyl methionine is shown in ball and sticks**.**

5.2.1.3 Catalytic mechanism of methionine synthase in the remethylation of homocysteine to generate methionine

Methionine synthase utilizes 5-methyltetrahydrofolate (5-MeTHF) as a co-substrate and methylcobalamin a derivative of vitamin B12 as a cofactor to catalyze methyl group transfer from N^5 methyltetrahydrofolate to homocysteine to form methionine and tetrahydrofolate (**Equation 2** and **3)** (Banerjee et al., 1990; Rowena G Matthews, 2001).

The catalytic mechanism of MS involves a ternary complex where substrates binds to catalytically active enzyme-bound methylcob(III)alamin in an ordered sequential manner (**Figure 20**). Steady state product inhibition studies revealed that N^5-methyltetrahydrofolate is the first substrate to bind and tetrahydrofolate is last product to be released (Banerjee et al., 1990). MS enzyme bound to MeCbl is the free form of the enzyme. Pre-steady state kinetic studies also showed that cob(I)alamin bound MS enzyme is the kinetically competent intermediate as it was found to react rapidly with methyl tetrahydrofolate. Furthermore the intermediate relevance of enzyme-bound cob(I)alamin was demonstrated by its rapid formation when homocysteine was added to the enzyme-bound methylcob(III)alamin (Ruma V Banerjee et al., 1990).

MS reaction proceeds in two half reactions **Figure 20**, the first half reaction involves methyl group transfer from enzyme-bound methylcob(III)alamin to homocysteine to form cob(I)alamin and Methionine (**Equation 2).** In the second half reaction, methylcobalamin and tetrahydrofolate are regenerated by remethylation of the enzyme-bound Cob(I)alamin by methyl tetrahydrofolate (**Equation 3**) also shown in (Banerjee et al., 1990; Matthews, 2001). Occasionally, cob(I)alamin which is a highly reactive nucleophile is oxidized to cob(II)alamin form which consequently inactivates the enzyme. In humans MS enzyme activity is restored by reductive methylation of cob(II)alamin by methionine synthase reductase using S-Adenosyl methionine as methyl donor (Eclerc et al., 1998; Ludwig and & Matthews, 1997; Olteanu & Banerjee, 2001). In *E. coli* reduced flavodoxins have been proposed to be the electron donors in this reaction. The cycles of reactivation and deactivation occur after every 100-2000 turnovers (Banerjee et al., 1990; R. G. Matthews, 2001).

Equation 2 $\text{Methylcob(III)alamin} + \text{Homocysteine} \longrightarrow \text{Cob(I)alamin} + \text{Methionine} + H^+$

Equation 3 $CH_3\text{-}H_4\text{folate} + \text{cob(I)alamin} + H^+ \longrightarrow H_4\text{folate} + \text{Methylcob(III)alamin}$

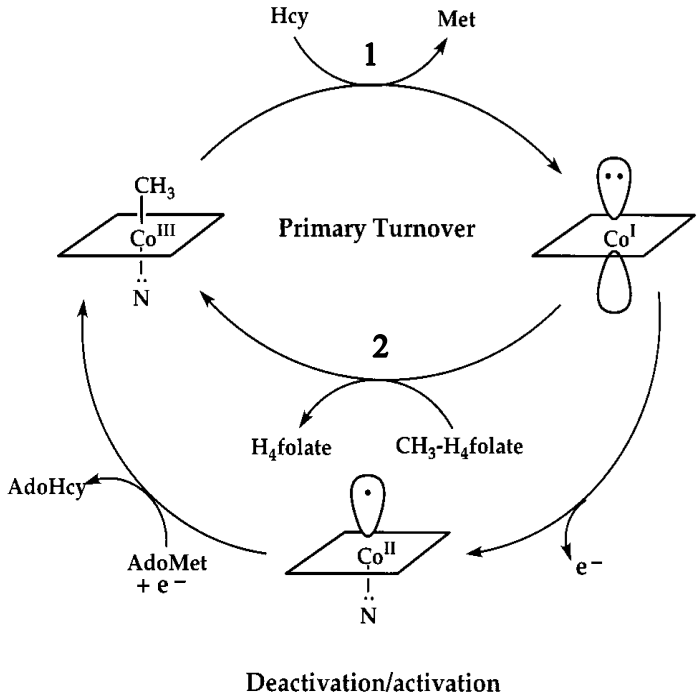

Figure 20: Reactions catalyzed by cobalamin dependent Methionine synthase in the conversion of homocysteine to methionine and N5-MeTHF to THF. Scheme Adapted from (R. G. Matthews, 2001)

During primary turnover, the cobalamin prosthetic groups that binds the MS enzyme alternates between cob(III)alamin and cob(I)alamin forms. In the first half reaction (1) methyl group is transferred from enzyme-bound methylCob(III)alamin to homocysteine to form methionine and cob(I)alamin. In the second half reaction (2) methyl group is transferred from MeTHF to cob(I)alamin generating methylcobalamin and tetrahydrofolate (THF). The cob(I)alamin form is occasionally oxidized by molecular oxygen forming an inactive enzyme in the cob(II)alamin form which needs reactivation by reductive methylation using adenosyl methionine (adomet) to regenerate the active enzyme.

5.2.2 MMACHC protein

MMACHC OMIM 609831 (Methyl Malonic Aciduria Combined Hyperhomocystinuria type C) gene encodes the MMACHC protein. MMACHC protein catalyzes the decyanation and dealkylation of diatery cyanocobalamin and alkylcobalamin respectively to generate the biologically active cobalamins: [methylcobalamins (MeCbl) and adenosylcobalamin (AdoCbl)] which are coenzymes for the cytoplasmic MS and the mitochondrial methylmalonyl-CoA mutase (MUT) (Hannibal, DiBello, & Jacobsen, 2013). MMACHC protein dysfunction causes impaired intracellular transport and biosynthesis of MeCbl and AdoCbl. MMACHC deficiency therefore impairs activity of MS and MUT leading to accumulation of homocysteine and

methylmalonic acid in the blood and urine. Methylmalonic aciduria may be fatal because it causes severe acidosis. MMACHC protein is essential for pre-implantation embryogenesis and for development of the cardiac, respiratory and nervous systems in organogenesis (Garcia 2014 et al ., 2014; Pupavac et al., 2011). We have shown that MMACHC protein interacts with methionine synthase to regulate the processing of cobalamin (Fofou-Caillierez et al., 2013). Mutation in *MMACHC* gene causes Methyl Malonic Aciduria Combined Hyperhomocystinuria type C (OMIM 277400) which is the most common inborn error of intracellular metabolism of cobalamin (Lerner-Ellis et al., 2006). CblC patients presents with combined hyperhomocytenuria and methymalonic aciduria, multisystem organ failure, neurological and haematological disorders that includes megaloblastic anaemia. CblC disease is heterogeneous with a severe early onset and late onset with better survival and response to treatment (Carrillo-Carrasco, Chandler, & Venditti, 2012). Proteomic analysis of the CblC mutant cells evident differential expression of proteins associated with cardiovascular diseases, neurological disorders, muscular and skeletal disorders (Hannibal et al., 2012). Prenatal dilated cardiomyopathy can be presenting manifestation of CblC disorders (Bie et al.,2009). Biochemical hallmarks of CblC disorder includes elevated plasma levels of both homocysteine and methylmalonic acid and a decrease in plasma methionine levels (Carrillo-Carrasco et al., 2012).

5.2.2.1 *MMACHC* gene

MMACHC gene OMIM 609831 is located in chromosome 1p34.1 consists of five exons. The open reading frame of MMACHC cDNA consist of 806 base pairs encoding a 282 aa protein. The predicted molecular weight of the MMACHC protein is 31.7 KDa (Lerner-Ellis et al., 2006).

5.2.2.2 Structure and function of MMACHC

High resolution X-ray Crystallographic structures of MMACHC have been independently resolved by the teams of (Froese et al., 2012; Koutmos et al., 2011). Human MMACHC protein in apo and cobalamin bound forms were crystallized. Crystal structure analysis revealed that MMCHC protein is composed of two modules connected by a linker **Figure 21**.

The first module is the N-terminal (core) module consisting of (1-172). In this module four stranded antiparallel ß sheets are flanked by an alpha helix and short two stranded antiparallel beta sheets. The fold of this domain is similar to the NADPH oxidase / flavin reductase despite the large difference in their sequence similarity. It is in this flavodoxin reductase domain that

the reductive decyanation of CNCbl (cyanocobalamin) using FMN or FAD occurs (Hannibal, DiBello, & Jacobsen, 2013; Koutmos et al., 2011).

The second module of MMACHC is the C-terminal (cap), which is made up of four helices that caps the N-terminal module. At the interface between the cap and the core is a large cavity for binding cobalamin. MeCbl is bound to this cavity in base off conformation thus enhancing the MMACHC reactivity of cobalt in the reductive decyanation.

On the other hand, CNCbl binds the MMACHC cavity in both the base off and base on conformations. MeCbl binding induces conformational changes on the loops. MMACHC overall fold is composed of highly conserved arginine rich pocket for binding glutathione and a dimerization cap for binding the beta axial 5' adenosyl ligand (Froese et al., 2012). The conserved arginine residues Arg161, Arg206 and Arg230 in the arginine pocket have been described as sites for point mutations that leads to CblC disease observed in humans (Hannibal et al., 2013). Decreased dealkylation but not decyanation activities of MMACHC were reported in missense mutations in Arg161Q and Arg161QG residues linked to the early and late onset of CblC disorder (Gherasim et al., 2015).

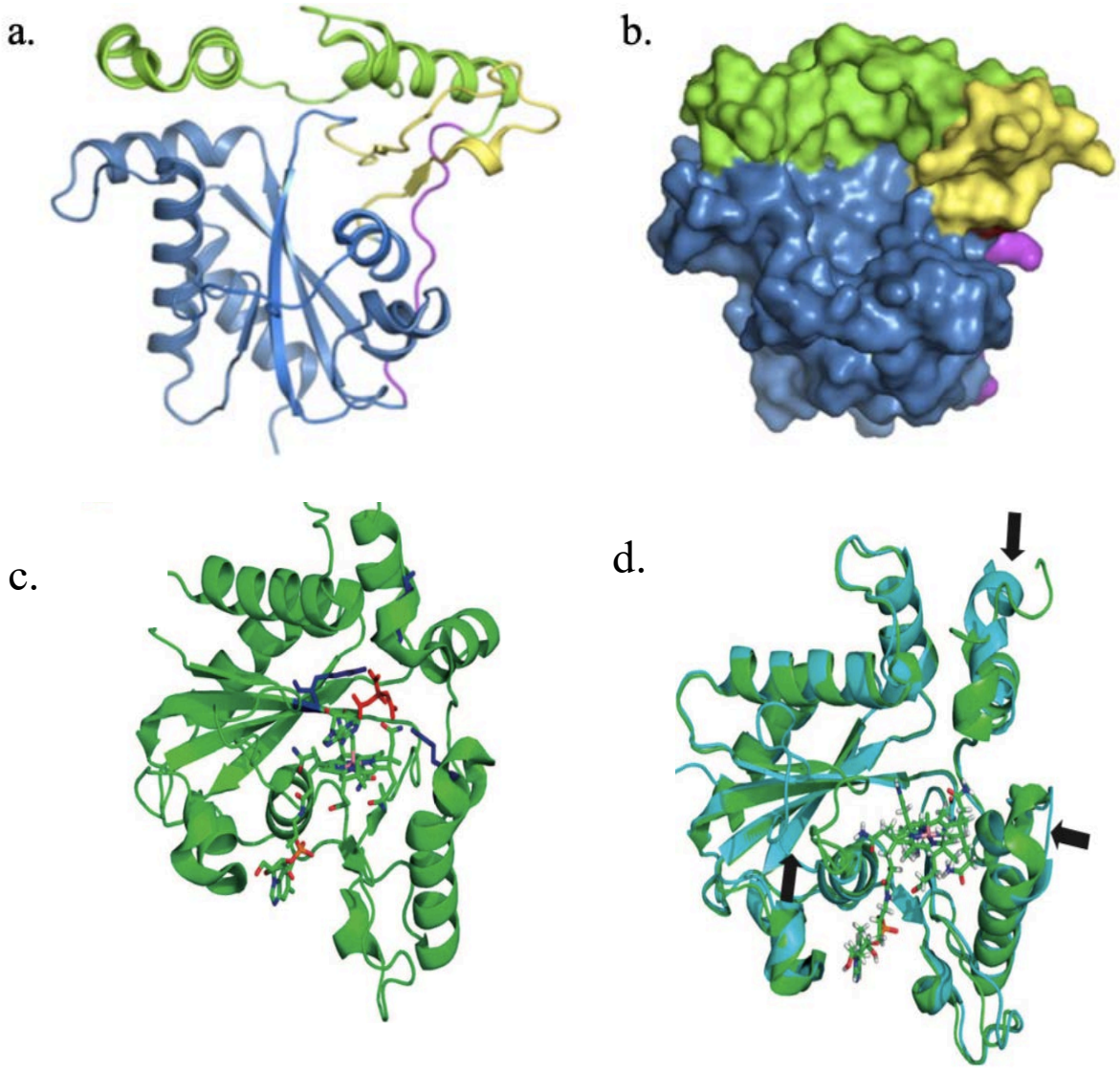

Figure 21: Structure of the apo-MMACHC protein adapted from (Hannibal et al., 2013; Koutmos et al., 2011)

The different modules of MMACHC protein are shown in a). ribbon structure and b). Space filled structure. Shown in blue is the core module, in green is the cap module, in pink is the linker and in yellow is the two beta sheets antiparallel insertion of the core domain. c). MMACHC-AdoCbl complex, shown in blue sticks are the three conserved arginine residues in the arginine pocket with the citrate molecule shown in red at the glutathione predicted binding site in the MMACHC. d). Superimposed Apo-MMACHC (cyan) and MeCbl-MMACHC (green), shown in arrows are the main sites that undergoes conformational changes after binding cobalamin.

5.2.2.3 MMACHC protein catalytic mechanism

The MMACHC protein has dual catalytic activities shown in **Figure 22**. MMACHC plays a crucial role in the processing of vitamin B12 which is a prerequisite to generate the

intermediates that will be converted into biologically active cobalamins: [methyl cobalamins (meCbl) and adenosylcobalamin (AdoCbl)] which are coenzymes for the cytoplasmic methionine synthase and the mitochondrial methylmalonyl-CoA mutase (Hannibal et al., 2013, 2009). The first reaction catalyzed by MMACHC is the reductive deacyanation of cyanocobalamin (CNCbl) in the presence of flavoprotein oxidoreductase (Kim et al., 2008). MMACHC being one of the most divergent member of NADPH dependent flavin reductase family, it uses FAD and FMN as prosthetic group in the reductive deacynation of CNCbl (Koutmos et al., 2011). The second reaction catalyzed by MMACHC is the dealkylation of alkylcobalamins like methyl cobalamin and adenosylcobalamin. In this reaction alkyl group is displaced by glutathione to generate cob(I)alamin and glutathione thioester (Jihoe Kim et al., 2009; Koutmos et al., 2011).

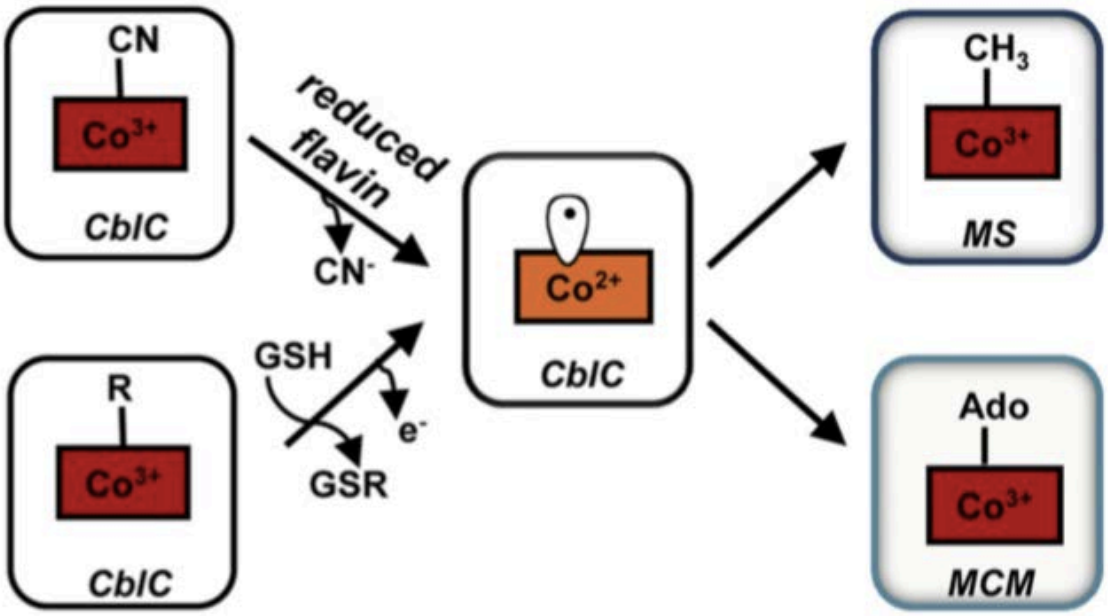

Figure 22: Processing of cobalamins by MMACHC adapted from (Koutmos et al., 2011)

6 GENETIC DEFECTS AND PATHOLOGIES LINKED TO INTRACELLULAR METABOLISM OF VITAMIN B12 AND REMETHYLATION OF HOMOCYSTEINE

6.1 Genetic defects linked to intracellular metabolism of vitamin B 12

6.1.1 Classification of inborn errors of intracellular metabolism of vitamin B12

Intracellular metabolism of vitamin B12 as mentioned earlier is a complex multistep process involving several proteins from lysosomal release of cobalamin to cytosol and processing of cobalamin into two active co-factors: AdoCbl and MeCbl. Inborn errors of vitamin B12 metabolism represent an important group of rare autosomal recessive disorders.

Genetic defects of intracellular metabolism of vitamin B12 can alter the synthesis of vitamin B12 cofactors : Adocbl the cofactor for mitochondrial methy-malonyl CoA mutase or MeCbl the cofactor for cytoplasmic MS or both cofactors (Froese et al., 2012; Koutmos et al., 2011).

Genetic defects that interfere with the synthesis of AdoCbl or have a direct effect on methyl malonyl-CoA mutase causes isolated aciduria and methylmalonic acidemia without elevated homocysteine includes mut, CblA and CblB. On the other hand, the defects that impact on the synthesis of MeCbl leads to development of homocystinuria, hyperhomocysteinemia and hypomethioninemia they include: CblG, CblE and CblD - HC/ CblD variant 1. In addition, the defects that interfere with the synthesis of the two coenzymes causes combined homocystinuria and methylmalonic aciduria (David Watkins & Rosenblatt, 2011).

Complementation analysis is a powerful diagnostic technique used to identify specific gene mutations at the different steps of intracellular cobalamin metabolism. In this analysis the patients' cells are fused with fibroblasts of patients with known inborn errors of cobalamin metabolism in order to identify the mutations (Gravel et al., 1975; David Watkins & Rosenblatt, 2011). The restoration of function of either methionine synthase or methyl malonylCoA is then evaluated in the fused or unfused cultures. If the mutation occurs in the same loci in the two cell lines complementation does not occur. However, if the mutation occurs in different loci, complementation occurs and the deficient function in the patients' cells is corrected. Until now, ten complementation groups for inborn errors of cobalamin metabolism that have been identified include : cblA, cblB, CblC, cblD, CblE, cblF , CblG, cblJ and cblX (**Figure 23**)

(Coelho et al., 2012, 2008; Froese & Gravel, 2010; Miousse et al., 2009; Tuchman et al., 1988; Watkins & Rosenblatt, 1986; David Watkins & Rosenblatt, 2011, 2016).

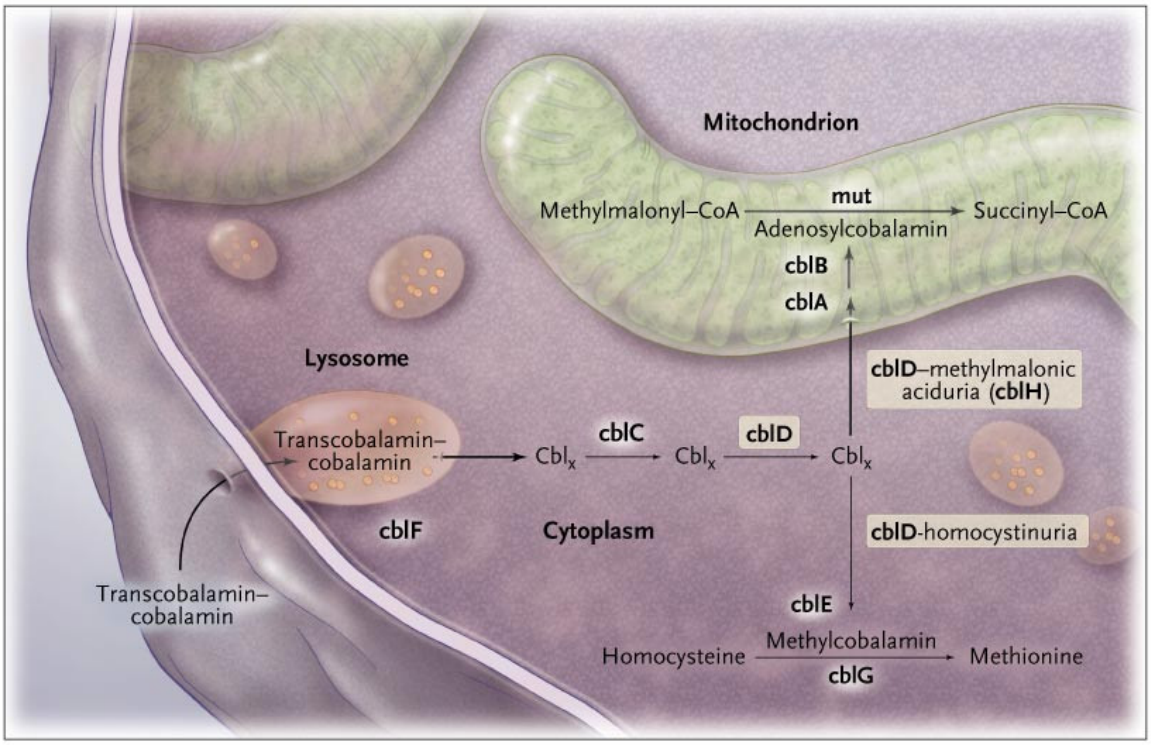

Figure 23: Genetic defects of metabolism of vitamin B12 adapted from (Coelho et al., 2008)

6.1.2 Genetic defects affecting the remethylation of homocysteine into methionine by methionine synthase

Inborn errors of intracellular metabolism of cobalamins linked to remethylation of homocysteine to methionine include CblG, CblE and cblD variant 1. They are rare autosomal recessive hereditary disorders.

6.1.2.1 Methylcobalamin deficiency G (CblG) and methylcobalamin deficiency E (CblE) disorders

Complementation analysis classified the disorders linked to impaired remethylation of homocysteine to methionine and MS dysfunction into homocystinuria-megaloblastic anemia, CblG complementation type / CblG complementation type methylcobalamin deficiency / CblG complementation type methionine synthase deficiency (OMIM 250940) and homocystinuria-megaloblastic anemia, CblE complementation type / methylcobalamin deficiency CblE type (OMIM 236270). CblG is caused by mutations in *MTR* gene encoding MS while CblE is caused by mutation in *MTRR* gene encoding methionine synthase reductase enzyme. Methionine

synthase reductase is important for the activity of MS as it catalyzes the reductive reactivation of oxidized MS.

Both CblG and CblE patients manifest early in life, mainly during their first two years of life (D. Watkins & Rosenblatt, 1989a). However, manifestation of CblG disorder in adulthood was reported in a 21 years old patient who presented with neurological symptoms which were initially misdiagnosed for multiple sclerosis (Carmel et al., 1988). Patients with CblG and CblE disorders are biochemically characterized by hyperhomocysteinemia and hypomethioninemia without methylmalonic aciduria (Watkins & Rosenblatt, 1989). In the 80s one CblE patient with mild methylmalonic aciduria was reported (Tuchman et al., 1988).

Around 25 cases for CblG and 20 CblE have been reported (Huemer et al., 2017). In CblG the activity of MS is impaired. An important decrease in MS specific activity was reported in cultured fibroblasts of CblG patients, MS enzyme activity was evaluated using standard enzyme assay. On the other hand, the specific activity of MS was high in CblE and comparable with the controls. However, in the presence of suboptimal amounts of reducing agent, this activity was reduced in the CblE patients fibroblasts in comparison to controls (Gulati et al., 1996; Rosenblatt et al., 1984; D. Watkins & Rosenblatt, 1989a).

6.1.2.2 Clinical presentation of CblG and CblE disorders

The most common clinical manifestations of CblG and CblE patients includes megaloblastic anemia, feeding difficulties, failure to thrive and diverse neurological disorders like cerebral atrophy, hypotonia, nystagmus, seizures, electroencephalographic abnormalities, cognitive impairment and developmental delays (Martina Huemer et al., 2017; Watkins & Rosenblatt, 1989). In rare cases patients may presents with microcephalus (Müller, Horneff, & Hennermann, 2007), opthalmological problems including vision disturbances (Outteryck et al., 2012).

6.1.2.3 Genetic causes of CblG and CblE disorders

Mutations of *MTR* and *MTRR* genes causes CblG and CblE disorders respectively.

i) Mutation of *MTR* gene and CblG disorder

CblG disorder is caused by mutations on *MTR* gene, this gene as mentioned earlier is located on human chromosome 1q43 and it encodes the cytoplasmic MS (David Watkins et al., 2002). Cloning of human *MTR* gene has contributed to the identification of several mutations in this

gene in the CblG patients (Leclerc et al., 1996a; Li et al., 1996). These mutations included: missense mutations, deletions leading to frame shifts and nonsense mutations (Gulati et al., 1996; Leclerc, 1996; David Watkins et al., 2002). Some of the deletion mutations detected include: c.12-13delGC, c.2101delT, c.381delA, c.2669 and c.2796-2800del. The missense mutation AAGTC. 2670delTG. c.3518C > T (P1173L) was found to be one of the most common missense mutation representing more than 40 % of the disease-causing alleles in CblG patients. R585X and E1204X are examples of nonsense mutations (David Watkins et al., 2002). *MTR* gene mutations were proposed to cause premature termination of the amino acid chain and hence leading to synthesis of truncated proteins lacking crucial domains essential for normal functioning of the enzyme (David Watkins et al., 2002a).

ii) Mutation of *MTRR* gene and CblE disorder

CblE disorder is caused by mutations in *MTRR* gene (OMIM# 602568) localized on human chromosome 5p15.2– 15.3 (Leclerc et al., 1999). *MTRR* encodes the methionine synthase reductase enzyme (MSR) which is a member of the ferredoxin–nicotinamide adenine dinucleotide phosphate ($NADP^+$) reductases. MSR is involved in reductive reactivation of MS. Human *MTRR* gene was identified and cloned by the team of (Leclerc et al., 1998).

Several mutations in this gene have been identified in CblE patients (Leclerc et al., 1998a; Ruiz-Mercado et al., 2016; Zavadáková et al., 2005). Some of the mutations that have been identified includes : c.1622_1623dupTA ,c.1557-4_1557+3del7, c.1459G4A, c.903+469T4C, c.1361C4T, c.1953-6_1953-2del5 ,c.7A4T and c.1573C4T (Zavadáková et al., 2005). The c.1361C > T mutation causes milder form of the disease and mainly with hematological presentation without neurological problems (Vilaseca et al., 2003). Deep Intronic mutation (c.9031+469T4C) has been described to be one of the most frequent mutation in CblE and has been proposed to induce aberrant splicing of *MTRR* transcript (Homolova et al., 2010). Recently (Ruiz-Mercado et al., 2016) identified c.1677–1G > A (p.Glu560fs) mutation.

6.1.2.4 Treatment of CblE and CblG disorders

Patients with early onset of CblG and CblE disorders presents with acute neurological distress which without proper diagnosis and medical intervention leads to rapid progressive neurological deterioration which could be fatal (Schiff et al., 2011). After diagnosis of CblE and CblG disorders, the patients are treated with intramuscular administration of hydroxycobalamin (OHCbl) (David Watkins & Rosenblatt, 2011). In some medical facilities,

the neonates with CblG and CblE disorders are given a daily injection of 1 mg/Kg of OHCbl until the patient normalizes (Huemer et al., 2017). In some cases the treatment involves injection of OHCbl in combination with oral administration of folate and betaine supplements or methionine (Huemer et al., 2017; Schiff et al., 2011; David Watkins & Rosenblatt, 2011, 2016). The delay in diagnosis and the time of initiation of treatment is important for the outcome (Huemer et al., 2015). In these cases, early treatment resulted in favorable outcome. Furthermore, early treatment prevents neurological development and also helps in developmental recovery. To the contrary, patients who receive late treatment have severe and irreversible neuromotor impairments (Schiff et al., 2011). In majority of cases, this treatment has been reported to cause a rapid improvement of hematological and biochemical abnormalities in some patients. This treatment was reported to cause a reduction in total plasma homocysteine and increased methionine concentrations. However, for the neurological disorders, a slow response to treatment has been observed with some of these defects persisting even after treatment (David Watkins & Rosenblatt, 2011a).

6.1.3 Genetic defects linked to deficiency in synthesis of both adenosyl-cobalamin and methyl cobalamin

Combined deficiency of Adenosylcobalamin and methylcobalamin results in the development of three disorders namely CblC, CblD-MMA/ CblD variant 1, CblF and CblJ (Martina Huemer et al., 2017). The main characteristics of CblC and cblD disorders includes 1). A decrease in the synthesis of both MeCbl and AdoCbl, 2). A reduced intracellular retention of cobalamin and 3). A decrease in enzymatic activities of both MS and methymalonylCoA mutase. Biochemically, these defects are characterized by combined methymalonic aciduria (due to impaired activity of methylmalonylCoA mutase) and hyperhomocysteinemia (resulting from impaired remethylation of homocysteine to methionine by MS) (David Watkins & Rosenblatt, 2011). In cblF, apart from lysosomal accumulation of large quantity of unmetabolized cobalamins, the deficiency in the synthesis of the two cobalamin cofactors and impairment in the activities of MS and methylmalonylCoA mutase are similar with that of CblC and cblD (David Watkins & Rosenblatt, 2011a).

6.1.3.1 Combined methylmalonic aciduria and homocystinuria, CblC type

Combined methylmalonic aciduria and homo- cystinuria, CblC type (OMIM# 277400), is an autosomal recessive inherited disorder of intracellular metabolism of cobalamin. CblC complementation group is one of the most common disorder of cobalamin metabolism, more

than 500 cases have been reported. (Lerner-Ellis et al., 2009; Liu et al., 2018; Zong et al., & Kong, 2015).

6.1.3.2 Clinical presentation of CblC

Combined methylmalonic aciduria and homo- cystinuria, CblC type disorder can either manifest in the first year of life defined as early onset (< 1 year of life) or later in childhood and adulthood defined as late onset (> 4 years of life) (Carrillo-Carrasco, Chandler, & Venditti, 2012). Clinical symptoms of early onset group of CblC are severe and are associated with high mortality rates (Fischer et al., 2014). These symptoms includes failure to thrive, neurological problems (hypotonia, delayed development, seizure), feeding difficulties, Opthalmological problems (decreased visual acuity, nystagmus and pigmentary retinopathy), Haematological (microcytic anemia and thrombocytopenia), hydrocephaly, microcephaly and hemolytic and Uremic syndrome (Adrovic et al., 2016; Carrillo-Carrasco & Venditti, 2012; Fischer et al., 2014; Rosenblatt et al., 1997; K. Zhang et al., 2018).

In the late onset, the patients present with acute neurological dysfunction like extrapyramidal signs (myelopathy), confusion, psychosis, dementia or derilium (state of acute confusion/ serious disturbance of mental abilities), cognitive decline and less severe haematological problems (Rosenblatt et al., 1997). In some cases, the patients present with pulmonary artery hypertension, haemolytic uremic syndrome, brain atrophy and white matter lesions (Martina Huemer et al., 2014; K. Zhang et al., 2018). Early onset is associated with poor survival rates with more than 25 % deaths observed within the first nine months of life. To the contrary, a good outcome is observed in the patients with late onset of CblC (Rosenblatt et al., 1997).

6.1.3.3 Genetic causes of CblC

Combined methylmalonic aciduria and homocystinuria, CblC type disorder is caused by mutations in *MMACHC* gene encoding MMACHC protein. About 70 mutations that cause CblC have been identified in *MMACHC* gene (David Watkins & Rosenblatt, 2011). At infancy / early onset c.271dupA and c.331C>T in homozygous or compound heterozygous state are the most frequent mutations and are associated with the severe form of the disease (Lerner-Ellis et al., 2006). The c.271dupA mutation accounts for around 40 % of disease-causing alleles. In childhood or adulthood (late onset) c.394C>T mutation was found to be the most frequent mutation in CblC patients (Lerner-Ellis et al., 2009, 2006; Morel, Lerner-Ellis, & Rosenblatt, 2006). A milder phenotype was observed in patients that were compound heterozygotes for (c.394 C>T, c.347 T>C, c.440 G>C, c.482 G>A) missense alleles and c.271dupA (Morel et al., 2006). Recently two novel mutations: a small-scale deletion [c.463_465delGGG

(p.Gly155del)], and a nonsense mutation [c.637G>T (p.Glu213Ter)] in *MMACHC* gene were identified in CblC patients (Hu et al., 2018).

6.1.3.4 Treatment of CblC patients

Patients with CblC disease are treated with parenteral OHCbl and betaine, the treatment is usually initiated immediately CblC is suspected without waiting for confirmatory testing (Carrillo-Carrasco et al., 2012). OHCbl treatment will increase the intracellular levels of cobalamin hence maximizing the activities of MS and MMA mutase. Betaine is the substrate for conversion of homocysteine to methionine by betaine methyltransferase and in some case folates is used improve homocysteine remethylation pathway (Martinelli, Deodato, & Dionisi-Vici, 2011). A dose of 1mg/Kg/day of OHCbl intramuscular injection and 250 mg/Kg/d of betaine is effective in children (Bartholomew et al., 1988). Parenteral OHCbl treatment has been reported to normalize the plasma biochemical parameters (serum methionine, total homocysteine and Methylmalonic acid) and improve clinical manifestations (Carrillo-Carrasco & Venditti, 2012). An improvement in HUS and cardiomyopathy is also observed. To the contrary the frequency of neurological and ophthalmological problems that include: seizures, developmental delay, failure to thrive, microcephaly and optic atrophy remained the same after treatment (Fischer et al., 2014). Regardless of treatment and amelioration of biochemical parameters, a poor long term neurological prognosis is observed (Martinelli et al., 2011). The treatment modalities seems not to completely alter the disease clinical manifestation (Fischer et al., 2014).

6.2 Cardiovascular diseases and congenital heart defects linked to genetic defects of vitamin B12 metabolism and remethylation of homocysteine

Hyperhomocysteinemia is the main biochemical presentation of patients with inborn errors of vitamin B12 metabolism that include CblC and CblG disorders. In a family based association study, the genetic polymorphisms of *MTR* (rs-1770449 and rs1050993) and *MTR* variants (186T > G and 905G > A) were found to be significantly associated with increased risk of congenital heart diseases (Deng et al., 2019; Zhao et al., 2014). Moreover, polymorphisms of *MTHFR* (involved in metabolism of folates) and *MTRR (*for reactivation of MS*)* were also associated with risk of development of conotruncial heart defects in Chinese population (Wang et al.,2018). Polymorphisms of *MTRR* in population were also shown to cause congenital heart defects (Hassan et al., 2017).

Congenital heart defects are highly prevalent in CblC patients and were suggested to be caused by abnormal methylation of DNA and histones during embryogenesis due to decreased synthesis of SAM (Profitlich, Kirmse, Wasserstein, Diaz, & Srivastava, 2009). Structural heart defects were detected in half of CblC patients aged between 2 weeks and 24 years in a retrospective observational study conducted by the team of (Profitlich et al., 2009). In this study, the patients underwent a complete 2-D echocardiogram. Some of the defects detected included dysplastic pulmonary valve without pulmonary stenosis, muscular ventricular septal defect, secundum atrial septal defect, left ventricular non-compaction, secundum atrial septal defect and mitral valve prolapse with mild mitral regurgitation. Quantitatively, normal systolic function was observed in these patients (Profitlich et al., 2009). Ventricular noncompaction and left ventricular dysfunction was also reported in CblC infant who presented with clinical heart failure at birth (Almassinokiani et al., 2015). Fetal dilated cardiomyopathy can be the presenting symptom of cobalamin C deficiency. Fetal echocardiography done at 30 weeks of gestation on a fetus with intrauterine growth retardation revealed dilated cardiomyopathy with an increased cardiothoracic index and decreased systolic function (Bie et al., 2009). Some patients with late onset of CblC manifest with pulmonary hypertension (Gündüz et al., 2014; Liu et al., 2017; Petropoulos et al., 2018).

7 TRANSGENIC ANIMAL MODELS TO STUDY DEFECTIVE METABOLISM OF FOLATE AND VITAMIN B12 METABOLISM AND REMETHYLATION OF HOMOCYSTEINE

Genetic models of dysregulated metabolism of cobalamins and folates and remethylation of homocysteine have been developed. These models include mice with invalidation of genes involved in remethylation pathway and metabolism of folates and cobalamins including *MTHFR, MTRR* and *CBS.*

7.1 Mice deficient in methionine synthase reductase (*Mtrr* deficient mice)

MTRR gene encodes methionine synthase reductase enzyme (EC 2.1.1.135) which catalyzes reductive reactivation of MS using SAM as a methyl donor (Leclerc et al., 1998).

The team of Elmore developed a model of impaired remethylation of homocysteine using gene trap insertion method in *Mtrr* gene (Elmore et al., 2007). Homozygous Methionine synthase reductase deficient mice the *Mtrr* $^{gt/gt}$ had decreased methionine synthase reductase activity with increased plasma homocysteine and MeTHF. In addition the mice *Mtrr*$^{gt/gt}$ had decreased plasma methionine levels, however SAM:SAH ratio was not decreased (Elmore et al., 2007). Litters from *Mtrr* deficient mothers *Mtrr* $^{gt/gt}$ were found to have higher incidences of cardiac ventricular septal defects and myocardial hypoplasia (Deng et al., 2008). *Mtrr* deficiency caused adverse reproductive outcomes. These outcomes include delayed embryos per litter, smaller placenta in the *Mtrr* $^{gt/gt}$ mothers and smaller embryos (Deng et al., 2008). Similar results were demonstrated by the team of (Padmanabhan et al., 2013) who used the same model of *Mtrr* deficiency. Most importantly, they found that *Mtrr* deficiency in maternal grandparents causes adverse developmental delay and congenital defects in their grand progeny including those from wildtype daughters. These congenital defects included heart defects such as pericardial edema, thicker enlarged hearts with nonproportional size, NTDs like failure of closure of the neural tube and placental defects (Padmanabhan et al., 2013). They suggested that the defects were due to transgenerational epigenetic inheritance.

1.1 Mice deficient in methyltetrahydrofolate reductase (*Mthfr* deficient mice)

MTHFR gene encodes the methyl tetrahydrofolate reductase (EC 1.5.1.20) which catalyzes the reduction of 5,10-methylenetetrahydrofolate to 5-methyltetrahydrofolate, the co-substrate for homocysteine remethylation to methionine by MS (Goyette et al., 1994).

In 2001, the team of (Chen et al., 2001) generated a *Mthfr* deficient mice using the targeted gene disruption at exon 3 of *Mthfr* gene. The metabolic phenotype of both the *Mthfr* heterozygous and homozygous mice fed with a normal diet include a significant increase in plasma homocysteine, increase in SAH in all tissue accompanied by decreased SAM:SAH. Global hypomethylation was also reported in these animals. In addition to a decreased survival within the first five weeks of life, the homozygotes were small with abnormalities of the neural tube and cerebellar. Both Heterozygotes and homozygotes had lipid deposition in the aorta confirming the atherogenic effect of hyperhomocysteinemia in this model (Chen et al., 2001). *Mthfr* deficient mice have been used to study the vascular effects of hyperhomocysteinemia. The group of (Devlin et al., 2004) reported endothelial dysfunction in the cerebral microvessels in the *Mthfr* mice fed with either low folate or high methionine diet. Other studies showed that the biochemical and developmental abnormalities in *Mthfr* mice are attenuated by betaine rich diet (Schwahn et al., 2004).

7.2 Mice deficient in Cystathionine beta synthase (*Cbs* deficient mice)

CBS gene encodes cystathionine beta synthase which catalyzes the irreversible conjugation of homocysteine to serine to form cystathionine in the first step of transsulfuration. The first *Cbs* deficient mice was generated using gene target disruption by the team of (Watanabe et al., 1995). $Cbs^{-/-}$ mice developed severe hyperhomocysteinemia with about 40-fold increase in plasma homocysteine. The enzyme activity of CBS was decreased by half in the liver of the homozygotes (Watanabe et al., 1995). The $Cbs^{-/-}$ mice had severe developmental delay with enlarged multinucleated hepatocytes and that majority of them died within the first five weeks of life (Watanabe et al., 1995). Neonatal lethality observed in $Cbs^{-/-}$ mice was rescued by overexpression of human CBS transgene. The CBS transgene was overexpressed under the control of Zinc inducible metallothionein promoter (Wang et al., 2004). Elevated homocysteine levels in the transgenic mice with human CBS transgene was significantly reduced by adding zinc in their drinking water. Furthermore, overexpression of CBS gene rescued hyperhomocystinuria caused by high methionine and low folate diet (Wang et al., 2004). Wangs' team also generated two other transgenic mice models that express human 1278T and 1278T/T424T transgenes under the control of Zinc inducible metallothionein promoter (Wang et al., 2005). The 1278T and 1278T/T424T transgenic mice were crossed with heterozygous mice $Cbs^{-/+}$ were in order to obtain the Tg-1278 $Cbs^{-/-}$ and Tg-1278/t4 $Cbs^{-/-}$ mice. Both 1278T and 1278T/T424T transgenes were able to rescue the neonatal mortality in $Cbs^{-/-}$ however the

plasma homocysteine levels remained significantly high. Tg-1278 *Cbs*$^{-/-}$ and Tg-1278/t4 *Cbs*$^{-/-}$ plasma homocysteine levels were 250μM and 278 μM respectively (Wang et al., 2005).

7.3 Betaine-homocysteine methyltransferase knock out mice (*Bhmt* deficient mice)

BHMT gene encodes betaine-homocysteine methyltransferase (BHMT;EC 2.1.1.5) involved in alternative remethylation of homocysteine to methionine. *Bhmt*$^{-/-}$ transgenic mice were generated by Teng and colleagues using the gene targeted disruption at exons 6 and 7 of *Bhmt* gene (Teng et al.,2011). *Bhmt*$^{-/-}$ *mice* had elevated plasma and liver homocysteine level with increase betaine accumulation in majority of tissues. These mice also developed hepatic carcinomas (Teng et al.,2011).

STUDY OBJECTIVES AND HYPOTHESES

Problem statement

Heart failure is a global life-threatening public health problem with poor prognosis and its prevalence is increasing with the ageing population. Approximately 26 million people have heart failure worldwide with half of reported cases dying within 5 years after diagnosis (Blair, Huffman, & Shah, 2013; Task et al., 2012; Velagaleti & Vasan, 2008). Heart failure is produced by a wide spectrum of metabolic, cardiovascular and heart diseases (Dickstein et al., 2008; Elliott et al., 2008; Maron et al., 2006; Ziaeian & Fonarow, 2016). The most frequent causes include coronary artery disease, hypertension, valvular disease and congenital heart disease (Dickstein et al., 2008; Elliott et al., 2008; Maron et al., 2006; Ziaeian & Fonarow, 2016). Nevertheless, other primary and secondary conditions produce heart failure and consequent dilated cardiomyopathy (DCM) (Dickstein et al., 2008; Elliott et al., 2008; Maron et al., 2006a; Ziaeian & Fonarow, 2016). The primary causes of DCM are generally confined to heart muscle while the secondary causes include systemic conditions with multiple origins. Among the primary causes, inherited metabolic diseases including the inborn errors of one-carbon metabolism constitute the major cause of DCM (Guéant et al., 2018; Watkins & Rosenblatt, 2016). The genetic defects of remethylation (RM) comprise mutations of methionine synthase (*MTR*) or genes involved in the processing of cobalamin (vitamin B12, Cbl), including *CD320, LMBRD1, ABCD4, MMACHC, MMADHC* and *MTRR* (Coelho et al., 2012; Green et al., 2017; David Watkins et al., 2002b). The later alters the activity of the methionine synthase enzyme (MS) (Ruiz-Mercado et al., 2016; Watkins & Rosenblatt, 1989; David Watkins & Rosenblatt, 2016).

MS utilizes 5-methyltetrahydrofolate (5-Me-THF) and methylcobalamin (a derivative of vitamin B12) to catalyze methyl group transfer from N^5 methyltetrahydrofolate to homocysteine to form methionine and tetrahydrofolate (Guéant et al., 2013). Methionine is the direct precursor of S-Adenosyl Methionine (SAM), the universal methyl group donor for the methylation of histones, RNA and DNA, which are crucial for epigenomic regulatory mechanisms of gene expression (Forges et al., 2007; Guéant et al., 2013)

Genetic defects of RM pathways linked to mutations of MS and other genes of cobalamin processing and deficiencies of vitamin B12 and folates produce decreased synthesis of methionine consequently leading to decreased concentration of SAM and increased homocysteine in tissues and blood. We and others have demonstrated a significant association between elevated plasma homocysteine with impaired left ventricular systolic function

(Bokhari et al.,2005; Guéant-Rodriguez et al., 2007). Heart failure is generally preceded by hypertrophic cardiomyopathy and stiffening of the peripheral arteries. Many studies have focused on the cardiomyopathies in adults. However, little work has been done concerning the hereditary cardiomyopathies. The deficiency in folates and vitamin B12 during pregnancy and lactation lead to hypertrophic cardiomyopathy with enlarged cardiomyocytes and increased thickness of myocardium, impaired activity of respiratory chain and fatty acid oxidation in weaning rat pubs (Garcia et al., 2011). A potential association between vitamin B12 and folate and pathological mechanisms of cardiomyopathies has been suggested in clinical reports and populations studies. However, the mechanisms that underlie these outcomes are unknown.

Nutritional models do not allow for the understanding of the mechanisms specifically related to the activity of methionine synthase, including those related to decreased synthesis of SAM in the cardiomyopathies observed in the two inborn errors of cobalamin metabolism: CblC and CblG caused by mutations in *MMACHC* and *MTR* genes respectively. We therefore used two transgenic mouse models in our study; 1) with constitutive cardiac specific invalidation of *Mtr* gene and 2) with systemic knockout of *MMACHC* gene. These models enabled us to study cardiac functional and metabolic consequences of long-term impaired synthesis of methionine, Methylcobalamin and adenosylcobalamin during specific windows of embryo-fetal development.

STUDY OBJECTIVES

The specific objectives of our study are:

1. To evaluate the effectiveness of the deletion of *Mtr* gene in the cardiomyocytes of *Mtr cKO* animals
2. To investigate cardiac metabolic and functional consequences of the impaired remethylation of homocysteine and methionine synthesis in transgenic mice with constitutive cardiac specific knock out of *Mtr* gene.
3. To investigate cardiac metabolic and functional consequences of the impaired processing of cobalamins in transgenic mice with systemic invalidation of *MMACHC* gene.

STUDY HYPOTHESES

1. Constitutive cardiac specific invalidation of *Mtr gene* and systemic invalidation of *MMACHC* gene causes impaired remethylation of homocysteine and decreased synthesis of methionine and Methylcobalamin in the myocardium.

2. Constitutive cardiac specific invalidation of *Mtr gene* and systemic invalidation of *MMACHC* gene causes severe deficit in myocardial energy metabolism, left ventricular dysfunction, cardiac hypertrophy and / or heart failure.

MATERIALS AND METHODS

1 Animals

Animal studies were approved by the Ministry of Higher Education and Research (MESR) of France after having received a favorable opinion from the Ethics Committee of Lorraine Region (CELMEA) reference no (APAFIS2776-2015111915482808). The authorization number of animal experimentation housing is 54-547-22 issued by the Departmental Direction for the protection of the populations, Meurthe and Moselle, France. All experiments and animal care were carried out in compliance with French and European laws, directives, and regulations on care and use of animals for scientific research. The mice were housed in standard laboratory conditions, on a 12h light, 12h darkness schedule at a temperature of (20 ± 24) °C and humidity of (50 ± 5) % with food and water available *ad libidum*. We used the C57BL/6 mouse strain in our study.

1.1 Generation of the transgenic mice models

1.1.1 Generation of Cardiac specific *Mtr* constitutive knock out mice by Cre-Lox System

Constitutive cardiac specific *Mtr* Knock-out (*Mtr cKO*) mice were generated in collaboration with the "Institut Clinique de la Souris" (ICS) in Strasbourg-Illkirch. Constitutive cardiac specific deletion of *Mtr* gene in the cardiomyocytes was achieved using tissue-specific and time controlled Cre-LoxP system. Cre recombinase is 38 kDa protein derived from P1 bacteriophage that catalyzes the site-specific recombination of LoxP sites. The loxP site is a 34 base pairs sequences, each LoxP site consists of a dyad of 13 base pair palindromic sequences separated by a region consisting of 8 base pairs. The DNA sequence floxed by the LoxP sites is excised following the recombination of the LoxP by Cre recombinase. Excision, inversion and integration/insertion are the three types of recombination catalyzed by Cre recombinase. These recombinations depend on the orientation of the LoxP sites. If the orientation is in the same direction, the floxed DNA is excised in a circular loop and if the orientation is in the opposite direction the floxed DNA is inverted.

In order to invalidate *Mtr* gene in the cardiomyocytes, mice bearing the *Mtr* conditional allele were crossed with Myh6-Cre line (JAXMICE Stock Number 11038, B6.FVB-Tg (Myh6-cre) 2182Mds / J expressing Cre recombinase in the cardiomyocytes which caused the deletion of this allele in the cardiomyocytes (**Figure 24**). The Cre recombinase is produced under control

of the promoter specific Myh6 in cardiomyocytes from embryonic day (E) 9.5 with a maximum at E 11.5, and this enzyme recombines the LoxP sites introduced in *Mtr* gene, around exons 4 and 5 which are essential (Agah et al., 1997). This causes the deletion of exons 4 and 5 in the DNA sequence, followed by a shift in the reading frame therefore messenger RNA transcribed from the deleted gene produces nonfunctional methionine synthase protein. PCR analysis was used to genotype the mice using DNA extracted from animals' tail. The sequences of primers that were used to genotype the Mhy6 transgene and floxed *Mtr* allele are shown in **Table 6**. Products of PCR were resolved in 1 % tris acetate EDTA (TAE) agarose gel electrophoresis. Methionine synthase enzyme activity assay and immunoblot analysis were used to confirm the level of expression MTR/MS at protein levels.

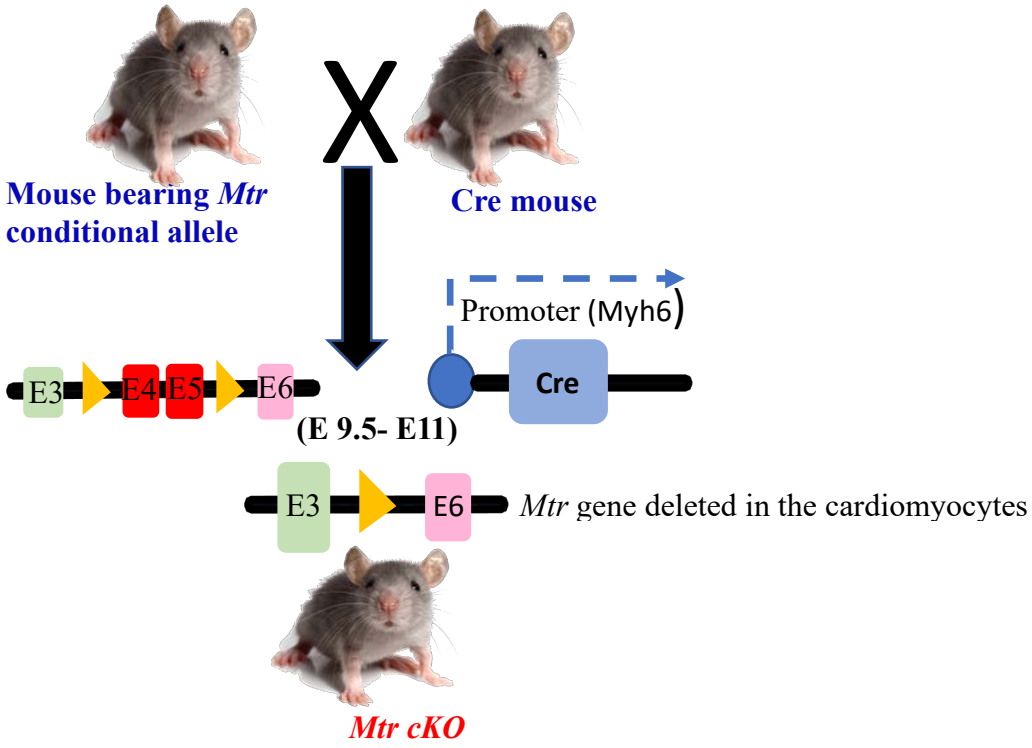

Figure 24: Cardiac specific invalidation of *Mtr* gene by Cre -loxP system

1.1.2 Systemic knock out of *MMACHC* gene mouse model

The *MMACHC* $^{-/+}$ mouse was produced by genetics department of McGill University.

1.2 Genotyping

1.2.1 DNA extraction

Genomic DNA was extracted using KAPA Mouse Genotyping Kit (KAPA Biosystem, KB7302). This Kit has a specific protease and extraction buffer (KAPA) the composition of the genomic DNA extraction reaction mix is shown on **Table 3**. The mouse tail piece was placed in a 200µL Eppendorf followed by addition of 10 µl of 10 X KAPA buffer, 2µL of enzyme (1 U / µL) and 88µL of water. The samples were then incubated at 75 ° C for 15 minutes and then at 95 ° C for 5 minutes and 12 ° C infinity in thermal cycler (C1000 Touch ™ BIO-RAD Laboratories). The extracted genomic DNAs were stored at -20 ° C.

Extraction of gDNA using KAPA kit (Clinicsciences for KAPABiosystems KK7302)				
Reaction volume for 50 (µL)	Reaction concentration	Stock concentration	*Volume* (µL)	Mix/16 (µL)
KAPA Express Extract Enzyme	0,02 U/µl	1 U/µl	*1*	16
KAPA Express Extract Buffer	1.x	10.x	*5*	80
H2O qsp 24 (µL)			*44,00*	704
Final volume			50	50

Table 3: **The reaction volumes of KAPA kit reagents used for extraction for genomic DNA for genotyping.**

PCR protocol on C1000 Touch thermal cycler: Amplification at 75°C for 15 minutes and enzyme denaturation at 95°C for 5 minutes.

1.2.2 Polymerase chain reaction (PCR)

For the amplification of genomic DNA by polymerase chain reaction (PCR), KAPA Mouse Genotyping Kit (KAPA BiosysteMTR, KK7302) was used. This kit contains a polymerase, 0.2 mM dNTPs each, the enzyme cofactor: MgCl2 (1.5 mM) and a stabilizer. To carry out this technique, (0.5 µM) of appropriate primers were mixed with the kits' PCR reaction mix, DNAse and RNAse free water and 1 µl of extracted gDNA shown in **Table 4.** The amplification was carried out in a thermocycler (C1000 Touch ™ BIO-RAD Laboratories) based on the appropriate PCR program for the sequence to be amplified (**Table 5**). The sequences for the primers used for genotyping are shown in **Table 6**.

After amplification, 12.5 µl of the amplification reaction mixture for each sample were resolved in a 1.5 % agarose migration gel (Eurobio, GEPAGA07), as well as 6 µl of size marker (100 µl DNA ladder, Invitrogen, 15628-050). The electrophoresis migration was carried out at 110V for 60 minutes in 1X Tris Borate EDTA buffer (TBE). The revelation of the gel was carried out under UV lamp (Imagemaster VDS) thanks to the presence of ethidium bromide (BET) (Eurobio, GEPBET000M), intercalating agent of the DNA incorporated in the gel during polymerization

PCR par le kit KAPA (Clinisciences pour KAPABiosystems KK7302)

Reaction volume 25 µL	C réaction	C stock	*Volume*	**Mix / 18**
2x KAPA2G Fast Genotyping Mix	1.x	2.x	*12,5 µL*	**225 µL**
089 - Myh6-F	0,5 µM	10 µM	*1,25 µL*	**22,5 µL**
090 - (Myh6) Cre-R	0,5 µM	10 µM	*1,25 µL*	**22,5 µL**
085 CONTINT-MC-F	0,5 µM	10 µM	*1,25 µL*	**22,5 µL**
086 - CONTINT-MC-R	0,5 µM	10 µM	*1,25 µL*	**22,5 µL**
H2O qsp 24 µL			*5,50 µL*	**99 µL**
ADN g			***2 µL***	/
			(25 µL)	(23 µL)

Table 4: PCR KAPA kit conditions

Conditions for amplification of genotyping primers

i. **PCR condition for CRE**

Cre			
Step	Temperature° C	Time	Number of cycles
Initial denaturation	94	3 minutes	1
Denaturation	94	20 seconds	35
Hybridization	TD (65-55)	20 seconds	
Elongation	72	20 seconds	
Final elongation	72	2 minutes	1

ii. PCR conditions for MC

MC			
Step	Temperature° C	Time	Number of cycles
Initial denaturation	94	3 minutes	1
Denaturation	94	20 seconds	35
Hybridization	55	20 seconds	
Elongation	72	20 seconds	
Final elongation	72	2 minutes	1

iii) **PCR conditions for MLML**

PCR conditions for MLML			
Step	Temperature ° C	Time	Number of cycles
Initial denaturation	94	3 minutes	1
Denaturation	94	15seconds	32
Hybridization	65	10 seconds	
Elongation	72	10 seconds	
Final elongation	72	2 minutes	1

iv) **PCR conditions for MMACHC**

MMACHC			
Step	Temperature ° C	Time	Number of cycles
Initial denaturation	94	3 minutes	1
Denaturation	94	15 seconds	35
Hybridization	60	15 seconds	
Elongation	72	15 seconds	
Final elongation	72	2 minutes	1

Table 5: PCR Conditions for genotyping

i), ii and iii, are PCR conditions for genotyping cre mc and MLML, this were used to genotype *Mtr cKO* while iv) conditions for MMACHC

Name	Primer Sequences	
Cre (Myh6)	Forward	5'-ATGACAGACAGATCCCTCCTATCTCC-3'
	Reverse	5'-CTCATCACTCGTTGCATCATCGAC-3'
MTR	Forward	5'-CATACAACCACAGACCTTGGGGAAGTG-3'
	Reverse	5'-CAGCAAGGTTGCTCCTAAACTGCTG-3'
MMACHC	Forward	5'-CTTGCCATCAATACGGGACT-3'
	Reverse	5'-CTGGAAAGCTCAATGGCCTA-3'
MC	Forward	5'-ATA CCG GAG ATC ATG CAA GC-3'
	Reverse	5'-AGG TGG ACC TGA TCA TGG AG-3'

Table 6: Sequences of primers used for genotyping

1.3 Sacrificing and harvesting of blood and tissue samples

After cardiac function studies the animals were weighed, anesthetized and then euthanized by decapitation. Blood samples were collected into heparinized tubes and stored at 4 °C. To separate plasma, blood was centrifuged at 2500 g at 4 ° C for 10 minutes and the plasma was collected and kept at -80 ° C until analysis. For SAM and SAH assay, 50 µl of plasma was acidified with 5 µl of 1 M Acetic acid and stored at -80 ° C until analysis. The hearts were harvested and submerge in ice cold 1X PBS buffer (2,7 mmol/L KCl, 140 mmol/L NaCl, 6,8 mmol/L $Na_2HPO_42H_2O$, 1,5 mmol/L KH_2PO_4, pH 7,4) to drain excess blood. The hearts were then weighed and cross-sectionally cut to obtain the apex and ventricles. The ventricles were fixed in either in 4% Formalin or beta MetaCarnoy for histology analysis and the remaining parts ventricles and apex were frozen in liquid nitrogen and stored at -80°C for biochemical analysis.

2 Evaluation of cardiac function parameters (hemodynamic and left ventricular function analysis)

2.1 Measurement of blood pressure using tail cuff plethysmography

i) Principle

Tail cuff plethysmography is a noninvasive technique used to measure systolic blood pressure in the caudal artery in conscious animals. This method is an automated computerized system

that measures blood flow pulsation at the caudal artery and determines systolic blood pressure based on volume changes around the tail. This method involves placing the occlusion cuff around the base of animals' tail and a photoelectric sensor is also placed adjacent to the occlusion cuff for blood pressure detection. The occlusion cuff is connected to a pressure gauge which calibrates the recorder and monitors the pressure in the occlusion cuff all the time. The recorder inflates the occlusion cuff with air, as the pressure increases it compresses the caudal artery therefore gradually preventing the blood from passing. When the pressure of the artery and the occlusion cuff are equal the occlusion cuff is crushed preventing blood circulation.

In this system the detection of systolic blood pressure is based on the transformation of light energy into electric energy by the photoelectric sensor. This sensor sends beam of light through the skin and measures the amount of reflected light which is then converted into electric signals. This electric signal is then processed and displayed by the recorder. There is a correlation between the intensity of the light reflected back to the photoelectric sensor and the volume of blood in the artery. A decrease in the intensity of reflected light corresponds to the decrease in blood volume in the artery. For this reason, when the pressure increases in the occlusion cuff, the artery is crushed, which decreases the passage of blood and causes a decrease in the signal, until it is below the extinction threshold (automatically defined by the device according to the signal-to-noise ratio). This is interpreted by the logger as being the value of the systolic pressure.

ii) Protocol

Systolic blood pressure and heart pulse rates were measured in conscious 5-month-old mice using noninvasive tail cuff plethysmography (SC-1000 BP analysis system, Hatteras Instruments, Inc., USA). The animals were acclimatized to the system for 7 consecutive days before experimental measurements were taken. The mice were artificially heated 15 minutes before and during systolic blood pressure measurement at 37 °C to increase the blood flow into the tail. The animal is placed in a magnetized compression box to restrain it. During each session, three series of 7 measurements were taken, and systolic blood pressure and the heart pulse rates were recorded. Stata data analysis and statistical software were used for data analysis

2.2 Evaluation of left ventricular function by echocardiography

i) Principle of the transthoracic echocardiography

Ultrasound echocardiography is a noninvasive powerful imaging tool used to evaluate and monitor cardiac left ventricular systolic and diastolic functions and mapping the progression of heart dysfunction. The cardiac function parameters that are assessed by echocardiography

includes left ventricular ejection fraction (LVEF), fractional shortening (FS), ventricular volume, ventricular filling, and isovolumic relaxation, regional contractility and myocardial thickening. The measurements from this technique are very sensitive and hence it enables early detection of minute myocardial defects in genetically engineered mice and other rodents with surgical injury before the development of global cardiac dysfunction (Ram et al., 2011). Transthoracic echocardiography uses three principle imaging techniques that include: motion mode (M-mode), brightness mode (B-mode) and doppler imaging and 3D images. Ultrasound echocardiographic images are based on the high frequency beams which penetrates the thoracic cavity and are reflected back to the echocardiographic transducer when they reach the interface between tissues of different acoustic resistance like the myocardium blood and valves. Real time images of the heart are obtained when the software processes this reverberated signal (Ram et al., 2011).

ii) Protocol

Cardiac performance and ventricular remodeling in 5-month-old mice were assessed by transthoracic echocardiography using the Vevo 770® micro-echocardiography imaging system (Visualsonics Inc, Canada) in collaboration with Inserm U1116. For anesthesia, 1.5 -2 % isoflurane in 100 % oxygen was used for induction and was maintained at 1- 1.5 % during the procedure. Chest hair was shaved and the mouse was placed in supine position on a heating pad to maintain the body temperature at 37 °C. RMV 707B scanhead, a high frequency ultra sound probe was used to obtain the echocardiograms. M-Mode echocardiography obtained from parasternal short axis view was used to measure the ventricle dimensions: Left ventricular internal diameters at end of diastole and systole {LVIDd and LVIDs}, LV Posterior wall thickness in diastole and systole (LVPWd and LVPWs), LV volumes in diastole and systole (Lvvold and Lvvols respectively). These measurements were then used to calculate the left ventricular mass (LV mass), left ventricular ejection fraction (LVEF) and fractional shortening (FS). B mode images of the apical four chamber view were taken to determine the accurate angle for pulsed wave Doppler of the mitrial and tricuspid valve. The pulse wave Doppler mode images of the aorta outflow from high right parasternal view were taken to calculate the stoke volume and cardiac output.

2.3 Evaluation of left ventricular function by Mini-PET

i) The principle for positron emission tomography

Positron emission tomography also called PET scan is a non-invasive nuclear medicine imaging technique. This technique uses radioactive tracers also known as radionuclides to produce three

dimensional images of body organs. The measurement of metabolic activity of organs in three dimensions by PET technique is achieved thanks to the emissions produced by the positrons resulting from the disintegration of radioactive tracers that was injected beforehand. This technique is widely used in preclinical research across different disciplinaries for dynamic examinations of metabolic and biochemical processes under normal and pathological conditions.

PET imaging technique is based on the general principle of scintigraphy, which involves injecting a tracer whose biological properties and behavior are known to obtain an image of the functioning of an organ. This tracer is labelled with a radioactive atom like fluorine, carbon, oxygen, nitrogen oxygen among others which emits positrons, annihilation (conversion of particles into electromagnetic radiations) of these radioactive atoms produces two photons. The collimator of the PET camera detects the trajectory of these photons making it possible to locate their emission points and hence the concentration of the tracer at the different parts in the organ of interest. It is this quantitative information that is represented in the form of an image shown in color in the areas of high concentration of the tracer. Fluorine (18F) the main tracer that is used in PET is incorporated into a glucose molecule forming Fluorodeoxyglucose labeled with Fluor 18 (18^{F}-FDG). 18-Fluorodeoxyglucose is chemically known as 2-deoxy-2 deoxy 2 (^{18}F) Fluoro-D-glucose is an analog of glucose, unlike glucose 18^{F}-FDG is radioactive because the normal hydroxyl group of its glucose is substituted with fluorine which is a positron emitting radionuclide. It is the radioactivity of this particular fluorine added to glucose that allows its detection by the PET camera. In order to survive, function and reproduce, cells need energy in the form of glucose, which is assimilable by the body. Glucose is the energy source essential for many cells of the body and is naturally found in the blood. Consumption of glucose by cells increases with the cells' metabolic activities. 18F-FDG behaves like glucose, but unlike glucose, it is not a source of energy usable by the cell. It accumulates in the cell that becomes radioactive. In fact, the 18F-FDG molecule is phosphorylated by the cell that "tries" to assimilate it in its metabolism, which prevents it from coming out of the cell and the 18F-FDG-6P accumulates there becoming radioactive, the cell then emits radiation that can be detected by the PET camera. All information collected by the PET camera relies on the radioactivity identified in the tissues after 18F-FDG injection into the animal. The computer system connected to the PET camera produces sections and three-dimensional images of the sites of the body where the 18F-FDG has accumulated, the (**Figure 25**) shows the process of acquisition.

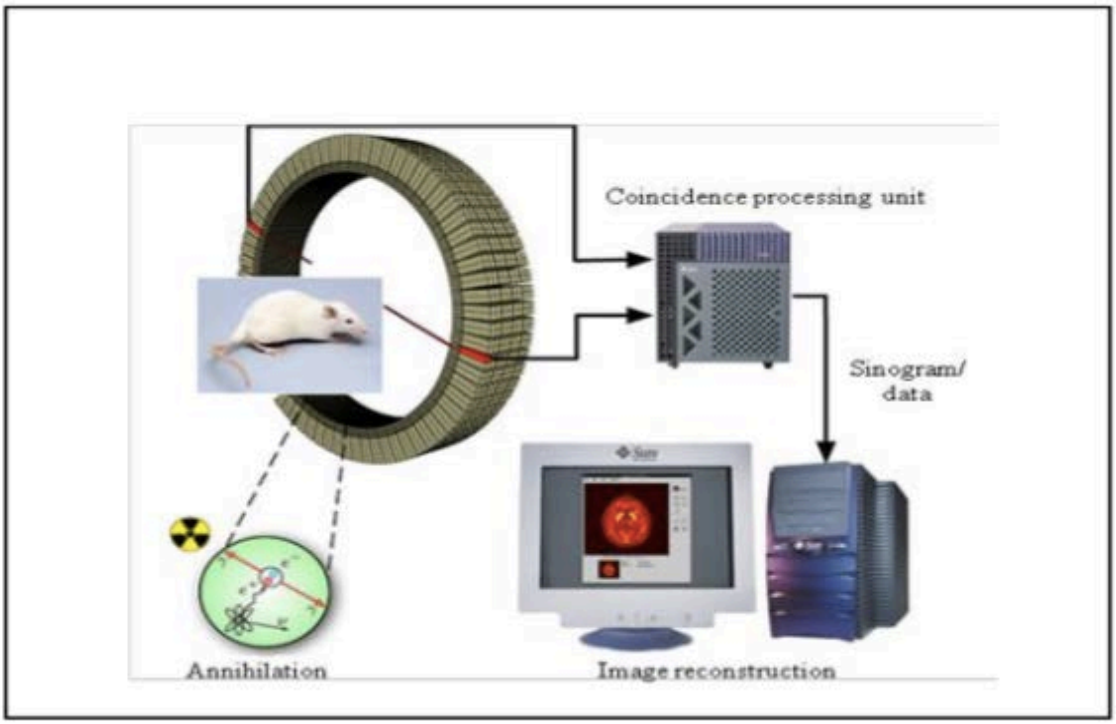

Figure 25: Representation of the MiniPET acquisition process adapted from thesis MM. Garcia 2011

ii) miniPET protocol

Cardiac function and tissue perfusion parameters in our study model were studied using MiniPET, the scans were performed on 5 -month- old mice using small animal monitoring and gating system M1025T (Inveon, Siemens Medical, USA). The animals were weighed, anesthetized using isoflurane according to their body weights and then injected with 37 MBq 18F-labelled PEGylated tetrameric RGD Peptide (18F-FPRGD4). The animals were placed in a ventral position on the examination bed a then four electrodes were placed on the legs of the animals. The examination was carried out in 180 °C circular orbit from 110 °C to 290 °C. MiniPET scans/ acquisitions were taken 30 minutes after the injection. The regions of interest at cardiac levels of each scan was drawn using the Vendor software (ASI Pro 5.2.4.0, Siemens Medical, Germany). Blood glucose levels were measured before and after the emission scans. After imaging, the animals were placed in a recovery chamber for 24 hours after which they were isolated until they were sacrificed to harvest blood and heart tissue samples for the biochemical analysis.

3 Determination of the concentration of metabolites of one-carbon metabolism in cardiac tissue

3.1 Determination of the concentration of adenylated molecules S-adenosyl homocysteine (SAH) and S-adenosyl methionine (SAM) cardiac tissue using chloroacetaldehyde by LC-MS / MS

i) Principle of Liquid Chromatography tandem Mass Spectrometry (LC-MS / MS).

Liquid Chromatography tandem Mass Spectrometry (LC-MS / MS) is an analytical method that combines the performance of liquid chromatography and mass spectrometry to identify and / or accurately quantify many substances. The LC-MS/MS unit consists of two main parts: a liquid chromatograph and a mass spectrometer. Determination of the concentration of SAM and SAH in tissue was achieved by following the steps below.

ii) Preparation of stock solutions (SAM, SAH).

The standard stock solutions for SAM and SAH (Sigma Aldrich, Louis USA) were prepared at a concentration of 50mM in 1N hydrochloric acid. A volume 0.5v of 2N NaOH, 0.2v of 1M sodium citrate (pH = 5) and 0.3v of ultrapure water was added to reach a final concentration of 25mM then aliquoted and stored at -20 °C. Stock working solution with a final concentration of 5µM was prepared from the standard solution using ultra-pure water.

iii) Deproteinization of samples.

A volume of 100 µl of sample (or standard) was mixed with 5 µl of 60 % $HClO_4$, vortexed and then incubated for 5 minutes in ice. The mixture was then centrifuged at 20000 g for 10 minutes at (4 ° C) and the pellet was eliminated. A volume of KOH (0.5N) was then added to neutralize and precipitate the perchlorate salts and then vortexed. A volume of 20 µl of KH_2PO_4 (1M) was then added to buffer the solution followed by vortexing and then centrifugation at 20000 g for 10 minutes (4 ° C) to remove the pellet.

iv) Derivation od adenyls

A volume of 200µl of sample or standard, 200 µl of 1M sodium acetate and 10 µl of 50 % chloroacetaldehyde was successively added into black microtubes of 0.5 ml, Vortexed and incubated at 80 ° C for 20 minutes then cooled to 4 ° C.

v) HPLC separation and analysis procedure

A total volume of (50 µL) of sample was injected into a high performance liquid chromatography (HPLC) system consisting of a high pressure pump (Spectra system P1000XR.TSP), an automated sample injector, a column containing a 5 µM silica resin with

grafts hydrophobic (column resolve N° 85711 C18 (150 x3.9 mm. 5 µM), Lichrospher Interchim), a fluorescence detector, RF10AXL (278 nm: Ex / 418 nm) an integrator (Borwin software 3.1) g and maintained at 30 ° C in a column oven, at a constant flow rate of 0, 8 mL / min (generating about 95 bar pressure). The absorbance was measured at 254 nm (maximum absorbance of purines by a UV-visible spectrophotometer, Spectra series UV100. TSP). The elution order of the different metabolites started with SAH followed by SAM. In parallel, standards containing different concentrations of SAH and SAM (8- 6-4-2-1 and 0.5µM) were passed. The standard range was made by measuring the area under the peak as a function of the concentration of standards. The concentration of the samples was determined by using line equation y = ax + b.

3.2 Determination of the concentration of folates

The concentration levels of folates in the plasma of 5 months old mice was determined using LC: MS / MS. First the standards at 250 µM and internal standards at 50 µM were removed from -80 °C, these standards were:

Folic acid + ascorbic acid 1 g/L + DTT 1 g/L

- Tetrahydrofolate.
- 5 Methyl THF.
- 5 Formyl THF.
- 5,10 Methenyl THF.
- Methylene THF was not used since it is unstable hence is difficult to analyze.
- ^{13}C5 Methyl THF, ^{13}C5 Formyl THF, ^{13}C5 FA.

To determine the concentration of folates the steps listed below were followed.

i) Preparation of reagents

a) Preparation of ascorbic acid and DTT solutions

A concentration of 20 mM Ascorbic Acid Solution (35.224 mg / 10 ml) and 450 mg of DTT in 3 mL of milliQ H2O (1 mol / L) were prepared.

b) Preparation of folate free serum standard range (S0 to S9) for Serum

A 2 mL beaker and a small magnetic bar were used to prepare serum free standards. To prepare 10 mL of SERUM (not EDTA), 80 mg activated carbon (Ref: 1.02186.0250 K21549186; Merck) was weighed followed by agitation for 20 min then centrifugation for 10 min at 3500 rpm (SV11RH centrifuge). This was followed by decantation and a second centrifugation in microtubes at 13000 rpm for 20 min at room temperature and then the pellet was eliminated.
The Standards were then prepared in folate free serum as follows:

- Prepare a concentration of 10 µmol / L solution of each standard by taking 40 µL of 5. standards at 250 µmol / L QSP and top up to to 1mL with milliQ H_2O.
- Prepare 100 nmol / L solution by taking 10 µL of the 10 µmol / L solution and top up to 1 mL with folate free serum.
- Then do dilution ½ to ½ of S9 to S1 (150 µL each): 100/50/25 / 12.5 / 6.25 / 3.125 / 1.563 / 0.781 / 0.391 nmol / L.

c) Preparation of internal standards

A volume of 50 µL of DTT was removed and set aside. Then 6 µL of DTT was added to each internal standard (13C5 Methyl THF, 13C5 Formyl THF, 13C-FA). For every 2,950 mL, 1 mg of DTT is added to have a concentration of (150 mg / mL).

d) Preparation of external standards

BioRad level 1/2/3: Immunoassay plus Control (IAPC) were used as external standards (NIBSC-B12 / Serum Folate 03/178).

ii) Procedure

The evaporator was prepared before dispensing reagents: under fume hood, (Tecne DRIBlock equipment, DB2B) was set at 60 ° C. The reagents were added to the tubes under nitrogen gas.

In 1.5 mL Eppendorf tubes: the reagents were added as follows:

- 100 µL of Standard, or serum or DTT alone.
- 25 µL of internal standard (no SI in samples used for incorporation tests of 13C, replace with 25 µL DTT 1 M) then shake
- 50 µL Ac. Ascorbic 20 mM. Vortex and incubate for 15 minutes at room temperature away from light.
- 225 µL MeOH, shake and incubate for 30 min at 4 ° (cold precipitation of proteins)
- Shake and Centrifuge 13000 rpm / min 10 min
- Dispense 200 µL of supernatant onto 96-well plates.
- Evaporate at 60 ° C under nitrogen for > 1h.
- Preheat the heat sealer before dispensing the reagents (be careful, to avoid the risk of overheating the device, disconnect completely after use).
- Resuspension, of the dry extract per 100 µL H_2O / 0.1% Formic acid.
- Close the plate with a film and centrifuge for 5 min at 600 rpm.

iii) Analysis by LC:MS/MS

The parameters of the column were noted using the column tracking on the folate workbook. The analysis manual and workbook routine were used to locate the operating parameters for

analysis and composition of buffers and volumes. The height of the probe was then adjusted (probe height 1, Column HSST3 5 cm). A1, B1, weak and strong solutions were prepared and then incubated in the ultrasonic tank for 10 minutes.

Solutions for the mobile phase were as follows:

• Solvent A1: Ac. 100 mM acetic acid (5.7 mL) + 0.1% Formic acid adjust to 1 L using milliQ H_2O

• Solvent B1: 0.1% Ac. Formal in MeOH

• Weak solution: 0.1% Ac. Formic in H2O milliQ

• Strong solutions: 100% MeOH

Balancing of the column:

• Disconnect and remove the fitting in the column compartment using the dedicated keys.

• Connect the column and tighten with the keys

• Reconnect the outlet pipe and close the compartment.

• Turn off the PC

• Clip the column magnet into the dedicated compartment (on the top / right side of the UPLC) and wait for the beep that signals the connection of the column and the UPLC

• Place the plate to be analyzed in rack 1, protected from light

The column output is connected to the bin.

To run the analysis the following steps were followed:

• Start PC> Windows> Analyst

⊗Menu: FOLATES

Configure TAB> Hardware configuration> LCMS> Activate profile (wait for initialization)

On the left panel, click "build acquisition batch (left panel)"

Open folder

⊗ Load the template

Right click: add sample (add the number of missing lines on the template)

⊗ Copy / paste the work list (check the list and position of the samples on the plate). Save changes to acquisition settings

⊗ Submit (send the list of samples to the waiting list)

Acquisition Method: FOLATES_FL_AC ACET_H1_13C

Quantification method: Folate 20150226

⊗click Warming up: Psi must reach a value close to the last recorded on the workbook

⊗ "ready": the UPLC / MS pipe can be connected to the probe.

NB: monitor the delta value which must be <10, Flow rate: 0.6 ml / min, Injection: 10

4 Determination of the concentration levels of free carnitine and acylcarnitine

The profile of free carnitine and acylcarnitine is used to diagnose the presence of deficit in mitochondrial fatty acid oxidation. The analysis of acylcarnitine on whole blood (blotting paper) or on plasma allows the diagnosis of a certain number of deficits. In the current study the concentration of free carnitine as well as acylcarnitine in plasma was achieved using liquid chromatography coupled to mass spectrometry (Chromosystems ®Diagnostics by HPLC and LC- MS / MS, Germany) and using Chromosystems ®Diagnostics kit that allows semi-quantitative analysis. The kit (Chromsystems ®) contains: the mobile phases, the freeze-dried internal standards, the bypass reagent, the reconstitution buffer, the rinsing solution, the extraction buffer, the plates 96 wells, lids for plates and dried blood test on blotting paper. The preparation of the samples for this analysis was based on the efficient extraction of the molecules on blotting paper, post-derivatization in butyl esters and to ensure a reproducible quantification of the molecules, the method is based on the use of stable internal standards with isotopic labeling (deuterated) for calibration and measurements. An internal standard is a molecule that has a deuterium, that is, a H^+ proton. This makes it possible to modify the mass of the molecule and to distinguish it from the analyte to be assayed while retaining the same properties.

The operating mode was in the following order:

i. Reconstitution of the mixture of internal standards

The standards are in is in powder form and hence were reconstituted with methanol. A constant amount was added to each sample as per the manufactures' instructions.

ii. The extraction of acylcarnitine

The proteins in the sample were precipitated with methanol, centrifuged and the supernatant was recovered.

iii. Evaporation

The supernatant was then transferred to a 96-well plate and evaporation was carried out using nitrogen jets.

iv. The derivation

The plate must be completely dry. Butanol was used as the bypass reagent that allows to addition of a butyl group on carnitine molecules to allow better detection (sensitivity gain).

v. Evaporation

It was done in the same way as in step (iii). Then the samples were taken up in a given volume of solvent.

vi. Injection

For acylcarnitine there is no need for separation beforehand, putting in a column is not required. The samples will go directly into the mass spectrometer by a continuous injection.

vii. Quantification

The quantification mode that was used is the Precursor Ion Scan mode. The butyl acylcarnitine have a common characteristic moiety of m / z = 85. This specific fragment ion was selected at Q3 and all parent ions that give this daughter ion were scanned at Q1. This gives a profile of all the acylcarnitine. Each peak was quantified according to its height relative to that of the corresponding internal standard.

5 Evaluation of methionine synthase enzyme activity in heart tissue

Methionine synthase enzyme assay was carried out according to the method described by Chen and Banerjee (Zhiqiang et al., 1995). This method is based on the transfer of a radio-labelled methyl group from Me-THF to homocysteine to form methionine. The separation of two radio-labelled elements is achieved after passing through an anion exchange chromatography column. The eluted fraction (containing methionine) is then counted.

As mentioned earlier, MS enzyme catalyzes the remethylation of homocysteine into methionine using MeTHF as a cosubstrate and MeCbl as a cofactor.

All the reagents were prepared with deoxygenated milli-Q water which was achieved under a stream of nitrogen gas for 30 minutes. The reaction was maintained under a stream of nitrogen throughout the preparation. The reactants and the proteins were incubated for 1 hour at 37 ° C in a thermostatically controlled heating block. Under these conditions the reaction is linear, proportional to the incubation time and the enzyme concentration. The enzymatic reaction was stopped by heating the samples at 95 ° C for 5 minutes to inactivate the enzyme. It was then cooled in ice followed by a centrifugation at 12,000 g at 4 ° C for 10 minutes and subsequently the pellet was removed.

The [14C] methionine formed and the excess [14C] MeTHF were separated by ion exchange chromatography. For this, a column AG1x8 (cationic cation exchange resin Cl-, Bio-Rad) is equilibrated with a wash of 4x5 mL of 0.5N HCl and then another wash of 5x2 mL of milli-Q

water. The column was then loaded with the (100 µL) of sample and the gel is then rinsed with 3 × 1 mL of milli-Q water. [14C] methionine is eluted first because it is not retained by the gel, in contrast to [14C] methyl-tetrahydrofolate. The gel is regenerated by washing with 4x5 ml of 0.5 N hydrochloric acid and the elution of [14 C] methyl-tetrahydrofolate. The radioactivity is counted in Poly-Ethylene tubes (Packard) by mixing 1 volume of eluate with 4 volumes of Pico-FluorTM (Scintillation agent, Packard). The specific radioactivity (Rs) is measured by counting the [14C] methyltetrahydrofolate aliquot. The Rs is expressed in cpm / nmol of methyl group and allows the calculation of the activity of the enzyme which is expressed in nmol / h / mg of proteins.

6 Real time Polymerase chain reaction

6.1 Extraction of RNA

Total RNA from cardiac tissue was isolated using the TRIzol reagent (Invitrogen Life Technologies) and purelink® RNA mini kit (Invitrogen ThermoFisher Scientific) in accordance to TRIzol plus total transcriptome isolation protocol. Frozen heart tissues were pulverized into powder in liquid nitrogen using mortar and pestle. The extraction of RNA was carried out in three steps

i) Homogenization of cardiac tissue in TRIzol

In the first step, for each sample 1000 µL of TRIzol reagent was added to 10 mg of heart tissue powder and homogenized using a needle 23G (0.6 x 16 mm) and 1 ml syringe followed by incubation at room temperature for 5 minutes to allow for complete dissociation of nucleospin complexes in phase locked Eppendoff tubes.

ii) Phase separation

A volume of 0.2 ml of chloroform was then added and then vigorously shaken by hand for about 15 seconds. It was then incubated at room temperature for 2-3 minutes. The homogenate was then centrifuged at more than 12000 g for 15 minutes at 4 °C to separate mixture into three phases (The aqueous phase containing RNA, interphase containing the DNA and the organic phase containing proteins an lipids). The aqueous phase is then transferred to RNAse free tubes. An equal volume of 100 % ethanol was added to the aqueous phase to obtain a 50 % final concentration and then vortexed to mix well. The tubes were inverted in order to disperse any visible air bubbles.

iii) Binding, washing and elution of RNA

The third step involved the binding, washing and elution of RNA from the sample. Less than 700 µL of sample was transferred into a spin cartridge with a collection tube, this was followed by centrifugation at > 12000 g for 1 minute at room temperature and the flow through was discarded. This step is repeated for any remaining sample and the flow through is discarded and the cartridge placed in a new collection tube. A volume 500 µL of wash buffer II with ethanol was added to clean the cartridge and bind the RNA on the column. This was followed by centrifugation at 12000 g for 15 seconds at room temperature and then the flow through was discarded. The washing step was repeated one more time and centrifuged for 1 minute to dry the membrane with bound RNA. The collection tube and the flow through were discarded and the cartridge was inserted into a RNAse free recovery tube. About 30 to 100 µL of RNAse free water was added to the centre of the cartridge and then incubated for 2 minutes at room temperature and the RNA eluted by centrifugation at 15000 g at room temperature. The eluted RNA is then quantified, aliquoted and stored at -80°C until downstream application.

6.2 Quantification of RNA

The extracted RNAs were quantified by reading the optical density (OD) using a spectrophotometer (NanoDrop, Thermo Fisher Scientific) and the concentrations were determined using the measured absorbance at 260 nm (1unit OD corresponds to 40 µg / mL of RNA, Beer Lambert's law). The concentration of RNA was calculated using the following formula

[ARN] = 44 µg / mL x A260 nm x dilution factor.

Protein and organic salt contamination in the RNA was verified by calculating 260 nm / 280 nm and 260 nm / 230 nm absorbance ratios. The 260 nm / 280 nm ratio is used to check the purity of RNA, a ratio of 2.0 indicates the purity of RNA, however a ratio less than 1.8 indicates contamination of RNA by proteins and phenols or with other molecules with absorbance near or at 280 nm. For the 260 nm / 230 nm ratio, a ratio of 2 to 2.2 indicates the purity of RNA however ratios below these values indicates presence of contaminants like phenols, EDTA, carbohydrates and guanidine isothiocyanate salts and other contaminants that absorbs at or near 230 nm.

6.3 Determination of RNA quality and integrity

The quality and integrity of RNA are key factors that influences the utilization of RNA in downstream application that include: RT-qPCR, microarray analysis and transcriptomics. We evaluated the quality of our RNA using the 260 nm / 280 nm and 260 nm / 230 nm ratio and the RNA integrity (RIN) number generated by the bioanalyzer 21000 (Agilent biotechnologies).

The RIN software algorithm classifies the riboeukaryotic total RNA using a numbering system that ranges from 1 to 10, with number 1 being the most degraded RNA and number 10 being the most intact RNA. A RIN of 8 is considered perfect total RNA quality for downstream application while in some cases a RIN of 5 is considered good total RNA quality. The working principle of bioanalyzer involves the use of electrophoretic separation of RNA on microfabricated chips, the separated RNA are subsequently detected through a laser induced fluorescence detection (Yahaya et al., 2011). An electropherogram which gives a detailed visual evaluation of the integrity and quality of total RNA and gel like images are generated by the bioanalyzer software. This software also displays concentration of sample and ribosomal ratios.

6.4 Real time Polymerase chain reaction (RT-qPCR)

From each sample, 1.0 µg total RNA was reverse transcribed into cDNA using 5x PrimeScript RT Master Mix (TAKARA Ozyme). The mixture was incubated at 37 °C for 15 minutes followed by inactivation at 85° C for 5 seconds in PCR thermocycler (C1000 Touch thermal cycler, Bio-Rad). Quantitative PCR (qPCR) was performed with SYBR green (TAKARA Ozyme) on StepOnePlus Real Time PCR system (Applied Biosystems) according to manufactures' instructions. A volume of 20 µL of the qPCR reaction mix consisted of: 1x SYBR premix Taq, 1 ROX ref Dye, 2 µL cDNA, and 0.2 µM for both the forward and reverse primers. The sequences of primers used are listed in **Table 7**. The conditions for PCR were as follows : Initial denaturation and activation of Polymerase enzyme at 95 ° C for 30 seconds , followed by 40 cycles (fast cycling) of denaturation and elongation / hybridization at 95 ° C for 5 seconds and X ° C for 30 seconds respectively (where X ° C dependents on primer hybridization temperature) and the final elongation step at 72 ° C for 7 minutes followed by a denaturation of the polymerase at 95 ° C for 5 seconds gives the melting curves. The Step One Plus Software (Applied biosystems) was used in all the analysis. The fold change levels for the target genes relative to two housekeeping genes (RNA pol II (RNA polymerase II) and RPS29 gene encoding ribosomal protein S29) were calculated using as $2^{-\Delta\Delta Ct}$ method. The Δ Ct of the gene of interest was calculated by subtracting the cycle thresholds (CT) values of reference genes from the Ct of gene of interest. Average Δ Ct of *Mtr* knock out samples minus average Δ Ct of control samples yielded the ΔΔCt.

Gene	Name	Primer sequence		Hybridization Temperature	Product size (bp)
Mtr	Methionine synthase	F	5'-ACACTTGGCCTACCGGATG-3'	63 ° C	99
		R	5'-CCAGCCACAAACCTCTTGAC-3'		
BNP	Natriuretic peptide type B	F	5'-GCTGCTTTGGGCACAAGATAG-3'	65 ° C	81
		R	5'-GGTCTTCCTACAACAACTTCAG-3'		
ANP	Natriuretic peptide type A	F	5'ACCTGCTAGACCACCTGGAGGAG-3'	66 ° C	347
		R	5'-CCTTGGCTGTTATCTTCGGTACCGG-3'		
α-MHC	Alpha-myosin heavy chain	F	5'-ACGGTGACCATAAAGGAGGA-3'	63 °C	67
		R	5'-TGTCCTCGATCTTGTCGAAC-3'		
β-MHC	Beta-myosin heavy chain	F	5'-GCCAACACCAACCTGTCCAAGTTC-3'	63 °C	203
		R	5'-TGCAAAGGCTCCAGGTCTGAGGGC-3'		
Sirt3	Sirtuin 3	F	5'-ATCCCGGACTTCAGATCCCC-3'	62 °C	126
		R	5'-CAACATGAAAAAGGGCTTGGG-3'		
Col1a1	Collagen, type I, alpha 1 (Col1a1)	F	5'-TAAGGGTCCCCAATGGTGAGA-3'	59 °C	203
		R	5'-GGGTCCCTCGACTCCTACAT-3'		
Col3a1	Collagen, type III, alpha 1 (Col3a1)	F	5'-ACGTAGATGAATTGGGATGCAG-3'	59 °C	154
		R	5'-GGGTTGGGGCAGTCTAGTG-3'		
Cox7a1	Cytochrome c oxidase subunit 7A1	F	5'-GCTCTGGTCCGGTCTTTTAGC-3'	61 °C	100
		R	5'-GTACTGGGAGGTCATTGTCGG-3'		
Hk1	Hexokinase 1	F	5'-CGGAATGGGGAGCCTTTGG-3'	58 °C	269
		R	5'-GCCTTCCTTATCCGTTTCAATGG-3'		
Atp5j	ATP synthase, H+ transporting, mitochondrial F0 complex, subunit F	F	5'-TATTGGCCCAGAGTATCAGCA-3'	60 °C	134
		R	5'-GGGGTTTGTCGATGACTTCAAAT-3'		
Pdk3	Pyruvate dehydrogenase kinase, isoenzyme 3	F	5'-TCCTGGACTTCGGAAGGGATA-3'	58°C	133
		R	5'-GAAGGGCGGTTCAACAAGTTA-3'		

R: Reverse and F: Forward.

Table 7: Sequences and conditions of primers used for RT-qPCR

7 Western blot analysis

7.1 Extraction and preparation of protein for western blot analysis

Frozen heart tissues were pulverized into powder in liquid nitrogen using mortar and pestle. The powder was homogenized at 4 °C with RIPA (Radio immuno precipitation assay) lysis buffer containing 1 % NP40, 0.5 % DOC, 0.1 % SDS (w/v) ,1 mM Na3VO4, 1 mM PMSF and 1 % PIC (pH 8.0). About 50 mg of heart tissue powder per sample was homogenized in 550 µL of RIPA buffer and incubated for 10 minutes at 4 °C. After incubation the lysates were mechanically sheared 10 to 20 times using needle 23G (0.6 x 16 mm) and 1 ml syringe then sonicated for 15 minutes at 4 °C. After sonication, the lysates underwent three cycles of freezing and thawing (liquid nitrogen/ water-bath at 37 °C for 1 minute each) followed by centrifugation at 12000 rpm for 30 minutes to recover the supernatant which was aliquoted and stored at -80

°C until analysis. Equal volumes of 2x Laemmli buffer containing 0.05 % Betamecarptoethanol were mixed with 30 µg of protein samples and heated at 96 °C for 5 minutes.

7.2 Determination of protein concentration using Bicinchoninic acid protein assay reagent

Bicinchoninic acid protein assay reagent (BCA; Interchim, Montluçon cedex France) was used to determine the total protein concentration of the supernatant. The BCA protein assay is a method for the colorimetric determination of proteins concentration in a sample. The principle of this technique is based on the ability of proteins to reduce Cu (II) cupric ion (Cu^{+2}) to Cu (I) cuprous ion (Cu^{+}) in alkaline solution and the ability of bicinchoninic acid to form a purple complex with cuprous ions. The reduction of Cu^{+2} to Cu^{+} is mainly caused by the amino acid residue like cystine, tryptophan and tyrosine in the protein sample. The bicinchoninic acid and cuprous ions complex has a high absorbance between 540 and 590 nm thus allowing the determination of proteins concentration. This method enables the determination of protein concentration that ranges from 0.2 to 1.0 mg/ml. First, a standard range (0, 50, 100, 200, 400, 800, 1200, 1600 and 2000 µg / mL) in triplicate was prepared from a stock solution of bovine serum albumin (BSA) at 2 mg / ml diluted in RIPA lysis buffer. A volume of 25 µL of each dilution of BSA and of each sample to be assayed were distributed on a 96-well plate. To prepare the working reagent, 50 volumes of Reagent A BCA, Protein Assay® Reagent (Uptima) was mixed with 1 volume of Reagent B (CuSO4). A volume of 200 µL of the working reagent was distributed on the wells and the plate was then incubated at 37 ° C for 30 minutes. The absorbance of the proteins at 570 nm was measured by spectrophotometer (MultiSkan Go, thermo Scientific). Then, the protein concentration of each sample was determined from the standard curve equation.

7.3 Preparation of protein sample for western blot analysis

Equal volumes of 2x Laemmli buffer containing 0.05 % Betamecarptoethanol were mixed with 30 µg of protein samples and heated at 96 °C for 5 minutes to denature the proteins.

7.4 Preparation of the sodium dodecyl sulfate polyacrylamide gel

Sodium dodecyl sulfate (SDS) Polyacrylamide gel percentage was chosen based on the size of the protein of interest. For small size proteins a high percentage of gel is used while for larger proteins a lower percentage gel is used as shown in **Table 8**. The composition of the stacking and separation gels for SDSPAGE Tris / Glycine are shown in **Table 9**.

Size of the protein in KDa	Percentage (%) of gel
4-40	20
12-45	15
10-70	12
15-100	10
25-200	8
>200	6

Table 8: Concentration of polyacrylamide gels for different sizes of proteins

Solution pour préparation des gels de concentration et de séparation pour SDS-PAGE Tris/Glycine **Acrylamide 40%**					
		1 gel	2 gels	3 gels	4 gels
gel de séparation		10 ml	20 ml	30 ml	40 ml
6%	H_2O MQ	5,8	11,6	17,4	23,2
	Acrylamide Mix 29:1	1,5	3	4,5	6
	Tris 1,5M pH 8,8	2,5	5	7,5	10
	SDS 10%	0,1	0,2	0,3	0,4
	APS 10%	0,1	0,2	0,3	0,4
	TEMED	0,008	0,016	0,024	0,032
8%	H_2O MQ	5,3	10,6	15,9	21,2
	Acrylamide Mix 29:1	2	4	6	8
	Tris 1,5M pH 8,8	2,5	5	7,5	10
	SDS 10%	0,1	0,2	0,3	0,4
	APS 10%	0,1	0,2	0,3	0,4
	TEMED	0,006	0,012	0,018	0,024
10%	H_2O MQ	4,8	9,6	14,4	19,2
	Acrylamide Mix 29:1	2,5	5	7,5	10
	Tris 1,5M pH 8,8	2,5	5	7,5	10
	SDS 10%	0,1	0,2	0,3	0,4
	APS 10%	0,1	0,2	0,3	0,4
	TEMED	0,004	0,008	0,012	0,016
12%	H_2O MQ	4,3	8,6	12,9	17,2
	Acrylamide Mix 29:1	3	6	9	12
	Tris 1,5M pH 8,8	2,5	5	7,5	10
	SDS 10%	0,1	0,2	0,3	0,4
	APS 10%	0,1	0,2	0,3	0,4
	TEMED	0,004	0,008	0,012	0,016
15%	H_2O MQ	3,5	7,1	10,6	14,2
	Acrylamide Mix 29:1	3,8	7,5	11,3	15
	Tris 1,5M pH 8,8	2,5	5	7,5	10
	SDS 10%	0,1	0,2	0,3	0,4
	APS 10%	0,1	0,2	0,3	0,4
	TEMED	0,004	0,008	0,012	0,016
		4 ml	8 ml		16 ml
Stacking (concentration)	H_2O MQ	2,92	5,83		11,66
	Acrylamide Mix 29:1	0,5	1		2
	Tris 0.5M pH 6.8	0,5	1		2
	SDS 10%	0,04	0,08		0,16
	APS 10%	0,04	0,08		0,16
	TEMED	0,004	0,008		0,016

Table 9*:* **Conditions for preparation of the stacking and separation gels for PAGE**

7.5 Electrophoresis

Electrophoresis is a technique that allows the differentiation and characterization of negatively charged proteins in an electric field based on their molecular weights. SDS-PAGE is a useful technique that allows the separation of proteins based on their molecular weight through the polyacrylamide gel. In SDS-PAGE the secondary and non-sulfide linked tertiary structure of proteins are denatured by SDS, this detergent also confers a negative charge to the denatured protein hence allowing easy migration through the polyacrylamide gel (Brunelle & Green, 2014). We used a discontinuous gel with upper stacking gel and lower resolving gel. The stacking gel allows the proteins to migrate quickly to the resolving gel, it has a lower percentage of polyacrylamide and a lower pH of 6.8. On the other hand, the resolving gel allows for the separation of protein, it has a higher percentage of polyacrylamide and a pH of 8.8. A total of 30 μg of each protein sample and 5μL of the molecular weight was deposited on the prepared SDS polyacrylamide gel. Electrophoresis was performed at room temperature in a vertical migration system (Mini- PROTEAN® II, Bio-Rad Laboratories, Marnes-la-Coquette, France) in 1X migration buffer pH 8.3. The stock solution (10X) of migration buffer consists of 250 mM Tris, 1.92 M glycine and 1 % SDS. A constant voltage of 80 V for 15 minutes was used to migrate the proteins across the stacking gel after which the voltage was increased to between (110 to 120) V until the migration front reached the bottom of the gel.

7.6 Transfer of proteins to the membrane

Proteins were transferred to either nitrocellulose or PVDF membranes (Amersham Hybond, GE Healthcare life science, Germany) using the semi-liquid transfer technique (BIO-RAD Trans-Blot ® Turbo™ Transfer system). The membranes were cut to the size of the gel (7 x 8.5 cm). The PVDF membranes were activated by immersion in 100 % ethanol for 5 seconds. The membranes and the filter paper were socked briefly in cold (4 ° C) 1X transfer buffer. To carry out the transfer in the Trans-Blot system, different elements of the sandwich were superimposed on the anodic platform of the transfer system in the order listed below.

- 3 layers of 3mm Whatman® filter paper
- Activated PVDF or nitrocellulose membrane
- The polyacrylamide gel
- 3 layers of 3mm Whatman® filter paper

The anodic platform with the sandwich is covered and then placed on RAD Trans-Blot ® Turbo^{TM} Transfer system. The transfer was achieved using the standard transblot protocol at 25 V and 0.1 A for 30 minutes.

7.7 Immunoblotting

Depending on the antibody used, the blocking buffer was made either with 5 % w/v non-fat/ skimmed milk or with 5 % w/v BSA in 1X TBS buffer containing 0.1 % Tween-20 (TBST). The membranes were blocked in the respective blocking buffer for one hour at room temperature with slow agitation. The purpose of the blockage was to saturate the membrane hence prevent nonspecific binding of the antibody. After blocking, the membranes were incubated with a primary antibody specific for the protein of interest overnight at 4 ° C with mild agitation. The conditions of the antibodies used are shown in **Table 10**. Subsequently the membranes were washed four times for 10 minutes each with 1x TBST buffer. The washed membranes were then incubated with the appropriate secondary antibody conjugated to horse radish peroxidase for 1 hour at room temperature. The membranes were then washed four times for 10 minutes each in 1X TBST. Enhanced chemiluminescence (ECL kit, Bio-Rad laboratories, USA) was used to visualize the immuno-reactive proteins in FusionFx7 detector (ThermoFischer). ImageJ software was used for densitometric analysis of the protein bands. The data was normalized to beta actin.

`

Antibody	Supplier	Reference NO	Dilution1° antibody	Host	Dilution 2° antibody	Blocking	Membrane	% GEL	Size kDa
Annexin 4	Euromedex	GTX30048	1/1000	Rabbit Poly	1/10000	5% bsa	0,2 µm Nitro	12	35
Annexin A5	Cell signaling	8555S	1/1000	Rabbit Poly	1/10000	5% BSA	0,2 µm PVDF	12	30
AT1	GeneTex	GTX87790	1/1000	Rabbit Poly	1/10000	5% BSA	0,2 µm Nitro	12	41
AT2	US biological	146514	1/1000	Rabbit Poly	1/10000	5% BSA	0,45 µm PVDF	10	41
αSMA	Cell signaling	14968	1/700	Rabbit Poly	1/7000	5% milk	0,45 µm Nitro	10	42
β Actine-HRP	Abcam	ab197277	1/7000	Mouse mono	none	5% BSA	any (ref protein)		42
BMP7	Abcam	ab54904	1/1000	Mouse	1/10000	5% BSA	0,2 µm Nitro	12	49
Caspase 1	Abcam	ab108362	1/1000	Rabbit Poly	1/10000	5% milk	0,2 µm PVDF	12	45
CD36	Abcam	ab124515	1/1000	Rabbit Poly	1/10000	5% BSA	0,45 µm Nitro	10	88(53)
HSPB3	Abcam	ab213591	1/1000	Rabbit poly	1/1000	5% BSA	0,2 µm PVDF	12	17
Hsp27	Cell signaling	2442	1/1000	Rabbit	1/10000	5% BSA /5%milk	0,2 µm Nitro	12	27
HSP90 (C45G5)	Cell signaling	4877	1/700	Rabbit	1/7000	5% BSA	0,45 Nitro	10	90
IL 1β	Abcam	ab9722	1/1000	Rabbit poly	1/10000	5% milk	0,2 µm PVDF	12	31/18
MMP2	Abcam	ab37150	1/1000	rabbit	1/10000	5% BSA	0,45 µm PVDF	10	72
Mpv17	Sigma	SAB2501439	1/1000	goat	1/10000	5% milk	0,2 µm PVDF	12	20 &26
TGFβ1	Abcam	ab66043	1/700	rabbit poly	1/7000	5% BSA	0,2 µm Nitro	10	44 (13)
Sirt1	Cell signalling	8469S	1/700	rabbit	1/2000	5% BSA	0,45 µm Nitro	10	120
Sirt3	Abcam	ab118334	1/1000	Goat	1/10000	5% BSA	0,2 µm Nitro	12	29
MT-ATP6	Abcam	ab 192423	1/700	Rabbit	1/7000	5% BSA	0,2 µm Nitro	12	25
MTR	Abcam	Ab66039	1/1000	Rabbit	1/10000	5% milk	0,45 µm PVDF		141
Cyt b	Interchim	BS-3951R	1/1000	Rabbit	1/10000	5% milk	0,2 µm PVDF	12	43
Cre	Cell signalling	12870	1/1000	Rabbit	1/10000	5% milk	0,45 µm PVDF	12	37

Table 10: List of antibodies used for western blotting analysis

8 Immunohistology

8.1 Treatment of fixed tissues for histological analysis

After fixation, the tissues were placed in cassettes. They were then dehydrated and embedded with paraffin in a (Excelsior ES type automaton) by passing the tissues through a series of successive baths of formaldehyde, alcohol, toluene and paraffin. After dehydration step, the tissues were placed in a mold filled with paraffin maintained in the liquid state. Once the tissues were properly positioned, the mold was placed on a cooling plate to solidify the paraffin.

8.2 Cutting of tissues

Tissue sections of 5 µM thick were cut with a microtome (Thermo Scientific, Microm HM325) and then deposited on SuperFrost Plus slides placed on hot plate heated at 50 ° C. Once the tissue sections were well fixed, the slides were incubated overnight at 37°C then kept at 4 ° C until histological analysis was carried out.

8.3 Deparaffination of tissue and unmasking of antigens

The slides were placed in slide holders and then heated at 60 ° C for 30 minutes. After this, the slides underwent deparaffination at room temperature in Histo-clear solution (National Diagnostics, HS-200). The slides were incubated 2x in Histo-clear solution for 3 minutes each. The slides were then dehydrated by successive incubation in decreasing concentrations of ethanol (100 %, 95 %, 70 % and 50 %) for 3 minutes each and then in a bath of distilled water for 5 minutes. After this step, the antigenic sites were unmasked by incubating the slides in 10 mM EDTA-Na2 buffer at pH = 8 for 30 minutes at 95 ° C in a water bath. The slides were then placed in ice for 20 minutes to cool after which they were washed three times in 1X PBS.

8.4 Immunofluorescence

After deparaffination, unmasking and washing steps described above, the cell membranes were permeabilized by incubating the slides in 1X PBS with 0.1 % Triton for 10 minutes at room temperature. The slides were then washed three times in 1X PBS for 5 minutes each. The area around the tissue was dried and with the help of the hydrophobic pen DakoPen ™ a boundary was marked around the tissues. Non-specific sites were blocked with around 200 µl of a solution containing a mixture of 10 % BSA-1X PBS for 1 hour at room temperature. A volume of 200 µl of primary antibody diluted 1/200 in 10 % BSA-1X PBS was then added to the tissue sections and incubated overnight at 4 ° C in a moist dark box. The primary antibodies used were Y14; ab181038, Hnrnpa1; ab5832 and HUR/ELAV1; ABIN577055. On the second day, the slides were washed in three times in 1X PBS for 5 minutes each. After washing, 200 µl of the

appropriate secondary antibody (Alexa fluorine 488 donkey anti-rabbit IgG, Molecular Probes) diluted 1/2000 in 10% BSA-1X PBS was deposited and incubated for 1 hour at room temperature in the dark. The slides were then washed three times in 1X PBS for 5 minutes each. The cells nuclei were then stained with DAPI (4 ', 6'-diamidino-2-phenylindole) diluted 1/5000 in 1X PBS for 5 minutes at room temperature in the dark room. Finally, the slides were washed three times in 1X PBS for 5 minutes each and then slides were mounted using mounting liquid (Dako Fluorescent Mounting Medium, Dako S3023) and then stored in obscurity overnight at 4 ° C and then observed on the confocal microscope (Nikon C2).

8.5 Picrosirius red staining

Picrosirius red stain is a histological staining technique that is used to investigate the presence of fibrosis in tissue. The Sirius Red stains the collagen and reticulin fibers in red while the nuclei and cytoplasm are stained yellow. Formalin-fixed paraffin-embedded mouse heart ventricles were cut into 5 µM-thick sections. Picrosirius red staining involves three steps described below.

i) Deparaffinization and rehydration of the slides:

The slides were immersed in three xylene baths for 5 minutes each with agitation. Subsequently, the slides were immersed in successive decreasing percentage of ethanol, first they were immersed in two baths of absolute alcohol (100 %) for 3 minutes each with agitation followed by 80 % ethanol bath for 2 minutes with agitation. Finally, the slides were rehydrated using distilled running distilled water.

ii) Coloration

The slides were immersed in 0.2 % phosphomolybdic acid for 1 minute then rinsed in running water. After which the slides were stained with Sirius Red (filtered before use) for 30 minutes then rinsed under running water. Subsequently, the slides were immersed in 1N hydrochloric acid for 1 minute then rinsed under running water followed by a second rinsing in a jet of 95 % ethanol. Finally, the slides were rinsed with two baths of 100 % ethanol with agitation.

iii) Xylene and mounting

The slides were first immersed in three xylene baths with agitation then the slides were mounted on 24x60mm slides using Eukitt ® mounting medium (VWR Prolabo, Fontenay-sous-Bois).

iv) Imaging

After staining with Picrosirius red stain, the stained sections were observed under normal brightfield microscopy. The collagen-enriched areas were stained red with Picrosirius red stain while the nuclei and cytoplasm were stained in yellow. Collagen was quantified by measuring

the area of collagen relative to the entire sample area with the color deconvolution plug-in in ImageJ. The area of collagen was expressed as fold-increase in fibrotic area compared to control samples.

8.6 Masson's Trichrome staining

Masson's Trichrome staining is a histological staining technique that is used to investigate the presence of fibrosis in fixed tissues. Formalin-fixed paraffin-embedded mouse heart ventricles were cut into 5 µM-thick sections using microtome. Hematoxyline stains the nuclei purple, Fuchsine Ponceau colors the cytoplasm in pink-red, red blood cells and keratin in bright red while Aniline blue stains collagen fibers in blue.

Masson's Trichrome staining procedure involves three steps described below.

i) Deparaffinization and rehydration of the slides

The slides were immersed in three xylene baths for 5 minutes each with agitation. Subsequently, the slides were immersed in successive decreasing percentages of ethanol, first they were immersed in two baths of absolute alcohol (100 %) for 3 minutes each with agitation followed by 80 % ethanol bath for 2 minutes with agitation. Finally, the slides were rehydrated with running distilled water.

ii) Coloration

The slides were stained with haematoxylin (Shardon Gill 2 Hematoxylin, Thermoscientific) for 10 minutes. The slides were then rinsed under running water then immersed in ammonia water until the cup is blue. After this the slides were rinsed with running water and then with distilled water. Subsequently, the slides were stained with Fuchsine Ponceau for 10 minutes then rinsed with distilled water. After the rinsing, the slides were immersed in phosphomolybdic acid (red lightening) for 3 minutes before they were stained with Aniline Blue for 1 minute. After staining with Aniline Blue, the slides were quickly dipped in acetic acid water (Merck, Darmstadt) to remove excess dye then rinsed in absolute ethanol with agitation.

iii) Xylene and mounting

The slides were dipped in three xylene baths with agitation. The cuts must be uniformly transparent. The slides were then mounted with 24x60mm coverslips using the Eukitt ® mounting medium (Eukitt ®, Freiburg).

iv) Imaging

After staining with Massons' Trichome, the stained sections were observed under normal brightfield microscopy. The collagen-enriched areas appeared blue. Collagen was quantified by measuring the area of collagen relative to the entire sample area with the color deconvolution

plug-in in ImageJ. The collagen area was expressed as fold-increase in fibrotic area compared to control samples.

9 Omics studies

9.1 Proteomic analysis by LC-MS / MS

Total proteins from the heart tissue were extracted using RIPA lysis buffer and quantified using BCA Protein Assay kit as described above (Interchim, Muntluçon Cedex France). For each sample, 75 µg of protein was resolved in 10 % SDS-PAGE gel electrophoresis by a short migration of 6-7 mm. After migration the gel was stained with Coomassie blue and then the 6-7 mm zone was cut into three equal parts. Direct digestion of gel sections was performed in triplicate overnight at 37°C by sequencing grade trypsin (12.5 µg/ml; Promega, Madison, Wi, USA) in 20 µl of 25 mmol/L NH_4HCO_3). LC-MS/MS acquisition was performed with a 2-hour gradient as described by (Télot et al., 2018). MS/MS data were processed with an in-house Mascot search server (Matrix Science, Boston, MA; version 2.4.1). Label-free quantification in between subject analysis was performed on raw data with Progenesis-Qi software 4.1 (Nonlinear Dynamics Ltd, Newcastle, U.K.) using the following procedure: (i) chromatograms alignment, (ii) peptide abundances normalization, (iii) statistical analyses of features, and (iv) peptides identification using the Mascot server. A decoy search was carried out and the significance threshold was fixed to 0.05. The resulting files were imported into Progenesis-LC software. Peptides with ion score less than 15 were rejected. Conflicts for the identification of some peptides were resolved.

Resultant proteome was filtered for remnants of missing or zero-expressed values, giving a final count of 1998 unique proteins. Data were then standardized using the VMR-ratio volume normalization method and log2-transformed (Meunier et al., 2007). Hierarchical cluster analyses were performed and heatmaps were explored with PermutMatrix on centered protein abundances (Caraux & Pinloche, 2005), with Euclidian distance as metrics and Ward's agglomeration. Functional annotations of disease associations were achieved with the Open Targets online platform (Carvalho-Silva et al., 2019) (https://www.targetvalidation.org). GO terms and biological pathways were performed using Enrichr (Kuleshov et al., 2016).

9.2 RNA Hi Seq sequencing and transcriptome analysis

First, total mice heart tissue RNAs were extracted and quantified as described above. After quantification and determination of quality of RNA, the RNAs with RIN >8.0 were subjected to DNAse I treatment where 5µg of each RNA were treated with MBU Baseline -ZERO^{TM}

DNAse (ref#DB0715K, Epicentre) for 25 minutes at 37°C followed by Phenol/chloroform and chloroform extraction. Three volumes of 96 % ethanol were used to precipitate the RNA using 15 mg of glycoblue and 0.3M AcONa. After a wash with 80 % ethanol, the pellet was re-suspended in 21 µl of RNAse free water. The quality of RNA before and after DNAse I treatment was checked by capillary electrophoresis using a PicoRNA chip on Bioanalyzer 2100 (Agilent). A volume of 2 µg of each DNAse I treated RNA was used for ribosomal RNA (rRNA) depletion using human Ribo-Zero rRNA removal kit (ref#MRZH116, Illumina) following the manufacturer's instructions. Elution of rRNA-depleted RNA was done in 8 µl of RNase free water. Effectiveness of depletion of rRNA was checked by capillary electrophoresis using a PicoRNA chip on Bioanalyzer 2100 (Agilent). A total of 20 ng of each rRNA-depleted RNA were then converted to library using the Scriptseq V2 RNA-Seq kit (ref#SSV21106, Illumina) following the manufacturer's instructions. After 15 cycles of PCR amplification, the libraries were purified using the Agencourt AMPure XP beads (ref#A63880, Beckman Coulter) at a ratio of 0.9x.

The quality of libraries were assessed using a high sensitivity DNA chip on a Bioanalyzer 2100 (Agilent) after which they were quantified using a fluorometer (Qubit 3.0 fluorometer, Invitrogen) Libraries were multiplexed and subjected to high-throughput sequencing using an Illumina HiSeq 1000 instrument with 2*101 bp paired-end read runs and loaded at 12 pM per lane.

After demultiplexing, reads were compiled in standard FASTQ files. Quality control was performed using FastQC v0.11.5 (http://www.bioinformatics.babraham.ac.uk/projects/fastqc). Bad quality sequences and reads contaminated by adapters were trimmed using cutadapt 1.11 with parameters "-a AGATCGGAAGAG -A AGATCGGAAGAG -m 30 --no-indels -O 5". Mapping of the resulting reads was performed by HISAT2 v2.0.4 (Kim, Langmead, & Salzberg, 2015). On a version of the GRCm38 reference genome which accounts for splicing donor and acceptor sites and SNP polymorphism (https://cloud.biohpc.swmed.edu/index.php/s/grcm38_snp/download).

Spliced isoforms were assembled from the reconstructed transcripts obtained with Stringtie v1.3.3b (Pertea et al., 2015), allowing for the identification of new isoforms in addition to those overlapping known transcripts (by at least 80% of their length) from the Ensembl official annotations (Mus_musculus.GRCm38.92.gtf). Transcripts with very low expression across all samples (mean read coverage < 30) were removed from further analysis. Data were normalized with the trimmed means of M-values (TMM) (Robinson & Oshlack, 2010)method, then log2-transformed and rendered in counts per million. Unsupervised clusterings and functional

annotations were carried out as previously described (Gauchotte et al., 2017). Additional functional annotations and GO terms enrichment analyses were performed with EnrichR (https://amp.pharm.mssm.edu/Enrichr) and PANTHER while diseases associations were achieved using Open Targets Platform.

10 Statistical analysis

For both proteome and transcriptome, linear modelling with empirical Bayes (from the bioconductor limma package) (Ritchie et al., 2015) was applied to assess differential expression at protein and at gene level between Control and *Mtr cKO* groups, respectively. Differential expression *P*-values were obtained by using a moderated Student t-test and adjusted for the false discovery rate (FDR) with the Benjamini-Hochberg procedure. Integrations of paired proteomic and transcriptomic samples were performed both ways on the 1720 total shared features: 1) without prior knowledge by computing the entire Spearman's correlation matrix between genes and proteins expression levels, and 2) by driving the proteome mining with the significant down and upregulated transcriptome clusters. Functional annotations and disease association analyses were then carried out on extracted features with Enrichr and Open Targets. PANTHER gene list analysis was used to analyze functional annotation so of the transcriptome. All *P*-values or FDR < 5 % indicated statistical significance, with relevance according to the feature observed (protein, gene, cluster, correlation, functional term).

Non-omics data were analyzed using Stata 12.0 statistics and data analysis software (stataCorp, College station TX, USA) and continuous variables were expressed as means ± standard error of means (SEM). One-way analysis of variance (ANOVA) was used to compare the raw data. Student t-test was used for statistical analysis of the western blotting densitometric and RT-qPCR data. Logarithmic transformations were used to normalize skewed distributions. Statistical significance was denoted by Asterisks Asterisks * P <0.05, ** P <0.01, *** P <0.001, the minimum statistical significance level was set at P <0.05.

RESULTS

RESULTS

MODEL 1

1 Validation of the study Model

1.1 Confirmation of the effective deletion of Mtr gene in the cardiomyocytes

To study cardiac consequences of specific invalidation of *Mtr* in the cardiomyocytes, confirmation of the effective deletion of *Mtr* gene in heart was a prerequisite. To achieve this, both the transcript and protein expression levels of *Mtr* gene and MTR protein in the heart tissues of 5-months old *Mtr cKO* and control animals were evaluated using RT-qPCR and western blot analysis respectively. Methionine synthase activity was also evaluated using a standard enzyme assay.

1.1.1 Expression of *Mtr* gene in the heart

The expression level of *Mtr* gene in the hearts of 5 months old mice was evaluated using RT-qPCR. As expected, *Mtr* gene was significantly downregulated in the hearts of *Mtr cKO* mice in comparison to control mice ($P = 0.001$; **Figure 26**). Our transcriptomic results also revealed 5.4-fold decrease in the expression of *Mtr* gene in the hearts of *Mtr cKO* in comparison to control animals ($P = 6.64E^{-06}$, FDR = 0.0055).

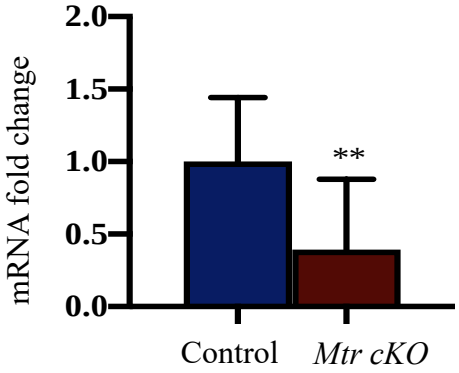

Figure 26: Expression levels of *Mtr* gene analyzed by RT-qPCR

Expression level of *Mtr* gene in the heart tissues of 5-months old mice analyzed by RT-qPCR. Means ± SEM, n = 6 to 10 per group, *P< 0.05 **P< 0.01, ***P< 0.001.

1.1.2 Expression of MTR /MS and Cre-recombinase proteins in the heart

Given the decreased expression of *Mtr* gene in the hearts of *Mtr cKO* animals. We further evaluated the expression levels of both Cre-recombinase and MTR / MS by western blotting. As expected, the expression level of MTR protein was significantly decreased in the hearts of *Mtr cKO* mice in comparison to the control mice (P = 0.04; **Figure 27**). Interestingly, Cre recombinase, a 38 KDa enzyme that catalyzes site-specific recombination of LoxP sites was only expressed in the hearts of *Mtr cKO* mice (P = 0.001; **Figure 27**). These results confirm the successful invalidation of *Mtr* gene in the cardiomyocytes of our study model. To confirm the tissue specificity of *Mtr* gene deletion, we assessed the expression levels of methionine synthase in the liver, we found no significant difference between *Mtr cKO* and control liver (P = 0.230; **Figure 28**).

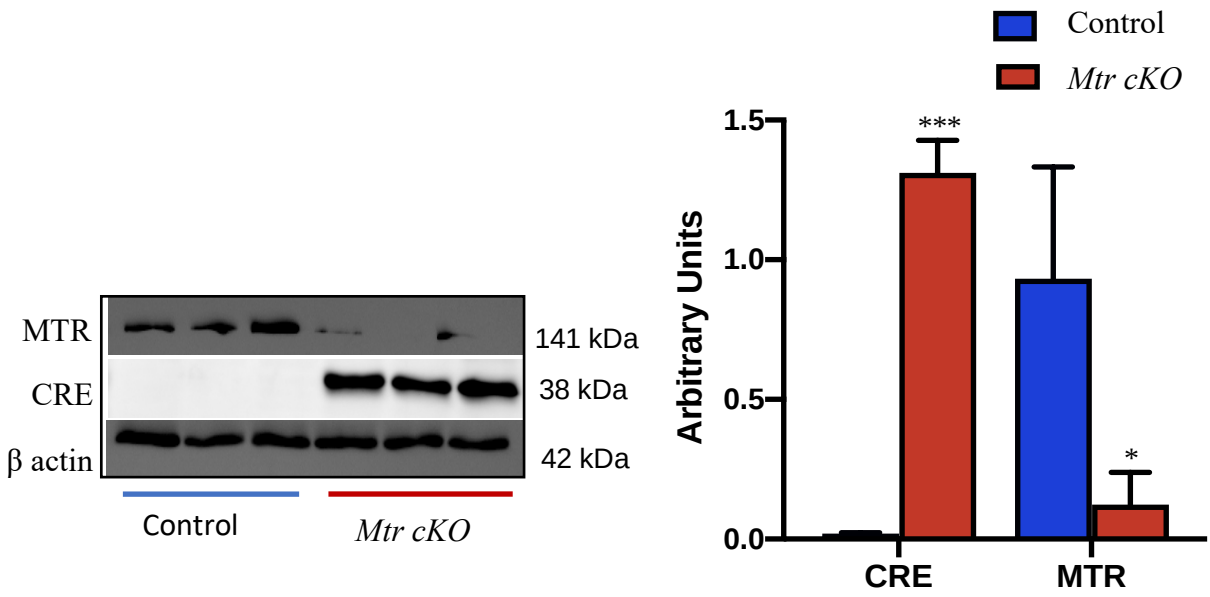

Figure 27: Expression levels of *MTR* and Cre proteins in the hearts of controls and *Mtr cKO* analyzed by western blotting

Western blots and densitometric analysis showing the expression levels of MTR protein and Cre recombinase in the heart tissues of 5-month old mice (Means ± SEM, n = 3 to 6 per group, * $P < 0.05$ ** $P < 0.01$, *** $P < 0.001$)

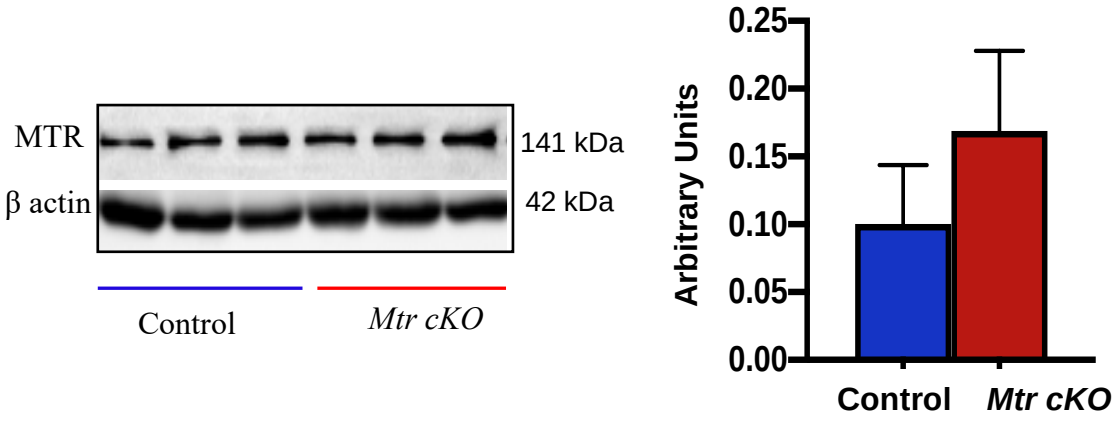

Figure 28: Expression level of MTR protein in the liver analyzed by western blot

Western blot and densitometric analysis showing the expression levels of MTR protein in the liver of 5 months old *Mtr cKO* and control mice (Means ± SEM, n = 3 to 6 per group, **P* < 0.05 ** *P* < 0.01, *** *P* < 0.001).

1.1.3 Evaluation of methionine synthase activity in the heart

Given the decreased expression of methionine synthase in the hearts of *Mtr cKO* animals, we further evaluated the activity of methionine synthase in the heart tissues of the *Mtr cKO* and control animals. The activity of methionine synthase was expressed as nmol/h/mg of the protein. This analysis revealed more than 6-fold decrease in methionine synthase activity in the hearts of *Mtr cKO* in comparison to the control hearts (0.074 ± 0.045 vs 0.438 ± 0.040 mmol/h/mg, *P* = 0.0018; **Figure 29**). This finding confirms methionine synthase dysfunction in the hearts of *Mtr cKO*. Together, these results confirm effective cardiac specific homologous invalidation of *Mtr* gene in our study model.

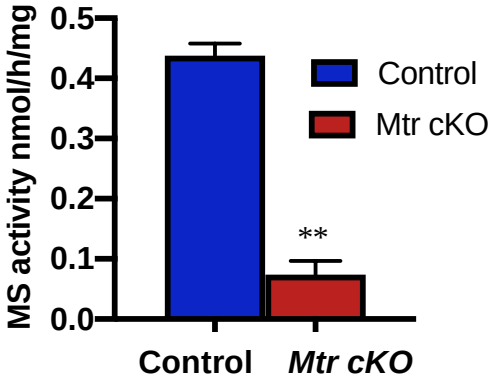

Figure 29: Activity of Methionine synthase enzyme in the myocardium

Enzyme activity of methionine synthase in the heart of 5 months old mice evaluated using a standard enzyme assay (Means ± SEM, n = 6 to 10 per group, * *P* < 0.05, ** *P* <0.01, *** *P* < 0.001).

1.2 Consequences of cardiac specific deletion of *Mtr* gene on one- carbon metabolism (metabolic phenotype).

Methionine synthase plays a crucial role in one-carbon metabolism. As mentioned earlier, it catalyzes the remethylation of homocysteine to methionine and tetrahydrofolate using 5-methyl tetrahydrofolate from folate cycle as co-substrate and methyl cobalamin (a derivative of vitamin B12) as cofactor. Given, the effective invalidation of *Mtr* gene and the decreased methionine synthase activity in our study model, we investigated the consequences of cardiac invalidation of *Mtr* gene on one-carbon metabolism. This was achieved by determining the concentration of metabolites (SAM and SAH) of one-carbon metabolism in the myocardium using LC-MS/MS.

1.2.1 Determination of the concentration of S-adenosyl homocysteine (SAH) and S-adenosyl methionine in heart tissue (SAM).

The concentration of SAH and SAM in heart tissue was investigated using LC-MS/MS.

We found that cardiac specific invalidation of *Mtr* gene produced increased SAH concentration in the Myocardium (251.20 ± 51.90 vs 107.73 ± 21.48 nmol/g of tissue, $P = 0.05$), however the concentration of SAM was comparable between the two groups (847.40 ± 129.91 vs 663.75 ± 52.58 nmol/g of tissue , $P = 0.327$; **Figure 30A**). As consequence, the SAM:SAH ratio was significantly decreased in *Mtr cKO* as compared to controls (3.6 ± 0.32 vs 6.75 ± 0.99, $P = 0.0143$; **Figure 30B**). Together, these results show that cardiomyocytes specific invalidation of *Mtr* gene impairs one-carbon metabolism and remethylation of homocysteine to methionine in the hearts of *Mtr cKO*

A.

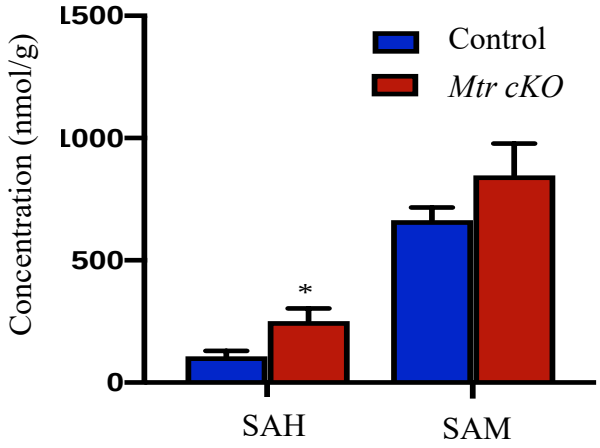

B.

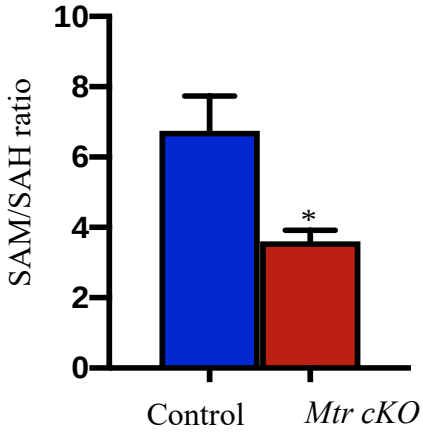

Figure 30: Concentration of metabolites of one-carbon metabolism and remethylation of homocysteine in the heart analyzed using LC-MS/MS.

A. Concentration of S-adenosyl homocysteine (SAH) and S-adenosyl methionine (SAM) in hearts of *Mtr cKO* and control mice. B. The ratio of SAM to SAH. (Means ± SEM, n = 3 to 6 per group, * $P < 0.05$ ** $P < 0.01$, *** $P < 0.001$)

1.2.2 Determination of folate concentration in heart

The concentration of folates in the heart tissues of *Mtr cKO* and control mice were analyzed using LC-MS/MS. Formyl tetrahydrofolate (fTHF) which is upstream the folate cycle was significantly increased in *Mtr cKO* as compared to controls (0.90 vs 0.279 nmol/L, $P = 0.0040$) while 5-methylterahydrofolate (5-methylTHF) and THF remained unchanged between the *Mtr cKO* and control (2.98 vs 2.6523, $P = 0.985$ and 0.2527 vs 0.170 $P = 0.573$ respectively; **Figure 31**).

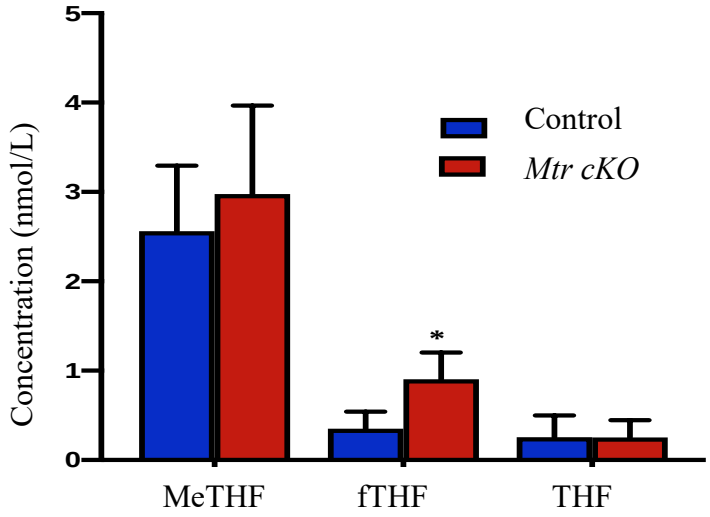

Figure 31: Concentration levels of folates in the heart tissue of 5 months old *Mtr cKO* and control mice

The graph bar shows the concentration levels of folates in the heart tissue of 5 months old control and *Mtr cKO* mice the analysis was achieved by LC-MS/MS**.** meTHF (methyl tetrahydrofolate), fTHF (formyl tetrahydrofolate) and THF (tetrahydrofolate). Means ± SEM, n = 3 to 6 per group, *$P < 0.05$ ** $P < 0.01$, *** $P < 0.001$).

2 Consequences of cardiac specific invalidation of *Mtr* gene on cardiac function parameters (Phenotypic study).

2.1 Systolic blood pressure

To investigate whether cardiac specific deletion of *Mtr* gene impacts blood pressure, systolic blood pressure was measured in conscious mice aged 5 months using tail cuff plethysmography. A significant increase in systolic blood pressure was observed in *Mtr cKO* mice compared to control mice (111.37 ± 0.82 vs 94.45 ± 2.96 mmHg, $P < 0.0000$; **Figure 32**). There was no observable difference in cardiac frequency (CF) between the two groups (613. 89 ± 22.06 vs 615.83 ± 23.23 BPM, $P = 0.8489$).

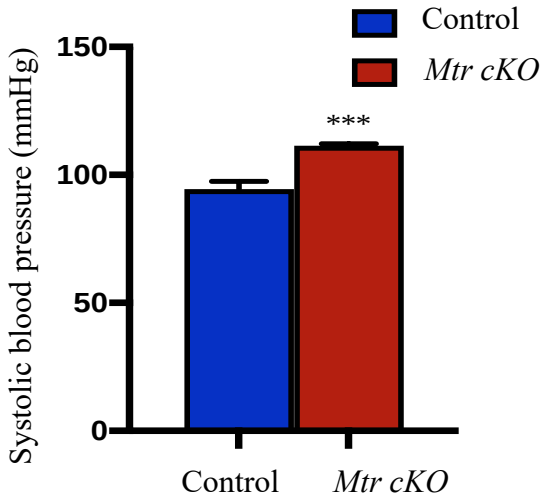

Figure 32: Systolic blood pressure in 5 months old mice measured using tail cuff plethysmography.

A significant increase in systolic blood pressure was observed in *Mtr cKO* mice compared to control mice (111.37 ± 0.82 vs 94.45 ± 2.96 mmHg, $P < 0.0000$). Means ± SEM, n = 6 to 10 per group, *$P <$ 0.05 ** $P < 0.01$, *** $P < 0.001$).

2.2 Evaluation of left ventricular function by Echocardiography

To further investigate whether the deletion of *Mtr* gene in the cardiomyocytes induces cardiac dysfunction in our study model, we evaluated left ventricular function using transthoracic echocardiography on 5 months old mice. A significant decrease in both left ventricular ejection fraction (LVEF) and left ventricular fractional shortening (LVFS) was observed in *Mtr cKO* mice relative to the control (38.97± 2.07 vs 55.38 ± 3.68, $P = 0.002$ and 18.79 ± 1.14 vs 28.64

± 2.40, *P* = 0.002 respectively; **Figure 33B**). LVEF is used to evaluate left ventricular systolic function and assess the severity of ventricular dysfunction. Interestingly, both the end systolic volumes (ESV) and end diastolic volumes (EDV) were significantly increased in *Mtr cKO* as compared to control animals (57.33 ± 7.28 vs 26.33 ± 4.00 µL, *P* = 0.0067 and 81.41 ± 2.90 vs 57.03 ± 5.72 µL, *P* = 0.0015, respectively) hence the observed decrease in LVEF in *Mtr cKO* animals. Transthoracic echocardiography also revealed an increase in the left ventricular mass in *Mtr cKO* in comparison to controls (103. 76 ± 2.23 vs 79.44 ± 8.29 mg, *P* = 0.07; **Figure 33 C**). A summary of echocardiographic measurements is shown in **Table 11.** These results indicate that cardiomyocyte deletion of *Mtr* gene induces dilatation of the left ventricle with severe left ventricular systolic dysfunction.

Parameters	Control	*Mtr cKO*	*P* value
LVEDV (µL)	57.03 ± 5.72	81.41 ± 2.89	0.0067
LVESV (µL)	26.33 ± 4.00	57.33 ± 7.28	0.0015
LVEF %	55.38 ± 3.68	38.97 ± 2.06	0.0022
LVFS %	28.64 ± 2.46	18.79 ± 1.13	0.0022
LVPWd (mm)	0.72 ± 0.04	0.78 ± 0.04	0.3139
LVPWs (mm)	1.05 ± 0.07	0.94 ± 0.03	0.2620
LVIDd (mm)	3.65 ± 0.16	4.34 ± 0.04	0.0032
LVIDs (mm)	2.64 ± 0.18	3.53 ± 0.08	0.0015

Table 11: Left ventricular parameters of *Mtr cKO* and control mice evaluated by echocardiography.

Left ventricular end diastolic volume (LVEDV), Left ventricular end systolic volume (LVESV), left ventricular ejection fraction (LVEF), left ventricular fractional shortening (LVFS), left ventricular posterior wall thickness in diastole (LVPWd), left ventricular posterior wall thickness in systoles (LVPWs) and left ventricular end-diastolic internal diameter in diastole (LVIDd) and left ventricular end-diastolic internal diameter in systole (LVIDs). Means ± SEM, n = 6 to 10 per group, * $P < 0.05$ ** $P < 0.01$, *** $P < 0.001$).

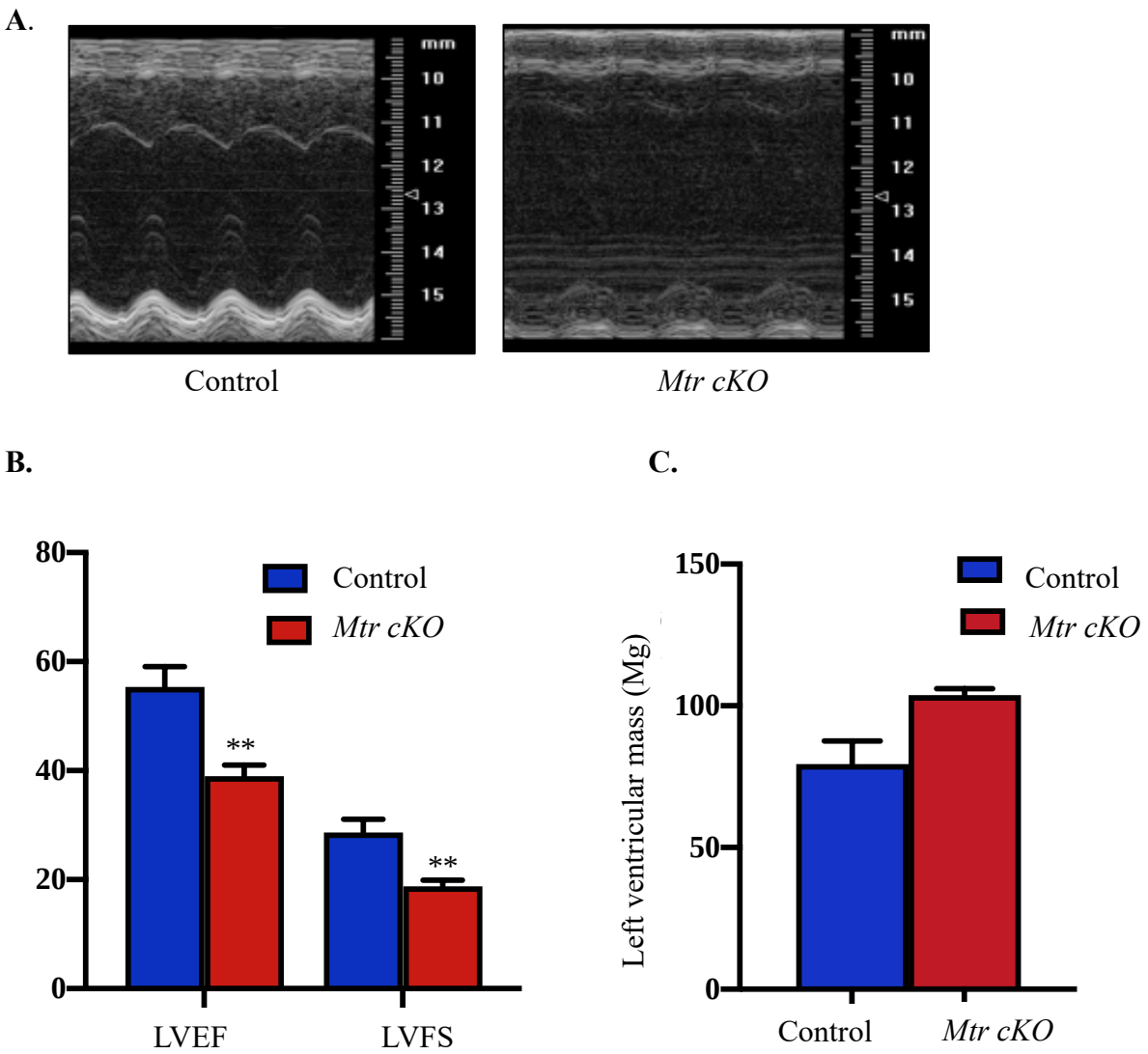

Figure 33: **Cardiac left ventricular function of *Mtr cKO* and control mice evaluated by transthoracic echocardiography.**

A. Echocardiographs in M mode. **B.** Left ventricular ejection fraction (LVEF) and fractional shortening (LVFS) (38.97 ± 2.07 vs 55.38 ± 3.68, $P = 0.002$ and 18.77 ± 1.14 vs 28.64 ± 2.4, $P = 0.002$ respectively) between *Mtr cKO* and control mice. **C**. Left ventricular mass of the hearts of *Mtr cKO* and control animals. Means ± SEM, n = 6 to 10 per group, *$P < 0.05$ **$P < 0.01$, ***$P < 0.001$)

2.3 Evaluation of left ventricular function using positron emission tomography (Mini-PET)

To further evaluate left ventricular function and tissue perfusion, we used Mini-PET scan. Both left ventricular end systolic and end diastolic volumes were significantly increased in *Mtr cKO* mice in comparison to control mice (81.84 ± 6.66 vs 58.42 ± 7.49 µL, $P = 0.004$, **Figure 34A**) and (118.03 ± 8.93 vs 102.89 ± 7.51 µL, $P = 0.028$; **Figure 34B**) respectively. As a consequence, LVEF was significantly decreased in the *Mtr cKO* relative to control (30.57 ± 1.54 vs 44. 44 ± 3.75 µL, $P = 0.028$; **Figure 34C**). Mini-PET results are summarized in **Table 12**. Combined, these results are consistent with those observed in the transthoracic ultrasonographic examination and confirms left ventricular systolic dysfunction in *Mtr cKO*.

Parameters	Control	*Mtr cKO*	*P* value
LVEDV (µL)	102.88 ± 7.51	118.03 ± 8.93	0.0284
LVESV (µL)	58.42 ± 7.49	81.84 ± 6.66	0.0044
LVEF %	44.44 ± 3.75	30.57 ± 1.54	0.0283
Glycemia (g/L)	2.28 ± 0.12	2.51 ± 0.12	0.6779
Area	229.44 ± 13.28	265.29 ± 13.76	0.0044
EDV (g)	3.59 ± 0.23	4.21 ± 0.34	0.1685
ESV (g)	1.98 ± 0.19	2.93 ± 0.25	0.0095

Table 12: **Left ventricular parameters of *Mtr cKO* and control mice assessed by Mini-PET scan.**

Left ventricular end diastolic volume (LVEDV), Left ventricular end systolic volume (LVESV), left ventricular ejection fraction (LVEF), Means ± SEM, n = 6 to 10 per group, $*P < 0.05$ $**P < 0.01$, $***P < 0.001$)

A. Left ventricular End Diastolic Volume

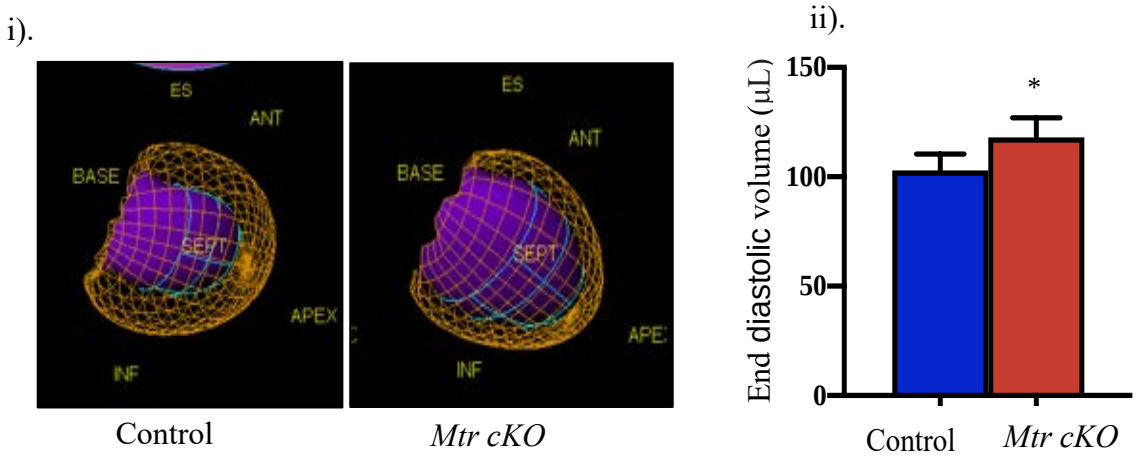

B. Left ventricular End Systolic

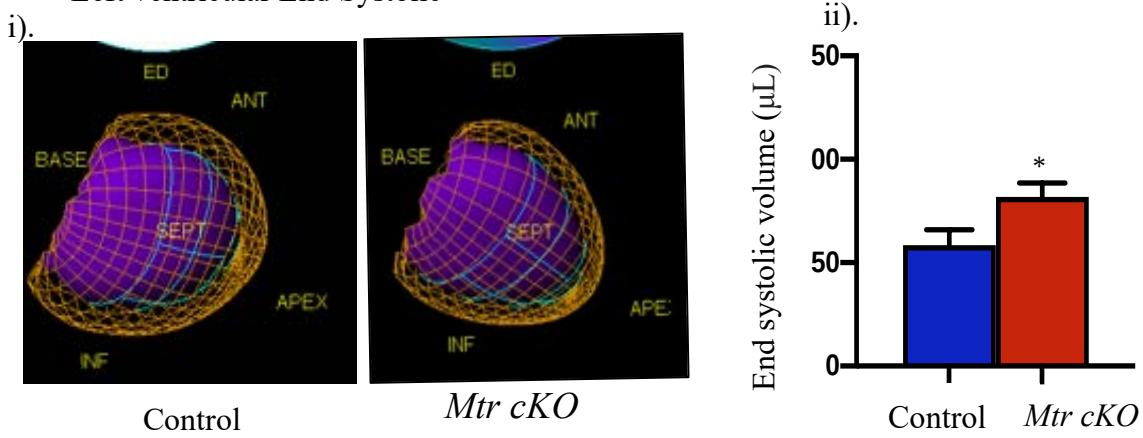

C. Left ventricular ejection fraction

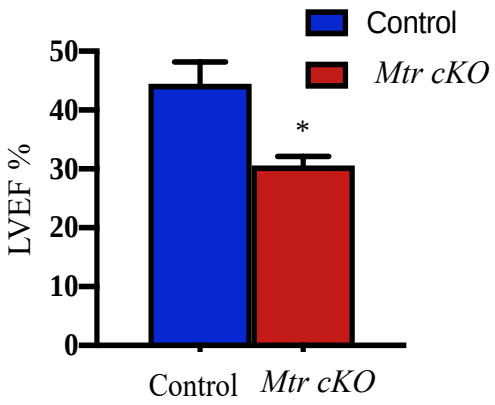

Figure 34: Left ventricular parameters of *Mtr cKO* and controls assessed by Mini-PET

A. (i) The representative PET scan images of the hearts of control and *Mtr cKO* at the end of systole and (ii) is the end systolic volumes of control and *Mtr cKO* mice. **B.** (i) Representative PET scan images of the hearts of control and *Mtr cKO* mice at the end of diastole and (ii) end diastolic volumes in the control and *Mtr cKO* mice. **C.** Left ventricular ejection fraction (LVEF) of control and *Mtr cKO* mice. Means ± SEM, n = 6 to 10 per group, **P* < 0.05 ** *P* < 0.01, *** *P* < 0.001).

2.4 Survival rate of *Mtr cKO*

The impaired remethylation of homocysteine and decreased synthesis of methionine by MS may impact on the survival of *Mtr cKO*. We analyzed the life expectancy of these animals and we found that in comparison to control animals, *Mtr cKO* mice did not survive beyond 9 months (14.1 ± 6.9 vs 8.7 ± 1.6 months, $P = 0.0001$; **Figure 35**). We hypothesize that the *Mtr cKO* mice might have died from cardiac complications related to left ventricular systolic dysfunction and heart failure.

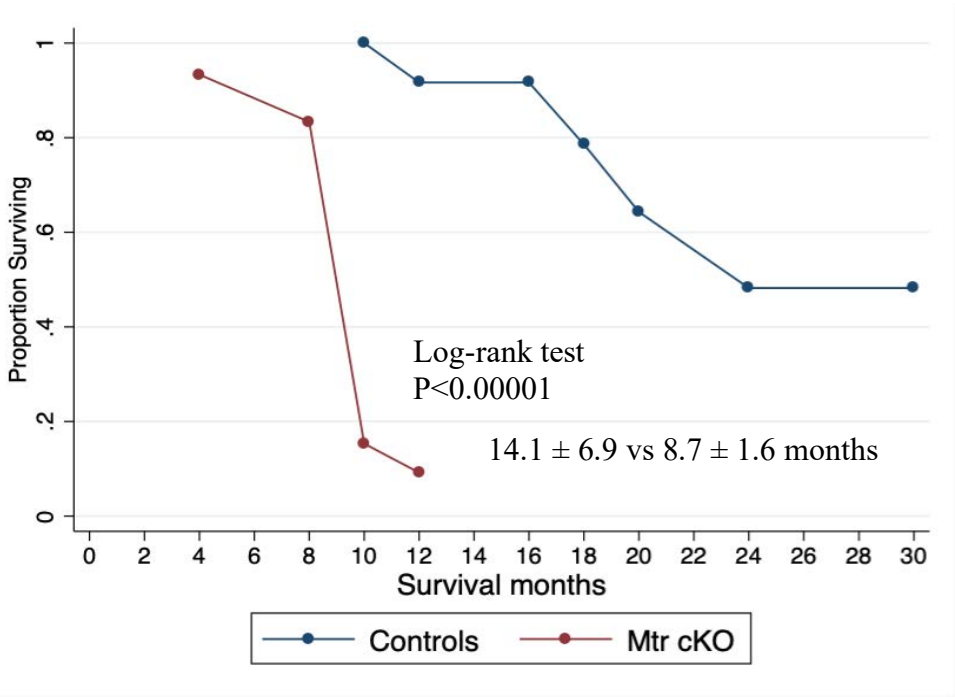

Figure 35: Comparison of survival rates of *Mtr cKO* and control mice.

Graph showing the survival rates between the *Mtr cKO* and control animals. *Mtr cKO* have decreased survival rate with a median length of survival of 8.7 months in comparison controls.

2.5 Expression levels of biomarkers of heart failure

Using RT-qPCR, we measured the expression levels of natriuretic peptides and alpha and beta MHCs (Myosin heavy chain) used as biomarkers of heart failure. The expression levels of atrial natriuretic peptide (ANP) and brain natriuretic peptides (BNP) were significantly elevated in the heart tissue of *Mtr cKO* in comparison to controls ($P = 0.003$ and $P = 0.001$ respectively; **Figure 36A).** Moreover, beta *Mhc7* was significantly overexpressed ($P = 0.017$; **Figure 36A**) and the alpha *Mhc6* : beta *Mhc7* ratio was decreased ($P = 0.0156$; **Figure 36B**). The shift in the expression of cardiac myosin heavy chain from alpha MHC to beta MHC is a hallmark of heart failure. These results are consistent with the hypertrophic cardiomyopathy, systolic dysfunction and heart failure revealed by echocardiography and mini-PET imaging. Together, these results reveal that cardiac specific invalidation of *Mtr* gene induces heart failure.

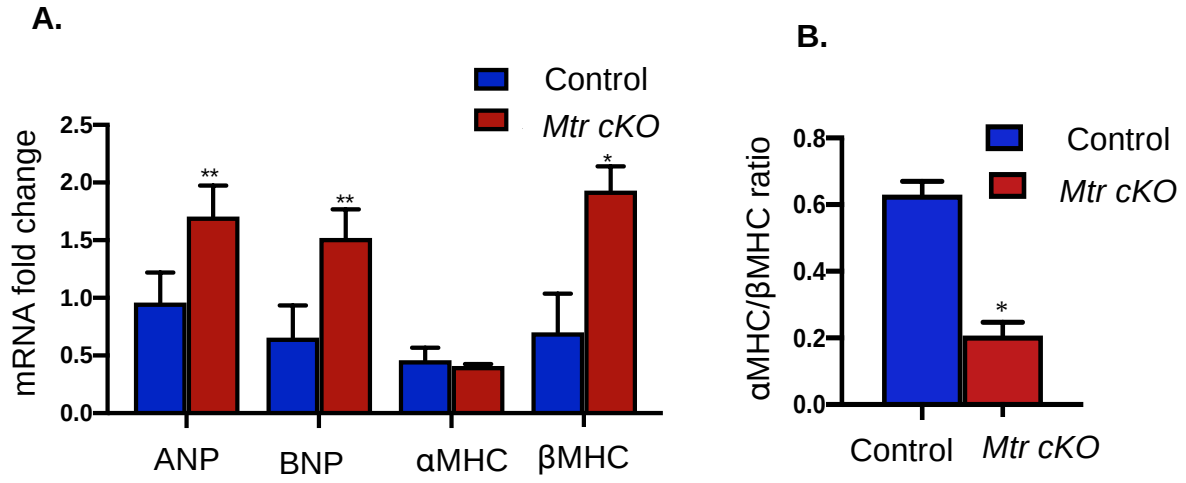

Figure 36: Expression levels of biomarkers of heart failure in the heart tissues of *Mtr cKO* and control mice analyzed by RT-qPCR

A. mRNA expression levels for genes encoding Atrial natriuretic peptide (ANP), Brain natriureticpeptides (BNP), Alpha myosin heavy chain (α-MHC) and beta myosin heavy chain (β-MHC) in the heart tissues of *Mtr cKO* and control mice. **B.** The α-MHC to β-MHC ratio. Means ± SEM, n = 6 to 10 per group, $*P < 0.05$ $**P < 0.01$, $***P < 0.001$

3 Consequences of cardiac specific invalidation of *Mtr* on expression changes in Omics studies

In order to dissect molecular consequences of cardiac specific deletion of *Mtr* gene that may explain the cardiomyopathy and heart failure observed in *Mtr cKO,* transcriptomics and proteomics analysis was carried out in the heart tissues.

3.1 Transcriptomics

3.1.1 Transcriptomic expression profile in the heart

A total of 16539 expressed genes were detected after quality control and removal of lowly expressed transcripts. These genes were clustered by K-means, and each of the resulting cluster was re-analyzed by hierarchical clustering, which delineated three strongly correlated gene signatures (cluster 2, cluster 3 and cluster 4) in *Mtr cKO* relative to the controls (**Figure 37A**). The three signatures represented about 36 % of the total dysregulated transcriptome in the hearts of *Mtr cKO* animals. Of the three signatures, cluster 3 and cluster 4 were upregulated and they consisted of 1666 and 2478 genes representing 10 % and 15 % of dysregulated transcriptome respectively. On the other hand, cluster 2 was downregulated and it consisted of 1889 genes representing 11.4 % of dysregulated transcriptome ($P = 1.9 \times 10^{-4}$, **Figure 37C**).

Sub-cluster 3, consisting of 418 genes and sub-cluster 4, consisting of 887 genes ($P = 1.4 \times 10^{-4}$ and $P = 2.6 \times 10^{-2,}$ respectively; **Figure 37D** and **37E**), were obtained after elimination of outliers by cutting of branches of the hierarchical trees in cluster 3 and 4, respectively. Statistical analyses output a total of 145 differentially expressed genes, 102 were under-expressed (Fold change < 0.5, FDR < 0.05) and 43 were overexpressed (Fold change > 2, FDR < 0.05) in *Mtr cKO.*

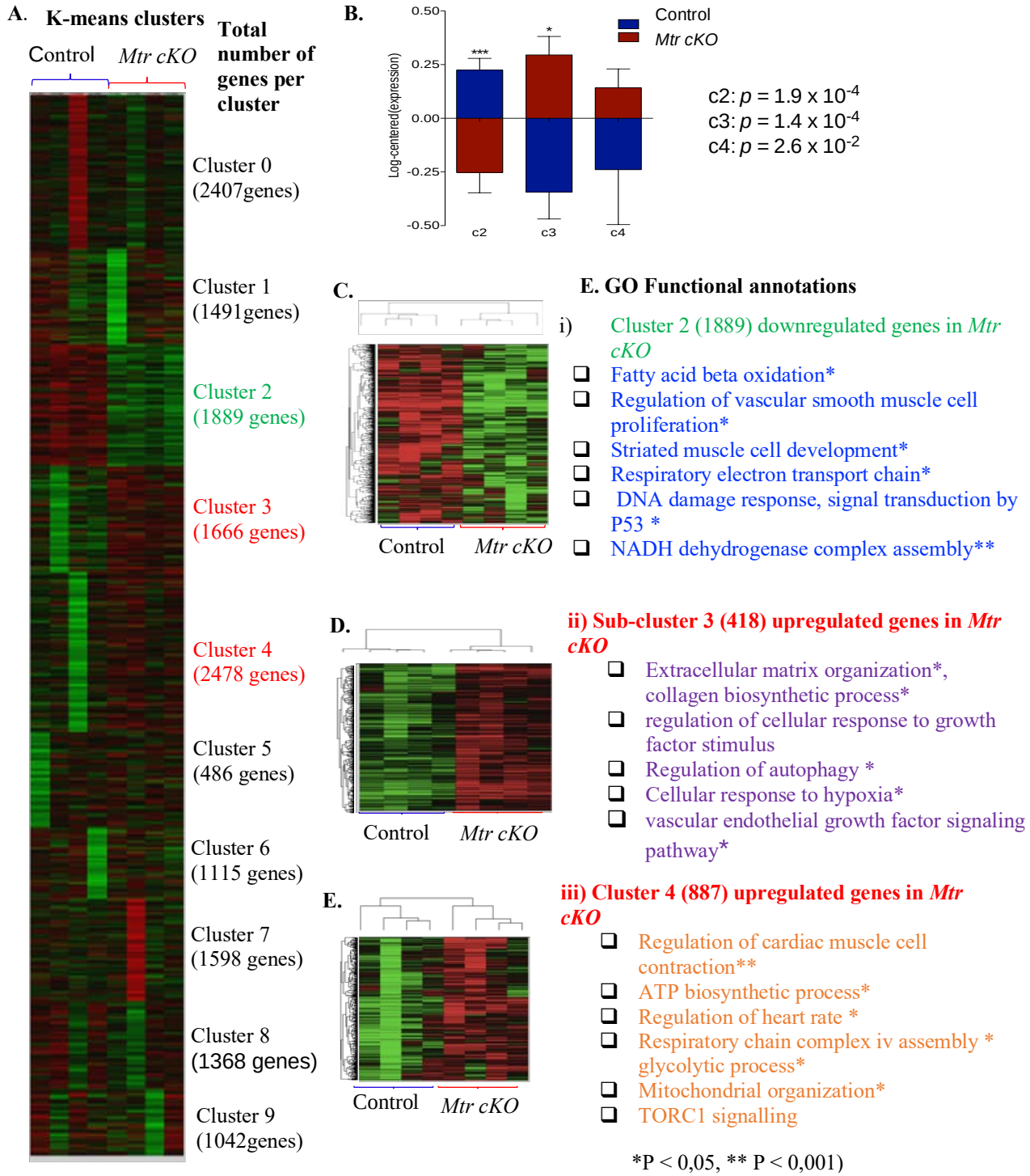

Figure 37: Consequence of cardiac specific deletion of *Mtr* gene in the transcriptome of the heart.

A. Heat-map of whole heart transcriptome showing 10 clusters of the 16539 detected genes. K-means clustering of the whole heart transcriptome delineated three strongly correlated gene signatures (cluster 2, 3 and 4). Black, red and green indicates median, upregulated and downregulated genes respectively. **B**. Log centred gene expression of the significant dysregulated clusters (cluster 2, sub-cluster 3 and sub-cluster 4) in *Mtr cKO*· **C**, **D** and **E** are heat-maps of the hierarchically clustered gene signatures; **C2**, **sub C3** and **Sub C4** respectively. An overview of the most significant and relevant GO enrichment and functional annotations related to the three significant dysregulated gene clusters (C2, sub C3 and sub C4). N = 8 $P < 0.05$.

3.1.2 Gene ontology enrichment and pathway analysis

Gene ontology (GO) enrichment and pathway analysis of our transcriptomic data was carried out using PANTHER (**P**rotein **An**alysis **Th**rough **E**volutionary **R**elationships) classification system and Enrichr bioinformatic tool.

3.1.2.1 Gene ontology enrichment and pathway analysis of the 1889 under-expressed genes

PANTHER facilitates high throughput classification of genes and proteins on the basis of their evolutionary relationships, biological processes, molecular function and pathway analysis. It is maintained by Thomas laboratory at the University of California.

The GO enrichment and pathway analysis of the 1889 under-expressed genes using PANTHER revealed that the most relevant and significantly overexpressed biological processes in *Mtr cKO* were mainly related to impaired mitochondrial energy metabolism, fatty acid oxidation and cardiac remodeling (FDR < 0.05) shown in (**Figure 38**).

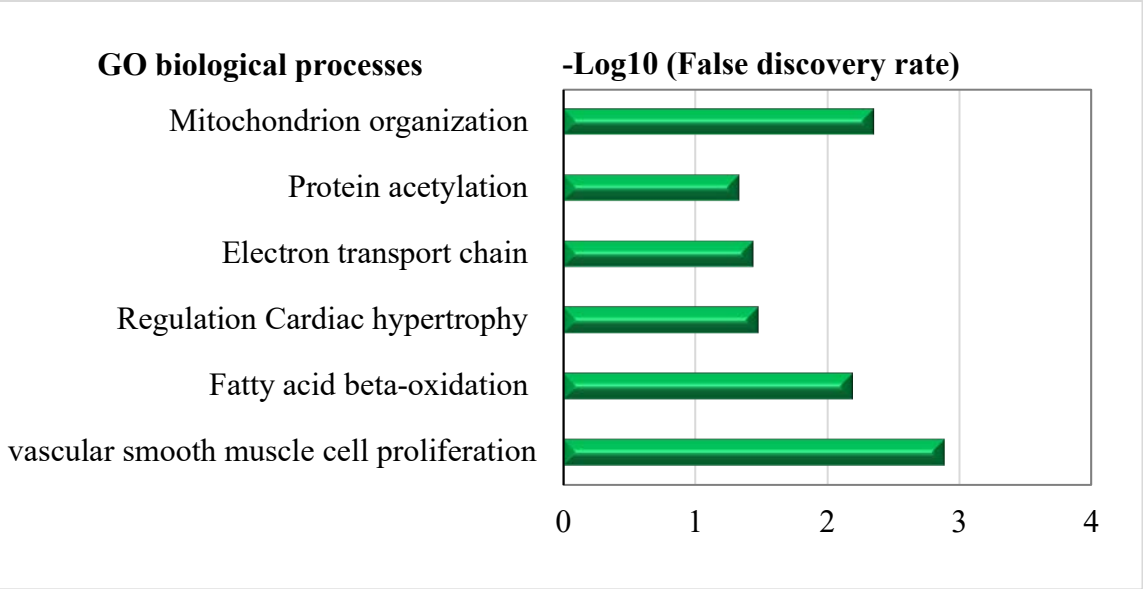

Figure 38: **PANTHER Gene Ontology term enrichment analysis of the 1889 under-expressed genes in the hearts of *Mtr cKO*.**

The most relevant and significantly overexpressed GO biological processes related to mitochondrial energy metabolism and cardiac remodelling associated with the 1889 (cluster 2) under-expressed genes in the hearts of *Mtr cKO* mice.

3.1.2.2 Gene ontology enrichment and pathway analysis of the 1889 under-expressed genes by Enrichr

Enrichr is a freely available easy to use intuitive enrichment analysis web based and mobile application software for curated gene set. It provides an alternative approach to rank enriched terms and provide different types of visualization summary of collective functions of gene lists by Ma'ayan laboratory computational systems biology.

Functional annotations of cluster 2 under-expressed genes by Enrichr analysis ($P < 0.05$) were similar to the results revealed by PANTHER classification system. The GO biological processes related to impaired mitochondrial energy metabolism in hearts of *Mtr cKO* included; mitochondrial complex respiratory chain complex I assembly, mitochondrial ATP synthesis coupled electron transport and fatty acid beta oxidation ($P < 0.05$; **Figure 39**). GO biological processes implicated in response to cellular stress included: cellular response to reactive oxygen species, IL 18 signaling pathway, DNA damage response signal transduction by P53 class mediator resulting in cell arrest and regulation of vascular smooth muscle cell proliferation (*P*

< 0.05; **Figure 40**). Other GO biological processes were involved in heart process, heart contraction and striated muscle development ($P < 0.05$).

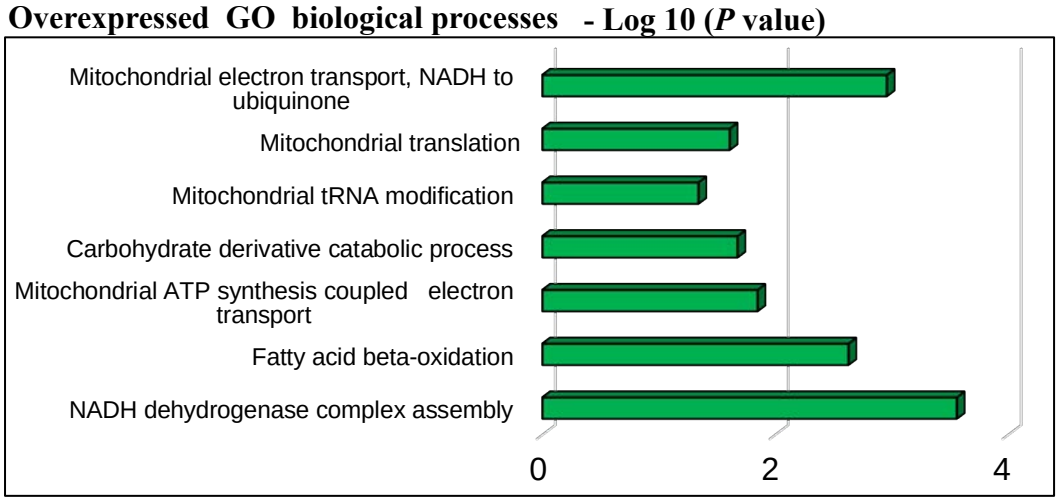

Figure 39: **Enrichr Gene Ontology term enrichment analysis for the cluster 2 under-expressed genes in the hearts of *Mtr cKO*.**

Overexpressed GO biological processes involved in myocardial energy metabolism and mitochondrial bioenergetics for the 1889 (cluster 2) under-expressed genes in *Mtr cKO*. The presented data are negative log of *P* value of the most significant GO biological processes with *P* value less than 0.05.

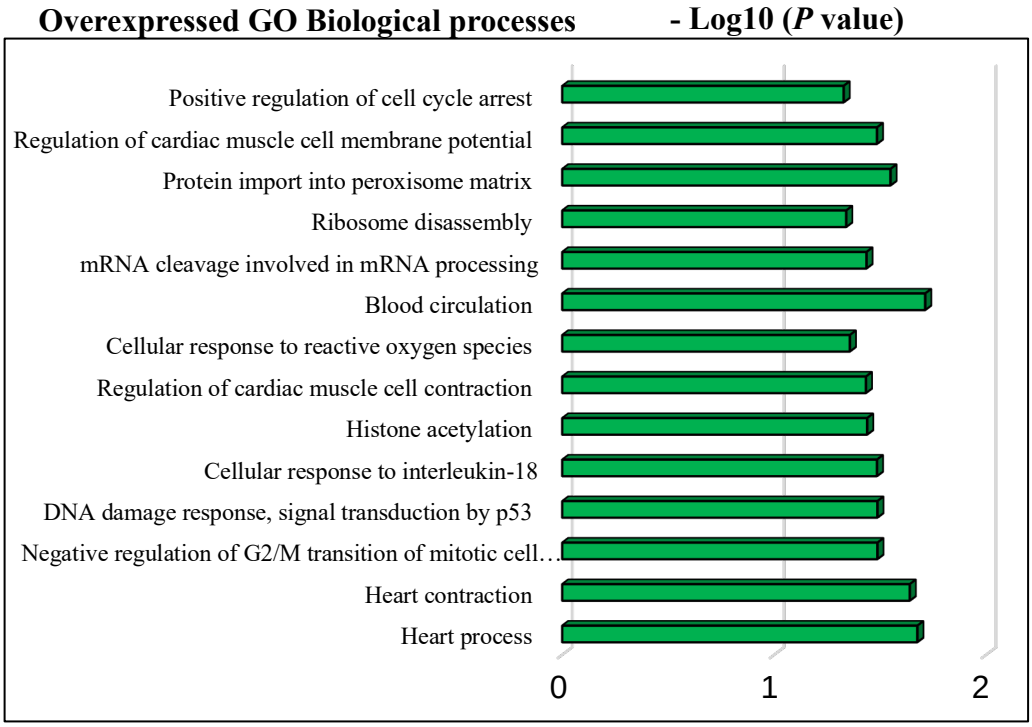

Figure 40: **Enrichr GO enrichment analysis for the cluster 2 under-expressed genes in hearts *Mtr cKO* implicated in response to cellular stress.**

The most relevant and significantly overexpressed GO biological processes implicated in response to cellular stress linked to the 1889 under-expressed genes (Cluster 2) in the myocardium of *Mtr cKO* mice. The data shown for the significant GO biological processes ($P < 0.05$) are presented as negative log (P value).

3.1.2.3 Gene ontology and pathway analysis of the overexpressed genes in sub-clusters 3 and 4.

Functional annotations for the genes in the two upregulated clusters were analyzed using Enrichr. The 418 overexpressed genes (sub-cluster 3) were related to adaptative mechanisms to cellular stress and cardiac fibrosis including negative regulation of oxidative stress induced cell death, cellular response to hypoxia, cellular response to unfolded proteins, proteasome mediated ubiquitin dependent protein catabolic process, regulation of stress fiber assembly, vascular endothelial growth factor (VEGF) signaling, extracellular matrix organization and collagen biosynthesis ($P < 0.05$; **Figure 41**).

Functional annotations of the 887 overexpressed genes (sub-cluster 4) were involved in adaptative mechanisms and pathways of cardiac remodeling and impaired mitochondria energy

metabolism ($P < 0.05$). The overexpressed GO biological processes related to impaired mitochondrial energy metabolism included: mitochondrial organization, mitochondrial complex IV biogenesis, glycolytic and ATP biosynthetic processes ($P < 0.05$); **Table 13**). Furthermore, the pathways and mechanisms linked to cardiac remodelling included: regulation of autophagy, TORC1 signaling and regulation of programmed cell death, positive regulation of extracellular matrix assembly, cardiac muscle cell development and contraction, regulation of heart rate by conduction and positive regulation of calcium mediated signaling ($P < 0.05$); **Table 13**). We further evaluated the pathways associated with the overexpressed genes in the hearts of *Mtr cKO* using PANTHER classification system. We found that most relevant reactome pathways associated with these overexpressed genes (sub-cluster 3 and sub-cluster 4) in *Mtr cKO* included: signaling pathways such as vascular endothelial growth factor (VEGFA-VEGFR2) and Rho GTPases signaling pathways, heat shock factor 1 (HSF1) activation, HSP90 chaperone cycle for steroid hormone receptors cellular response to stress, pyruvate metabolism and Citric acid cycle, glycogen and glucose metabolism (FDR < 0.05; **Figure 42**).

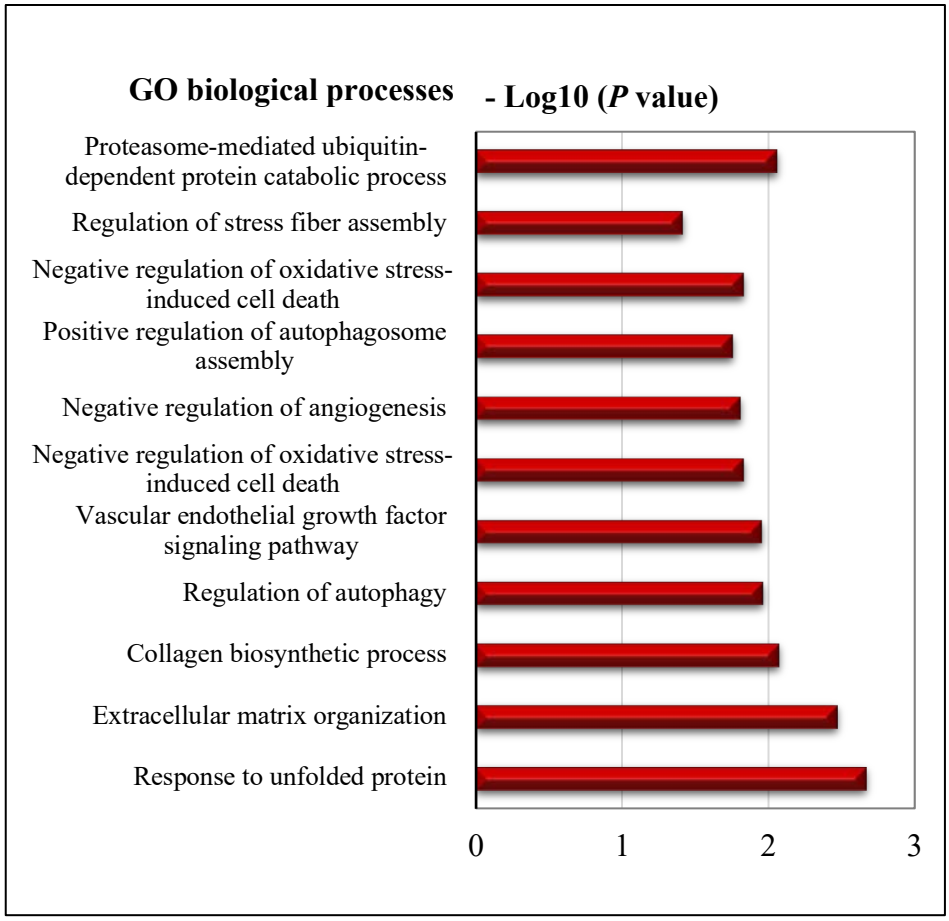

Figure 41: Enrichr Gene Ontology term enrichment analysis for the 418 overexpressed genes (Sub-cluster 3) in the hearts of *Mtr cKO*.

Shown in the bar graph are the most relevant and significantly overexpressed biological processes related to response to cellular stress and cardiac fibrosis for to the 418 overexpressed genes in the myocardium of *Mtr cKO* mice (P value < 0.05). The data are presented as negative P value.

Go biological processes linked to the upregulated genes in sub-cluster 4 analyzed by Enrichr		
Go biological process	**Genes**	***(P* value)**
Mitochondrial respiratory chain complex IV biogenesis (GO:0097034)	COA3, SCO1, COX17, COX14	0,0126
Regulation of cell cycle G2/M phase transition (GO:1902749)	YWHAE; DYNC1H1; DCTN2; PPP2R1A; DCTN1 ; PRKACA; PCNT; TUBB4B; YWHAG	0,0129
Mitochondrial respiratory chain complex IV assembly (GO:0033617)	COA3; SCO1; COX17; COX14	0,0105
ATP biosynthetic process (GO:0006754)	ATP5E; ATP5D; ATP5G3; ALDOA; ATP6V0A1	0,0143
Glycolytic process (GO:0006096)	PFKL; ALDOA; GCK; HK1	0,0174
Mitochondrion organization (GO:0007005)	ALAS1; CLUH; TOMM40; MUL1; SIRT5; MIEF2; S 7; TRAK1; TRAK2; AFG3L2; OXA1L; PITRM1; MYH14; HAP1	0,0176
Positive regulation of programmed cell death (GO:0043068)	ARHGEF12; GADD45B; ITSN1; DAPK3; ARHGEF19; HTT; SCRIB; HDAC6; TIAM2; ABR; AKAP13; NCSTN; ARHGEF9; TCTN3; ANKRD1; TRIM35; ARHGEF1; FADD; SOS1	0,0215
ER-associated misfolded protein catabolic process (GO:0071712)	POMT2; VCP; UGGT1	0,0178
Regulation of autophagy (GO:0010506)	USP36; KDM4A; ROCK1; DAPK3; PIK3R2; ZDHHC8; HDAC6; MTOR; GOLGA2; TRIM8; CPTP; WDR6; VDAC1; CAPN1; PRKACA; ATP6V0A1	0,0198
Smooth muscle contraction (GO:0006939)	SMTN; ROCK1; HMCN2	0,0219
Cardiac muscle contraction (GO:0060048)	MYBPC3; GAA; MYL3; SCN5A ; ATP1B1 ;SCN1B; TTN	0,0231
ATP generation from ADP (GO:0006757)	PFKL; ALDOA; GCK; HK1	0,0071
Regulation of autophagy of mitochondrion (GO:1903146)	USP36; HTT; VDAC1; ZDHHC8; HDAC6	0,0010
cardiac muscle cell development (GO:0055013	PDGFRB; SORBS2; NKX2-5; OBSL1; MYPN; TTN; MYOM3	1,72E-04
Positive regulation of calcium-mediated signaling (GO:0050850)	P2RX5; GSTO1; HTT; CDH13; AKAP6; HAP1	0,0015
Positive regulation of extracellular matrix assembly (GO:1901203)	SMAD3; DAG1; CLASP2	0,0041
TORC1 signaling (GO:0038202)	LARP1; CLEC16A; MTOR	0,0041
Negative regulation of striated muscle cell differentiation (GO:0051154))	CAV3; FZD7;BHLHE41;NKX2-5	0,0047
Regulation of heart rate by cardiac conduction (GO:0086091)	JUP; CACNA2D1; SCN5A; SCN1B; DSC2	0,0047
Cardiac muscle tissue development (GO:0048738)	AKAP13; TBX20; ANKRD1; NKX2-5; TTN; MYOM3	0,0054

Table 13: Enrichr Gene ontology term enrichment analysis for the 887 overexpressed genes (Sub-cluster 4) in the hearts of *Mtr cKO*.

The Table shows the most relevant and significantly overexpressed GO biological processes linked to sub-cluster 4 overexpressed genes in the myocardium of *Mtr cKO* mice (*P* value < 0.05).

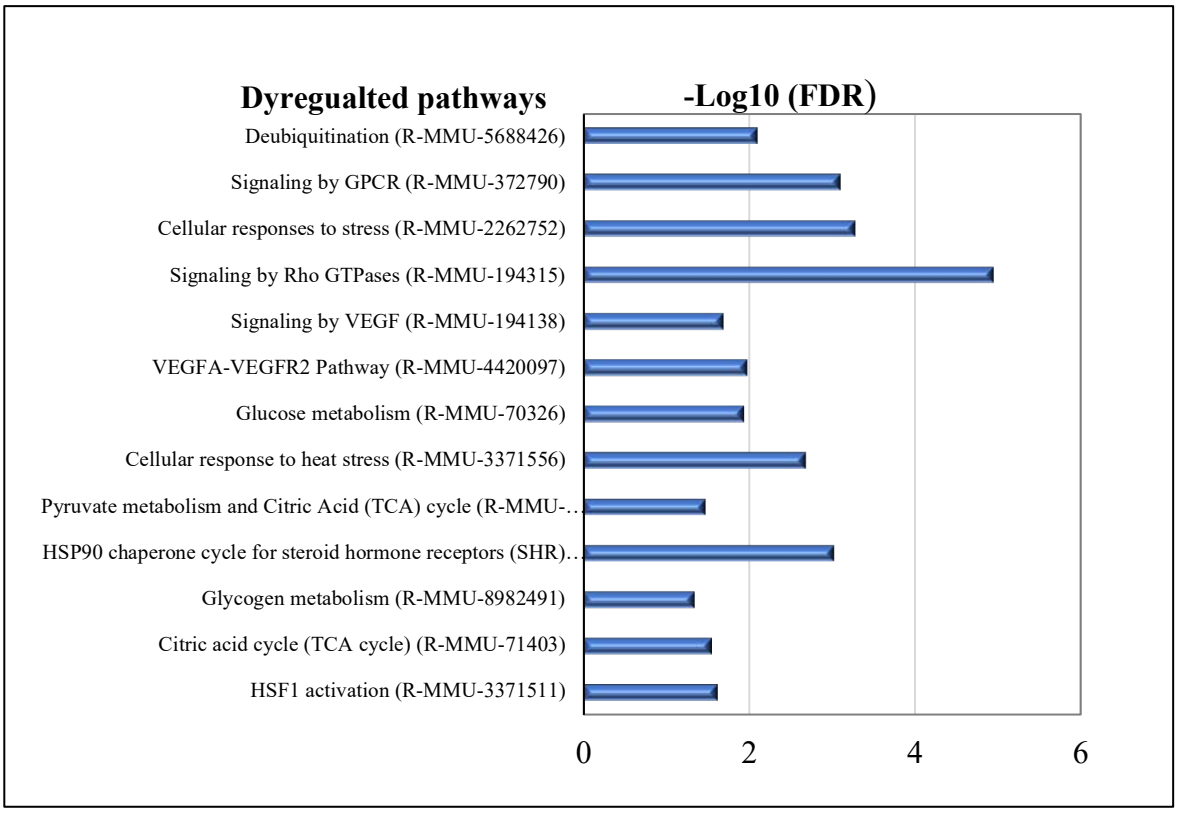

Figure 42: PANTHER Gene Ontology term enrichment and pathway analysis for the overexpressed genes (Sub-cluster 4 and sub-cluster 3) in the hearts of *Mtr cKO*.

Shown in the bar graph are the reactome pathways associated with the overexpressed genes in sub-cluster 3 and sub-cluster 4 in the hearts of *Mtr cKO*. Majority of these pathways were linked to response to cellular stress, cardiac remodeling and myocardial bioenergetics (FDR < 0.05)

3.1.3 Mapping the dysregulated genes in the myocardium *Mtr cKO* using KEGG pathway database

Given the GO biological processes and pathways related to the dysregulated genes in the myocardium of *Mtr cKO* mice revealed by PANTHER classification system and Enrichr bioinformatic analytical tool. We further used KEGG pathway database to map the significantly dysregulated genes in the myocardium of *Mtr cKO*. Some of the most relevant KEGG pathways that were dysregulated in *Mtr cKO* included energy metabolism pathways including oxidative phosphorylation and fatty acid beta oxidation and cardiac hypertrophy.

3.2 PROTEOMICS

3.2.1 Proteomic expression profile in the heart tissues.

A total of 1998 proteins were detected of which 34 proteins were differentially expressed in the hearts *Mtr cKO*. Of these, 26 were downregulated (Fold change < 0.8, $P < 0.05$) and 8 were upregulated (Fold change >1.25, $P < 0.05$). Furthermore, according to the t-statistics ($P < 0.01$), the top 94 dysregulated proteins in the hearts of *Mtr cKO* were hierarchically clustered This clustering delineated three protein clusters of which the largest (cluster 1) consisted of downregulated proteins (**Figure 43A**).

3.2.2 Gene ontology enrichment and pathway analysis of the dysregulated proteins in heart tissues.

3.2.2.1 Gene ontology enrichment and pathway analysis of the 34 differentially expressed proteins in hearts of *Mtr cKO*.

Functional annotation of the 34 differentially expressed proteins in the hearts of *Mtr cKO* were performed using Enrichr. The most relevant GO biological processes associated with these proteins were related to energy metabolism (ketone body and galactose metabolisms, mitochondrial biogenesis) and myocardium remodeling (muscle cell differentiation, Fibroblast Growth Factor Receptor (FGFR) signaling, proteasome assembly, cell to cell adhesion mediated by cadherin, negative regulation of intrinsic apoptotic signaling pathway in response to DNA damage and protein repair) others included negative regulation of interleukin 8 production and protein deacetylation (**Figure 43B)**. To assess the diseases associated with the dysregulated proteins, Open Targets platform was used. This tool is a comprehensive and robust data integration tool for access and visualization of drug targets associated with diseases. A total of 22 out of the 34 targets were associated with cardiovascular diseases ($P = 0.0006$), these diseases included genetic cardiomyopathies, including those related to mitochondrial disorders, heart failure, pulmonary arterial hypertension and hypertension (**Figure 43C**, **Table 14**).

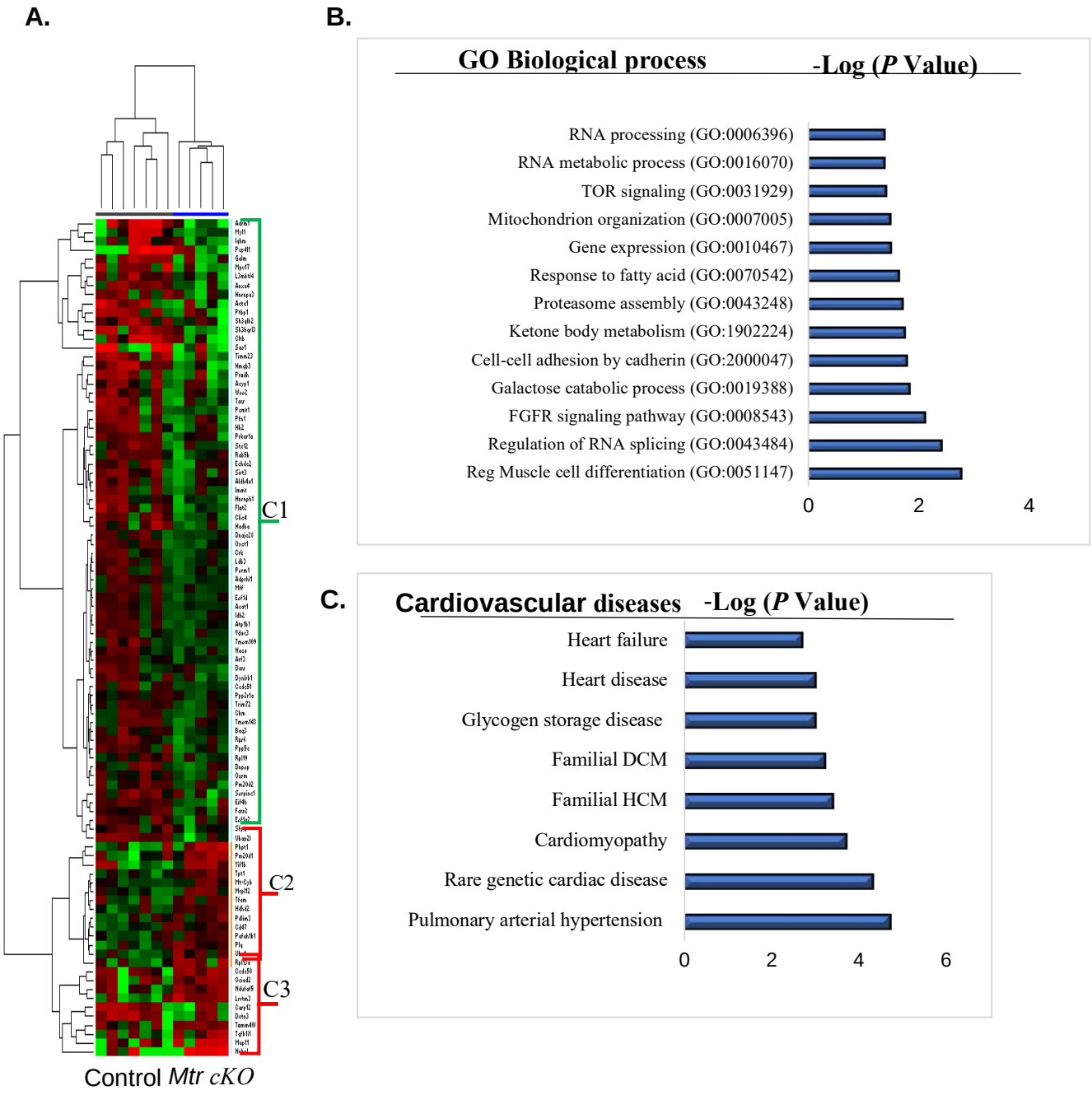

Figure 43*:* **Proteomic analysis of dysregulated proteins in the heart of *Mtr cKO*.**

A. Heatmap of the top 94 dysregulated proteins in the heart of *Mtr cKO.* Black, red and green indicates median, upregulated and downregulated proteins respectively. **B.** Most relevant GO biological processes linked to the 34 differentially expressed proteins. **C.** Cardiovascular diseases associated with the 34 differential expressed proteins in the hearts of *Mtr cKO*. (HCM = hypertrophic cardiomyopathy, DCM= dilated cardiomyopathy). N=12, $P < 0.05$.

Cardiovascular diseases associated with the 34 differentially expressed proteins in the myocardium of *Mtr cKO* analyzed by Open Targets bioinformatic tool			
Cardiovascular diseases (P = 0.001)		P value	Number of associated targets
1	Rare genetic cardiac disease	0.00005	16
2	Cardiomyopathy	0.00020	14
3	Rare familial disorder with hypertrophic cardiomyopathy	0.00040	10
4	Familial dilated cardiomyopathy	0.00060	10
5	Glycogen storage disease with hypertrophic cardiomyopathy	0.00100	4
6	Hypertension	0.00100	12
7	Heart failure	0.00200	8
8	Mitochondrial disease with hypertrophic cardiomyopathy	0.02000	4
9	pulmonary arterial hypertension	0.00002	10

Table 14: Cardiovascular diseases associated with the 34 differentially expressed proteins in the myocardium of *Mtr cKO* analysis achieved using Open Targets platform.

3.2.3 GO enrichment and pathway analysis of the top 94 dysregulated proteins in the myocardium of *Mtr cKO*.

The top 94 dysregulated proteins were functionally analyzed for associated diseases using open Target platform. Interestingly, 62 out of the 94 targets were associated with cardiovascular diseases similar to those obtained with the 34 differentially expressed proteins, only with drastic improvements in both statistics and enrichments ($P = 3.E^{-9}$ **; Figure 43C**, **Table 14**). In addition, 62 targets were linked to metabolic diseases ($P = 3.E^{-8}$; **Table 15**) and 72 to genetic disorders

($P = 4.E^{-10}$) which included those of inborn errors of metabolism and disorders of mitochondrial energy metabolism including oxidative phosphorylation disorders, glycogen storage diseases and disorders of carbohydrate metabolism (**Table 16**).

Metabolic diseases associated with top 94 differentially expressed proteins in the myocardium of MTR CKO analyzed by Open target bioinformatic tool			
Metabolic disorders ($P = 3.e^{-8}$)		*P* value	Number of associated targets
1	Inborn errors of metabolism	8E-07	48
2	Mitochondrial oxidative phosphorylation disorder due to mitochondrial DNA anomalies	0.000009	14
3	Mitochondrial disease	0.000007	30
4	Pyruvate dehydrogenase deficiency	0.00002	9
5	Disorder of energy metabolism	0.00001	31
6	Mitochondrial oxidative phosphorylation disorder	0.000002	27
7	Disorder of fatty acid oxidation and ketone body metabolism	0.001	11
8	Disorder of other vitamins and cofactors metabolism and transport	0.0004	7
9	Glycogen storage disease	0.00001	24
10	Fatal infantile cytochrome C oxidase deficiency	0.006	6
11	Disorder of amino acid and other organic acid metabolism	0.00001	24

Table 15: Metabolic diseases associated with the top 94 dysregulated proteins

Most relevant metabolic diseases associated with the top 94 dysregulated proteins in the myocardium of *Mtr cKO* analysis achieved using Open targets platform ($P < 0.05$).

Genetic diseases associated with top 94 differentially expressed proteins in the myocardium of *Mtr cKO* analyzed by Open Target bioinformatic tool			
Genetic disorders ($P = 4.e\text{-}^{10}$)		*P* value	Number of associated targets
1	Metabolic myopathy	9E-10	27
2	Rare genetic developmental defect during embryogenesis	8E-10	57
3	Rare genetic cardiac disease	1E-08	40
4	Mitochondrial myopathy	1E-08	22
5	Inborn errors of metabolism	7E-08	48
6	Mitochondrial oxidative phosphorylation disorder	2E-5	27
7	Genetic neurodegenerative disease	5E-4	31
8	Disorder of energy metabolism	1E-6	31

Table 16: Genetic diseases associated with the top 94 dysregulated proteins

Most relevant genetic diseases associated with the top 94 dysregulated proteins in the myocardium of *Mtr cKO* analysis achieved using Open Targets platform ($P < 0.05$).

3.3 Intergration of proteome and transcriptome results

3.3.1 Transcriptomic driven proteomic analysis

To confirm these results and further analyze the proteomic data, we integrated the proteome by correlating its features with the transcriptomic ones. We also mined the proteome according to transcriptome-clustering results (from cluster 2, sub-cluster 3 and sub-cluster 4), and extracted gene-protein features with positively and negatively correlated expressions. Among the 1720 shared genes and proteins with altered expression in *Mtr cKO* mice, 213 were under-expressed while 245 were overexpressed. Transcriptomic driven analysis of proteome revealed that the 213 downregulated genes translated into 90 under-expressed proteins (fold-change < 0.8), 50 proteins that correlated inversely with upregulation (fold-change > 1.25) and 71 proteins with no change of expression. On the other hand, the 245 overexpressed genes were translated into 85 under-expressed (fold-change < 0.8), 59 overexpressed proteins (fold-change > 1.25) and 101 with no change of expression (**Figure 44**). This observation could either be due to posttranslational modification, distinct half-life and/or degradation of proteins.

Functional annotation of the positively correlated genes-proteins (90 under-expressed and 59 overexpressed) was performed using Enrichr. The most significant and relevant GO biological processes linked to the 90 positively under-expressed proteins in the myocardium of *Mtr cKO* mice were related to mitochondrial energy metabolism (mitochondrial respiratory chain complex I assembly, ATP biosynthesis and short chain fatty acid metabolism) and regulation of cardiac function (cardiac ventricular muscle development, cardiac muscle contraction and relaxation) ($P < 0.05$; **Figure 45**). Furthermore, GO molecular processes associated with these under-expressed proteins included: RNA binding, ATPase and NADH dehydrogenase activity, NO synthase binding, cadherins binding, long chain fatty acid binding and acylcoA transferase activity ($P < 0.05$; **Figure 46**). Pathway analysis revealed that the KEGG pathways associated with these under-expressed proteins in the myocardium of *Mtr cKO* included: oxidative phosphorylation, fatty acid degradation, dilated cardiomyopathy, hypertrophic cardiomyopathy, cardiac muscle contraction and apoptosis ($P < 0.05$; **Figure 47A**).

Similarly, functional annotations for the 59 positively overexpressed proteins in the myocardium of *Mtr cKO* mice were analyzed. The most relevant GO biological processes associated with these positively overexpressed proteins were related to adaptive response to unfolded proteins, oxidative stress, cardiac contraction and mitochondrial biogenesis and energy metabolism including mitochondrial complex I assembly, electron transport chain and glucose homeostasis ($P < 0.05$; **Figure 47B**).

To further investigate why genes were inversely translated in *Mtr cKO*, we analyzed the transcription factors protein-protein interactions target enrichment for the negatively translated proteins. We found that majority of the 85 negatively downregulated proteins were enriched in transcription regulation by ESR1 (encoding estrogen receptor 1), Myc (encoding Myc Proto-Oncogene Protein) and HTT (encoding huntingtin) transcription factors protein-protein interactions ($P = 6.38e^{-11,}$ $P = 1.09e^{-9}$ and $P = 4.38e^{-8}$ respectively; Supplementary file 2). On the other hand, no transcription factors were found to be significantly associated with the 50 negatively overexpressed protein, however transcription factor perturbation followed by expression were enriched in PPARG, ESR2 and GATA4 ($P < 0.05$; supplementary file 3).

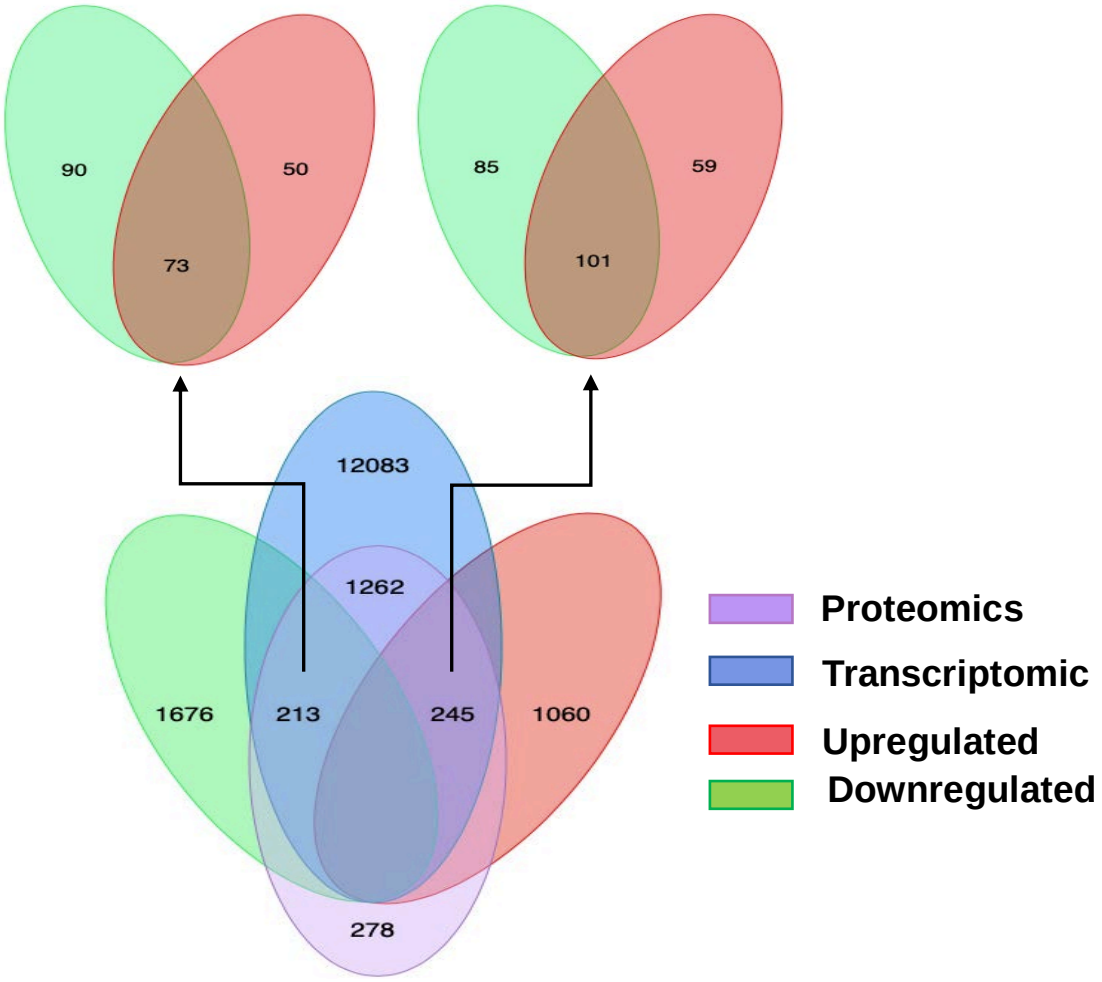

Figure 44: Venn diagram representing the overlapping between the commonly dysregulated genes and proteins in the hearts of *Mtr cKO* mice.

A total of 16539 genes and 1998 proteins were detected in the heart of *Mtr cKO* as revealed by transcriptomic and proteomic analysis respectively. Of these, a total 1720 genes-proteins were commonly dysregulated of which 213 were downregulated and 245 were upregulated. Transcriptomic driven analysis of proteome revealed that the 213 downregulated were positively translated into 90 downregulated proteins and negatively translated into 50 upregulated proteins and 73 proteins with no change. The 245 upregulated genes were negatively translated into 85 downregulated and positively translated into 59 upregulated proteins and 101 proteins with no change (0.8 < FC > 1.25.

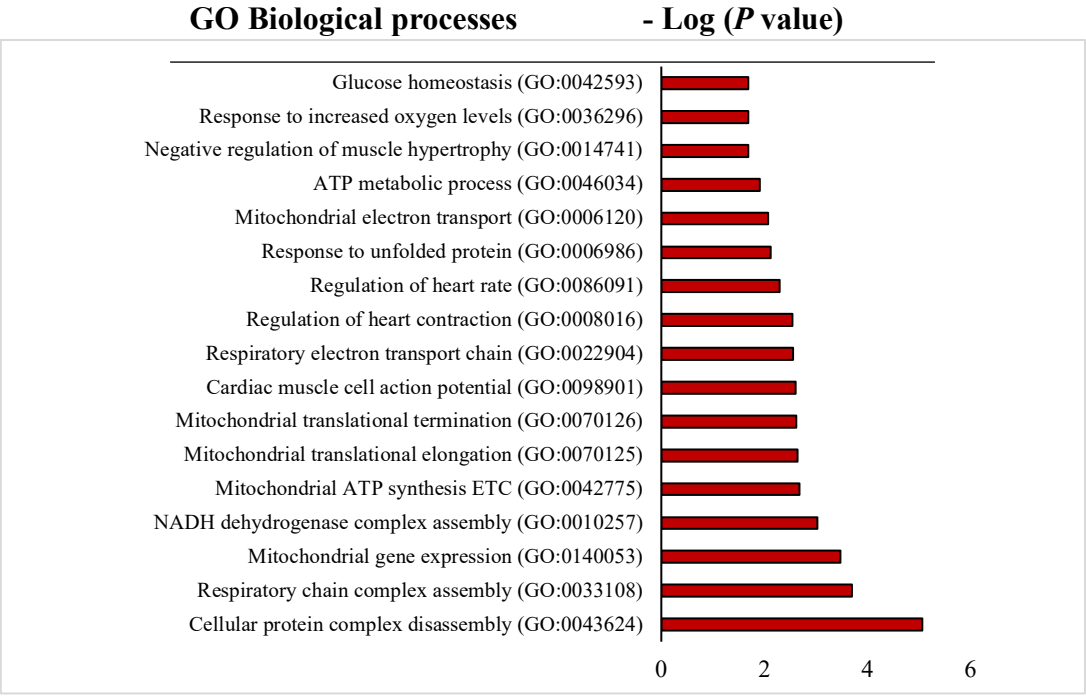

Figure 45: Enrichr GO biological processes of the 59 positively overexpressed proteins in the hearts of *Mtr cKO* in comparison to controls.

The bar graph shows GO biological processes associated with the 59 positively over-expressed proteins in the hearts of *Mtr cKO* animals.

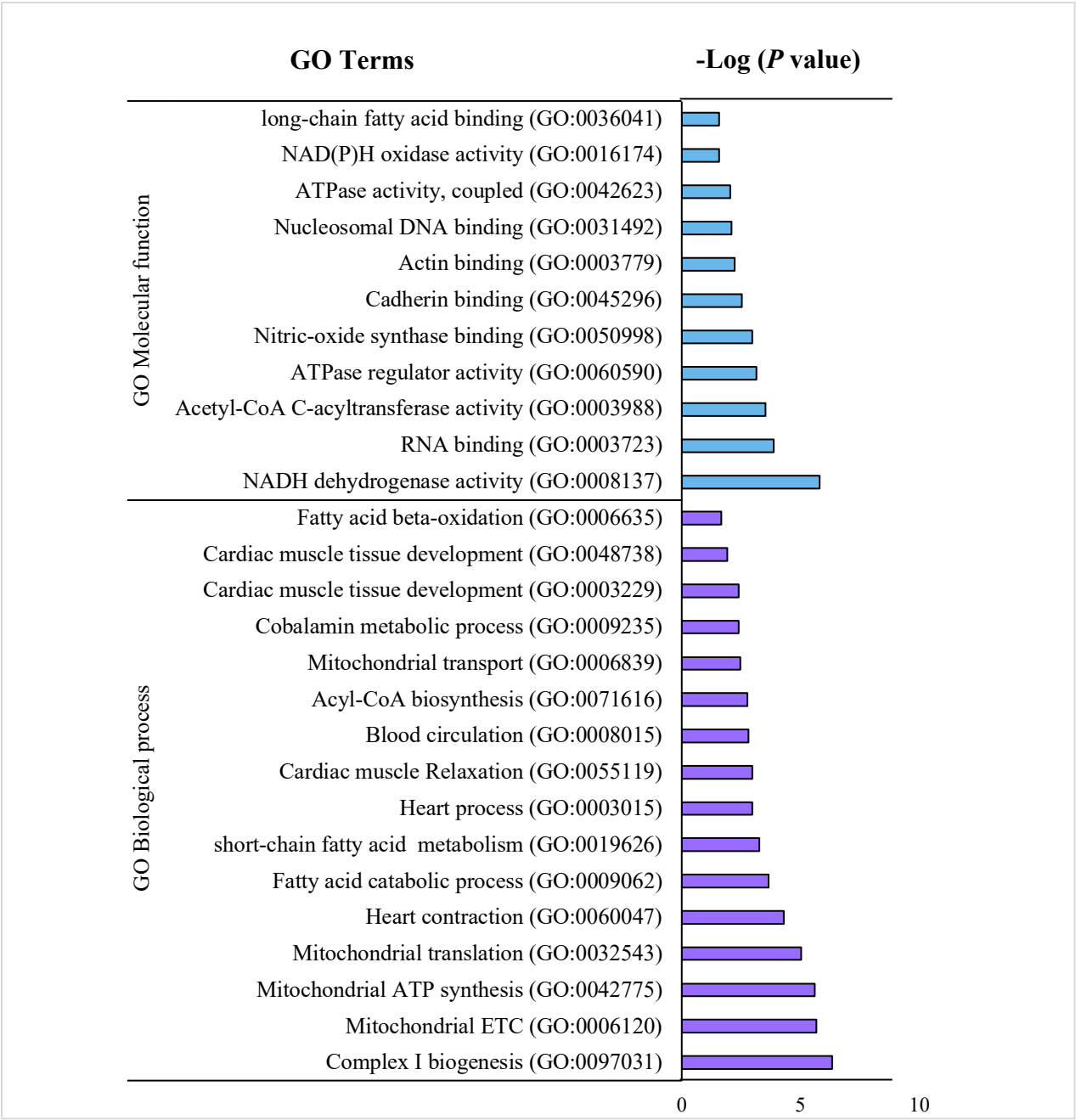

Figure 46: **Enrichr GO biological processes and molecular functions associated with the 90 positively under-expressed proteins in the hearts of *Mtr cKO*.**

Shown in the bar graph are the GO biological processes and molecular functions of the 90 positively under-expressed proteins in the hearts of *Mtr cKO* mice ($P < 0.05$).

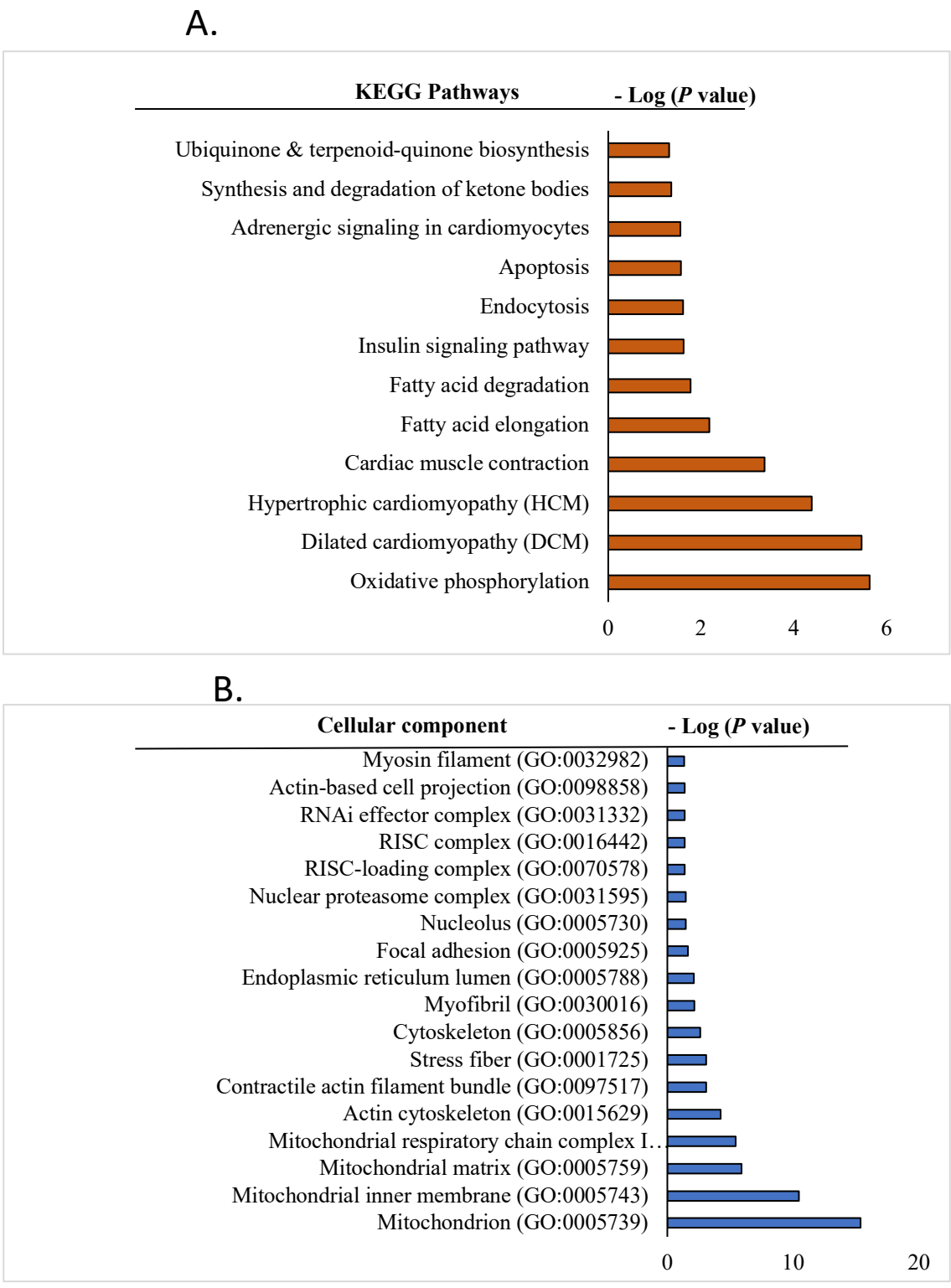

Figure 47: Enrichr GO cellular components and the KEGG pathways associated with the 90 under-expressed proteins in the heart of *Mtr cKO*.

A). KEGG pathways associated with the 90 under-expressed proteins in the heart of *Mtr cKO* mice analyzed by Enrichr. **B).** GO cellular component of the 90 under-expressed proteins in the heart of *Mtr cKO*.

3.3.2 Correlation analysis of the proteome and transcriptome

Spearman's correlation was used to evaluate the correlation between the expression values for the genes and proteins that were commonly dysregulated between proteome and transcriptome data sets. Once the correlations were computed, only genes and proteins with significant Spearmans rho values over a specific threshold were selected. With these criteria, 22 genes and proteins were significantly correlated in *Mtr cKO,* of which 17 were positively and 5 were negatively correlated respectively (**Table 17 and Figure 48)**

Gene/ protein	**rho**	***P* value**	**Transcriptome FC**	**Proteome FC**
Ak4	0.76	0.0368	1.96	1.40
Aldh1l2	-0.90	0.0046	0.77	1.52
Anxa4	-0.81	0.0218	1.30	0.45
Atic	-0.86	0.0107	1.25	0.93
Ckb	0.69	0.0694	1.37	1.58
Col15a1	-0.64	0.0962	0.77	0.63
Cops8	0.74	0.0458	0.78	1.07
Csrp3	0.79	0.0279	0.75	0.85
Dhrs1	0.76	0.0368	1.36	2.68
Echdc1	0.76	0.0368	0.79	0.93
Enpp4	0.64	0.0962	0.71	0.55
Gpd2	0.64	0.0962	0.73	0.77
Hist2h2ab	-0.71	0.0576	1.26	0.93
Hmox2	0.71	0.0576	1.31	3.16
Mrpl4	0.73	0.0396	1.28	14.35
Myl1	0.86	0.0107	0.32	0.32
Myl2	0.95	0.0011	0.75	0.55
Plin1	0.76	0.0368	0.26	0.57
Sh3glb2	0.67	0.0831	0.77	0.57
Slc25a1	0.86	0.0107	0.59	0.69
Slc4a1	0.88	0.0072	0.56	0.46
Snca	0.88	0.0072	0.65	0.447

Table 17: Correlation analysis of the proteome and transcriptome.

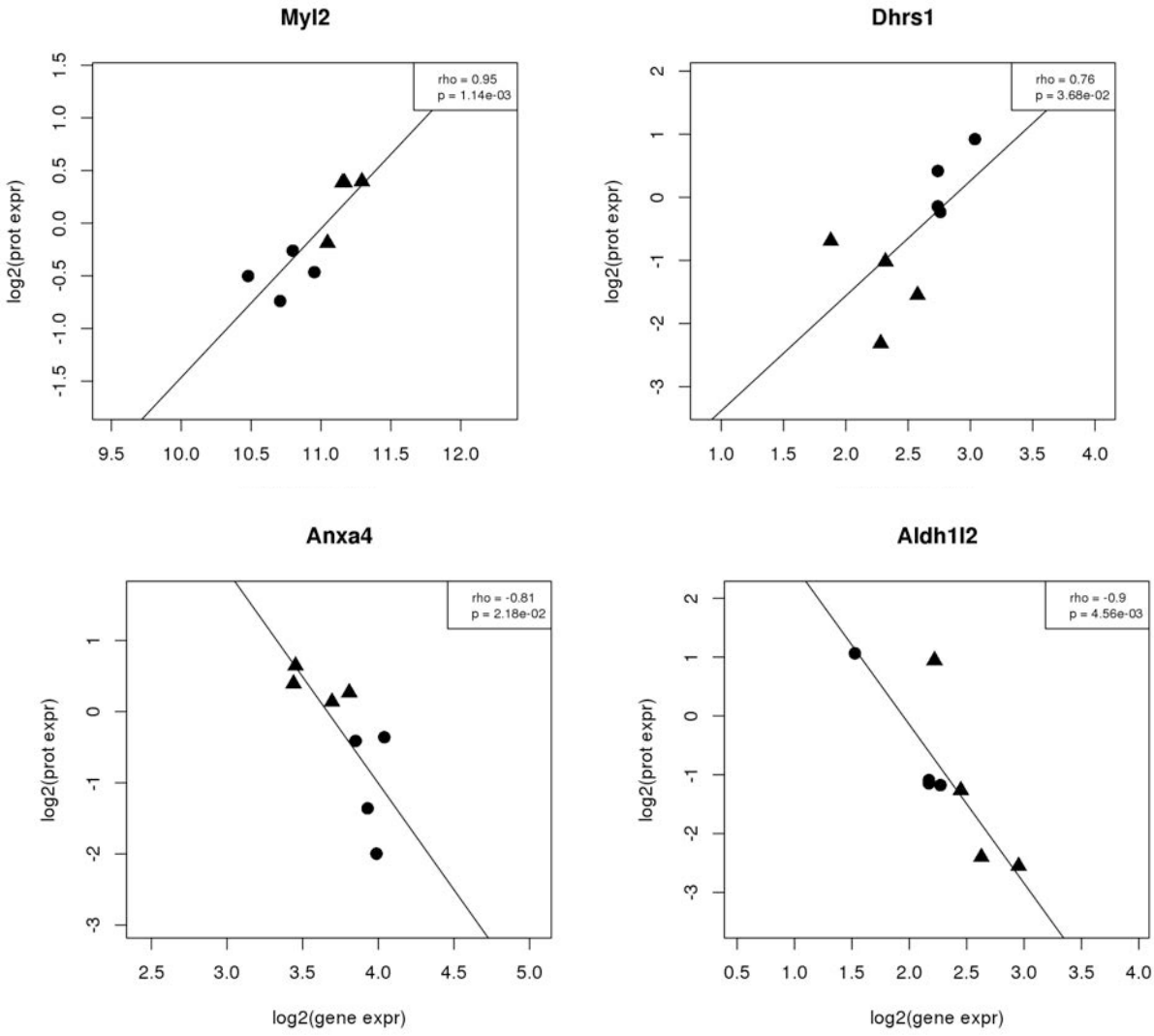

Figure 48: **Graphical representation of the positively and negatively correlated genes-proteins in *Mtr cKO* analyzed by Spearman correlation.**

Myl2 and Dhrs1 are among the 17 positively correlated genes-proteins and Anxa4 and Aldh1l2 are among the 5 negatively correlated genes-proteins in the hearts of *Mtr cKO*.

4 Consequences of cardiac specific invalidation of *Mtr* on cardiac remodelling.

Given the effect of cardiac specific deletion of *Mtr* gene on cardiac remodeling revealed by our omics studies. We further investigated the evidence of cardiac remodeling in *Mtr cKO* using immunostaining, western blotting and RT-qPCR. Cardiac hypertrophy and cardiac fibrosis were the main mechanisms linked to cardiac remodeling.

4.2 Cardiac specific deletion of *Mtr* gene induces myocardium hypertrophy

Silencing of methionine synthase in the heart induced cardiac hypertrophy evidenced by the increased heart to body weight ratios (HW/BW) of 5 months old *Mtr cKO* mice compared to the control (57.44 ± 2.8 vs 49.18 ± 2.58 Mg/g, $P = 0.02$; **Figure 49A**). Moreover, cardiac hypertrophy was evidenced by the increase in left ventricular mass revealed by transthoracic echocardiography (**Figure 49B)**. Our transcriptomic data showed that the Zinc finger transcription factor Gata4 a key regulator of hypertrophic growth and gene expression in the cardiomyocytes was significantly upregulated in *Mtr cKO* as compared to control (Fold change 2, $P < 0.00035$). We also used the KEGG pathway database to plot the dysregulated genes in the myocardium of *Mtr cKO* linked to cardiac hypertrophy. Of these genes Hgb5, Dmd, TPm2 and Myl2 were downregulated while cacna2d, Lmna and Pkag2 were upregulated as shown in the hypertrophic cardiomyopathy pathway (**Figure 50**). Collectively, these results indicate that *Mtr* gene deletion in the cardiomyocytes induces cardiac hypertrophy.

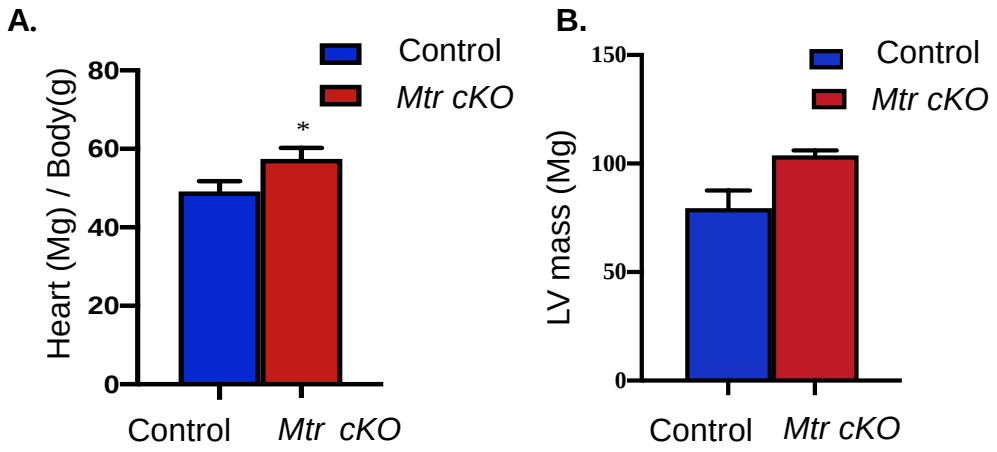

Figure 49: Deletion of *Mtr cKO* in the heart induces cardiac hypertrophy.

A). Heart to body weight ratio. **B).** Left ventricular mass evaluated using echocardiography between *Mtr cKO* and controls. Means ± SEM, n = 6 to 10 per group, * $P < 0.05$ ** $P < 0.01$, *** $P < 0.001$.

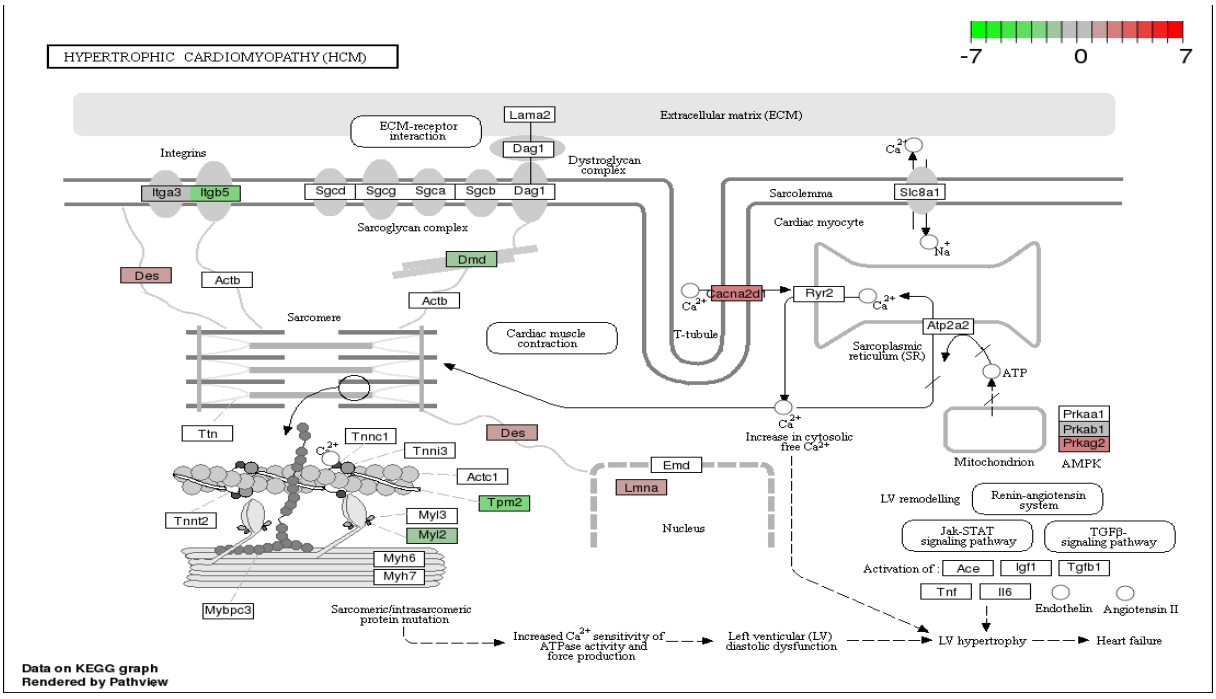

Figure 50: KEGG pathway showing the dysregulated genes in the *Mtr cKO* associated with the development of hypertrophic cardiomyopathy.

Shown in green are downregulated genes and in red are upregulated genes in *Mtr cKO* linked to cardiac hypertrophy.

4.3 Cardiac specific deletion of *Mtr* gene induces myocardial fibrosis

Given the evidence of cardiac hypertrophy in *Mtr cKO*, we further investigated the presence of cardiac fibrosis using histopathological staining, immuno-blotting and RT-qPCR. Both Masson's Trichrome and Picrosirius Red staining revealed a significant increase in collagen deposition in *Mtr cKO* hearts compared to control hearts (P = 0.018 and P = 0.0004 respectively; **Figure 51A** and **51B**). Furthermore, RT-qPCR analysis revealed an upregulated expression of Col3a1 and Col1a1 in *Mtr cKO* mice compared to controls (4.72-fold increase, P = 0.001, and 4.9-fold increase, P = 0.002 respectively; **Figure 51D**). This fibrosis was related to the upregulated expression of transforming growth factor beta 1 (TGFB1), angiotensin receptor 2 (AGTR2) and matrix metalloproteinase-2 (MMP2), as demonstrated by western blot analysis (P = 0.006, P = 0.023 and P = 0.005 respectively; **Figure 51C**). Immunofluorescence showed an increased expression MMP2 (**Figure 52**). Together, these results indicate that cardiac invalidation of *Mtr* gene induces cardiac interstitial fibrosis.

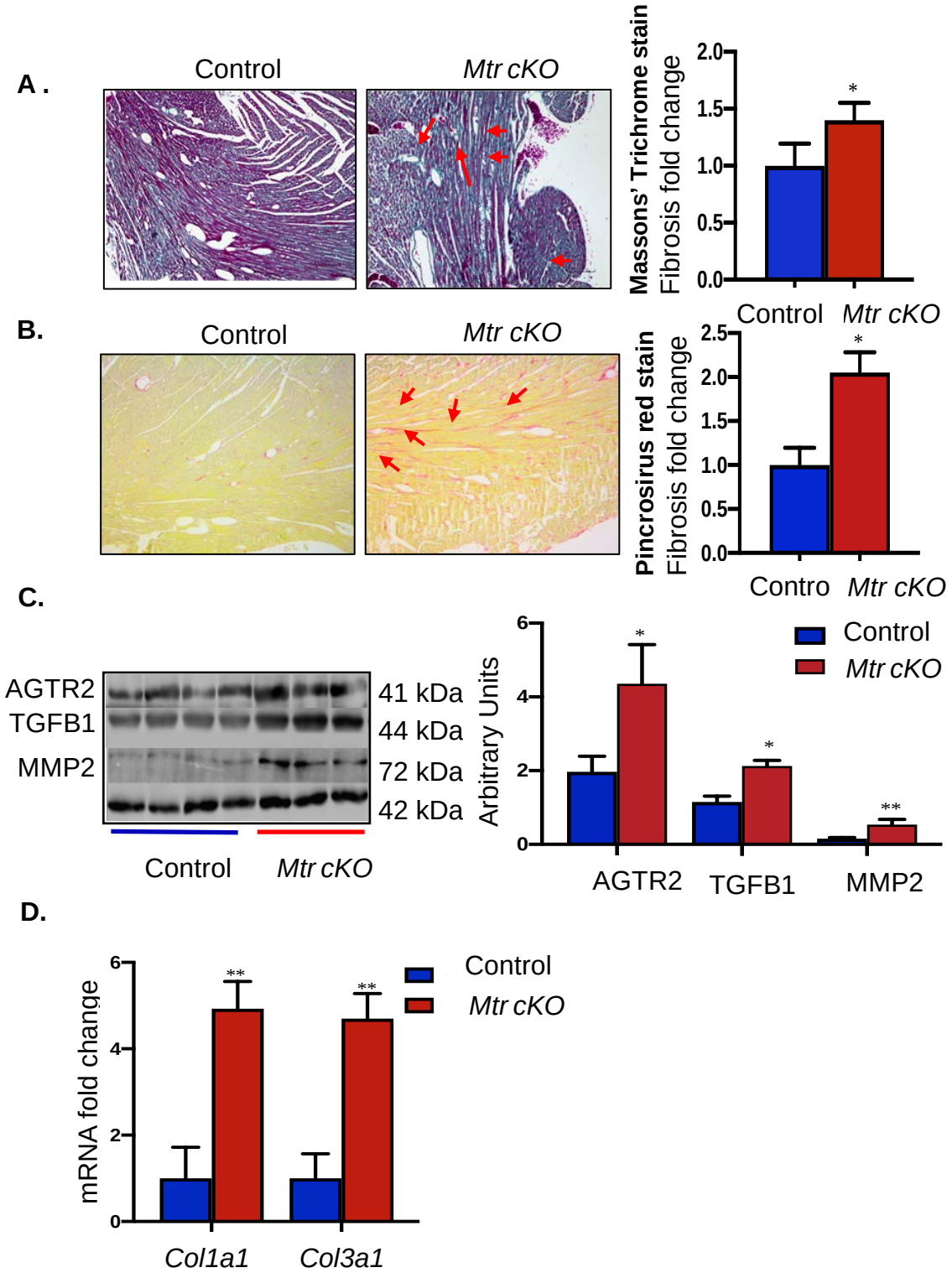

Figure 51*:* **Cardiac specific deletion of *Mtr* gene induces interstitial fibrosis in the myocardium evidenced by increased collagen deposition in the myocardium.**

A. Transversely sectioned left ventricular tissues from the controls and *Mtr cKO* mice stained with Masson's Trichrome, collagen enriched areas are stained in blue. **B**. Transversely sectioned left ventricular tissues from the controls and *Mtr cKO* mice stained with Picrosirius Red, collagen enriched areas are stained in red. **C**. Western blots showing expression levels of fibrotic proteins; AGTR2, TGFB1 and MMP2 in the myocardium of *Mtr cKO* and control. **D**. mRNA expression levels of collagen

encoding genes Cola1 and Col3a1 evaluated by RT-qPCR. Western blot protein bands were quantified densitometrically and the data was normalized to β actin and expressed as arbitrary units. Means ± SEM, n = 6 to 10 per group, *$P < 0.05$ **$P < 0.01$, *** $P < 0.001$.

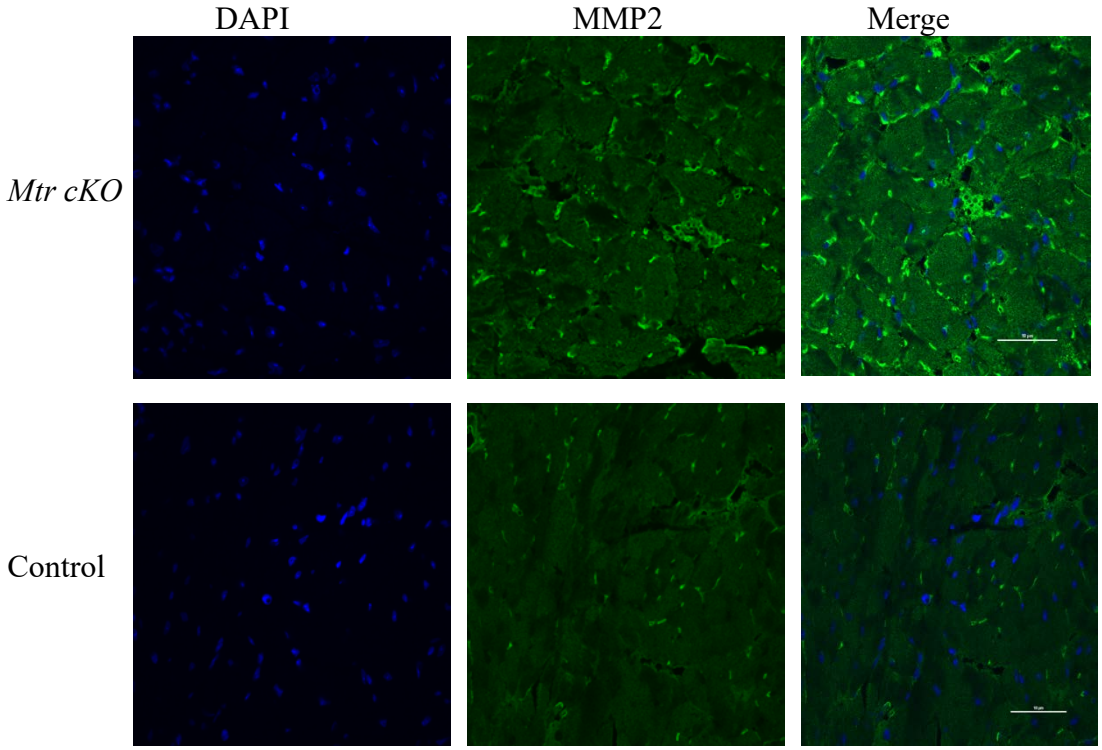

Figure 52: Cardiac specific deletion of *Mtr* gene induces interstitial fibrosis in the myocardium evidenced by increased expression of MMP2 in the myocardium of *Mtr cKO*.

Immunostaining showing the expression levels of MMP2 in the left ventricles of *Mtr cKO* and controls. MMP2 is shown in green and cell nucleus in blue.

4.4 Cardiac specific invalidation of *Mtr* gene induces cellular stress in the myocardium.

Cardiac invalidation of *Mtr* gene dysregulated the expression of genes and proteins involved in response to cellular stress. Transcriptomic data analysis showed a significant increased expression of genes encoding proteins involved in response to cellular stress and apoptosis, these genes included *Gata4 and Bcl2* and a downregulated expression of *Glrx3* in *Mtr cKO* compared with controls animals ($P < 0.05$). Consistently, proteomic studies also demonstrated an increased expression of proteins involved in response to cellular stress, including heat shock proteins and ubiquitin like modifier activity enzyme 1(Uba1) and SH3 Domain Binding Glutamate

Rich Protein Like 3 (SH3bgrl3) in the heart of *Mtr cKO* compared to control mice. SH3bgrl3 is a protein that modulates the biological activity of glutaredoxins. Furthermore, western blot analysis showed a significant increased expression of heat shock proteins Hspb3, and Hsp27 in *Mtr cKO* compared with control mice (2.0-fold increase, $P = 0.024$ and 8.1-fold increase, $P = 0.00023$, respectively, In contrast, no significant difference was observed for Hsp90 between the two groups ($P = 0.54$; **Figure 53A**). Annexin A5 a Ca2+ binding protein with anti-apoptotic, anti-inflammatory and anticoagulant effect was significantly upregulated (3.2-fold increase, $P = 0.0025$) in *Mtr cKO* compared to control. Moreover, MPV17 an inner mitochondrial membrane protein that plays crucial role in mitochondrial homeostasis through metabolism of reactive oxygen species and maintenance of mitochondrial DNA was significantly decreased of *Mtr cKO* ($P = 0.019$; **Figure 53B**). Inflammatory proteins caspase 1 and IL1 beta were also upregulated in *Mtr cKO* hearts compared to control hearts ($P = 0.016$ and $P = 0.184$ respectively; **Figure 53C**). Proteomic and western blot analysis revealed that sirt3 was significantly downregulated in the hearts of *Mtr cKO* in comparison to controls. Sirt3 is a mitochondrial NAD dependent deacetylase with antioxidant and antiapoptotic properties, it therefore plays crucial role in regulating mitochondrial homeostasis.

Given the cellular stress observed in *Mtr cKO*, we further investigated whether invalidation of *Mtr* gene influenced the subcellular localization of 3 stress-related RNA binding proteins (RBPs), ELVAL1/HuR, Y14 and hnRNPA1, using immunofluorescence detection. We found that hnRNPA1 was exclusively localized in the nucleus of cardiomyocytes of *Mtr cKO*, while it was localized in the cytoplasm and the perinucleus, in the cardiomyocytes of controls (**Figure 54A**). In contrast, ELVAL1/HuR was localized in the nucleus of the cardiomyocytes of both the *Mtr cKO* and controls, and its expression levels was comparable between the two groups (**Figure 54B**). We also found that Y14 was localized in the perinucleus and cytoplasm of the cardiomyocytes of both *Mtr cKO* and control animals (**Figure 54C**). Taken together, these data suggested that invalidation of *Mtr* gene in the cardiomyocytes blocks the shuttling of hnRNPA1 from the nucleus into the cytoplasm in stress conditions.

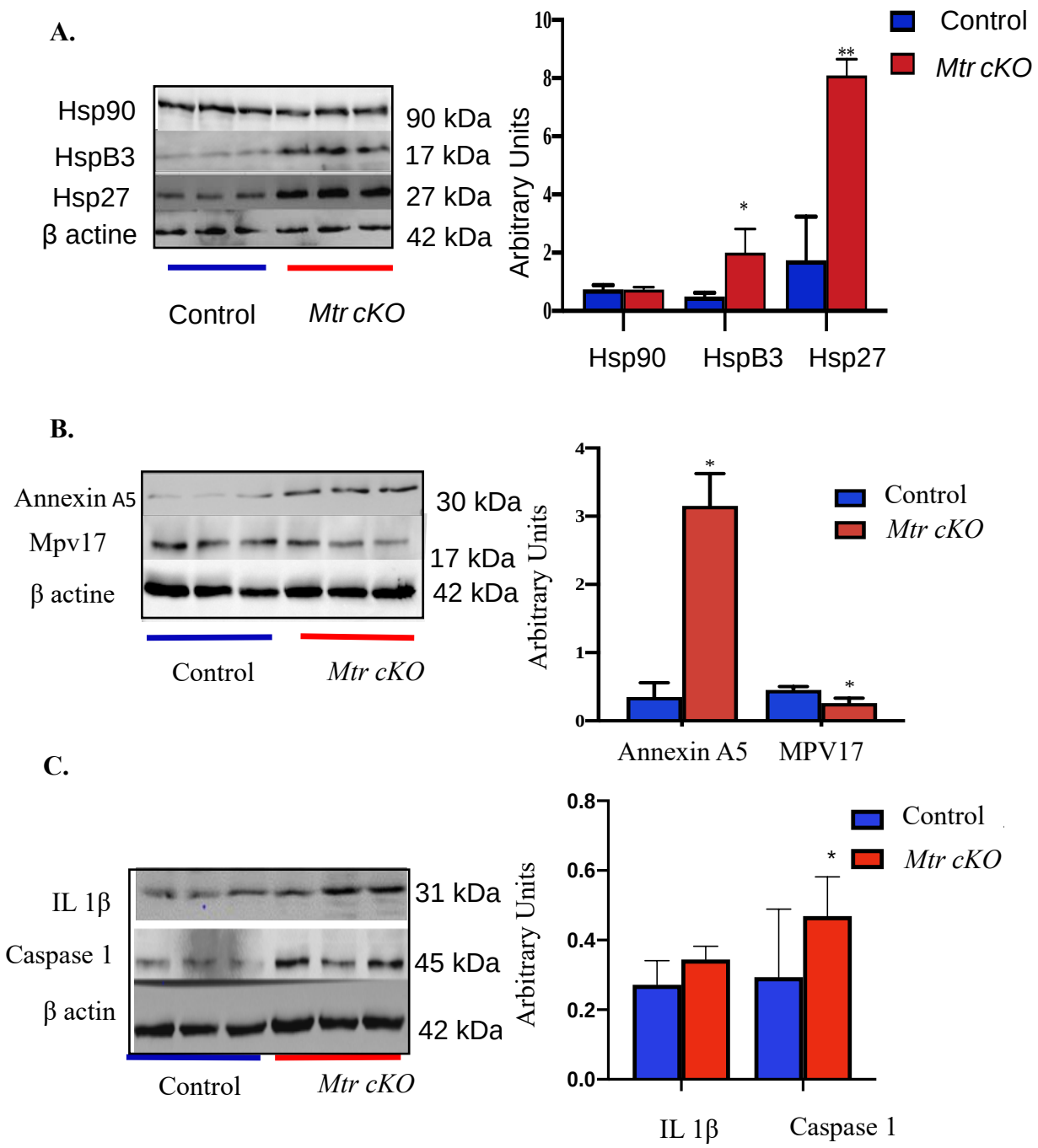

Figure 53: Cardiac specific deletion of *Mtr* gene induces cellular stress

A). Western blots of heat shock proteins Hsp90, Hspb3 and Hsp27. **B**. Western blots for annexin A5 and MPV17. **C**. Western blots for caspase 1 and IL1 beta. Protein bands were quantified densitometrically, the data was normalized to β actin and expressed as arbitrary units. n= 3 per group, Means ± SEM, * $P < 0.05$, ** $P < 0.01$, *** $P < 0.001$.

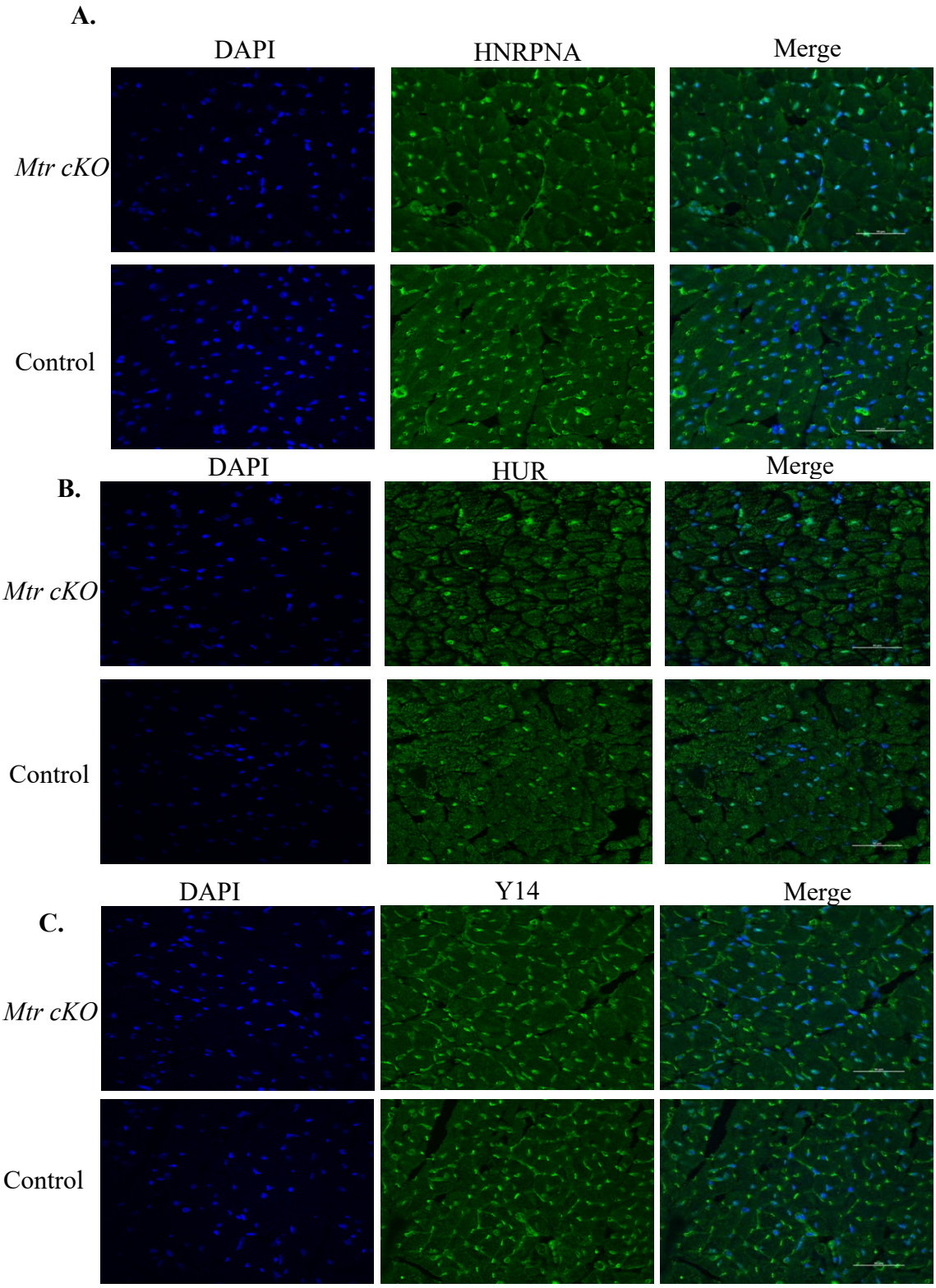

Figure 54: Subcellular localization of HNRNPA1, HuR/ ELAV1 and Y14 RNA binding proteins in the left ventricles of *Mtr cKO* and controls evaluated by immunofluorescence

A, B and C are subcellular localization of Hnrpna1, HuR/ ELAV1 and Y14 RNA binding proteins respectively in the left ventricles of *Mtr cKO* and control animals. HnrpnaA1, HUR and Y14 are stained in green while the cell nuclei are stained blue.

5 Consequences of cardiac specific invalidation of *Mtr* gene on energy metabolism in the myocardium

Invalidation of *Mtr* gene in the heart caused extensive deficit in myocardial energy metabolism. We evaluated the evidence of impaired energy metabolism in the myocardium by determining the concentration levels of acylcarnitine in plasma using LC-MS / MS and evaluating the expression levels of genes and proteins involved in energy metabolism using RT-qPCR and immuno-blotting respectively.

5.1 Concentration of acylcarnitine in plasma

Impaired energy metabolism in the myocardium was evidenced by the increased plasma concentration levels of short chain (C4) and medium chain (C8) acyl carnitines in *Mtr cKO* compared to controls mice ($P < 0.001$ and $P = 0.041$ respectively; **Figure 55A** and **Figure 55B** respectively). The C0 / (C16+C18) ratio which is an index for carnitine palmitoyl transferase 1 (CPT1) activity was significantly increased *(*$P = 0.025$) while C14.1 / C12.1 and C14.1 / C16 ratios were significantly decreased ($P < 0.001$ and $P = 0.039$) in *Mtr cKO* compared to controls (**Figures 55C, 55D** and **55E** respectively). Consistently, CD36, an important transmembrane fatty acid importer, was significantly downregulated in the *Mtr cKO* mice hearts ($P = 0.008$, **Figure 55F**). Together, these results confirm that invalidation of *Mtr cKO* gene in heart impairs myocardial fatty acid beta oxidation.

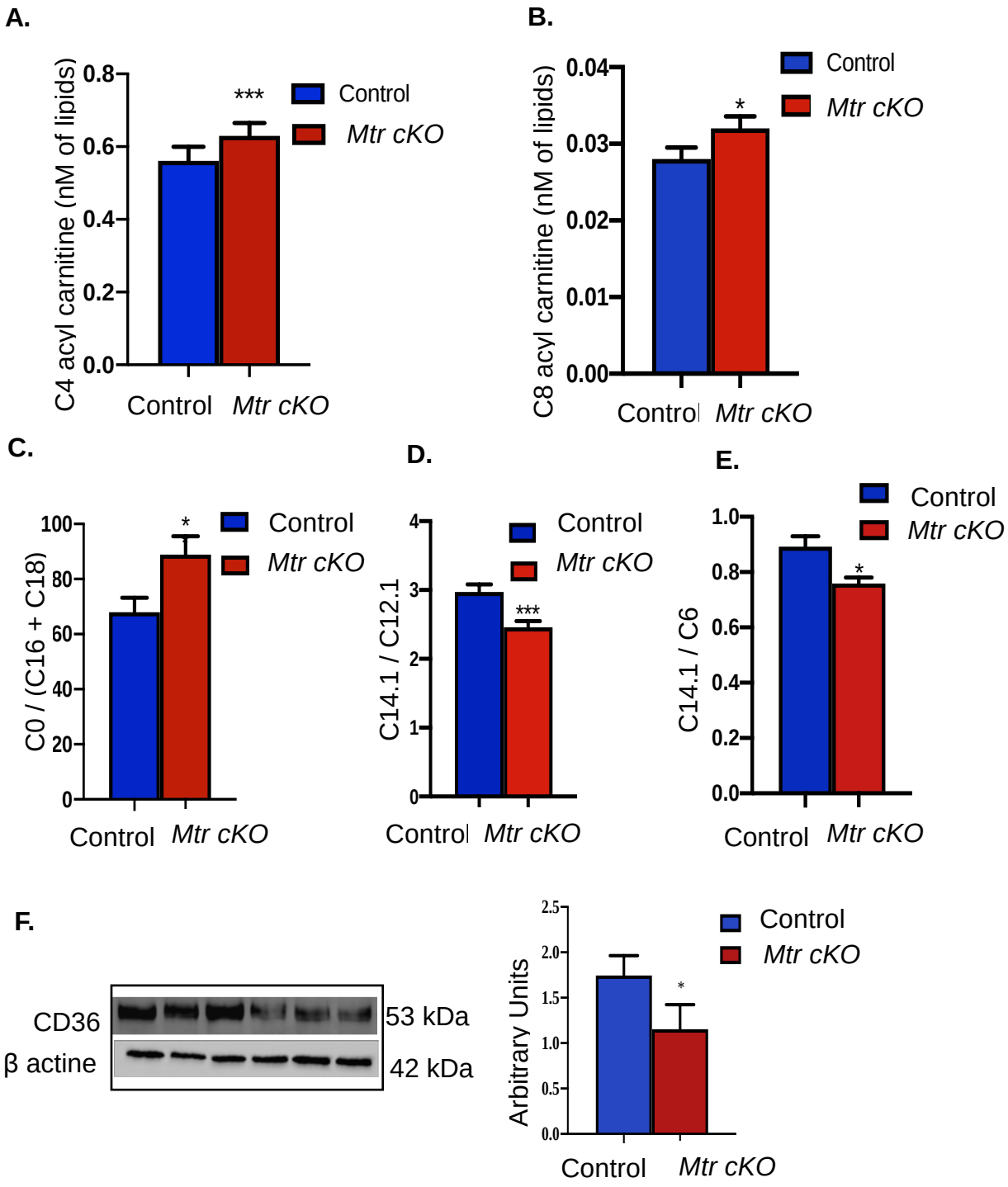

Figure 55: Plasma acylcarnitine concentration levels and expression of CD36 in hearts *Mtr cKO* and control mice.

A. Short chain (C4) and **B.** medium chain (C8) acylcarnitine levels in plasma of control and *Mtr cKO* mice analysed by LC-MS / MS. **C, D and E**. Acylcarnitine ratios in control and *Mtr cKO* mice. **F.** Western blots for CD36 in the heart of *Mtr cKO* and control mice. Protein bands were quantified densitometrically and normalized to β actin and expressed as arbitrary units. n = 3 per group, Means ± SEM, * $P < 0.05$ ** $P < 0.01$, *** $P < 0.001$.

5.2 Expression levels of genes, proteins and regulators of energy metabolism in the heart

5.2.1 Cardiac specific invalidation of *Mtr* gene induces dysregulated expression of fatty acid beta oxidation genes and proteins.

We observed a dysregulated expression of genes and proteins involved in fatty acid beta oxidation, oxidative phosphorylation and glycolysis in the hearts of *Mtr cKO* animals in comparison to controls.

In agreement with the impaired fatty acid oxidation in the *Mtr cKO* transcriptomics data analysis revealed a decreased expression of genes encoding fatty acid beta oxidation enzymes, including *Acat1, Acadm, Ehhadh, Acaa2* and *Decr1* ($P < 0.05$; **Figure 56 and Table 18**). Moreover, proteomic data analysis revealed a decreased expression of proteins involved in fatty acid oxidation, including 3 Oxoacyl (acyl carrier protein) synthase and Peroxisomal acyl coenzyme A oxidase ($P < 0.05$).

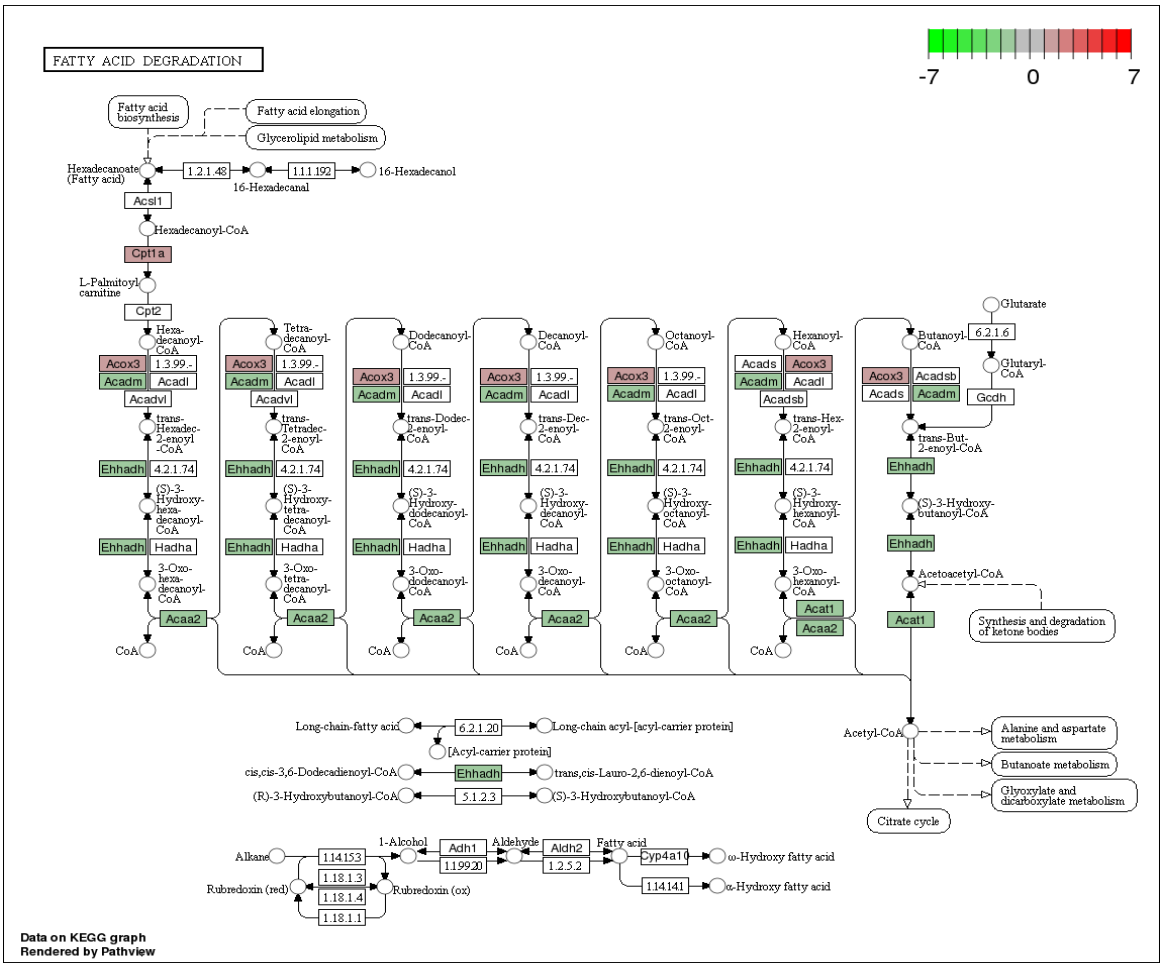

Figure 56: KEGG pathway showing dysregulated expression of genes encoding enzymes involved in fatty acid oxidation in the hearts of *Mtr cKO*.

Genes_Symbols_IDs	P Value	Fold change	Control_mean	MTR CKOmean
Acaa2//ENSMUSG00000036880	0.010	-1.340	351.53	262.47
Acat1//ENSMUSG00000032047	0.039	-1.191	338.69	284.46
Acadm//ENSMUSG00000062908	0.023	-1.309	816.37	623.48
Ehhadh//ENSMUSG00000022853	0.010	-1.848	19.64	10.63
Decr1//ENSMUSG00000028223	0.005	-1.392	189.69	136.29
Ndufv1//ENSMUSG00000037916	0.0195	-1.199	148.60	123.90
Ndufb4//ENSMUSG00000022820	0.015	-1.253	39.84	31.80
Ndufa7//ENSMUSG00000041881	0.033	-1.195	31.19	26.11
Cox6a2//ENSMUSG00000030785	0.035	-1.222	715.30	585.42
Cox7a1//ENSMUSG00000074218	0.051	-1.214	125.57	103.46
Atp5j//ENSMUSG00000022890	0.012	-1.342	111.84	83.32
Atp5s//ENSMUSG00000054894	0.046	-1.282	11.16	8.70
Atp5h//ENSMUSG00000034566	0.043	-1.217	292.03	240.05
Pfkfb1//ENSMUSG00000025271	3.96E-06	-3.637	8.23	2.26
Hk1//ENSMUSG00000037012	0.0004	1.657	33.72	55.86
Pdk3//ENSMUSG00000035232	0.0001	1.953	2.77	5.40
Sirt1//ENSMUSG00000020063	0.591	-1.037	12.38	11.94

Table 18: Transcriptomics data showing dysregulated genes involved in fatty acid beta oxidation, oxidative phosphorylation and glycolysis in the myocardium of *Mtr cKO*.

5.3 Cardiac specific invalidation of *Mtr* gene induces dysregulated expression of genes encoding oxidative phosphorylation and glycolysis enzymes.

Cardiomyocyte specific deletion of *Mtr* gene impaired oxidative phosphorylation in *Mtr cKO* compared to controls. Transcriptomic analysis evidenced a decreased expression of genes involved in mitochondrial oxidative phosphorylation including *NADH dehydrogenases; Ndufv1, Ndufb4 and Ndufa7* (complex I) and *Cox6a2* (complex IV), in *Mtr cKO* compared with control animals ($P < 0.05$; **Table 18** and Figure **58**). In addition, RT-qPCR showed an increased expression of Cox7a1 and Atp5j genes ($P < 0.05$, **Figure 57B**). Conversely, the analysis of heart transcriptome showed an adaptative upregulation of *Hk1 and Pdk3* genes of glycolysis, which was confirmed by RT-qPCR, in *Mtr cKO* compared with control animals ($P < 0.05$; **Figure 57A**). Western blot analysis confirmed the increased expression of mitochondrial membrane ATP synthase subunit a (mt ATP6) and the decreased expression of cytochrome b in *Mtr cKO* hearts compared to control ($P < 0.05$, **Figure 57C).** Functional annotations of the dysregulated proteins and genes in the hearts of *Mtr cKO* by Panther and Enricher showed that the GO biological processes were related to fatty acid beta oxidation, electron transport chain, mitochondrial complex 1 assembly and mitochondrial biogenesis.

Combined, these results indicate that invalidation of *Mtr* gene in the cardiomyocytes causes severe deficit in mitochondrial energy metabolism. *Mtr* gene invalidation impairs oxidative phosphorylation and fatty acid beta oxidation and induces adaptative upregulation of glycolysis. Therefore, energy metabolism in the myocardium of *Mtr cKO* shifts back to fetal energy metabolism that largely depends on glycolysis as source of ATP. This shift is a hallmark of heart failure.

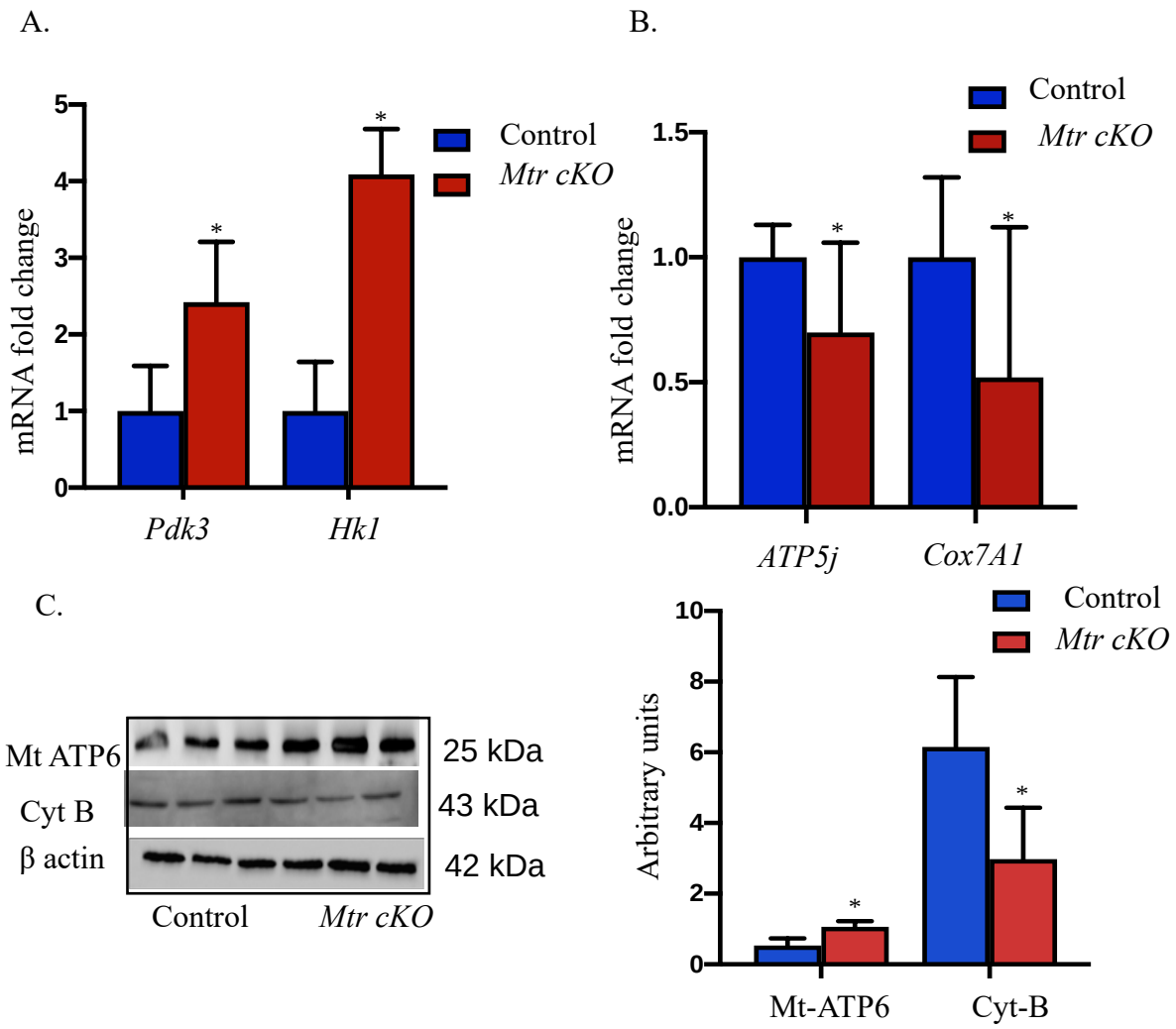

Figure 57: Cardiac invalidation of *Mtr* induces dysregulated expression of oxidative phosphorylation and glycolytic genes and proteins.

A. mRNA expression level of glycolytic genes *Pdk3* and *Hk1* in the heart of *Mtr cKO* and control analyzed by RT-qPCR. **B.** mRNA expression level of *Cox7a1* and *ATP5j* genes in the heart of *Mtr cKO* and control mice analyzed by RT-qPCR. **C.** Western blots for Mt-ATP6 and cytochrome B in the heart of *Mtr cKO* and control mice. Protein bands were quantified densitometrically, normalized to β actin and expressed as arbitrary units. n = 3 to 6 per group, Means ± SEM, * $P < 0.05$ ** $P < 0.01$, *** $P < 0.001$.

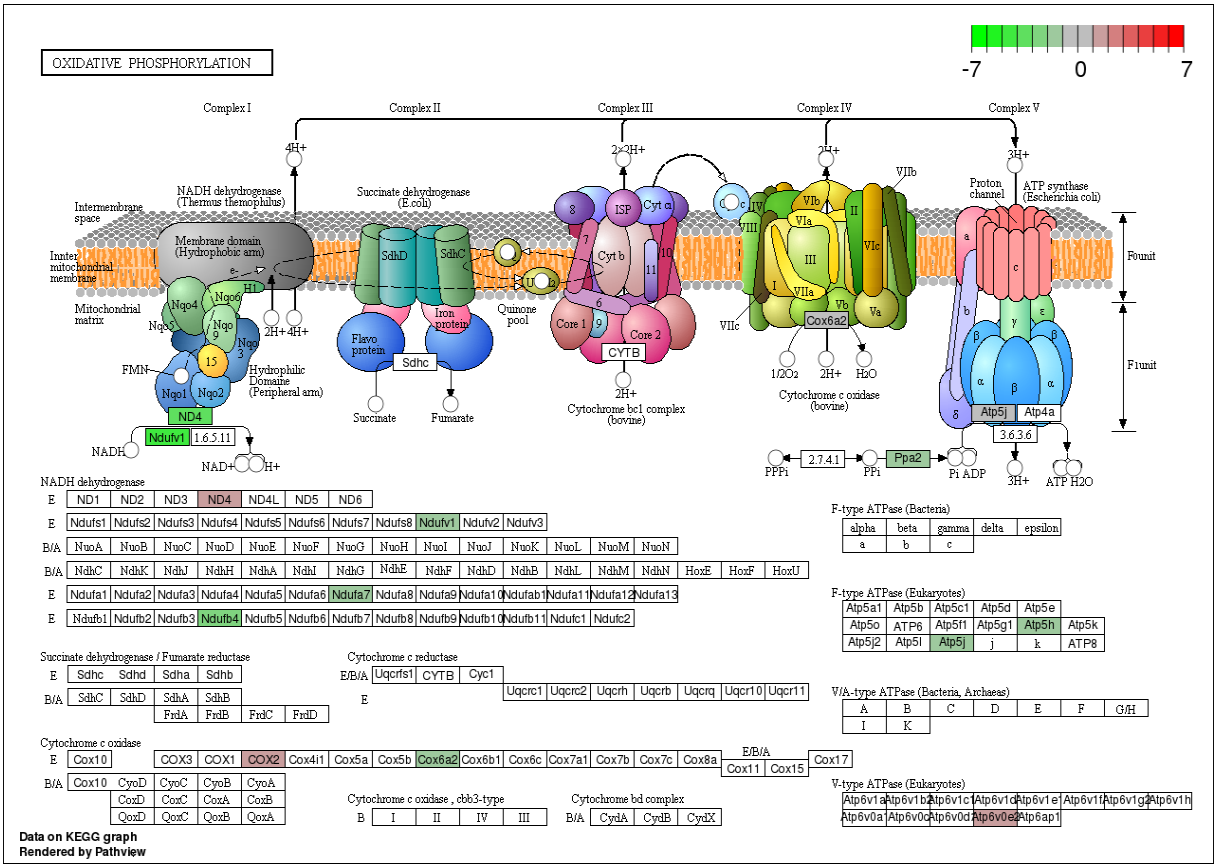

Figure 58: KEGG pathway showing dysregulated genes involved oxidative phosphorylation in the hearts of *Mtr cKO*. Shown in green are downregulated genes and red are upregulated genes.

Shown in green are downregulated genes and in red are upregulated genes encoding proteins involved in oxidative phosphorylation in the hearts of *Mtr cKO*.

5.4 Expression levels of regulators of energy metabolism in the heart

Mitochondrial NADH deacetylase Sirt3 is a prominent regulator of mitochondrial energy metabolism. In addition to regulation of mitochondrial homeostasis and biogenesis, Sirt3 activates key proteins involved in mitochondrial energy metabolism, including fatty acid oxidation, oxidative phosphorylation, glycolysis and ketone metabolism by deacetylation. Sirt3 was significantly downregulated in *Mtr cKO* compared with control animals, in proteomic and western blot analysis ($P = 0.008$; **Figure 59**). On the other hand, the expression levels of NAD-dependent deacetylase sirtuin-1 was comparable between the two groups ($P = 0.537$; **Figure 59**). Furthermore, peroxisome proliferator activated receptor gamma coactivator 1 alpha (PGC1 alpha), a key regulator of energy metabolism was slightly decreased in the hearts of *Mtr cKO,* however, this change was not significant ($P = 0.10$; **Figure 59**). Together, these results indicate

that the decreased expressed of Sirt3 induced significant impaired myocardial mitochondrial energy metabolism in *Mtr cKO*.

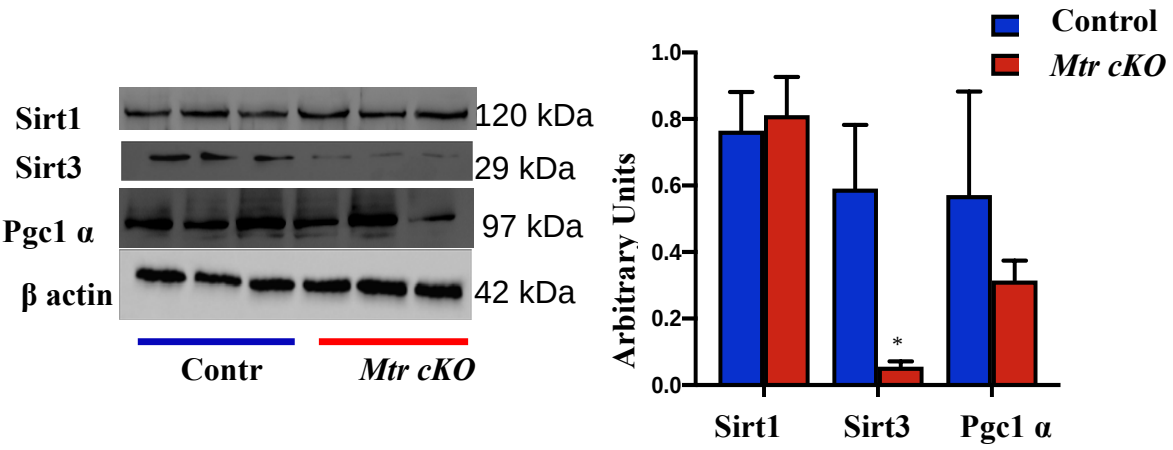

Figure 59: Silencing of MS in the heart impairs energy metabolism by decreasing the expression of Sirt3 protein.

Expression levels of Sirt3, Sirt1 and Pgc1 alpha in the heart of *Mtr cKO* and control analyzed by immune blotting**.** Protein bands were quantified densitometrically and normalized to β actin. n = 3 per group, Means ± SEM, * $P < 0.05$ ** $P < 0.01$, *** $P < 0.001$.

MODEL II : Study of cardiovascular consequences of systemic invalidation of *MMACHC* gene in 5 months old mice

1. Consequences of systemic invalidation of *MMACHC* gene on cardiac function parameters

1.1. Systolic Blood pressure

In order to evaluate the consequences of systemic mutation of MMACHC gene on cardiac function parameters, systolic blood pressure in five months old conscious mice was measured using non-invasive tail cuff plethysmography method. No significant difference was observed between the two groups (118.77 vs 126.00 mmHg, $P = 0.3812$; **Figure 60**).

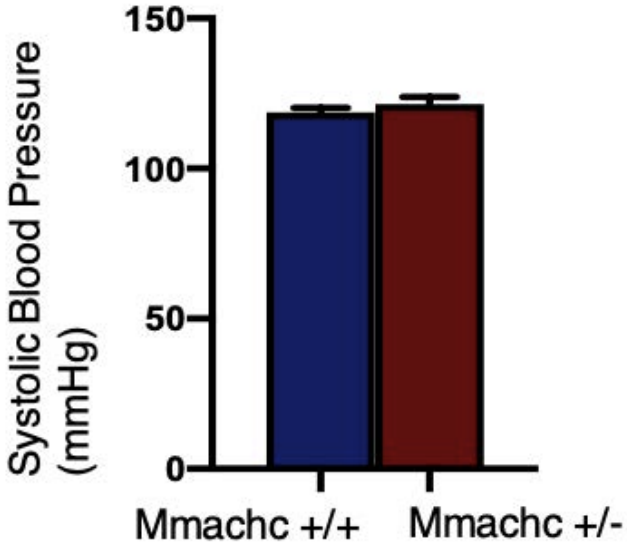

Figure 60: Systolic blood pressure in the M*M*ACHC $^{+/+}$ and MMACHC $^{+/-}$ mice measured using tail cuff plethysmography.

n = 6 to 10 per group, Mean ± SEM, * $P < 0.05$ ** $P < 0.01$, *** $P < 0.001$.

1.2. Expression levels of biomarkers of heart failure

RT-qPCR was used to measure the expression levels of natriuretic peptides (ANP and BNP), α-MHC and β-MHC genes in heart tissues of *MMACHC* $^{+/+}$ and *MMACHC* $^{+/-}$ mice. The expression levels of both ANP and BNP genes were comparable between the two groups (P = 0.4 6 and $P = 0.42$, respectively; **Figure 61**). α-MHC was upregulated while the β-MHC gene was downregulated in the hearts of *MMACHC* $^{+/-}$ mice in comparison to *MMACHC* $^{+/+}$, however this change was not significant ($P = 0.56$ and $P = 0.20$ respectively; **Figure 61**). Together, these

results suggest that systemic invalidation of MMACHC gene in heterozygous state did not induce cardiac dysfunction in 5 months old mice.

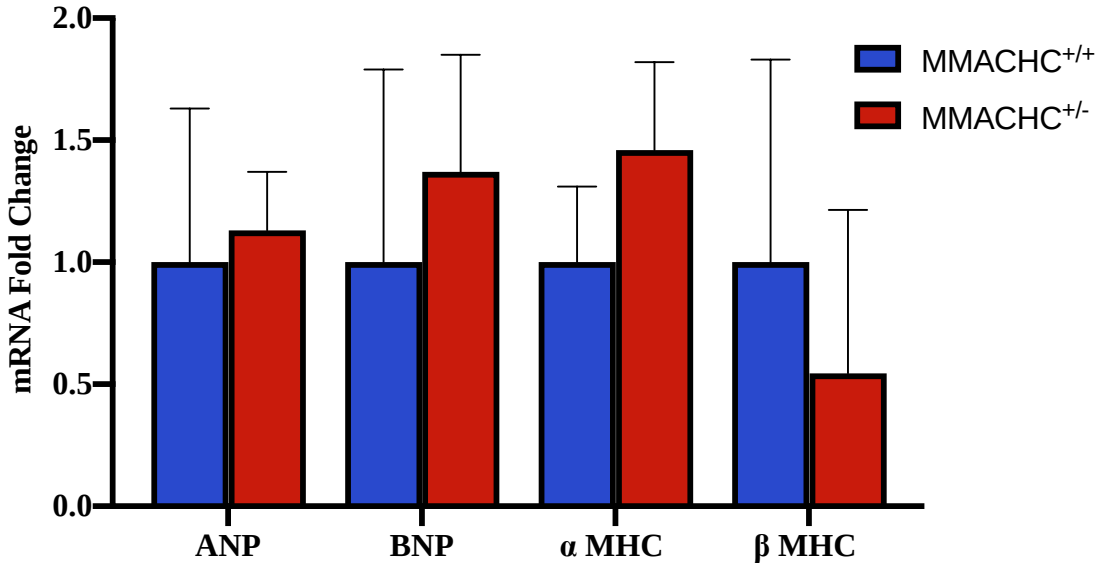

Figure 61: Expression levels of biomarkers of heart failure in the hearts of MMACHC $^{+/-}$ and MMACHC $^{+/+}$ mice.

Level expression of genes encoding atrial natriuretic peptide (ANP), brain natriuretic peptides (BNP), alpha myosin heavy chain (α-MHC) and beta myosin heavy chain (β-MHC) in the heart tissues of MMACHC $^{+/-}$ and MMACHC $^{+/+}$ mice analyzed by RT-qPCR. Means ± SEM, n = 6 to 10 per group, * $P < 0.05$ ** $P < 0.01$, *** $P < 0.001$.

2 Consequences of cardiac specific invalidation of *Mtr* gene on one carbon metabolism

Given that we did not observe any difference in systolic blood pressure and biomarkers of heart failure in the five months old *MMACHC* $^{+/+}$ and *MMACHC* $^{+/-}$ mice. We measured vitamin B12 concentration levels in the heart tissues of 21 days old mice whose dams were either fed normal diet or a vitamin B12 deficient diet using LC-MS/MS. A decrease in concentration of vitamin B12 was observed in the hearts of 21 days old *MMACHC* $^{+/-}$ whose mothers were fed with normal diet as compared to *MMACHC* $^{+/+}$, however this decrease was not significant (355 vs 1723 nmol/g, $P = 0.307$; **Figure 62A**). Vitamin B12 was not detected in the heart tissues of 21 days old *MMACHC* $^{+/-}$ mice whose mothers were fed vitamin B12 deficient diet during gestation and lactation (118.00 vs 0.0 nmol/g, $P = 0.027$; **Figure 62B**).

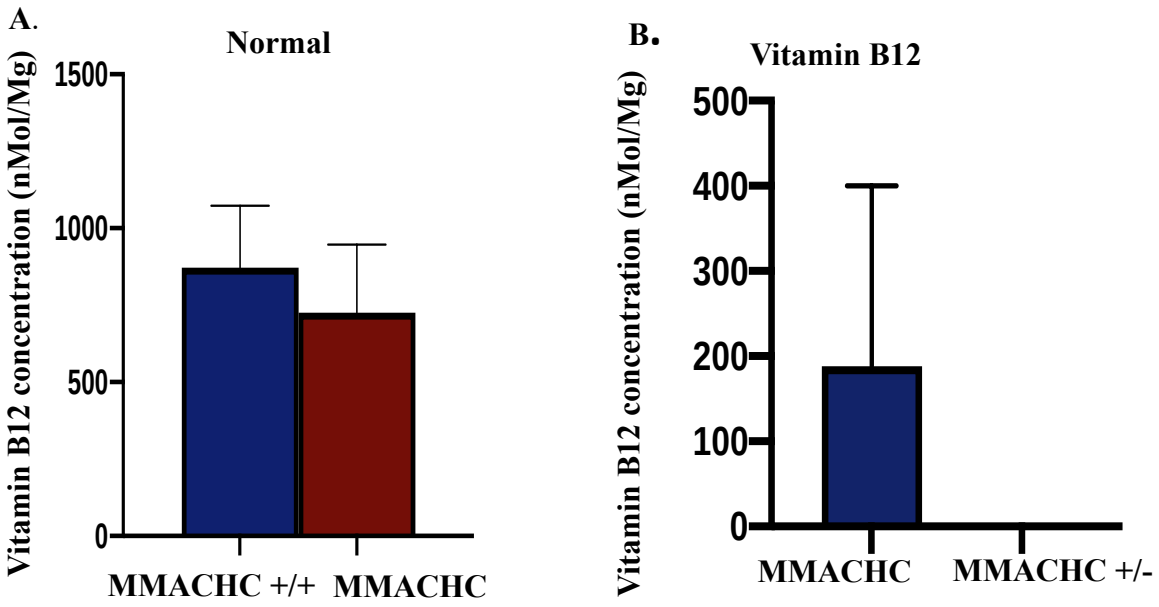

Figure 62: Concentration of Vitamin B12 in the hearts of 21 days old MMACHC $^{+/+}$ and MMACHC $^{+/-}$ mice analyzed by LC-MS/MS.

A. Vitamin B12 levels in the heart of 21 days old MMACHC $^{+/+}$ and MMACHC $^{+/-}$ mice whose mothers were fed normal diet during gestation and lactation. **B**. Vitamin B12 levels in the heart of 21 days old MMACHC $^{+/+}$ and MMACHC $^{+/-}$ mice whose mothers were fed vitamin B12 deficient diet during gestation and lactation. Means ± SEM, n = 6 to 10 per group, * $P < 0.05$ ** $P < 0.01$, *** $P < 0.001$.

DISCUSSION

Our study is focused on understanding the molecular and metabolic mechanisms in cardiomyopathies associated with genetic defects of remethylation of homocysteine observed in CblG and CblC inborn errors of cobalamin (vitamin B12) metabolism. In this context, the aim of this Ph.D work was to investigate and characterize cardiac metabolic and functional consequences in two transgenic mice models 1) of constitutive cardiac specific invalidation of *Mtr* gene (encoding methionine MS) and 2) of systemic invalidation of *MMACHC* gene (encoding MMACHC protein). Mutations in *Mtr* gene causes CblG (Leclerc et al., 1996) while mutations of *MMACHC* gene cause CblC (Carrillo-Carrasco et al., 2012b; Lerner-Ellis et al., 2009). Given that the metabolism of homocysteine into cystathionine in the transsulfuration pathway catalyzed by cystathionine beta synthase and the alternative remethylation pathway by betaine dependent betaine homocysteine methyl transferase (BHMT) is undetectable in the myocardium, these proteins play limited role in the synthesis of methionine and elimination of homocysteine (Guéant et al.,2013). We therefore hypothesized that vitamin B12 dependent remethylation of homocysteine by MS is the major pathway for metabolism and elimination of homocysteine in the cardiomyocytes of *Mtr cKO*. Studying consequences of systemic homozygous deletion of *Mtr* gene is complicated because homozygous *Mtr* Knockout mice are lethal at embryogenic stage (Swanson et al., 2001), for this reason we used transgenic mice model of cardiac specific constitutive invalidation of *Mtr* gene.

We found that selective *Mtr* invalidation in heart produces cardiomyopathy with heart failure, myocardium hypertrophy and fibrosis in young adult mice. The selective silencing of *Mtr* was evidenced by the decreased expression and activity of MS enzyme at protein levels whereas at the metabolic level, by the decreased SAM:SAH ratio and increase in tissue concentration of SAH. The increased accumulation of SAH in the hearts of knock out animals was a consequence of insufficient remethylation of homocysteine by MS and the reversible hydrolysis of homocysteine into SAH by SAH hydrolase (Forges et al., 2007). The cardiomyopathy observed in *Mtr cKO* was related to impaired mitochondrial energy metabolism with disruption of fatty acid oxidation and oxidative phosphorylation, cellular stress and cardiac remodelling with fibrosis.

Selective invalidation of *Mtr* gene induced dilated cardiomyopathy with severe left ventricular systolic dysfunction (Kemp & Conte, 2012; Yancy et al., 2013). This cardiomyopathy was documented by the increase in both end systolic and diastolic volumes which consequently led to decrease in ejection fraction (LVEF < 40). According to Frank-Starling mechanism, the

increase in both left ventricular diastolic volume and end systolic volumes results in the stretching of the hearts' muscle fibers leading to dilatation of the left ventricles (Kemp & Conte, 2012). Left ventricular ejection fraction < 40 is considered as a marker for heart failure (Yancy et al., 2013). Patients with heart failure with reduced ejection fraction (HFrEF) have left ventricular ejection fraction < 40 (Butler, Anker, & Packer, 2019; Jessup et al., 2016). Impaired left ventricular function and heart failure might have contributed to the decreased survival rates observed in *Mtr cKO*.

The significant increased expression of genes encoding the natriuretic peptides (ANP and BNP) in the myocardium of *Mtr cKO* evidenced heart failure induced by selective invalidation of *Mtr* gene in the cardiomyocytes. ANP and BNP are neurohormonal peptides that play vital role as diagnostic and prognostic biomarkers of heart failure and cardiac dysfunction (Baba et al., 2019; Cao et al., 2019; Maisel et al., 2018). ANP is produced predominantly in the atria and to a lesser extend in the ventricles while the BNP is produced in the ventricles. These peptides are produced in response to pressure and volume overload particularly in reponse to mechanical stretching of the atria and ventricle walls (Maisel et al., 2018). Furthermore, the shift in the expression of myosin heavy chain from alpha isoform to beta isoform in the hearts of *Mtr cKO* illustrated the contractile dysfunction and heart failure induced by MS silencing (Krenz & Robbins, 2004). This shift was accompanied by the decrease in the alpha MHC: beta MHC ratio which is a hallmark of heart failure. Experimental studies of failing hearts including those of end stage chronic heart failuire and failing adult mouse hearts have reported a shift from alpha MHC to beta MHC (Krenz & Robbins, 2004). This shift is believed to be an adaptive response to preserve energy, however under cardiovascular stress conditions, this shift is detrimental (Krenz & Robbins, 2004).

The decreased expression of Sirt3 was consistent with the impaired energy metabolisms in *Mtr cKO (Ahn et al., 2008)*. The mislocalization and nuclear sequestration of mRNAs of hnRNPA1 could explain part of the expression changes of genes and proteins involved in energy metabolism and response to cellular stress. It is noteworthy that we previously found a similar disruption of myocardial fatty acid beta oxidation and impaired oxidative phosphorylation with decreased complex I and complex II respiratory activities in rat pubs from dams fed with methyl donor deficient diet during gestation and lactation. These observations were related to decreased SAM:SAH ratio and decreased expression of PMRT1 and Sirt1 proteins which consequently led to hyperacetylation and hypomethylation of PGC1 alpha (Garcia et al., 2011).

Mitochondria play a central role in myocardium physiology. The heart continuously generates ATP to meet its constant energy and intermediate metabolites requirements to support its

contractile function (Lopaschuk et al., 2010). The increased plasma concentration of both short and medium chain acyl carnitines in *Mtr cKO* was a consequence of the impaired fatty acid beta oxidation and the decreased activity of carnitine Palmitoyl transferase 1 (CPT1) reflected by the increase in C0/(C16+C18) ratio (Hollak & Lachmann, 2016). The increased concentration of short and medium chain acyl carnitines was consistent with the transcriptomic and proteomic expression changes of genes and proteins involved in fatty acid oxidation in *Mtr cKO*. The changes evidenced in transcriptomic analyses were found with genes encoding proteins of the mitochondrial matrix of fatty acid oxidation. Both transcriptomic and proteomic analyses showed a decreased expression of ACAT1, which plays a crucial role in the final step of fatty acid beta oxidation and ketone body metabolism. The impaired fatty acid beta oxidation was also illustrated by the decreased expression of Cd36 in the myocardium of *Mtr cKO*. Cd36 is a transmembrane fatty acid transporter, which plays a major role in fatty acid uptake across cardiomyocyte membrane (Glatz, Nabben, Heather, Bonen, & Luiken, 2016). Fatty acid uptake via Cd36 is critical for sufficient production of ATP in the heart and that its deletion accelerates contractile dysfunction (Umbarawan et al., 2018b). Cardiomyocyte specific deletion of *Cd36* gene in adult mice hastens the progression from compensated cardiac hypertrophy to heart failure in response to pressure overload (Sung et al., 2017). Conversely, cardio-specific inhibition of CD36 can protect mice against high fat diet induced cardiac remodelling (Y. Zhang et al., 2015). The overexpression of genes encoding glycolytic pathway enzymes, including *Gck*, *Hk1* and *Pdk3* could be a compensatory mechanism of impaired fatty acid oxidation of *Mtr cKO* mice (Fillmore et al., 2014; Kato et al., 2010; Lopaschuk et al., 2010; Riehle Christian et al., 2011). These changes illustrates the shift of myocardial energy production from impaired fatty acid oxidation to glycolysis, a very known metabolic hallmark of heart failure (Lopaschuk et al., 2018; Kato et al., 2010; Lopaschuk et al., 2010).

Cardiomyocyte specific silencing of *Mtr* also impaired oxidative phosphorylation in myocardium through decreased expression of genes and proteins involved in complex I, complex IV and complex V. Of particular interest was the decreased expression of Ndufv1 gene encoding NADH Dehydrogenase Ubiquinone Flavoprotein 1, which plays a crucial role in delivering electrons from NADH to ubiquinone. A decreased expression of NDUFV1 protein was previously reported in patients with dilated cardiomyopathy (Ono et al., 2010). Complex 1 deficiency is associated with hypertrophic cardiomyopathy and neonatal cardiomyopathy (Bugiani et al., 2004; Pitkanen et al., 1996; B. H. Robinson, 1998) and ischemic heart failure (T. Liu et al., 2014). Mutations in *Ndufv1* gene have also been linked to mitochondrial diseases (Ortega-Recalde et al., 2013; Srivastava et al., 2018). The upregulated expression of ATP

synthase subunit alpha (Mt-ATP6) *in Mtr cKO* could be a compensatory mechanism of impaired ATP synthesis in the myocardium. The team of (Roselló-Lletí et al., 2015) reported a significant association between overexpression of Mt-ATP6 and reduction of left ventricular mass in patients with ischemic heart failure. Mutation of MT-ATP a were reported in (Alila-Fersi et al., 2017)

The dysregulated mitochondrial energy metabolism was linked to a dramatic decreased expression of the mitochondrial matrix NADH deacetylase sirtuin 3 in hearts of *Mtr cKO* mice. Given the crucial role played by sirt3 in regulating mitochondrial energy metabolism, it can be hypothesized that the decreased expression of Sirt3 led to impairement of energy metabolism observed in the hearts of *Mtr cKO* via imbalanced acetylation/ deacetylation of key proteins involved in fatty acid oxidation, tricarboxylic acid cycle and oxidative phosphorylation (Hirschey et al., 2011; Koentges et al., 2015; Parodi-Rullán, Chapa-Dubocq, & Javadov, 2018; Sun et al., 2018). As showed in our model, the decreased expression of *Sirt3* causes impairs myocardial energetic and systolic dysfunction in mice through impaired expression of long and medium chain acyl CoA dehydrogenases (Hirschey et al., 2011;Hirschey et al., 2010; Yang et al., 2016). In the absence of S*irt3*, hyperacetylation of LCAD at lysine 42 reduces its activity (Matthew D. Hirschey et al., 2010). Similar effects have been reported in proteins of complexes I, II, III and IV of electron transport chain (Parodi-Rullán et al., 2018). ATP synthase activity is also regulated by SIRT3-mediated deacetylation (Bao et al., 2010; Yang et al., 2016). This explains the 50 % reduction of basal ATP levels observed in heart from mice lacking *Sirt3* (Ahn et al., 2008). Finally, plays also a crucial in the response to the cell stress and cardiac remodeling, including *Mtr* cKO by regulating the activity of antioxidant enzymes (Sundaresan et al., 2009; Tao et al., 2010). Activation of Sirt3 by resveratrol reduces TGF-β expression in cardiac tissue (T. Chen, Li, et al., 2015).

Deletion of *Mtr* in the cardiomyocytes induced cardiac remodelling. Cardiac remodelling is an adaptive response against ventricular wall stress, however if the process continues it progressively leads to deterioration of ventricular performance leading to either systolic or diastolic dysfunction (Azevedo et al 2016; Cohn et al., 2000; Dorsa Pontes & Vieira Pontes, 2016). The hypertrophic cardiomyopathy in *Mtr cKO* was documented by the increase in left ventricular mass and the increase in heart to body weight ratio. Furthermore transcriptomic and proteomic studies revealed overexpression of some genes linked to cardiac hypertrophy including Gata4 gene which encodes Zinc finger transcription factor GATA4 which is a key regulator for hypertrophic growth and gene expression in the cardiomyocytes. Some of the genes linked to cardiac hypertrophy regulated by GATA 4 include angiotensin II receptors and

beta MHC (Hasegawa, Lee, Jobe, Markham, & Kitsis, 1997; Suzuki, 2011). The increased expression of ANP also demonstrated cardiac hypertrophy in *Mtr cKO* (Hayashi et al., 2004). Previous studies in our laboratory showed that deficiency in vitamin B12 and folates during gestation and lactation induces cardiac hypertrophy with increase in cardiomyocyte size (Garcia et al., 2011). In other animal studies, cardiac hypertrophy and systolic dysfunction induced by pressure overload in mice was attenuated by cobalamin and folate supplementation (Piquereau et al., 2017).

We observed an increased expression of TGFß1 and AT2 in heart tissue of *Mtr* cKO mice. TGF ß1 promotes the development of cardiac fibrosis (Edgley et al., 2012), cardiac hypertrophy (Huntgeburth et al., 2011) and cardiomyocyte apoptosis (Heger et al., 2011). The classical TGF ß /SMADs signalling pathway stimulates fibroblasts to increase the production of the extracellular matrice (ECM) proteins like fibrillar collagens and fibronectin (Verrecchia & Mauviel, 2002). Moreover, TGF ß decreases the degradation of ECM by inhibiting the expression of metalloproteases MMP and by increasing the expression of protease inhibitors like TIMPs and plasminogen activator inhibitor (Bujak & Frangogiannis, 2007; Verrecchia & Mauviel, 2002). Increased tissue expression and serum concentration of TGFß1 have been reported in idiopathic hypertrophic cardiomyopathy and its correlation with left ventricular mass in hypertensive patients with cardiomyopathy (Almendral, Shick, Rosendorff, & Atlas, 2010). As a consequence of increased TGFß1, we observed an increased expression *Col1a1*, *Col3a1* and *Mmp2* genes and an increased collagen deposition in the myocardium of *Mtr* cKO Consistently, the development of heart failure revealed an upregulated expression of several genes including *Col1a1*, *Col3a1* and *Mmp2* in Dahl rats (Yim et al., 2018). Cardiac-specific constitutive increased expression of *Mmp-2* impairs ventricular contraction, induces myocardial fibrosis and increases myocardial stiffness in mice (G.-Y. Wang et al., 2006). Moreover, the increase expression of *Col1a1* and *Col3a1* genes could be driven by decrease expression of Sirt3, as shown in *Sirt3*-KO mice (Guo, Yan, Li, Zhang, & Bu, 2017). Imbalanced synthesis and degradation of extracellular matrix particularly collagens contributes to the development of myocardial fibrosis (An, Yang, Zheng, Nie, & Liu, 2017; Creemers & Pinto, 2011). Experimental models have demostrated the link between upregulated expression of collagens and cardiac fibrosis, an upregulated expression of mRNA for collagen type I and type III was reported in the hearts of both non infarcted and infarcted rats (Cleutjens, Verluyten, Smiths, & Daemen, 1995). Increased collagen concentration or fibrosis in the myocardium of hypertensive patients and rat models were reported to be associated with increased myocardial stiffness which led to impaired ventricular contractile function (Conrad et al., 1995; Díez et al., 2002;

Fan et al., 2012). MMP2 is a proteolytic enzyme involved in Extracellular matrix turnover and cardiac remodelling (Roldán et al., 2008; Visse & Nagase, 2003). The substrates for MMP2 includes elastin and collagens type I, III, IV and V (Senior et al., 1991; Steffensen, Wallon, & Overall, 1995). Clinical and experimental studies of cardiac remodeling, ventricular dysfunction and heart failure have reported an upregulated expression of MMP2. In agreement with our results, severe cardiac fibrosis characterized by significant increased deposition of collagens was observed in transgenic mice with cardiac overexpression of MMP-2 at the age of 4 months (Bergman et al., 2007). Similarly, cardiac fibrosis in these mice resulted in severe systolic dysfunction with increased LV end diastolic and systolic volume and decreased LVEF (Bergman et al., 2007).

Cardiovascular diseases including heart failure are characterized by increased oxidative and mechanical stress which induces the accumulation of misfolded proteins (Hu et al., 2017; Ranek et al., 2018; Rodríguez-Iturbe & Johnson, 2018). Cardiomyocyte toxicity caused by these misfolded proteins leads to heart failure (Bernini et al., 2016; Pattison et al., 2008). Heat shock proteins are molecular chaperones that regulate the synthesis and degradation of misfolded proteins hence offering protection against oxidative and mechanical stress induced cell death. They also play crucial role in signal transduction and cell homeostasis (Hu et al., 2017; Ranek et al., 2018; Rodríguez-Iturbe & Johnson, 2018). The small heat shock protein Hsp27/Hspb1 and Hspb3 were upregulated in response to cellular stress. Hsp27 has anti-apoptotic, anti-inflammatory and antioxidant properties and thus offer cardio-protection. Hsp27 improved contractile function by preserving mitochondrial function of myocardial infarction induced heart failure in rats (Marunouchi, Inomata, Sanbe, Takagi, & Tanonaka, 2014).

The mislocalization of hnRNPA1 could explain part of the changes of gene expression and protein translation evidenced in omics studies through its role in the splicing, nucleocytoplasmic transport and translation of mRNAs (Jeffrey D. Levengood, Seminars in Cell & Developmental Biology Volume 86, February 2019, Pages 150-161). It could also contribute to the alterations of gene expression through its role in the processing of microRNAs (Jean-Philippe, Paz, & Caputi, 2013). Heterozygous hnRNPA1 mutations in a mouse model and in two human cases produced congenital heart defects (Yu et al., 2018). We previously found that impaired cobalamin metabolism and pathogenic mutations of MS disrupt nucleocytoplasmic transport of mRNA through mislocalization of *ELAVL1*/*HuR* and *hnRNPA1*, in NIE115 neuroblastoma cells and fibroblasts from CblG patients exposed to cell stress inducers (Battaglia-Hsu et al., 2018; Ghemrawi et al., 2019). In contrast to our results in

myocardium of *Mtr cKO* mice, we observed a cytoplasm export of *hnRNPA1* and a nuclear sequestration of *ELAVL1*/*HuR* in these cells (Battaglia-Hsu et al., 2018; Ghemrawi et al., 2019).

CONCLUSION AND PERSPECTIVES

In conclusion, our results provide experimental evidence in a Knock-out model that *Mtr* deficiency has detrimental consequences on cardiac function. We found that the selective *Mtr* invalidation in the heart produces cardiomyopathy with heart failure, myocardium hypertrophy and fibrosis in young adult mice. At the tissue and molecular levels, the cardiomyopathy was related to impaired mitochondrial energy metabolism with disruption of fatty acid oxidation and oxidative phosphorylation, cellular stress and remodeling with fibrosis. The decreased expression of Sirt3 was consistent with the impaired energy metabolisms. The mislocalization and nuclear sequestration of hnRNPA1 which is a mRNAs binding protein could explain part of the expression changes of genes and proteins. These findings suggest to further evaluate whether CblG could be a new genetic causes of primary heart failure in adult patients.

REFERENCES

Adrovic, A., Canpolat, N., Caliskan, S., Sever, L., Kıykım, E., Agbas, A., & Baumgartner, M. R. (2016). Cobalamin C defect-hemolytic uremic syndrome caused by new mutation in MMACHC. *Pediatrics International: Official Journal of the Japan Pediatric Society*, *58*(8), 763–765. https://doi.org/10.1111/ped.12953

Agah, R., Frenkel, P. A., French, B. A., Michael, L. H., Overbeek, P. A., & Schneider, M. D. (1997). Gene recombination in postmitotic cells. Targeted expression of Cre recombinase provokes cardiac-restricted, site-specific rearrangement in adult ventricular muscle in vivo. *The Journal of Clinical Investigation*, *100*(1), 169–179. https://doi.org/10.1172/JCI119509

Ahn, B.-H., Kim, H.-S., Song, S., Lee, I. H., Liu, J., Vassilopoulos, A., … Finkel, T. (2008). A role for the mitochondrial deacetylase Sirt3 in regulating energy homeostasis. *Proceedings of the National Academy of Sciences*, *105*(38), 14447–14452. https://doi.org/10.1073/pnas.0803790105

Akhmedov, A. T., Rybin, V., & Marín-García, J. (2015). Mitochondrial oxidative metabolism and uncoupling proteins in the failing heart. *Heart Failure Reviews*, *20*(2), 227–249. https://doi.org/10.1007/s10741-014-9457-4

Alila-Fersi, O., Chamkha, I., Majdoub, I., Gargouri, L., Mkaouar-Rebai, E., Tabebi, M., … Fakhfakh, F. (2017). Co segregation of the m.1555A>G mutation in the MT-RNR1 gene and mutations in MT-ATP6 gene in a family with dilated mitochondrial cardiomyopathy and hearing loss: A whole mitochondrial genome screening. *Biochemical and Biophysical Research Communications*, *484*(1), 71–78. https://doi.org/10.1016/j.bbrc.2017.01.070

Allen, L. H. (2008). *Causes of vitamin B 12 and folate deficiency*. *29*(2), 20–34.

Allen, R. H., Seetharam, B., Podell, E., & Alpers, D. H. (1978). Effect of Proteolytic Enzymes on the Binding of Cobalamin to R Protein and Intrinsic Factor. *Journal of Clinical Investigation*, *61*(1), 47–54. https://doi.org/10.1172/JCI108924

Almassinokiani, F., Kashanian, M., Akbari, P., Mossayebi, E., & Sadeghian, E. (2016). Folic acid supplementation reduces plasma homocysteine in postmenopausal women. *Journal of Obstetrics and Gynaecology: The Journal of the Institute of Obstetrics and Gynaecology*, *36*(4), 492–495. https://doi.org/10.3109/01443615.2015.1091811

Almendral, J. L., Shick, V., Rosendorff, C., & Atlas, S. A. (2010). Association between transforming growth factor-β1 and left ventricular mass and diameter in hypertensive patients. *Journal of the American Society of Hypertension*, *4*(3), 135–141. https://doi.org/10.1016/j.jash.2010.02.007

Alrob, O. A., Sankaralingam, S., Ma, C., Wagg, C. S., Fillmore, N., Jaswal, J. S., … Lopaschuk, G. D. (2014). Obesity-induced lysine acetylation increases cardiac fatty acid oxidation and impairs insulin signalling. *Cardiovascular Research*, *103*(4), 485–497. https://doi.org/10.1093/cvr/cvu156

Amouzou, E. K., Chabi, N. W., Adjalla, C. E., Rodriguez-Guéant, R. M., Feillet, F., Villaume, C., … Guéant, J.-L. (2004). High prevalence of hyperhomocysteinemia related to folate deficiency and the 677C-->T mutation of the gene encoding methylenetetrahydrofolate reductase in coastal West Africa. *The American Journal of Clinical Nutrition*, *79*(4), 619–624. https://doi.org/10.1093/ajcn/79.4.619

An, Z., Yang, G., Zheng, H., Nie, W., & Liu, G. (2017). Biomarkers in patients with myocardial fibrosis. *Open Life Sciences*, *12*(1). https://doi.org/10.1515/biol-2017-0039

Augustus, A. S., Kako, Y., Yagyu, H., & Goldberg, I. J. (2003). Routes of FA delivery to cardiac muscle: Modulation of lipoprotein lipolysis alters uptake of TG-derived FA.

American Journal of Physiology-Endocrinology and Metabolism, *284*(2), E331–E339. https://doi.org/10.1152/ajpendo.00298.2002

Azevedo, P., Minicucci, M., Santos, P., Paiva, S. A., & Zornoff, L. A. (2013). Energy Metabolism in Cardiac Remodeling and Heart Failure. *Cardiology in Review*, *21*(3), 135–140. https://doi.org/10.1097/CRD.0b013e318274956d

Azevedo, P. S., Polegato, B. F., Minicucci, M. F., Paiva, S. A. R., & Zornoff, L. A. M. (2016). Cardiac Remodeling: Concepts, Clinical Impact, Pathophysiological Mechanisms and Pharmacologic Treatment. *Arquivos Brasileiros de Cardiologia*, *106*(1), 62–69. https://doi.org/10.5935/abc.20160005

Baba, M., Yoshida, K., & Ieda, M. (2019). Clinical Applications of Natriuretic Peptides in Heart Failure and Atrial Fibrillation. *International Journal of Molecular Sciences*, *20*(11), 2824. https://doi.org/10.3390/ijms20112824

Banerjee, R., & Ragsdale, S. W. (2003). The Many Faces of Vitamin B $_{12}$: Catalysis by Cobalamin-Dependent Enzymes. *Annual Review of Biochemistry*, *72*(1), 209–247. https://doi.org/10.1146/annurev.biochem.72.121801.161828

Banerjee, R. V., Johnston, N. L., Sobeski, J. K., Datta, P., & Matthews, R. G. (1989). Cloning and sequence analysis of the Escherichia coli metH gene encoding cobalamin-dependent methionine synthase and isolation of a tryptic fragment containing the cobalamin-binding domain. *The Journal of Biological Chemistry*, *264*(23), 13888–13895.

Banerjee, R. V., & Matthews, R. G. (1990). Cobalamin-dependent methionine synthase. *FASEB Journal: Official Publication of the Federation of American Societies for Experimental Biology*, *4*(5), 1450–1459. https://doi.org/10.1096/fasebj.4.5.2407589

Banerjee, R. V, & Matthews, R. G. (2016). *Methionine Synthase*. *4*(5), 1450–1459. https://doi.org/10.1093/hmg/5.12.1851.

Banerjee, R. V., Rowena, A., & Matthews, R. G. (1990). Cobalamin dependent methionine synthase. *Biophysics*. FASEB J. 1990 Mar;4(5):1450-9. https://doi.org/ 10. 1096/fasebj.4.5.2407589

Bao, J., Scott, I., Lu, Z., Pang, L., Dimond, C. C., Gius, D., & Sack, M. N. (2010). SIRT3 is regulated by nutrient excess and modulates hepatic susceptibility to lipotoxicity. *Free Radical Biology & Medicine*, *49*(7), 1230–1237. https://doi.org/10.1016/j.freeradbiomed.2010.07.009

Barger, P. M., & Kelly, D. P. (2000). PPAR Signaling in the Control of Cardiac Energy Metabolism. *Trends in Cardiovascular Medicine*, *10*(6), 238–245. https://doi.org/10.1016/S1050-1738(00)00077-3

Bartholomew, D. W., Batshaw, M. L., Allen, R. H., Roe, C. R., Rosenblatt, D., Valle, D. L., & Francomano, C. A. (1988). Therapeutic approaches to cobalamin-C methylmalonic acidemia and homocystinuria. *The Journal of Pediatrics*, *112*(1), 32–39. https://doi.org/10.1016/s0022-3476(88)80114-8

Bassila, C., Ghemrawi, R., Flayac, J., Froese, D. S., Baumgartner, M. R., Guéant, J. L., & Coelho, D. (2017). Methionine synthase and methionine synthase reductase interact with MMACHC and with MMADHC. *Biochimica et Biophysica Acta - Molecular Basis of Disease*, *1863*(1), 103–112. https://doi.org/10.1016/j.bbadis.2016.10.016

Battaglia-Hsu, S.-F., Ghemrawi, R., Coelho, D., Dreumont, N., Mosca, P., Hergalant, S., … Guéant, J.-L. (2018). Inherited disorders of cobalamin metabolism disrupt nucleocytoplasmic transport of mRNA through impaired methylation/phosphorylation of ELAVL1/HuR. *Nucleic Acids Research*, *46*(15), 7844–7857. https://doi.org/10.1093/nar/gky634.

Battersby, A. R. (1994). *Nature Builds The Conquest the of Pigments of Vitamin Life : 264*(5165), 1551–1557. https://doi.org/10.1126/science.8202709

Beedholm-Ebsen, R., van de Wetering, K., Hardlei, T., Nexo, E., Borst, P., & Moestrup, S. K. (2010). Identification of multidrug resistance protein 1 (MRP1/ABCC1) as a

molecular gate for cellular export of cobalamin. *Blood*, *115*(8), 1632–1639. https://doi.org/10.1182/blood-2009-07-232587

Beer, M., Seyfarth, T., Sandstede, J., Landschütz, W., Lipke, C., Köstler, H., … Neubauer, S. (2002). Absolute concentrations of high-energy phosphate metabolites in normal, hypertrophied, and failing human myocardium measured noninvasively with (31)P-SLOOP magnetic resonance spectroscopy. *Journal of the American College of Cardiology*, *40*(7), 1267–1274. https://doi.org/10.1016/s0735-1097(02)02160-5

Bekaert, S., Storozhenko, S., Mehrshahi, P., Bennett, M. J., Lambert, W., Gregory, J. F., … Hanson, A. D. (2008). Folate biofortification in food plants. *Trends in Plant Science*, *13*(1), 28–35. https://doi.org/10.1016/j.tplants.2007.11.001

Bergman, M. R., Teerlink, J. R., Mahimkar, R., Li, L., Zhu, B.-Q., Nguyen, A., … Lovett, D. H. (2007). Cardiac matrix metalloproteinase-2 expression independently induces marked ventricular remodeling and systolic dysfunction. *American Journal of Physiology-Heart and Circulatory Physiology*, *292*(4), H1847–H1860. https://doi.org/10.1152/ajpheart.00434.2006

Bernini, F., Malferrari, D., Pignataro, M., Bortolotti, C. A., Di Rocco, G., Lancellotti, L., … Castellini, E. (2016). Pre-amyloid oligomers budding:a metastatic mechanism of proteotoxicity. *Scientific Reports*, *6*, 35865. https://doi.org/10.1038/srep35865

Bertolo, R. F., & McBreairty, L. E. (2013). The nutritional burden of methylation reactions. *Current Opinion in Clinical Nutrition and Metabolic Care*, *16*(1), 102–108. https://doi.org/10.1097/MCO.0b013e32835ad2ee

Blair, J. E. A., Huffman, M., & Shah, S. J. (2013). *Heart Failure in North America*. 128–146.

Blom, H. J., & Smulders, Y. (2011). Overview of homocysteine and folate metabolism. With special references to cardiovascular disease and neural tube defects. *Journal of*

Inherited Metabolic Disease, *34*(1), 75–81. https://doi.org/10.1007/s10545-010-9177-4

Böger, R. H., Bode-Böger, S. M., Szuba, A., Tsao, P. S., Chan, J. R., Tangphao, O., … Cooke, J. P. (1998). Asymmetric dimethylarginine (ADMA): A novel risk factor for endothelial dysfunction: its role in hypercholesterolemia. *Circulation*, *98*(18), 1842–1847. https://doi.org/10.1161/01.cir.98.18.1842

Bokhari, S. W., Bokhari, Z. W., Zell, J. A., Lee, D. W., & Faxon, D. P. (2005). Plasma homocysteine levels and the left ventricular systolic function in coronary artery disease patients. *Coronary Artery Disease*, *16*(3), 153. https://doi.org/10.1097/00019501-200505000-00004

Boldyrev, A. A. (2009). Molecular mechanisms of homocysteine toxicity. *Biochemistry. Biokhimiia*, *74*(6), 589–598. https://doi.org/10.1134/s0006297909060017

Botto, L. D., Mulinare, J., & Erickson, J. D. (2000). Occurrence of congenital heart defects in relation to maternal mulitivitamin use. *American Journal of Epidemiology*, *151*(9), 878–884. https://doi.org/10.1093/oxfordjournals.aje.a010291

Brahmbhatt, D. H., & Cowie, M. R. (2018a). Heart failure: Classification and pathophysiology. *Medicine*, *46*(10), 587–593. https://doi.org/10.1016/j.mpmed.2018.07.004

Brahmbhatt, D. H., & Cowie, M. R. (2018b). Heart failure: Classification and pathophysiology. *Medicine*, *46*(10), 587–593. https://doi.org/10.1016/j.mpmed.2018.07.004

Brandt, R. R., Wright, R. S., Redfield, M. M., & Burnett, J. C. (1993). Atrial natriuretic peptide in heart failure. *Journal of the American College of Cardiology*, *22*(4 Suppl A), 86A-92A.https://doi.org/10.1016/0735-1097(93)90468-g

Bristow, M. R., Ginsburg, R., Umans, V., Fowler, M., Minobe, W., Rasmussen, R., Jamieson, S. (1986). Beta 1- and beta 2-adrenergic-receptor subpopulations in nonfailing and failing human ventricular myocardium: Coupling of both receptor subtypes to muscle contraction and selective beta 1-receptor down-regulation in heart failure. *Circulation Research*, *59*(3), 297–309. https://doi.org/10.1161/01.res.59.3.297

Bristow, Michael R., Ginsburg, R., Minobe, W., Cubicciotti, R. S., Sageman, W. S., Lurie, K.Stinson, E. B. (1982). Decreased Catecholamine Sensitivity and β-Adrenergic-Receptor Density in Failing Human Hearts. *New England Journal of Medicine*, *307*(4), 205–211. https://doi.org/10.1056/NEJM198207223070401

Brunaud, L., Alberto, J. M., Ayav, A., Gérard, P., Namour, F., Antunes, L., Guéant, J. L. (2003a). Vitamin B12 is a strong determinant of low methionine synthase activity and DNA hypomethylation in gastrectomized rats. *Digestion*, *68*(2–3), 133–140. https://doi.org/10.1159/000075307

Brunaud, L., Alberto, J.-M., Ayav, A., Gérard, P., Namour, F., Antunes, L.,Guéant, J.-L. (2003b). Vitamin B12 is a strong determinant of low methionine synthase activity and DNA hypomethylation in gastrectomized rats. *Digestion*, *68*(2–3), 133–140. https://doi.org/10.1159/000075307

Brunelle, J. L., & Green, R. (2014). One-dimensional SDS-polyacrylamide gel electrophoresis (1D SDS-PAGE). *Methods in Enzymology*, *541*, 151–159. https://doi.org/10.1016/B978-0-12-420119-4.00012-4

Bugiani, M., Invernizzi, F., Alberio, S., Briem, E., Lamantea, E., Carrara, F., … Zeviani, M. (2004). Clinical and molecular findings in children with complex I deficiency. *Biochimica et Biophysica Acta (BBA) - Bioenergetics*, *1659*(2–3), 136–147. https://doi.org/10.1016/j.bbabio.2004.09.006

Bui, A. L., Horwich, T. B., & Fonarow, G. C. (2011). Epidemiology and risk profile of heart failure. *Nature Reviews. Cardiology*, *8*(1), 30–41. https://doi.org/10.1038/nrcardio.2010.165

Bujak, M., & Frangogiannis, N. G. (2007). The role of TGF-beta signaling in myocardial infarction and cardiac remodeling. *Cardiovascular Research*, *74*(2), 184–195. https://doi.org/10.1016/j.cardiores.2006.10.002

Burger, R. L., Schneider, R. J., Mehlman, C. S., & Allen, R. H. (1975). Human plasma R-type vitamin B12-binding proteins. II. The role of transcobalamin I, transcobalamin III, and the normal granulocyte vitamin B12-binding protein in the plasma transport of vitamin B12. *The Journal of Biological Chemistry*, *250*(19), 7707–7713.

Butler, J., Anker, S. D., & Packer, M. (2019). Redefining Heart Failure With a Reduced Ejection Fraction. *JAMA*. https://doi.org/10.1001/jama.2019.15600

Byrne, N. J., Levasseur, J., Sung, M. M., Masson, G., Boisvenue, J., Young, M. E., & Dyck, J. R. B. (2016). Normalization of cardiac substrate utilization and left ventricular hypertrophy precede functional recovery in heart failure regression. *Cardiovascular Research*, *110*(2), 249–257. https://doi.org/10.1093/cvr/cvw051

Cameron, V. A., & Ellmers, L. J. (2003). Minireview: Natriuretic Peptides during Development of the Fetal Heart and Circulation. *Endocrinology*, *144*(6), 2191–2194. https://doi.org/10.1210/en.2003-0127

Cantoni, G. L., & Chiang, P. K. (1980). The Role of S-Adenosylhomocysteine and S-Adenosylhomocysteine Hydrolase in the Control of Biological Methylations. In D. Cavallini, G. E. Gaull, & V. Zappia (Eds.), *Natural Sulfur Compounds: Novel Biochemical and Structural Aspects* (pp. 67–80). https://doi.org/10.1007/978-1-4613-3045-5_6

Cao, Z., Jia, Y., & Zhu, B. (2019). BNP and NT-proBNP as Diagnostic Biomarkers for Cardiac Dysfunction in Both Clinical and Forensic Medicine. *International Journal of Molecular Sciences*, *20*(8). https://doi.org/10.3390/ijms20081820

Cappola Thomas P., Li Mingyao, He Jing, Ky Bonnie, Gilmore Joan, Qu Liming, … Dorn Gerald W. (2010). Common Variants in HSPB7 and FRMD4B Associated With Advanced Heart Failure. *Circulation: Cardiovascular Genetics*, *3*(2), 147–154. https://doi.org/10.1161/CIRCGENETICS.109.898395

Caraux, G., & Pinloche, S. (2005). PermutMatrix: A graphical environment to arrange gene expression profiles in optimal linear order. *Bioinformatics*, *21*(7), 1280–1281. https://doi.org/10.1093/bioinformatics/bti141

Carmel, R., Watkins, D., Goodman, S. I., & Rosenblatt, D. S. (1988). Hereditary defect of cobalamin metabolism (cblG mutation) presenting as a neurologic disorder in adulthood. *The New England Journal of Medicine*, *318*(26), 1738–1741. https://doi.org/10.1056/NEJM198806303182607

Carmen Gherasim, Luciana Hannibal, Deepa Rajagopalan, Donald W. Jacobsen, and R. B. (2013). The C-terminal domain of CblD interacts with CblC and influences intracellular cobalamin partitioning. *Biochimie*, *95*(05), 1023–1032. https://doi.org/10.1016/j.neuroimage.2013.08.045.The

Carrillo-Carrasco, N., Chandler, R. J., & Venditti, C. P. (2012a). Combined methylmalonic acidemia and homocystinuria, cblC type. I. Clinical presentations, diagnosis and management. *Journal of Inherited Metabolic Disease*, *35*(1), 91–102. https://doi.org/10.1007/s10545-011-9364-y

Carrillo-Carrasco, N., Chandler, R. J., & Venditti, C. P. (2012b). Combined methylmalonic acidemia and homocystinuria, cblC type. I. Clinical presentations, diagnosis and

management. *Journal of Inherited Metabolic Disease*, *35*(1), 91–102. https://doi.org/10.1007/s10545-011-9364-y

Carrillo-Carrasco, N., & Venditti, C. P. (2012). Combined methylmalonic acidemia and homocystinuria, cblC type. II. Complications, pathophysiology, and outcomes. *Journal of Inherited Metabolic Disease*, *35*(1), 103–114. https://doi.org/10.1007/s10545-011-9365-x

Carvalho-Silva, D., Pierleoni, A., Pignatelli, M., Ong, C., Fumis, L., Karamanis, N., … Dunham, I. (2019). Open Targets Platform: New developments and updates two years on. *Nucleic Acids Research*, *47*(D1), D1056–D1065. https://doi.org/10.1093/nar/gky1133

Casademont, J., & Miró, Ò. (2002). Electron Transport Chain Defects in Heart Failure. *Heart Failure Reviews*, *7*(2), 131–139. https://doi.org/10.1023/A:1015372407647

Chandler, C. J., Harrison, D. A., Buffington, C. A., Santiago, N. A., & Halsted, C. H. (1991). Functional specificity of jejunal brush-border pteroylpolyglutamate hydrolase in pig. *American Journal of Physiology-Gastrointestinal and Liver Physiology*, *260*(6), G865–G872. https://doi.org/10.1152/ajpgi.1991.260.6.G865

Chen, J., Stampfer, M. J., Ma, J., Selhub, J., Malinow, M. R., Hennekens, C. H., & Hunter, D. J. (2001). Influence of a methionine synthase (D919G) polymorphism on plasma homocysteine and folate levels and relation to risk of myocardial infarction. *Atherosclerosis*, *154*(3), 667–672. https://doi.org/10.1016/S0021-9150(00)00469-X

Chen, L. H., Liu, M.-L., Hwang, H.-Y., Chen, L.-S., Korenberg, J., & Shane, B. (1997). Human Methionine Synthase cDNA CLONING, GENE LOCALIZATION, AND EXPRESSION. *Journal of Biological Chemistry*, *272*(6), 3628–3634. https://doi.org/10.1074/jbc.272.6.3628

Chen, T., Li, J., Liu, J., Li, N., Wang, S., Liu, H., … Bu, P. (2015). Activation of SIRT3 by resveratrol ameliorates cardiac fibrosis and improves cardiac function via the TGF-β/Smad3 pathway. *American Journal of Physiology. Heart and Circulatory Physiology*, *308*(5), H424-434. https://doi.org/10.1152/ajpheart.00454.2014

Chen, T., Liu, J., Li, N., Wang, S., Liu, H., Li, J., … Bu, P. (2015). Mouse SIRT3 Attenuates Hypertrophy-Related Lipid Accumulation in the Heart through the Deacetylation of LCAD. *PLoS ONE*, *10*(3). https://doi.org/10.1371/journal.pone.0118909

Chen, Z., Chakraborty, S., & Banerjee, R. (1995). Demonstration That Mammalian Methionine Synthases Are Predominantly Cobalamin-loaded. *Journal of Biological Chemistry*, *270*(33), 19246–19249. https://doi.org/10.1074/jbc.270.33.19246

Cheng, Z., Yang, X., & Wang, H. (2009). Hyperhomocysteinemia and Endothelial Dysfunction. *Current Hypertension Reviews*, *5*(2), 158–165. https://doi.org/10.2174/157340209788166940

Chiang, P. K., & Cantoni, G. L. (1979). Perturbation of biochemical transmethylations by 3-deazaadenosine in vivo. *Biochemical Pharmacology*, *28*(12), 1897–1902. https://doi.org/10.1016/0006-2952(79)90642-7

Cho, R. C., Cole, P. D., Sohn, K.-J., Gaisano, G., Croxford, R., Kamen, B. A., & Kim, Y.-I. (2007). Effects of folate and folylpolyglutamyl synthase modulation on chemosensitivity of breast cancer cells. *Molecular Cancer Therapeutics*, *6*(11), 2909–2920. https://doi.org/10.1158/1535-7163.MCT-07-0449

Clarke, R., Daly, L., Robinson, K., Naughten, E., Cahalane, S., Fowler, B., & Graham, I. (1991). Hyperhomocysteinemia: An Independent Risk Factor for Vascular Disease. *New England Journal of Medicine*, *324*(17), 1149–1155. https://doi.org/10.1056/NEJM199104253241701

Cleutjens, J. P., Verluyten, M. J., Smiths, J. F., & Daemen, M. J. (1995). Collagen remodeling after myocardial infarction in the rat heart. *The American Journal of Pathology*, *147*(2), 325–338.

Cody, R. J., Atlas, S. A., Laragh, J. H., Kubo, S. H., Covit, A. B., Ryman, K. S., … Camargo, M. J. (1986). Atrial natriuretic factor in normal subjects and heart failure patients. Plasma levels and renal, hormonal, and hemodynamic responses to peptide infusion. *The Journal of Clinical Investigation*, *78*(5), 1362–1374. https://doi.org/10.1172/JCI112723

Coelho, D., Kim, J. C., Miousse, I. R., Fung, S., du Moulin, M., Buers, I., … Baumgartner, M. R. (2012). Mutations in *ABCD4* cause a new inborn error of vitamin B_{12} metabolism. *Nature Genetics*, *44*(10), 1152–1155. https://doi.org/10.1038/ng.2386

Coelho, D., Suormala, T., Stucki, M., Lerner-Ellis, J. P., Rosenblatt, D. S., Newbold, R. F., … Fowler, B. (2008). Gene identification for the cblD defect of vitamin B12 metabolism. *The New England Journal of Medicine*, *358*(14), 1454–1464. https://doi.org/10.1056/NEJMoa072200

Cohn, J. N., Ferrari, R., & Sharpe, N. (2000). Cardiac remodeling--concepts and clinical implications: A consensus paper from an international forum on cardiac remodeling. Behalf of an International Forum on Cardiac Remodeling. *Journal of the American College of Cardiology*, *35*(3), 569–582. https://doi.org/10.1016/S0735-1097(99)00630-0

Conrad Chester H., Brooks Wesley W., Hayes John A., Sen Subha, Robinson Kathleen G., & Bing Oscar H. L. (1995). Myocardial Fibrosis and Stiffness With Hypertrophy and Heart Failure in the Spontaneously Hypertensive Rat. *Circulation*, *91*(1), 161–170. https://doi.org/10.1161/01.CIR.91.1.161

Creemers, E. E., & Pinto, Y. M. (2011). Molecular mechanisms that control interstitial fibrosis in the pressure-overloaded heart. *Cardiovascular Research*, *89*(2), 265–272. https://doi.org/10.1093/cvr/cvq308

Crider, K. S., Bailey, L. B., & Berry, R. J. (2011). Folic Acid Food Fortification—Its History, Effect, Concerns, and Future Directions. *Nutrients*, *3*(3), 370–384. https://doi.org/10.3390/nu3030370

Crowley, S. D., Gurley, S. B., Herrera, M. J., Ruiz, P., Griffiths, R., Kumar, A. P., … Coffman, T. M. (2006). Angiotensin II causes hypertension and cardiac hypertrophy through its receptors in the kidney. *Proceedings of the National Academy of Sciences of the United States of America*, *103*(47), 17985–17990. https://doi.org/10.1073/pnas.0605545103

Curran, J., Hinton, M. J., Ríos, E., Bers, D. M., & Shannon, T. R. (2007). β-Adrenergic Enhancement of Sarcoplasmic Reticulum Calcium Leak in Cardiac Myocytes Is Mediated by Calcium/Calmodulin-Dependent Protein Kinase. *Circulation Research*, *100*(3), 391–398. https://doi.org/10.1161/01.RES.0000258172.74570.e6

Cybulska, B., & Kłosiewicz-Latoszek, L. (2015). Homocysteine—Is it still an important risk factor for cardiovascular disease? *Kardiologia Polska*, 1092–1096. https://doi.org/10.5603/KP.2015.0229

Czeizel, A. E., Dudás, I., Vereczkey, A., & Bánhidy, F. (2013). Folate Deficiency and Folic Acid Supplementation: The Prevention of Neural-Tube Defects and Congenital Heart Defects. *Nutrients*, *5*(11), 4760–4775. https://doi.org/10.3390/nu5114760

Dayal Sanjana, Brown Kara L., Weydert Christine J., Oberley Larry W., Arning Erland, Bottiglieri Teodoro, … Lentz Steven R. (2002). Deficiency of Glutathione Peroxidase-1 Sensitizes Hyperhomocysteinemic Mice to Endothelial Dysfunction.

Arteriosclerosis, Thrombosis, and Vascular Biology, *22*(12), 1996–2002. https://doi.org/10.1161/01.ATV.0000041629.92741.DC

De Bie, I., Nizard, S. D. P., & Mitchell, G. A. (2009). Fetal dilated cardiomyopathy: An unsuspected presentation of methylmalonic aciduria and hyperhomocystinuria, cblC type. *Prenatal Diagnosis*, *29*(3), 266–270. https://doi.org/10.1002/pd.2218

De Wals, P., Tairou, F., Van Allen, M. I., Uh, S.-H., Lowry, R. B., Sibbald, B., … Niyonsenga, T. (2007). Reduction in Neural-Tube Defects after Folic Acid Fortification in Canada. *New England Journal of Medicine*, *357*(2), 135–142. https://doi.org/10.1056/NEJMoa067103

Deatrick, K. B., Luke, C. E., Elfline, M. A., Sood, V., Baldwin, J., Upchurch, G. R., … Henke, P. K. (2013). The Effect of MMP2 and MMP 2/9 deletion in Experimental Post-thrombotic Vein Wall Remodeling. *Journal of Vascular Surgery*, *58*(5). https://doi.org/10.1016/j.jvs.2012.11.088

Delicce, A. V., Basit, H., & Makaryus, A. N. (2019a). Physiology, Frank Starling Law. In *StatPearls*. Retrieved from http://www.ncbi.nlm.nih.gov/books/NBK470295/

Delicce, A. V., Basit, H., & Makaryus, A. N. (2019b). Physiology, Frank Starling Law. In *StatPearls*. Retrieved from http://www.ncbi.nlm.nih.gov/books/NBK470295/

Deme, J. C., Hancock, M. A., Xia, X., Shintre, C. A., Plesa, M., Kim, J. C., … Coulton, J. W. (2014). Purification and interaction analyses of two human lysosomal vitamin B12 transporters: LMBD1 and ABCD4. *Molecular Membrane Biology*, *31*(7–8), 250–261. https://doi.org/10.3109/09687688.2014.990998

Deng, C., Deng, Y., Xie, L., Yu, L., Liu, L., Liu, H., & Dai, L. (2019). Genetic polymorphisms in MTR are associated with non-syndromic congenital heart disease from a family-based case-control study in the Chinese population. *Scientific Reports*, *9*(1), 1–7. https://doi.org/10.1038/s41598-019-41641-z

Deng, L., Elmore, C. L., Lawrance, A. K., Matthews, R. G., & Rozen, R. (2008). Methionine synthase reductase deficiency results in adverse reproductive outcomes and congenital heart defects in mice. *Molecular Genetics and Metabolism*, *94*(3), 336–342. https://doi.org/10.1016/j.ymgme.2008.03.004

Dennis, S. C., Gevers, W., & Opie, L. H. (1991). Protons in ischemia: Where do they come from; where do they go to? *Journal of Molecular and Cellular Cardiology*, *23*(9), 1077–1086. https://doi.org/10.1016/0022-2828(91)91642-5

De-Regil, L. M., Peña-Rosas, J. P., Fernández-Gaxiola, A. C., & Rayco-Solon, P. (2015). Effects and safety of periconceptional oral folate supplementation for preventing birth defects. *Cochrane Database of Systematic Reviews*, (12). https://doi.org/10.1002/14651858.CD007950.pub3

Desjardins, F., & Balligand, J.-L. (2006). NITRIC OXIDE-DEPENDENT ENDOTHELIAL FUNCTION AND CARDIOVASCULAR DISEASE. *Acta Clinica Belgica*, *61*(6), 326–334. https://doi.org/10.1179/acb.2006.052

Devlin, A. M., Arning, E., Bottiglieri, T., Faraci, F. M., Rozen, R., & Lentz, S. R. (2004). Effect of Mthfr genotype on diet-induced hyperhomocysteinemia and vascular function in mice. *Blood*, *103*(7), 2624–2629. https://doi.org/10.1182/blood-2003-09-3078

Diakos, N. A., Navankasattusas, S., Abel, E. D., Rutter, J., McCreath, L., Ferrin, P., … Drakos, S. G. (2016). Evidence of Glycolysis Up-Regulation and Pyruvate Mitochondrial Oxidation Mismatch During Mechanical Unloading of the Failing Human Heart: Implications for Cardiac Reloading and Conditioning. *JACC: Basic to Translational Science*, *1*(6), 432–444. https://doi.org/10.1016/j.jacbts.2016.06.009

Dickstein, K., Cohen-Solal, A., Filippatos, G., McMurray, J. J. V., Ponikowski, P., Poole-Wilson, P. A., ESC Committee for Practice Guidelines (CPG). (2008). ESC guidelines for the diagnosis and treatment of acute and chronic heart failure 2008: The Task Force for the diagnosis and treatment of acute and chronic heart failure 2008 of the European Society of Cardiology. Developed in collaboration with the Heart Failure Association of the ESC (HFA) and endorsed by the European Society of Intensive Care Medicine (ESICM). *European Journal of Heart Failure*, *10*(10), 933–989. https://doi.org/10.1016/j.ejheart.2008.08.005

Díez Javier, Querejeta Ramón, López Begoña, González Arantxa, Larman Mariano, & Martínez Ubago José L. (2002). Losartan-Dependent Regression of Myocardial Fibrosis Is Associated With Reduction of Left Ventricular Chamber Stiffness in Hypertensive Patients. *Circulation*, *105*(21), 2512–2517. https://doi.org/10.1161/01.CIR.0000017264.66561.3D

Dixon, M. M., Huang, S., Matthews, R. G., & Ludwig, M. (1996). The structure of the C-terminal domain of methionine synthase: Presenting S-adenosylmethionine for reductive methylation of B12. *Structure (London, England: 1993)*, *4*(11), 1263–1275. https://doi.org/10.1016/s0969-2126(96)00135-9

Dixon, Melinda M., Huang, S., Matthews, R. G., & Ludwig, M. (1996). The structure of the C-terminal domain of methionine synthase: Presenting S-adenosylmethionine for reductive methylation of B12. *Structure*, *4*(11), 1263–1275. https://doi.org/10.1016/S0969-2126(96)00135-9

Doenst, T., Nguyen, T. D., & Abel, E. D. (2013a). Cardiac Metabolism in Heart Failure—Implications beyond ATP production. *Circulation Research*, *113*(6), 709–724. https://doi.org/10.1161/CIRCRESAHA.113.300376

Doenst, T., Nguyen, T. D., & Abel, E. D. (2013b). Cardiac Metabolism in Heart Failure—Implications beyond ATP production. *Circulation Research*, *113*(6), 709–724. https://doi.org/10.1161/CIRCRESAHA.113.300376

Doenst, T., Pytel, G., Schrepper, A., Amorim, P., Färber, G., Shingu, Y., … Schwarzer, M. (2010). Decreased rates of substrate oxidation ex vivo predict the onset of heart failure and contractile dysfunction in rats with pressure overload. *Cardiovascular Research*, *86*(3), 461–470. https://doi.org/10.1093/cvr/cvp414

Dorsa Pontes, H. B., & Vieira Pontes, J. C. D. (2016). Cardiac remodelling: General aspects and mechanisms. *Current Research: Cardiology*, *3*(3). https://doi.org/10.4172/2368-0512.1000073

Drennan, C. L., Matthews, R. G., & Ludwig, M. L. (1994). Cobalamin-dependent methionine synthase: The structure of a methylcobalamin-binding fragment and implications for other B12-dependent enzymes. *Current Opinion in Structural Biology*, *4*(6), 919–929. https://doi.org/10.1016/0959-440x(94)90275-5

Ducker, G. S., & Rabinowitz, J. D. (2017). One-Carbon Metabolism in Health and Disease. *Cell Metabolism*, *25*(1), 27–42. https://doi.org/10.1016/j.cmet.2016.08.009

Durand, P., Prost, M., & Blache, D. (1998). Folate deficiencies and cardiovascular pathologies. *Clinical Chemistry and Laboratory Medicine*, *36*(7), 419–429. https://doi.org/10.1515/CCLM.1998.072

Dyck, J. R. B., Cheng, J.-F., Stanley, W. C., Barr, R., Chandler, M. P., Brown, S., … Lopaschuk, G. D. (2004). Malonyl coenzyme a decarboxylase inhibition protects the ischemic heart by inhibiting fatty acid oxidation and stimulating glucose oxidation. *Circulation Research*, *94*(9), e78-84. https://doi.org/10.1161/01.RES.0000129255.19569.8f

Eclerc, D. L., Ilson, A. W., Umas, R. D., Afuik, C. G., Ong, D. S., Atkins, D. W., & Eng, H. H. Q. H. (1998). Cloning and mapping of a cDNA for methionine synthase reductase , a flavoprotein defective in patients with homocystinuria. *Pnas*, *95*(March), 3059–3064. https://doi.org/10.1073/pnas.95.6.3059

Edgley, A. J., Krum, H., & Kelly, D. J. (2012). Targeting Fibrosis for the Treatment of Heart Failure: A Role for Transforming Growth Factor-β. *Cardiovascular Therapeutics*, *30*(1), e30–e40. https://doi.org/10.1111/j.1755-5922.2010.00228.x

Edwards, B. S., Zimmerman, R. S., Schwab, T. R., Heublein, D. M., & Burnett, J. C. (1988). Atrial stretch, not pressure, is the principal determinant controlling the acute release of atrial natriuretic factor. *Circulation Research*, *62*(2), 191–195. https://doi.org/10.1161/01.RES.62.2.191

Elliott, P., Andersson, B., Arbustini, E., Bilinska, Z., Cecchi, F., Charron, P., … Keren, A. (2008). Classification of the cardiomyopathies: A position statement from the European Society Of Cardiology Working Group on Myocardial and Pericardial Diseases. *European Heart Journal*, *29*(2), 270–276. https://doi.org/10.1093/eurheartj/ehm342

Elmore, C. L., Wu, X., Leclerc, D., Watson, E. D., Bottiglieri, T., Krupenko, N. I., … Matthews, R. G. (2007a). Metabolic derangement of methionine and folate metabolism in mice deficient in methionine synthase reductase. *Molecular Genetics and Metabolism*, *91*(1), 85–97. https://doi.org/10.1016/j.ymgme.2007.02.001

Elmore, C. L., Wu, X., Leclerc, D., Watson, E. D., Bottiglieri, T., Krupenko, N. I., … Matthews, R. G. (2007b). Metabolic derangement of methionine and folate metabolism in mice deficient in methionine synthase reductase. *Molecular Genetics and Metabolism*, *91*(1), 85–97. https://doi.org/10.1016/j.ymgme.2007.02.001

Ertl, G., Gaudron, P., Eilles, C., Schorb, W., & Kochsiek, K. (1991). Compensatory mechanisms for cardiac dysfunction in myocardial infarction. In R. W. Gülch & G. Kissling (Eds.), *Current Topics in Heart Failure: Experimental and Clinical Aspects* (pp. 159–165). https://doi.org/10.1007/978-3-662-30769-4_15

Evans, J. C., Huddler, D. P., Hilgers, M. T., Romanchuk, G., Matthews, R. G., & Ludwig, M. L. (2004a). Structures of the N-terminal modules imply large domain motions during catalysis by methionine synthase. *Proceedings of the National Academy of Sciences of the United States of America*, *101*(11), 3729–3736. https://doi.org/10.1073/pnas.0308082100

Evans, J. C., Huddler, D. P., Hilgers, M. T., Romanchuk, G., Matthews, R. G., & Ludwig, M. L. (2004b). Structures of the N-terminal modules imply large domain motions during catalysis by methionine synthase. *Proceedings of the National Academy of Sciences of the United States of America*, *101*(11), 3729–3736. https://doi.org/10.1073/pnas.0308082100

Fan, D., Takawale, A., Lee, J., & Kassiri, Z. (2012). Cardiac fibroblasts, fibrosis and extracellular matrix remodeling in heart disease. *Fibrogenesis & Tissue Repair*, *5*, 15. https://doi.org/10.1186/1755-1536-5-15

Ferla, M. P., & Patrick, W. M. (2014). Bacterial methionine biosynthesis. *Microbiology*, *160*(Pt_8), 1571–1584. https://doi.org/10.1099/mic.0.077826-0

Fillmore, N., Mori, J., & Lopaschuk, G. D. (2014a). Mitochondrial fatty acid oxidation alterations in heart failure, ischaemic heart disease and diabetic cardiomyopathy. *British Journal of Pharmacology*, *171*(8), 2080–2090. https://doi.org/10.1111/bph.12475

Fillmore, N., Mori, J., & Lopaschuk, G. D. (2014b). Mitochondrial fatty acid oxidation alterations in heart failure, ischaemic heart disease and diabetic cardiomyopathy.

British Journal of Pharmacology, *171*(8), 2080–2090. https://doi.org/10.1111/bph.12475

Fillmore, Natasha, Levasseur, J. L., Fukushima, A., Wagg, C. S., Wang, W., Dyck, J. R. B., & Lopaschuk, G. D. (2018). Uncoupling of glycolysis from glucose oxidation accompanies the development of heart failure with preserved ejection fraction. *Molecular Medicine*, *24*. https://doi.org/10.1186/s10020-018-0005-x

Finck, B. N., & Kelly, D. P. (2006). PGC-1 coactivators: Inducible regulators of energy metabolism in health and disease. *The Journal of Clinical Investigation*, *116*(3), 615–622. https://doi.org/10.1172/JCI27794

Finck Brian N., & Kelly Daniel P. (2007). Peroxisome Proliferator–Activated Receptor γ Coactivator-1 (PGC-1) Regulatory Cascade in Cardiac Physiology and Disease. *Circulation*, *115*(19), 2540–2548. https://doi.org/10.1161/CIRCULATIONAHA.107.670588

Finley, L. W. S., Haas, W., Desquiret-Dumas, V., Wallace, D. C., Procaccio, V., Gygi, S. P., & Haigis, M. C. (2011). Succinate Dehydrogenase Is a Direct Target of Sirtuin 3 Deacetylase Activity. *PLOS ONE*, *6*(8), e23295. https://doi.org/10.1371/journal.pone.0023295

Fischer, S., Huemer, M., Baumgartner, M., Deodato, F., Ballhausen, D., Boneh, A., … Dionisi-Vici, C. (2014). Clinical presentation and outcome in a series of 88 patients with the cblC defect. *Journal of Inherited Metabolic Disease*, *37*(5), 831–840. https://doi.org/10.1007/s10545-014-9687-6

Fofou-Caillierez, M. B., Mrabet, N. T., Chéry, C., Dreumont, N., Flayac, J., Pupavac, M., … Gueánt, J. L. (2013). Interaction between methionine synthase isoforms and MMACHC: Characterization in cblG-variant, cblG and cblC inherited causes of

megaloblastic anaemia. *Human Molecular Genetics*, *22*(22), 4591–4601. https://doi.org/10.1093/hmg/ddt308

Forges, T., Monnier-Barbarino, P., Alberto, J. M., Guéant-Rodriguez, R. M., Daval, J. L., & Guéant, J. L. (2007a). Impact of folate and homocysteine metabolism on human reproductive health. *Human Reproduction Update*, *13*(3), 225–238. https://doi.org/10.1093/humupd/dml063

Forges, T., Monnier-Barbarino, P., Alberto, J. M., Guéant-Rodriguez, R. M., Daval, J. L., & Guéant, J. L. (2007b). Impact of folate and homocysteine metabolism on human reproductive health. *Human Reproduction Update*, *13*(3), 225–238. https://doi.org/10.1093/humupd/dml063

Fournier, P., Fourcade, J., Roncalli, J., Salvayre, R., Galinier, M., & Caussé, E. (2015). Homocysteine in Chronic Heart Failure. *Clinical Laboratory*, *61*(9), 1137–1145. https://doi.org/10.7754/clin.lab.2015.141238

Fowler, B. (1998). Genetic defects of folate and cobalamin metabolism. *European Journal of Pediatrics*, *157*(2), S60–S66. https://doi.org/10.1007/PL00014306

Freedman, N. J., & Lefkowitz, R. J. (2004). Anti–β1-adrenergic receptor antibodies and heart failure: Causation, not just correlation. *Journal of Clinical Investigation*, *113*(10), 1379–1382. https://doi.org/10.1172/JCI200421748

Froese, D. S., & Gravel, R. A. (2010). Genetic disorders of vitamin B 12 metabolism: Eight complementation groups—Eight genes. *Expert Reviews in Molecular Medicine*, *12*(November), 1–20. https://doi.org/10.1017/S1462399410001651

Froese, D. S., Huemer, M., Suormala, T., Burda, P., Coelho, D., Guéant, J.-L., … Baumgartner, M. R. (2016). Mutation Update and Review of Severe Methylenetetrahydrofolate Reductase Deficiency. *Human Mutation*, *37*(5), 427–438. https://doi.org/10.1002/humu.22970

Froese, D. S., Kopec, J., Rembeza, E., Bezerra, G. A., Oberholzer, A. E., Suormala, T., … Yue, W. W. (2018). Structural basis for the regulation of human 5,10-methylenetetrahydrofolate reductase by phosphorylation and S-adenosylmethionine inhibition. *Nature Communications*, *9*. https://doi.org/10.1038/s41467-018-04735-2

Froese, D. S., Krojer, T., Wu, X., Shrestha, R., Kiyani, W., von Delft, F., … Yue, W. W. (2012). Structure of MMACHC reveals an arginine-rich pocket and a domain-swapped dimer for its B12 processing function. *Biochemistry*, *51*(25), 5083–5090. https://doi.org/10.1021/bi300150y

Frosst, P., Blom, H. J., Milos, R., Goyette, P., Sheppard, C. A., Matthews, R. G., … Rozen, R. (1995). A candidate genetic risk factor for vascular disease: A common mutation in methylenetetrahydrofolate reductase. *Nature Genetics*, *10*(1), 111–113. https://doi.org/10.1038/ng0595-111

Fu, Y., & Eisen, H. J. (2018). Genetics of Dilated Cardiomyopathy. *Current Cardiology Reports*, *20*(11), 121. https://doi.org/10.1007/s11886-018-1061-0

Fyfe, J. C., Hemker, S. L., Venta, P. J., Stebbing, B., & Giger, U. (2014). Selective Intestinal Cobalamin Malabsorption with Proteinuria (Imerslund-Gräsbeck Syndrome) in Juvenile Beagles. *Journal of Veterinary Internal Medicine*, *28*(2), 356–362. https://doi.org/10.1111/jvim.12284

Fyfe, John C., Hemker, S. L., Venta, P. J., Fitzgerald, C. A., Outerbridge, C. A., Myers, S. L., & Giger, U. (2013). An exon 53 frameshift mutation in CUBN abrogates cubam function and causes Imerslund-Gräsbeck syndrome in dogs. *Molecular Genetics and Metabolism*, *109*(4), 390–396. https://doi.org/10.1016/j.ymgme.2013.05.006

Gabriel-Costa, D. (2018a). The pathophysiology of myocardial infarction-induced heart failure. *Pathophysiology: The Official Journal of the International Society for Pathophysiology*, *25*(4), 277–284. https://doi.org/10.1016/j.pathophys.2018.04.003

Gabriel-Costa, D. (2018b). The pathophysiology of myocardial infarction-induced heart failure. *Pathophysiology: The Official Journal of the International Society for Pathophysiology*, *25*(4), 277–284. https://doi.org/10.1016/j.pathophys.2018.04.003

Ganguly, P., & Alam, S. F. (2015). Role of homocysteine in the development of cardiovascular disease. *Nutrition Journal*, *14*. https://doi.org/10.1186/1475-2891-14-6

Garcia, M. M., Guéant-Rodriguez, R.-M., Pooya, S., Brachet, P., Alberto, J.-M., Jeannesson, E., Guéant, J.-L. (2011). Methyl donor deficiency induces cardiomyopathy through altered methylation/acetylation of PGC-1α by PRMT1 and SIRT1. *The Journal of Pathology*, *225*(3), 324–335. https://doi.org/10.1002/path.2881

Garcia-Ropero, A., Santos-Gallego, C. G., Zafar, M. U., & Badimon, J. J. (2019). Metabolism of the failing heart and the impact of SGLT2 inhibitors. *Expert Opinion on Drug Metabolism & Toxicology*, *15*(4), 275–285. https://doi.org/10.1080/17425255.2019.1588886

Gauchotte, G., Hergalant, S., Vigouroux, C., Casse, J.-M., Houlgatte, R., Kaoma, T., … Battaglia-Hsu, S.-F. (2017). Cytoplasmic overexpression of RNA-binding protein HuR is a marker of poor prognosis in meningioma, and HuR knockdown decreases meningioma cell growth and resistance to hypoxia. *The Journal of Pathology*, *242*(4), 421–434. https://doi.org/10.1002/path.4916

Gaughan, D. J., Kluijtmans, L. A. J., Barbaux, S., McMaster, D., Young, I. S., Yarnell, J. W. G.,Whitehead, A. S. (2001). The methionine synthase reductase (MTRR) A66G polymorphism is a novel genetic determinant of plasma homocysteine concentrations. *Atherosclerosis*, *157*(2), 451–456. https://doi.org/10.1016/S0021-9150(00)00739-5

Ghemrawi, R., Arnold, C., Battaglia-Hsu, S.-F., Pourié, G., Trinh, I., Bassila, C., … Coelho, D. (2019). SIRT1 activation rescues the mislocalization of RNA-binding proteins and

cognitive defects induced by inherited cobalamin disorders. *Metabolism: Clinical and Experimental*, *101*, 153992. https://doi.org/10.1016/j.metabol.2019.153992

Gherasim, C., Ruetz, M., Li, Z., Hudolin, S., & Banerjee, R. (2015). Pathogenic Mutations Differentially Affect the Catalytic Activities of the Human B12-processing Chaperone CblC and Increase Futile Redox Cycling. *The Journal of Biological Chemistry*, *290*(18), 11393–11402. https://doi.org/10.1074/jbc.M115.637132

Glatz, J. F. C., Nabben, M., Heather, L. C., Bonen, A., & Luiken, J. J. F. P. (2016). Regulation of the subcellular trafficking of CD36, a major determinant of cardiac fatty acid utilization. *Biochimica et Biophysica Acta (BBA) - Molecular and Cell Biology of Lipids*, *1861*(10), 1461–1471. https://doi.org/10.1016/j.bbalip.2016.04.008

Goetze, J. P., Hansen, L. H., Terzic, D., Zois, N. E., Albrethsen, J., Timm, A., … Hunter, I. (2015). Atrial natriuretic peptides in plasma. *Clinica Chimica Acta*, *443*, 25–28. https://doi.org/10.1016/j.cca.2014.08.017

Gomes, S., Lopes, C., & Pinto, E. (2016). Folate and folic acid in the periconceptional period: Recommendations from official health organizations in thirty-six countries worldwide and WHO. *Public Health Nutrition*, *19*(1), 176–189. https://doi.org/10.1017/S1368980015000555

Goulding, C. W., Postigo, D., & Matthews, R. G. (1997). Cobalamin-dependent methionine synthase is a modular protein with distinct regions for binding homocysteine, methyltetrahydrofolate, cobalamin, and adenosylmethionine. *Biochemistry*, *36*(26), 8082–8091. https://doi.org/10.1021/bi9705164

Goyette, P., Christensen, B., Rosenblatt, D. S., & Rozen, R. (1996). Severe and mild mutations in cis for the methylenetetrahydrofolate reductase (MTHFR) gene, and description of five novel mutations in MTHFR. *American Journal of Human Genetics*, *59*(6), 1268–1275.

Goyette, P., Sumner, J. S., Milos, R., Duncan, A. M., Rosenblatt, D. S., Matthews, R. G., & Rozen, R. (1994). Human methylenetetrahydrofolate reductase: Isolation of cDNA, mapping and mutation identification. *Nature Genetics*, *7*(2), 195–200. https://doi.org/10.1038/ng0694-195

Gravel, R. A., Mahoney, M. J., Ruddle, F. H., & Rosenberg, L. E. (1975). Genetic complementation in heterokaryons of human fibroblasts defective in cobalamin metabolism. *Proceedings of the National Academy of Sciences of the United States of America*, *72*(8), 3181–3185.https://doi.org/10.1073/pnas.72.8.3181

Green, R., Allen, L. H., Bjørke-Monsen, A.-L., Brito, A., Guéant, J.-L., Miller, J. W., … Yajnik, C. (2017). Vitamin B12 deficiency. *Nature Reviews. Disease Primers*, *3*, 17040. https://doi.org/10.1038/nrdp.2017.40

Grimm, M., & Brown, J. H. (2010). Beta-adrenergic receptor signaling in the heart: Role of CaMKII. *Journal of Molecular and Cellular Cardiology*, *48*(2), 322–330. https://doi.org/10.1016/j.yjmcc.2009.10.016

Gruber, K., & Kratky, C. (2006). Cobalamin-Dependent Methionine Synthase. *Handbook of Metalloproteins*. https://doi.org/10.1002/0470028637.met173

Gruber, K., Puffer, B., & Kräutler, B. (2011). Vitamin B12-derivatives—Enzyme cofactors and ligands of proteins and nucleic acids. *Chemical Society Reviews*, *40*(8), 4346. https://doi.org/10.1039/c1cs15118e

Guéant, J. L., Namour, F., Guéant-Rodriguez, R. M., & Daval, J. L. (2013). Folate and fetal programming: A play in epigenomics? *Trends in Endocrinology and Metabolism*, *24*(6), 279–289. https://doi.org/10.1016/j.tem.2013.01.010

Guéant, J.-L., Caillerez-Fofou, M., Battaglia-Hsu, S., Alberto, J.-M., Freund, J.-N., Dulluc, I., Daval, J.-L. (2013). Molecular and cellular effects of vitamin B12 in brain, myocardium and liver through its role as co-factor of methionine synthase. *Biochimie*, *95*(5), 1033–1040. https://doi.org/10.1016/j.biochi.2013.01.020

Guéant, J.-L., Chéry, C., Oussalah, A., Nadaf, J., Coelho, D., Josse, T., … Rosenblatt, D. S. (2018). APRDX1 mutant allele causes a MMACHC secondary epimutation in cblC patients. *Nature Communications*, *9*(1), 67. https://doi.org/10.1038/s41467-017-02306-5

Guéant, J.-L., Namour, F., Guéant-Rodriguez, R.-M., & Daval, J.-L. (2013). Folate and fetal programming: A play in epigenomics? *Trends in Endocrinology and Metabolism: TEM*, *24*(6), 279–289. https://doi.org/10.1016/j.tem.2013.01.010

Guéant-Rodriguez, R. M., Juillière, Y., Nippert, M., Abdelmouttaleb, I., Herbeth, B., Aliot, E., Guéant, J. L. (2007). Left ventricular systolic dysfunction is an independent predictor of homocysteine in angiographically documented patients with or without coronary artery lesions. *Journal of Thrombosis and Haemostasis*, *5*(6), 1209–1216. https://doi.org/10.1111/j.1538-7836.2007.02535.x

Guéant-Rodriguez, R.-M., Juillière, Y., Nippert, M., Abdelmouttaleb, I., Herbeth, B., Aliot, E., Guéant, J.-L. (2007). Left ventricular systolic dysfunction is an independent predictor of homocysteine in angiographically documented patients with or without coronary artery lesions. *Journal of Thrombosis and Haemostasis*, *5*(6), 1209–1216. https://doi.org/10.1111/j.1538-7836.2007.02535.x

Gulati, S., Baker, P., Li, Y. N., Fowler, B., Kruger, W., Brody, L. C., & Banerjee, R. (1996). Defects in human methionine synthase in cblG patients. *Human Molecular Genetics*, *5*(12), 1859–1865. https://doi.org/ 10.1093/hmg/5.12.1859

Gündüz, M., Ekici, F., Özaydın, E., Ceylaner, S., & Perez, B. (2014). Reversible pulmonary arterial hypertension in cobalamin-dependent cobalamin C disease due to a novel mutation in the MMACHC gene. *European Journal of Pediatrics*, *173*(12), 1707–1710. https://doi.org/10.1007/s00431-014-2330-6

Guo, X., Yan, F., Li, J., Zhang, C., & Bu, P. (2017). SIRT3 attenuates AngII-induced cardiac fibrosis by inhibiting myofibroblasts transdifferentiation via STAT3-NFATc2 pathway. *American Journal of Translational Research*, *9*(7), 3258–3269.

Handy, D. E., Castro, R., & Loscalzo, J. (2011). Epigenetic Modifications: Basic Mechanisms and Role in Cardiovascular Disease. *Circulation*, *123*(19), 2145–2156. https://doi.org/10.1161/CIRCULATIONAHA.110.956839

Hankey, G. J., & Eikelboom, J. W. (1999). Homocysteine and vascular disease. *The Lancet*, *354*(9176), 407–413. https://doi.org/10.1016/S0140-6736(98)11058-9

Hannibal, L., DiBello, P. M., & Jacobsen, D. W. (2013a). Proteomics of vitamin B12 processing. *Clinical Chemistry and Laboratory Medicine*, *51*(3), 477–488. https://doi.org/10.1515/cclm-2012-0568

Hannibal, L., DiBello, P. M., & Jacobsen, D. W. (2013b). Proteomics of vitamin B12 processing. *Clinical Chemistry and Laboratory Medicine*, *51*(3), 477–488. https://doi.org/10.1515/cclm-2012-0568

Hannibal, L., DiBello, P. M., & Jacobsen, D. W. (2013c). Proteomics of vitamin B12 processing. *Clinical Chemistry and Laboratory Medicine*, *51*(3), 477–488. https://doi.org/10.1515/cclm-2012-0568

Hannibal, L., Dibello, P. M., Yu, M., Miller, A., Wang, S., Rosenblatt, D. S., & Jacobsen, D. W. (2012). *NIH Public Access* (Vol. 103). https://doi.org/10.1016/j.ymgme.2011.03.008.THE

Hannibal, L., Kim, J., Brasch, N. E., Wang, S., Rosenblatt, D. S., Banerjee, R., & Jacobsen, D. W. (2009). Processing of alkylcobalamins in mammalian cells: A role for the MMACHC (cblC) gene product. *Molecular Genetics and Metabolism*, *97*(4), 260–266. https://doi.org/10.1016/j.ymgme.2009.04.005

Hartupee, J., & Mann, D. L. (2017a). Neurohormonal activation in heart failure with reduced ejection fraction. *Nature Reviews. Cardiology*, *14*(1), 30–38. https://doi.org/10.1038/nrcardio.2016.163

Hartupee, J., & Mann, D. L. (2017b). Neurohormonal activation in heart failure with reduced ejection fraction. *Nature Reviews. Cardiology*, *14*(1), 30–38. https://doi.org/10.1038/nrcardio.2016.163

Hasegawa, K., Lee, S. J., Jobe, S. M., Markham, B. E., & Kitsis, R. N. (1997). Cis-Acting sequences that mediate induction of beta-myosin heavy chain gene expression during left ventricular hypertrophy due to aortic constriction. *Circulation*, *96*(11), 3943–3953. https://doi.org/10.1161/01.cir.96.11.3943

Hassan, F. M., Khattab, A. A., Abo El Fotoh, W. M. M., & Zidan, R. S. (2017). A66G and C524T polymorphisms of methionine synthase reductase gene are linked to the development of acyanotic congenital heart diseases in Egyptian children. *Gene*, *629*, 59–63. https://doi.org/10.1016/j.gene.2017.07.081

Hauck, F. H., Tanner, S. M., Henker, J., & Laass, M. W. (2008). Imerslund-Gräsbeck syndrome in a 15-year-old German girl caused by compound heterozygous mutations in CUBN. *European Journal of Pediatrics*, *167*(6), 671–675. https://doi.org/10.1007/s00431-007-0571-3

Hayashi, D., Kudoh, S., Shiojima, I., Zou, Y., Harada, K., Shimoyama, M., … Komuro, I. (2004). Atrial natriuretic peptide inhibits cardiomyocyte hypertrophy through mitogen-activated protein kinase phosphatase-1. *Biochemical and Biophysical Research Communications*, *322*(1), 310–319. https://doi.org/10.1016/j.bbrc.2004.07.119

Heger, J., Warga, B., Meyering, B., Abdallah, Y., Schlüter, K.-D., Piper, H. M., & Euler, G. (2011). TGFβ receptor activation enhances cardiac apoptosis via SMAD activation

and concomitant NO release. *Journal of Cellular Physiology*, *226*(10), 2683–2690. https://doi.org/10.1002/jcp.22619

Hershberger, R. E., Hedges, D. J., & Morales, A. (2013). Dilated cardiomyopathy: The complexity of a diverse genetic architecture. *Nature Reviews. Cardiology*, *10*(9), 531–547. https://doi.org/10.1038/nrcardio.2013.105

Hertrampf, E., & Cortes, F. (2004). Folic Acid Fortification of Wheat Flour: Chile. *Nutrition Reviews*, *62*(suppl_1), S44–S48. https://doi.org/10.1111/j.1753-4887.2004.tb00074.x

Hfa, E. S. C., Care, I., France, A. C., Mcmurray, J. J. V, Poland, P. P., Uk, P. A. P., … Israel, Y. H. (2008). *ESC GUIDELINES ESC Guidelines for the diagnosis and treatment of acute and chronic heart failure 2008 ‡ The Task Force for the Diagnosis and Treatment of Acute and Chronic Heart Failure 2008 of the European Society of Cardiology. Developed in collaborati*. 933–989. https://doi.org/10.1016/j.ejheart.2008.08.005

Hirschey, M. D., Shimazu, T., Huang, J.-Y., Schwer, B., & Verdin, E. (2011). SIRT3 regulates mitochondrial protein acetylation and intermediary metabolism. *Cold Spring Harbor Symposia on Quantitative Biology*, *76*, 267–277. https://doi.org/10.1101/sqb.2011.76.010850

Hirschey, Matthew D., Shimazu, T., Goetzman, E., Jing, E., Schwer, B., Lombard, D. B., … Verdin, E. (2010). SIRT3 regulates mitochondrial fatty-acid oxidation by reversible enzyme deacetylation. *Nature*, *464*(7285), 121–125. https://doi.org/10.1038/nature08778

Hodgkin, D. C., Kamper, J., Lindsey, J., MacKay, M., Pickworth, J., Robertson, J. H., … Trueblood, K. N. (1957). The Structure of Vitamin B12 I. An Outline of the Crystallographic Investigation of Vitamin B12. *Proceedings of the Royal Society of*

London. Series A, Mathematical and Physical Sciences, *242*(1229), 228–263. Retrieved from JSTOR. https://doi.org/10.1098/rspa.1957.0174

Hollak, C. E. M., & Lachmann, R. (2016). *Inherited Metabolic Disease in Adults: A Clinical Guide*. Oxford University Press. https://doi.org/10.1093/med/9780199972135.001.0001

Homocysteine Lowering Trialists' Collaboration. (2005). Dose-dependent effects of folic acid on blood concentrations of homocysteine: A meta-analysis of the randomized trials. *The American Journal of Clinical Nutrition*, *82*(4), 806–812. https://doi.org/10.1093/ajcn/82.4.806

Homolova, K., Zavadakova, P., Doktor, T. K., Schroeder, L. D., Kozich, V., & Andresen, B. S. (2010). The deep intronic c.903+469T>C mutation in the MTRR gene creates an SF2/ASF binding exonic splicing enhancer, which leads to pseudoexon activation and causes the cblE type of homocystinuria. *Human Mutation*, *31*(4), 437–444. https://doi.org/10.1002/humu.21206

Honein, M. A., Paulozzi, L. J., Mathews, T. J., Erickson, J. D., & Wong, L.-Y. C. (2001). Impact of Folic Acid Fortification of the US Food Supply on the Occurrence of Neural Tube Defects. *JAMA*, *285*(23), 2981–2986. https://doi.org/10.1001/jama.285.23.2981

Hu, S., Mei, S., Liu, N., & Kong, X. (2018). Molecular genetic characterization of cblC defects in 126 pedigrees and prenatal genetic diagnosis of pedigrees with combined methylmalonic aciduria and homocystinuria. *BMC Medical Genetics*, *19*(1), 154. https://doi.org/10.1186/s12881-018-0666-x

Hu, X., Van Marion, D. M. S., Wiersma, M., Zhang, D., & Brundel, B. J. J. M. (2017). The protective role of small heat shock proteins in cardiac diseases: Key role in atrial fibrillation. *Cell Stress and Chaperones*, *22*(4), 665–674. https://doi.org/10.1007/s12192-017-0799-4

Hue, L., & Taegtmeyer, H. (2009). The Randle cycle revisited: A new head for an old hat. *American Journal of Physiology - Endocrinology and Metabolism*, *297*(3), E578–E591. https://doi.org/10.1152/ajpendo.00093.2009

Huemer, M., Bürer, C., Ješina, P., Kožich, V., Landolt, M. A., Suormala, T., … Baumgartner, M. R. (2015). Clinical onset and course, response to treatment and outcome in 24 patients with the cblE or cblG remethylation defect complemented by genetic and in vitro enzyme study data. *Journal of Inherited Metabolic Disease*, *38*(5), 957–967. https://doi.org/10.1007/s10545-014-9803-7

Huemer, Martina, Diodato, D., Schwahn, B., Schiff, M., Bandeira, A., Benoist, J.-F., … Dionisi-Vici, C. (2017). Guidelines for diagnosis and management of the cobalamin-related remethylation disorders cblC, cblD, cblE, cblF, cblG, cblJ and MTHFR deficiency. *Journal of Inherited Metabolic Disease*, *40*(1), 21–48. https://doi.org/10.1007/s10545-016-9991-4

Huemer, Martina, Scholl-Bürgi, S., Hadaya, K., Kern, I., Beer, R., Seppi, K., … Karall, D. (2014). Three new cases of late-onset cblC defect and review of the literature illustrating when to consider inborn errors of metabolism beyond infancy. *Orphanet Journal of Rare Diseases*, *9*, 161. https://doi.org/10.1186/s13023-014-0161-1

Hunt, S. A. (2005). ACC/AHA 2005 Guideline Update for the Diagnosis and Management of Chronic Heart Failure in the Adult: A Report of the American College of Cardiology/American Heart Association Task Force on Practice Guidelines (Writing Committee to Update the 2001 Guidelines for the Evaluation and Management of Heart Failure). *Journal of the American College of Cardiology*, *46*(6), e1–e82. https://doi.org/10.1016/j.jacc.2005.08.022

Hunt, S. A., Abraham, W. T., Chin, M. H., Feldman, A. M., Francis, G. S., Ganiats, T. G., … Yancy, C. W. (2009). 2009 Focused Update Incorporated Into the ACC/AHA 2005

Guidelines for the Diagnosis and Management of Heart Failure in Adults: A Report of the American College of Cardiology Foundation/American Heart Association Task Force on Practice Guidelines Developed in Collaboration With the International Society for Heart and Lung Transplantation. *Journal of the American College of Cardiology*, *53*(15), e1–e90. https://doi.org/10.1016/j.jacc.2008.11.013

Huntgeburth, M., Tiemann, K., Shahverdyan, R., Schlüter, K.-D., Schreckenberg, R., Gross, M.-L., Rosenkranz, S. (2011). Transforming Growth Factor β1 Oppositely Regulates the Hypertrophic and Contractile Response to β-Adrenergic Stimulation in the Heart. *PLOS ONE*, *6*(11), e26628. https://doi.org/10.1371/journal.pone.0026628

Hurlimann, J., Zuber, C., Hurlimann, J., & Zuber, C. (1969). *VITAMIN B12-BINDERS IN HUMAN BODY FLUIDS*. 125–140.

Iacobazzi, V., Infantino, V., Castegna, A., & Andria, G. (2014). Hyperhomocysteinemia: Related genetic diseases and congenital defects, abnormal DNA methylation and newborn screening issues. *Molecular Genetics and Metabolism*, *113*(1–2), 27–33. https://doi.org/10.1016/j.ymgme.2014.07.016

Ibrahim, S., Maqbool, S., Azam, M., Iqbal, M. P., & Qamar, R. (2018). CBS mutations and MTFHR SNPs causative of hyperhomocysteinemia in Pakistani children. *Molecular Biology Reports*, *45*(3), 353–360. https://doi.org/10.1007/s11033-018-4169-9

Imbard, A., Benoist, J.-F., & Blom, H. J. (2013). Neural Tube Defects, Folic Acid and Methylation. *International Journal of Environmental Research and Public Health*, *10*(9), 4352–4389. https://doi.org/10.3390/ijerph10094352

Jacques Paul F., Bostom Andrew G., Williams Roger R., Ellison R. Curtis, Eckfeldt John H., Rosenberg Irwin H., Rozen Rima. (1996). Relation Between Folate Status, a Common Mutation in Methylenetetrahydrofolate Reductase, and Plasma Homocysteine Concentrations. *Circulation*, *93*(1), 7–9. https://doi.org/10.1161/01.CIR.93.1.7

Jakubowski, H. (1999). Protein homocysteinylation: Possible mechanism underlying pathological consequences of elevated homocysteine levels. *FASEB Journal: Official Publication of the Federation of American Societies for Experimental Biology*, *13*(15), 2277–2283. https://doi.org/10.1096/fasebj.13.15.2277

Jakubowski, H. (2008). The pathophysiological hypothesis of homocysteine thiolactone-mediated vascular disease. *Journal of Physiology and Pharmacology: An Official Journal of the Polish Physiological Society*, *59 Suppl 9*, 155–167.

Jakubowski, H., & Goldman, E. (1993). Synthesis of homocysteine thiolactone by methionyl-tRNA synthetase in cultured mammalian cells. *FEBS Letters*, *317*(3), 237–240. https://doi.org/10.1016/0014-5793(93)81283-6

Jakubowski, Hieronim, Boers, G. H. J., & Strauss, K. A. (2008). Mutations in cystathionine beta-synthase or methylenetetrahydrofolate reductase gene increase N-homocysteinylated protein levels in humans. *FASEB Journal: Official Publication of the Federation of American Societies for Experimental Biology*, *22*(12), 4071–4076. https://doi.org/10.1096/fj.08-112086

Jakubowski, Hieronim, Perla-Kaján, J., Finnell, R. H., Cabrera, R. M., Wang, H., Gupta, S., Shih, D. M. (2009). Genetic or nutritional disorders in homocysteine or folate metabolism increase protein N-homocysteinylation in mice. *FASEB Journal: Official Publication of the Federation of American Societies for Experimental Biology*, *23*(6), 1721–1727. https://doi.org/10.1096/fj.08-127548

Jakubowski Hieronim, Zhang Li, Bardeguez Arlene, & Aviv Abram. (2000). Homocysteine Thiolactone and Protein Homocysteinylation in Human Endothelial Cells. *Circulation Research*, *87*(1), 45–51. https://doi.org/10.1161/01.RES.87.1.45

Januzzi, J. L. (2013). Natriuretic Peptides as Biomarkers in Heart Failure. *Journal of Investigative Medicine : The Official Publication of the American Federation for Clinical Research*, *61*(6), 950–955. https://doi.org/10.231/JIM.0b013e3182946b69

Jaswal, J. S., Keung, W., Wang, W., Ussher, J. R., & Lopaschuk, G. D. (2011). Targeting fatty acid and carbohydrate oxidation—A novel therapeutic intervention in the ischemic and failing heart. *Biochimica Et Biophysica Acta*, *1813*(7), 1333–1350. https://doi.org/10.1016/j.bbamcr.2011.01.015

Jean-Louis Gueant, Celine Chery, and F. N. (2001). Cubilin and the hydrophobic intrinsic factor receptor are distinct molecules Cubilin. *BLOOD*, *97*(10), 3316–3318. https://doi.org/10.1016/j.resuscitation.2010.01.015

Jean-Philippe, J., Paz, S., & Caputi, M. (2013). hnRNP A1: The Swiss army knife of gene expression. *International Journal of Molecular Sciences*, *14*(9), 18999–19024. https://doi.org/10.3390/ijms140918999

Jenkins, C. M., Yang, J., Sims, H. F., & Gross, R. W. (2011). Reversible High Affinity Inhibition of Phosphofructokinase-1 by Acyl-CoA. *The Journal of Biological Chemistry*, *286*(14), 11937–11950. https://doi.org/10.1074/jbc.M110.203661

Jessup, M., Marwick, T. H., Ponikowski, P., Voors, A. A., & Yancy, C. W. (2016). 2016 ESC and ACC/AHA/HFSA heart failure guideline update—What is new and why is it important? *Nature Reviews Cardiology*, *13*(10), 623–628. https://doi.org/10.1038/nrcardio.2016.134

Jiang, W., Nakayama, Y., Sequeira, J. M., & Quadros, E. V. (2013a). Mapping the functional domains of TCblR/CD320, the receptor for cellular uptake of transcobalamin-bound cobalamin. *The FASEB Journal*, *27*(8), 2988–2994. https://doi.org/10.1096/fj.13-230185

Jiang, W., Nakayama, Y., Sequeira, J. M., & Quadros, E. V. (2013b). Mapping the functional domains of TCblR/CD320, the receptor for cellular uptake of transcobalamin-bound cobalamin. *FASEB Journal: Official Publication of the Federation of American Societies for Experimental Biology*, *27*(8), 2988–2994. https://doi.org/10.1096/fj.13-230185

Jideama, N. M., Crawford, B. H., Hussain, A. K. M. A., & Raynor, R. L. (2006). Dephosphorylation specificities of protein phosphatase for cardiac troponin I, troponin T, and sites within troponin T. *International Journal of Biological Sciences*, *2*(1), 1–9. https://doi.org/10.7150/ijbs.2.1

Jing, E., O'Neill, B. T., Rardin, M. J., Kleinridders, A., Ilkeyeva, O. R., Ussar, S., … Kahn, C. R. (2013). Sirt3 Regulates Metabolic Flexibility of Skeletal Muscle Through Reversible Enzymatic Deacetylation. *Diabetes*, *62*(10), 3404–3417. https://doi.org/10.2337/db12-1650

Jing, Enxuan, O'Neill, B. T., Rardin, M. J., Kleinridders, A., Ilkeyeva, O. R., Ussar, S., … Kahn, C. R. (2013). Sirt3 Regulates Metabolic Flexibility of Skeletal Muscle Through Reversible Enzymatic Deacetylation. *Diabetes*, *62*(10), 3404–3417. https://doi.org/10.2337/db12-1650

John C. Fyfe, Mette Madsen, Peter Højrup, Erik I. Christensen, Stephan M. Tanner, Albert de la Chapelle, Qianchuan He, and S. K. M. (2004). The functional cobalamin (vitamin B12)–intrinsic factor receptor is a novel complex ofcubilin and amnionless. *BLOOD*, *103*(5), 1573–1580. https://doi.org/10.1182/blood-2003-08-2852.Supported

Joo, J.-H. E., Andronikos, R. H., & Saffery, R. (2011). Chapter 17—Metabolic Regulation of DNA Methylation in Mammals. In T. Tollefsbol (Ed.), *Handbook of Epigenetics* (pp. 281–293). https://doi.org/10.1016/B978-0-12-375709-8.00017-4

Kain, D., Simon, A. J., Greenberg, A., Ben Zvi, D., Gilburd, B., & Schneiderman, J. (2018). Cardiac leptin overexpression in the context of acute MI and reperfusion potentiates myocardial remodeling and left ventricular dysfunction. *PloS One*, *13*(10), e0203902. https://doi.org/10.1371/journal.pone.0203902

Karbowska, J., Kochan, Z., & Smoleński, R. T. (2003). Peroxisome proliferator-activated receptor alpha is downregulated in the failing human heart. *Cellular & Molecular Biology Letters*, *8*(1), 49–53.

Karwi, Q. G., Uddin, G. M., Ho, K. L., & Lopaschuk, G. D. (2018a). Loss of Metabolic Flexibility in the Failing Heart. *Frontiers in Cardiovascular Medicine*, *5*. https://doi.org/10.3389/fcvm.2018.00068

Karwi, Q. G., Uddin, G. M., Ho, K. L., & Lopaschuk, G. D. (2018b). Loss of Metabolic Flexibility in the Failing Heart. *Frontiers in Cardiovascular Medicine*, *5*. https://doi.org/10.3389/fcvm.2018.00068

Kaski, J. P., Syrris, P., Burch, M., Tomé-Esteban, M.-T., Fenton, M., Christiansen, M., … Elliott, P. M. (2008). Idiopathic restrictive cardiomyopathy in children is caused by mutations in cardiac sarcomere protein genes. *Heart (British Cardiac Society)*, *94*(11), 1478–1484. https://doi.org/10.1136/hrt.2007.134684

Kato Takao, Niizuma Shinichiro, Inuzuka Yasutaka, Kawashima Tsuneaki, Okuda Junji, Tamaki Yodo, … Shioi Tetsuo. (2010). Analysis of Metabolic Remodeling in Compensated Left Ventricular Hypertrophy and Heart Failure. *Circulation: Heart Failure*, *3*(3), 420–430. https://doi.org/10.1161/CIRCHEARTFAILURE.109.888479

Kemp, C. D., & Conte, J. V. (2012a). The pathophysiology of heart failure. *Cardiovascular Pathology: The Official Journal of the Society for Cardiovascular Pathology*, *21*(5), 365–371. https://doi.org/10.1016/j.carpath.2011.11.007

Kemp, C. D., & Conte, J. V. (2012b). The pathophysiology of heart failure. *Cardiovascular Pathology*, *21*(5), 365–371. https://doi.org/10.1016/j.carpath.2011.11.007

Kim, D., Langmead, B., & Salzberg, S. L. (2015). HISAT: A fast spliced aligner with low memory requirements. *Nature Methods*, *12*(4), 357–360. https://doi.org/10.1038/nmeth.3317

Kim, Jihoe, Gherasim, C., & Banerjee, R. (2008). Decyanation of vitamin B12 by a trafficking chaperone. *Proceedings of the National Academy of Sciences of the United States of America*, *105*(38), 14551–14554. https://doi.org/10.1073/pnas.0805989105

Kim, Jihoe, Hannibal, L., Gherasim, C., Jacobsen, D. W., & Banerjee, R. (2009). A human vitamin B12trafficking protein uses glutathione transferase activity for processing alkylcobalamins. *Journal of Biological Chemistry*, *284*(48), 33418–33424. https://doi.org/10.1074/jbc.M109.057877

Kim, Jihyun, Kim, H., Roh, H., & Kwon, Y. (2018). Causes of hyperhomocysteinemia and its pathological significance. *Archives of Pharmacal Research*, *41*(4), 372–383. https://doi.org/10.1007/s12272-018-1016-4

Kim Shokei, Ohta Kensuke, Hamaguchi Akinori, Yukimura Tokihito, Miura Katsuyuki, & Iwao Hiroshi. (1995). Angiotensin II Induces Cardiac Phenotypic Modulation and Remodeling In Vivo in Rats. *Hypertension*, *25*(6), 1252–1259. https://doi.org/10.1161/01.HYP.25.6.1252

Kim, Y.-I. (2004). Folate and DNA Methylation: A Mechanistic Link between Folate Deficiency and Colorectal Cancer? *Cancer Epidemiology and Prevention Biomarkers*, *13*(4), 511–519.

Klabunde, R. (2011). *Cardiovascular Physiology Concepts*. Lippincott Williams & Wilkins.

Koentges, C., Pfeil, K., Schnick, T., Wiese, S., Dahlbock, R., Cimolai, M. C., … Bugger, H. (2015). SIRT3 deficiency impairs mitochondrial and contractile function in the heart. *Basic Research in Cardiology*, *110*(4), 36. https://doi.org/10.1007/s00395-015-0493-6

Kojima, M., Minamino, N., Kangawa, J., & Matsuo, H. (1989). Cloning and sequence analysis of cDNA encoding a precursor for rat brain natriuretic peptide. *Biochemical and Biophysical Research Communications*, *159*(3), 1420–1426. https://doi.org/10.1016/0006-291X(89)92268-7

Kokame, K., Agarwala, K. L., Kato, H., & Miyata, T. (2000). Herp, a new ubiquitin-like membrane protein induced by endoplasmic reticulum stress. *The Journal of Biological Chemistry*, *275*(42), 32846–32853. https://doi.org/10.1074/jbc.M002063200

Kokame, K., Kato, H., & Miyata, T. (1996). Homocysteine-respondent genes in vascular endothelial cells identified by differential display analysis. GRP78/BiP and novel genes. *The Journal of Biological Chemistry*, *271*(47), 29659–29665. https://doi.org/10.1074/jbc.271.47.29659

Kolwicz Stephen C., Olson David P., Marney Luke C., Garcia-Menendez Lorena, Synovec Robert E., & Tian Rong. (2012). Cardiac-Specific Deletion of Acetyl CoA Carboxylase 2 Prevents Metabolic Remodeling During Pressure-Overload Hypertrophy. *Circulation Research*, *111*(6), 728–738. https://doi.org/10.1161/CIRCRESAHA.112.268128

Koutmos, M., Gherasim, C., Smith, J. L., & Banerjee, R. (2011a). Structural basis of multifunctionality in a vitamin B12- processing enzyme. *Journal of Biological Chemistry*, *286*(34), 29780–29787. https://doi.org/10.1074/jbc.M111.261370

Koutmos, M., Gherasim, C., Smith, J. L., & Banerjee, R. (2011b). Structural Basis of Multifunctionality in a Vitamin B12-processing Enzyme. *The Journal of Biological Chemistry*, *286*(34), 29780–29787. https://doi.org/10.1074/jbc.M111.261370

Kozyraki, R., & Gofflot, F. (2007). Multiligand endocytosis and congenital defects: Roles of cubilin, megalin and amnionless. *Curr Pharm Des*, *13*(29), 3038–3046. https://doi.org/10.2174/138161207782110507

Kraegen, E. W., Sowden, J. A., Halstead, M. B., Clark, P. W., Rodnick, K. J., Chisholm, D. J., & James, D. E. (1993). Glucose transporters and in vivo glucose uptake in skeletal and cardiac muscle: Fasting, insulin stimulation and immunoisolation studies of GLUT1 and GLUT4. *Biochemical Journal*, *295*(Pt 1), 287–293. https://doi.org/10.1042/bj2950287

Krenz, M., & Robbins, J. (2004). Impact of beta-myosin heavy chain expression on cardiac function during stress. *Journal of the American College of Cardiology*, *44*(12), 2390–2397. https://doi.org/10.1016/j.jacc.2004.09.044

Kuleshov, M. V., Jones, M. R., Rouillard, A. D., Fernandez, N. F., Duan, Q., Wang, Z., … Ma'ayan, A. (2016). Enrichr: A comprehensive gene set enrichment analysis web server 2016 update. *Nucleic Acids Research*, *44*(Web Server issue), W90–W97. https://doi.org/10.1093/nar/gkw377

Kumar, A., Palfrey, H. A., Pathak, R., Kadowitz, P. J., Gettys, T. W., & Murthy, S. N. (2017). The metabolism and significance of homocysteine in nutrition and health. *Nutrition & Metabolism*, *14*. https://doi.org/10.1186/s12986-017-0233-z

Kuznetsova Tatiana, Herbots Lieven, López Begoña, Jin Yu, Richart Tom, Thijs Lutgarde, … Staessen Jan A. (2009). Prevalence of Left Ventricular Diastolic Dysfunction in a General Population. *Circulation: Heart Failure*, *2*(2), 105–112. https://doi.org/10.1161/CIRCHEARTFAILURE.108.822627

Lai, W. K. C., & Kan, M. Y. (2015a). Homocysteine-Induced Endothelial Dysfunction. *Annals of Nutrition and Metabolism*, *67*(1), 1–12. https://doi.org/10.1159/000437098

Lai, W. K. C., & Kan, M. Y. (2015b). Homocysteine-Induced Endothelial Dysfunction. *Annals of Nutrition & Metabolism*, *67*(1), 1–12. https://doi.org/10.1159/000437098

Lanzkowsky, P. (1970). Congenital malabsorption of folate. *The American Journal of Medicine*, *48*(5), 580–583. https://doi.org/10.1016/0002-9343(70)90007-0

Leclerc, D. (1996). Human methionine synthase: CDNA cloning and identification of mutations in patients of the cblG complementation group of folate/cobalamin disorders. *Human Molecular Genetics*, *5*(12), 1867–1874. https://doi.org/10.1093/hmg/5.12.1867

Leclerc, D., Campeau, E., Goyette, P., Adjalla, C. E., Christensen, B., Ross, M., Gravel, R. A. (1996a). *Human methionine synthase: CDNA cloning and identification of mutations in patients of the cblG complementation group of folate / cobalamin disorders*. *5*(12), 1867–1874. https://doi.org/10.1093/hmg/5.12.1867

Leclerc, D., Odièvre, M., Wu, Q., Wilson, A., Huizenga, J. J., Rozen, R., Gravel, R. A. (1999). Molecular cloning, expression and physical mapping of the human methionine synthase reductase gene. *Gene*, *240*(1), 75–88. https://doi.org/10.1016/s0378-1119(99)00431-x

Leclerc, D., Wilson, A., Dumas, R., Gafuik, C., Song, D., Watkins, D., Gravel, R. A. (1998a). Cloning and mapping of a cDNA for methionine synthase reductase, a flavoprotein defective in patients with homocystinuria. *Proceedings of the National Academy of Sciences of the United States of America*, *95*(6), 3059–3064. https://doi.org/10.1073/pnas.95.6.3059

Leclerc, D., Wilson, A., Dumas, R., Gafuik, C., Song, D., Watkins, D., Gravel, R. A. (1998b). Cloning and mapping of a cDNA for methionine synthase reductase, a flavoprotein defective in patients with homocystinuria. *Proceedings of the National Academy of Sciences*, *95*(6), 3059–3064. https://doi.org/10.1073/pnas.95.6.3059

Ledley, F. D., Lumetta, M. R., Zoghbi, H. Y., VanTuinen, P., Ledbetter, S. A., & Ledbetter, D. H. (1988). Mapping of human methylmalonyl CoA mutase (MUT) locus on chromosome 6. *American Journal of Human Genetics*, *42*(6), 839–846.

Lee, J. E., Willett, W. C., Fuchs, C. S., Smith-Warner, S. A., Wu, K., Ma, J., & Giovannucci, E. (2011). Folate intake and risk of colorectal cancer and adenoma: Modification by time. *The American Journal of Clinical Nutrition*, *93*(4), 817–825. https://doi.org/10.3945/ajcn.110.007781

Lehotsky, J., Petras, M., Kovalska, M., Tothova, B., Drgova, A., & Kaplan, P. (2015). Mechanisms Involved in the Ischemic Tolerance in Brain: Effect of the Homocysteine. *Cellular and Molecular Neurobiology*, *35*(1), 7–15. https://doi.org/10.1007/s10571-014-0112-3

Lei, B., Lionetti, V., Young, M. E., Chandler, M. P., d'Agostino, C., Kang, E., Recchia, F. A. (2004). Paradoxical downregulation of the glucose oxidation pathway despite enhanced flux in severe heart failure. *Journal of Molecular and Cellular Cardiology*, *36*(4), 567–576. https://doi.org/10.1016/j.yjmcc.2004.02.004

Lerman, A., Gibbons, R. J., Rodeheffer, R. J., Bailey, K. R., McKinley, L. J., Heublein, D. M., & Burnett, J. C. (1993). Circulating N-terminal atrial natriuretic peptide as a marker for symptomless left-ventricular dysfunction. *The Lancet*, *341*(8853), 1105–1109. https://doi.org/10.1016/0140-6736(93)93125-K

Lerner-Ellis, J. P., Anastasio, N., Liu, J., Coelho, D., Suormala, T., Stucki, M., … Fowler, B. (2009). Spectrum of mutations in MMACHC, allelic expression, and evidence for genotype-phenotype correlations. *Human Mutation*, *30*(7), 1072–1081. https://doi.org/10.1002/humu.21001

Lerner-Ellis, J. P., Tirone, J. C., Pawelek, P. D., Doré, C., Atkinson, J. L., Watkins, D., … Rosenblatt, D. S. (2006). Identification of the gene responsible for methylmalonic

aciduria and homocystinuria, cblC type. *Nature Genetics*, *38*(1), 93–100. https://doi.org/10.1038/ng1683

Lerner-Ellis, J. P., Tirone, J. C., Pawelek, P. D., Doré, C., Atkinson, J. L., Watkins, D., Rosenblatt, D. S. (2006b). Identification of the gene responsible for methylmalonic aciduria and homocystinuria, cblC type. *Nature Genetics*, *38*(1), 93–100. https://doi.org/10.1038/ng1683

Levick, J. R. (2013). *An Introduction to Cardiovascular Physiology*. Butterworth-Heinemann.

Li, D.-X., Li, X.-Y., Dong, H., Liu, Y.-P., Ding, Y., Song, J.-Q., Yang, Y.-L. (2018). Eight novel mutations of CBS gene in nine Chinese patients with classical homocystinuria. *World Journal of Pediatrics*, *14*(2), 197–203. https://doi.org/10.1007/s12519-018-0135-9

Li, W.-X., Cheng, F., Zhang, A.-J., Dai, S.-X., Li, G.-H., Lv, W.-W., Huang, J.-F. (2017). Folate Deficiency and Gene Polymorphisms of MTHFR, MTR and MTRR Elevate the Hyperhomocysteinemia Risk. *Clinical Laboratory*, *63*(3), 523–533. https://doi.org/10.7754/Clin.Lab.2016.160917

Li, Y. N., Gulati, S., Baker, P. J., Brody, L. C., Banerjee, R., & Kruger, W. D. (1996). Cloning, mapping and RNA analysis of the human methionine synthase gene. *Human Molecular Genetics*, *5*(12), 1851–1858.https://doi.org/10.1093/hmg/5.12.1851

Liu, T., Chen, L., Kim, E., Tran, D., Phinney, B. S., & Knowlton, A. A. (2014). Mitochondrial Proteome Remodeling in Ischemic Heart Failure. *Life Sciences*, *101*(0), 27–36. https://doi.org/10.1016/j.lfs.2014.02.004

Liu, X. Q., Yan, H., Qiu, J. X., Zhang, C. Y., Qi, J. G., Zhang, X., Du, J. B. (2017). [Pulmonary arterial hypertension as leading manifestation of methylmalonic aciduria: Clinical characteristics and gene testing in 15 cases]. *Beijing Da Xue Xue Bao. Yi Xue Ban = Journal of Peking University. Health Sciences*, *49*(5), 768–777.

Liu, Y., Liu, Y. P., Zhang, Y., Song, J. Q., Zheng, H., Dong, H., … Yang, Y. L. (2018). [Heterogeneous phenotypes, genotypes, treatment and prevention of 1 003 patients with methylmalonic acidemia in the mainland of China]. *Zhonghua Er Ke Za Zhi = Chinese Journal of Pediatrics*, *56*(6), 414–420. https://doi.org/10.3760/cma.j.issn.0578-1310.2018.06.003

Lopaschuk, G. D., Ussher, J. R., Folmes, C. D. L., Jaswal, J. S., & Stanley, W. C. (2010). Myocardial Fatty Acid Metabolism in Health and Disease. *Physiological Reviews*, *90*(1), 207–258. https://doi.org/10.1152/physrev.00015.2009

Lopes, L. R., & Elliott, P. M. (2013). Genetics of heart failure. *Biochimica et Biophysica Acta (BBA) - Molecular Basis of Disease*, *1832*(12), 2451–2461. https://doi.org/10.1016/j.bbadis.2012.12.012

Lucia, C. de, Eguchi, A., & Koch, W. J. (2018). New Insights in Cardiac β-Adrenergic Signaling During Heart Failure and Aging. *Frontiers in Pharmacology*, *9*. https://doi.org/10.3389/fphar.2018.00904

Luciana Hannibal, Jihoe Kim, Nicola E. Brasch, Sihe Wang5 David S. Rosenblatt, Ruma Banerjee, and D. W. J. (2009). *Processing of alkylcobalamins in mammalian cells: A role for the MMACHC (cblC) gene product*. *97*(4), 260–266. https://doi.org/10.1158/2326-6066.CIR-13-0034.PD-L1

Lucock, M. (2000). Folic Acid: Nutritional Biochemistry, Molecular Biology, and Role in Disease Processes. *Molecular Genetics and Metabolism*, *71*(1), 121–138. https://doi.org/10.1006/mgme.2000.3027

Ludwig and, M. L., & Matthews, R. G. (1997). -Dependent Enzymes. *Annual Review of Biochemistry*, *66*(1), 269–313. https://doi.org/10.1146/annurev.biochem.66.1.269

Ludwig, M. L., & Matthews, R. G. (1997). Structure-based perspectives on B12-dependent enzymes. *Annual Review of Biochemistry*, *66*, 269–313. https://doi.org/10.1146/annurev.biochem.66.1.269

Luiken, J. J. F. P., Coort, S. L. M., Koonen, D. P. Y., van der Horst, D. J., Bonen, A., Zorzano, A., & Glatz, J. F. C. (2004). Regulation of cardiac long-chain fatty acid and glucose uptake by translocation of substrate transporters. *Pflügers Archiv*, *448*(1), 1–15. https://doi.org/10.1007/s00424-003-1199-4

Luschinsky, C. L., Drummond, J. T., Matthews, R. G., & Ludwig, M. L. (1992). Crystallization and preliminary X-ray diffraction studies of the cobalamin-binding domain of methionine synthase from Escherichia coli. *Journal of Molecular Biology*, *225*(2), 557–560. https://doi.org/10.1016/0022-2836(92)90940-l

Lymperopoulos, A. (Ed.). (2015). *The Cardiovascular Adrenergic System*. Retrieved from https://www.springer.com/gp/book/9783319136790

Madamanchi, A. (2007). β-Adrenergic receptor signaling in cardiac function and heart failure. *McGill Journal of Medicine : MJM*, *10*(2), 99–104.

Madrazo, J. A., & Kelly, D. P. (2008). The PPAR trio: Regulators of myocardial energy metabolism in health and disease. *Journal of Molecular and Cellular Cardiology*, *44*(6), 968–975. https://doi.org/10.1016/j.yjmcc.2008.03.021

Mahalle, N., Kulkarni, M. V., Garg, M. K., & Naik, S. S. (2013). Vitamin B12 deficiency and hyperhomocysteinemia as correlates of cardiovascular risk factors in Indian subjects with coronary artery disease. *Journal of Cardiology*, *61*(4), 289–294. https://doi.org/10.1016/j.jjcc.2012.11.009

Maier, L. S., Bers, D. M., & Brown, J. H. (2007). Calmodulin and Ca2+/calmodulin kinases in the heart – Physiology and pathophysiology. *Cardiovascular Research*, *73*(4), 629–630. https://doi.org/10.1016/j.cardiores.2007.01.005

Maisel, A. S., Duran, J. M., & Wettersten, N. (2018). Natriuretic Peptides in Heart Failure: Atrial and B-type Natriuretic Peptides. *Heart Failure Clinics*, *14*(1), 13–25. https://doi.org/10.1016/j.hfc.2017.08.002

Maisel, A. S., Krishnaswamy, P., Nowak, R. M., McCord, J., Hollander, J. E., Duc, P., … McCullough, P. A. (2002). Rapid Measurement of B-Type Natriuretic Peptide in the Emergency Diagnosis of Heart Failure. *New England Journal of Medicine*, *347*(3), 161–167. https://doi.org/10.1056/NEJMoa020233

Maiti, N., Widjaja, L., & Banerjee, R. (1999). Proton transfer from histidine 244 may facilitate the 1,2 rearrangement reaction in coenzyme B12-dependent methylmalonyl-CoA mutase. *Journal of Biological Chemistry*, *274*(46), 32733–32737. https://doi.org/10.1074/jbc.274.46.32733

Malik, R. A., Lone, M. R., Ahmed, A., Koul, K. A., & Malla, R. R. (2017). Maternal hyperhomocysteinemia and congenital heart defects: A prospective case control study in Indian population. *Indian Heart Journal*, *69*(1), 17–19. https://doi.org/10.1016/j.ihj.2016.07.014

Maron, B. J., Towbin, J. A., Thiene, G., Antzelevitch, C., Corrado, D., Arnett, D., … Young, J. B. (2006a). Contemporary Definitions and Classification of the Cardiomyopathies: An American Heart Association Scientific Statement From the Council on Clinical Cardiology, Heart Failure and Transplantation Committee; Quality of Care and Outcomes Research and Functional Genomics and Translational Biology Interdisciplinary Working Groups; and Council on Epidemiology and Prevention.

Circulation, *113*(14), 1807–1816. https://doi.org/10.1161/CIRCULATIONAHA.106.174287

Maron, B. J., Towbin, J. A., Thiene, G., Antzelevitch, C., Corrado, D., Arnett, D., … Young, J. B. (2006b). Contemporary Definitions and Classification of the Cardiomyopathies: An American Heart Association Scientific Statement From the Council on Clinical Cardiology, Heart Failure and Transplantation Committee; Quality of Care and Outcomes Research and Functional Genomics and Translational Biology Interdisciplinary Working Groups; and Council on Epidemiology and Prevention. *Circulation*, *113*(14), 1807–1816. https://doi.org/10.1161/CIRCULATIONAHA.106.174287

Martens, J. H., Barg, H., Warren, M., & Jahn, D. (2002). Microbial production of vitamin B12. *Applied Microbiology and Biotechnology*, *58*(3), 275–285. https://doi.org/10.1007/s00253-001-0902-7

Martinelli, D., Deodato, F., & Dionisi-Vici, C. (2011). Cobalamin C defect: Natural history, pathophysiology, and treatment. *Journal of Inherited Metabolic Disease*, *34*(1), 127–135. https://doi.org/10.1007/s10545-010-9161-z

Marunouchi, T., Inomata, S., Sanbe, A., Takagi, N., & Tanonaka, K. (2014). Protective effect of geranylgeranylacetone via enhanced induction of HSPB1 and HSPB8 in mitochondria of the failing heart following myocardial infarction in rats. *European Journal of Pharmacology*, *730*, 140–147. https://doi.org/10.1016/j.ejphar.2014.02.037

Masoud, W. G. T., Ussher, J. R., Wang, W., Jaswal, J. S., Wagg, C. S., Dyck, J. R., … Lopaschuk, G. D. (2014). Failing mouse hearts utilize energy inefficiently and benefit from improved coupling of glycolysis and glucose oxidation. *Cardiovascular Research*, *101*(1), 30–38. https://doi.org/10.1093/cvr/cvt216

Matthews, R. G. (2001a). Cobalamin-dependent methyltransferases. *Accounts of Chemical Research*, *34*(8), 681–689.

Matthews, R. G. (2001b). Cobalamin-dependent methyltransferases. *Accounts of Chemical Research*, *34*(8), 681–689. https://doi.org/10.1021/ar0000051

Matthews, Rowena G. (2001). *Cobalamin-Dependent Methyltransferases*. *34*(8), 681–689.

McCully, K. S. (1969). Vascular pathology of homocysteinemia: Implications for the pathogenesis of arteriosclerosis. *The American Journal of Pathology*, *56*(1), 111–128.

McCully, Kilmer S. (2015). Homocysteine Metabolism, Atherosclerosis, and Diseases of Aging. In *Comprehensive Physiology* (pp. 471–505). https://doi.org/10.1002/cphy.c150021

McDowell, I. F. W., & Lang, D. (2000). Homocysteine and Endothelial Dysfunction: A Link with Cardiovascular Disease. *The Journal of Nutrition*, *130*(2), 369S-372S. https://doi.org/10.1093/jn/130.2.369S

McGarry, J. D., Leatherman, G. F., & Foster, D. W. (1978). Carnitine palmitoyltransferase I. The site of inhibition of hepatic fatty acid oxidation by malonyl-CoA. *Journal of Biological Chemistry*, *253*(12), 4128–4136.

McGarry, J. Denis, & Brown, N. F. (1997). The Mitochondrial Carnitine Palmitoyltransferase System—From Concept to Molecular Analysis. *European Journal of Biochemistry*, *244*(1), 1–14. https://doi.org/10.1111/j.1432-1033.1997.00001.x

McKenna, W. J., Maron, B. J., & Thiene, G. (2017). Classification, Epidemiology, and Global Burden of Cardiomyopathies. *Circulation Research*, *121*(7), 722–730. https://doi.org/10.1161/CIRCRESAHA.117.309711

McKinley, M. C., McNulty, H., McPartlin, J., Strain, J. J., Pentieva, K., Ward, M., … Scott, J. M. (2001). Low-dose vitamin B-6 effectively lowers fasting plasma homocysteine in

healthy elderly persons who are folate and riboflavin replete. *The American Journal of Clinical Nutrition*, *73*(4), 759–764. https://doi.org/10.1093/ajcn/73.4.759

McMurray, J. J. V., Adamopoulos, S., Anker, S. D., Auricchio, A., Böhm, M., Dickstein, K., Ponikowski, P. (2012). ESC Guidelines for the diagnosis and treatment of acute and chronic heart failure 2012. *European Journal of Heart Failure*, *14*(8), 803–869. https://doi.org/10.1093/eurjhf/hfs105

McNally, E. M., & Mestroni, L. (2017). Dilated Cardiomyopathy: Genetic Determinants and Mechanisms. *Circulation Research*, *121*(7), 731–748. https://doi.org/10.1161/CIRCRESAHA.116.309396

Meunier, B., Dumas, E., Piec, I., Béchet, D., Hébraud, M., & Hocquette, J.-F. (2007). Assessment of Hierarchical Clustering Methodologies for Proteomic Data Mining. *Journal of Proteome Research*, *6*(1), 358–366. https://doi.org/10.1021/pr060343h

Miller-Davis, C., Marden, S., & Leidy, N. K. (2006). The New York Heart Association Classes and functional status: What are we really measuring? *Heart & Lung*, *35*(4), 217–224. https://doi.org/10.1016/j.hrtlng.2006.01.003

Miousse, I. R., Watkins, D., Coelho, D., Rupar, T., Crombez, E. A., Vilain, E., … Rosenblatt, D. S. (2009). Clinical and Molecular Heterogeneity in Patients with the CblD Inborn Error of Cobalamin Metabolism. *The Journal of Pediatrics*, *154*(4), 551–556. https://doi.org/10.1016/j.jpeds.2008.10.043

Moestrup, S. K., Birn, H., Fischer, P. B., Petersen, C. M., Verroust, P. J., Sim, R. B., Nexø, E. (1996). Megalin-mediated endocytosis of transcobalamin-vitamin-B12 complexes suggests a role of the receptor in vitamin-B12 homeostasis. *Proceedings of the National Academy of Sciences of the United States of America*, *93*(16), 8612–8617. https://doi.org/10.1073/pnas.93.16.8612

Montjean, D., Benkhalifa, M., Dessolle, L., Cohen-Bacrie, P., Belloc, S., Siffroi, J.-P., … McElreavey, K. (2011). Polymorphisms in MTHFR and MTRR genes associated with

blood plasma homocysteine concentration and sperm counts. *Fertility and Sterility*, *95*(2), 635–640. https://doi.org/10.1016/j.fertnstert.2010.08.054

Moore, S. J., Lawrence, A. D., Biedendieck, R., Deery, E., Frank, S., Howard, M. J., … Warren, M. J. (2013). Elucidation of the anaerobic pathway for the corrin component of cobalamin (vitamin B12). *Proceedings of the National Academy of Sciences*, *110*(37), 14906–14911. https://doi.org/10.1073/pnas.1308098110

Morel, C. F., Lerner-Ellis, J. P., & Rosenblatt, D. S. (2006). Combined methylmalonic aciduria and homocystinuria (cblC): Phenotype-genotype correlations and ethnic-specific observations. *Molecular Genetics and Metabolism*, *88*(4), 315–321. https://doi.org/10.1016/j.ymgme.2006.04.001

Moreno-Garcia, M. A., Pupavac, M., Rosenblatt, D. S., Tremblay, M. L., & Jerome-Majewska, L. A. (2014). The Mmachc gene is required for pre-implantation embryogenesis in the mouse. *Molecular Genetics and Metabolism*, *112*(3), 198–204. https://doi.org/10.1016/j.ymgme.2014.05.002

Mori Jun, Basu Ratnadeep, McLean Brent A., Das Subhash K., Zhang Liyan, Patel Vaibhav B., Oudit Gavin Y. (2012). Agonist-Induced Hypertrophy and Diastolic Dysfunction Are Associated With Selective Reduction in Glucose Oxidation. *Circulation: Heart Failure*, *5*(4), 493–503. https://doi.org/10.1161/CIRCHEARTFAILURE.112.966705

Morita, H., Rehm, H. L., Menesses, A., McDonough, B., Roberts, A. E., Kucherlapati, R., Seidman, C. E. (2008). Shared Genetic Causes of Cardiac Hypertrophy in Children and Adults. *New England Journal of Medicine*, *358*(18), 1899–1908. https://doi.org/10.1056/NEJMoa075463

Müller, P., Horneff, G., & Hennermann, J. B. (2007). [A rare inborn error of intracellular processing of cobalamine presenting with microcephalus and megaloblastic anemia: A

report of 3 children]. *Klinische Padiatrie*, *219*(6), 361–367. https://doi.org/10.1055/s-2007-973067

Murthy, M. S., & Pande, S. V. (1984). Mechanism of carnitine acylcarnitine translocase-catalyzed import of acylcarnitines into mitochondria. *Journal of Biological Chemistry*, *259*(14), 9082–9089. https://doi.org/10.1042/bj2300657

Naghshtabrizi, B., Shakerian, F., Hajilooi, M., & Emami, F. (2012). Plasma homocysteine level and its genotypes as a risk factor for coronary artery disease in patients undergoing coronary angiography. *Journal of Cardiovascular Disease Research*, *3*(4), 276–279. https://doi.org/10.4103/0975-3583.102695

Neely, J. R., & Morgan, H. E. (1974). Relationship Between Carbohydrate and Lipid Metabolism and the Energy Balance of Heart Muscle. *Annual Review of Physiology*, *36*(1), 413–459. https://doi.org/10.1146/annurev.ph.36.030174.002213

Neubauer, S. (2007). The Failing Heart—An Engine Out of Fuel. *New England Journal of Medicine*, *356*(11), 1140–1151. https://doi.org/10.1056/NEJMra063052

Nham, S.-U., Wilkemeyer, M. F., & Ledley, F. D. (1990). Structure of the human methylmalonyl-CoA mutase (MUT) locus. *Genomics*, *8*(4), 710–716. https://doi.org/10.1016/0888-7543(90)90259-W

Nielsen, M. J., Rasmussen, M. R., Andersen, C. B. F., Nexø, E., & Moestrup, S. K. (2012). Vitamin B12transport from food to the body's cells—A sophisticated, multistep pathway. *Nature Reviews Gastroenterology and Hepatology*, *9*(6), 345–354. https://doi.org/10.1038/nrgastro.2012.76

Nishikimi, T., Maeda, N., & Matsuoka, H. (2006). The role of natriuretic peptides in cardioprotection. *Cardiovascular Research*, *69*(2), 318–328. https://doi.org/10.1016/j.cardiores.2005.10.001

Nonaka, H., Tsujino, T., Watari, Y., Emoto, N., & Yokoyama, M. (2001). Taurine prevents the decrease in expression and secretion of extracellular superoxide dismutase induced by homocysteine: Amelioration of homocysteine-induced endoplasmic reticulum stress by taurine. *Circulation*, *104*(10), 1165–1170. https://doi.org/10.1161/hc3601.093976

Nozaki, S., Tanaka, T., Yamashita, S., Sohmiya, K., Yoshizumi, T., Okamoto, F., … Matsuzawa, Y. (1999). CD36 mediates long-chain fatty acid transport in human myocardium: Complete myocardial accumulation defect of radiolabeled long-chain fatty acid analog in subjects with CD36 deficiency. *Molecular and Cellular Biochemistry*, *192*(1), 129–135. https://doi.org/10.1023/A:1006816702425

Oka Shin-ichi, Zhai Peiyong, Yamamoto Takanobu, Ikeda Yoshiyuki, Byun Jaemin, Hsu Chiao-Po, & Sadoshima Junichi. (2015). Peroxisome Proliferator Activated Receptor-α Association With Silent Information Regulator 1 Suppresses Cardiac Fatty Acid Metabolism in the Failing Heart. *Circulation: Heart Failure*, *8*(6), 1123–1132. https://doi.org/10.1161/CIRCHEARTFAILURE.115.002216

O'Leary, F., & Samman, S. (2010). Vitamin B12 in health and disease. *Nutrients*, *2*(3), 299–316. https://doi.org/10.3390/nu2030299

Olivotto, I., Girolami, F., Nistri, S., Rossi, A., Rega, L., Garbini, F., … Yacoub, M. H. (2009). The many faces of hypertrophic cardiomyopathy: From developmental biology to clinical practice. *Journal of Cardiovascular Translational Research*, *2*(4), 349–367. https://doi.org/10.1007/s12265-009-9137-2

Olteanu, H., & Banerjee, R. (2001). Human Methionine Synthase Reductase, a Soluble P-450 Reductase-like Dual Flavoprotein, is Sufficient for NADPH-dependent Methionine Synthase Activation. *Journal of Biological Chemistry*, *276*(38), 35558–35563. https://doi.org/10.1074/jbc.M103707200

Ono, H., Nakamura, H., & Matsuzaki, M. (2010). A NADH dehydrogenase ubiquinone flavoprotein is decreased in patients with dilated cardiomyopathy. *Internal Medicine (Tokyo, Japan)*, *49*(19), 2039–2042.https://doi.org/10.2169/internalmedicine.49.3710

Ortega-Recalde, O., Fonseca, D. J., Patiño, L. C., Atuesta, J. J., Rivera-Nieto, C., Restrepo, C. M., … Laissue, P. (2013). A novel familial case of diffuse leukodystrophy related to NDUFV1 compound heterozygous mutations. *Mitochondrion*, *13*(6), 749–754. https://doi.org/10.1016/j.mito.2013.03.010

Osorio, J. C., Stanley, W. C., Linke, A., Castellari, M., Diep, Q. N., Panchal, A. R., … Recchia, F. A. (2002). Impaired Myocardial Fatty Acid Oxidation and Reduced Protein Expression of Retinoid X Receptor-α in Pacing-Induced Heart Failure. *Circulation*, *106*(5), 606–612. https://doi.org/10.1161/01.CIR.0000023531.22727.C1

Osorio Juan Carlos, Stanley William C., Linke Axel, Castellari Michele, Diep Quy N., Panchal Ashish R., … Recchia Fabio A. (2002). Impaired Myocardial Fatty Acid Oxidation and Reduced Protein Expression of Retinoid X Receptor-α in Pacing-Induced Heart Failure. *Circulation*, *106*(5), 606–612. https://doi.org/10.1161/01.CIR.0000023531.22727.C1

Outinen, P. A., Sood, S. K., Liaw, P. C., Sarge, K. D., Maeda, N., Hirsh, J.,Austin, R. C. (1998). Characterization of the stress-inducing effects of homocysteine. *Biochemical Journal*, *332*(Pt 1), 213–221.https://doi.org/10.1042/bj3320213

Outinen, P. A., Sood, S. K., Pfeifer, S. I., Pamidi, S., Podor, T. J., Li, J., Austin, R. C. (1999). Homocysteine-induced endoplasmic reticulum stress and growth arrest leads to specific changes in gene expression in human vascular endothelial cells. *Blood*, *94*(3), 959–967.https://doi.org/10.1182/blood.V94.3.959.415k20_959_967

Outteryck, O., de Sèze, J., Stojkovic, T., Cuisset, J.-M., Dobbelaere, D., Delalande, S., … Vermersch, P. (2012). Methionine synthase deficiency: A rare cause of adult-onset leukoencephalopathy. *Neurology*, *79*(4), 386–388. https://doi.org/10.1212/WNL.0b013e318260451b

Pacher, R., Bergler-Klein, J., Globits, S., Teufelsbauer, H., Schuller, M., Krauter, A., … Hartter, E. (1993). Plasma big endothelin-1 concentrations in congestive heart failure patients with or without systemic hypertension. *The American Journal of Cardiology*, *71*(15), 1293–1299. https://doi.org/10.1016/0002-9149(93)90543-L

Padmanabhan, N., Jia, D., Geary-Joo, C., Wu, X., Ferguson-Smith, A. C., Fung, E., … Watson, E. D. (2013). Mutation in Folate Metabolism Causes Epigenetic Instability and Transgenerational Effects On Development. *Cell*, *155*(1). https://doi.org/10.1016/j.cell.2013.09.002

Padovani, D., Labunska, T., Palfey, B. A., Ballou, D. P., & Banerjee, R. (2008). Adenosyltransferase tailors and delivers coenzyme B12. *Nature Chemical Biology*, *4*(3), 194–196. https://doi.org/10.1038/nchembio.67

Palm, F., Onozato, M. L., Luo, Z., & Wilcox, C. S. (2007). Dimethylarginine dimethylaminohydrolase (DDAH): Expression, regulation, and function in the cardiovascular and renal systems. *American Journal of Physiology-Heart and Circulatory Physiology*, *293*(6), H3227–H3245. https://doi.org/10.1152/ajpheart.00998.2007

Paolisso, G., Gambardella, A., Galzerano, D., D'Amore, A., Rubino, P., Verza, M., D'Onofrio, F. (1994). Total-body and myocardial substrate oxidation in congestive heart failure. *Metabolism: Clinical and Experimental*, *43*(2), 174–179. https://doi.org/10.1016/0026-0495(94)90241-0

Parmeggiani, A., & Bowman, R. H. (1963). Regulation of phosphofructokinase activity by citrate in normal and diabetic muscle. *Biochemical and Biophysical Research Communications*, *12*(4), 268–273. https://doi.org/10.1016/0006-291X(63)90294-8

Parodi-Rullán, R. M., Chapa-Dubocq, X. R., & Javadov, S. (2018). Acetylation of Mitochondrial Proteins in the Heart: The Role of SIRT3. *Frontiers in Physiology*, *9*. https://doi.org/10.3389/fphys.2018.01094

Pattison, J. S., Sanbe, A., Maloyan, A., Osinska, H., Klevitsky, R., & Robbins, J. (2008). Cardiomyocyte Expression of a Polyglutamine Pre-amyloid Oligomer Causes Heart Failure. *Circulation*, *117*(21), 2743–2751. https://doi.org/10.1161/CIRCULATIONAHA.107.750232

Pearse, S. G., & Cowie, M. R. (2014). Heart failure: Classification and pathophysiology. *Medicine*, *42*(10), 556–561. https://doi.org/10.1016/j.mpmed.2014.07.012

Peng, H., Man, C., Xu, J., & Fan, Y. (2015). Elevated homocysteine levels and risk of cardiovascular and all-cause mortality: A meta-analysis of prospective studies. *Journal of Zhejiang University. Science. B*, *16*(1), 78–86. https://doi.org/10.1631/jzus.B1400183

Pepper S. Gregory, L. W. R. (1999). Sympathetic Activation in Heart Failure and Its Treatment With β-Blockade | Cardiology | JAMA Internal Medicine | JAMA Network. Retrieved June 15, 2019, from https://jamanetwork.com/journals/jamainternalmedicine/article-abstract/484949

Perez, A. L., Grodin, J. L., Wu, Y., Hernandez, A. F., Butler, J., Metra, M., … Tang, W. H. W. (2016). Increased mortality with elevated plasma endothelin-1 in acute heart failure: An ASCEND-HF biomarker substudy. *European Journal of Heart Failure*, *18*(3), 290–297. https://doi.org/10.1002/ejhf.456

Pertea, M., Pertea, G. M., Antonescu, C. M., Chang, T.-C., Mendell, J. T., & Salzberg, S. L. (2015). StringTie enables improved reconstruction of a transcriptome from RNA-seq reads. *Nature Biotechnology*, *33*(3), 290–295. https://doi.org/10.1038/nbt.3122

Petropoulos, T. E., Ramirez, M. E., Granton, J., Licht, C., John, R., Moayedi, Y., … McQuillan, R. F. (2018). Renal thrombotic microangiopathy and pulmonary arterial hypertension in a patient with late-onset cobalamin C deficiency. *Clinical Kidney Journal*, *11*(3), 310–314. https://doi.org/10.1093/ckj/sfx119

Pinto, Y. M., Elliott, P. M., Arbustini, E., Adler, Y., Anastasakis, A., Böhm, M., … Charron, P. (2016). Proposal for a revised definition of dilated cardiomyopathy, hypokinetic non-dilated cardiomyopathy, and its implications for clinical practice: A position statement of the ESC working group on myocardial and pericardial diseases. *European Heart Journal*, *37*(23), 1850–1858. https://doi.org/10.1093/eurheartj/ehv727

Piquereau, J., Moulin, M., Zurlo, G., Mateo, P., Gressette, M., Paul, J.-L., … Garnier, A. (2017). Cobalamin and folate protect mitochondrial and contractile functions in a murine model of cardiac pressure overload. *Journal of Molecular and Cellular Cardiology*, *102*, 34–44. https://doi.org/10.1016/j.yjmcc.2016.11.010

Pitkanen, S., Merante, F., McLeod, D. R., Applegarth, D., Tong, T., & Robinson, B. H. (1996). Familial cardiomyopathy with cataracts and lactic acidosis: A defect in complex I (NADH-dehydrogenase) of the mitochondria respiratory chain. *Pediatric Research*, *39*(3), 513–521. https://doi.org/10.1203/00006450-199603000-00021

Plesa, M., Kim, J., Paquette, S. G., Gagnon, H., Ng-Thow-Hing, C., Gibbs, B. F., … Coulton, J. W. (2011). Interaction between MMACHC and MMADHC, two human proteins participating in intracellular vitamin B12 metabolism. *Molecular Genetics and Metabolism*, *102*(2), 139–148. https://doi.org/10.1016/j.ymgme.2010.10.011

Ponikowski, P., Anker, S. D., AlHabib, K. F., Cowie, M. R., Force, T. L., Hu, S., … Filippatos, G. (2014). Heart failure: Preventing disease and death worldwide. *ESC Heart Failure*, *1*(1), 4–25. https://doi.org/10.1002/ehf2.12005

Ponikowski, P., Voors, A. A., Anker, S. D., Bueno, H., Cleland, J. G. F., Coats, A. J. S., … Davies, C. (2016). 2016 ESC Guidelines for the diagnosis and treatment of acute and chronic heart failureThe Task Force for the diagnosis and treatment of acute and chronic heart failure of the European Society of Cardiology (ESC)Developed with the special contribution of the Heart Failure Association (HFA) of the ESC. *European Heart Journal*, *37*(27), 2129–2200. https://doi.org/10.1093/eurheartj/ehw128

Pousset, F., Isnard, R., Lechat, P., Kalotka, H., Carayon, A., Maistre, G., Komajda, M. (1997). Prognostic value of plasma endothelin-1 in patients with chronic heart failure. *European Heart Journal*, *18*(2), 254–258. https://doi.org/10.1093/oxfordjournals.eurheartj.a015228

Profitlich, L. E., Kirmse, B., Wasserstein, M. P., Diaz, G. A., & Srivastava, S. (2009). High prevalence of structural heart disease in children with cblC-type methylmalonic aciduria and homocystinuria. *Molecular Genetics and Metabolism*, *98*(4), 344–348. https://doi.org/10.1016/j.ymgme.2009.07.017

Pupavac, M., Garcia, M. A. M., Rosenblatt, D. S., & Jerome-Majewska, L. A. (2011). Expression of Mmachc and Mmadhc during mouse organogenesis. *Molecular Genetics and Metabolism*, *103*(4), 401–405. https://doi.org/10.1016/j.ymgme.2011.04.004

Qiu, A., Jansen, M., Sakaris, A., Min, S. H., Chattopadhyay, S., Tsai, E., … Goldman, I. D. (2006). Identification of an Intestinal Folate Transporter and the Molecular Basis for Hereditary Folate Malabsorption. *Cell*, *127*(5), 917–928. https://doi.org/10.1016/j.cell.2006.09.041

Quadros, E. V. (2010). Advances in the Understanding of Cobalamin Assimilation and Metabolism. *British Journal of Haematology*, *148*(2), 195–204. https://doi.org/10.1111/j.1365-2141.2009.07937.x

Quadros, E. V., & Sequeira, J. M. (2013). Cellular uptake of cobalamin: Transcobalamin and the TCblR/CD320 receptor. *Biochimie*, *95*(5), 1008–1018. https://doi.org/10.1016/j.biochi.2013.02.004

Quadros, E V, Regec, A. L., Khan, K. M. F., Quadros, E., & Rothenberg, S. P. (1999). Transcobalamin II synthesized in the intestinal villi facilitates transfer of cobalamin to the portal blood. *The American Journal of Physiology*, *277*(29), G161–G166. https://doi.org/10.1152/ajpgi.1999.277.1.G161

Quadros, Edward V, Nakayama, Y., & Sequeira, J. M. (2008). The protein and the gene encoding the receptor for the cellular uptake of transcobalamin bound cobalamin The Protein and the Gene Encoding the Receptor for the Cellular Uptake of E Mail: Edward.Quadros@downstate.edu. *October*, *113*(1), 186–193. https://doi.org/10.1182/blood-2008-05-158949

Quadros, Edward V., & Sequeira, J. M. (2013). Cellular uptake of cobalamin: Transcobalamin and the TCblR/CD320 receptor. *Biochimie*, Vol. 95, pp. 1008–1018. https://doi.org/10.1016/j.biochi.2013.02.004

Qureshi, A. A., Rosenblatt, D. S., & Cooperd, B. A. (1994). Inherited disorders of cobalamin metabolism. *Critical Reviews in Oncology/Hematology*, *7*. https://doi.org/10.1016/1040-8428(94)90022-1

Radziejewska, A., & Chmurzynska, A. (2019). Folate and choline absorption and uptake: Their role in fetal development. *Biochimie*, *158*, 10–19. https://doi.org/10.1016/j.biochi.2018.12.002

Raina, J. K., Sharma, M., Panjaliya, R. K., Bhagat, M., Sharma, R., Bakaya, A., & Kumar, P. (2016). Methylenetetrahydrofolate reductase C677T and methionine synthase A2756G

gene polymorphisms and associated risk of cardiovascular diseases: A study from Jammu region. *Indian Heart Journal*, *68*(3), 421–430. https://doi.org/10.1016/j.ihj.2016.02.009

Ram, R., Mickelsen, D. M., Theodoropoulos, C., & Blaxall, B. C. (2011). New approaches in small animal echocardiography: Imaging the sounds of silence. *American Journal of Physiology - Heart and Circulatory Physiology*, *301*(5), H1765–H1780. https://doi.org/10.1152/ajpheart.00559.2011

Randle, P. J., Garland, P. B., Hales, C. N., & Newsholme, E. A. (1963). THE GLUCOSE FATTY-ACID CYCLE ITS ROLE IN INSULIN SENSITIVITY AND THE METABOLIC DISTURBANCES OF DIABETES MELLITUS. *The Lancet*, *281*(7285), 785–789. https://doi.org/10.1016/S0140-6736(63)91500-9

Ranek, M. J., Stachowski, M. J., Kirk, J. A., & Willis, M. S. (2018). The role of heat shock proteins and co-chaperones in heart failure. *Philosophical Transactions of the Royal Society of London. Series B, Biological Sciences*, *373*(1738). https://doi.org/10.1098/rstb.2016.0530

Rardin, M. J., Newman, J. C., Held, J. M., Cusack, M. P., Sorensen, D. J., Li, B., … Gibson, B. W. (2013). Label-free quantitative proteomics of the lysine acetylome in mitochondria identifies substrates of SIRT3 in metabolic pathways. *Proceedings of the National Academy of Sciences of the United States of America*, *110*(16), 6601–6606. https://doi.org/10.1073/pnas.1302961110

Razeghi, P., Young, M. E., Alcorn, J. L., Moravec, C. S., Frazier, O. H., & Taegtmeyer, H. (2001). Metabolic gene expression in fetal and failing human heart. *Circulation*, *104*(24), 2923–2931.

Rébeillé, F., Ravanel, S., Jabrin, S., Douce, R., Storozhenko, S., & Straeten, D. V. D. (2006). Folates in plants: Biosynthesis, distribution, and enhancement. *Physiologia Plantarum*, *126*(3), 330–342. https://doi.org/10.1111/j.1399-3054.2006.00587.x

Refsum, H., Ueland, P. M., Nygård, O., & Vollset, S. E. (1998). Homocysteine and cardiovascular disease. *Annual Review of Medicine*, *49*, 31–62. https://doi.org/10.1146/annurev.med.49.1.31

Report of the Dietary Guidelines Advisory Committee on the Dietary Guidelines for Americans, 2010: (566752010-001) [Data set]. (2010). [Data set]. https://doi.org/10.1037/e566752010-001

Riehle Christian, Wende Adam R., Zaha Vlad G., Pires Karla Maria, Wayment Benjamin, Olsen Curtis, Abel E. Dale. (2011). PGC-1β Deficiency Accelerates the Transition to Heart Failure in Pressure Overload Hypertrophy. *Circulation Research*, *109*(7), 783–793. https://doi.org/10.1161/CIRCRESAHA.111.243964

Ritchie, M. E., Phipson, B., Wu, D., Hu, Y., Law, C. W., Shi, W., & Smyth, G. K. (2015). Limma powers differential expression analyses for RNA-sequencing and microarray studies. *Nucleic Acids Research*, *43*(7), e47. https://doi.org/10.1093/nar/gkv007

Robinson, B. H. (1998). Human Complex I deficiency: Clinical spectrum and involvement of oxygen free radicals in the pathogenicity of the defect. *Biochimica et Biophysica Acta (BBA) - Bioenergetics*, *1364*(2), 271–286. https://doi.org/10.1016/S0005-2728(98)00033-4

Robinson, M. D., & Oshlack, A. (2010). A scaling normalization method for differential expression analysis of RNA-seq data. *Genome Biology*, *11*(3), R25. https://doi.org/10.1186/gb-2010-11-3-r25

Rodeheffer, R. J., Lerman, A., Heublein, D. M., & Burnett, J. C. (1992). Increased Plasma Concentrations of Endothelin in Congestive Heart Failure in Humans. *Mayo Clinic Proceedings*, *67*(8), 719–724. https://doi.org/10.1016/S0025-6196(12)60795-2

Rodríguez-Iturbe, B., & Johnson, R. (2018). Heat shock proteins and cardiovascular disease. *Physiology International*, *105*(1), 19–37. https://doi.org/10.1556/2060.105.2018.1.4

Roselló-Lletí, E., Tarazón, E., Barderas, M. G., Ortega, A., Molina-Navarro, M. M., Martínez, A., … Rivera, M. (2015). ATP synthase subunit alpha and LV mass in ischaemic human hearts. *Journal of Cellular and Molecular Medicine*, *19*(2), 442–451. https://doi.org/10.1111/jcmm.12477

Rosenblatt, D. S., Aspler, A. L., Shevell, M. I., Pletcher, B. A., Fenton, W. A., & Seashore, M. R. (1997). Clinical heterogeneity and prognosis in combined methylmalonic aciduria and homocystinuria (cblC). *Journal of Inherited Metabolic Disease*, *20*(4), 528–538.https://doi.org/10.1023/a:1005353530303

Rosenblatt, D. S., Cooper, B. A., Pottier, A., Lue-Shing, H., Matiaszuk, N., & Grauer, K. (1984). Altered vitamin B12 metabolism in fibroblasts from a patient with megaloblastic anemia and homocystinuria due to a new defect in methionine biosynthesis. *The Journal of Clinical Investigation*, *74*(6), 2149–2156. https://doi.org/10.1172/JCI111641

Ruiz-Mercado, M., Vargas, M. T., de Soto, I. P., Pecellín, C. D., Sánchez, M. C., Delgado, M. A. B., Díaz-Aguado, A. H. (2016). Methionine synthase reductase deficiency (CblE): A report of two patients and a novel mutation. *Hematology (Amsterdam, Netherlands)*, *21*(3), 193–197. https://doi.org/10.1179/1607845415Y.0000000017

Ruma V Banerjee, Verna, F., David P, B., & Rowena, M. G. (1990). Participation of Cob(1)alamin in the Reaction Catalyzed by Methionine Synthase from. *Biochemistry*, *29*, 11101_11109. https://doi.org/10.1021/bi00502a013

Rutsch, F., Gailus, S., Miousse, I. R., Suormala, T., Sagné, C., Toliat, M. R., Nürnberg, P. (2009). Identification of a putative lysosomal cobalamin exporter altered in the cblF defect of vitamin B12metabolism. *Nature Genetics*, *41*(2), 234–239. https://doi.org/10.1038/ng.294

Sack, M. N., Rader, T. A., Park, S., Bastin, J., McCune, S. A., & Kelly, D. P. (1996). Fatty acid oxidation enzyme gene expression is downregulated in the failing heart. *Circulation*, *94*(11), 2837–2842. https://doi.org/10.1161/01.cir.94.11.2837

Safi, J., Joyeux, L., & Chalouhi, G. E. (2012). Periconceptional Folate Deficiency and Implications in Neural Tube Defects [Research article]. https://doi.org/10.1155/2012/295083

Salbaum, J. M., & Kappen, C. (2012). Genetic and Epigenomic Footprints of Folate. In C. Bouchard & J. M. Ordovas (Eds.), *Progress in Molecular Biology and Translational Science* (pp. 129–158). https://doi.org/10.1016/B978-0-12-398397-8.00006-X

Scaglione, F., & Panzavolta, G. (2014a). Folate, folic acid and 5-methyltetrahydrofolate are not the same thing. *Xenobiotica; the Fate of Foreign Compounds in Biological Systems*, *44*(5), 480–488. https://doi.org/10.3109/00498254.2013.845705

Scaglione, F., & Panzavolta, G. (2014b). Folate, folic acid and 5-methyltetrahydrofolate are not the same thing. *Xenobiotica*, *44*(5), 480–488. https://doi.org/10.3109/00498254.2013.845705

Schiff, M., Benoist, J.-F., Tilea, B., Royer, N., Giraudier, S., & Ogier de Baulny, H. (2011). Isolated remethylation disorders: Do our treatments benefit patients? *Journal of Inherited Metabolic Disease*, *34*(1), 137–145. https://doi.org/10.1007/s10545-010-9120-8

Schneider, E., & Ryan, T. J. (2006). Gamma-glutamyl hydrolase and drug resistance. *Clinica Chimica Acta*, *374*(1), 25–32. https://doi.org/10.1016/j.cca.2006.05.044

Schröder, M., & Kaufman, R. J. (2005). ER stress and the unfolded protein response. *Mutation Research*, *569*(1–2), 29–63. https://doi.org/10.1016/j.mrfmmm.2004.06.056

Schwahn, B. C., Laryea, M. D., Chen, Z., Melnyk, S., Pogribny, I., Garrow, T., Rozen, R. (2004). Betaine rescue of an animal model with methylenetetrahydrofolate reductase deficiency. *Biochemical Journal*, *382*(Pt 3), 831–840. https://doi.org/10.1042/BJ20030822

Schwer, B., & Verdin, E. (2008). Conserved Metabolic Regulatory Functions of Sirtuins. *Cell Metabolism*, *7*(2), 104–112. https://doi.org/10.1016/j.cmet.2007.11.006

Sciarretta, S., Paneni, F., Palano, F., Chin, D., Tocci, G., Rubattu, S., & Volpe, M. (2009). Role of the renin–angiotensin–aldosterone system and inflammatory processes in the development and progression of diastolic dysfunction. *Clinical Science*, *116*(6), 467–477. https://doi.org/10.1042/CS20080390

Seferović, P. M., Polovina, M., Bauersachs, J., Arad, M., Gal, T. B., Lund, L. H., Tschöpe, C. (2019). Heart failure in cardiomyopathies: A position paper from the Heart Failure Association of the European Society of Cardiology. *European Journal of Heart Failure*, *21*(5), 553–576. https://doi.org/10.1002/ejhf.1461

Senior, R. M., Griffin, G. L., Fliszar, C. J., Shapiro, S. D., Goldberg, G. I., & Welgus, H. G. (1991). Human 92- and 72-kilodalton type IV collagenases are elastases. *Journal of Biological Chemistry*, *266*(12), 7870–7875.

Sharma, G. S., Kumar, T., Dar, T. A., & Singh, L. R. (2015). Protein N-homocysteinylation: From cellular toxicity to neurodegeneration. *Biochimica Et Biophysica Acta*, *1850*(11), 2239–2245. https://doi.org/10.1016/j.bbagen.2015.08.013

Sharma, G. S., Kumar, T., & Singh, L. R. (2014). N-Homocysteinylation Induces Different Structural and Functional Consequences on Acidic and Basic Proteins. *PLOS ONE*, *9*(12), e116386. https://doi.org/10.1371/journal.pone.0116386

Shawky, R. M., Ramy, A. R. M., El-Din, S. M. N., Abd Elmonem, S. M., & Abd Elmonem, M. A. (2018). Abnormal maternal biomarkers of homocysteine and methionine metabolism and the risk of congenital heart defects. *Egyptian Journal of Medical Human Genetics*, *19*(1), 7–12. https://doi.org/10.1016/j.ejmhg.2017.08.004

Shenoy, V., Mehendale, V., Prabhu, K., Shetty, R., & Rao, P. (2014). Correlation of Serum Homocysteine Levels with the Severity of Coronary Artery Disease. *Indian Journal of Clinical Biochemistry*, *29*(3), 339–344. https://doi.org/10.1007/s12291-013-0373-5

Sihag, S., Cresci, S., Li, A. Y., Sucharov, C. C., & Lehman, J. J. (2009). PGC-1α and ERRα target gene downregulation is a signature of the failing human heart. *Journal of Molecular and Cellular Cardiology*, *46*(2), 201–212. https://doi.org/10.1016/j.yjmcc.2008.10.025

Škovierová, H., Vidomanová, E., Mahmood, S., Sopková, J., Drgová, A., Červeňová, T., Lehotský, J. (2016). The Molecular and Cellular Effect of Homocysteine Metabolism Imbalance on Human Health. *International Journal of Molecular Sciences*, *17*(10). https://doi.org/10.3390/ijms17101733

Smith Nicholas L., Felix Janine F., Morrison Alanna C., Demissie Serkalem, Glazer Nicole L., Loehr Laura R., Vasan Ramachandran S. (2010). Association of Genome-Wide Variation With the Risk of Incident Heart Failure in Adults of European and African Ancestry. *Circulation: Cardiovascular Genetics*, *3*(3), 256–266. https://doi.org/10.1161/CIRCGENETICS.109.895763

Smulders, Y. M., & Stehouwer, C. D. A. (2005). Folate metabolism and cardiovascular disease. *Seminars in Vascular Medicine*, *5*(2), 87–97. https://doi.org/10.1055/s-2005-872395

Soualmia, H., Barthélemy, C., Masson, F., Maistre, G., Eurin, J., & Carayon, A. (1997). Angiotensin II-induced phosphoinositide production and atrial natriuretic peptide release in rat atrial tissue. *Journal of Cardiovascular Pharmacology*, *29*(5), 605–611. https://doi.org/10.1097/00005344-199705000-00007

Srivastava, A., Srivastava, K. R., Hebbar, M., Galada, C., Kadavigrere, R., Su, F., … Bielas, S. L. (2018). Genetic diversity of NDUFV1-dependent mitochondrial complex I deficiency. *European Journal of Human Genetics: EJHG*, *26*(11), 1582–1587. https://doi.org/10.1038/s41431-018-0209-0

Stabler, S. P., Korson, M., Jethva, R., Allen, R. H., Kraus, J. P., Spector, E. B., … Mudd, S. H. (2013). Metabolic Profiling of Total Homocysteine and Related Compounds in Hyperhomocysteinemia: Utility and Limitations in Diagnosing the Cause of Puzzling Thrombophilia in a Family. *JIMD Reports*, *11*, 149–163. https://doi.org/10.1007/8904_2013_235

Stanley, W. C., Morgan, E. E., Huang, H., McElfresh, T. A., Sterk, J. P., Okere, I. C., … Lopaschuk, G. D. (2005). Malonyl-CoA decarboxylase inhibition suppresses fatty acid oxidation and reduces lactate production during demand-induced ischemia. *American Journal of Physiology. Heart and Circulatory Physiology*, *289*(6), H2304-2309. https://doi.org/10.1152/ajpheart.00599.2005

Stasch, J. P., Hirth-Dietrich, C., Kazda, S., & Neuser, D. (1989). Endothelin stimulates release of atrial natriuretic peptides in vitro and in vivo. *Life Sciences*, *45*(10), 869–875. https://doi.org/10.1016/0024-3205(89)90200-2

Steffensen, B., Wallon, U. M., & Overall, C. M. (1995). Extracellular matrix binding properties of recombinant fibronectin type II-like modules of human 72-kDa gelatinase/type IV collagenase. High affinity binding to native type I collagen but not native type IV collagen. *Journal of Biological Chemistry*, *270*(19), 11555–11566. https://doi.org/10.1074/jbc.270.19.11555

Stipanuk, M. H., Dominy, J. E., Lee, J.-I., & Coloso, R. M. (2006). Mammalian Cysteine Metabolism: New Insights into Regulation of Cysteine Metabolism. *The Journal of Nutrition*, *136*(6), 1652S-1659S. https://doi.org/10.1093/jn/136.6.1652S

Stühlinger, M. C., Tsao, P. S., Her, J. H., Kimoto, M., Balint, R. F., & Cooke, J. P. (2001). Homocysteine impairs the nitric oxide synthase pathway: Role of asymmetric dimethylarginine. *Circulation*, *104*(21), 2569–2575. https://doi.org/10.1161/hc4601.098514

Sudoh, T., Maekawa, K., Kojima, M., Minamino, N., Kangawa, K., & Matsuo, H. (1989). Cloning and sequence analysis of cDNA encoding a precursor for human brain natriuretic peptide. *Biochemical and Biophysical Research Communications*, *159*(3), 1427–1434. https://doi.org/10.1016/0006-291X(89)92269-9

Sun, W., Liu, C., Chen, Q., Liu, N., Yan, Y., & Liu, B. (2018). SIRT3: A New Regulator of Cardiovascular Diseases [Research article]. https://doi.org/10.1155/2018/7293861

Sundaresan, N. R., Gupta, M., Kim, G., Rajamohan, S. B., Isbatan, A., & Gupta, M. P. (2009). Sirt3 blocks the cardiac hypertrophic response by augmenting Foxo3a-dependent antioxidant defense mechanisms in mice. *The Journal of Clinical Investigation*, *119*(9), 2758–2771. https://doi.org/10.1172/JCI39162

Sunden, S. L., Renduchintala, M. S., Park, E. I., Miklasz, S. D., & Garrow, T. A. (1997). Betaine-homocysteine methyltransferase expression in porcine and human tissues and

chromosomal localization of the human gene. *Archives of Biochemistry and Biophysics*, *345*(1), 171–174. https://doi.org/10.1006/abbi.1997.0246

Sung, M. M., Byrne, N. J., Kim, T. T., Levasseur, J., Masson, G., Boisvenue, J. J., … Dyck, J. R. B. (2017). Cardiomyocyte-specific ablation of CD36 accelerates the progression from compensated cardiac hypertrophy to heart failure. *American Journal of Physiology. Heart and Circulatory Physiology*, *312*(3), H552–H560. https://doi.org/10.1152/ajpheart.00626.2016

Sung, M. M., Das, S. K., Levasseur, J., Byrne, N. J., Fung, D., Kim, T. T., … Dyck, J. R. B. (2015). Resveratrol Treatment of Mice With Pressure-Overload–Induced Heart Failure Improves Diastolic Function and Cardiac Energy Metabolism. *Circulation: Heart Failure*, *8*(1), 128–137. https://doi.org/10.1161/CIRCHEARTFAILURE.114.001677

Suzuki, Y. J. (2011). Cell signalling pathways for the regulation of GATA4 transcription factor: Implications for cell growth and apoptosis. *Cellular Signalling*, *23*(7), 1094–1099. https://doi.org/10.1016/j.cellsig.2011.02.007

Swanson, D. A., Liu, M.-L., Baker, P. J., Garrett, L., Stitzel, M., Wu, J., … Brody, L. C. (2001). Targeted Disruption of the Methionine Synthase Gene in Mice. *Molecular and Cellular Biology*, *21*(4), 1058–1065. https://doi.org/10.1128/MCB.21.4.1058-1065.2001

Takahashi-Iñiguez, T., García-Hernandez, E., Arreguín-Espinosa, R., & Flores, M. E. (2012). Role of vitamin B12 on methylmalonyl-CoA mutase activity. *Journal of Zhejiang University SCIENCE B*, *13*(6), 423–437. https://doi.org/10.1631/jzus.B1100329

Tao, R., Coleman, M. C., Pennington, J. D., Ozden, O., Park, S.-H., Jiang, H., … Gius, D. (2010). Sirt3-mediated deacetylation of evolutionarily conserved lysine 122 regulates MnSOD activity in response to stress. *Molecular Cell*, *40*(6), 893–904. https://doi.org/10.1016/j.molcel.2010.12.013

Task, A., Members, F., Mcmurray, J. J. V, Uk, C., Germany, S. D. A., Auricchio, A., … Popescu, B. A. (2012). *ESC GUIDELINES ESC Guidelines for the diagnosis and treatment of acute and chronic heart failure 2012 The Task Force for the Diagnosis and Treatment of Acute and Chronic Heart Failure 2012 of the European Society of Cardiology. Developed in collaboration*. 1787–1847. https://doi.org/10.1093/eurheartj/ehs104

Tayal, U., Prasad, S., & Cook, S. A. (2017). Genetics and genomics of dilated cardiomyopathy and systolic heart failure. *Genome Medicine*, *9*(1), 20. https://doi.org/10.1186/s13073-017-0410-8

Télot, L., Rousseau, E., Lesuisse, E., Garcia, C., Morlet, B., Léger, T., … Serre, V. (2018). Quantitative proteomics in Friedreich's ataxia B-lymphocytes: A valuable approach to decipher the biochemical events responsible for pathogenesis. *Biochimica et Biophysica Acta (BBA) - Molecular Basis of Disease*, *1864*(4, Part A), 997–1009. https://doi.org/10.1016/j.bbadis.2018.01.010

Temple, M. E., Luzier, A. B., & Kazierad, D. J. (2000). Homocysteine as a Risk Factor for Atherosclerosis. *Annals of Pharmacotherapy*, *34*(1), 57–65. https://doi.org/10.1345/aph.18457

Teng, Y.-W., Mehedint, M. G., Garrow, T. A., & Zeisel, S. H. (2011). Deletion of Betaine-Homocysteine S-Methyltransferase in Mice Perturbs Choline and 1-Carbon Metabolism, Resulting in Fatty Liver and Hepatocellular Carcinomas. *The Journal of Biological Chemistry*, *286*(42), 36258–36267. https://doi.org/10.1074/jbc.M111.265348

Tousoulis, D., Kampoli, A.-M., Tentolouris, C., Papageorgiou, N., & Stefanadis, C. (2012). The role of nitric oxide on endothelial function. *Current Vascular Pharmacology*, *10*(1), 4–18.https://doi.org/10.2174/157016112798829760

Triposkiadis, F., Karayannis, G., Giamouzis, G., Skoularigis, J., Louridas, G., & Butler, J. (2009). The Sympathetic Nervous System in Heart Failure: Physiology, Pathophysiology, and Clinical Implications. *Journal of the American College of Cardiology*, *54*(19), 1747–1762. https://doi.org/10.1016/j.jacc.2009.05.015

Tuchman, M., Kelly, P., Watkins, D., & Rosenblatt, D. S. (1988). Vitamin B12-responsive megaloblastic anemia, homocystinuria, and transient methylmalonic aciduria in cb1E disease. *The Journal of Pediatrics*, *113*(6), 1052–1056. https://doi.org/10.1016/s0022-3476(88)80582-1

Turner, M. A., Yang, X., Yin, D., Kuczera, K., Borchardt, R. T., & Howell, P. L. (2000). Structure and function of S-adenosylhomocysteine hydrolase. *Cell Biochemistry and Biophysics*, *33*(2), 101–125. https://doi.org/10.1385/CBB:33:2:101

Tuunanen, H., Engblom, E., Naum, A., Scheinin, M., Någren, K., Airaksinen, J., Knuuti, J. (2006). Decreased Myocardial Free Fatty Acid Uptake in Patients With Idiopathic Dilated Cardiomyopathy: Evidence of Relationship With Insulin Resistance and Left Ventricular Dysfunction. *Journal of Cardiac Failure*, *12*(8), 644–652. https://doi.org/10.1016/j.cardfail.2006.06.005

Tuunanen, H., Ukkonen, H., & Knuuti, J. (2008). Myocardial fatty acid metabolism and cardiac performance in heart failure. *Current Cardiology Reports*, *10*(2), 142–148. https://doi.org/10.1007/s11886-008-0024-2

Tyagi, N., Sedoris, K. C., Steed, M., Ovechkin, A. V., Moshal, K. S., & Tyagi, S. C. (2005). Mechanisms of homocysteine-induced oxidative stress. *American Journal of Physiology-Heart and Circulatory Physiology*, *289*(6), H2649–H2656. https://doi.org/10.1152/ajpheart.00548.2005

Umbarawan, Y., Syamsunarno, M. R. A. A., Koitabashi, N., Obinata, H., Yamaguchi, A., Hanaoka, H., Iso, T. (2018a). Myocardial fatty acid uptake through CD36 is

indispensable for sufficient bioenergetic metabolism to prevent progression of pressure overload-induced heart failure. *Scientific Reports*, *8*. https://doi.org/10.1038/s41598-018-30616-1

Umbarawan, Y., Syamsunarno, M. R. A. A., Koitabashi, N., Obinata, H., Yamaguchi, A., Hanaoka, H., Iso, T. (2018b). Myocardial fatty acid uptake through CD36 is indispensable for sufficient bioenergetic metabolism to prevent progression of pressure overload-induced heart failure. *Scientific Reports*, *8*(1), 12035. https://doi.org/10.1038/s41598-018-30616-1

van der Vusse, G. J., van Bilsen, M., & Glatz, J. F. C. (2000). Cardiac fatty acid uptake and transport in health and disease. *Cardiovascular Research*, *45*(2), 279–293. https://doi.org/10.1016/S0008-6363(99)00263-1

van Riet, E. E. S., Hoes, A. W., Wagenaar, K. P., Limburg, A., Landman, M. A. J., & Rutten, F. H. (2016). Epidemiology of heart failure: The prevalence of heart failure and ventricular dysfunction in older adults over time. A systematic review. *European Journal of Heart Failure*, *18*(3), 242–252. https://doi.org/10.1002/ejhf.483

Vasan, R. S., Beiser, A., D'Agostino, R. B., Levy, D., Selhub, J., Jacques, P. F., … Wilson, P. W. F. (2003). Plasma homocysteine and risk for congestive heart failure in adults without prior myocardial infarction. *JAMA*, *289*(10), 1251–1257. https://doi.org/10.1001/jama.289.10.1251

Velagaleti, R., & Vasan, R. S. (2008). *Heart Failure in the 21 st Century: Is it a Coronary Artery Disease*. *25*(4), 1–13. https://doi.org/10.1016/j.ccl.2007.08.010

Ventura-Clapier, R., Garnier, A., Veksler, V., & Joubert, F. (2011). Bioenergetics of the failing heart. *Biochimica et Biophysica Acta (BBA) - Molecular Cell Research*, *1813*(7), 1360–1372. https://doi.org/10.1016/j.bbamcr.2010.09.006

Verrecchia, F., & Mauviel, A. (2002). Transforming Growth Factor-β Signaling Through the Smad Pathway: Role in Extracellular Matrix Gene Expression and Regulation. *Journal of Investigative Dermatology*, *118*(2), 211–215. https://doi.org/10.1046/j.1523-1747.2002.01641.x

Vilaseca, M. A., Vilarinho, L., Zavadakova, P., Vela, E., Cleto, E., Pineda, M., Kozich, V. (2003). CblE type of homocystinuria: Mild clinical phenotype in two patients homozygous for a novel mutation in the MTRR gene. *Journal of Inherited Metabolic Disease*, *26*(4), 361–369. https://doi.org/10.1023/a:1025159103257

Villard, E., Perret, C., Gary, F., Proust, C., Dilanian, G., Hengstenberg, C., Cambien, F. (2011). A genome-wide association study identifies two loci associated with heart failure due to dilated cardiomyopathy. *European Heart Journal*, *32*(9), 1065–1076. https://doi.org/10.1093/eurheartj/ehr105

Vincent, J.-L. (2008). Understanding cardiac output. *Critical Care*, *12*(4), 174. https://doi.org/10.1186/cc6975

Visentin, M., Diop-Bove, N., Zhao, R., & Goldman, I. D. (2014). The Intestinal Absorption of Folates. *Annual Review of Physiology*, *76*(1), 251–274. https://doi.org/10.1146/annurev-physiol-020911-153251

Volpe, M., Carnovali, M., & Mastromarino, V. (2016a). The natriuretic peptides system in the pathophysiology of heart failure: From molecular basis to treatment. *Clinical Science*, *130*(2), 57–77. https://doi.org/10.1042/CS20150469

Volpe, M., Carnovali, M., & Mastromarino, V. (2016b). The natriuretic peptides system in the pathophysiology of heart failure: From molecular basis to treatment. *Clinical Science (London, England : 1979)*, *130*(2), 57–77. https://doi.org/10.1042/CS20150469

Wald, D. S., Law, M., & Morris, J. K. (2002). Homocysteine and cardiovascular disease: Evidence on causality from a meta-analysis. *BMJ : British Medical Journal*, *325*(7374), 1202. https://doi.org/10.1136/bmj.325.7374.1202

Wang, G.-Y., Bergman, M. R., Nguyen, A. P., Turcato, S., Swigart, P. M., Rodrigo, M. C., … Baker, A. J. (2006). Cardiac transgenic matrix metalloproteinase-2 expression directly induces impaired contractility. *Cardiovascular Research*, *69*(3), 688–696. https://doi.org/10.1016/j.cardiores.2005.08.023

Wang, L., Jhee, K.-H., Hua, X., DiBello, P. M., Jacobsen, D. W., & Kruger, W. D. (2004). Modulation of cystathionine beta-synthase level regulates total serum homocysteine in mice. *Circulation Research*, *94*(10), 1318–1324. https://doi.org/10.1161/01.RES.0000129182.46440.4a

Wang, X., Wei, H., Tian, Y., Wu, Y., & Luo, L. (2018). Genetic variation in folate metabolism is associated with the risk of conotruncal heart defects in a Chinese population. *BMC Pediatrics*, *18*(1), 287. https://doi.org/10.1186/s12887-018-1266-9

Wang, X.-C., Sun, W.-T., Yu, C.-M., Pun, S.-H., Underwood, M. J., He, G.-W., & Yang, Q. (2015). ER stress mediates homocysteine-induced endothelial dysfunction: Modulation of IKCa and SKCa channels. *Atherosclerosis*, *242*(1), 191–198. https://doi.org/10.1016/j.atherosclerosis.2015.07.021

Wang, Y. H., Yan, Q. H., Xu, J. Y., Li, X. J., & Cheng, M. N. (2019). High Prevalence and Factors Contributing to Hyperhomocysteinemia, Folate Deficiency, and Vitamin B12 Deficiency among Healthy Adults in Shanghai, China. *Biomedical and Environmental Sciences: BES*, *32*(1), 63–67. https://doi.org/10.3967/bes2019.010

Watanabe, M., Osada, J., Aratani, Y., Kluckman, K., Reddick, R., Malinow, M. R., & Maeda, N. (1995). Mice deficient in cystathionine beta-synthase: Animal models for mild and

severe homocyst(e)inemia. *Proceedings of the National Academy of Sciences of the United States of America*, *92*(5), 1585–1589. https://doi.org/10.1073/pnas.92.5.1585

Watkins, D., & Rosenblatt, D. S. (1986). Failure of lysosomal release of vitamin B12: A new complementation group causing methylmalonic aciduria (cblF). *American Journal of Human Genetics*, *39*(3), 404–408.

Watkins, D, & Rosenblatt, D. S. (1989). Functional methionine synthase deficiency (cblE and cblG): Clinical and biochemical heterogeneity. *American Journal of Medical Genetics*, *34*(3), 427–434. https://doi.org/10.1002/ajmg.1320340320

Watkins, D., & Rosenblatt, D. S. (1989a). Functional methionine synthase deficiency (cblE and cblG): Clinical and biochemical heterogeneity. *American Journal of Medical Genetics*, *34*(3), 427–434. https://doi.org/10.1002/ajmg.1320340320

Watkins, D., & Rosenblatt, D. S. (1989b). Functional methionine synthase deficiency (cblE and cblG): Clinical and biochemical heterogeneity. *American Journal of Medical Genetics*, *34*(3), 427–434. https://doi.org/10.1002/ajmg.1320340320

Watkins, David, & Rosenblatt, D. S. (2011a). Inborn errors of cobalamin absorption and metabolism. *American Journal of Medical Genetics. Part C, Seminars in Medical Genetics*, *157C*(1), 33–44. https://doi.org/10.1002/ajmg.c.30288

Watkins, David, & Rosenblatt, D. S. (2011b). *Inborn Errors of Cobalamin Absorption and Metabolism*. *44*, 33–44. https://doi.org/10.1002/ajmg.c.30288

Watkins, David, & Rosenblatt, D. S. (2016). Lessons in biology from patients with inherited disorders of vitamin B12 and folate metabolism. *Biochimie*, *126*, 3–5. https://doi.org/10.1016/j.biochi.2016.05.001

Watkins, David, Ru, M., Hwang, H.-Y., Kim, C. D., Murray, A., Philip, N. S., … Rosenblatt, D. S. (2002a). Hyperhomocysteinemia due to methionine synthase deficiency, cblG: Structure of the MTR gene, genotype diversity, and recognition of a common

mutation, P1173L. *American Journal of Human Genetics*, *71*(1), 143–153. https://doi.org/10.1086/341354

Watkins, David, Ru, M., Hwang, H.-Y., Kim, C. D., Murray, A., Philip, N. S., … Rosenblatt, D. S. (2002b). Hyperhomocysteinemia Due to Methionine Synthase Deficiency, cblG: Structure of the MTR Gene, Genotype Diversity, and Recognition of a Common Mutation, P1173L. *American Journal of Human Genetics*, *71*(1), 143–153. https://doi.org/10.1086/341354

Wehrens, X. H. T., Lehnart, S. E., Reiken, S. R., & Marks, A. R. (2004). Ca2+/calmodulin-dependent protein kinase II phosphorylation regulates the cardiac ryanodine receptor. *Circulation Research*, *94*(6), e61-70. https://doi.org/10.1161/01.RES.0000125626.33738.E2

Wei, C. M., Lerman, A., Rodeheffer, R. J., McGregor, C. G., Brandt, R. R., Wright, S., … Burnett, J. C. (1994). Endothelin in human congestive heart failure. *Circulation*, *89*(4), 1580–1586. https://doi.org/10.1161/01.CIR.89.4.1580

Wei, L., Zhou, Y., Dai, Q., Qiao, C., Zhao, L., Hui, H., … Guo, Q.-L. (2013). Oroxylin A induces dissociation of hexokinase II from the mitochondria and inhibits glycolysis by SIRT3-mediated deacetylation of cyclophilin D in breast carcinoma. *Cell Death & Disease*, *4*(4), e601–e601. https://doi.org/10.1038/cddis.2013.131

Weinberger, M. H., Aoi, W., & Henry, D. P. (1975). Direct effect of beta-adrenergic stimulation on renin release by the rat kidney slice in vitro. *Circulation Research*, *37*(3), 318–324. https://doi.org/10.1161/01.RES.37.3.318

Wende, A. R., Brahma, M. K., McGinnis, G. R., & Young, M. E. (2017). Metabolic Origins of Heart Failure. *JACC: Basic to Translational Science*, *2*(3), 297–310. https://doi.org/10.1016/j.jacbts.2016.11.009

Wenstrom, K. D., Johanning, G., Johnston, K. E., & Dubard, M. (2001). Association of the C677T methylenetetrahydrofolate reductase mutation and elevated homocysteine levels with congenital cardiac malformations. *American Journal of Obstetrics and Gynecology*, *184*(5), 806–812; discussion 812-7. https://doi.org/10.1067/mob.2001.113845

Wolthers, K. R., Toogood, H. S., Jowitt, T. A., Marshall, K. R., Leys, D., & Scrutton, N. S. (2007). Crystal structure and solution characterization of the activation domain of human methionine synthase. *The FEBS Journal*, *274*(3), 738–750. https://doi.org/10.1111/j.1742-4658.2006.05618.x

Wu, Q.-Q., Xiao, Y., Yuan, Y., Ma, Z.-G., Liao, H.-H., Liu, C., … Tang, Q.-Z. (2017). Mechanisms contributing to cardiac remodelling. *Clinical Science (London, England: 1979)*, *131*(18), 2319–2345. https://doi.org/10.1042/CS20171167

Xiao, Y., Su, X., Huang, W., Zhang, J., Peng, C., Huang, H., … Ling, W. (2015). Role of S-adenosylhomocysteine in cardiovascular disease and its potential epigenetic mechanism. *The International Journal of Biochemistry & Cell Biology*, *67*, 158–166. https://doi.org/10.1016/j.biocel.2015.06.015

Xiong, Y., & Guan, K.-L. (2012). Mechanistic insights into the regulation of metabolic enzymes by acetylation. *J Cell Biol*, *198*(2), 155–164. https://doi.org/10.1083/jcb.201202056

Xu, J., Carretero, O. A., Liao, T.-D., Peng, H., Shesely, E. G., Xu, J., … Yang, X.-P. (2010). Local angiotensin II aggravates cardiac remodeling in hypertension. *American Journal of Physiology. Heart and Circulatory Physiology*, *299*(5), H1328-1338. https://doi.org/10.1152/ajpheart.00538.2010

Yahaya, B. H., McLachlan, G., Vrettou, C., & Collie, D. (2011). *METHOD Optimising the quality and integrity of RNA samples from bronchial airway tissues*.

Yakub, M., Moti, N., Parveen, S., Chaudhry, B., Azam, I., & Iqbal, M. P. (2012). Polymorphisms in MTHFR, MS and CBS genes and homocysteine levels in a Pakistani population. *PloS One*, *7*(3), e33222. https://doi.org/10.1371/journal.pone.0033222

Yamada, K., Tobimatsu, T., & Toraya, T. (1998). Cloning, sequencing, and heterologous expression of rat methionine synthase cDNA. *Bioscience, Biotechnology, and Biochemistry*, *62*(11), 2155–2160. https://doi.org/10.1271/bbb.62.2155

Yamada, Kazuhiro, Gherasim, C., Banerjee, R., & Koutmos, M. (2015). Structure of human B12trafficking protein CblD reveals molecular mimicry and identifies a new subfamily of nitro-FMN reductases. *Journal of Biological Chemistry*, *290*(49), 29155–29166. https://doi.org/10.1074/jbc.M115.682435

Yamada, Kazuhiro, & Koutmos, M. (2018). The folate-binding module of *Thermus thermophilus* cobalamin-dependent methionine synthase displays a distinct variation of the classical TIM barrel: A TIM barrel with a `twist'. *Acta Crystallographica Section D Structural Biology*, *74*(1), 41–51. https://doi.org/10.1107/S2059798317018290

Yancy, C. W., Jessup, M., Bozkurt, B., Butler, J., Casey, D. E., Drazner, M. H., … Wilkoff, B. L. (2013). 2013 ACCF/AHA guideline for the management of heart failure: Executive summary: a report of the American College of Cardiology Foundation/American Heart Association Task Force on practice guidelines. *Circulation*, *128*(16), 1810–1852. https://doi.org/10.1161/CIR.0b013e31829e8807

Yancy Clyde W., Jessup Mariell, Bozkurt Biykem, Butler Javed, Casey Donald E., Drazner Mark H., Wilkoff Bruce L. (2013). 2013 ACCF/AHA Guideline for the Management of Heart Failure. *Circulation*, *128*(16), e240–e327. https://doi.org/10.1161/CIR.0b013e31829e8776

Yang, D., Song, L.-S., Zhu, W.-Z., Chakir, K., Wang, W., Wu, C., … Cheng, H. (2003). Calmodulin regulation of excitation-contraction coupling in cardiac myocytes. *Circulation Research*, *92*(6), 659–667. https://doi.org/10.1161/01.RES.0000064566.91495.0C

Yang, J., Xu, W., & Hu, S. (2015). Heart Failure: Advanced Development in Genetics and Epigenetics [Research article]. https://doi.org/10.1155/2015/352734

Yang, W., Nagasawa, K., Münch, C., Xu, Y., Satterstrom, K., Jeong, S., … Haigis, M. C. (2016). Mitochondrial Sirtuin Network Reveals Dynamic SIRT3-Dependent Deacetylation in Response to Membrane Depolarization. *Cell*, *167*(4), 985-1000.e21. https://doi.org/10.1016/j.cell.2016.10.016

Yim, J., Cho, H., & Rabkin, S. W. (2018). Gene expression and gene associations during the development of heart failure with preserved ejection fraction in the Dahl salt sensitive model of hypertension. *Clinical and Experimental Hypertension (New York, N.Y.: 1993)*, *40*(2), 155–166. https://doi.org/10.1080/10641963.2017.1346113

Yu, X., & Long, Y. C. (2016). Crosstalk between cystine and glutathione is critical for the regulation of amino acid signaling pathways and ferroptosis. *Scientific Reports*, *6*, 30033. https://doi.org/10.1038/srep30033

Yu, Z., Tang, P. L. F., Wang, J., Bao, S., Shieh, J. T., Leung, A. W. L., … Song, Y.-Q. (2018). Mutations in *Hnrnpa1* cause congenital heart defects. *JCI Insight*, *3*(2). https://doi.org/10.1172/jci.insight.98555

Zavadáková, P., Fowler, B., Suormala, T., Novotna, Z., Mueller, P., Hennermann, J. B., … Kozich, V. (2005). cblE type of homocystinuria due to methionine synthase reductase deficiency: Functional correction by minigene expression. *Human Mutation*, *25*(3), 239–247. https://doi.org/10.1002/humu.20131

Zbidi, H., Redondo, P. C., López, J. J., Bartegi, A., Salido, G. M., & Rosado, J. A. (2010). Homocysteine induces caspase activation by endoplasmic reticulum stress in platelets from type 2 diabetics and healthy donors. *Thrombosis and Haemostasis*, *103*(5), 1022–1032. https://doi.org/10.1160/TH09-08-0552

Zeng, R., Xu, C.-H., Xu, Y.-N., Wang, Y.-L., & Wang, M. (2015). The effect of folate fortification on folic acid-based homocysteine-lowering intervention and stroke risk: A meta-analysis. *Public Health Nutrition*, *18*(8), 1514–1521. https://doi.org/10.1017/S1368980014002134

Zhang, K., Gao, M., Wang, G., Shi, Y., Li, X., Lv, Y., … Liu, Y. (2018). Hydrocephalus in cblC type methylmalonic acidemia. *Metabolic Brain Disease*. https://doi.org/10.1007/s11011-018-0351-y

Zhang, L., Keung, W., Samokhvalov, V., Wang, W., & Lopaschuk, G. D. (2010). Role of fatty acid uptake and fatty acid β-oxidation in mediating insulin resistance in heart and skeletal muscle. *Biochimica et Biophysica Acta (BBA) - Molecular and Cell Biology of Lipids*, *1801*(1), 1–22. https://doi.org/10.1016/j.bbalip.2009.09.014

Zhang, S., Bai, Y.-Y., Luo, L.-M., Xiao, W.-K., Wu, H.-M., & Ye, P. (2014). Association between serum homocysteine and arterial stiffness in elderly: A community-based study. *Journal of Geriatric Cardiology: JGC*, *11*(1), 32–38. https://doi.org/10.3969/j.issn.1671-5411.2014.01.007

Zhang, Y., Bao, M., Dai, M., Wang, X., He, W., Tan, T., … Zhang, R. (2015). Cardiospecific CD36 suppression by lentivirus-mediated RNA interference prevents cardiac hypertrophy and systolic dysfunction in high-fat-diet induced obese mice. *Cardiovascular Diabetology*, *14*(1), 69. https://doi.org/10.1186/s12933-015-0234-z

Zhao, J.-Y., Qiao, B., Duan, W.-Y., Gong, X.-H., Peng, Q.-Q., Jiang, S.-S., Wang, H.-Y. (2014). Genetic variants reducing MTR gene expression increase the risk of congenital

heart disease in Han Chinese populations. *European Heart Journal*, *35*(11), 733–742. https://doi.org/10.1093/eurheartj/eht221

Zhao, R., Diop-Bove, N., Visentin, M., & Goldman, I. D. (2011). Mechanisms of membrane transport of folates into cells and across epithelia. *Annual Review of Nutrition*, *31*, 177–201. https://doi.org/10.1146/annurev-nutr-072610-145133

Zhao, R., Matherly, L. H., & Goldman, I. D. (2009). Membrane Transporters and Folate Homeostasis; Intestinal Absorption, Transport into Systemic Compartments and Tissues. *Expert Reviews in Molecular Medicine*, *11*, e4. https://doi.org/10.1017/S1462399409000969

Zheng, Y., Ramsamooj, S., Li, Q., Johnson, J. L., Yaron, T. M., Sharra, K., & Cantley, L. C. (2019). Regulation of folate and methionine metabolism by multisite phosphorylation of human methylenetetrahydrofolate reductase. *Scientific Reports*, *9*(1), 4190. https://doi.org/10.1038/s41598-019-40950-7

Zhu, M., Mao, M., & Lou, X. (2019). Elevated homocysteine level and prognosis in patients with acute coronary syndrome: A meta-analysis. *Biomarkers: Biochemical Indicators of Exposure, Response, and Susceptibility to Chemicals*, *24*(4), 309–316. https://doi.org/10.1080/1354750X.2019.1589577

Zhu, Y.-C., Zhu, Y.-Z., Lu, N., Wang, M.-J., Wang, Y.-X., & Yao, T. (2003). Role of angiotensin AT1 and AT2 receptors in cardiac hypertrophy and cardiac remodelling. *Clinical and Experimental Pharmacology and Physiology*, *30*(12), 911–918. https://doi.org/10.1111/j.1440-1681.2003.03942.x

Ziaeian, B., & Fonarow, G. C. (2016). Epidemiology and aetiology of heart failure. *Nature Reviews. Cardiology*, *13*(6), 368–378. https://doi.org/10.1038/nrcardio.2016.25

Zong, Y., Liu, N., Zhao, Z., & Kong, X. (2015). Prenatal diagnosis using genetic sequencing and identification of a novel mutation in MMACHC. *BMC Medical Genetics*, *16*, 48. https://doi.org/10.1186/s12881-015-0196-8

Annex 1: Hypertrophic cardiomypathy and systolic dysfunction in mice with heart selective invalidation of *methionine synthase* (*Mtr*) is related to impaired energy metabolism, cellular stress and fibrosis

Viola J. Kosgei[1], Carole Arnold[1], Sebastien Hergalant[1], Brittany Balint[1], Jean-Michel Camadro[3], Fatiha Elkhafifi[1], Patrick Lacolley[4], Luc Monnasier[5], Fatiha Maskali [6], Jean-Louis Guéant [1,2*], Rosa-Maria Guéant-Rodriguez [1,2*]

[1]UMR Inserm 1256 N-GERE (Nutrition, Génetique et Exposition aux Risques Environmentaux), Université de Lorraine, 54500 Vandoeuvre-lès-Nancy, France.

[2]Departments of Digestive Diseases and Molecular Medicine and National Center of Inborn Errors of Metabolism, University Hospital Center, Université de Lorraine, 54500 Vandoeuvre-lès-Nancy, France.

[3]Mass Spectrometry Laboratory, Institut Jacques Monod, UMR 7592, Université Paris Diderot, CNRS, Sorbonne Paris Cité, 75205 Paris, France

[4]UMRS Inserm 1116 DCAC (Défaillance cardiovasculaire aiguë et chronique), Université de Lorraine, 54500 Vandoeuvre-lès-Nancy, France.

[5]Mouse clinical institute MCI, IGBMC, Strasbourg' France

[6]Nancyclotep-GIE, CHRU of Nancy, France

***Equal contribution**

Corresponding author: Pr Rosa-Maria Guéant Rodriguez**,** rosa-maria.gueant-rodriguez@univ-lorraine.fr, Tel: (33)3 72 74 61 35

Key words: Cardiomyopathy, heart failure, Inborn Errors of Metabolism, methionine synthase, vitamin B12, one carbon metabolism

Abstract

Introduction. Inherited metabolic disorders of vitamin B12 that lead to decreased methionine synthase activity, including type *cblG* with mutations in *MTR*, produce dramatic cardio-metabolic decompensation in first years of life. However, whether these inherited disorders produce a cardiomyopathy in later life is not known.

Objective : To investigate the cardiac metabolic and functional consequences of constitutive selective invalidation of *Mtr* gene in an original transgenic mouse model at adult age.

Methods. We performed functional, morphological, metabolic and molecular examinations of selective *Mtr* invalidation in heart of young adult mice.

Results. Cardiac invalidation of *Mtr* gene decreased both methionine synthase expression and activity and SAM :SAH ratio in the heart. This invalidation also led to cardiac hypertrophy and systolic dysfunction evidenced by echocardiography and mini-Positron Emission Tomography imaging. An increased expression of natriuretic peptides (ANP and BNP) and decreased cardiac myosin heavy chains alpha /beta ratio was observed in *Mtr cKO* animals. The cardiomyopathy in *Mtr cKO* was related to impaired energy metabolism, cellular stress and fibrosis revealed by metabolic and immunohistochemical examination. Transcriptomic and proteomic analyses revealed altered expression of genes involved in inherited heart failure and/or mitochondria energy metabolism, fatty acid oxidation, cardiac contraction and remodeling. We also observed an important decreased expression of *Sirt3*, a prominent regulator of myocardium energy metabolism. Cellular stress was associated with disrupted nucleocytoplasmic shuttling of the RNA binding protein hnRNPA1.

Conclusion. The selective invalidation of *Mtr* in heart produces hypertrophic cardiomyopathy with systolic dysfunction and impaired myocardial energy metabolsim in young adult mice. This suggests to further evaluate whether *cblG* could be a new genetic cause of primary heart failure in adult patients.

Introduction

Heart failure (HF) is one of the most common causes of morbidity and mortality in Western countries (Schocken et al., 2008; Ziaeian & Fonarow, 2016). The most frequent causes of HF are secondary to coronary artery disease, hypertension and valvular diseases. Primary causes are rare and produced by genetic defects. HF leads to dilated cardiomyopathy (DCM)

(Dickstein et al., 2008; Elliott et al., 2007; Maron et al., 2006; Ziaeian & Fonarow, 2016). The primary causes of DCM are generally confined to heart muscle while the secondary causes involve complex mechanisms, including at the systemic level.

Inherited metabolic diseases constitute the major cause of primary HF and DCM (Fu & Eisen, 2018). Among them, little attention has been dedicated to the inborn errors of one-carbon metabolism (1CM) despite several experimental and clinical evidences of the importance of this metabolism in myocardium (Guéant et al., 2018; Watkins & Rosenblatt, 2016). The main inborn errors of 1CM are produced by genetic defects of the remethylation pathway involved in the endogenous synthesis of methionine. They result from mutations in methionine synthase gene (*MTR*), which encodes methionine synthase (MS) or genes involved in the processing of cobalamin (vitamin B12, Cbl), including *CD320, LMBRD1, ABCD4, MMACHC, MMADHC* and *MTRR* (Coelho et al., 2012; Green et al., 2017; Watkins et al., 2002). MS utilizes 5-methyltetrahydrofolate (5-Me-THF) and methylcobalamin (a derivative of vitamin B12) to catalyze the transfer of methyl group from N^5 methyltetrahydrofolate to homocysteine to form methionine and tetrahydrofolate (Banerjee & Matthews, 1990; Guéant, Namour, Guéant-Rodriguez, & Daval, 2013). Methionine is the direct precursor of S-Adenosyl Methionine (SAM), the universal methyl group donor for the synthesis of intermediate metabolites and the methylation of histones, RNA and DNA, which are crucial for epigenomic regulatory mechanisms of gene expression (Forges et al., 2007; Guéant et al., 2013). Genetic defects with decreased activity of MS lead to decreased SAM and dramatic increase of homocysteine in blood and tissues (Huemer et al., 2017; Richard et al., 2017), cellular oxidative stress (Moselhy & Demerdash, 2003) and endoplasmic reticulum stress in endothelium (Wu et al., 2019). The deficiency in folates and vitamin B12 during pregnancy and lactation lead to hypertrophic cardiomyopathy with enlarged cardiomyocytes and increased thickness of the myocardium, impaired activity of respiratory chain and fatty acid oxidation in rat pups (Garcia et al., 2011).

Clinical reports and population studies suggest an association between the deficit in methyl donors (vitamin B12 and folates) and HF. We and others have demonstrated a significant association between elevated plasma homocysteine, low vitamin B12 and impaired left ventricular systolic function (Bokhari, Bokhari, Zell, Lee, & Faxon, 2005; GUÉANT-RODRIGUEZ et al., 2007). However, whether this association is cause or consequence of HF and whether it results from decrease activity of MS is unknown. Moreover, the patients with cblG and other inherited disorders of vitamin B12 metabolism that lead to dramatic decreased of methionine synthase may have lethal dramatic cardiometabolic decompensation in the first two years of life, but nothing is known regarding the cardiac consequences at adult age. To

address these issues, we designed and produced an original transgenic mouse model with constitutive selective invalidation of *Mtr* gene in myocardium. We investigated the functional, morphological and molecular cardiac consequences at young adult age.

MATERIALS AND METHODS

Animals

Animal studies were approved by the Ministry of Higher Education and Research (MESR) of France after having received a favorable opinion from the Ethics Committee of Lorraine Region (APAFIS2776-2015111915482808). All experiments and animal care were carried out in compliance with French and European laws, directives, and regulations on care and use of animals for scientific research. The mice were housed in standard laboratory conditions, on a 12h light, 12h darkness schedule at a temperature of (20 ± 2) °C and humidity of (50 ± 5) % with food and water available *ad libidum*.

Generation of the cardiac specific *Mtr* Knock out mice

Cardiac specific *Mtr* Knock-out (*Mtr* cKO) mice were generated in collaboration with the "Institut Clinique de la Souris" (ICS) in Strasbourg-Illkirch. Conditional cardiac specific deletion of *Mtr* gene in the cardiomyocytes was achieved using tissue-specific and time controlled Cre-LoxP system (Agah et al., 1997). The mice bearing the *Mtr* conditional allele were crossed with Myh6-Cre line (JAXMICE Stock Number 11038, B6.FVB-Tg (Myh6-cre) 2182Mds / J expressing Cre recombinase in the cardiomyocytes causing the deletion of this allele in the cardiomyocytes. The Cre recombinase is produced under control of the promoter specific Myh6 in cardiomyocytes from embryonic day (E) 9.5 with a maximum at E 11.5, and this enzyme recombines the LoxP sites introduced in the *Mtr* gene, around exons 4 and 5 which are essential. The deletion of exons 4 and 5 in the DNA sequence causes a shift in the reading frame hence the messenger RNA transcribed from the deleted gene produces nonfunctional methionine synthase protein. PCR analysis was used to genotype the mice using DNA extracted from animals' tail. Supplementary Table 8 shows the sequences of primers that were used to genotype the Mhy6 transgene and floxed *Mtr* allele. Products of PCR were resolved in 1 % tris acetate EDTA (TAE) agarose gel electrophoresis. Methionine synthase enzyme activity assay and immunoblot analysis were used to confirm the effective deletion of *Mtr* gene.

Echocardiography

Cardiac function parameters and ventricular remodeling in 5-month-old mice were assessed by transthoracic echocardiography using the Vevo 770® micro-echocardiography imaging system (Visualsonics Inc, Canada). The animals were anaesthesized with 1.5 -2 % isoflurane in 100 %

oxygen during induction and was maintained at 1- 1.5 % during echocardiographic scans. Chest hair was shaved and the mouse was placed in supine position on a heating pad to maintain the body temperature at 37 °C. M-Mode echocardiography obtained from parasternal short axis view was used to determine left ventricular ejection fraction (LVEF), fractional shortening (FS) and left ventricular mass (LV mass).

MiniPET Positron Emission Tomograph (PET) Imaging

The cardiac function and tissue perfusion parameters were performed on 5 -month- old mice using small animal monitoring and gating system M1025T (Inveon, Siemens Medical, USA). The animals were weighed, anaesthesized and then injected with 37 MBq 18F-labelled PEGylated tetrameric RGD Peptide (18F-FPRGD4). MiniPET scans were taken 30 minutes after the injection. The regions of interest of each scan was drawn using the Vendor software (ASI Pro 5.2.4.0, Siemens Medical, Germany). Blood glucose levels were measured before and after the emission scans. After imaging, the animals were placed in a recovery chamber for 24 hours after which they were isolated until the day they were sacrificed.

Blood and tissue harvest

After cardiac functional studies the animals were weighed, anesthetized and then euthanized by decapitation. Blood was collected, centrifuged at 2500 g for 10 minutes and plasma was aliquoted and kept at -80 ° C until analysis. For SAM and SAH assay, 50 µl of plasma was acidified with 5 µl of 1 M Acetic acid and stored at -80 ° C until analysis.

Hearts were harvested and submerge in ice cold 1X PBS buffer to drain excess blood. The hearts were then weighed and cut cross-sectionally to obtain the ventricles which were fixed in 4 % Formalin for histological analysis. The remaining parts (ventricles and apex) were frozen in liquid nitrogen and stored at -80°C until analysis.

Western blotting

Frozen mouse heart tissues were homogenised and proteins were extracted and quantified as described previously (Bison et al., 2016). A total of 30 µg of proteins were resolved /electrophoresed by SDS PAGE and subsequently transferred to either nitrocellulose or PVDF membranes (Amersham Hybond, GE Healthcare life science, Germany). The latter were blocked and incubated with antibodies as described previously (Garcia et al., 2011). Target proteins were detected using specific primary antibodies and the respective secondary antibodies, as listed in supplementary Table 6. The enhanced chemiluminescence (ECL kit, Bio-Rad laboratories, USA) was used to visualize the immuno-reactive proteins in FusionFx7 detector (Fischer). ImageJ software was used for densitometric analysis.

RNA extraction and RT qPCR

Total RNA from cardiac tissue was isolated using the TRIzol reagent (Invitrogen life technologies) and pure link RNA mini kit (Invitrogen thermoFisher Scientific) in accordance to TRIzol plus total transcriptome isolation protocol. Reverse transcription and quantitative PCR was done as described previously (Zgheib et al., 2019). The sequences and hybridization conditions of primers used are tabulated in supplementary data Table 7.

The fold change levels for the target genes relative to RNA polymerase II and Ribosomal protein S29 housekeeping genes were calculated using as $2^{-\Delta\Delta Ct}$ method. ΔC_T of the gene of interest was calculated by subtracting the cycle thresholds (C_T) values of reference genes from the C_T of gene of interest. The $\Delta\Delta C_T$ was obtained by subtracting the average ΔC_T of control samples from that of *Mtr cKO*.

Histological examination and quantification of myocardial fibrosis

Formalin-fixed paraffin-embedded mouse heart ventricles were cut into 5 µM-thick sections., The sections were deparaffinised, rehydrated and stained with Picrosirus red and Massons Trichome and were observed under normal brightfield microscopy. The picrosirus red collagen-enriched areas appeared red or pale yellow, while for Masson Trichome, the collagen-enriched areas appeared blue. Collagen was quantified by measuring the area of collagen relative to the entire sample area with the colour deconvolution plug-in in ImageJ. The area of collagen was expressed as fold-increase in fibrotic area compared to control samples. Immunofluorescence of formalin-fixed paraffin-embedded mouse heart ventricles was carried out as described previously (Battaglia-Hsu et al., 2018). The primary antibodies used for immunofluorescence were : Y14; ab181038, Hnrnpa1; ab5832 and HUR/ELAV1; ABIN577055.

Cell lysates and proteomic analysis by LC-MS/MS

Total proteins from the heart tissues were extracted using RIPA lysis buffer and quantified using BCA Protein Assay kit (Interchim, Muntluçon Cedex France). Peptide mixtures were analyzed in triplicates, LC-MS/MS acquisitions were carried out as described elsewhere (Télot et al., 2018). MS/MS data were processed with an in-house Mascot search server (Matrix Science, Boston, MA; version 2.4.1). Label-free quantification in between subject analysis was performed on raw data with Progenesis-Qi software 4.1 (Nonlinear Dynamics Ltd, Newcastle, U.K.) using the following procedure: (i) chromatograms alignment, (ii) peptide abundances normalization, (iii) statistical analyses of features, and (iv) peptides identification using the Mascot server. A decoy search was performed and the significance threshold was fixed to 0.05. The resulting files were imported into Progenesis-LC software. Peptides with ion score less than 15 were rejected. Conflicts for the identification of some peptides were resolved.

Resultant proteome was filtered for remnants of missing or zero-expressed values, giving a final count of 1998 unique proteins. Data were then stardardized using the VMR-ratio volume normalization method (Meunier et al., 2007) and log2-transformed. Hierarchical cluster analyses were performed and heatmaps were explored with PermutMatrix (Caraux & Pinloche, 2004) on centered protein abundances, with Euclidian distance as metrics and Ward's agglomeration. Functional annotations of disease association, GO terms and biological pathways were achieved with the Open Targets online platform (Carvalho-Silva et al., 2018) (https://www.targetvalidation.org).

RNA sequencing and transcriptome analysis

Total mice heart tissue RNAs were extracted as described above and quantified using a Nanodrop 2000. RNAs were then subjected to DNAse I treatment where 5µg of each RNA were treated with MBU Baseline -ZERO^{TM} DNAse (ref#DB0715K, Epicentre) for 25 minutes at 37°C followed by Phenol/chloroform and chloroform extraction. Three volumes of 96 % ethanol were used to precipitate the RNA using 15 mg of glycoblue and 0.3M AcONa. After a wash with 80 % ethanol, the pellet was re-suspended in 21 µl of RNAse free water. The quality of RNA before and after DNAse I treatment was checked by capillary electrophoresis using a PicoRNA chip on Bioanalyzer 2100 (Agilent). A total of 2 µg of each DNAse I treated RNA was used for ribosomal RNA (rRNA) depletion using human Ribo-Zero rRNA removal kit (ref#MRZH116, Illumina) following the manufacturer's instructions. Elution of rRNA-depleted RNA was done in 8 µl of RNase free water. Effectiveness of depletion of rRNA was checked by capillary electrophoresis using a PicoRNA chip on Bioanalyzer 2100 (Agilent). A total of 20 ng of each rRNA-depleted RNA were then converted to library using the Scriptseq V2 RNA-Seq kit (ref#SSV21106, Illumina) following the manufacturer's instructions. After 15 cycles of PCR amplification, the libraries were purified using the Agencourt AMPure XP beads (ref#A63880, Beckman Coulter) at a ratio of 0.9x.The quality of libraries were assessed using a high sensitivity DNA chip on a Bioanalyzer 2100 (Agilent) after which they were quantified using a fluorometer (Qubit 3.0 fluorometer, Invitrogen). DNA libraries were multiplexed and subjected to high-throughput sequencing using an Illumina HiSeq 1000 instrument with 2*101 bp paired-end read runs and loaded at 12 pM per lane. After demultiplexing, reads were compiled in standard FASTQ files.Quality control was performed using FastQCv0.11.5 (http://www.bioinformatics.babraham.ac.uk/projects/fastqc) (Gauchotte et al., 2017). Bad quality sequences and reads contaminated by adapters were trimmed using cutadapt 1.11 with parameters "-a AGATCGGAAGAG -A AGATCGGAAGAG -m 30 --no-indels -O 5". Mapping of the resulting reads was performed by HISAT2 v2.0. (Kim, Langmead, & Salzberg,

2015). On a version of the GRCm38 reference genome which accounts for splicing donor and acceptor sites and SNP polymorphism (https://cloud.biohpc.swmed.edu/index.php/s/grcm38_snp/download).

Spliced isoforms were assembled from the reconstructed transcripts obtained with Stringtie v1.3.3b (Pertea et al., 2015), allowing for the identification of new isoforms in addition to those overlapping known transcripts (by at least 80% of their length) from the Ensembl official annotations (Mus_musculus.GRCm38.92.gtf). Transcripts with very low expression across all samples (mean read coverage < 30) were removed from further analysis. Data were normalized with the trimmed means of M-values (TMM) (M. D. Robinson & Oshlack, 2010) method, then log2-transformed and rendered in counts per million. Unsupervised clusterings and functional annotations were carried out as previously described (Gauchotte et al., 2017). Additional functional annotations and GO terms enrichment analyses were performed with EnrichR (https://amp.pharm.mssm.edu/Enrichr) and PANTHER classification systems (Mi, Muruganujan, Casagrande, & Thomas, 2013), while diseases associations were achieved using Open Targets Platform (Carvalho-Silva et al., 2018).

Statistical analysis

For both proteome and transcriptome, linear modelling with empirical Bayes (from the bioconductor limma package) (Ritchie et al., 2015) was applied to assess differential expression at protein and at gene level between Control and *Mtr cKO* groups, respectively. Differential expression *P*-values were obtained by using a moderated Student t-test and adjusted for the false discovery rate (FDR) with the Benjamini-Hochberg procedure. Integrations of paired proteomic and transcriptomic samples were performed both ways on the 1720 total shared features: 1) without prior knowledge by computing the entire Spearman's correlation matrix between genes and proteins expression levels, and 2) by driving the proteome mining with the significant down and upregulated transcriptome clusters. Functional annotations and disease association analyses were then carried out on extracted features with Enrichr and Open Targets. PANTHER gene list analysis was used to analyze functional annotationso of the transcriptome. All *P*-values or FDR < 5% indicated statistical significance, with relevance according to the feature observed (protein, gene, cluster, correlation, functional term).

Non-omics data were analyzed using Stata 12.0 statistics and data analysis software (stataCorp, College station TX, USA) and continuous variables were expressed as means ± standard error of means (SEM). One-way analysis of variance (ANOVA) was used to compare the raw data. Student t-test was used for statistical analysis of the westernblot densitometric and RT-qPCR

data. Logarithmic transformations were used to normalize skewed distributions. Statistical significance was denoted by Asterisks Asterisks * P <0.05, ** P <0.01, *** P <0.001, the minimum statistical significance level was set at P <0.05.

RESULTS

Cardiac-specific *Mtr* deletion decreases Methionine synthase expression in the heart, but not the liver, and is associated with a decreased SAM/SAH ratio

As expected, both the transcript and protein expression levels of methionine synthase were significantly decreased in the hearts of 5-month old *Mtr cKO* mice as compared with the control group (P = 0.001 and P = 0.040, respectively; Figure 1A and 1B). Cre recombinase was only expressed in the hearts of *Mtr cKO* mice (P = 0.001; Figure 1B). Consistently, methionine synthase activity was significantly decreased in *Mtr cKO* hearts as compared to controls (0.07 ± 0.04 vs 0.43 ± 0.04 mmol/h/mg, P = 0.0018; Figure 1D). To confirm the tissue specificity of *Mtr* invalidation, we assessed methionine synthase protein expression in the liver and found no significant difference between *Mtr cKO* and controls animals (P = 0.230; Figure 1C). Together, these results demonstrate the successful homozygous deletion of the *Mtr* gene in the heart of our mouse model.

We further investigated the metabolic consequence of the *Mtr* gene deletion in the myocardium. We found that *Mtr* deletion produced an increase in the concentration of SAH (351.20 ± 51.90 vs 107.73 ± 21.48 nm/mg of tissue, P = 0.05), while that of SAM remained unchanged in the hearts of *Mtr cKO* mice in comparison to controls (847.40 ± 129.91 vs 663.75 ± 52.58 nm/mg of tissue, P = 0.327; Figure 1E). Consequently, the SAM/SAH ratio, the index for cellular methylation capacity, was significantly decreased in *Mtr* $^{-/-}$ compared to controls (3.60 ± 0.32 vs 6.75 ± 0.99, P = 0.0143; Figure 1F). Formyl tetrahydrofolate (fTHF), was significantly increased in *Mtr cKO* as compared to controls (0.90 vs 0.28 nmol/L, P = 0.0040) while 5-methyltetrahydrofolate (5-methylTHF) and THF remained unchanged (2.98 vs 2.65, P = 0.985 and 0.25 vs 0.17 nmol/L, P = 0.573, respectively; Figure 1G).

The cardiac-specific *Mtr* deletion produces cardiac dysfunction and heart failure.

We evaluated the left ventricular function using transthoracic echocardiography to further investigate whether the deletion of *Mtr* induced cardiac dysfunction. We observed an increase in left ventricular mass (Figure 2C) and a notable decrease in both LVEF and LVFS in *Mtr cKO* relative to control animals, indicating cardiac hypertrophy and systolic dysfunction in *Mtr cKO* (38.97 ± 2.07 vs 55.38 ± 3.677, P = 0.002 and 18.79 ± 1.14 vs 28.64 ± 2.40, P = 0.002 respectively; Figure 2B). In addition, the left ventricular dimensions in M mode showed

increased LV volumes at the end of diastole (LVEDV) and systole (LVESV) in *Mtr cKO* mice (57.33 ± 7.28 vs 26.33 ± 4.00 µL, $P = 0.0067$ and 81.41 ± 2.90 vs 57.03 ± 5.72 µL, $P = 0.0015$, respectively; Table 1).

We further evaluated the cardiac perfusion and ventricular dysfunction of *Mtr cKO* mice, using mini-Positron Emission Tomography imaging. These data were consistent with those observed in the transthoracic ultrasonographic examination. No difference for perfusion was observed. The end diastolic volume (EDV) and the end systolic volume (ESV) were significantly increased in *Mtr cKO* compared with control mice (114.60 ± 4.60 vs 99.20 ± 2.60 µL, $P = 0.028$ and 72.20 ± 4.10 vs 53.90 ± 4.70 µL, $P = 0.004$, respectively; Figure 2D and 2E, and 2G and 2H respectively). These data may explain the significant decrease of LVEF in *Mtr cKO* in comparison to control animals (33.16 ± 2.10 vs 52.08 ± 2.80, P = 0.010; Figure 2F). Furthermore, a significant increase in systolic blood pressure was observed in *Mtr cKO* mice compared to control mice (111.37 ± 0.82 vs 94.45 ± 2.96 mmHg, $P = 0.0001$; Figure 2I). Taken together, these results indicate that *Mtr* silencing in myocardium induced dilatation of the left ventricles and LV systolic dysfunction in *Mtr cKO* mice.

Biomarkers confirm heart failure of *Mtr cKO* mice.

Through RT-qPCR, we measured the expression levels of natriuretic peptides and alpha and beta MHCs used as biomarkers of heart failure. The expression of atrial natriuretic peptide (ANP) and brain natriuretic peptides (BNP) were significantly elevated in the heart tissue of *Mtr cKO* in comparison with controls ($P = 0.003$ and $P = 0.001$ respectively; Figure 2J). Meanwhile, beta *Mhc7* was significantly overexpressed ($P = 0.017$; Figure 2J) and the alpha *Mhc6*/beta *Mhc7* ratio was decreased ($P = 0.0156$; Figure 2H). The shift in the expression of cardiac myosin heavy chain from alpha MHC to beta MHC is a hallmark of heart failure. These results are consistent with the hypertrophic cardiomyopathy, systolic dysfunction and heart failure revealed by echocardiography and mini-PET imaging.

The cardiac-specific *Mtr* deletion dysregulates the expression of genes and proteins in the myocardium

We carried out transcriptomic and proteomic studies in order to dissect the molecular consequences of the cardiac specific deletion of the *Mtr* gene that may explain the cardiomyopathy observed in *Mtr cKO* mice. For transcriptomics studies 4 samples were used per group, while for proteomics 5 *Mtr cKO* and 7 controls samples were used.

Transcriptomic expression profile

We detected a total of 16539 expressed genes after quality control and removal of lowly expressed transcripts. These genes were clustered by K-means, and each of the resulting cluster

was re-analysed by hierarchical clustering, which delineated three strongly correlated gene signatures of *Mtr* silencing (Figure 3A). The 3 signatures represented about 35 % of the total dysregulated transcriptome. The downregulated signature consisted of 1889 genes representing 11.4 % of the transcriptome (cluster 2; $P = 1.9 \times 10^{-4}$, Figure 3C) while the upregulated signatures consisted of 1666 (cluster 3) and 2478 genes (cluster 4) representing 10 % and 15 % of the transcriptome, respectively. Sub-cluster 3, consisting of 418 genes and sub-cluster 4, consisting of 887 genes ($P = 1.4 \times 10^{-4}$ and $P = 2.6 \times 10^{-2,}$ respectively; Figure 3D and 3E), were obtained after elimination of outliers by cutting of branches of the hierarchical trees in cluster 3 and 4, respectively. Statistical analyses output a total of 145 differentially expressed genes, 102 were underexpressed (Fold change < 0.5, FDR < 0.05) and 43 were overexpressed (Fold change > 2, FDR < 0.05) in *Mtr cKO* (Supplementary statistical files).

The Gene Ontology (GO) enrichment and pathway analysis of the 1889 underexpressed genes in *Mtr cKO* mice ($P < 0.05$) were mainly related to impaired mitochondria energy metabolism, fatty acid beta oxidation and cardiac remodeling (Supplementary Figure S1). The changes found with genes encoding proteins of the mitochondrial matrix of fatty acid oxidation included *Acadm* (medium chain acyl dehydrogenase involved in the first step of medium chain acyl CoA metabolism), *Ehhadh (E*noyl-CoA Hydratase And 3-Hydroxyacyl CoA Dehydrogenase involved in fatty acid beta-oxidation), *Acaa2* (ketoacyl CoA thiolase involved in fatty acid beta-oxidation) and *Decr1* (dienoyl CoA reductase involved in the last steps of fatty acid oxidation) (Supplementary Table 1). The 418 overexpressed genes (sub-cluster 3) were related to adaptive mechanisms to cellular stress and cardiac hypertrophy including response to oxidative stress, autophagy, growth factor stimuli, regulation of vascular endothelial growth factor signalling and extracellular matrix organization ($P < 0.05$; Supplementary Figure S2A). The 887 overexpressed genes (sub-cluster 4) were involved in adaptative pathways of cardiac remodeling and impaired mitochondria energy metabolism ($P < 0.05$; Supplementary Figure S2B and S3 and Table 2). These pathways included ATP biosynthesis, TORC1 and calcium mediated signaling pathways, cardiac muscle cell contraction and development, and regulation of heart rate by cardiac conduction ($P < 0.05$). The *Mtr cKO* GO biological processes and reactome pathways highlighted in the 3 clusters are detailed in Supplementary Figure S4.

Proteomic expression profile

A total of 1998 proteins were detected of which 34 proteins were differentially expressed (Supplementary statistical file). Among them, 26 were downregulated (Fold change < 0.8, $P < 0.05$) and 8 upregulated (Fold change > 1.25, $P < 0.05$). The most relevant GO biological processes associated with these proteins were related to energy metabolism (ketone body and

galactose metabolisms, mitochondrial biogenesis) and myocardium remodeling (muscle cell differentiation, Fibroblast Growth Factor Receptor signalling, proteasome assembly, cell to cell adhesion mediated by cadherins; Supplementary Figure S5B). The cardiovascular diseases associated with the 34 dysregulated proteins included genetic cardiomyopathies related to mitochondrial disorders and heart failure (Supplementary Figure S5C and Supplementary Table 3). The altered expression of the 34 proteins was correlated with transcription change of the related genes, in *Mtr* cKO mice compared with control mice. According to the t-statistics ($P < 0.01$), the top 94 dysregulated proteins were hierarchically clustered (Supplementary Figure S5A), and resulting clusters were functionally analyzed for associated diseases using open Target platform (Supplementary Table 4 and 5). Cardiovascular diseases and number of targets associated with these proteins were similar to those obtained with the 34 differentially expressed proteins (Supplementary Table 3).

Transcriptomic driven proteomic analysis

To further analyse the proteomic data, we integrated the proteome by correlating its features with the transcriptomic ones. We also mined the proteome according to transcriptome-clustering results (from cluster 2, sub-cluster3 and sub-cluster4), and extracted gene-protein features with positively and negatively correlated expressions. Among the 1720 shared genes and proteins in both omics, 213 were underexpressed while 245 were overexpressed in the hearts of *Mtr cKO* mice. Transcriptomic driven analysis of proteome revealed that the 213 downregulated genes translated into 90 underexpressed proteins (fold-change < 0.8), 50 proteins that correlated inversely with upregulation (fold-change > 1.25) and 71 proteins with no change of expression. On the other hand, the 245 overexpressed genes were translated into 85 underexpressed, 59 overexpressed proteins and 101 with no change of expression (Supplementary Figure S6).

Functional annotation of the positively correlated genes-proteins (90 underexpressed and 59 overexpressed) was performed using Enrichr. The most significant and relevant GO biological processes linked to the 90 positively under-expressed proteins in the myocardium of *Mtr cKO* mice were related to mitochondrial energy metabolism (mitochondrial respiratory chain complex I assembly, ATP biosynthesis and short chain fatty acid metabolism) and regulation of cardiac function (cardiac ventricular muscle development, cardiac muscle contraction and relaxation) ($P < 0.05$; Supplementary Figure S8). Furthermore, GO molecular processes associated with these under-expressed proteins included: RNA binding, ATPase and NADH dehydrogenase activity, NO synthase binding, cadherins binding, long chain fatty acid binding and acylcoA transferase activity ($P < 0.05$; Supplementary Figure S8). Pathway analysis by

Enrichr revealed that the KEGG pathways associated with these under-expressed proteins in the myocardium of *Mtr cKO* included: oxidative phosphorylation, fatty acid degradation, dilated cardiomyopathy, hypertrophic cardiomyopathy, cardiac muscle contraction and apoptosis ($P < 0.05$; Supplementary Figure S9A). Majority of these proteins were localized in the mitochondria and myofibrils ($P < 0.05$; Supplementary Figure S9B).

Similarly, functional annotations for the 59 positively overexpressed proteins in the myocardium of *Mtr cKO* mice were analyzed using Enrichr. The most relevant GO biological processes associated with these positively overexpressed proteins were related to adaptive response to unfolded proteins, oxidative stress, cardiac contraction, mitochondrial biogenesis and energy metabolism including mitochondrial complex I assembly, electron transport chain and glucose homeostasis (Supplementary Figure S10).

To further investigate why genes were inversely translated in *Mtr cKO*, we analyzed the transcription factors protein-protein interactions target enrichment for the negatively translated proteins using Enrichr. We found that majority of the 85 negatively downregulated proteins were enriched in transcription regulation by ESR1 (encoding estrogen receptor 1), Myc (encoding Myc Proto-Oncogene Protein) and HTT (encoding huntingtin) transcription factors protein-protein interactions ($P = 6.38e^{-11,}$ $P = 1.09e^{-9}$and $P = 4.38e^{-8}$ respectively; Supplementary file 2). On the other hand, no transcription factors were found to be significantly associated with the 50 negatively overexpressed protein, however transcription factor perturbation followed by expression were enriched in PPARG, ESR2 and GATA4 ($P < 0.05$; supplementary file 3).

Furthermore, Spearman's correlation analysis revealed that 22 genes and proteins were significantly correlated in *Mtr cKO.* Of these, 17 genes/proteins were positively and 5 were negatively correlated (Supplementary Table 6 and Figure S11).

The cardiac-specific *Mtr* silencing produces cardiac remodelling, with myocardium hypertrophy and fibrosis.

Silencing of methionine synthase in the myocardium induced cardiac hypertrophy, evidenced by the increased heart to body weight ratios in *Mtr cKO* mice compared to controls (57.44 ± 2.80 vs 49.18 ± 2.58 mg/g, $P = 0.02$; Figure 4E). We further investigated the presence of cardiac fibrosis as a consequence of this remodeling using histopathological staining and immuno blotting. Both Masson's Trichome and Picrosirus Red staining revealed a significant increase of collagen deposition in *Mtr cKO* hearts compared to control hearts ($P = 0.018$, $P = 0.0004$; Figure 4A and 4B). Furthermore, RT-qPCR analysis revealed an increasedexpression of *Col3a1* and *Col1a1* in *Mtr cKO* mice compared to controls (4.72 fold increase, $P = 0.001$, and 4.9 fold

increase, P = 0.002 respectively; Figure 4D). The fibrosis was related to the increased expression of transforming growth factor beta 1 (TGFβ1), angiotensin receptor 2 (AGTR2) and matrix metalloproteinase-2 (MMP2), as evidenced by western blot analysis (P = 0.006, P = 0.023 and P = 0.005 respectively; Figure 4C). Together, these results indicate that the cardiac invalidation of *Mtr* induced left ventricular systolic dysfunction and myocardium hypertrophy with remodeling and fibrosis.

The myocardium hypertrophy was related to impaired energy metabolism

Invalidation of *Mtr* in the heart caused extensive impaired myocardial energy metabolism. This was evidenced by the increased plasma levels of short chain (C4) and medium chain (C8) acyl carnitines in *Mtr cKO* compared to control mice (P = 0.001 and P = 0.041 respectively; Figure 5A and 5B respectively). The C0/(C16+C18) ratio, which is an index for carnitine palmitoyl transferase 1 (CPT1) activity was significantly increased (P = 0.025) while C14.1/C12.1 and C14.1/C16 ratios were significantly decreased (P = 0.001 and P = 0.039) in *Mtr cKO* compared to controls (Figures 5C, 5D and 5E respectively). CD36, an important transmembrane fatty acid importer, was significantly downregulated in *Mtr cKO* mice hearts (Figure 6A). In agreement with these results, transcriptomics and proteomic data analysis revealed a decreased expression of proteins involved in fatty acid oxidation, including 3 Oxoacyl (acyl carrier protein) synthase and Peroxisomal acyl coenzyme A oxidase, and a decreased expression of genes and proteins involved in mitochondrial oxidative phosphorylation including *NADH dehydrogenases; Ndufv1, Ndufb4 and Ndufa7* (complex I) and *Cox6a2* (complex IV), in *Mtr cKO* animals (Supplementary Table 1). Transcriptomics data analysis revealed also a decreased expression of genes encoding fatty acid beta oxidation enzymes, including *Acat1, Acadm, Ehhadh, Acaa2* and *Decr1* ($P < 0.05$; Supplementary Table 1). Conversely, the analysis of heart transcriptome showed an adaptative upregulation of *Hk1 and Pdk3* genes of glycolysis in *Mtr cKO* compared with control animals, which was confirmed by RTqPCR (Figure 6C and supplementary Table 1). In addition, RT-qPCR showed an increased expression of *Cox7a1* and a decreased expression of *Atp5j* genes (Figure 6B). The proteomic analysis also revealed altered expression of other proteins involved in the mitochondrial respiratory chain including decreased expression of cytochrome b (complex III) and an adaptative increased expression of ATP synthase sub-unit a (complex V). Western blot analysis confirmed the increased expression of mitochondrial membrane ATP synthase subunit a (mt ATP6) and the decreased expression of cytochrome b in the hearts of *Mtr cKO* compaired to control animals (Figure 6A).

Mitochondrial NADH deacetylase Sirt3 is a prominent regulator of mitochondrial energy metabolism. Sirt3 deacetylates key proteins involved in fatty acid oxidation and oxidative

phosphorylation. Proteomic and western blot analysis revealed a decreased expression of Sirt3 in *Mtr cKO* compared to control ($P < 0.05$; Figure 6A). Collectively, these results shows that invalidation of *Mtr* in cardiomyoytes dramatically impairs mitochondrial fatty acid beta oxidation and oxidative phosphorylation.

The myocardium fibrosis was related to increased cellular stress.

The cardiac invalidation of *Mtr* dysregulated the expression of genes and proteins involved in the response to cellular stress. Transcriptomic data analysis showed an increased expression of *Gata4 and Bcl2* and a decreased expression of *Glrx3* in *Mtr cKO* compared to controls animals ($P < 0.05$). Proteomic studies showed an increased expression of heat shock proteins and ubiquitin like modifier activity enzyme 1 (Uba1), SH3 domain-binding glutamic acid-rich-like protein 3 (Sh3bgrl3) and High Mobility Group Box 3 (Hmgb3) in the heart of *Mtr cKO* mice. Western blot analysis confirmed the increased expression of Hspb3, annexin A 5 and Hsp27 in *Mtr cKO* (2.0-fold, 3.2-fold and 8.1-fold increase, respectively; Figure 6D). In contrast, no significant difference was observed for Hsp90 between the two groups.

Given the cellular stress observed in *Mtr cKO*, we further investigated whether invalidation of *Mtr* gene influenced the subcellular localization of 3 stress-related RNA binding proteins (RBPs), ELVAL1/HuR, Y14 and hnRNPA1, using immunofluorescence detection. hnRNPA1 was exclusively localized in the nucleus of cardiomyocytes of *Mtr cKO*, while it was localized in the cytoplasm and the perinucleus, in the cardiomyocytes of controls (Supplementary Figure S7A). In contrast, ELVAL1/HuR was localized in the nucleus of the cardiomyocytes of both the *Mtr cKO* and controls, and its expression levels was comparable between the two groups (Supplementary Figure S7B). We also found that Y14 was localized in the perinucleus and cytoplasm of the cardiomyocytes of both *Mtr cKO* and control animals (Supplementary Figure S7C). Taken together, these data suggested that invalidation of *Mtr* gene in the cardiomyocytes blocks the shuttling of hnRNPA1 from the nucleus into the cytoplasm in stress conditions.

Discussion

We found that the selective *Mtr* invalidation in the heart produces cardiomyopathy with heart failure, myocardium hypertrophy and fibrosis in young adult mice. The selective silencing of *Mtr* was evidenced by the decreased protein expression and enzyme activity of MS and at the metabolic level, by the decreased SAM:SAH ratio. The cardiomyopathy was related to impaired energy metabolism with disruption of fatty acid oxidation and oxidative phosphorylation, cellular stress and remodeling with fibrosis. The decreased expression of Sirt3 was consistent with the impaired energy metabolism and the mislocalization and nuclear sequestration of

mRNAs of hnRNPA1 could explain part of the expression changes of genes and proteins involved in energy metabolism and cellular stress. It is noteworthy that we previously found a similar disruption of the fatty acid oxidation and impaired oxidative phosphorylation that was related to decreased expression of *Sirt1* in heart tissue of pups from rat dams subjected to methyl donor (folate and viamin B12) deficient diet during gestation and lactation (Garcia et al., 2011) Mitochondria play a central role in myocardium physiology. The heart continuously generates ATP to support its constant needs in energy and intermediate metabolites related to its contractile function (Lopaschuk, Ussher, Folmes, Jaswal, & Stanley, 2010).

The increased plasma concentration of both short and medium chain acyl carnitines was a consequence of the impaired fatty acid beta oxidation and the decreased activity of carnitine Palmitoyl transferase 1 (CPT1) reflected by the increase of C0/(C16+C18) ratio, in *Mtr cKO vs*. wild type animals (Hollak & Lachmann, 2016). The increased concentration of short and medium chain acyl carnitines was consistent with the transcriptomic and proteomic expression changes of genes and proteins involved in fatty acid oxidation in *Mtr cKO*. The changes evidenced in transcriptomic analyses included genes encoding mitochondrial matrix proteins involved in fatty acid oxidation. Both transcriptomic and proteomic analyses showed a decreased expression of ACAT1 (Acetyl-CoA Acetyltransferase 1), which plays a crucial role in the final step of fatty acid beta oxidation and ketone body metabolism. The impaired fatty acid beta oxidation was also illustrated by the decreased expression of *Cd36* in the myocardium of *Mtr cKO*. Cd36 is a transmembrane fatty acid transporter, which plays a major role in fatty acid uptake across cardiomyocyte membrane (Glatz, Nabben, Heather, Bonen, & Luiken, 2016). Fatty acid uptake via Cd36 is critical for sufficient production of ATP in the heart and that its deletion accelerates contractile dysfunction (Umbarawan et al., 2018). The specific deletion of *Cd36* gene in cardiomyocytes in adult mice hastens the progression from compensated cardiac hypertrophy to heart failure in response to pressure overload (Sung et al., 2017). Conversely, cardio-specific inhibition of Cd36 can protect mice against high fat diet induced cardiac remodeling (Zhang et al., 2015). The overexpression of genes encoding glycolytic pathway enzymes, including *Gck*, *Hk1* and *Pdk3* could be a compensatory mechanism of impaired fatty acid oxidation in *Mtr cKO* mice (Fillmore, Mori, & Lopaschuk, 2014; Kato et al., 2010; Lopaschuk et al., 2010; Riehle et al., 2011). These changes illustrate the shift of myocardial energy production from fatty acid oxidation to glycolysis, a very known metabolic hallmark of heart failure (Karwi, Uddin, Ho, & Lopaschuk, 2018; Kato et al., 2010; Lopaschuk et al., 2010).

The specific silencing of *Mtr* also impaired oxidative phosphorylation in myocardium through decreased expression of genes and proteins involved in complex I, complex IV and complex V. Of particular interest was the decreased expression of Ndufv1 gene encoding NADH Dehydrogenase Ubiquinone Flavoprotein 1, which plays a crucial role in delivering electrons from NADH to ubiquinone. A decreased expression of NDUFV1 protein was previously reported in patients with dilated cardiomyopathy (Ono, Nakamura, & Matsuzaki, 2010). Complex 1 deficiency is associated with hypertrophic cardiomyopathy and neonatal cardiomyopathy (Bugiani et al., 2004; Pitkänen et al., 1996; B. H. Robinson, 1998) and ischemic heart failure (Liu et al., 2014). Mutations in Ndufv1 have also been linked to mitochondrial diseases (Ortega-Recalde et al., 2013; Srivastava et al., 2018). The upregulated expression of ATP synthase subunit alpha (Mt-ATP6) *in Mtr cKO* could be a compensatory mechanism of impaired ATP synthesis, as suggested by the association between its overepression and left ventricular mass in patients with ischemic heart failure (Roselló-Lletí et al., 2015).

The dysregulated mitochondrial energy metabolism was linked to a dramatic decreased expression of the mitochondrial matrix NADH deacetylase Sirtuin 3 (Sirt3) in hearts of *Mtr cKO* mice. Given the crucial role played by sirt3 in regulating mitochondrial energy metabolism, it can be hypothesized that the decreased expression of Sirt3 led to impaired energy metabolism observed in the hearts of *Mtr cKO* via imbalanced acetylation/ deacetylation of key proteins involved in fatty acid oxidation, tricarboxylic acid cycle and oxidative phosphorylation (M. Hirschey, Shimazu, Huang, Schwer, & Verdin, 2011; Koentges et al., 2015; Parodi-Rullán, Chapa-Dubocq, & Javadov, 2018; Sun et al., 2018). As showed in our model, the decreased expression of *Sirt3* causes impaired myocardial energetics and systolic dysfunction in mice through impaired expression of short and medium chain acyl CoA dehydrogenases (M. Hirschey et al., 2011; M. D. Hirschey et al., 2010; Yang et al., 2016). In the absence of Sirt3, hyperacetylation of LCAD at lysine 42 reduces its activity (M. D. Hirschey et al., 2010). Similar effects have been reported in proteins of complexes I, II, III and IV of electron transport chain (Parodi-Rullán, Chapa-Dubocq, & Javadov, 2018). ATP synthase activity is also regulated by SIRT3-mediated deacetylation (Bao et al., 2010; Yang et al., 2016). This explains the 50 % reduction of basal ATP levels observed in heart from mice lacking *Sirt3* (Ahn et al., 2008*)*. Finally, Sirt3 plays also a crucial in the response to the cell stress and cardiac remodeling in *Mtr* cKO by regulating the activity of mnSOD (Sundaresan et al., 2009; Tao et al., 2010). Its activation by resveratrol reduces TGF-β expression in cardiac tissue (Chen et al., 2014).

Deletion of *Mtr* in the cardiomyocytes induced cardiac remodelling. We observed an increased expression of TGFß1 and AT2 in heart tissue of *Mtr* cKO mice. TGF ß1 promotes the development of cardiac fibrosis (Edgley, Krum, & Kelly, 2012), cardiac hypertrophy (Huntgeburth et al., 2011) and cardiomyocyte apoptosis (Heger et al., 2011). The classical TGF ß /SMADs signalling pathway stimulates fibroblasts to increase the production of the extracellular matrice (ECM) proteins like fibrillar collagens and fibronectin (Verrecchia & Mauviel, 2002). Moreover, TGFß decreases the degradation of ECM by inhibiting the expression of metalloproteases (MMPs) and by increasing the expression of protease inhibitors like TIMPs and plasminogen activator inhibitor (Bujak & Frangogiannis, 2007; Verrecchia & Mauviel, 2002). Increased tissue expression and serum concentration of TGFß1 have been reported in idiopathic hypertrophic cardiomyopathy and its correlation with left ventricular mass in hypertensive patients with cardiomyopathy (Almendral, Shick, Rosendorff, & Atlas, 2010). As a consequence of increased TGFß1, we observed an increased expression *Col1a1*, *Col3a1* and *Mmp2* genes and an increased collagen deposition in the myocardium of *Mtr* cKO. Consistently, the development of heart failure revealed an upregulated expression of several genes including *Col1a1*, *Col3a1* and *Mmp2* in Dahl rats (Yim, Cho, & Rabkin, 2018). Cardiac-specific constitutive increased expression of *Mmp-2* impairs ventricular contraction, induces myocardial fibrosis and increases myocardial stiffness in mice (Wang et al., 2006),
the increase expression of *Col1a1* and *Col3a1* genes could be driven by decreased expression of Sirt3, as shown in *Sirt3*-KO mice (Guo, Yan, Li, Zhang, & Bu, 2017).

The mislocalization of hnRNPA1 could explain part of the changes of gene expression and protein translation evidenced in omics studies through its role in the splicing, nucleocytoplasmic transport and translation of mRNAs (Levengood & Tolbert, 2019). It could also contribute to the alterations of gene expression through its role in the processing of microRNAs (Jean-Philippe, Paz, & Caputi, 2013). Heterozygous *hnRNPA1* mutations in a mouse model and in two human cases produced congenital heart defects (Yu et al., 2018). We previously found that impaired cobalamin metabolism and pathogenic mutations of MS disrupt nucleocytoplasmic transport of mRNA through mislocalization of *ELAVL1*/*HuR* and *hnRNPA1*, in NIE115 neuroblastoma cells and fibroblasts from *cblG* patients exposed to cell stress inducers (Battaglia-Hsu et al., 2018; Ghemrawi et al., 2019). In contrast to our results in myocardium of *Mtr cKO* mice, we observed a cytoplasm export of *hnRNPA1* and a nuclear sequestration of *ELAVL1*/*HuR* in these cells (Battaglia-Hsu et al., 2018; Ghemrawi et al., 2019)..

In conclusion, we found that the selective invalidation of *Mtr* in heart produces a cardiomyopathy with cardiac hypertrophy and systolic dysfunction in young adult mice. At the tissue and molecular levels, the cardiomyopathy was related to disruption of fatty acid oxidation and oxidative phosphorylation, cellular stress and remodeling with fibrosis. The decreased expression of Sirt3 was consistent with the impaired energy metabolism and the mislocalization of hnRNPA1 could explain part of the expression changes of genes and proteins. These findings suggest to further evaluate whether cblG could be a new genetic cause of primary heart failure in adult patients.

ACKNOWLEDGEMENTS

The study is part of the project entitled "GEENAGE" of the University of Excellence I-Site LUE funded by the French Ministry for research and higher education. The work was also supported by fundings from the FHU ARRIMAGE, Inserm, European funds FEDER, and the Région Lorraine, France. The authors have no conflict of interest to declare.

Author contributions

RM Guéant-Rodriguez and JL Guéant had full access to all of the data and take responsibility for the integrity and accuracy of the data analysis. Study concept and design: RM Guéant-Rodriguez, JL Guéant and C Arnold. Acquisition, analysis, interpretation of data: Viola Kosgei, RM Guéant-Rodriguez, JL Guéant and all authors. Drafting of the manuscript: Viola Kosgei, RM Guéant-Rodriguez and JL Guéant. Critical revision of the manuscript for important intellectual content: All authors. Statistical analysis: RM Guéant-Rodriguez and Viola Kosgei. Obtained funding: RM Guéant-Rodriguez and JL Guéant. Study supervision: RM Guéant-Rodriguez and JL Guéant.

References

Agah, R., Frenkel, P. A., French, B. A., Michael, L. H., Overbeek, P. A., & Schneider, M. D. (1997). Gene recombination in postmitotic cells. Targeted expression of Cre recombinase provokes cardiac-restricted, site-specific rearrangement in adult ventricular muscle in vivo. *The Journal of clinical investigation, 100*(1), 169-179.

Ahn, B.-H., Kim, H.-S., Song, S., Lee, I. H., Liu, J., Vassilopoulos, A., Finkel, T. (2008). A role for the mitochondrial deacetylase Sirt3 in regulating energy homeostasis. *Proceedings of the National Academy of Sciences, 105*(38), 14447-14452.

Almendral, J. L., Shick, V., Rosendorff, C., & Atlas, S. A. (2010). Association between transforming growth factor-β1 and left ventricular mass and diameter in hypertensive patients. *Journal of the American Society of Hypertension, 4*(3), 135-141.

Banerjee, R. V., & Matthews, R. G. (1990). Cobalamin-dependent methionine synthase. *The FASEB journal, 4*(5), 1450-1459.

Bao, J., Scott, I., Lu, Z., Pang, L., Dimond, C. C., Gius, D., & Sack, M. N. (2010). SIRT3 is regulated by nutrient excess and modulates hepatic susceptibility to lipotoxicity. *Free Radical Biology and Medicine, 49*(7), 1230-1237.

Battaglia-Hsu, S.-F., Ghemrawi, R., Coelho, D., Dreumont, N., Mosca, P., Hergalant, S., Houlgatte, R. (2018). Inherited disorders of cobalamin metabolism disrupt nucleocytoplasmic transport of mRNA through impaired methylation/phosphorylation of ELAVL1/HuR. *Nucleic acids research, 46*(15), 7844-7857.

Bison, A., Marchal-Bressenot, A., Li, Z., Elamouri, I., Feigerlova, E., Peng, L., Alberto, J.-M. (2016). Foetal programming by methyl donor deficiency produces steato-hepatitis in rats exposed to high fat diet. *Scientific reports, 6*, 37207.

Bokhari, S. W., Bokhari, Z. W., Zell, J. A., Lee, D. W., & Faxon, D. P. (2005). Plasma homocysteine levels and the left ventricular systolic function in coronary artery disease patients. *Coronary artery disease, 16*(3), 153-161.

Bugiani, M., Invernizzi, F., Alberio, S., Briem, E., Lamantea, E., Carrara, F., Donati, M. (2004). Clinical and molecular findings in children with complex I deficiency. *Biochimica et Biophysica Acta (BBA)-Bioenergetics, 1659*(2-3), 136-147.

Bujak, M., & Frangogiannis, N. G. (2007). The role of TGF-β signaling in myocardial infarction and cardiac remodeling. *Cardiovascular research, 74*(2), 184-195.

Caraux, G., & Pinloche, S. (2004). PermutMatrix: a graphical environment to arrange gene expression profiles in optimal linear order. *Bioinformatics, 21*(7), 1280-1281.

Carvalho-Silva, D., Pierleoni, A., Pignatelli, M., Ong, C., Fumis, L., Karamanis, N., McAuley, E. (2018). Open Targets Platform: new developments and updates two years on. *Nucleic acids research, 47*(D1), D1056-D1065.

Chen, T., Li, J., Liu, J., Li, N., Wang, S., Liu, H., Bu, P. (2014). Activation of SIRT3 by resveratrol ameliorates cardiac fibrosis and improves cardiac function via the TGF-β/Smad3 pathway. *American Journal of Physiology-Heart and Circulatory Physiology, 308*(5), H424-H434.

Coelho, D., Kim, J. C., Miousse, I. R., Fung, S., du Moulin, M., Buers, I., Stucki, M. (2012). Mutations in ABCD4 cause a new inborn error of vitamin B 12 metabolism. *Nature genetics, 44*(10), 1152.

Dickstein, K., Members, A. T. F., Cohen-Solal, A., Filippatos, G., McMurray, J. J., Ponikowski, P., Atar, D. (2008). ESC Guidelines for the diagnosis and treatment of acute and chronic heart failure 2008‡: The Task Force for the Diagnosis and Treatment of Acute and Chronic Heart Failure 2008 of the European Society of Cardiology. Developed in collaboration with the Heart Failure Association of the ESC (HFA) and endorsed by the European Society of Intensive Care Medicine (ESICM). *European journal of heart failure, 10*(10), 933-989.

Edgley, A. J., Krum, H., & Kelly, D. J. (2012). Targeting Fibrosis for the Treatment of Heart Failure: A Role for Transforming Growth Factor-β. *Cardiovascular therapeutics, 30*(1), e30-e40.

Elliott, P., Andersson, B., Arbustini, E., Bilinska, Z., Cecchi, F., Charron, P., McKenna, W. J. (2007). Classification of the cardiomyopathies: a position statement from the European Society Of Cardiology Working Group on Myocardial and Pericardial Diseases. *European heart journal, 29*(2), 270-276.

Fillmore, N., Mori, J., & Lopaschuk, G. (2014). Mitochondrial fatty acid oxidation alterations in heart failure, ischaemic heart disease and diabetic cardiomyopathy. *British journal of pharmacology, 171*(8), 2080-2090.

Forges, T., Monnier-Barbarino, P., Alberto, J., Gueant-Rodriguez, R., Daval, J., & Gueant, J. (2007). Impact of folate and homocysteine metabolism on human reproductive health. *Human reproduction update, 13*(3), 225-238.

Fu, Y., & Eisen, H. J. (2018). Genetics of dilated cardiomyopathy. *Current cardiology reports, 20*(11), 121.

Garcia, M. M., Guéant-Rodriguez, R. M., Pooya, S., Brachet, P., Alberto, J. M., Jeannesson, E., Lacolley, P. (2011). Methyl donor deficiency induces cardiomyopathy through altered methylation/acetylation of PGC-1α by PRMT1 and SIRT1. *The Journal of pathology, 225*(3), 324-335.

Gauchotte, G., Hergalant, S., Vigouroux, C., Casse, J. M., Houlgatte, R., Kaoma, T., Peyre, M. (2017). Cytoplasmic overexpression of RNA-binding protein HuR is a marker of poor prognosis in meningioma, and HuR knockdown decreases meningioma cell growth and resistance to hypoxia. *The Journal of pathology, 242*(4), 421-434.

Ghemrawi, R., Arnold, C., Battaglia-Hsu, S.-F., Pourié, G., Trinh, I., Bassila, C., Robert, A. (2019). SIRT1 activation rescues the mislocalization of RNA-binding proteins and cognitive defects induced by inherited cobalamin disorders. *Metabolism*, 153992.

Glatz, J. F., Nabben, M., Heather, L. C., Bonen, A., & Luiken, J. J. (2016). Regulation of the subcellular trafficking of CD36, a major determinant of cardiac fatty acid utilization. *Biochimica et Biophysica Acta (BBA)-Molecular and Cell Biology of Lipids, 1861*(10), 1461-1471.

Green, R., Allen, L. H., Bjørke-Monsen, A. L., Brito, A., Guéant, J. L., Miller, J. W., Toh, B. H. (2017). Erratum: Correction: Vitamin B 12 deficiency (Nature reviews. Disease primers (2017) 3 (17040)). *Nature reviews. Disease primers, 3*.

GUÉANT-RODRIGUEZ, R. M., Juilliere, Y., Nippert, M., Abdelmouttaleb, I., Herbeth, B., Aliot, E., GUÉANT, J. L. (2007). Left ventricular systolic dysfunction is an independent predictor of homocysteine in angiographically documented patients with or without coronary artery lesions. *Journal of Thrombosis and Haemostasis, 5*(6), 1209-1216.

Guéant, J.-L., Chéry, C., Oussalah, A., Nadaf, J., Coelho, D., Josse, T., Gastin, I. (2018). A PRDX1 mutant allele causes a MMACHC secondary epimutation in cblC patients. *Nature communications, 9*(1), 67.

Guéant, J.-L., Namour, F., Guéant-Rodriguez, R.-M., & Daval, J.-L. (2013). Folate and fetal programming: a play in epigenomics? *Trends in Endocrinology & Metabolism, 24*(6), 279-289.

Guo, X., Yan, F., Li, J., Zhang, C., & Bu, P. (2017). SIRT3 attenuates AngII-induced cardiac fibrosis by inhibiting myofibroblasts transdifferentiation via STAT3-NFATc2 pathway. *American journal of translational research, 9*(7), 3258.

Heger, J., Warga, B., Meyering, B., Abdallah, Y., Schlüter, K. D., Piper, H. M., & Euler, G. (2011). TGFβ receptor activation enhances cardiac apoptosis via SMAD activation and concomitant NO release. *Journal of cellular physiology, 226*(10), 2683-2690.

Hirschey, M., Shimazu, T., Huang, J.-Y., Schwer, B., & Verdin, E. (2011). *SIRT3 regulates mitochondrial protein acetylation and intermediary metabolism.* Paper presented at the Cold Spring Harbor symposia on quantitative biology.

Hirschey, M. D., Shimazu, T., Goetzman, E., Jing, E., Schwer, B., Lombard, D. B., Ilkayeva, O. R. (2010). SIRT3 regulates mitochondrial fatty-acid oxidation by reversible enzyme deacetylation. *Nature, 464*(7285), 121.

Hollak, C. E., & Lachmann, R. (2016). *Inherited Metabolic Disease in Adults: A Clinical Guide*: Oxford University Press.

Huemer, M., Diodato, D., Schwahn, B., Schiff, M., Bandeira, A., Benoist, J.-F., Garcia-Cazorla, A. (2017). Guidelines for diagnosis and management of the cobalamin-related remethylation disorders cblC, cblD, cblE, cblF, cblG, cblJ and MTHFR deficiency. *Journal of inherited metabolic disease, 40*(1), 21-48.

Huntgeburth, M., Tiemann, K., Shahverdyan, R., Schlüter, K.-D., Schreckenberg, R., Gross, M.-L., Ghanem, A. (2011). Transforming growth factor β1 oppositely regulates the hypertrophic and contractile response to β-adrenergic stimulation in the heart. *PloS one, 6*(11), e26628.

Jean-Philippe, J., Paz, S., & Caputi, M. (2013). hnRNP A1: the Swiss army knife of gene expression. *International journal of molecular sciences, 14*(9), 18999-19024.

Karwi, Q. G., Uddin, G. M., Ho, K. L., & Lopaschuk, G. D. (2018). Loss of metabolic flexibility in the failing heart. *Frontiers in cardiovascular medicine, 5*.

Kato, T., Niizuma, S., Inuzuka, Y., Kawashima, T., Okuda, J., Tamaki, Y., Soga, T. (2010). Analysis of metabolic remodeling in compensated left ventricular hypertrophy and heart failure. *Circulation: Heart Failure, 3*(3), 420-430.

Kim, D., Langmead, B., & Salzberg, S. L. (2015). HISAT: a fast spliced aligner with low memory requirements. *Nature methods, 12*(4), 357.

Koentges, C., Pfeil, K., Schnick, T., Wiese, S., Dahlbock, R., Cimolai, M. C., Jaeger, C. (2015). SIRT3 deficiency impairs mitochondrial and contractile function in the heart. *Basic research in cardiology, 110*(4), 36.

Levengood, J. D., & Tolbert, B. S. (2019). *Idiosyncrasies of hnRNP A1-RNA recognition: can binding mode influence function.* Paper presented at the Seminars in cell & developmental biology.

Liu, T., Chen, L., Kim, E., Tran, D., Phinney, B. S., & Knowlton, A. A. (2014). Mitochondrial proteome remodeling in ischemic heart failure. *Life sciences, 101*(1-2), 27-36.

Lopaschuk, G. D., Ussher, J. R., Folmes, C. D., Jaswal, J. S., & Stanley, W. C. (2010). Myocardial fatty acid metabolism in health and disease. *Physiological reviews, 90*(1), 207-258.

Maron, B. J., Towbin, J. A., Thiene, G., Antzelevitch, C., Corrado, D., Arnett, D., Young, J. B. (2006). Contemporary definitions and classification of the cardiomyopathies: an American Heart Association scientific statement from the council on clinical cardiology, heart failure and transplantation committee; quality of care and outcomes research and functional genomics and translational biology interdisciplinary working groups; and council on epidemiology and prevention. *Circulation, 113*(14), 1807-1816.

Meunier, B., Dumas, E., Piec, I., Bechet, D., Hebraud, M., & Hocquette, J.-F. (2007). Assessment of hierarchical clustering methodologies for proteomic data mining. *Journal of proteome research, 6*(1), 358-366.

Mi, H., Muruganujan, A., Casagrande, J. T., & Thomas, P. D. (2013). Large-scale gene function analysis with the PANTHER classification system. *Nature protocols, 8*(8), 1551.

Moselhy, S., & Demerdash, S. (2003). Plasma homocysteine and oxidative stress in cardiovascular disease. *Disease markers, 19*(1), 27-31.

Ono, H., Nakamura, H., & Matsuzaki, M. (2010). A NADH dehydrogenase ubiquinone flavoprotein is decreased in patients with dilated cardiomyopathy. *Internal Medicine, 49*(19), 2039-2042.

Ortega-Recalde, O., Fonseca, D. J., Patiño, L. C., Atuesta, J. J., Rivera-Nieto, C., Restrepo, C. M., . . . Laissue, P. (2013). A novel familial case of diffuse leukodystrophy related to NDUFV1 compound heterozygous mutations. *Mitochondrion, 13*(6), 749-754.

Parodi-Rullán, R. M., Chapa-Dubocq, X. R., & Javadov, S. (2018). Acetylation of mitochondrial proteins in the heart: the role of SIRT3. *Frontiers in physiology, 9*, 1094.

Pertea, M., Pertea, G. M., Antonescu, C. M., Chang, T.-C., Mendell, J. T., & Salzberg, S. L. (2015). StringTie enables improved reconstruction of a transcriptome from RNA-seq reads. *Nature biotechnology, 33*(3), 290.

Pitkänen, S., Merante, F., McLeod, D. R., Applegarth, D., Tong, T., & Robinson, B. H. (1996). Familial cardiomyopathy with cataracts and lactic acidosis: a defect in complex I (NADH-dehydrogenase) of the mitochondria respiratory chain. *Pediatric research, 39*(3), 513.

Richard, E., Brasil, S., Leal, F., Navarrete, R., Vega, A., Ecay, M. J., Merinero, B. (2017). Isolated and Combined Remethylation Disorders: Biochemical and Genetic Diagnosis and Pathophysiology. *Journal of Inborn Errors of Metabolism and Screening, 5*, 2326409816685732.

Riehle, C., Wende, A. R., Zaha, V. G., Pires, K. M., Wayment, B., Olsen, C., Moreira, A. B. (2011). PGC-1β deficiency accelerates the transition to heart failure in pressure overload hypertrophy. *Circulation research, 109*(7), 783-793.

Ritchie, M. E., Phipson, B., Wu, D., Hu, Y., Law, C. W., Shi, W., & Smyth, G. K. (2015). limma powers differential expression analyses for RNA-sequencing and microarray studies. *Nucleic acids research, 43*(7), e47-e47.

Robinson, B. H. (1998). Human complex I deficiency: clinical spectrum and involvement of oxygen free radicals in the pathogenicity of the defect. *Biochimica et Biophysica Acta (BBA)-Bioenergetics, 1364*(2), 271-286.

Robinson, M. D., & Oshlack, A. (2010). A scaling normalization method for differential expression analysis of RNA-seq data. *Genome biology, 11*(3), R25.

Roselló-Lletí, E., Tarazón, E., Barderas, M. G., Ortega, A., Molina-Navarro, M. M., Martínez, A., . . . Salvador, A. (2015). ATP synthase subunit alpha and LV mass in ischaemic human hearts. *Journal of cellular and molecular medicine, 19*(2), 442-451.

Schocken, D. D., Benjamin, E. J., Fonarow, G. C., Krumholz, H. M., Levy, D., Mensah, G. A., . . . Hong, Y. (2008). Prevention of heart failure: a scientific statement from the American Heart Association Councils on epidemiology and prevention, clinical cardiology, cardiovascular nursing, and high blood pressure research; Quality of Care and Outcomes Research Interdisciplinary Working Group; and Functional Genomics and Translational Biology Interdisciplinary Working Group. *Circulation, 117*(19), 2544-2565.

Srivastava, A., Srivastava, K. R., Hebbar, M., Galada, C., Kadavigrere, R., Su, F., Shukla, A. (2018). Genetic diversity of NDUFV1-dependent mitochondrial complex I deficiency. *European Journal of Human Genetics, 26*(11), 1582.

Sun, W., Liu, C., Chen, Q., Liu, N., Yan, Y., & Liu, B. (2018). SIRT3: a new regulator of cardiovascular diseases. *Oxidative medicine and cellular longevity, 2018*.

Sundaresan, N. R., Gupta, M., Kim, G., Rajamohan, S. B., Isbatan, A., & Gupta, M. P. (2009). Sirt3 blocks the cardiac hypertrophic response by augmenting Foxo3a-dependent antioxidant defense mechanisms in mice. *The Journal of clinical investigation, 119*(9), 2758-2771.

Sung, M. M., Byrne, N. J., Kim, T. T., Levasseur, J., Masson, G., Boisvenue, J. J., Dyck, J. R. (2017). Cardiomyocyte-specific ablation of CD36 accelerates the progression from compensated cardiac hypertrophy to heart failure. *American Journal of Physiology-Heart and Circulatory Physiology, 312*(3), H552-H560.

Tao, R., Coleman, M. C., Pennington, J. D., Ozden, O., Park, S.-H., Jiang, H., McDonald, W. H. (2010). Sirt3-mediated deacetylation of evolutionarily conserved lysine 122 regulates MnSOD activity in response to stress. *Molecular cell, 40*(6), 893-904.

Télot, L., Rousseau, E., Lesuisse, E., Garcia, C., Morlet, B., Léger, T., Serre, V. (2018). Quantitative proteomics in Friedreich's ataxia B-lymphocytes: A valuable approach to

decipher the biochemical events responsible for pathogenesis. *Biochimica et Biophysica Acta (BBA)-Molecular Basis of Disease, 1864*(4), 997-1009.

Umbarawan, Y., Syamsunarno, M. R. A., Koitabashi, N., Obinata, H., Yamaguchi, A., Hanaoka, H., Sunaga, H. (2018). Myocardial fatty acid uptake through CD36 is indispensable for sufficient bioenergetic metabolism to prevent progression of pressure overload-induced heart failure. *Scientific reports, 8*(1), 12035.

Verrecchia, F., & Mauviel, A. (2002). Transforming growth factor-β signaling through the Smad pathway: role in extracellular matrix gene expression and regulation. *Journal of Investigative Dermatology, 118*(2), 211-215.

Wang, G.-Y., Bergman, M. R., Nguyen, A. P., Turcato, S., Swigart, P. M., Rodrigo, M. C., . Baker, A. J. (2006). Cardiac transgenic matrix metalloproteinase-2 expression directly induces impaired contractility. *Cardiovascular research, 69*(3), 688-696.

Watkins, D., & Rosenblatt, D. S. (2016). Lessons in biology from patients with inherited disorders of vitamin B12 and folate metabolism. *Biochimie, 126*, 3-5.

Watkins, D., Ru, M., Hwang, H.-Y., Kim, C. D., Murray, A., Philip, N. S., Hilton, J. F. (2002). Hyperhomocysteinemia due to methionine synthase deficiency, cblG: structure of the MTR gene, genotype diversity, and recognition of a common mutation, P1173L. *The American Journal of Human Genetics, 71*(1), 143-153.

Wu, X., Zhang, L., Miao, Y., Yang, J., Wang, X., Wang, C.-c., Wang, L. (2019). Homocysteine causes vascular endothelial dysfunction by disrupting endoplasmic reticulum redox homeostasis. *Redox biology, 20*, 46-59.

Yang, W., Nagasawa, K., Münch, C., Xu, Y., Satterstrom, K., Jeong, S., Zaganjor, E. (2016). Mitochondrial sirtuin network reveals dynamic SIRT3-dependent deacetylation in response to membrane depolarization. *Cell, 167*(4), 985-1000. e1021.

Yim, J., Cho, H., & Rabkin, S. W. (2018). Gene expression and gene associations during the development of heart failure with preserved ejection fraction in the Dahl salt sensitive model of hypertension. *Clinical and Experimental Hypertension, 40*(2), 155-166.

Yu, Z., Tang, P. L., Wang, J., Bao, S., Shieh, J. T., Leung, A. W., Hui, A. L. (2018). Mutations in Hnrnpa1 cause congenital heart defects. *JCI insight, 3*(2).

Zgheib, R., Battaglia-Hsu, S.-F., Hergalant, S., Quéré, M., Alberto, J.-M., Chéry, C., Namour, F. (2019). Folate can promote the methionine-dependent reprogramming of glioblastoma cells towards pluripotency. *Cell death & disease, 10*(8), 1-12.

Zhang, Y., Bao, M., Dai, M., Wang, X., He, W., Tan, T., Zhang, R. (2015). Cardiospecific CD36 suppression by lentivirus-mediated RNA interference prevents cardiac hypertrophy and systolic dysfunction in high-fat-diet induced obese mice. *Cardiovascular diabetology, 14*(1), 69.

Ziaeian, B., & Fonarow, G. C. (2016). Epidemiology and aetiology of heart failure. *Nature Reviews Cardiology, 13*(6), 368.

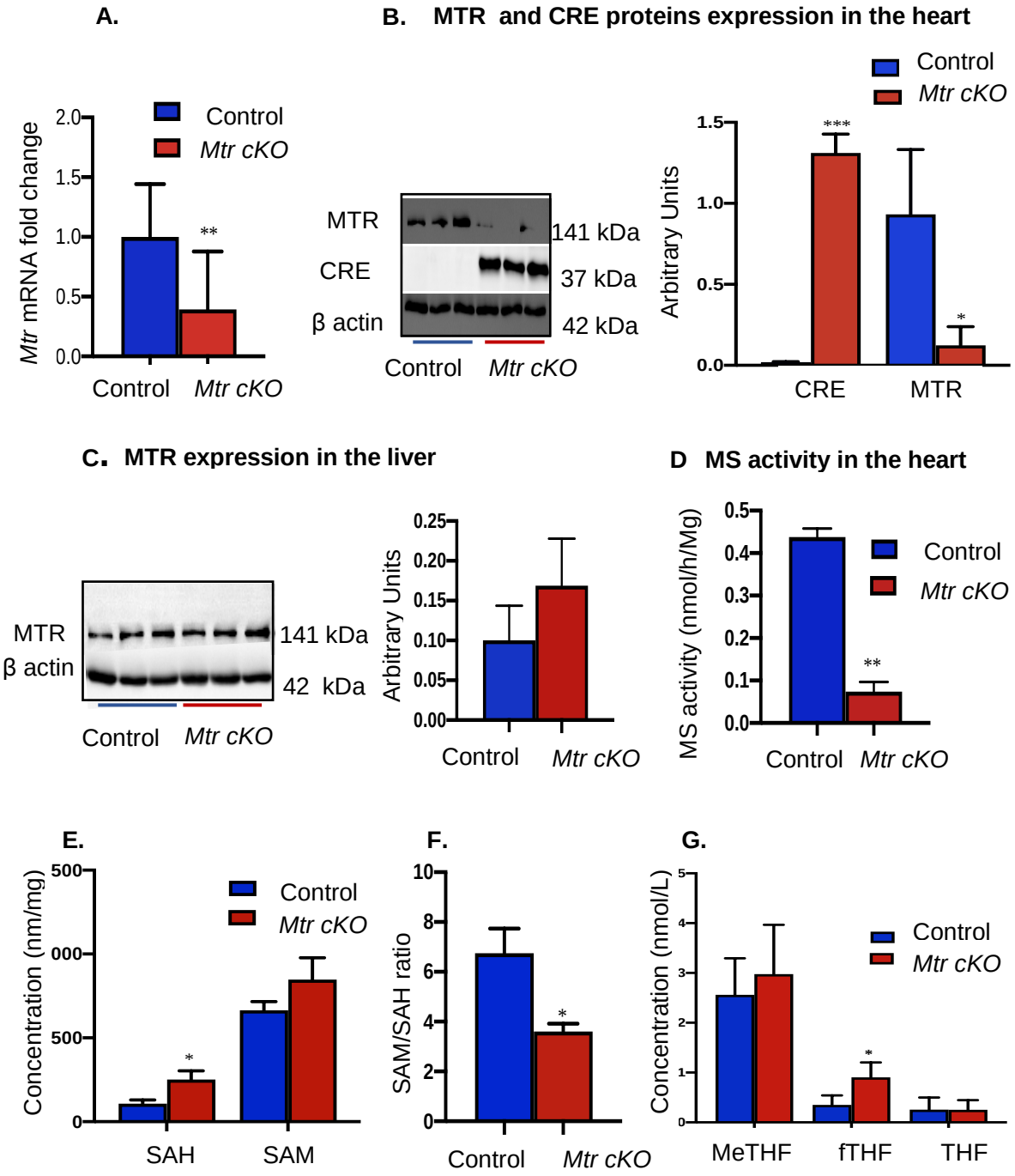

Figure 1. Cardiac specific invalidation of *Mtr* decreases methionine synthase expression in the heart, but not in the liver, and is associated with a decreased SAM:SAH ratio. A. mRNA expression levels for *Mtr* gene in the heart tissue analysed by RT-qPCR. **B.** Western blot and densitometric analysis of MTR protein and Cre recombinase expression levels in the heart tissue. **C.** Western blots and densitometric analysis of MTR protein expression levels in the liver tissue. **D.** Methionine synthase activity in the heart tissue evaluated by MS activity enzyme assay. **E.** S- Adenosyl homocysteine (SAH) and S-Adenosyl methionine (SAM) concentration in heart tissue. **F**. SAM:SAH ratio. **G**. Concentration of folates in the heart. The western blot protein bands were quantified densitometrically, normalized to β actin and expressed as arbitrary units. Means ± SEM, n = 4 to 6 per group, * $P < 0.05$ ** $P < 0.01$, ***$P < 0.001$.

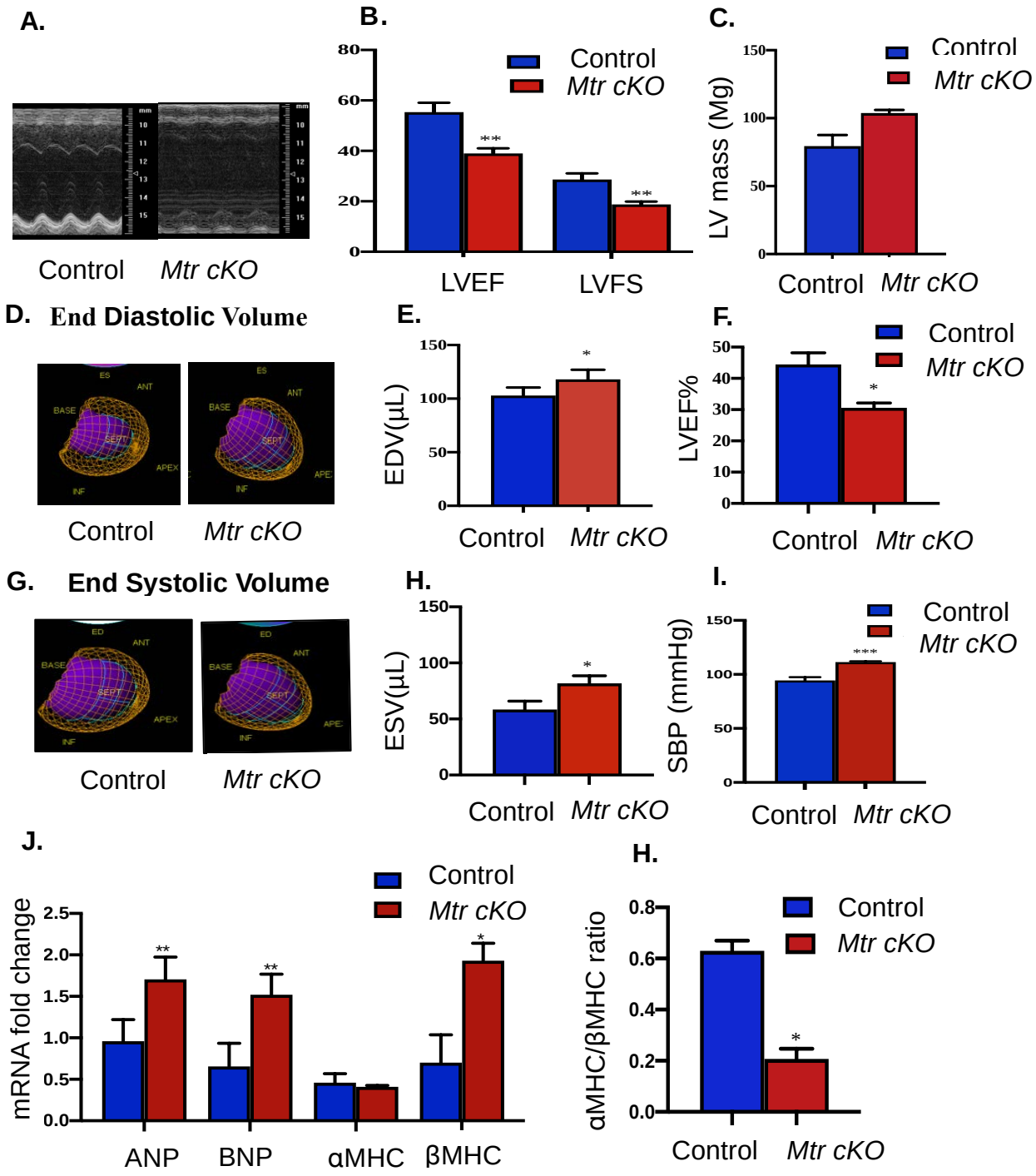

Figure 2. Cardiovascular consequences and evidence of heart failure associated with cardiac specific deletion of *Mtr*. A. Echocardiographs (M-mode images). **B.** Left ventricular Ejection Fraction (LVEF) and fractional shortening (LVFS) and **C**. Left ventricular mass assessed by Echocardiography in control and *Mtr cKO* animals. **D** and **G** are representative images at the end of systole and diastole respectively obtained using by small animal PET scanner Inveon (Siemens Medical, USA) in the controls and *Mtr cKO* mice. **E.** End diastolic volumes (EDV)**, F**. LVEF and **H**. End systolic volumes (ESV) assessed by Mini-PET in the controls and *Mtr cKO* mice. **I.** Systolic blood pressure between *Mtr cKO* and control mice. **J**. mRNA expression levels for the markers of heart failure ANP, BNP, alpha MHC6 and beta MHC7 analyzed by RT-qPCR and **H.** Alpha MHC6 and beta MHC7 ratio. n = 6 to 10 per group, Means ± SEM, * $P < 0.05$ ** $P < 0.01$, *** $P < 0.001$

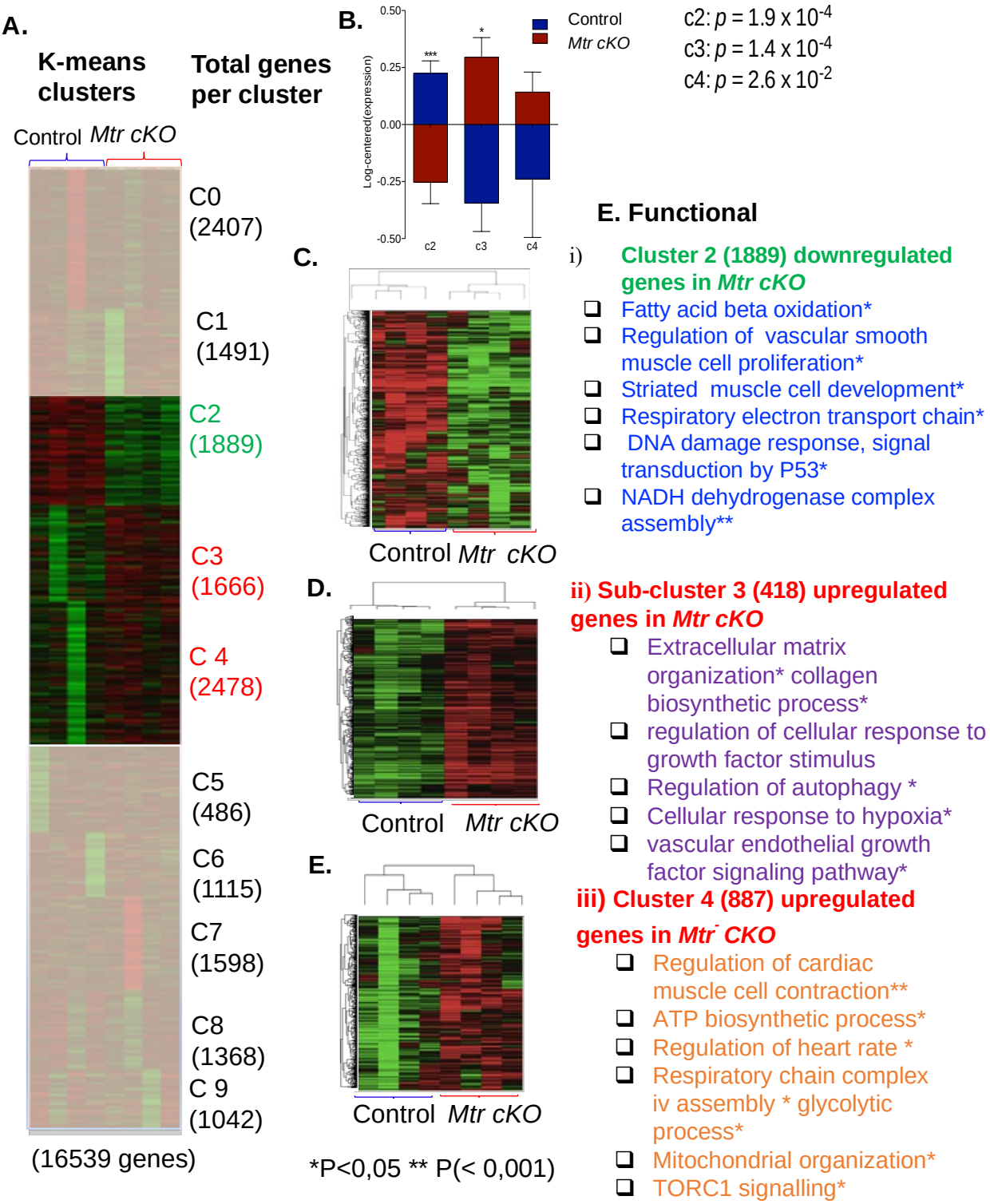

Figure 3. Consequence of cardiac specific deletion of *Mtr* gene in the transcriptome of the heart. **A**. Heat-map of whole heart transcriptome showing 10 clusters of the 16539 detected genes. K-means clustering of the whole heart transcriptome delineated three strongly correlated gene signatures (cluster 2, 3 and 4) black, red and green indicates median, upregulated and downregulated genes respectively. **B**. Log centred gene expression of the significantly dysregulated clusters (cluster 2, 3 and 4) in *Mtr cKO*. **C**, **D** and **E.** Heat-maps of hierarchically clustered **C2**, **sub C3** and **Sub C4** respectively. An overview of the most significant and relevant GO enrichment and functional annotations related to the three significant dysregulated gene clusters (C2, sub-C3 and sub-C4)n= 4 per group

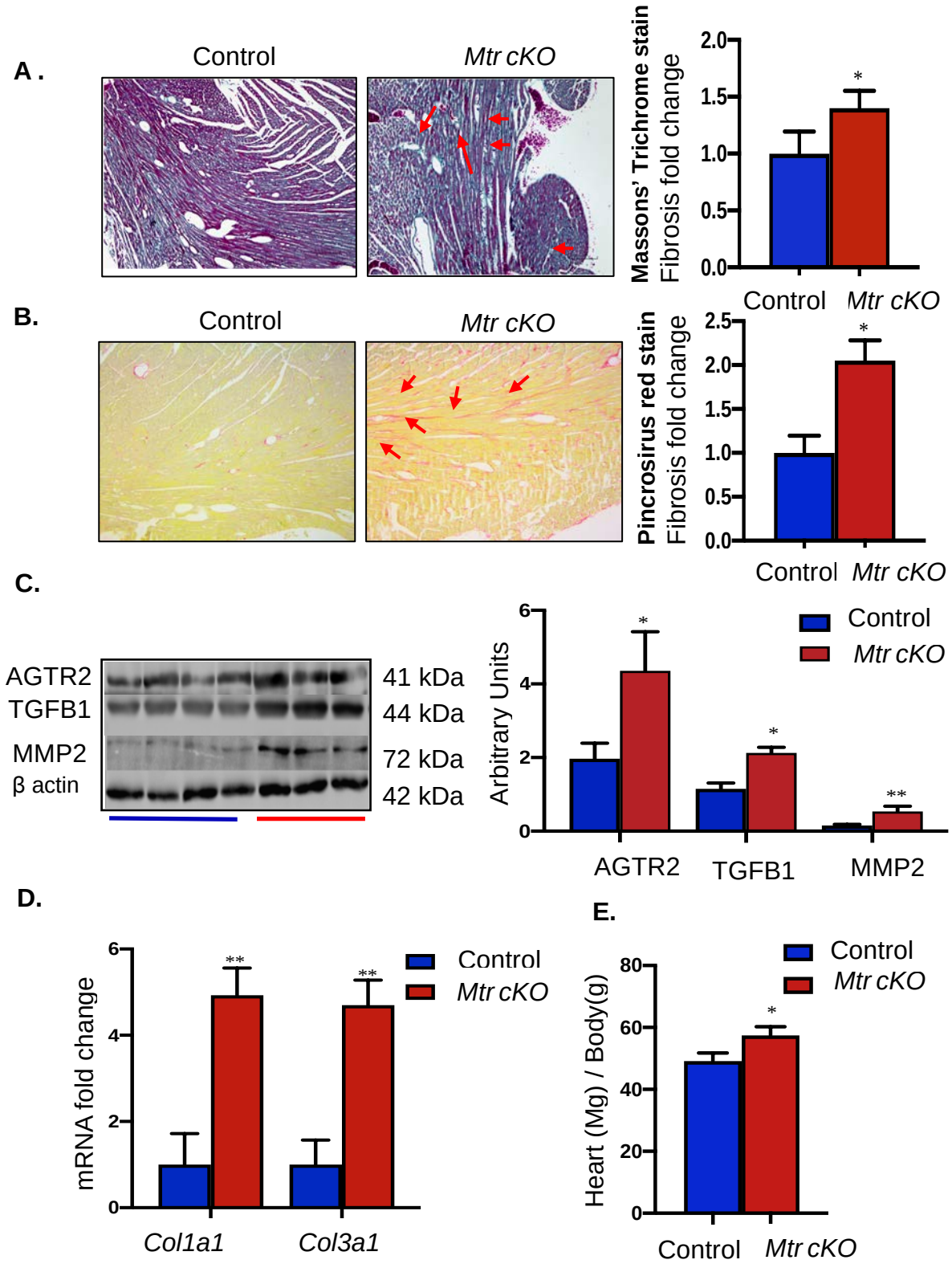

Figure 4. Silencing of methionine synthase in the heart causes cardiac remodelling evidenced by cardiac hypertrophy and fibrosis. A. Transversely sectioned left ventricle tissue from the controls and *Mtr cKO* mice stained with Masson's Trichrome. B. Transversely sectioned left ventricle tissue from the controls and *Mtr cKO* mice stained with Picrosirius Red Staining. C. Evaluation of expression levels of fibrotic proteins: AGTR2, TGFB1 and MMP2, the protein bands were quantified densitometrically, normalized to β actin and expressed as ratio of protein to beta actin. D. mRNA expression levels for *Col1a1* and *Col1a3* which are known fibrotic markers E. Relative heart weight (body weight: heart weight ratio) in the controls and *Mtr cKO;* n = 3 to 6 per group, means ± SEM, **P* < 0.05, ** *P* < 0.01

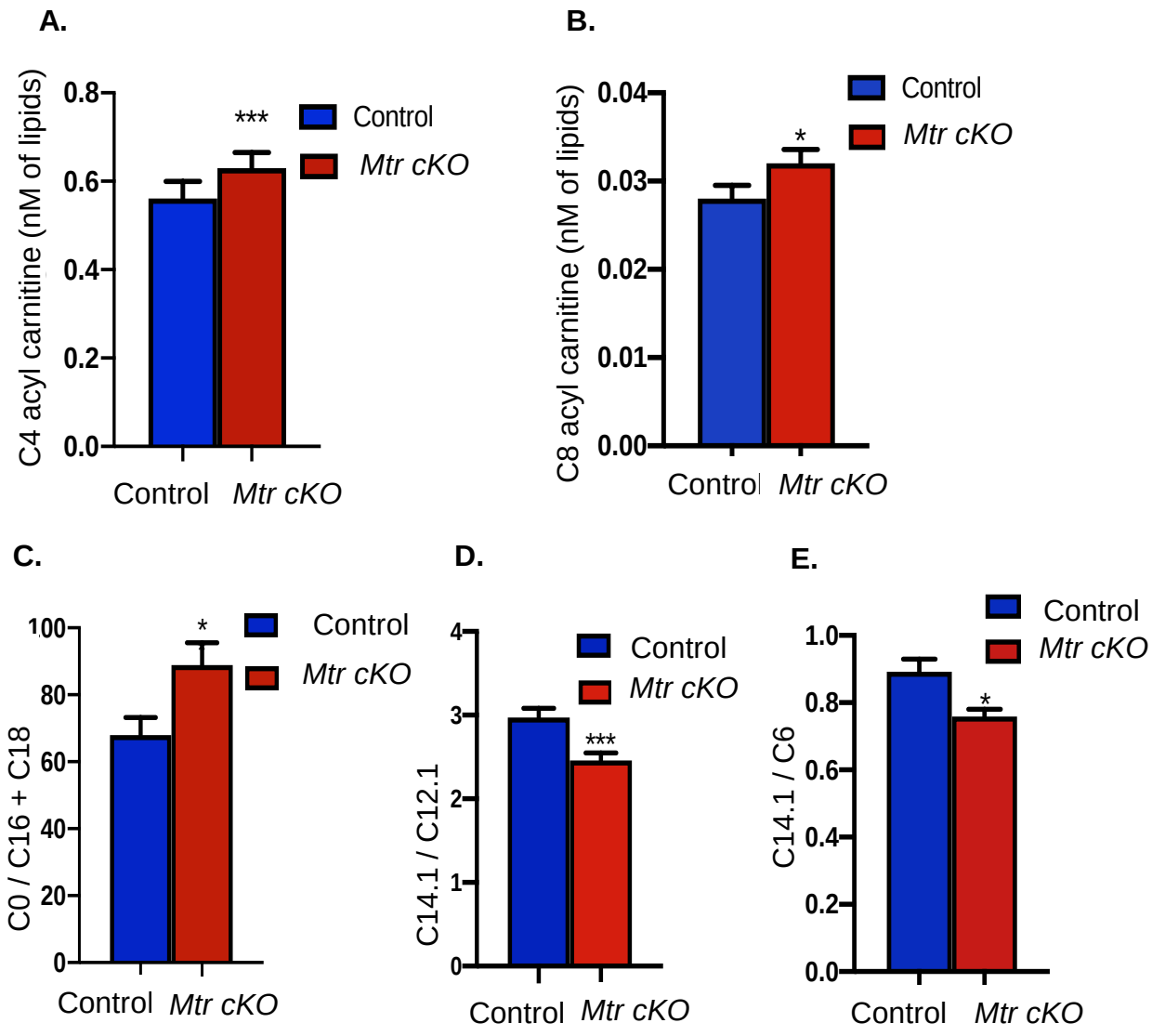

Figure 5. Silencing of methionine synthase in the heart impairs myocardial fatty acid oxidation.

A. Short chain (C4) **B.** Medium chain (C8) acylcarnitine levels in plasma of control and *Mtr cKO* mice. **C, D** and **E** are C0 / (C16 +C18), C14.1 / C12.1 and C14.1 / C6 acylcarnitine ratios in control and *Mtr cKO* mice. mice n = 3 to 6 per group, means ± SEM, * $P < 0.05$,** $P < 0.01$, *** $P < 0.001$.

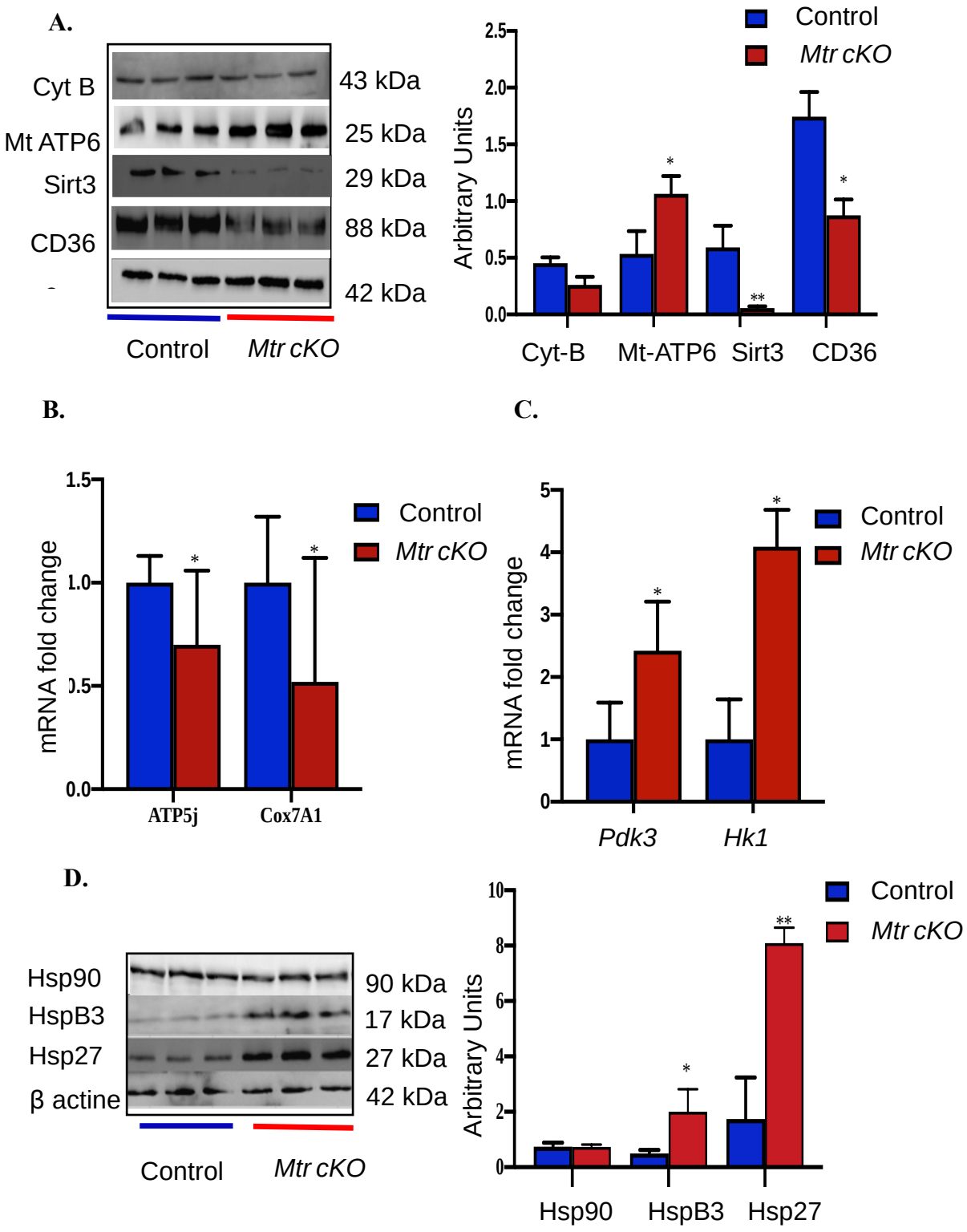

Figure 6. Silencing of methionine synthase in the heart impairs myocardial energy metabolism and induces cellular stress.
A. Western blot for Cytochrome B (Cyt B), Mt ATP6, Sirt3 and CD36 protein**. B.** Glycolytic genes **(***Pdk3* and *Hk1*) and **C.** *Cox7a1* and *ATP5j* mRNA expression level in the heart of *Mtr cKO*. **D** Western blots of Hsp90, Hspb3 and Hsp27. protein bands were quantified densitometrically, normalized to β actin and expressed as arbitrary unit; n = 3 per group, Means ± SEM,* $P < 0.05$ ** $P < 0.01$,*** $P < 0.001$.

Parameters	Control	*Mtr* cKO	*P* value
LVEDV (µL)	57.03 ± 5.72	81.41 ± 2.89	0.0067
LVESV(µL)	26.33 ± 4.00	57.33 ± 7.28	0.0015
LVEF %	55.38 ± 3.68	38.97 ± 2.06	0.0022
LVFS %	28.64 ± 2.46	18.79 ± 1.13	0.0022
LVPWd (mm)	0.72 ± 0.04	0.78 ± 0.04	0.3139
LVPWs (mm)	1.05 ± 0.07	0.94 ± 0.03	0.2620
LVIDd (mm)	3.65 ± 0.16	4.34 ± 0.04	0.0032
LVIDs (mm)	2.64 ± 0.18	3.53 ± 0.08	0.0015

TABLE 1. Echocardiographic left ventricular parameters for *Mtr cKO* and control. Left ventricular end diastolic volume (LVEDV), Left ventricular end systolic volume (LVESV), left ventricular ejection fraction (LVEF), left ventricular fractional shortening (LVFS), left ventricular posterior wall thickness in diastole (LVPWd), left ventricular posterior wall thickness in systoles (LVPWs) and left ventricular end diastolic internal diameter in diastole (LVIDd) and left ventricular end diastolic internal diameter in systole (LVIDs). Means ± SEM, n = 6 to 10 per group, * $P < 0.05$ ** $P < 0.01$, *** $P < 0.001$).

Annex 3: Supplementary data for Kosgei J Viola et al

Kosgei. J. V *et al*, Hypertrophic cardiomyopathy and systolic dysfunction in mice with heart selective invalidation of methionine synthase (*Mtr*) related to impaired energy metabolism, cellular stress and fibrosis.

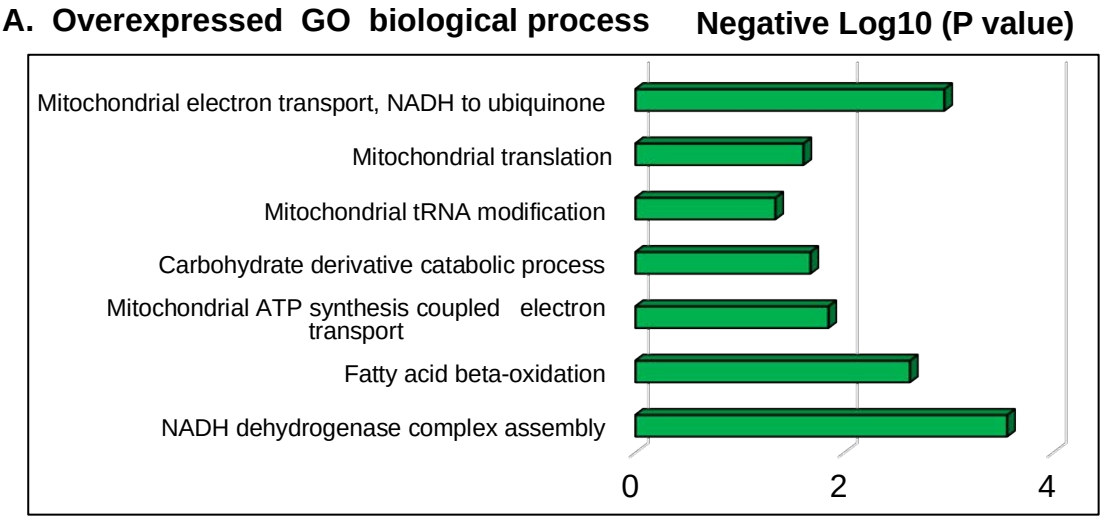

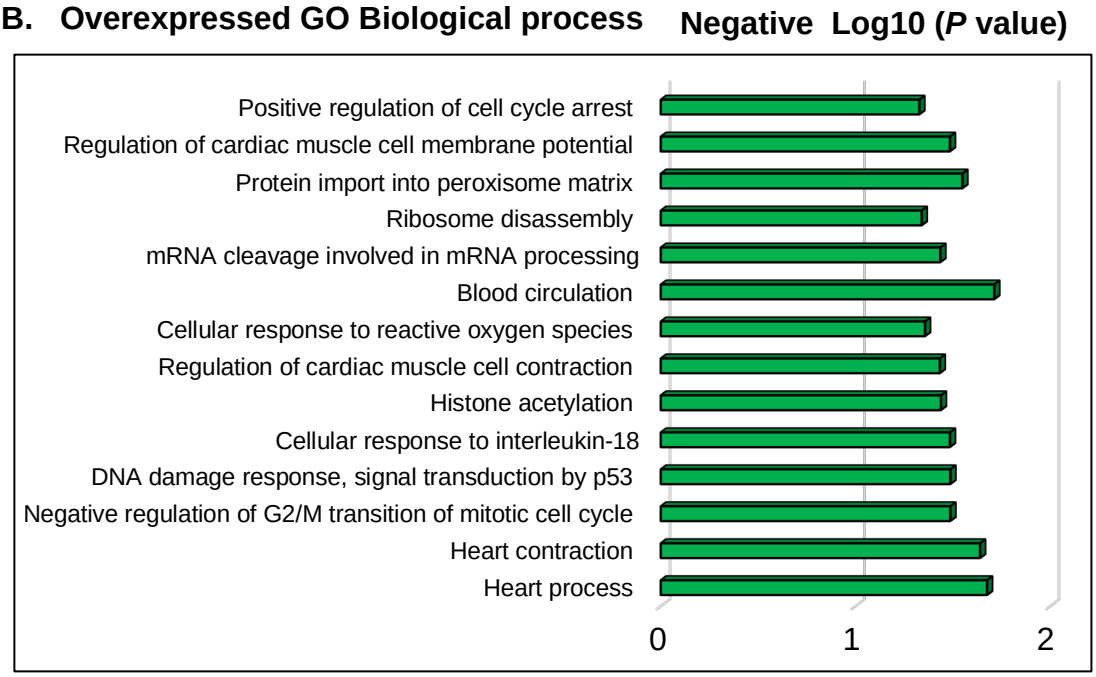

Supplementary Figure S1. Functional annotations of under-expressed genes in the heart of *Mtr* cKO (cluster 2) in comparison to control hearts. A. Enrichr overexpressed GO biological processes related to Myocardial energy metabolism and mitochondrial bioenergetics for the under-expressed genes in *Mtr cKO*. B. Enrichr overexpressed GO biological processes related to cardiac remodelling and heart processes associated with the under-expressed genes in *Mtr cKO*.

A. Overexpressed GO Biological Processes **Negative Log10 (*P* value)**

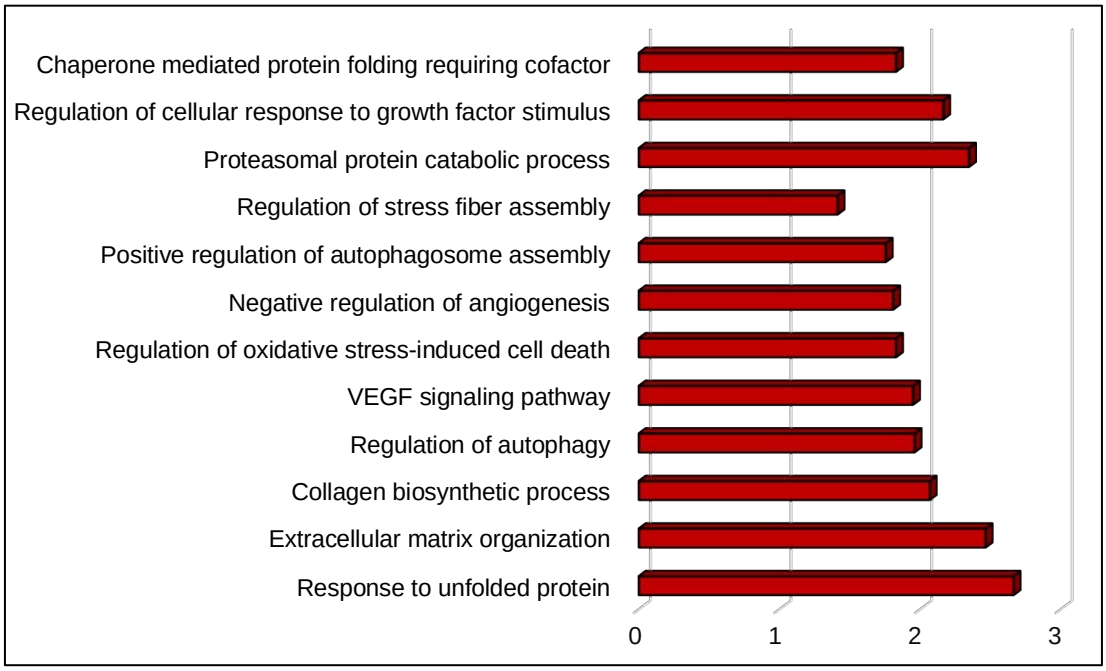

B. Overexpressed GO Biological Processes **Negative Log10 (*P* value)**

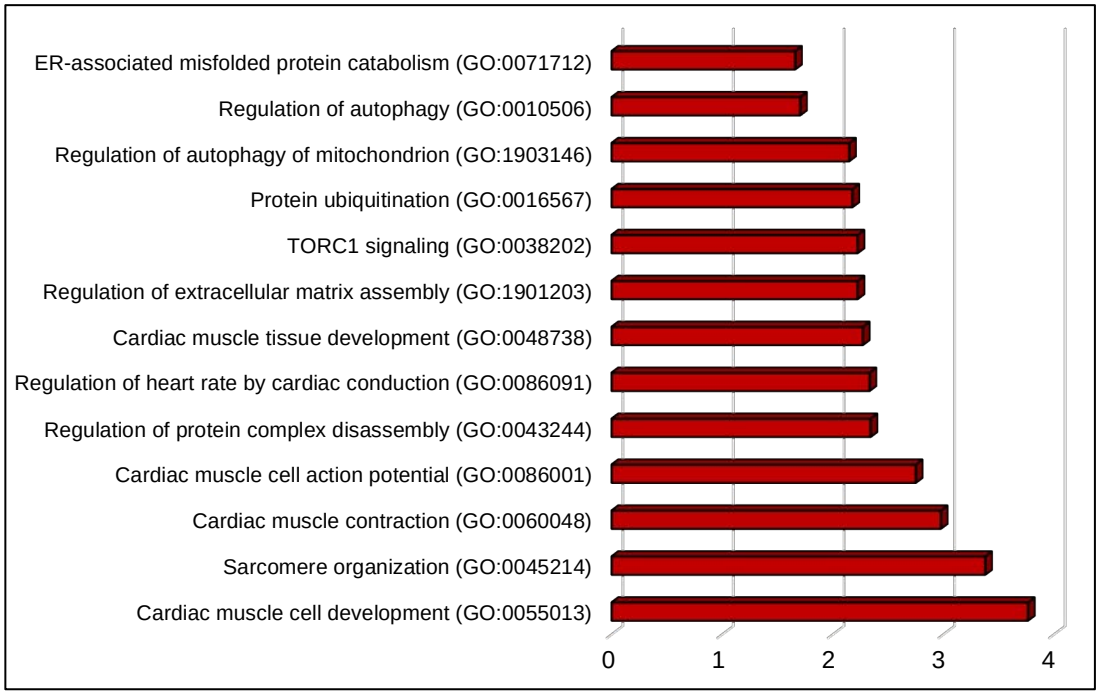

Supplementary Figure S2. Functional annotations of overexpressed genes in the myocardium of *Mtr cKO* performed by Enrichr. A. Enrichr over-expressed GO biological processes for the overexpressed genes of sub-cluster 3 in *Mtr cKO*. B. Enrichr overexpressed GO biological processes related to cardiac remodelling and heart processes for the overexpressed genes of sub-cluster 4 in *Mtr cKO*

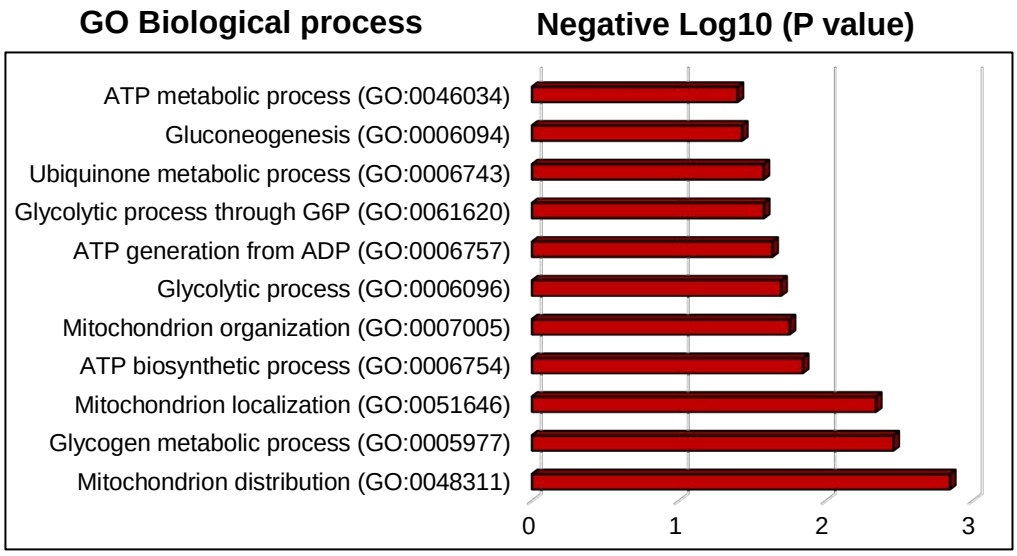

Supplementary Figure S3. Enrichr overexpressed GO biological processes enriched in mitochondrial energy metabolism for the overexpressed sub-cluster 4 genes in *Mtr cKO*.

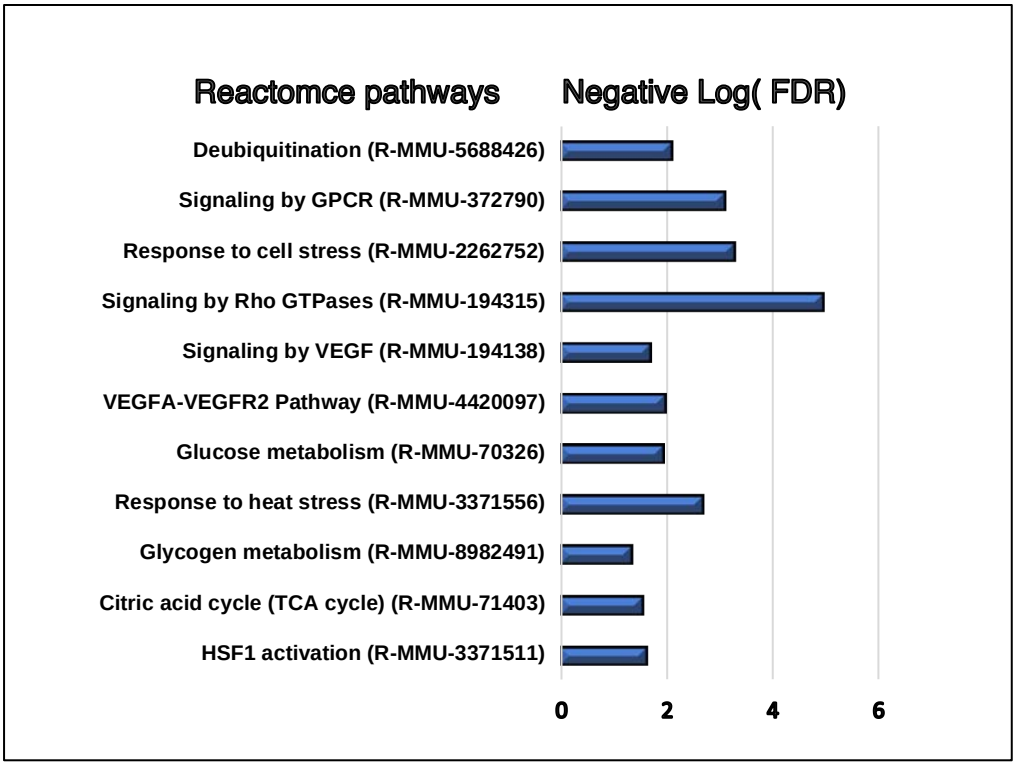

Supplementary Figure S4. PANTHER Gene ontology term enrichment and pathway analysis for the upregulated genes (Sub-cluster 4 and sub-cluster 3) in the hearts of *Mtr cKO*. Shown in the bar graph are the dysregulated reactome pathways associated with the upregulated genes in sub-cluster 3 and sub-cluster 4 in the hearts of *Mtr cKO.* Majority of these dysregulated pathways are linked to response to cellular stress, cardiac remodelling and myocardial bioenergetics. The analysis of pathways was performed using Panther classification system (FDR < 0.05).

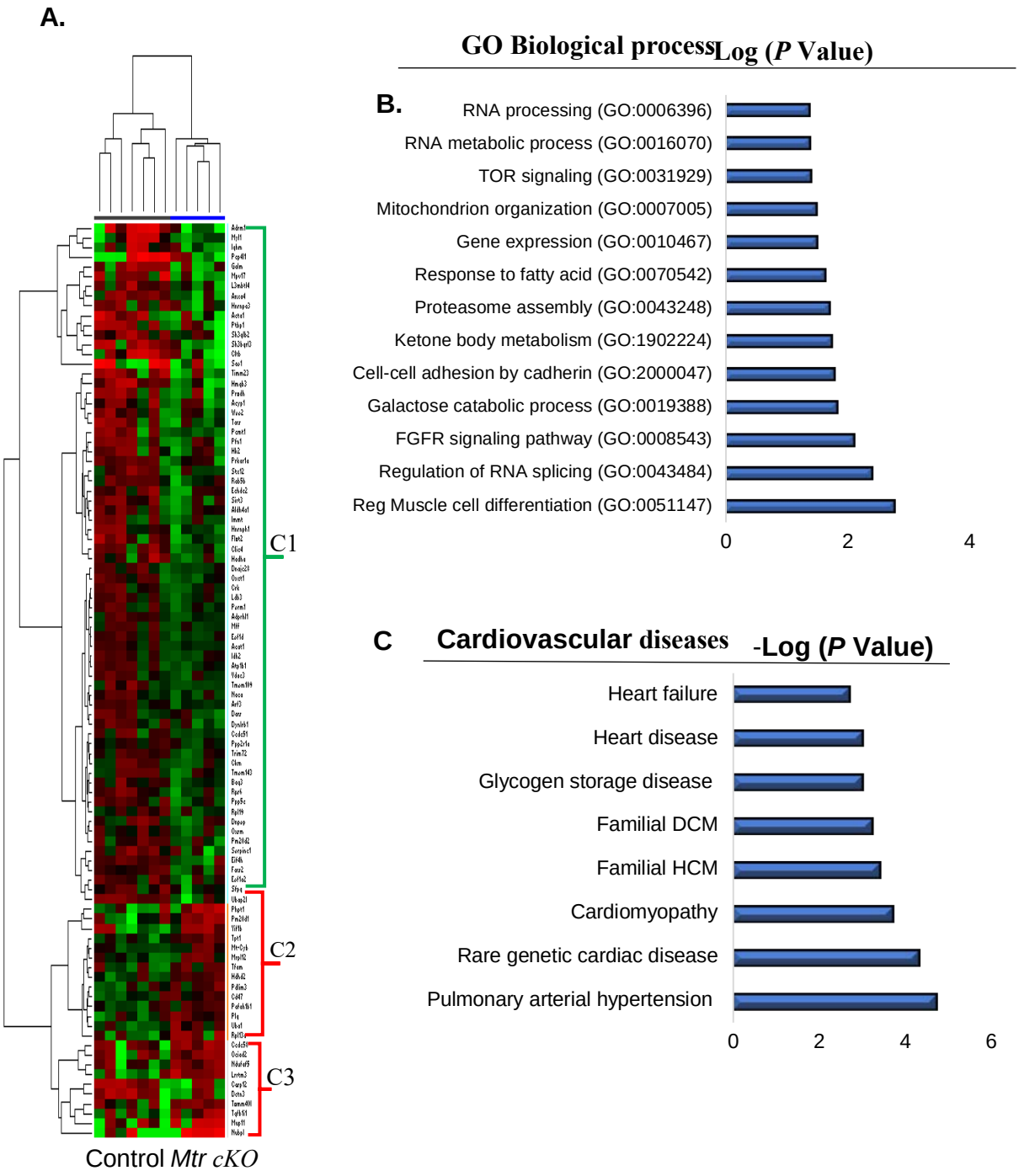

Supplementary Figure S5. Cardiac-specific invalidation of *Mtr* dysregulates protein expression in the myocardium. **A.** Heatmap of the top 94 dysregulated proteins in the myocardium of *Mtr cKO* in comparison to control mice. Black, red and green indicates median, overexpressed and under-expressed proteins respectively. **B.** Overexpressed GO biological processes linked to 34 differentially expressed proteins in the myocardium of *Mtr cKO* associated with energy metabolism and cardiac remodelling. **C**. Cardiovascular diseases associated with 34 differentially expressed proteins in the myocardium of *Mtr cKO*. *n* = 7 controls and n = 5 *Mtr cKO*. (HCM = hypertrophic cardiomyopathy and DCM = dilated cardiomyopathy).

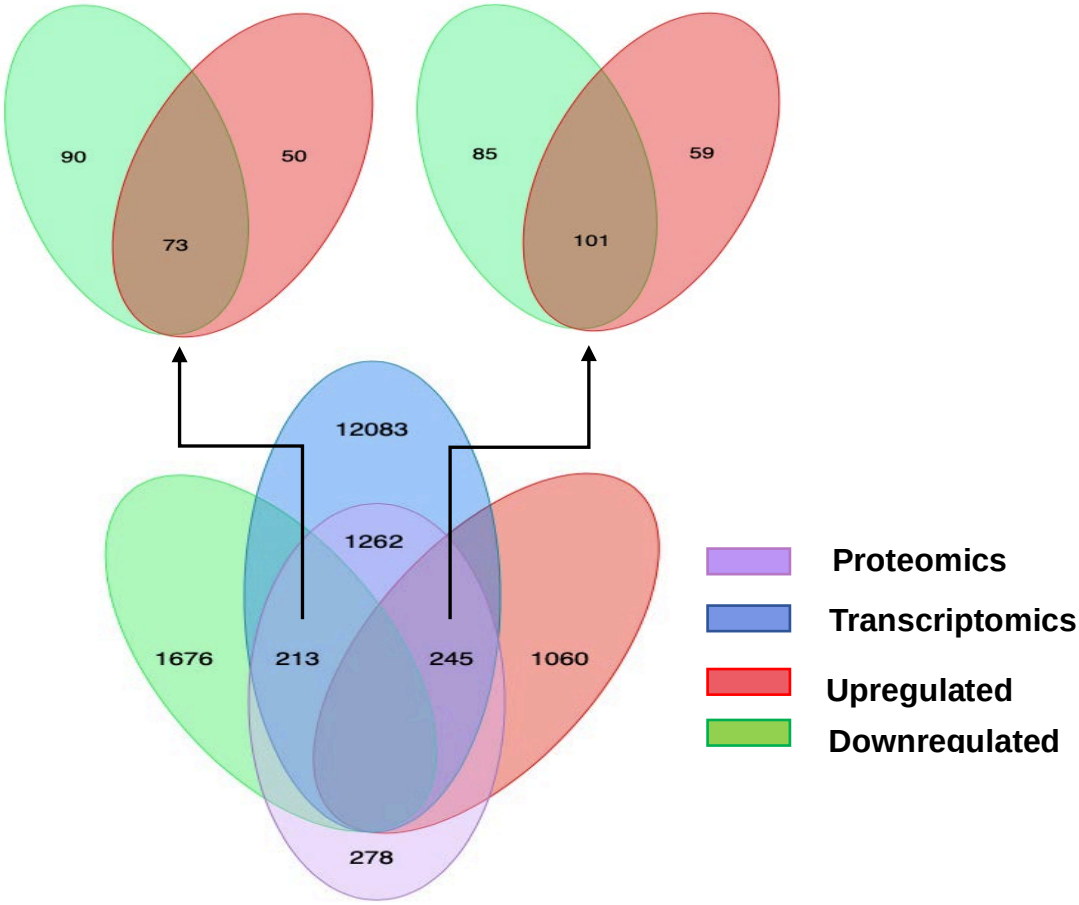

Supplementary Figure S6. Venn diagram representing the overlapping between dysregulated genes and proteins in the heart of *Mtr cKO* mice based on transcriptomic driven analysis of proteome. A total of 16539 genes and 1998 proteins were detected in the heart of *Mtr cKO* as revealed by transcriptomic and proteomic analysis respectively. Of these, a total 1720 genes-proteins were commonly dysregulated of which 213 were downregulated and 245 were upregulated. Transcriptomic driven analysis of proteome revealed that the 213 downregulated were positively translated into 90 downregulated proteins and negatively translated into 50 upregulated proteins and 73 proteins with no change. The 245 upregulated genes were negatively translated into 85 downregulated and positively translated into 59 upregulated proteins and 101 proteins with no change (0.8 < FC > 1.25.

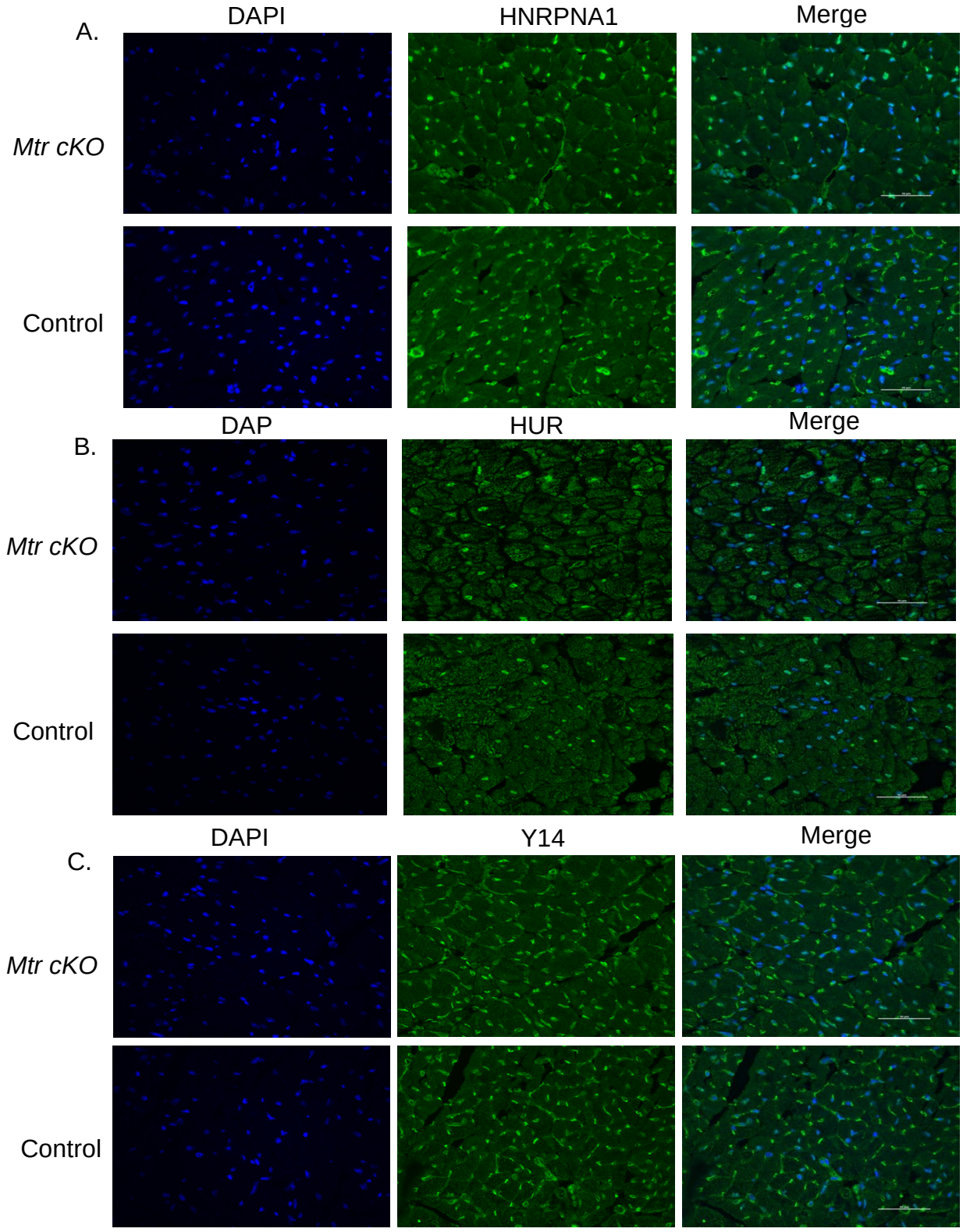

Supplemenatry Figure S7. Invalidation of *Mtr* gene in the heart induces subcellular mislocalization of Hnrpna1 RNA binding protein. A, B and C shows the subcellular localization of Hnrpna1, Hur and Y14 RNA binding proteins in the hearts of *Mtr cKO* and control animals.

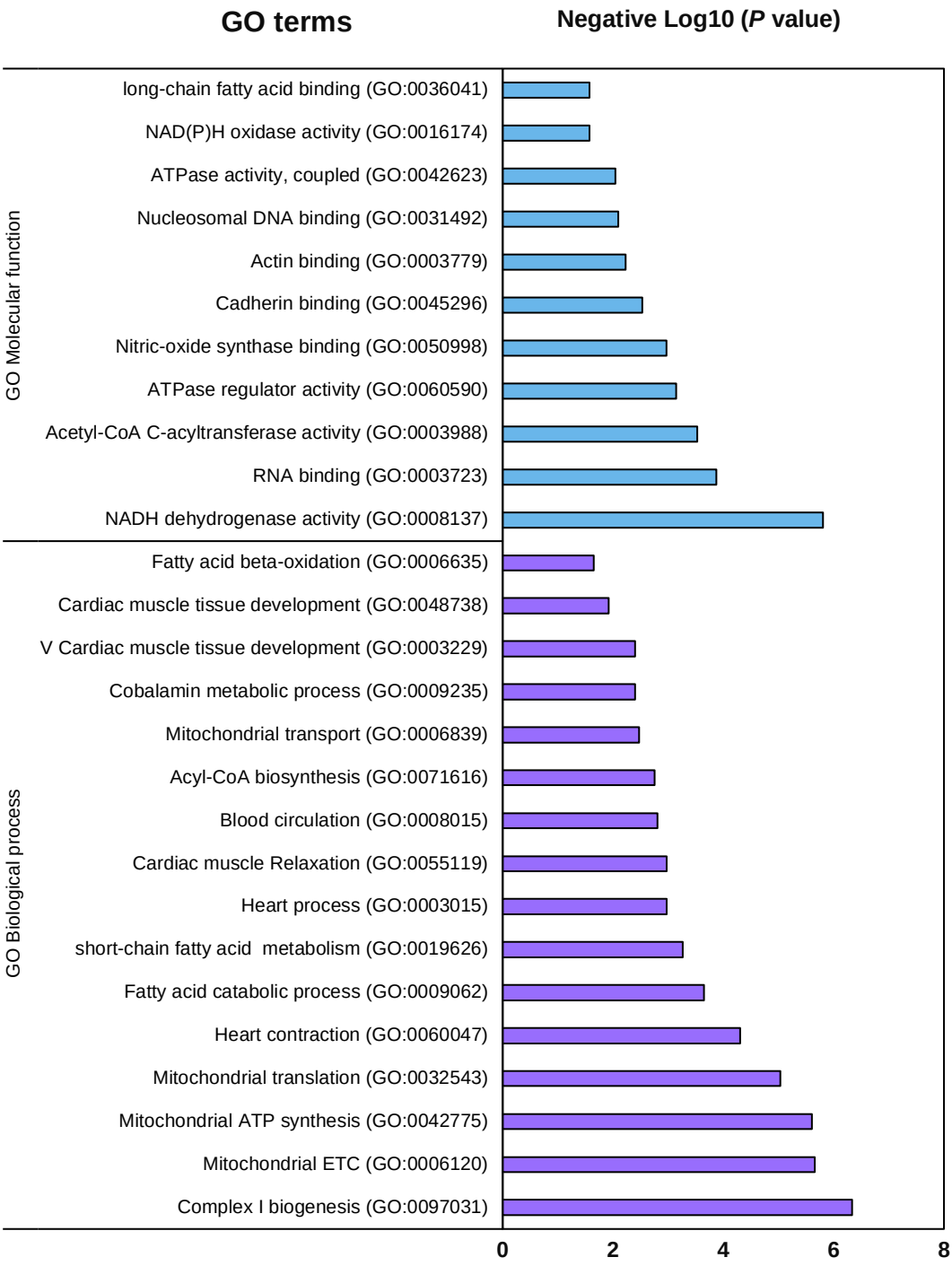

Supplementary Figure S8. Enrichr GO biological processes and molecular function associated with the 90 under-expressed proteins in the heart of *Mtr cKO*. Shown in the bar graph are the GO biological processes and molecular functions of the 90 positively under-expressed proteins in the hearts of *Mtr cKO* mice in comparison to control mice, the analysis was performed using Enrichr ($P < 0.05$).

A.

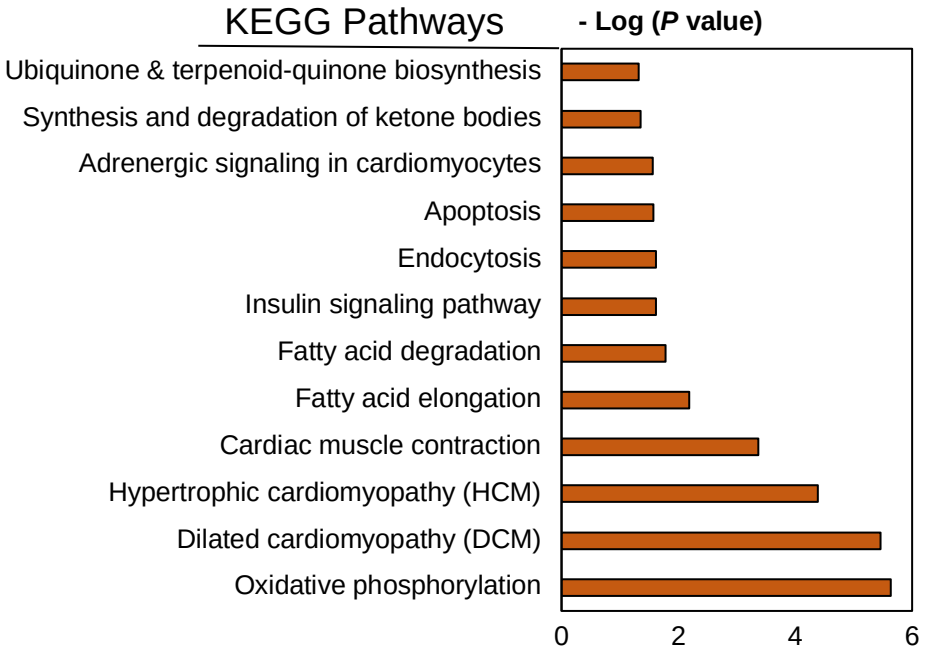

B.

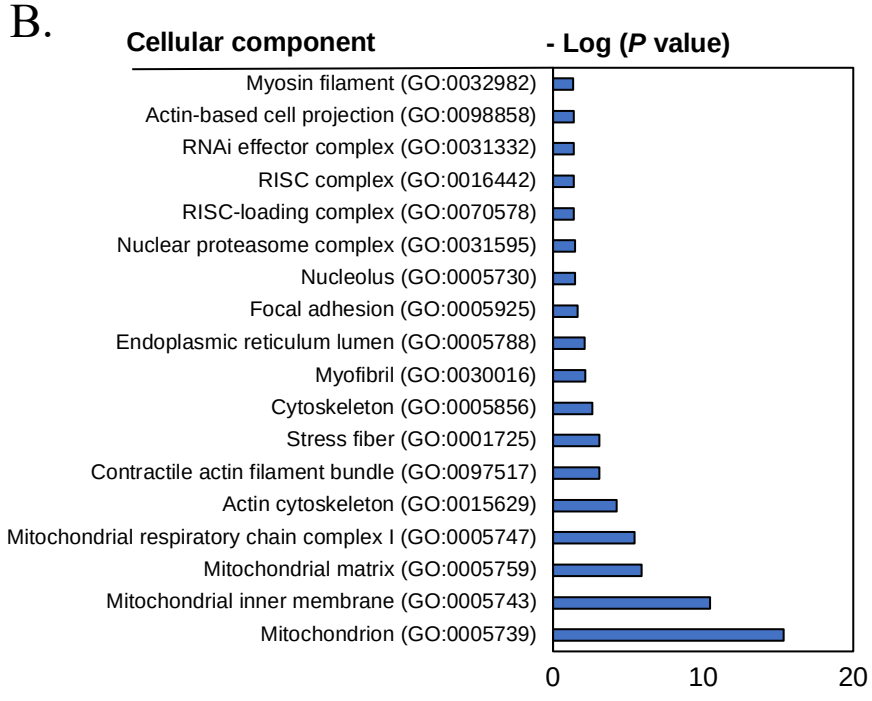

Supplementary Figure S9. Enrichr KEGG pathways and cellular component associated with the positively 90 under-expressed proteins in the heart of *Mtr cKO* in comparison to controls. A. KEGG pathways associated with the 90 under-expressed proteins in the

heart of *Mtr cKO* mice analyzed by Enrichr. B. GO cellular component of the 90 under-expressed proteins in the heart of *Mtr cKO.*

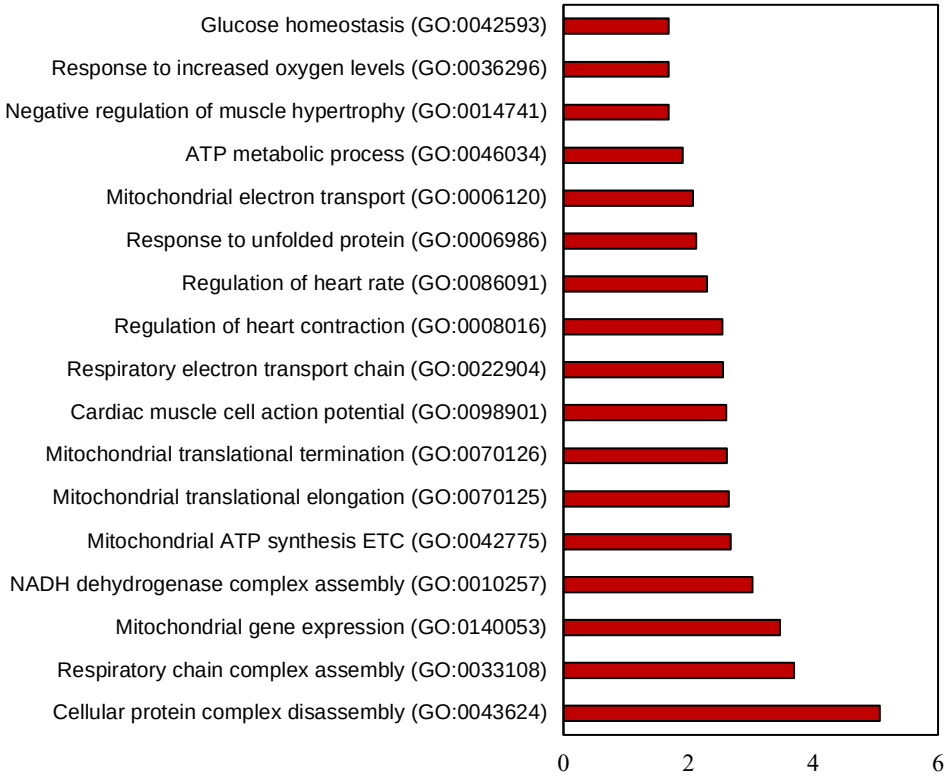

Supplementary Figure S10. Enrichr GO biological processes of the 59 positively overexpressed proteins in the hearts of *Mtr cKO* in comparison to control hearts.

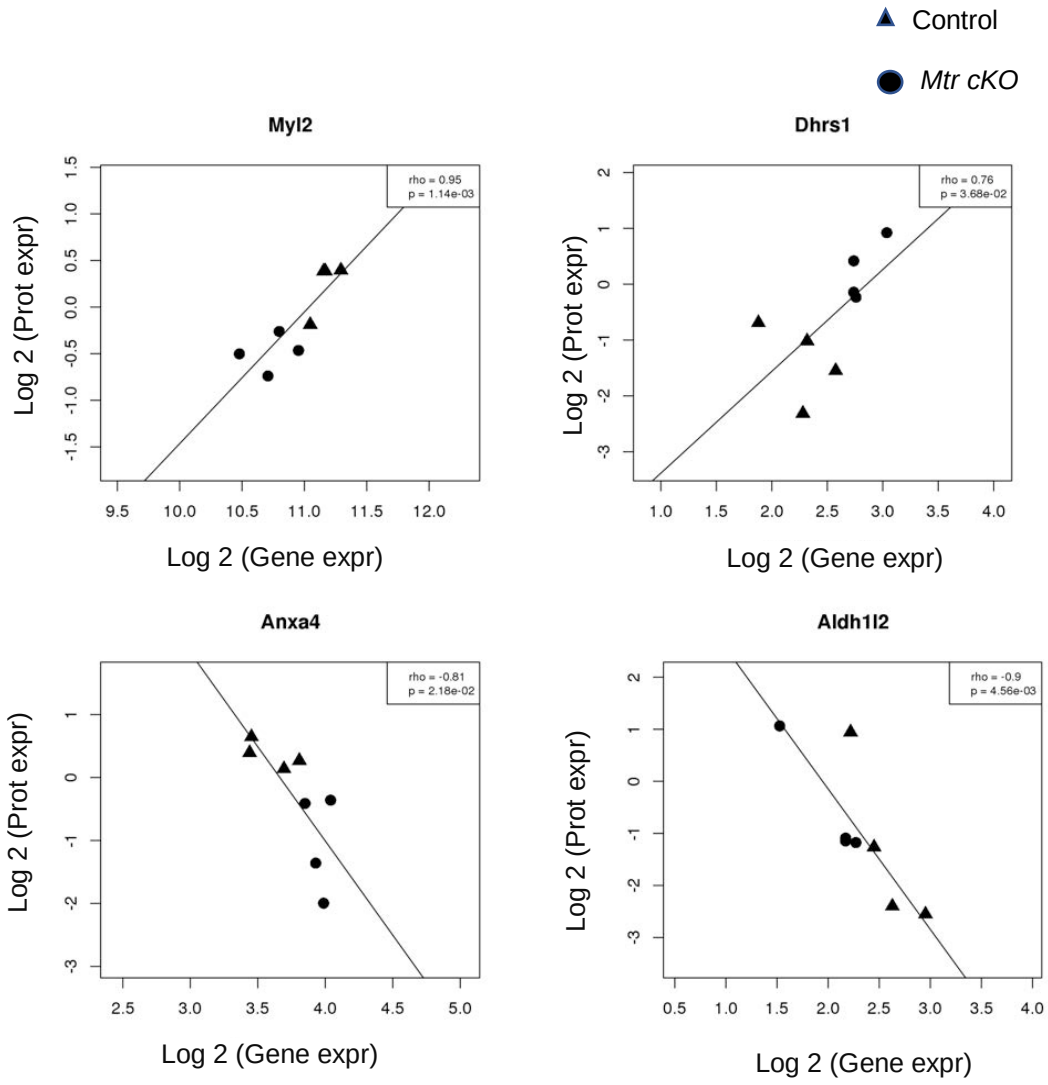

Supplementary Figure S11. Graphical representation of the positively and negatively correlated genes-proteins in *Mtr cKO* analyzed by Spearman correlation. Myl2 and Dhrs1 are among the 17 positively correlated genes-proteins and Anxa4 and Aldh1l2 are among the 5 negatively correlated genes-proteins in the hearts of *Mtr cKO*.

Genes_Symbols_IDs	P Value	Fold change	Control_mean	Mtr-cKO mean
Acaa2//ENSMUSG00000036880	0.010	-1.340	351.53	262.47
Acat1//ENSMUSG00000032047	0.039	-1.191	338.69	284.46
Acadm//ENSMUSG00000062908	0.023	-1.309	816.37	623.48
Ehhadh//ENSMUSG00000022853	0.010	-1.848	19.64	10.63
Decr1//ENSMUSG00000028223	0.005	-1.392	189.69	136.29
Ndufv1//ENSMUSG00000037916	0.0195	-1.199	148.60	123.90
Ndufb4//ENSMUSG00000022820	0.015	-1.253	39.84	31.80
Ndufa7//ENSMUSG00000041881	0.033	-1.195	31.19	26.11
Cox6a2//ENSMUSG00000030785	0.035	-1.222	715.30	585.42
Cox7a1//ENSMUSG00000074218	0.051	-1.214	125.57	103.46
Atp5j//ENSMUSG00000022890	0.012	-1.342	111.84	83.32
Atp5s//ENSMUSG00000054894	0.046	-1.282	11.16	8.70
Atp5h//ENSMUSG00000034566	0.043	-1.217	292.03	240.05
Pfkfb1//ENSMUSG00000025271	3.96E-06	-3.637	8.23	2.26
Hk1//ENSMUSG00000037012	0.0004	1.657	33.72	55.86
Pdk3//ENSMUSG00000035232	0.0001	1.953	2.77	5.40

Supplementary Table 1. List of differentially expressed genes involved in mitochondrial energy metabolism including fatty acid beta oxidation, oxidative phosphorylation and glycolysis in the myocardium *Mtr cKO* in comparison to controls

Overexpressed GO biological processes linked to the upregulated genes in sub-cluster 4 analyzed by Enrichr		
Go biological process	Genes	P value)
Mitochondrial respiratory chain complex IV biogenesis (GO:0097034)	COA3, SCO1, COX17, COX14	0,01257
Regulation of cell cycle G2/M phase transition (GO:1902749)	YWHAE; DYNC1H1; DCTN2; PPP2R1A; DCTN1; PRKACA; PCNT; TUBB4B; YWHAG	0,0129
Mitochondrial respiratory chain complex IV assembly (GO:0033617)	COA3; SCO1; COX17; COX14	0,0105
ATP biosynthetic process (GO:0006754)	ATP5E; ATP5D; ATP5G3; ALDOA; ATP6V0A1	0,01434
Glycolytic process (GO:0006096)	PFKL; ALDOA; GCK; HK1	0,0174
Mitochondrion organization (GO:0007005)	ALAS1; CLUH; TOMM40; MUL1; SIRT5; MIEF2; S; TRAK1; TRAK2; AFG3L2; OXA1L; PITRM1; MYH14; HAP1	0,01763
Positive regulation of programmed cell death (GO:0043068)	ARHGEF12; GADD45B; ITSN1; DAPK3; ARHGEF19; HTT; SCRIB; HDAC6; TIAM2; ABR; AKAP13; NCSTN; ARHGEF9; TCTN3; ANKRD1; TRIM35; ARHGEF1; FADD; SOS1	0,0215
ER-associated misfolded protein catabolic process (GO:0071712)	POMT2; VCP; UGGT1	0,0178
Regulation of autophagy (GO:0010506)	USP36; KDM4A; ROCK1; DAPK3; PIK3R2; ZDHHC8; HDAC6; MTOR; GOLGA2; TRIM8; CPTP; WDR6; VDAC1; CAPN1; PRKACA; ATP6V0A1	0,0198
Smooth muscle contraction (GO:0006939)	SMTN; ROCK1; HMCN2	0,0219
Cardiac muscle contraction (GO:0060048)	MYBPC3; GAA; MYL3; SCN5A ; ATP1B1 ;SCN1B; TTN	0,0231
ATP generation from ADP (GO:0006757)	PFKL; ALDOA; GCK; HK1	0,0071
Regulation of autophagy of mitochondrion (GO:1903146)	USP36; HTT; VDAC1; ZDHHC8; HDAC6	0,0010
CAardiac muscle cell development (GO:0055013)	PDGFRB; SORBS2; NKX2-5; OBSL1; MYPN; TTN; MYOM3	1,72E-04
Positive regulation of calcium-mediated signaling (GO:0050850)	P2RX5; GSTO1; HTT; CDH13; AKAP6; HAP1	0,0015
Positive regulation of extracellular matrix assembly (GO:1901203)	SMAD3; DAG1; CLASP2	0,0041
TORC1 signaling (GO:0038202)	LARP1; CLEC16A; MTOR	0,0041
Negative regulation of striated muscle cell differentiation (GO:0051154))	CAV3; FZD7;BHLHE41;NKX2-5	0,0047
Regulation of heart rate by cardiac conduction (GO:0086091)	JUP; CACNA2D1; SCN5A; SCN1B; DSC2	0,0047
Cardiac muscle tissue development (GO:0048738)	AKAP13; TBX20; ANKRD1; NKX2-5; TTN; MYOM3	0,0054

Supplementary Table 2. Enrichr Gene ontology term enrichment analysis for the 887 upregulated genes (Sub-cluster 4) in the hearts of *Mtr cKO*. The Table shows the most relevant and significantly overexpressed GO biological processes linked to sub-cluster 4 upregulated genes in the myocardium of *Mtr cKO* mice (*P* value < 0.05)

Cardiovascular diseases associated with the 34 differentially expressed proteins in the myocardium of *Mtr cKO* analyzed by Open Targets Platform			
Cardiovascular diseases (*P*= 0.001)		*P* value	Number of associated targets
1	Rare genetic cardiac disease	0.00005	16
2	Cardiomyopathy	0.0002	14
3	Rare familial disorder with hypertrophic cardiomyopathy	0.0004	10
4	Familial dilated cardiomyopathy	0.0006	10
5	Glycogen storage disease with hypertrophic cardiomyopathy	0.001	4
6	Hypertension	0.001	12
7	Heart failure	0.002	8
8	Mitochondrial disease with hypertrophic cardiomyopathy	0.02	4
9	Pulmonary arterial hypertension	0.00002	10

Supplementary Table 3. Cardiovascular diseases and number of targets associated with the 34 differentially expressed proteins in the myocardium of *Mtr cKO* analysis achieved using Open Targets Platform.

Metabolic diseases associated with top 94 differentially expressed proteins in the myocardium of *Mtr cKO* analyzed by Open Target Platform			
Metabolic disorders (P =3.e^{-8})		P value	Number of associated targets
1	Inborn errors of metabolism	8E-07	48
2	Mitochondrial oxidative phosphorylation disorder due to mitochondrial DNA anomalies	0.000009	14
3	Mitochondrial disease	0.000007	30
4	Pyruvate dehydrogenase deficiency	0.00002	9
5	Disorder of energy metabolism	0.00001	31
6	Mitochondrial oxidative phosphorylation disorder	0.000002	27
7	Disorder of fatty acid oxidation and ketone body metabolism	0.001	11
8	Disorder of other vitamins and cofactors metabolism and transport	0.0004	7
9	Glycogen storage diseases	0.00001	24
10	Fatal infantile cytochrome C oxidase deficiency	0.006	6
11	Disorder of amino acid and other organic acid metabolism	0.00001	24

Supplementary Table 4. Most relevant metabolic disorders and the number of targets associated with the top 94 dysregulated proteins in the myocardium of *Mtr cKO,* analysis was achieved using Open Targets Platform ($P < 0.05$).

Genetic diseases associated with top 94 differentially expressed proteins in the myocardium of *Mtr cKO* analyzed by Open target bioinformatic tool			
Genetic disorders ($P = 4.e\text{-}^{10}$)		P value	Number of associated targets
1	Metabolic myopathy	9E-10	27
2	Rare genetic developmental defect during embryogenesis	8E-10	57
3	Rare genetic cardiac diseases	1E-08	40
4	Mitochondrial myopathy	1E-08	22
5	Inborn errors of metabolism	7E-08	48
6	Mitochondrial oxidative phosphorylation disorder	0.000002	27
7	Genetic neurodegenerative disease	0.00005	31
8	Disorder of energy metabolisms	0.000001	31

Supplementary Table 5. The most relevant genetic diseases and number of targets associated with the top 94 dysregulated proteins in the myocardium of *Mtr cKO* analysis was performed using Open Targets Platform ($P < 0.05$).

Gene/ protein	rho	pval	transFC	protFC
Ak4	0.761904761904762	0.0367559523809524	1.96213293802764	1.4002399552368
Aldh1l2	-0.904761904761905	0.00456349206349206	0.773115989421706	1.51928961255414
Anxa4	-0.80952380952381	0.0217757936507936	1.30148308934009	0.453000492497343
Atic	-0.857142857142857	0.0107142857142857	1.25167321485731	0.928880526289553
Ckb	0.690476190476191	0.0693948412698413	1.37247919764253	1.5849782218571
Col15a1	-0.642857142857143	0.0961805555555556	0.770048844621929	0.630709846658297
Cops8	0.738095238095238	0.0458333333333333	0.786489862079733	1.06963590511243
Csrp3	0.785714285714286	0.0279265873015873	0.754319148344273	0.848288851134725
Dhrs1	0.761904761904762	0.0367559523809524	1.36530675876541	2.67796290343909
Echdc1	0.761904761904762	0.0367559523809524	0.790413758540751	0.92877787555414
Enpp4	0.642857142857143	0.0961805555555556	0.714441418391645	0.55361095131433
Gpd2	0.642857142857143	0.0961805555555556	0.733166740722631	0.768581674347435
Hist2h2ab	-0.714285714285714	0.0575892857142857	1.26204060610359	0.927441823575625
Hmox2	0.714285714285714	0.0575892857142857	1.31056135639104	3.16132087793648
Mrpl4	0.730552019767088	0.0395556279042975	1.28452000229843	14.3520447043443
Myl1	0.857142857142857	0.0107142857142857	0.324574674950568	0.319293685701231
Myl2	0.952380952380953	0.00114087301587302	0.754030935512335	0.547426523067139
Plin1	0.761904761904762	0.0367559523809524	0.269881832467477	0.568381759714516
Sh3glb2	0.666666666666667	0.0830853174603175	0.772600734979913	0.573385431774321
Slc25a1	0.857142857142857	0.0107142857142857	0.589383683034287	0.693281499660582
Slc4a1	0.880952380952381	0.00724206349206349	0.555804745214445	0.461214061789782
Snca	0.880952380952381	0.00724206349206349	0.650893625213038	0.437772715208782

Supplementary Table 6. Correlation analysis of the commonly dysregulated genes-proteins in the myocardium of *Mtr cKO* analyzed using Spearman's correlation. Shown in the table are the rho values of the negatively and the positively correlated genes-proteins in the hearts of *Mtr cKO.*

SUMMARY

Heart failure is one of the most common causes of morbidity and mortality in Western countries and its incidence is increasing in developing countries. Deficiency in folates and vitamin B12 (cobalamin) during gestation and lactation causes a fetal programming effect with metabolic cardiomyopathy related to decreased synthesis of methionine and impaired remethylation (RM) of homocysteine. Inborn errors of cobalamin metabolism, including CblG caused by mutations of *MTR* gene, which encodes methionine synthase (that catalyzes vitamin B12 dependent remethylation of homocysteine to methionine), and CblC caused by mutations of *MMACHC* gene cause cardiometabolic decompensation in infants. However, cardiac consequences and mechanisms underlying this process in adults are unknown. The aim of this Ph.D. project was to investigate the cardiac functional, metabolic and molecular consequences of the inhibition of methionine synthesis in a transgenic mouse model of constitutive cardiac specific invalidation of *Mtr* gene and systemic invalidation of *MMACHC* gene. We found that the selective *Mtr* invalidation in the heart produces cardiomyopathy with heart failure, myocardium hypertrophy and systolic dysfunction in young adult mice. At the tissue and molecular levels, the observed cardiomyopathy was related to impaired energy metabolism with disruption of fatty acid oxidation and oxidative phosphorylation, cellular stress and cardiac remodeling with fibrosis. Impaired energy metabolism was linked to decreased expression of Sirt3. The mislocalization and nuclear sequestration of hnRNPA1 could explain part of the expression changes of genes and proteins. These findings suggest a further need to evaluate whether CblG could be a new genetic cause of primary heart failure in adult patients.

Key words: Vitamin B12, methionine synthase, cardiomyopathy, heart failure, cardiac hypertrophy, energy metabolism, *MMACHC, MTR*

RÉSUMÉ

L'insuffisance cardiaque est l'une des causes les plus courantes de morbidité et de mortalité dans les pays occidentaux et son incidence augmente dans les pays en développement. Une carence en folates et en vitamine B12 (cobalamine) au cours de la gestation et de l'allaitement entraîne un effet de programmation fœtale avec une cardiomyopathie métabolique liée à une diminution de la synthèse de méthionine et à une altération de la réméthylation de l'homocystéine. Les défauts génétiques du métabolisme de la cobalamine, y compris la CblG causée par des mutations du gène *MTR*, qui code pour la méthionine synthase (qui catalyse la reméthylation de l'homocystéine dépendante de la vitamine B12 en méthionine), et CblC causée par des mutations du gène *MMACHC* provoquent une décompensation cardiométabolique chez les nourrissons. Cependant, les conséquences cardiaques et les mécanismes sous-jacents à ce processus chez l'adulte sont inconnus. Le but de ce projet de doctorat consistait à étudier les conséquences fonctionnelles, métaboliques et moléculaires cardiaques de l'inhibition de la synthèse de la méthionine dans un modèle murin transgénique d'invalidation constitutive du gène *Mtr* par spécificité cardiaque et invalidation systémique du gène *MMACHC*. Nous avons constaté que l'invalidation sélective de *Mtr* dans le cœur produisait une cardiomyopathie avec insuffisance cardiaque, une hypertrophie du myocarde et un dysfonctionnement systolique chez les jeunes souris adultes. Au niveau tissulaire et moléculaire, la cardiomyopathie observée était liée à une altération du métabolisme énergétique avec perturbation de l'oxydation des acides gras et de la phosphorylation oxydative, au stress cellulaire et au remodelage cardiaque avec fibrose. Un métabolisme énergétique altéré, il était lié à une diminution de l'expression de Sirt3. La mauvaise localisation et la séquestration nucléaire de hnRNPA1 pourraient expliquer une partie des modifications de l'expression des gènes et des protéines. Ces résultats suggèrent un mécanisme de cardiomyopathie chez jeunes adultes CblG.

Mots-clés : Vitamine B12, méthionine synthase, cardiomyopathie, insuffisance cardiaque, hypertrophie cardiaque, métabolisme énergétique, *MMACHC, MTR*